NEURAL SUBSTRATES OF ACUPUNCTURE: FROM PERIPHERAL TO CENTRAL NERVOUS SYSTEM MECHANISMS

EDITED BY: Younbyoung Chae, Vitaly Napadow, Florian Beissner, Yi-Wen Lin and Richard E. Harris

PUBLISHED IN: Frontiers in Neuroscience, Frontiers in Psychology, Frontiers in Cellular Neuroscience and Frontiers in Human Neuroscience

frontiers Research Topics

ISSN 1664-8714
ISBN 978-2-88963-505-4
DOI 10.3389/978-2-88963-505-4

About Frontiers

Frontiers is more than just an open-access publisher of scholarly articles: it is a pioneering approach to the world of academia, radically improving the way scholarly research is managed. The grand vision of Frontiers is a world where all people have an equal opportunity to seek, share and generate knowledge. Frontiers provides immediate and permanent online open access to all its publications, but this alone is not enough to realize our grand goals.

Frontiers Journal Series

The Frontiers Journal Series is a multi-tier and interdisciplinary set of open-access, online journals, promising a paradigm shift from the current review, selection and dissemination processes in academic publishing. All Frontiers journals are driven by researchers for researchers; therefore, they constitute a service to the scholarly community. At the same time, the Frontiers Journal Series operates on a revolutionary invention, the tiered publishing system, initially addressing specific communities of scholars, and gradually climbing up to broader public understanding, thus serving the interests of the lay society, too.

Dedication to Quality

Each Frontiers article is a landmark of the highest quality, thanks to genuinely collaborative interactions between authors and review editors, who include some of the world's best academicians. Research must be certified by peers before entering a stream of knowledge that may eventually reach the public - and shape society; therefore, Frontiers only applies the most rigorous and unbiased reviews.
Frontiers revolutionizes research publishing by freely delivering the most outstanding research, evaluated with no bias from both the academic and social point of view. By applying the most advanced information technologies, Frontiers is catapulting scholarly publishing into a new generation.

What are Frontiers Research Topics?

Frontiers Research Topics are very popular trademarks of the Frontiers Journals Series: they are collections of at least ten articles, all centered on a particular subject. With their unique mix of varied contributions from Original Research to Review Articles, Frontiers Research Topics unify the most influential researchers, the latest key findings and historical advances in a hot research area! Find out more on how to host your own Frontiers Research Topic or contribute to one as an author by contacting the Frontiers Editorial Office: researchtopics@frontiersin.org

NEURAL SUBSTRATES OF ACUPUNCTURE: FROM PERIPHERAL TO CENTRAL NERVOUS SYSTEM MECHANISMS

Topic Editors:
Younbyoung Chae, Kyung Hee University, South Korea
Vitaly Napadow, Harvard Medical School, United States
Florian Beissner, Hannover Medical School, Germany
Yi-Wen Lin, China Medical University, Taiwan
Richard E. Harris, University of Michigan, United States

Citation: Chae, Y., Napadow, V., Beissner, F., Lin, Y.-W., Harris, R. E., eds. (2020). Neural Substrates of Acupuncture: From Peripheral to Central Nervous System Mechanisms. Lausanne: Frontiers Media SA. doi: 10.3389/978-2-88963-505-4

Table of Contents

frontiers in Neuroscience

EDITORIAL
published: 17 January 2020
doi: 10.3389/fnins.2019.01419

Editorial: Neural Substrates of Acupuncture: From Peripheral to Central Nervous System Mechanisms

Vitaly Napadow[1]*, *Florian Beissner*[2], *Yiwen Lin*[3], *Younbyoung Chae*[4] and *Richard E. Harris*[5]

[1] Martinos Center for Biomedical Imaging, Massachusetts General Hospital, Harvard Medical School, Boston, MA, United States, [2] Somatosensory and Autonomic Therapy Research, Hannover Medical School, Hanover, Germany, [3] Graduate Institute of Acupuncture Science, College of Chinese Medicine, China Medical University, Taichung, Taiwan, [4] Acupuncture and Meridian Science Research Center, Kyung Hee University, Seoul, South Korea, [5] Department of Anesthesiology, Chronic Pain and Fatigue Research Center, University of Michigan, Ann Arbor, MI, United States

Keywords: acupuncture, neuroscience, somatosensation, endorphin, autonomic nervous system

Editorial on the Research Topic

Neural Substrates of Acupuncture: From Peripheral to Central Nervous System Mechanisms

"Acupuncture" is a therapeutic intervention involving percutaneous mechanical, thermal, or electrical stimulation via needling of specific locations on the body. Acupuncture has been used in China and other Asian countries for thousands of years, and is one component of traditional Chinese medicine. Usage of acupuncture in Western countries, such as the United States, has been growing slowly but steadily (Ma et al., 2016; Nahin et al., 2016), with most common applications for chronic pain and neurological conditions. Mechanistic research exploring how acupuncture may reduce pain and contribute to other clinically meaningful outcomes is ongoing. This special issue further explores the neural basis of acupuncture, focusing on both peripheral and central nervous system mechanisms.

Historically, in the West, acupuncture research began mainly in the 1970's. An early popular theory to explain acupuncture analgesia was the "gate control theory," which posited that stimulation from acupuncture needling produces pre-synaptic inhibition of nociceptive afference in the central nervous system (Melzack and Wall, 1965). However, the gate control theory would predict analgesia on the order of milliseconds, while acupuncture analgesia develops much more slowly, reaching a maximum analgesic effect 30 min after initial stimulation (Pomeranz, 1989). Such results seemingly refuted the previously popular gate control theory. However, other research studies in the 1970's clearly linked peripheral and central nervous system signaling in acupuncture mechanisms of action for pain relief. Naloxone, an opioid receptor antagonist, has been shown to block acupuncture analgesia by binding to selective opioid receptors (Mayer et al., 1977). In fact, acupuncture analgesia has been demonstrated to be mediated by afferent sensory nerves, as vascular occlusion has no effect on acupuncture analgesia (Chiang et al., 1973), while procaine (a local anesthetic) has indeed been shown to negate acupuncture analgesia (Ulett et al., 1998).

These early studies have been bolstered by more recent human and pre-clinical basic science studies, further defining the mechanistic role of endogenous opioid receptors in acupuncture analgesia (Harris et al., 2009), and suggesting other mechanisms of action including adenosine receptor modulation (Goldman et al., 2010), dopamine signaling for immune regulation (Torres-Rosas et al., 2014), and neuroplasticity in the primary somatosensory cortex of the brain (Maeda et al., 2017). Indeed, clinical trials of acupuncture for chronic pain conditions indicate that acupuncture analgesic effects persist for months following the end of treatment suggesting long term plastic changes in pain processing (MacPherson et al., 2017). This type of long term change

OPEN ACCESS

Edited and reviewed by:
Rufin VanRullen,
Centre National de la Recherche Scientifique (CNRS), France

***Correspondence:**
Vitaly Napadow
vitaly@mgh.harvard.edu

Specialty section:
This article was submitted to Perception Science, a section of the journal Frontiers in Neuroscience

Received: *02 December 2019*
Accepted: *16 December 2019*
Published: *17 January 2020*

Citation:
Napadow V, Beissner F, Lin Y, Chae Y and Harris RE (2020) Editorial: Neural Substrates of Acupuncture: From Peripheral to Central Nervous System Mechanisms. Front. Neurosci. 13:1419. doi: 10.3389/fnins.2019.01419

in sensory processing is a hallmark of central neurobiology. These studies over the last 50 years of acupuncture research clearly highlight the nervous system as the main conduit for clinical efficacy underlying this therapeutic intervention.

This Issue furthers the research base on the neural basis of acupuncture mechanisms. Studies include both behavioral and neuroimaging research in humans, as well as basic molecular, cellular, and physiological research in animal models. Clinical applications included in this Issue extend beyond pain, to cover chronic itch, depression, stroke, drug addiction, and cardiovascular regulation. Molecular and cellular targets are identified for acupuncture analgesia and anti-depressive effects (Wan et al.; Zheng et al.), as well as inflammatory modulation (Ma et al.) and characterization of specific body locations (i.e., acupoints) for needle stimulation (Fan et al.). Other preclinical studies highlight specific brain regions such as paraventricular nucleus for cardiovascular modulation by acupuncture (Cheng et al.) and cuneate nucleus in drug dependence (Chang et al.). Human research studies explore the role of the brain's default mode network, previously implicated in acupuncture-evoked brain response and analgesia (Hui et al., 2009; Napadow et al., 2012), in acupuncture clinical response more broadly (Zhang et al.). Human neuroimaging studies in this issue also evaluate potential brain-based mechanisms of acupuncture for motor outcomes (Nierhaus et al.) and itch (Min et al.). Human behavioral studies evaluate acupuncture modulation of temporal summation and its role in analgesia (Baeumler et al.). The role of cognitive effects and expectancy, vis-à-vis the placebo effect, are also investigated as they relate to acupuncture (Aichner et al.; Lee et al.; Musial; Song et al.). Other studies evaluate neural modulation by combined acupuncture with mental imagery (Takahashi et al.) or transcranial magnetic stimulation (Huang et al.), and the more general role of acupuncture in stress reduction (Lee et al.). Finally, structural parameters of the needle are evaluated for their role in analgesia (Bae et al.) and an interesting study explores how the connective tissue system and nervous system may be differentially involved in acupuncture efficacy (Chang et al.).

We hope the reader enjoys this compendium of novel acupuncture research studies, which both extends the substantive research base supporting acupuncture mechanisms of action, and bridges to future basic and translational research that more precisely defines the pathways and neural circuitry underpinning acupuncture clinical efficacy.

AUTHOR CONTRIBUTIONS

All authors listed have made a substantial, direct and intellectual contribution to the work, and approved it for publication.

ACKNOWLEDGMENTS

We thank the following organizations for supporting the investigators on this editorial: Horst Görtz Stiftung to FB, NCCIH, NIH R01 AT007550 to RH and VN, and NCCIH NIH P01-AT009965 and R33-AT009306 to VN.

REFERENCES

Chiang, C., Chang, C., Chu, H., and Yang, L. (1973). Peripheral afferent pathway for acupuncture analgesia. *Sci. Sin.* 16, 210–217.

Goldman, N., Chen, M., Fujita, T., Xu, Q., Peng, W., Liu, W., et al. (2010). Adenosine A1 receptors mediate local anti-nociceptive effects of acupuncture. *Nat. Neurosci.* 13, 883–888. doi: 10.1038/nn.2562

Harris, R. E., Zubieta, J. K., Scott, D. J., Napadow, V., Gracely, R. H., and Clauw, D. J. (2009). Traditional Chinese acupuncture and placebo (sham) acupuncture are differentiated by their effects on mu-opioid receptors (MORs). *Neuroimage* 47, 1077–1085. doi: 10.1016/j.neuroimage.2009.05.083

Hui, K. K., Marina, O., Claunch, J. D., Nixon, E. E., Fang, J., Liu, J., et al. (2009). Acupuncture mobilizes the brain's default mode and its anti-correlated network in healthy subjects. *Brain Res.* 1287, 84–103. doi: 10.1016/j.brainres.2009.06.061

Ma, Y., Dong, M., Zhou, K., Mita, C., Liu, J., and Wayne, P. M. (2016). Publication trends in acupuncture research: a 20-year bibliometric analysis based on PubMed. *PLoS ONE* 11:e0168123. doi: 10.1371/journal.pone.0168123

MacPherson, H., Vertosick, E. A., Foster, N. E., Lewith, G., Linde, K., Sherman, K. J., et al. (2017). The persistence of the effects of acupuncture after a course of treatment: a meta-analysis of patients with chronic pain. *Pain* 158, 784–793. doi: 10.1097/j.pain.0000000000000747

Maeda, Y., Kim, H., Kettner, N., Kim, J., Cina, S., Malatesta, C., et al. (2017). Rewiring the primary somatosensory cortex in carpal tunnel syndrome with acupuncture. *Brain* 140, 914–927. doi: 10.1093/brain/awx015

Mayer, D., Price, D., and Rafii, A. (1977). Antagonism of acupuncture analgesia in man by the narcotic antagonist naloxone. *Brain Res.* 121, 368–372. doi: 10.1016/0006-8993(77)90161-5

Melzack, R., and Wall, P. D. (1965). Pain mechanisms: a new theory. *Science* 150, 971–979. doi: 10.1126/science.150.3699.971

Nahin, R. L., Boineau, R., Khalsa, P. S., Stussman, B. J., and Weber, W. J. (2016). Evidence-based evaluation of complementary health approaches for pain management in the United States. *Mayo Clin. Proc.* 91, 1292–1306. doi: 10.1016/j.mayocp.2016.06.007

Napadow, V., Kim, J., Clauw, D. J., and Harris, R. E. (2012). Decreased intrinsic brain connectivity is associated with reduced clinical pain in fibromyalgia. *Arthritis Rheum.* 64, 2398–2403. doi: 10.1002/art.34412

Pomeranz, B. (1989). "Acupuncture related research to pain, drug addiction, and nerve regeneration," in *Scientific Bases of Acupuncture*, eds B. Pomeranz and G. Stux (New York, NY: Springer-Verlag), 35–52. doi: 10.1007/978-3-642-73757-2

Torres-Rosas, R., Yehia, G., Pena, G., Mishra, P., del Rocio Thompson-Bonilla, M., Moreno-Eutimio, M. A., et al. (2014). Dopamine mediates vagal modulation of the immune system by electroacupuncture. *Nat. Med.* 20, 291–295. doi: 10.1038/nm.3479

Ulett, G., Han, S., and Han, J.-S. (1998). Electroacupuncture: mechanisms and clinical application. *Biol. Psychiatry* 44, 129–138. doi: 10.1016/S0006-3223(97)00394-6

Conflict of Interest: The authors declare that the research was conducted in the absence of any commercial or financial relationships that could be construed as a potential conflict of interest.

frontiers in Neuroscience

ORIGINAL RESEARCH
published: 12 December 2018
doi: 10.3389/fnins.2018.00907

Neuropeptides SP and CGRP Underlie the Electrical Properties of Acupoints

Yu Fan[1†], Do-Hee Kim[1†], Yeonhee Ryu[2†], Suchan Chang[1], Bong Hyo Lee[1], Chae Ha Yang[1] and Hee Young Kim[1]*

[1] Department of Physiology, College of Korean Medicine, Daegu Haany University, Daegu, South Korea, [2] Korean Medicine Fundamental Research Division, Korea Institute of Oriental Medicine, Daejeon, South Korea

Electrical skin measurements at acupuncture points (acupoints) have been utilized as a diagnostic and therapeutic aid for more than 50 years. Although acupoints are described as having distinct electrical properties, such as high conductance and low impedance, the underlying mechanisms are currently unknown. The present study investigated in a rat model of hypertension whether the high conductance at acupoints is a result of the release of the neuropeptides substance P (SP) and calcitonin gene-related peptide (CGRP) during neurogenic inflammation in the referred pain area. When plasma extravasation from neurogenic inflammation was examined by exploring the leakage of intravenously injected Evans blue dye (EBD) to the skin, extravasated EBD was found most frequently in acupoints on the wrist. The increased conductance and temperature at these acupoints occurred during the development of hypertension. The increase in conductance and plasma extravasation at acupoints in hypertensive rats was ablated by cutting median and ulnar nerves, blocking small diameter afferent fibers with resiniferatoxin (RTX) injection into median and ulnar nerves, or antagonizing SP or CGRP receptors in acupoints. In turn, intradermal injection of SP or CGRP resulted in increased conductance and plasma extravasation in naïve rats. Elevated levels of SP and CGRP were found in the acupoints of hypertensive rats. These findings suggest that the high conductance at acupoints is due to vascular leakage following local release of SP and CGRP during neurogenic inflammation.

Keywords: substance P, CGRP, acupoints, electrical properties, skin conductance, Evans blue dye, plasma extravasation, neurogenic inflammation

OPEN ACCESS

Edited by:
Yi-Wen Lin,
China Medical University, Taiwan

Reviewed by:
Yung-Hsiang Chen,
China Medical University, Taiwan
Dongwoon Han,
Hanyang University, South Korea

***Correspondence:**
Hee Young Kim
hykim@dhu.ac.kr

[†]These authors have contributed equally to this work

Specialty section:
This article was submitted to Perception Science, a section of the journal Frontiers in Neuroscience

Received: *19 September 2018*
Accepted: *19 November 2018*
Published: *12 December 2018*

Citation:
Fan Y, Kim D-H, Ryu Y, Chang S, Lee BH, Yang CH and Kim HY (2018) Neuropeptides SP and CGRP Underlie the Electrical Properties of Acupoints. Front. Neurosci. 12:907. doi: 10.3389/fnins.2018.00907

SIGNIFICANCE STATEMENT

Electrical skin measurements at acupuncture points have been utilized as a diagnostic and therapeutic aid for more than 50 years. Although acupoints are described as having distinct electrical properties, such as higher conductance and lower impedance than that of surrounding skin, the underlying mechanisms are completely unknown. Using a newly constructed electrode, intravenous injection of Evans blue dye, and cutaneous thermal recordings and imaging, the present study suggests a novel mechanism underlying the electrical properties of acupoints: the neuropeptides SP and CGRP produce high conductance at acupoints by causing neurogenic inflammation, plasma extravasation and accumulation of subskin water contents.

INTRODUCTION

Acupuncture, a therapeutic intervention of traditional medicine, has been used for centuries to relieve a variety of conditions. For acupuncture treatment, thin needles are inserted into specific but poorly defined sites on or under the skin called acupoints or acupuncture points. Based on acupuncture theory, there are about 360 acupuncture points, most of which lie along the Qi channels (called meridians) connecting the surface of the body to internal organs. Each acupoint communicates with a specific internal organ; an acupoint reflects the status of an internal organ, and the internal disorders can be treated by stimulating the acupoints (Stux and Pomeranz, 2012). In support of this, we and others have proven that acupoints become hypersensitive under abnormal visceral conditions and that stimulation of the acupoints can relieve the symptoms of the associated visceral organs (Chae et al., 2007; Kim et al., 2017).

As the acupoints themselves are grossly anatomically invisible, several scientific approaches, such as electrodermal measurements (Ahn et al., 2008) and infrared thermal imaging (Yang et al., 2007), have been attempted to identify the acupoints. Notably, numerous studies have reported the electrical properties of acupoints. Since the 1950s, when Nakatani (1956) reported that there were some points on the skin with special electrical properties, experimental and clinical studies have been carried out in many countries including China, Japan, France, Germany, and the United States and suggest that acupoints have distinct electrical properties, including a higher conductance, lower impedance and resistance and increased capacitance compared to the surrounding skin (Ahn et al., 2008). As this view gained traction, many instruments such as acupoint detectors and electrodiagnostic devices have been developed and are increasingly used in acupuncture clinics. However, the mechanisms by which acupoints have these distinct electrical properties are currently unknown.

Our previous studies showed that in rat models of hypertension or colitis, the skin over acupoints exhibits neurogenic inflammation due to viscerosomatic convergence in sensory pathways (Kim et al., 2006, 2017). Neurogenic inflammation is characterized by vasodilation and vascular leakage (plasma extravasation) in the skin arising from the release of neuropeptides calcitonin gene-related peptide (CGRP) and substance P (SP) from activated small diameter sensory afferents (Schmelz and Petersen, 2001). The insights that many acupoints show neurogenic inflammation under certain conditions (Kim et al., 2006, 2017) and electrically high conductance/low impedance (Ahn et al., 2008; Colbert et al., 2008, 2009) have led to the hypothesis that the neuropeptides CGRP and SP evoke vascular dilation and leakage, causing the increased subskin tissue water content in acupoints and thus producing electrically high conductance and low impedance, potentially underlying the electrical properties of acupoints. To prove this hypothesis, the present study used a rat model of immobilization-induced hypertension (IMH) to investigate (1) whether acupoints exhibit active neurogenic inflammatory responses by using intravenous injection of Evans blue dye (EBD) and cutaneous thermal recordings and imaging and (2) whether acupoints have high conductance by using a newly constructed electrode and plasma extravasation. Furthermore, we explored (3) whether the increased conductance at acupoints is mediated by activation of small diameter afferents and generated by localized release of CGRP and SP.

MATERIALS AND METHODS

Animals

Adult male Sprague-Dawley rats (Hyochang, Seoul, South Korea) weighing 250–350 g were used. Animals were housed at constant humidity (40∼60%) and temperature (22 ± 2°C) on a 12-h light/dark cycle and allowed free access to food and water. All procedures were carried out in accordance with the National Institutes of Health Guide for Care and Use of Laboratory Animals and approved by the Institutional Animal Care and Use Committee (IACUC) at Daegu Haany University.

Chemicals

Evans blue dye (50 mg/ml saline; Sigma-Aldrich, St. Louis, MO, United States), human calcitonin gene-related peptide (CGRP; 1 mg/ml saline; Bachem, Torrance, CA, United States; a 37-amino acid peptide), and α-CGRP 8-37 (1 mg/ml distilled water, Bachem, Torrance, CA, United States; a CGRP receptor antagonist) were used in this study (Shen et al., 2001). Substance P acetate salt hydrate (SP; 0.5 mg/ml saline; Sigma-Aldrich; a SP receptor agonist) and (+)-(2S,3S)-3-(2-methoxybenzylamino)-2-phenylpiperidine (CP-99994; 33 mmol/ml saline; Sigma-Aldrich; an SP receptor antagonist) were also used (McLean et al., 1993). Resiniferatoxin (RTX; 100 μg/ml vehicle; Sigma-Aldrich), an ultrapotent capsaicin analog known to block small diameter afferent fibers containing transient receptor potential vanilloid type 1 receptor (TRPV1) (Suter et al., 2009), was dissolved in a vehicle that contained 0.3% Tween 80, 10% DMSO and saline. Capsaicin (0.05 and 0.1%; Sigma-Aldrich; a TRPV1 agonist) was dissolved in a vehicle consisting of 10% alcohol and 10% Tween 80 in saline (Knotkova et al., 2008), and FITC-conjugated isolectin B4 (FITC IB4 tracer; 1%, 3 μl, Vector Laboratories, Burlingame, CA, United States) was used.

Immobilization Stress-Induced Hypertension (IMH) and Measurement of Systolic Blood Pressure

Hypertension was induced by immobilization with a cone-shaped polyethylene bag, as described previously (Kvetnansky et al., 1979). Systolic blood pressure was measured non-invasively with a tail cuff blood pressure monitor (Model 47, IITC, Inc., Woodland Hills, CA, United States). Briefly, the rat was placed in a chamber, and an occluding cuff and a pneumatic pulse transducer were positioned on the base of the tail. A programmed electrosphygmomanometer (Narco Bio-Systems, Inc., Austin, TX, United States) was inflated and deflated automatically, and the tail cuff signals from the transducer were automatically collected every 10 min using an IITC apparatus (Model 47, IITC,

Inc.). The mean of two readings was taken at each blood pressure measurement.

Detection of Neurogenic Inflammation in the Skin by EBD Injection

Neurogenic inflammatory sites were visualized by intravenously injecting EBD (50 mg/kg) in male Sprague-Dawley rats as described previously (Kim et al., 2017). While the rats were immobilized by the cone-shaped bags, the distal portion of the tail was dipped into 40°C warm water for at least 30 s. EBD was then injected into the tail vein with a catheter (26 gauge), and skin color changes were observed up to 2 h after the injection. The blue-dyed areas on the skin were sketched using body charts, photographed and compared with a human acupoint chart based on the transpositional method, which locates acupoints on the surface of animal skin corresponding to the anatomic site of human acupoints (Yin et al., 2008).

Measurement of Skin Surface Temperature

Skin temperature was measured using a K-type thermocouple microprobe (TC-11p, Minnesota Measurement Instruments, Minneapolis, MN, United States) coupled with an analog-digital interface converter (Physitemp BAT-12, American Laboratory Trading, San Diego, CA, United States) and digitized through a PowerLab 4/30 acquisition system (ADInstruments, Colorado Springs, CO, United States). While the rats were placed in a plastic chamber, a flexible thermoprobe was attached to the skin over wrist acupoints, mostly PC6 acupoints, the nearby site approximately 5 mm away from PC6 (**Figures 2A,B**) or capsaicin-injected sites (**Figure 2C**). Body temperature was also monitored with a regular thermocouple probe inserted into the rectum. For the experiment shown in **Figures 2A,B**, after the basal temperatures were recorded for at least 10 min, the rats were subjected to the IMH procedure, and the temperatures were measured up to 30 min after restraint. The skin-body temperature differentials were estimated by subtracting the body temperature from the skin temperature at each time point. At 30 min after restraint, infrared thermal images were obtained using a thermal camera (Ti55, Fluke IR Fusion Technology, Washington DC, United States) under slight isoflurane anesthesia. In another set of experiments (for **Figure 2C**), either capsaicin (0.05 or 0.1% capsaicin, 30 μl) or vehicle was intradermally injected into the bilateral PC6 acupoint near the wrist under slight isoflurane anesthesia, and temperature changes in the injected sites were monitored up to 30 min after injection.

Measurement of Electrical Skin Conductance

Skin moisture and temperature in the rats may be influenced according to external environment. To control the factors, all experiments were carried out under constant humidity (40∼60%) and temperature (22 ± 2°C). The animal hair was shaved prior to the placement of electrode. To simultaneously measure conductance and the applied pressure, a device was newly constructed by coupling a force transducer (FT-100, iWorx/CB Sciences, Inc., Dover, NH, United States) with an electrical conductance probe (3.7 mm diameter, stainless). The rats were placed in cone-shaped bags or plastic chambers. While the positive electrode was attached to the tail surface, the device (negative electrode) was placed on the skin over acupoints and was pressed at a force of 300 g. Signals from the conductance (current) probe and the force transducer were fed to an ETH-200 Bridge Amplifier (CB Science, Inc., Lemont, PA, United States) and a GSR AMP device (Model FE116, ADInstruments, Colorado Springs, CO, United States), respectively, and digitized through a PowerLab 4/30 acquisition system (ADInstruments). After basal electrical currents were recorded for at least 5 min, skin conductance (measured as a current) following treatments was recorded up to 30 min.

Estimation of EBD Extravasation in Skin Tissues

To assess the extent of EBD extravasation in the skin, rats were sacrificed 120 min after intravenous injection of EBD. The skin near the wrist was photographed using a digital camera (SONY ILCE-5000, China). The original EBD images were used to obtain a three-dimensional (3D) surface plot with ImageJ software (National Institute of Mental Health, Rockville, MD, United States) using the command Plugins/3D/interactive 3D surface plot (parameters; Mesh, Spectrum LUT, Scale 1.75, and Z 0.19). To determine the concentration of EBD that infiltrated the skin tissues, the skin tissue was processed using the dye-extraction method described previously (Martin et al., 2010). In brief, the skin (approximately 3 mm in size) near the wrist was excised, dry-weighed, homogenized in 1: 3 volume of 50% trichloroacetic acid (TCA; dissolved in 0.9% saline) and centrifuged (10,000 rpm for 10 min). The supernatants were diluted with 1: 3 volume of 95% ethanol and measured using a spectrophotometric method (620 nm excitation/680 nm emission).

Surgical or Pharmacological Blockade of Median and Ulnar Nerves

Median and ulnar nerves were blocked surgically or pharmacologically as described previously (Kim et al., 2013). Briefly, under isoflurane anesthesia, a small skin incision was made longitudinally on the medial part of the elbow to expose the median and ulnar nerves. For surgical lesions of median and ulnar nerves, the nerves were bilaterally ligated with 4–0 silk and cut around the medial head of the triceps muscle of both forelimbs. The sham group underwent the same procedure but without nerve injury. For blocking small diameter afferent fibers, RTX (0.01%, 30 μl) was administered perineurally in the median and ulnar nerves. All incisions were closed aseptically and 2 or 3 days after surgery, experiments for skin conductance were performed.

Another set of experiments was performed to confirm the blockade of small diameter afferent fibers by RTX by using an IB4 tracing method (Pan et al., 2003). In brief, 48 h after perineural injection of either RTX (n = 3) or vehicle (n = 3) into the ulnar nerve, an FITC IB4 tracer (3 μl) was administered into ulnar

nerves under isoflurane anesthesia in rats ($n = 3$). Three to four days later, dorsal root ganglion (DRG) neurons of C8 and T1 were removed, post-fixed in 4% buffered paraformaldehyde (PFA) for 2 h, immersed in 30% sucrose overnight and cryosectioned at 30 μm. The cryosections were then mounted on gelatin-coated glass slides. Skin images were taken from 3 to 4 sections per animal under an Olympus AX70 fluorescence microscope (Olympus, Japan) and quantified by using ImageJ software.

Immunohistochemistry for CGRP or SP in the Skin

One hour after restraint, skin samples were taken from the wrist, which most commonly showed EBD leakage in IMH rats ($n = 6$) and naïve rats ($n = 6$). The skin samples were paraffin-embedded, sectioned (5 μm), and incubated with either anti-CGRP mouse antibody (1:500; Chemicon, Temecula, CA, United States; RRID:AB_1658411) or anti-SP mouse monoclonal antibody (1:500; GeneTex, Irvine, CA, United States; RRID:AB_785913), followed by incubation with secondary antibody (1:500, Alexa Fluor 488-conjugated donkey anti-mouse IgG antibody, Thermo Scientific, Waltham, MA, United States; RRID:AB_141607). The sections were mounted on gelatin-coated slides, air-dried, and coverslipped. Skin images were taken from three sections from each animal with a laser-scanning confocal microscope (LSM700, Carl Zeiss, Germany) and quantified by using ImageJ software (National Institute of Mental Health, Rockville, MD, United States). The number of pixels with green fluorescence intensity greater than the cut-off value (100) was counted to quantify positive staining. Data were expressed as the number of positive pixels over a field area of 1280 × 1024 pixels.

Statistical Analysis

Statistical analysis was carried out using SigmaStat 3.5 software (Systat Software, Inc., United States). All data are presented as the mean ± SEM (standard error of the mean) and analyzed by one or two-way repeated measures analysis of variance (ANOVA) with Tukey *post hoc* tests or unpaired *t*-tests where appropriate. Statistical significance was considered at $p < 0.05$.

RESULTS

Cutaneous Neurogenic Inflammation at Acupoints

First, we explored whether some of acupoints displayed neurogenic inflammation in IMH rats. When a rat was placed in an immobilization bag, systolic blood pressure gradually increased for the next several hours (**Figures 1A,B**), consistent with our previous study (Kim et al., 2017). Approximately 10 min after the initiation of restraint, cutaneous neurogenic inflammatory sites [neurogenic spots (Neuro-Sp)] were visualized by intravenous injection of EBD (50 mg/kg). The blue spots started to appear approximately 5 min after EBD injection, ranged in diameter from 0.5 to 3 mm and were maintained throughout the experiment. IMH rats exhibited approximately nine spots per animal (**Figure 1D**), while control rats only showed a few spots. When the Neuro-Sp in IMH rats ($n = 21$) were mapped and compared with the corresponding human anatomical acupoints, the majority appeared bilaterally or unilaterally on the wrist, and 69% (123 of 178 spots) were found in acupoints of the forelimbs, such as PC6 (33 spots), PC7 (25 spots), and HT7 (30 spots) (**Figures 1D–F**). These results indicate that acupoints, most frequently on the wrist, display cutaneous neurogenic inflammation and plasma extravasation in the rat model of IMH.

Increased Skin Temperature at Acupoints Following Neurogenic Inflammation

To determine whether the acupoints undergo active neurogenic inflammation processes, cutaneous temperature, as an outcome measure of inflammation (Birklein and Schmelz, 2008; Montalto et al., 2013), was compared between acupoints on the wrist and nearby sites approximately 5 mm away from the acupoints in IMH rats. Skin temperature rapidly elevated following restraint and then continued to increase slowly over 30 min after restraint. This increase was higher at acupoints than at nearby sites (two-way ANOVA; group $F_{(1,4)} = 26.231$, $p = 0.07$; time $F_{(15,60)} = 28.589$, $p < 0.001$; interaction $F_{(15,60)} = 1.061$, $p = 0.41$; **Figure 2A**). Thermal infrared imaging found elevated temperature in the skin over wrist acupoints such as PC6 (**Figure 2B**). To verify whether neurogenic inflammation itself can increase skin temperature, the effect of intradermally injected capsaicin (0.05, 0.1%; 30 μl), which is known to trigger neurogenic inflammation (Lin et al., 1999), on skin temperature was investigated. Local injection of capsaicin into the skin of the wrist significantly increased temperature at the injection site in a dose-dependent manner compared to injection of vehicle (two-way ANOVA, group $F_{(2,8)} = 29.018$, $p < 0.001$; time $F_{(20,80)} = 38.794$, $p < 0.001$; interaction $F_{(40,160)} = 9.737$, $p < 0.001$; **Figure 2C**), suggesting that acupoints on the wrist of IMH rats are undergoing active processes of neurogenic inflammation.

Increased Electrical Conductance and Plasma Extravasation at Acupoints in IMH Rats

Next, we investigated whether acupoints showed increased electrical conductance under pathological conditions. The pressure exerted by the probe on the skin is considered to be a potential confounder affecting the reproducibility and reliability of data on the measurement of electrical skin conductance/impedance (Ahn and Martinsen, 2007). To hold the electrode to the skin at a constant pressure at every measurement, we constructed a conductance probe that could measure electrical currents and touch pressure simultaneously (**Figure 3A**). Skin conductance was estimated as the plateau value of electrical current recorded while holding the electrode at a constant pressure of 300 g (**Figure 3B**). To assess the validity of the device, various amounts of distilled water (1∼10 μl) were applied to the skin near the wrist in isoflurane-anesthetized rats ($n = 6$), and the electrical conductance was measured at the wrist skin. Electrical currents proportionally increased with increasing water

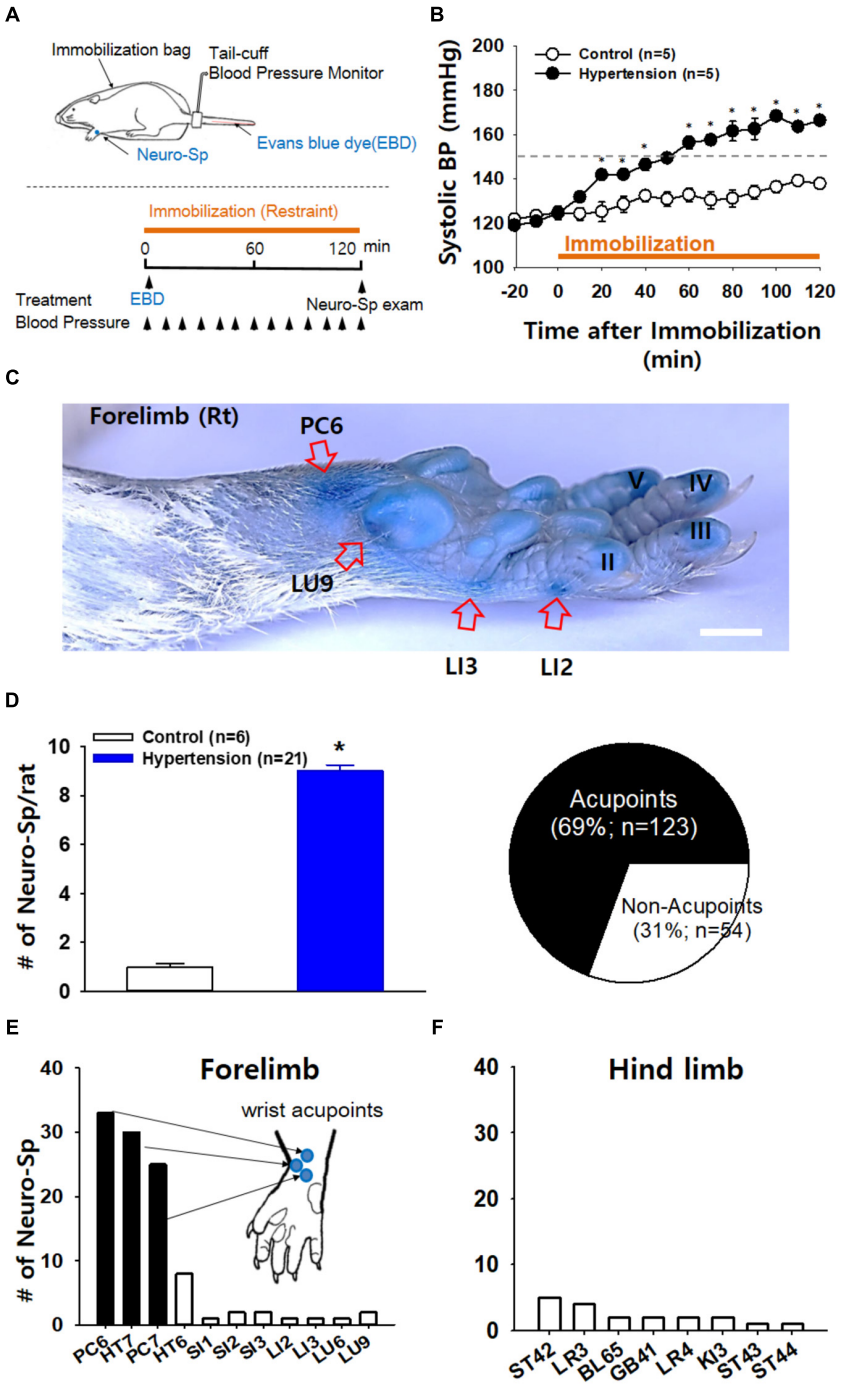

FIGURE 1 | Neurogenic inflammation at acupoints in IMH rats. **(A)** Schematic of the experimental procedure in the rat model of immobilization-induced hypertension (IMH). Evans blue dye (EBD); neurogenic inflammatory spots [neurogenic spots (Neuro-Sp)]. **(B)** Development of hypertension following immobilization (restraint). In restrained rats, systolic blood pressure (systolic BP) was significantly elevated, reaching the level of hypertension over 150 mmHg within 1 h, compared to that in unrestrained control rats (control). *$p < 0.001$ vs. control. **(C)** A representative image of Neuro-Sp in an IMH rat. **(D)** Numbers of Neuro-Sp per animal (bar graph) and correlation of the anatomic location between Neuro-Sp and acupoints in hypertensive rats ($n = 21$ animals; pie graph). Numbers of Neuro-Sp corresponding to acupoints in the forelimb **(E)** or hind limb **(F)**. Bar = 20 mm.

volumes, reaching a maximum level at approximately 5 μl water (**Figure 3C**), indicating an increase in conductance according to the extent of skin hydration.

To explore whether acupoints exhibit a high conductance under pathological conditions, electrical currents at an acupoint on the wrist were compared between IMH and control rats. When

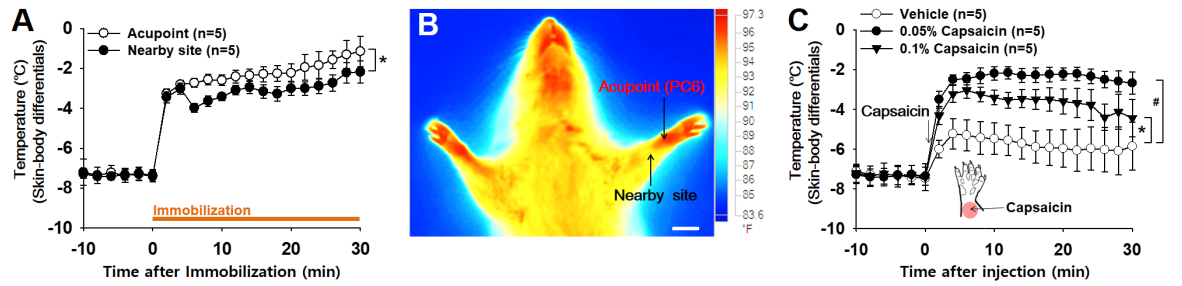

FIGURE 2 | Increased temperature at acupoints in IMH rats. **(A)** Changes in temperature at acupoints on the wrist following restraint. Skin (acupoint)-body temperature differentials were calculated by subtracting the body temperatures from the temperatures over wrist acupoints. $^{*}p < 0.05$ vs. nearby site. **(B)** A representative thermal infrared image of the wrist 2 h after restraint. **(C)** Effect of intradermal capsaicin on skin–body temperature differentials. Capsaicin (0.05 or 0.1%) or vehicle was injected into the skin over the wrist of naïve rats. $^{*}p < 0.05$, 0.05% capsaicin vs. vehicle; $^{\#}p < 0.05$, 0.1% capsaicin vs. vehicle. Bar = 20 mm.

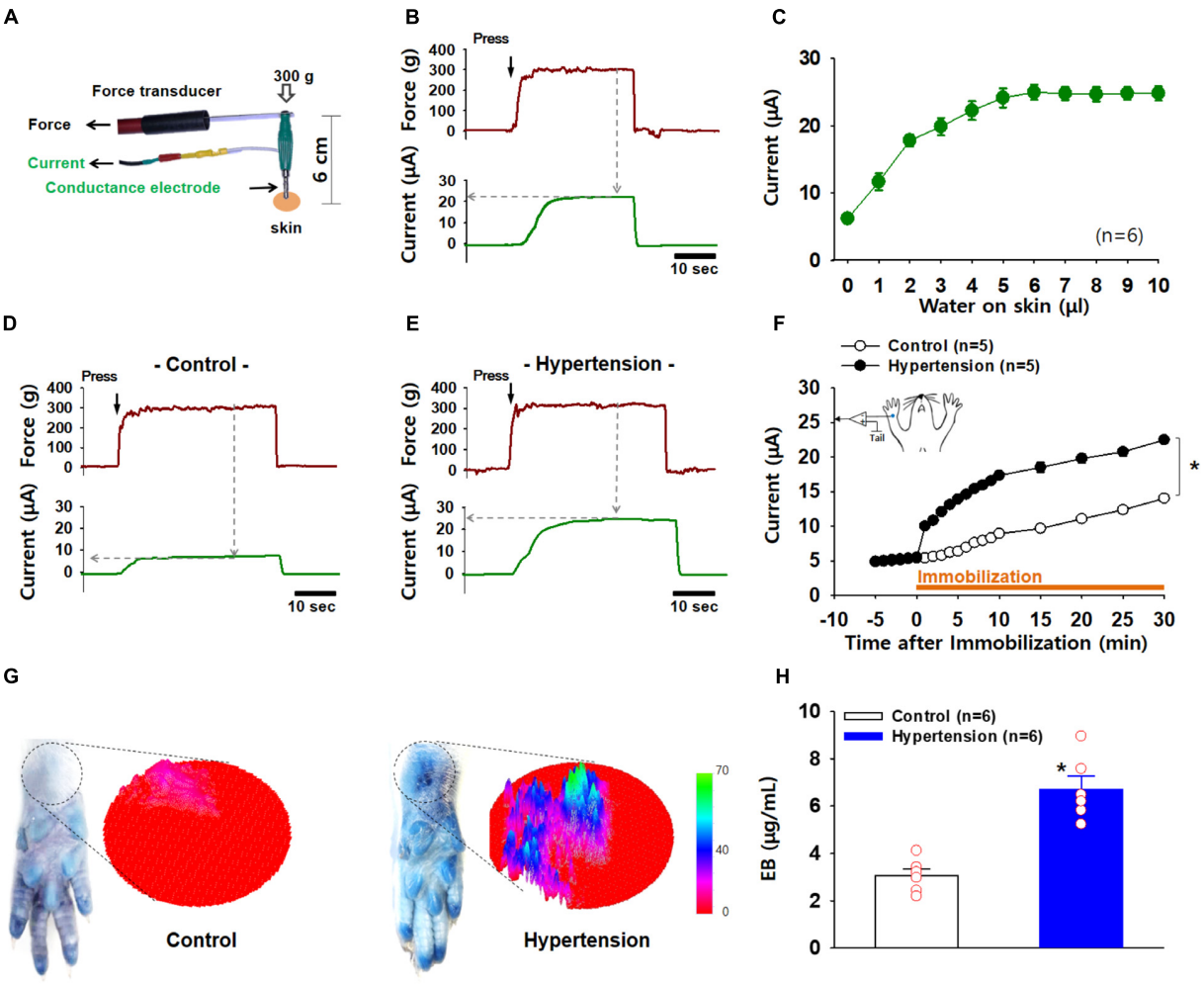

FIGURE 3 | Increased electrical conductance and plasma extravasation at acupoints in IMH rats. **(A)** A newly constructed electrode for the simultaneous measurement of conductance and applied pressure. **(B)** A representative trace of applied force and electrical currents. Conductance was estimated as the maximum current value (μA) reached when a pressure of 300 g on the electrode was held constant. **(C)** Changes in conductance induced by various amounts of water topically applied to rat skin. **(D–F)** Increased conductance at acupoints following IMH. A representative trace of applied pressure (upper panels) and electrical currents (low panels) recorded in wrist acupoints of control and IMH rats. Significantly increased conductance at the wrist acupoint was observed in IMH rats compared to that in control **(F)**. $p < 0.05$ vs. control. **(G)** Extravasation of EBD over the wrist acupoint of hypertensive rats. Representative photographs of wrist areas in control and IMH rats 2 h after intravenous injection of EBD and the 3D images created from the circles in the photographs by using ImageJ. **(H)** Concentration of EBD in the wrist acupoints of naïve control and IMH rats. $^{*}p = 0.027$ vs. control.

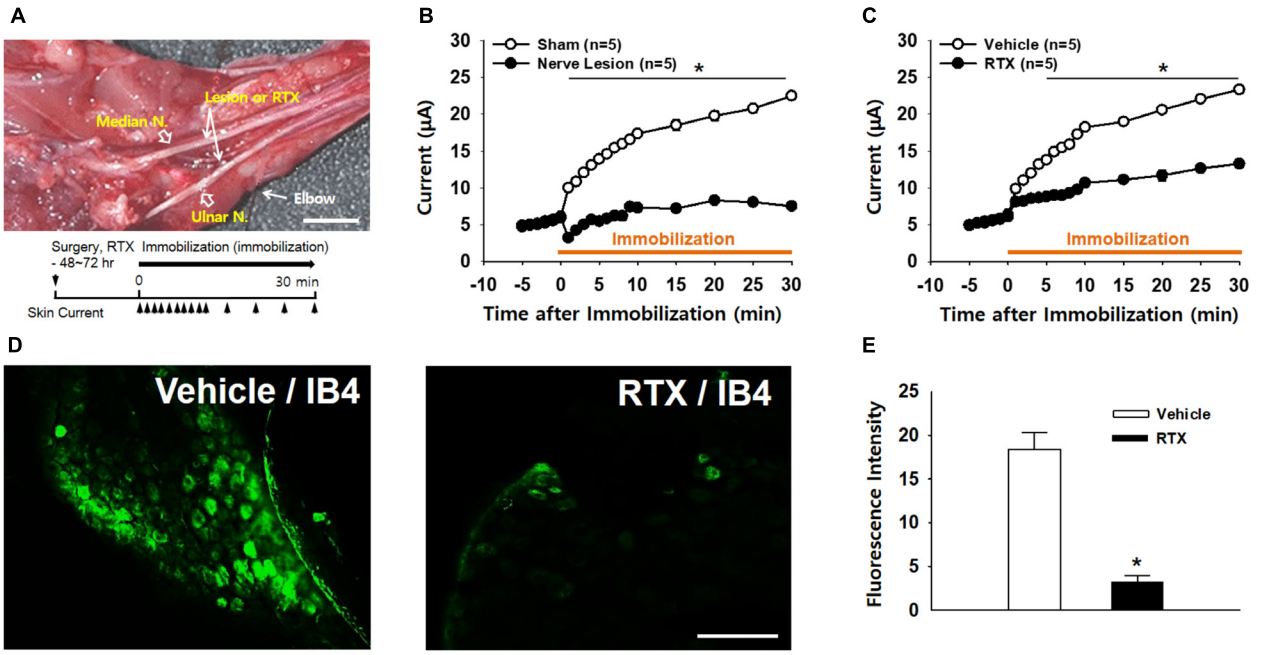

FIGURE 4 | Blockade of high conductance at acupoints by either surgical nerve injury or perineural injection of RTX in IMH rats. **(A)** A photograph of the median and ulnar nerves at the plane of the elbow segment. Arrows indicate sites for surgical lesions or perineural injection of resiniferatoxin (RTX). Bar = 20 mm. **(B)** Effect of surgical nerve injury on the development of high conductance at acupoints in IMH rats. Peripheral nerve injuries abolished the development of high conductance at acupoints, compared to leaving the nerve intact (sham). $^*p < 0.05$. **(C)** Effect of perineural injection of RTX on electrical skin conductance in IMH rats. **(D,E)** Epifluorescent images showing IB4-labeled neurons in the C8 DRG of a rat injected with IB4 into RTX- (RTX/IB4) and vehicle-treated (vehicle/IB4) ulnar nerves. An FITC IB4 tracer was bilaterally administered into nerves of rats 48 h after perineural injection of either RTX or vehicle into ulnar nerves. Significantly fewer IB4-labeled cells were found in the RTX-treated DRGs (n = 10 slices from three animals) than in those treated with vehicle (n = 10 slices from three animals, Vehicle). $^*p < 0.001$ vs. vehicle. Bar = 100 μm.

the conductance probe was applied over the PC6 acupoint on the wrist at a constant pressure of 300 g, the acupoint in the IMH rats showed a higher electrical conductance than that in the control rats (two-way ANOVA; group $F_{(1,4)} = 1147.149$, $p < 0.001$; time $F_{(19,76)} = 228.471$, $p < 0.001$; interaction $F_{(19,76)} = 232.043$, $p < 0.001$; **Figures 3D–F**). In another set of experiments, we imaged and quantified neurogenic extravasation at acupoints on the wrist 2 h after EBD injection with or without restraint. **Figure 3G** shows that there was blue EBD staining over the wrist acupoints in IMH rats (hypertension) but not naïve control rats (control). The 3D plots derived from the photographs also show the predominant EBD staining in IMH rats (right panels in **Figure 3G**). When measured by spectrophotometry, the EBD concentration at the wrist acupoints was significantly higher in IMH rats (hypertension, $n = 6$) than in naïve control rats (control, $n = 6$; $p < 0.001$; **Figure 3H**). These results suggest that both conductance and plasma extravasation were enhanced at the acupoints of IMH rats.

C-Fiber Mediation of the High Electrical Conductance of Acupoints

To identify whether afferent nerves mediate the development of high conductance at acupoints, surgical lesions of the ulnar and median nerves were made 48∼72 h prior to restraint and skin conductance measurements (**Figure 4A**). While conductance at the wrist acupoint wrist gradually increased following restraint (sham; **Figure 4B**), such effects were not observed in the rats with nerve lesions (nerve lesion; two-way ANOVA; group $F_{(1,4)} = 939.849$, $p < 0.001$; time $F_{(13,52)} = 64.358$, $p < 0.001$; interaction $F_{(13,52)} = 32.538$, $p < 0.001$; **Figure 4B**). To further examine the role of small diameter afferent fibers in producing high acupoint conductance, we injected a specific C/Aδ-fiber blocker RTX into ulnar and median nerves 48–72 h prior to the IMH procedure. Unlike pretreatment of the nerves with saline (vehicle), pretreatment with RTX abolished the development of the high conductance at the acupoint in IMH rats (two-way ANOVA; group $F_{(1,4)} = 398.84$, $p < 0.001$; time $F_{(13,52)} = 82.402$, $p < 0.001$; interaction $F_{(13,52)} = 25.643$, $p < 0.001$; **Figure 4C**). Furthermore, Aδ/C-fiber blockade by RTX was confirmed by significantly less FITC IB4 tracer labeling in the DRG in RTX-treated rats (RTX/IB4) compared to in the vehicle group (vehicle/IB4, **Figures 4D,E**). Taken together, our results indicate that small diameter afferent fibers mediate the development of high conduction at acupoints.

Production of High Conductance by SP and CGRP

To explore whether the increased conductance at acupoints is associated with levels of SP and CGRP, we injected either SP or CGRP intradermally into the skin on the wrist and

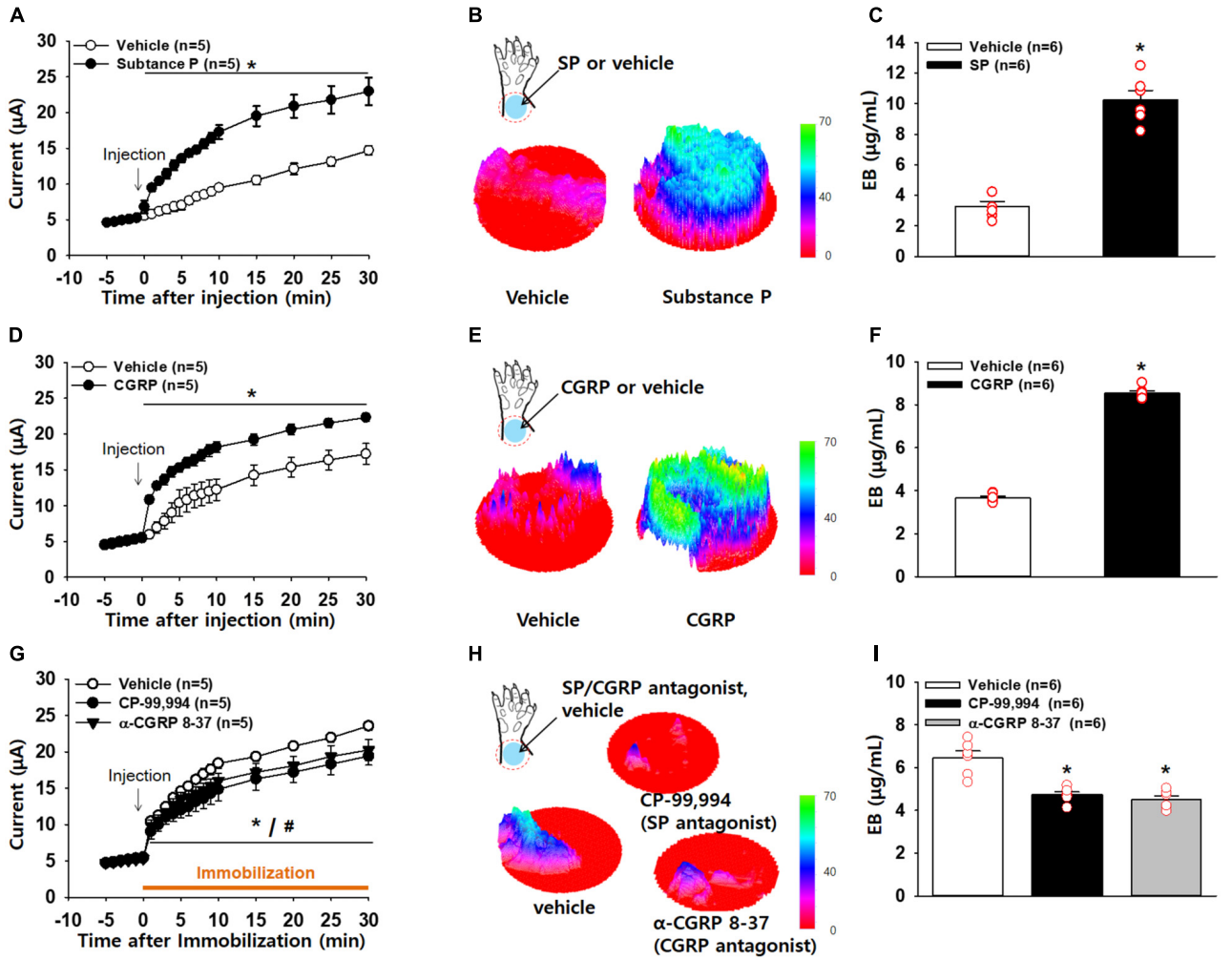

FIGURE 5 | Increased conductance at acupoints by SP or CGRP. **(A–C)** Effect of intradermal substance P (SP) on electrical conductance in naïve rats. Injection of SP into the skin of the wrist acupoints significantly increased conductance compared to injection of vehicle **(A)**. $p < 0.05$ vs. vehicle. The three-dimensional (3D) images of EBD extravasation in the wrist skin in vehicle- or SP–treated rats **(B)** and the concentration of EBD in the wrist acupoints of vehicle- or SP-treated rats **(C)**. $^*p < 0.001$ vs. vehicle. **(D–F)** Effect of intradermal calcitonin gene-related peptide (CGRP) on electrical conductance in naïve rats. Injection of CGRP into the skin of the wrist acupoints significantly increased conductance compared to injection of vehicle **(D)**. The 3D images of EBD extravasation in the wrist skin in vehicle- or CGRP-treated rats **(E)** and the concentration of EBD in the wrist acupoints of vehicle- or CGRP-treated rats **(F)**. $^*p < 0.001$ vs. vehicle. **(G–I)** Effects of intradermal SP or CGRP antagonists on the development of high conductance in hypertensive rats. Injection of SP or CGRP antagonists into the skin of the wrist acupoints prevented the development of high conductance in IMH rats compared to injection of vehicle **(G)**. The 3D images of EBD in the wrist skin in vehicle- or SP or CGRP antagonist-treated rats **(H)** and the concentration of EBD in the wrist acupoints of vehicle- or SP or CGRP antagonist-treated rats **(I)**. $^*p = 0.003$ vs. vehicle.

measured the skin conductance. An artificial increase in SP in the skin significantly increased conductance (two-way ANOVA; group $F_{(1,4)} = 63.285$, $p = 0.001$; time $F_{(19,73)} = 117.661$, $p < 0.001$; interaction $F_{(19,76)} = 22.732$, $p < 0.001$; **Figure 5A**). In another set of experiments, we determined the levels of plasma extravasation 2 h after the injection of vehicle ($n = 6$) or SP ($n = 6$) and found significantly higher levels of plasma extravasation in the wrist acupoints of SP-injected rats than in those of vehicle-injected rats, as shown in 3D skin images (**Figure 5B**) and the EBD concentration assessed by spectrophotometry (t-test, $p < 0.01$; **Figure 5C**). Such effects were replicated by injection of a CGRP agonist (two-way ANOVA; group $F_{(1,4)} = 20.372$, $p = 0.011$; time $F_{(19,76)} = 122.989$, $p < 0.001$; interaction $F_{(19,76)} = 18.115$, $p < 0.001$; **Figures 5D–F**).

To see if inhibition of SP or CGRP prevents the increase in conductance at acupoints, we injected either vehicle (saline), a SP antagonist CP-99,994 or a CGRP antagonist α-CGRP 8-37 into acupoints on the wrist prior to restraint and measured conductance up to 30 min after restraint. Saline-injected rats showed enhanced conductance at the wrist acupoints following restraint, which was significantly reduced by pretreatment with the SP or CGRP antagonist (two-way ANOVA; group $F_{(2,8)} = 2.307$, $p = 0.162$; time $F_{(19,76)} = 277.166$, $p < 0.001$; interaction $F_{(38,152)} = 2.361$, $p < 0.001$; **Figure 5G**). This decrease was further confirmed by 3D skin images (t-test; $^*p < 0.05$,

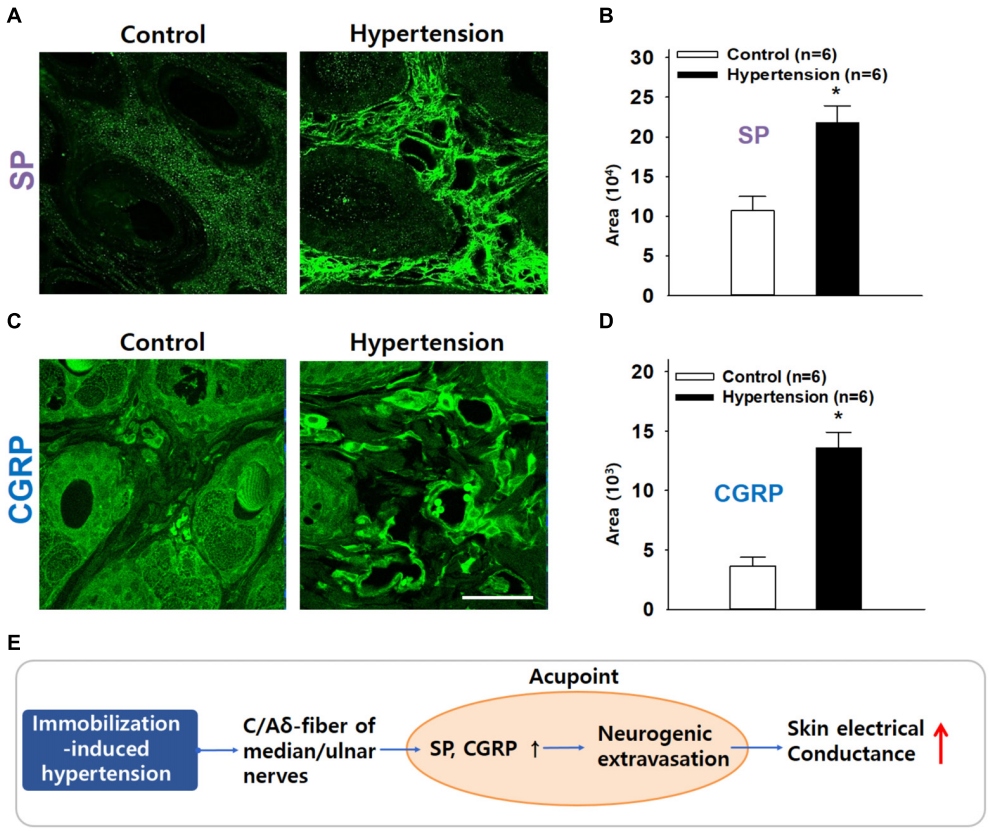

FIGURE 6 | Increased immunofluorescence of SP or CGRP in the skin over acupoints. **(A,B)** Greater SP expression in the wrist acupoint in IMH rats than in control rats. **(C,D)** Greater CGRP expression in the wrist acupoint in IMH rats than in control rats. $^*p < 0.001$ vs. control. Bar = 50 μm. **(E)** Overall hypothesis. A pathological condition of hypertension antidromically activates peripheral nerves, especially small diameter sensory afferents, which causes SP and CGRP release in the acupoints containing the activated sensory afferents and thus induces vasodilation and plasma extravasation. It leads to the development of high conductance at acupoints.

Figure 5H) and the EBD concentration in the skin (one-way ANOVA; $^*p < 0.05$ vs. Vehicle, **Figure 5I**). Taken together, these results suggest that local release of SP and CGRP in acupoints leads to an increase in conductance by inducing vascular leakage.

Increased Levels of SP and CGRP at Acupoints in IMH Rats

Finally, to confirm the increased expression of SP and CGRP at acupoints in IMH rats, we compared the expression of CGRP and SP in the skin on the wrist between normal ($n = 6$) and IMH rats ($n = 6$). Significantly greater SP (**Figures. 6A,B**) and CGRP (**Figures 6C,D**) fluorescence was found in the dermis of IMH rats than in that of control naïve rats (t-test; $p < 0.001$ in **Figures 6B,D**). Notably, the dermal blood vessels in IMH rats but not control naïve rats were predominantly enlarged (**Figures 6A,C**).

DISCUSSION

Our findings demonstrated that SP and CGRP released from afferents fibers increased electrical conductance at acupoints in IMH rats. In the IMH rat model, cutaneous neurogenic inflammation was found most frequently in the acupoints on the wrist. These acupoints revealed higher temperature and more plasma extravasation than the acupoints in naïve rats. Electrical conductance at the acupoints gradually increased with the development of hypertension but was blocked by surgical transection of the median and ulnar nerves or blockade of small diameter afferent fibers with RTX. Skin conductance and plasma extravasation were increased by intradermal injection of SP or CGRP in normal rats. In turn, inhibition of SP or CGRP by antagonists prevented the increase in both the conductance and plasma extravasation at acupoints in IMH rats. Levels of SP and CGRP were elevated in the dermis of acupoints in hypertensive rats. Our findings suggest that the local release of SP and CGRP induces vasodilation and plasma extravasation, resulting in accumulation of subskin tissue water content, thereby leading to an increase in electrical conductance at acupoints (**Figure 6E**).

While traditional acupoints have long been thought to be anatomically invisible, our recent study suggested that acupoints can be identified as neurogenic inflammatory spots (Neuro-Sp) on the skin, which are produced by activation of somatic afferents in abnormal conditions of visceral organs and can be visualized by intravenous injection of EBD (Kim et al., 2017). Consistent with our previous study (Kim et al., 2017), hypertensive rats

revealed highly localized neurogenic inflammation (indicated by Neuro-Sp) in the dermatome of the forelimbs (**Figure 1**), which is innervated by the same spinal segments (C8-T2) that innervate the heart (Alles and Dom, 1985). Cutaneous neurogenic inflammation was observed most frequently in acupoints on the wrist, such as PC6, HT7, and PC7 (**Figures 1D,E**), which are commonly used in acupuncture clinics for cardiac disorders (Stux and Pomeranz, 2012). Furthermore, neurogenic inflammation tended to rapidly develop in acupoints after an IMH procedure and to be maintained during IMH, as shown by EBD staining and thermal recordings. Similar to our findings, a previous study reported that neurogenic inflammation appears in the skin of the abdomen, groin, lower back, and perineal areas several minutes after uterine inflammation with mustard oil, as assessed by EBD extravasation (Wesselmann and Lai, 1997). Cutaneous neurogenic inflammation is manifested as flare, vasodilation and increased local skin temperature (Wesselmann and Lai, 1997; Serra et al., 1998). In our thermal recordings and imaging, a rapid and long-lasting rise in temperature at acupoints was observed after the IMH procedure and was mimicked by intradermal injection of capsaicin, which produces cutaneous neurogenic inflammation (Lin et al., 1999). These results suggest that acupoints on the wrist displayed active neurogenic inflammation characterized by plasma extravasation in this rat model of hypertension.

Multiple studies have suggested that acupoints have higher conductance and lower impedance (resistance) than the surrounding skin (Reichmanis et al., 1975; Colbert et al., 2008, 2009), although this issue is currently controversial (Ahn et al., 2008; Wong, 2014). Reichmanis et al. (1975) reported that certain acupoints had significantly higher electrical conductance than nearby sites in healthy subjects. Colbert et al. (2008, 2009) recorded skin impedance at multiple acupoints simultaneously by using a fully automatic multichannel device and reported that several acupoints showed lower impedance than nearby sites in healthy subjects. The above studies are supported by our previous and current studies showing a high conductance of acupoints in IMH rats (Kim et al., 2017) (**Figures 3D–F**). However, others have also shown inconsistent results in the electrical conductance and impedance of acupoints. Pearson et al. (2007) observed that none of the three acupoints tested had lower skin impedance than the surrounding skin in healthy subjects. Kramer et al. (2009) reported that when skin impedance was measured in healthy subjects by using an array electrode of 64 channels, the majority of acupoints tested showed no changes in impedance, but some showed transient high or low impedance. A systematic review found that five out of nine studies showed a positive association between acupoints and low electrical impedance (Ahn et al., 2008). In these previous studies, a major problem is that almost all were conducted in healthy subjects and not in disease states, which may generate mixed results in electrodermal measurements at acupoints. As acupoints are generally accepted to reflect pathological states of the body and to become hypersensitive under pathological conditions (Stux and Pomeranz, 2012; Kim et al., 2017), pathological body conditions may cause considerable changes in skin conductance or impedance at acupoints. In support of this, our previous and present studies found that the conductance of acupoints significantly increased with the development of hypertension in rats, and such an increase was not seen in the same acupoints of control rats (Kim et al., 2017) (**Figures 3D–F**). In addition, the acupoints with high conductance in IMH rats but not naïve rats showed higher neurogenic inflammation and plasma extravasation than those of naïve rats (**Figures 3G,H**). Our hypothesis is further supported by another study showing that more significant changes in skin impedance at acupoint GB34 were observed in patients that had undergone surgery than in healthy subjects (Kramer et al., 2012). Importantly, previous studies point out that the precision of skin conductance measurements can be influenced by numerous factors such as skin dryness, skin thickness, size of the sensing electrode, pressure applied on the electrode, interelectrode distance, room temperature, and humidity (Ahn and Martinsen, 2007). In the present experiment, we developed a device that applied constant pressure on the electrode and performed the experiments under controlled environmental conditions, which might rule out the impact of the above factors. Therefore, the present study suggests that during diseases, the conductance at acupoints is abnormally high and that these electrical changes are associated with neurogenic inflammation and plasma extravasation.

In the somatic areas of referred pain from viscera, Neuro-Sp are generated by activation of small diameter sensory afferents (C/Aδ-fibers) in the dermatome convergent with visceral afferents (Wesselmann and Lai, 1997; Arendt-Nielsen et al., 2008). The sensory neurons are branched, with one projection leading to the internal organs and the other extending to the skin. The visceral inputs activate the viscerosomatic convergent neurons in the sensory pathway, and the neurons antidromically activate the branches, leading to the release of neuropeptides (e.g., SP and CGRP) from small diameter sensory fibers and subsequent neurogenic extravasation (Wesselmann and Lai, 1997; Arendt-Nielsen et al., 2008). Linkage of Neuro-Sp to internal organs was proven by our previous study showing convergent DRG neurons innervating both the heart and the Neuro-Sp (Kim et al., 2017). In the present study, the development of high conductance at acupoints in hypertensive rats was almost completely ablated by surgical lesions of the median and ulnar nerves (**Figures 4A,B**), suggesting that the afferent nerves mediate the high conductance at acupoints. Furthermore, pretreatment of the median and ulnar nerves with a specific C/Aδ-fiber blocker RTX prevented the development of high conductance at acupoints (**Figure 4C**), while RTX effectively blocked transmission of small sensory afferents in the median and ulnar nerves (**Figures 4D,E**), as reported previously (Suter et al., 2009). Taken together, these findings indicate that high conductance at acupoints is caused by antidromic activation of peripheral nerves, especially small diameter sensory afferents, in the dermatome associated with visceral disorders.

Activation of small diameter sensory afferents is known to induce the release of neuropeptides SP and CGRP into the periphery and lead to the development of neurogenic inflammation (Richardson and Vasko, 2002). SP as well as other tachykinins activates neurokinin receptors to increase microvascular permeability and edema formation, while CGRP

acts on CGRP1 receptors to dilate arterioles (Schmelz and Petersen, 2001). The neuropeptides released by activated afferent fibers evoke neurogenic inflammation in the skin by activating vasodilation, axon reflex flare, and microvascular plasma extravasation (Wesselmann and Lai, 1997; Schmelz and Petersen, 2001). In the present study, intradermal injection of SP or CGRP increased both conductance and plasma extravasation in naïve rats, similar to the pattern observed in hypertensive rats (**Figures 5A–F**). In contrast, intradermal injection of SP or CGRP antagonists into acupoints prevented the development of high conductance and plasma extravasation at acupoints (**Figures 5G–I**). Moreover, increased levels of SP and CGRP were found in the acupoints of hypertensive rats. Thus, our findings suggest that SP and CGRP induce vasodilation and plasma extravasation to increase skin hydration, resulting in the development of high conductance at acupoints. Paradoxically, the locally released SP and CGRP into acupoints may in turn play a role in acupuncture effect. It has been suggested that active acupoints are associated with tissues where the sensory nerve endings are sensitized by neurogenic inflammatory mediators (Rong et al., 2013; He et al., 2017). Given that the sensitized sensory nerve endings are more sensitive to external stimuli than intact sensory nerves, we suggest that sensory nerve endings in acupoints would be sensitized by SP or CGRP released during neurogenic inflammation. Accordingly, stimulation of these sensitive acupoints would evoke the therapeutic effects of acupuncture by reaching physiological thresholds quickly, compared with stimulation of normal surrounding tissues including as sham or inactive acupoints.

A limitation of this study is that neurogenic extravasation of EBD was examined in only the skin over acupoints. Acupuncture needles often penetrate multiple layers including skin, subcutaneous tissue and muscles. As these layers may contain structures that respond to needling and produce acupuncture effects, future study will be needed to identify whether the neurogenic inflammatory processes also occur in the tissues below skin (i.e., subcutaneous tissue and muscles) and in turn are associated with acupuncture effects.

CONCLUSION

The present study suggests a novel mechanism underlying the electrical properties of acupoints: the neuropeptides SP and CGRP produce high conductance at acupoints by causing neurogenic inflammation, plasma extravasation and accumulation of subskin water contents. This study would help solve some of controversial issues concerning electrical properties of acupoints.

AUTHOR CONTRIBUTIONS

HK designed the experiment, responsible for the overall direction of the project, and for edits to the manuscript. YF, D-HK, YR, SC, BL and CHY performed the experiments and analyzed the data. YF and HK drafted the manuscript.

FUNDING

This research was supported by Basic Science Research Program through the National Research Foundation of Korea (NRF; 2018R1A5A2025272, and 2018R1E1A2A02086499), the Korea Institute of Oriental Medicine (KIOM; K18181) and Korea Brain Research Institute (KBRI; 18-BR-03).

REFERENCES

Ahn, A. C., Colbert, A. P., Anderson, B. J., Martinsen, O. G., Hammerschlag, R., Cina, S., et al. (2008). Electrical properties of acupuncture points and meridians: a systematic review. *Bioelectromagnetics* 29, 245–256. doi: 10.1002/bem.20403

Ahn, A. C., and Martinsen, O. G. (2007). Electrical characterization of acupuncture points: technical issues and challenges. *J. Altern. Complement. Med.* 13, 817–824. doi: 10.1089/acm.2007.7193

Alles, A., and Dom, R. M. (1985). Peripheral sensory nerve fibers that dichotomize to supply the brachium and the pericardium in the rat: a possible morphological explanation for referred cardiac pain? *Brain Res.* 342, 382–385. doi: 10.1016/0006-8993(85)91142-4

Arendt-Nielsen, L., Schipper, K. P., Dimcevski, G., Sumikura, H., Krarup, A. L., Giamberardino, M. A., et al. (2008). Viscero-somatic reflexes in referred pain areas evoked by capsaicin stimulation of the human gut. *Eur. J. Pain* 12, 544–551. doi: 10.1016/j.ejpain.2007.08.010

Birklein, F., and Schmelz, M. (2008). Neuropeptides, neurogenic inflammation and complex regional pain syndrome (CRPS). *Neurosci. Lett.* 437, 199–202. doi: 10.1016/j.neulet.2008.03.081

Chae, Y., Kim, H. Y., Lee, H. J., Park, H. J., Hahm, D. H., An, K., et al. (2007). The alteration of pain sensitivity at disease-specific acupuncture points in premenstrual syndrome. *J. Physiol. Sci.* 57, 115–119. doi: 10.2170/physiolsci.RP012706

Colbert, A. P., Larsen, A., Chamberlin, S., Decker, C., Schiffke, H. C., Gregory, W. L., et al. (2009). A multichannel system for continuous measurements of skin resistance and capacitance at acupuncture points. *J. Acupunct. Meridian Stud.* 2, 259–268. doi: 10.1016/S2005-2901(09)60066-2

Colbert, A. P., Yun, J., Larsen, A., Edinger, T., Gregory, W. L., and Thong, T. (2008). Skin impedance measurements for acupuncture research: development of a continuous recording system. *Evid. Based Complement. Alternat. Med.* 5, 443–450. doi: 10.1093/ecam/nem060

He, W., Wang, X. Y., Shi, H., Bai, W. Z., Cheng, B., Su, Y. S., et al. (2017). Cutaneous neurogenic inflammation in the sensitized acupoints induced by gastric mucosal injury in rats. *BMC Complement. Altern. Med.* 17:141. doi: 10.1186/s12906-017-1580-z

Kim, D. H., Ryu, Y., Hahm, D. H., Sohn, B. Y., Shim, I., Kwon, O. S., et al. (2017). Acupuncture points can be identified as cutaneous neurogenic inflammatory spots. *Sci. Rep.* 7:15214. doi: 10.1038/s41598-017-14359-z

Kim, H. Y., Hahm, D. H., Sohn, B. Y., Choi, Y., Pyun, K. H., Lee, H. J., et al. (2006). Skin on GV01 acupoint in colonic inflammatory states: tenderness and neurogenic inflammation. *J. Physiol. Sci.* 56, 317–320. doi: 10.2170/physiolsci.SC001606

Kim, S. A., Lee, B. H., Bae, J. H., Kim, K. J., Steffensen, S. C., Ryu, Y. H., et al. (2013). Peripheral afferent mechanisms underlying acupuncture inhibition of cocaine behavioral effects in rats. *PLoS One* 8:e81018. doi: 10.1371/journal.pone.0081018

Knotkova, H., Pappagallo, M., and Szallasi, A. (2008). Capsaicin (TRPV1 Agonist) therapy for pain relief: farewell or revival? *Clin. J. Pain* 24, 142–154. doi: 10.1097/AJP.0b013e318158ed9e

Kramer, S., Winterhalter, K., Schober, G., Becker, U., Wiegele, B., Kutz, D. F., et al. (2009). Characteristics of electrical skin resistance at acupuncture points in healthy humans. *J. Altern. Complement. Med.* 15, 495–500. doi: 10.1089/acm.2008.0331

Kramer, S., Zaps, D., Kutz, D. F., Wiegele, B., Kolb, F. P., Zimmer, K., et al. (2012). Impact of surgical intervention and postoperative pain on electrical skin resistance at acupuncture points: an exploratory study. *Acupunct. Med.* 30, 120–126. doi: 10.1136/acupmed-2011-010118

Kvetnansky, R., Mccarty, R., Thoa, N. B., Lake, C. R., and Kopin, I. J. (1979). Sympatho-adrenal responses of spontaneously hypertensive rats to immobilization stress. *Am. J. Physiol.* 236, H457–H462. doi: 10.1152/ajpheart.1979.236.3.H457

Lin, Q., Wu, J., and Willis, W. D. (1999). Dorsal root reflexes and cutaneous neurogenic inflammation after intradermal injection of capsaicin in rats. *J. Neurophysiol.* 82, 2602–2611. doi: 10.1152/jn.1999.82.5.2602

Martin, Y., Avendaño, C., Piedras, M. J., and Krzyzanowska, A. (2010). Evaluation of Evans blue extravasation as a measure of peripheral inflammation. *Protocol Exchange* 10, 1919–1931. doi: 10.1038/protex.2010.209

McLean, S., Ganong, A., Seymour, P. A., Snider, R. M., Desai, M. C., Rosen, T., et al. (1993). Pharmacology of CP-99,994; a nonpeptide antagonist of the tachykinin neurokinin-1 receptor. *J. Pharmacol. Exp. Ther.* 267, 472–479.

Montalto, M., Davies, F., Marijanovic, N., and Meads, A. (2013). Skin surface temperature: a possible new outcome measure for skin and soft tissue infection. *Aust. Fam. Phys.* 42, 653–657.

Nakatani, Y. (1956). Skin electric resistance and ryodoraku. *J. Auton. Nerve* 6:52.

Pan, H. L., Khan, G. M., Alloway, K. D., and Chen, S. R. (2003). Resiniferatoxin induces paradoxical changes in thermal and mechanical sensitivities in rats: mechanism of action. *J. Neurosci.* 23, 2911–2919. doi: 10.1523/JNEUROSCI.23-07-02911.2003

Pearson, S., Colbert, A. P., Mcnames, J., Baumgartner, M., and Hammerschlag, R. (2007). Electrical skin impedance at acupuncture points. *J. Altern. Complement. Med.* 13, 409–418. doi: 10.1089/acm.2007.6258

Reichmanis, M., Marino, A. A., and Becker, R. O. (1975). Electrical correlates of acupuncture points. *IEEE Trans. Biomed. Eng.* 22, 533–535. doi: 10.1109/TBME.1975.324477

Richardson, J. D., and Vasko, M. R. (2002). Cellular mechanisms of neurogenic inflammation. *J. Pharmacol. Exp. Ther.* 302, 839–845. doi: 10.1124/jpet.102.032797

Rong, P. J., Li, S., Ben, H., Li, L., Yu, L. L., Cui, C. X., et al. (2013). Peripheral and spinal mechanisms of acupoint sensitization phenomenon. *Evid. Based Complement. Altern. Med.* 2013:742195. doi: 10.1155/2013/742195

Schmelz, M., and Petersen, L. J. (2001). Neurogenic inflammation in human and rodent skin. *News Physiol. Sci.* 16, 33–37. doi: 10.1152/physiologyonline.2001.16.1.33

Serra, J., Campero, M., and Ochoa, J. (1998). Flare and hyperalgesia after intradermal capsaicin injection in human skin. *J. Neurophysiol.* 80, 2801–2810. doi: 10.1152/jn.1998.80.6.2801

Shen, Y. T., Pittman, T. J., Buie, P. S., Bolduc, D. L., Kane, S. A., Koblan, K. S., et al. (2001). Functional role of alpha-calcitonin gene-related peptide in the regulation of the cardiovascular system. *J. Pharmacol. Exp. Ther.* 298, 551–558.

Stux, G., and Pomeranz, B. (2012). *Acupuncture: Textbook and Atlas*. Berlin: Springer Science & Business Media.

Suter, M. R., Berta, T., Gao, Y. J., Decosterd, I., and Ji, R. R. (2009). Large A-fiber activity is required for microglial proliferation and p38 MAPK activation in the spinal cord: different effects of resiniferatoxin and bupivacaine on spinal microglial changes after spared nerve injury. *Mol. Pain* 5:53. doi: 10.1186/1744-8069-5-53

Wesselmann, U., and Lai, J. (1997). Mechanisms of referred visceral pain: uterine inflammation in the adult virgin rat results in neurogenic plasma extravasation in the skin. *Pain* 73, 309–317. doi: 10.1016/S0304-3959(97)00112-7

Wong, Y. M. (2014). Is an acupuncture point identifiable with skin electrical resistance measurement? *Acupunct. Med.* 32, 203–205. doi: 10.1136/acupmed-2014-010532

Yang, H. Q., Xie, S. S., Hu, X. L., Chen, L., and Li, H. (2007). Appearance of human meridian-like structure and acupoints and its time correlation by infrared thermal imaging. *Am. J. Chin. Med.* 35, 231–240. doi: 10.1142/S0192415X07004771

Yin, C. S., Jeong, H. S., Park, H. J., Baik, Y., Yoon, M. H., Choi, C. B., et al. (2008). A proposed transpositional acupoint system in a mouse and rat model. *Res. Vet. Sci.* 84, 159–165. doi: 10.1016/j.rvsc.2007.04.004

Conflict of Interest Statement: The authors declare that the research was conducted in the absence of any commercial or financial relationships that could be construed as a potential conflict of interest.

The reviewer Y-HC and handling Editor declared their shared affiliation.

frontiers in Neuroscience

ORIGINAL RESEARCH
published: 21 January 2019
doi: 10.3389/fnins.2018.01057

Moxibustion Modulates Sympathoexcitatory Cardiovascular Reflex Responses Through Paraventricular Nucleus

Ling Cheng[1†], Peng Li[2], Yash Patel[2], Yiwei Gong[2], Zhi-Ling Guo[2], Huangan Wu[3], Shaista Malik[2] and Stephanie C. Tjen-A-Looi[2*†]*

[1] Eastern Hospital Affiliated to Tongji University, Shanghai, China, [2] Susan Samueli Integrative Health Institute, University of California, Irvine, Irvine, CA, United States, [3] Shanghai Research Institute of Acupuncture and Meridian, Shanghai University of Traditional Chinese Medicine, Shanghai, China

Electroacupuncture (EA) point specific (ST36-37) stimulation decreases cardiovascular reflex responses through supraspinal regions such as the hypothalamic paraventricular nucleus (PVN) while mechanical stimulation of acupoints decreases pressor responses through peripheral thermal transient receptor potential vanilloid type-1 (TRPV1). Moxibustion generating heat applied at acupoint in combination with antihypertensive drugs decreases elevated blood pressure. We hypothesized that moxibustion modulates sympathoexcitatory cardiovascular responses through the hypothalamic PVN and peripheral heat sensitive TRPV1 in the absence of antihypertensive drugs. Rats were anesthetized, ventilated, and heart rate and mean blood pressure were monitored. Gastric distention induced consistent pressor reflex responses every 10-min. Thirty-minutes of bilateral moxibustion at the acupoint ST36, overlying the deep peroneal nerves, reduced the gastric distention evoked elevation in blood pressure. Blood pressure reflex responses were not reduced by both EA and moxibustion at G39. The moxibustion inhibition but not EA inhibition of the cardiovascular responses was reversed with blockade of local heat sensitive TRPV1 at ST36. Accordingly, activation of thermal TRPV1 by moxibustion at an average of 44.2°C in contrast to 40°C reduced the pressor responses. Naloxone, an opioid receptor antagonist, microinjected into PVN inhibited transiently the effect of moxibustion. Thus, activation of peripheral heat sensitive TRPV1 mediated the moxibustion-inhibition, but not EA-inhibition, of sympathoexcitatory cardiovascular reflex responses through hypothalamic PVN opioid system.

Keywords: gastric distention, deep peroneal nerve, acupoint specific, paraventricular nucleus, sympathoexcitatory cardiovascular reflex response

OPEN ACCESS

Edited by:
Younbyoung Chae,
Kyung Hee University, South Korea

Reviewed by:
Hee Young Kim,
Daegu Haany University, South Korea
Min-Ho Nam,
Korea Institute of Science and Technology (KIST), South Korea

***Correspondence:**
Ling Cheng
chlrosy.east@sina.com
Stephanie C. Tjen-A-Looi
stjenalo@uci.edu

† These authors have contributed equally to this work

Specialty section:
This article was submitted to Perception Science, a section of the journal Frontiers in Neuroscience

Received: *27 June 2018*
Accepted: *31 December 2018*
Published: *21 January 2019*

Citation:
Cheng L, Li P, Patel Y, Gong Y, Guo Z-L, Wu H, Malik S and Tjen-A-Looi SC (2019) Moxibustion Modulates Sympathoexcitatory Cardiovascular Reflex Responses Through Paraventricular Nucleus. Front. Neurosci. 12:1057. doi: 10.3389/fnins.2018.01057

INTRODUCTION

Moxibustion has been used to treat gastrointestinal problems such as irritable bowel syndrome (Liu et al., 2015; Shi et al., 2015) but not much is known about its effect on hypertension. Few clinical studies indicate that moxibustion in the presence of antihypertensive drugs may reduce hypertension, but the efficacy and mechanisms underlying moxibustion in the absence of drugs are

unknown (Xiong et al., 2014; Lee et al., 2016). We have shown in a series of studies in men and animals that electroacupuncture (EA) at specific acupoints activating peripheral nerves modifies sustained hypertension and reflex elevated blood pressure through reduction of sympathetic activity (Chao et al., 1999; Tjen-A-Looi et al., 2004; Li et al., 2004, 2016; Crisostomo et al., 2005). In this respect, specific central regions and neurotransmitter systems in the hypothalamus and medulla participate in the central processing of the action of acupuncture (Chao et al., 1999; Crisostomo et al., 2005; Li et al., 2009, 2010, 2015; Tjen-A-Looi et al., 2009; Moazzami et al., 2010; Tjen-A-Looi et al., 2013). The current study investigates in the absence of antihypertensive drugs the effect as well as underlying mechanisms of moxibustion at specific acupoint on sympathoexcitatory cardiovascular reflex responses in rats.

Cardiovascular regions in the central nervous system (CNS) such as rostral ventrolateral medulla (rVLM), and paraventricular nucleus (PVN) are activated during stimulation of visceral spinal afferents that leads to increases in blood pressure (Tjen-A-Looi et al., 2003, 2016). A series of studies have shown that through actions in rVLM stimulation of both gallbladder and gastric afferent activates splanchnic nerve and increases blood pressure (Li et al., 2002, 2010; Tjen-A-Looi et al., 2004; Crisostomo et al., 2005; Zhou et al., 2005a; Tjen-A-Looi et al., 2006; Moazzami et al., 2010). The PVN projects directly to the rVLM and to a lesser extent to the intermediolateral column of the spinal cord (Pyner and Coote, 1999; Hardy, 2001; Pan, 2004; Chen and Toney, 2010) and contributes to the descending neuronal pathway regulating sympathetic outflow in the rVLM (Tjen-A-Looi et al., 2016). In particular, the parvocellular PVN is critical in regulation of sympathoexcitatory cardiovascular pressor reflex responses such as during activation of splanchnic and cardiac sensory fibers (Xu et al., 2012; Tjen-A-Looi et al., 2016).

Manual acupuncture (MA) and EA modulate pressor responses that are induced by chemical, mechanical, or electrical stimulation of visceral afferent nerves (Li et al., 1998, 2001, 2002; Chao et al., 1999; Tjen-A-Looi et al., 2003, 2004; Crisostomo et al., 2005; Zhou et al., 2005a,b). We observe that EA at P5-6 decreases ischemic myocardial dysfunction (Chao et al., 1999) through decrease of oxygen demand demonstrating that acupuncture reduces demand-induced myocardial ischemia and blunts the sympathoexcitatory reflex elevation of blood pressure (Li et al., 1998). EA stimulation at P5-6 or ST36-37 activating respectively median or deep peroneal nerves and reducing elevated sympathetic activity decreases cardiovascular reflex vasoconstriction and elevation in blood pressure (Li et al., 1998, 2002; Chao et al., 1999; Tjen-A-Looi et al., 2004). With this regard, sympathoexcitatory cardiovascular responses are decreased by EA stimulation at both P5-6 and ST36-376. In addition, sympathetic premotor cardiovascular rVLM cells important for sympathetic outflow participate in central processing of the actions of EA and MA (Tjen-A-Looi et al., 2003, 2004; Zhou et al., 2005b). Recently, we demonstrate that EA-modulation of visceral induced excitatory cardiovascular responses also involves the hypothalamic PVN (Tjen-A-Looi et al., 2016). We showed that the rVLM-projecting PVN neurons important in regulation of cardiovascular responses participate in central processing of the modulatory actions of EA (Tjen-A-Looi et al., 2016). Thus, parvocellular PVN appears to be an important cardiovascular region in the hypothalamus that processes cardiovascular reflex responses and contributes to the actions of acupuncture.

Moxibustion, like EA and MA, is a form of acupoint stimulation. The acupoints are stimulated with heat generated by moxibustion (Wang et al., 2013). Moxibustion at specific acupoints relieves pain and modulates gastric motility and irritable bowel syndrome (Su et al., 2014; Liu et al., 2016; Zhao et al., 2016). Moxibustion applied at acupoint ST36 modulated gastric motility in rats (Su et al., 2014) suggesting that activation of peripheral nerves underlying the acupoint modulates gastrointestinal responses (Tjen and Fu, 2017). Moreover, stimulation of acupoints with either EA or MA modulates elevated blood pressure (Tjen-A-Looi et al., 2004; Zhou et al., 2005b) but through different peripheral mechanisms (Guo et al., 2018). In this regard in contrast to EA, peripheral transient receptor potential vanilloid type-1 (TRPV1) at acupoint P6 contributes to the effect of MA (Guo et al., 2018) suggesting differential underlying mechanisms are involved during stimulation of acupoints. The TRPV1 polymodal receptor is activated by heat greater than 42°C, mechanical stimuli, during EA in analgesia at ST36, and others (Tominaga et al., 2001; Birder et al., 2002; Pan and Chen, 2004; Nakagawa and Hiura, 2006; Caterina, 2007; Xin et al., 2016). Although activation of mechanosensitive TRPV1 during MA at P6 reduces elevated blood pressure, no information is available on the role of thermosensitive TRPV1 at acupoint ST36 during EA or moxibustion on sympathoexcitatory cardiovascular reflex responses. We hypothesize that moxibustion activating peripheral thermal-sensitive TRPV1 at acupoint ST36 decreases reflex hypertension through the opioid system in the PVN. A preliminary report of this work has been presented (Gong et al., 2018).

MATERIALS AND METHODS

Surgical Procedures

Experimental preparations and protocols were reviewed and approved by the Institutional Animal Care and Use Committee of the University of California, Irvine, CA, United States. The study conformed to the American Physiological Society "Guiding Principles for Research Involving Animals and Human Beings." The minimal possible number of rats was used to obtain reproducible and statistically significant results. Studies were performed on adult Sprague-Dawley male rats (400–600 g). Rats were anesthetized with ketamine (100 mg/kg im) and anesthesia was maintained with αα-chloralose (5 mg/kg iv). Additional doses of α-chloralose were given as necessary to maintain an adequate level of anesthesia, as determined by the lack of response to noxious toe pinch and corneal reflex, and the ability to artificially maintain a consistent respiratory rate. The trachea was intubated for artificial respiration using a ventilator (Model 661, Harvard Apparatus). The respiration was maintained with room air enriched with oxygen. The right jugular vein was cannulated for administration of fluids. The

right or left carotid artery was cannulated and attached to a pressure transducer (P23XL, Ohmeda) to monitor arterial blood pressure. Heart rate was derived from the pulsatile blood pressure pulse using a biotech Gould Instrument (Cleveland, OH, United States). Blood pressures and heart rates were recorded and analyzed offline with a computer and CED Spike 2 Windows software. Throughout the experiment arterial blood gases and pH were measured periodically with a blood gas analyzer (ABL5, Radiometer America) and were kept within normal physiological limits (PCO_2 35–40 mmHg, and PO_2 100–150 mmHg) by adjusting ventilatory rate or volume and enriching the inspired O_2 supply. Arterial pH was maintained between 7.35–7.45 by infusion of 8% sodium bicarbonate. Body temperature was kept between 36° and 38°C with a heating pad and an external heat lamp. Fur was removed in the region of the ST 36 or G39 acupoint located bilaterally on the hind limbs.

To stimulate gastric afferent by gastric distention, a 2-cm diameter unstressed dimension latex balloon attached to a polyurethane tube (3 mm diameter) was inserted into the stomach through the mouth and esophagus (Tjen-A-Looi et al., 2009). During insertion and passage through the esophagus, the balloon was palpated manually to confirm positioning of the balloon inside the stomach. A syringe was attached to the cannula to inflate and deflate the balloon with air, while a manometer through a T-connection was used to monitor balloon pressure. Transmural pressure was determined by measuring the pressure required to inflate the balloon with the various volumes of air before it was inserted into the stomach (Li et al., 2002). Distention pressures were selected to fall within the range that a rat normally experiences during ingestion of food and fluids in a single meal (Davison and Grundy, 1978; Baird et al., 2001). The balloon was deflated within 30 s after reaching the maximum increase in blood pressure. The positioning of the balloon was verified post mortem to be in the stomach.

To investigate the action of moxibustion in the hypothalamus, the animal was stabilized with a Kopf stereotaxic head frame. A craniotomy was performed to expose the dorsal surface of the cortex and gain access to the PVN. An injection cannula and microsyringe (Hamilton) fixed to a microinjection probe with inner diameter of 0.4 mm was inserted into the PVN to deliver antagonist, vehicle control or Chicago blue dye. Using visual approximation, the microinjection probe was positioned perpendicularly to the dorsal surface of the cortex 1.8 mm posterior to the Bregma, 0.5 mm lateral to the midline, and advanced ventrally 7.5–7.8 mm to reach the PVN. These coordinates provide access to a region that has been found by others to contain sympathetic related cells (Kenney et al., 2003; Chen and Toney, 2010; Cardoso et al., 2012). At the end of experiment, the microinjection site was marked with Chicago blue dye for later histological confirmation following delivery of drugs into the PVN.

Stimulating Methods

Gastric distensions were repeated 10 times to establish consistent pressor responses. Recovery of at least 10 min between gastric distensions prevented tachyphylaxis of the cardiovascular responses. To examine effects of moxibustion, acupoint ST36 (the anterolateral side of the hind-limb near the anterior crest of the tibia below the knee, under the tibialis anterior muscle that overlies the deep peroneal nerves) was stimulated with moxibustion for 30 min during three gastric distensions following two initial consistent pressor responses. Additional five pressor responses were evaluated after cessation of thermal stimulation to determine long-lasting effect of thermal stimulation at ST36. Total of 10 gastric distention induced pressor responses were evaluated. To examine the point specific thermal-sensitive effect, acupoint G39 (above the ankle at the lower one third of the hind limb overlying superficial peroneal nerves) also was stimulated similarly with heat generated by moxibustion. Responsiveness to specific temperature was evaluated with moxibustion–induced heat at 1 or 2 cm distance from the surface of the hind limbs at acupoint ST36 or G39 (Su et al., 2014). Temperature was measured with probe and thermometer (Fluke 51 II Thermometer) placed on the skin without fur during thermal stimulation at 15 and 30 min. To achieve and maintain the temperatures, the adjustment of the distance from the moxibustion stick to the surface of the skin and the tapping off the ash at end of the stick were performed frequently. Once the temperatures were achieved, the distance was determined and held constant. To determine the similarity of EA and moxibustion on sympathoexcitatory reflex responses, EA at G37-39 and ST36-37 on increases in blood pressure were evaluated in 11 other rats. Needles (40-gauge made by Suzhou Medical Appliance, Suzhou, China) were inserted at ST36-37 at a depth of 3–5 mm and G37-39 at depth of 1–2 mm bilaterally and connected to an isolation unit and stimulator (model S88, Grass, West Warwick, RI) to deliver bipolar stimuli at frequency of 2 Hz, duration of 0.5 ms, and current of 1–4 mA for 30 min. To ensure that twitches by the stimulation of motor fibers (Li et al., 2016) do not contribute to the effects of EA, gallamine triethiodide (4 mg/kg) was administered into the vein after insertion of needles and before the application of EA (Li et al., 2006).

Methods of Blockade

The role of TRPV1 at acupoint ST36 during action of bilateral moxibustion on gastric distention induced pressor responses was determined with bilateral administration of TRPV1 antagonist iodoresiniferatoxin (Iodo-RTX; 0.1 mM; 10 μl) (Guo et al., 2018). The vehicle control 5% dimethylsulfoxide (DMSO) was administered bilaterally at ST36. The antagonist or vehicle was administered with a hypodermic needle at acupoint ST36 following moxibustion or EA. The proper site and depth of hypodermic needle insertion was confirmed with brief EA stimulation at ST36-37 (placed at a depth of about 3–5 mm) inducing slight repetitive paw twitches in the rats treated with moxibustion. The twitches confirmed stimulation of motor fibers in the mixed deep peroneal nerve bundle (Li et al., 2016). In the hypothalamus, the roles of opioid receptors in the PVN during effect of moxibustion were evaluated by microinjection of the non-specific antagonist naloxone (100 nM, 50-75 nl, Sigma Aldrich, St. Louise, MO, United States) (Tjen-A-Looi et al., 2007) or 0.9% saline vehicle control. An injection cannula and microsyringe (Hamilton) fixed to a pipette were used to administer naloxone or saline into the PVN. Unilateral

microinjection allows maintenance of optimal physiological state in studies of EA-modulation of cardiovascular responses (Li et al., 2001; Tjen-A-Looi et al., 2012). With this regard, we investigated the PVN during the effect of heat generating moxibustion on pressor responses with unilateral blockade of opioid receptors.

Experimental Protocols

1. Gastric distention evoked reflexes

After the surgical procedures, experiment was conducted following a 30 min stabilization period. Repeated gastric distention was evaluated for consistent increase in blood pressure (Li et al., 2002). After obtaining the maximal cardiovascular pressor response, air was withdrawn from the balloon. Typically, the pressor response was observed within 10 sec following inflation of the balloon. The pressor reflex in mean arterial pressure (MAP) was calculated as the difference in MAP before gastric distention and MAP at the peak of the reflex response. After the completion of each experiment, rats were euthanized with intravenous KCl under deep anesthesia.

2. Moxibustion-inhibition of gastric distention responses

Consistency of increase in blood pressure to gastric distention was evaluated in a group of five animals. Moxibustion-inhibition (ST36) of the increases in MAP was examined in nine other rats. Five of the nine rats were treated with moxibustion 1-cm distance from acupoint ST36 while the other four rats were subjected to the thermal stimulation at 2-cm distance from the skin.

3. Point specific moxibustion-inhibition of pressor responses

Point specific moxibustion-modulation of gastric distention reflex responses was determined by stimulating two different acupoints, including ST36 or G39 at 1-cm distance from the skin. The moxibustion effect at ST36 was evaluated in five rats listed in above protocol (2). In four other animals, eight pressor responses were evaluated during and after 30 min moxibustion at acupoint G39 after obtaining two consistent responses to gastric distension.

4. Electroacupuncture-inhibition of gastric distention responses

Following consistent increases in blood pressure with at least two gastric distentions, cardiovascular reflex responses were measured during 30 min EA at G37-39 ($n = 5$) or EA at ST 36-37 ($n = 6$) in rats. The reflex responses to EA were determined during three gastric distentions. Thereafter, five more gastric distentions were performed every 10 min to evaluate the long lasting inhibitory responses.

5. Thermal sensitive TRPV1 in moxibustion-inhibition and EA-inhibition of pressor responses

Role of TRPV1 during moxibustion-inhibition of the increases in MAP was examined in 12 animals. At ST36 acupoint, TRPV1 was blocked with Iodo-RTX 5 min following termination of moxibustion to evaluate its role in mediating the actions of moxibustion on pressor responses in six of the 12 rats. As a control for the receptor blockade study, DMSO (5%) was injected at the acupoint in six of the 12 subjects tested for ST36 moxibustion-inhibition. In addition, TRPV1 was blocked with Iodo-RTX 5 min following termination of EA ST36-37 to evaluate its role in EA-inhibition of pressor responses in six other rats, listed in protocol (4).

6. Influence of opioid receptor blockade in PVN on moxibustion-inhibition of pressor responses

Role of PVN in moxibustion-inhibition of the increase in MAP was evaluated in eight animals. Two reproducible pre-moxibustion control values were obtained followed by 30 min of moxibustion at the ST36 acupoints. Saline was microinjected into PVN after 20 min of moxibustion. Five min after the end of moxibustion, naloxone was administered into the PVN of five rats. To confirm the role of opioids in moxibustion-inhibition, the effect of naloxone on the pressor responses in the absence of moxibustion was examined in four other animals.

7. Histology

At the end of each experiment, animals were euthanized under deep α-chloralose anesthesia followed by iv injection of saturated KCl. Microinjection sites were marked by microinjection of 2% Chicago blue dye. The brain was removed and fixed in 10% paraformaldehyde for at least 48 hr. Brains were sliced with a microtome cryostat into 40 μm sections. The sites of microinjection were identified and reconstructed with the aid of a microscope (Nikon) and software (Corel presentation) according to the atlas of Paxinos and Watson (2009).

Statistical Analysis

Means and standard errors of mean blood pressure and heart rate at rest were compared over time using a repeated-measures analysis of variance (ANOVA) followed by the Student Newman Keuls Test to examine for non-random variation. In the distension-response protocol, comparisons by ANOVA were made between blood pressure responses before and after EA at each increment in gastric volume. Student *t*-test was used to compare responses among groups. The 0.05 probability level was chosen to determine statistical significance.

RESULTS

Moxibustion-Inhibition of Gastric Distention Evoked Pressor Responses

Gastric distention increased blood pressure through activation of splanchnic afferent and induced sympathoexcitatory cardiovascular reflex responses (Li et al., 2002). Repeated stimulation of gastric afferent every 10 min displayed consistent increases in MAP during application of 30-min moxibustion 2-cm distance from the skin at acupoint ST36 showing temperatures lower than 40 ± 0.4°C (MAP, **Figure 1A**). On the other hand, application of 30-min moxibustion 1-cm distance from the skin at acupoint ST36 yielding temperature of 44.2 ± 0.6°C reduced the elevated blood pressure responses for 40 min (**Figure 1B**). Thus, moxibustion applied with different temperature at acupoint ST36 displayed differential inhibitory outcomes. Baseline blood pressures throughout the experiments were not significantly different. Heart rates also were not altered during the cardiovascular responses.

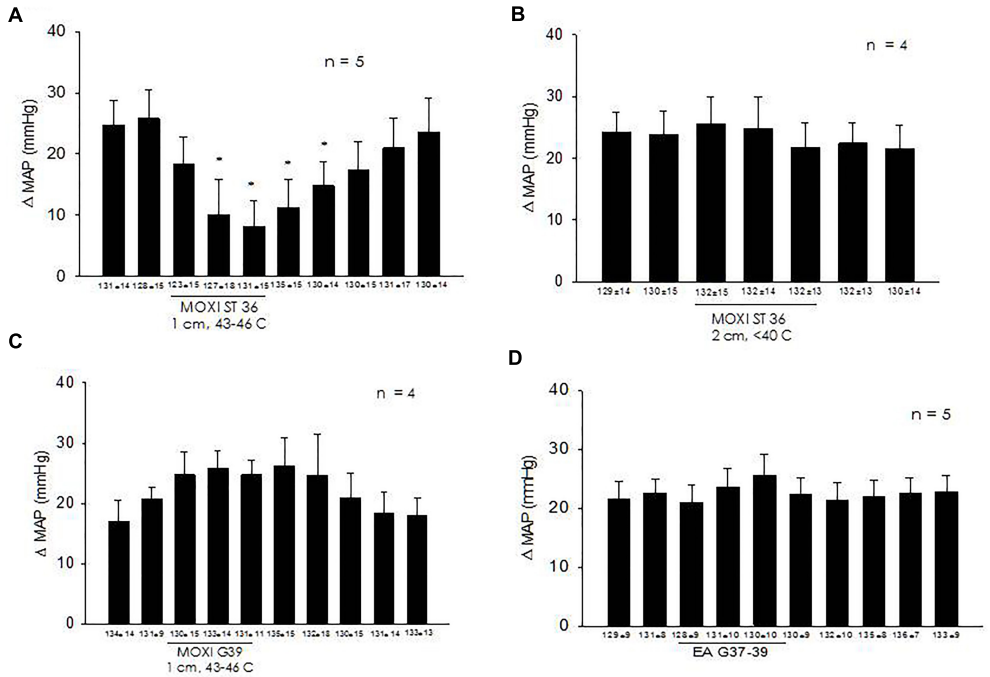

FIGURE 1 | Moxibustion inhibition of sympathoexcitatory cardiovascular reflex responses is temperature dependent and acupoint specific. Consistent elevated blood pressure reflex responses (every 10 min) were reduced by moxibustion at ST36 generating heat at temperature between 43 and 46°C **(A)**. Moxibustion temperature between 39 and 41°C did not influence the consistent gastric distention induced pressor responses **(B)**. Moxibustion application at acupoint G39 at temperature between 43 and 46°C also did not reduce the consistent increases in blood pressure **(C)**. Application of EA at ST36-37 also did not reduce the pressor responses **(D)**. Line underneath the histogram bars display the time of duration (30 min) of moxibustion and EA. Numbers below each bar represent the means and SEM of baseline blood pressures. * indicates significant different in pressor responses compared with blood pressure increases prior to application of moxibustion or EA.

Point Specific Moxibustion-Inhibition of Pressor Responses

Consistent gastric distention sympathoexcitatory cardiovascular reflex responses were examined for point specific effects. Moxibustion at average temperature of 44.2 ± 0.6°C applied at ST36 or G39 modulated the reflex responses differentially. Heat stimulation with moxibustion at G39 acupoint did not reduce the pressor responses (**Figure 1C**) in contrast to ST36 (**Figure 1B**). Thirty minutes of EA (G37-39) stimulating superficial peroneal nerve also did not reduce the blood pressure reflex responses (**Figure 1D**) supporting the importance of acupoints ST36 in reducing pressor responses.

Thermal Sensitive TRPV1 in Moxibustion-Inhibition of Pressor Responses

To determine the peripheral mechanism at acupoint ST36 on the inhibitory effect of moxibustion on sympathoexcitatory cardiovascular responses, the heat sensitive TRPV1 receptor underneath the acupoint was blocked with iodoresiniferatoxin. The TRPV1 blockade transiently reversed the inhibitory effect of moxibustion in contrast to DMSO vehicle (**Figures 2A,B**). The reversal of moxibustion-inhibition with the TRPV1 antagonist compared with vehicle DMSO on the pressor responses was significantly different ($P = 0.019$).

Thermal Sensitive TRPV1 in EA-Inhibition of Gastric Distention Responses

To examine the peripheral mechanism at acupoint ST36 on the inhibitory effect of EA on sympathoexcitatory cardiovascular responses, the heat sensitive TRPV1 receptor underneath this acupoint was blocked with iodoresiniferatoxin. Our previous study shows that EA ST36-37 reduced the elevated blood pressure responses during repeated gastric distention (Zhou et al., 2005a). Present study showed that the TRPV1 blockade did not reverse the inhibitory effect of EA (**Figure 2C**). Since DMSO did not affect the inhibition on the cardiovascular reflex responses, DMSO was not re-examined in the presence of EA. In addition, the reversal of moxibustion-inhibition compared with EA-inhibition on the pressor responses following TRPV1 antagonist administration was significantly different ($P = 0.012$) suggesting that the peripheral mechanisms at ST36 in reducing elevated blood pressure are dissimilar.

Role of Opioids in PVN on Moxibustion-Inhibition of Pressor Responses

To establish participation of the hypothalamus during the moxibustion inhibition on elevated blood pressure responses, opioid receptors were examined in the PVN. Naloxone in

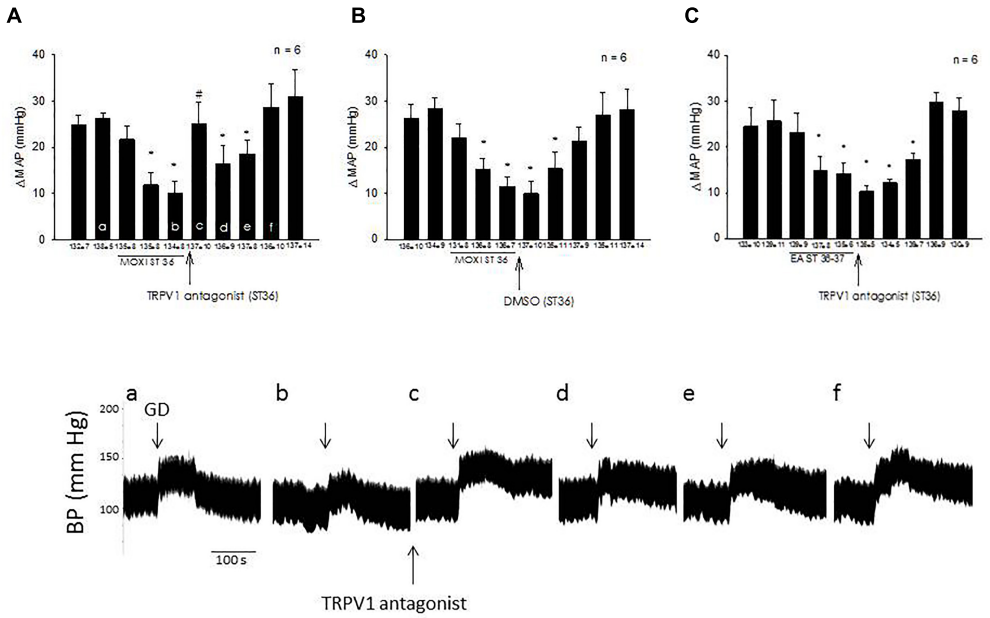

FIGURE 2 | Moxibustion inhibits the pressor responses through peripheral TRPV1. Gastric distention (every 10 min) induced increases in blood pressures reduced by moxibustion was reversed transiently following blockade of TRPV1 underneath acupoint. The moxibustion inhibition lasted at least another 20 min after the antagonism **(A)** in contrast to administration of vehicle DMSO **(B)**. Blockade of TRPV1 at ST36 during EA did not reverse the EA-inhibition of the gastric distention induced increases in blood pressure **(C)**. Letters shown in the histogram bars in Panel **A** correspond with the blood pressure tracings a-f. Numbers below each bar represent the means and SEM of baseline blood pressures. * indicates significant different in pressor responses compared with blood pressure increases prior to application of moxibustion. # indicates significant reversal of moxibustion-inhibition compared with pressor response immediately before the TRPV1 blockade.

contrast to saline in the PVN reversed the moxibustion inhibition on pressor responses (**Figure 3**).

Histology

Sites of microinjection marked with Chicago blue dye were confirmed histologically. The sites were determined by the location of microinjection tracks and dye spots. The PVN microinjection sites were confirmed to be 0.4–0.6 mm lateral to the midline and 1.6–1.75 mm from the ventral surface. Data from two microinjections of naloxone that were outside the PVN and did not reverse the effects of moxibustion were not included. **Figure 4A** displays a coronal section of 60 microns showing the site of microinjection. **Figure 4B** represents a composite map of all sites closely matched with the rat brain atlas (Paxinos and Watson, 2009).

DISCUSSION

The present study investigates the effect and underlying mechanisms in the reduction of elevated blood pressure by heat generating moxibustion. The study examined four aspects that are important in the actions of moxibustion inhibition of sympathoexcitatory cardiovascular reflex responses. First, we have observed that the effect of moxibustion is temperature dependent. A temperature greater or at 43°C at the surface of the skin at acupoint ST36 decreases gastric distention induced reflex increases in blood pressure. Secondly, the temperature-dependent moxibustion inhibitory effect on gastric distention induced cardiovascular responses also is related to point specificity. Moxibustion similar to EA applied at ST36, in contrast to G39, significantly decreases the gastric distention induced pressor response (Tjen-A-Looi et al., 2004; Zhou et al., 2005a). As such, previous (Tjen-A-Looi et al., 2004; Zhou et al., 2005a) and current data show that EA and moxibustion share similar point specific modification of pressor responses. Third, blockade of TRPV1 receptor at acupoint ST36 reverses the inhibitory effect of moxibustion. On the other hand, blockade at ST36 is unable to reverse EA-inhibition of reflex elevation of blood pressure. In this respect, heat sensitive receptor TRPV1 activation by moxibustion appears to be important in the inhibition of the pressor response while this receptor activation is not involved during EA-inhibition. Importantly, we demonstrate that the inhibitory effect of moxibustion on cardiovascular reflex responses includes opioid receptor activation in hypothalamic PVN. We have observed that blockade of opioid receptors reverses the moxibustion blood pressure lowering effect suggesting that the action of moxibustion, in part, likely is processed in this brain region. Thus, temperature-dependent moxibustion at specific acupoint reduces elevated blood pressure through hypothalamic opioid receptors in the PVN and, unlike cardiovascular EA-inhibition, peripheral local TRPV1 receptors.

Point specific stimulation with moxibustion or EA differentially inhibits elevated blood pressure. Current study shows that stimulation at ST36 acupoint with moxibustion

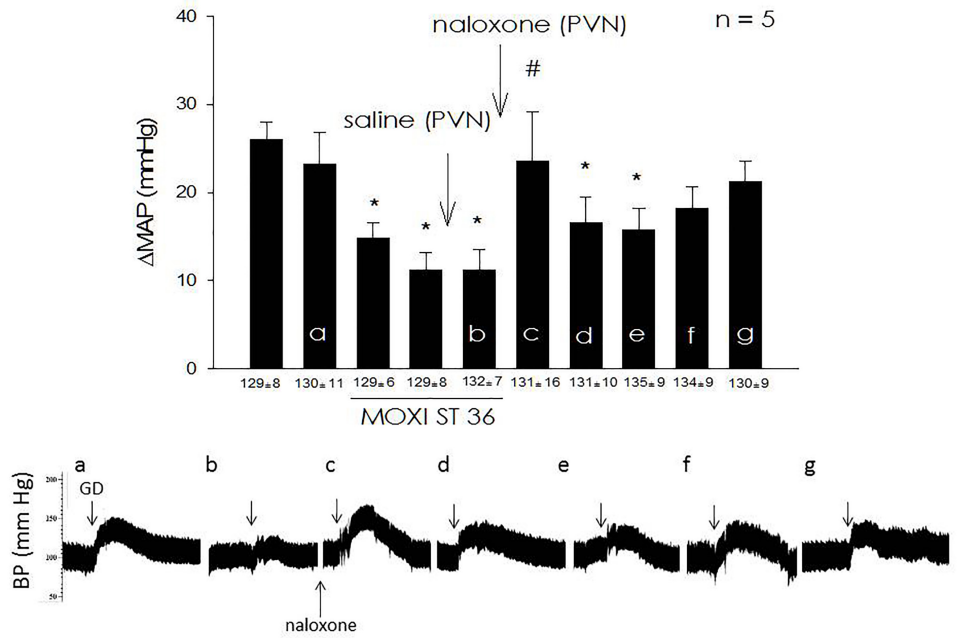

FIGURE 3 | Moxibustion inhibits cardiovascular reflex responses through opioids in PVN. Microinjection of naloxone in PVN reversed the moxibustion inhibition on pressor responses induced every 10 min. The moxibustion inhibition lasted at least another 30 min after the opioid receptors blockade. Microinjection of saline did not influence moxibustion inhibition on the gastric distention evoked elevated blood pressures. Numbers below each bar represent the means and SEM of baseline blood pressures. * indicates significant different in pressor responses compared with blood pressure increases prior to application of moxibustion. # indicates significant reversal of moxibustion-inhibition compared with pressor response immediately before the TRPV1 blockade.

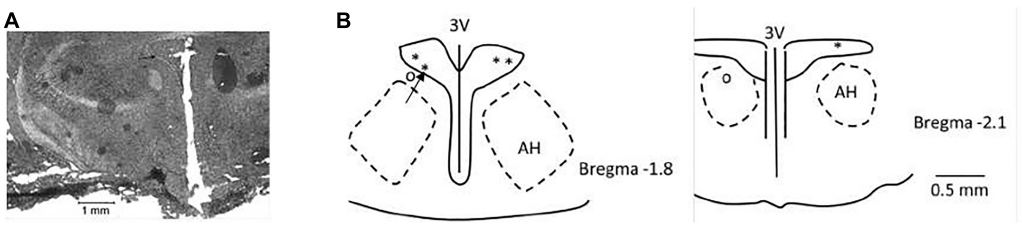

FIGURE 4 | Microinjection site marked with an arrow in PVN is displayed in the coronal section **(A)**. Composite map displays the sites of microinjections **(B)**. Coronal sections of the hypothalamus PVN caudal to bregma at 1.8 and 2.1 show the sites with *. Sites shown with o indicate microinjections outside the PVN.

is effective in reducing elevated blood pressure in contrast to moxibustion application at G39. In line with these observations, moxibustion at different acupoints induces facilitatory and inhibitory effects on gastric motility (Su et al., 2015) supporting the point specific effect of moxibustion. In addition, stimulation with EA at P5-6 or ST36-37 acupoints inhibits sympathoexcitatory blood pressure responses (Tjen-A-Looi et al., 2004; Zhou et al., 2005a) while current data show the inability of EA-inhibition at G37-39. EA modulates also reflex hypotension and bradycardia with point specific actions (Tjen-A-Looi et al., 2018) suggesting that EA influences both cardiovascular inhibitory and excitatory reflex responses. Collectively, these observations suggest that both moxibustion and EA modify excitatory as well as inhibitory reflex responses by stimulation at specific acupoints.

Transient receptor potential vanilloid 1, a known capsaicin receptor, is heat-sensitive and depolarizes neurons at temperatures greater than 42°C. Interestingly, studies have suggested that ruthenium red, the non-competitive antagonist for the capsaicin receptor, abolish the capsaicin but not the heat induced reflex response (Hiura, 2009). The polymodal TRPV1 receptor, sensor of chemical, mechanical and heat stimuli, is expressed most abundantly in small diameter peripheral sensory neurons (Sanchez et al., 2001; Caterina, 2007). The TRPV1 located on sensory neuronal tissue is a ligand-gated, voltage-gated and cationic channel (Voets et al., 2004; Matta and Ahern, 2007). TRPV1 located on sensory fibers is important during 50 Hz EA ST36 on systemic analgesia (Xin et al., 2016). In these respects, current study shows an important role for TRPV1, likely located in the small diameter fibers underneath acupoint ST36, during moxibustion inhibition of pressor responses, however,

this receptor does not participate during the inhibitory actions of 2 Hz EA. Notably, MA also modulates sympathoexcitatory cardiovascular reflex responses through peripheral TRPV1 underneath the blood pressure lowering acupoint P6 (Guo et al., 2018). Hence, TRPV1 activated by heat or mechanical stimuli during moxibustion or MA application respectively modulates sympathoexcitatory cardiovascular reflex responses in contrast to EA-inhibition on pressor responses. Further studies are warranted to examine the role of TRPV1 during actions of EA focusing on physiological conditions and stimulating parameters.

The importance of supraspinal regions during effects of moxibustion has been unclear while EA inhibits cardiovascular responses, in part, through hypothalamus, midbrain and medulla. Stimulation of ST36-37 with EA activates hypothalamic arcuate nucleus, modulates brainstem rVLM activity and decreases sympathoexcitatory cardiovascular reflex responses (Tjen-A-Looi et al., 2004; Li et al., 2006). We also have demonstrated that the PVN projecting to rVLM is activated during EA (P5-6) while the present study shows that moxibustion through local TRPV1 at ST36 reduces reflex increases in blood pressure through the hypothalamic PVN. In accordance with the previous and current studies, activation of peripheral TRPV1 at ST36 modifies hypothalamic PVN, PVN-rVLM projection and hence cardiovascular reflex responses. However, current observation indicates that activation of ST36 by EA does not include the activation of the heat sensitive TRPV1. Future studies are needed to determine the peripheral mechanisms during EA activation of ST36 involving central regions such as PVN in modulating the reflex elevation of blood pressure.

The PVN is rich in opioids. In particular, the opioids, enkephalin and β-endorphin, are present in the PVN and participate in regulation of cardiovascular function (Kiss et al., 1984; Lessard and Bachelard, 2002; Bowman et al., 2013). Furthermore, opioids reduce neuronal activity in PVN in rat hypothalamic brain slice preparation (Muehlethaler et al., 1980; Pittman et al., 1980). In intact animal, we show the relevance of PVN opioid receptors during effects of EA at P5-6 (Tjen-A-Looi et al., 2016). Although stimulation with EA at P5-6 decreases the sympathetic activity of cardiovascular neurons in PVN that, in turn, reduces pressor responses through activation of PVN opioid receptors (Tjen-A-Looi et al., 2016), the actions and effects during ST36 stimulation and activation of the local TRPV1 has been unclear. We currently demonstrate a reversal of the moxibustion-inhibition activating temperature specific TRPV1 on sympathetic cardiovascular responses following non-specific blockade of opioid receptors in the PVN. Thus, the present data show that moxibustion inhibition by stimulation of ST36 and activation of peripheral TRPV1 employs the opioid system in the PVN to reduce sympathoexcitatory reflex responses. The specific opioid receptor subtype(s) in the PVN relevant to the moxibustion-inhibition warrants further investigation.

PERSPECTIVE AND SUMMARY

Our results suggest that thermal dependent moxibustion stimulating ST36 activates TRPV1 in peripheral sensory nerves, reduces PVN neuronal activity through the opioid system, and decreases sympathoexcitatory cardiovascular reflex responses. Decrease in these cardiovascular reflex responses by stimulation of acupoint ST36 with EA or moxibustion appears to occur through different peripheral mechanisms. These observations imply that the activation of sensory neuron during acupoint stimulation by different modes such as EA, MA, or moxibustion eventually decreases sympathoexcitatory responses possibly through similar central processes (Tjen-A-Looi et al., 2016; Guo et al., 2018). Although previous reports show moxibustion blood pressure lowering effect in combination with antihypertensive drugs, present data show that moxibustion alone decreases sympathoexcitatory blood pressure responses. Studies are warranted to examine the long lasting effect of moxibustion on sustained hypertension.

AUTHOR CONTRIBUTIONS

ST-A-L, LC, and PL were responsible for experimental design and data evaluation. The experiments were conducted by ST-A-L, YG, Z-LG, and YP. All authors reviewed the manuscript.

FUNDING

National Heart, Lung, and Blood Institute and National Center for Complimentary and Integrative Health, Bethesda, MD, United States, grants HL-72125 and AT-009347. Shanghai Natural Science Foundation: Moxibustion at Zusanli on IML-rVLM neural regulation pathway in hypertensive rats (16ZR1428300). The National Basic Research Program of China, the "973 plan" project, the mechanism of the moxibustion effect and the mechanism of its endogenous regulation (2015CB554501).

ACKNOWLEDGMENTS

The authors are grateful for technical input from Sixian Audrey Li.

REFERENCES

Baird, J., Travers, J., and Travers, S. (2001). Parametric analysis of gastric distention responses in the parabrachial nucleus. *Am. J. Physiol. Regul. Integr. Comp. Physiol.* 281, R1568–R1580.

Birder, L. A., Nakamura, Y., Kiss, S., Nealen, M. L., Barrick, S., Kanai, A. J., et al. (2002). Altered urinary bladder function in mice lacking the vanilloid receptor TRPV1. *Nat. Neurosci.* 5, 856–860. doi: 10.1038/nn902

Bowman, B. R., Kumar, N. N., Hassan, S. F., McMullan, S., and Goodchild, A. K. (2013). Brain sources of inhibitory input to the rat rostral ventrolateral medulla. *J. Comp. Neurol.* 521, 213–232. doi: 10.1002/cne.23175 doi: 10.1002/cne.23175

Cardoso, L. M., Colombari, E., and Toney, G. M. (2012). Endogenous hydrogen peroxide in the hypothalamic paraventricular nucleus regulates sympathetic

nerve activity responses to L-glutamate. *J. Appl. Physiol.* 113, 1423–1431. doi: 10.1152/japplphysiol.00912.2012

Caterina, M. J. (2007). Transient receptor potential ion channels as participants in thermosensation and thermoregulation. *Am. J. Physiol. Regul. Integr. Comp. Physiol.* 292, R64–R76. doi: 10.1152/ajpregu.00446.2006

Chao, D. M., Shen, L. L., Tjen-A-Looi, S., Pitsillides, K. F., Li, P., Longhurst, J. C., et al. (1999). Naloxone reverses inhibitory effect of electroacupuncture on sympathetic cardiovascular reflex responses. *Am. J. Physiol.* 276, H2127–H2134. doi: 10.1152/ajpheart.1999.276.6.H2127

Chen, Q. H., and Toney, G. M. (2010). In vivo discharge properties of hypothalamic paraventricular nucleus neurons with axonal projections to the rostral ventrolateral medulla. *J. Neurophysiol.* 103, 4–15. doi: 10.1152/jn.00094.2009

Crisostomo, M., Li, P., Tjen-A-Looi, S. C., and Longhurst, J. C. (2005). Nociceptin in rVLM mediates electroacupuncture inhibition of cardiovascular reflex excitatory response in rats. *J. Appl. Physiol.* 98, 2056–2063. doi: 10.1152/japplphysiol.01282.2004

Davison, J. S., and Grundy, D. (1978). Modulation of single vagal efferent fibre discharge by gastrointestinal afferents in the rat. *J. Physiol.* 284, 69–82. doi: 10.1113/jphysiol.1978.sp012528

Gong, Y., Tjen-A-looi, S. C., Fu, L.-W., and Cheng, L. (2018). Role of hypothalamic opioids in moxibustion modulation of sympathoexcitatory cardiovascular reflex responses. *Soc. Neurosci.*

Guo, Z. L., Fu, L. W., Su, H. F., Tjen, A. L. S., and Longhurst, J. C. (2018). Role of TRPV1 in acupuncture modulation of reflex excitatory cardiovascular responses. *Am. J. Physiol. Regul. Integr. Comp. Physiol.* 314, R655–R666. doi: 10.1152/ajpregu.00405.2017

Hardy, S. G. P. (2001). Hypothalamic projections to cardiovascular centers of the medulla. *Brain Res.* 894, 233–240. doi: 10.1016/S0006-8993(01)02053-4

Hiura, A. (2009). Is thermal nociception only sensed by the capsaicin receptor, TRPV1? *Anat. Sci. Int.* 84, 122–128. doi: 10.1007/s12565-009-0048-8

Kenney, M. J., Weiss, M. L., Mendes, T., Wang, Y., and Fels, R. J. (2003). Role of paraventricular nucleus in regulation of sympathetic nerve frequency components. *Am. J. Physiol. Heart Circ. Physiol.* 284, H1710–H1720. doi: 10.1152/ajpheart.00673.2002

Kiss, J. Z., Cassell, M. D., and Palkovits, M. (1984). Analysis of the ACTH/beta-End/alpha-MSH-immunoreactive afferent input to the hypothalamic paraventricular nucleus of rat. *Brain Res.* 324, 91–99. doi: 10.1016/0006-8993(84)90625-5

Lee, E., Zhou, C., Zhao, T. P., Chen, X. C., Cheng, L., Liu, H., et al. (2016). Effect of direct moxibustion on blood pressure and clinical symptoms in elderly patients with essential hypertension. *J. Acupunct. Tuina Sci.* 14, 73–81. doi: 10.1007/s11726-016-0904-8

Lessard, A., and Bachelard, H. (2002). Tonic inhibitory control exerted by opioid peptides in the paraventricular nuclei of the hypothalamus on regional hemodynamic activity in rats. *Br. J. Pharmacol.* 136, 753–763. doi: 10.1038/sj.bjp.0704780

Li, M., Tjen-A-Looi, S. C., Guo, Z. L., and Longhurst, J. C. (2016). Repetitive electroacupuncture attenuates cold-induced hypertension through enkephalin in the rostral ventral lateral medulla. *Sci. Rep.* 6:35791. doi: 10.1038/srep35791

Li, P., Ayannusi, O., Reed, C., and Longhurst, J. C. (2004). Inhibitory effect of electroacupuncture (EA) on the pressor response induced by exercise stress. *Clin. Auton. Res.* 14, 182–188. doi: 10.1007/s10286-004-0175-1

Li, P., Pitsillides, K. F., Rendig, S. V., Pan, H.-L., and Longhurst, J. C. (1998). Reversal of reflex-induced myocardial ischemia by median nerve stimulation: a feline model of electroacupuncture. *Circulation* 97, 1186–1194. doi: 10.1161/01.CIR.97.12.1186

Li, P., Rowshan, K., Crisostomo, M., Tjen-A-Looi, S. C., and Longhurst, J. C. (2002). Effect of electroacupuncture on pressor reflex during gastric distention. *Am. J. Physiol.* 283, R1335–R1345.

Li, P., Tjen-A-Looi, S. C., Cheng, L., Liu, D., Painovich, J., Vinjamury, S., et al. (2015). Long-lasting reduction of blood pressure by electroacupuncture in patients with hypertension: randomized controlled trial. *Med. Acupunct.* 27, 253–266. doi: 10.1089/acu.2015.1106

Li, P., Tjen-A-Looi, S. C., Guo, Z. L., Fu, L. W., and Longhurst, J. C. (2009). Long-loop pathways in cardiovascular electroacupuncture responses. *J. Appl. Physiol.* 106, 620–630. doi: 10.1152/japplphysiol.91277.2008

Li, P., Tjen-A-Looi, S. C., and Longhurst, J. C. (2001). Rostral ventrolateral medullary opioid receptor subtypes in the inhibitory effect of electroacupuncture on reflex autonomic response in cats. *Auton. Neurosci.* 89, 38–47. doi: 10.1016/S1566-0702(01)00247-8

Li, P., Tjen-A-Looi, S. C., and Longhurst, J. C. (2006). Excitatory projections from arcuate nucleus to ventrolateral periaqueductal gray in electroacupuncture inhibition of cardiovascular reflexes. *Am. J. Physiol.* 209, H2535–H2542. doi: 10.1152/ajpheart.00972.2005

Li, P., Tjen-A-Looi, S. C., and Longhurst, J. C. (2010). Nucleus raphé pallidus participates in midbrain-medullary cardiovascular sympathoinhibition during electroacupuncture. *Am. J. Physiol.* 299, R1369–R1376. doi: 10.1152/ajpregu.00361.2010

Liu, S., Shi, Q., Zhu, Q., Zou, T., Li, G., Huang, A., et al. (2015). P2X(7) receptor of rat dorsal root ganglia is involved in the effect of moxibustion on visceral hyperalgesia. *Purinergic. Signal.* 11, 161–169. doi: 10.1007/s11302-014-9439-y

Liu, Z., Yan, S., Wu, J., He, L., Li, N., Dong, G., et al. (2016). Acupuncture for chronic severe functional constipation: a randomized, controlled trial. *Ann. Intern. Med.* 165, 761–769. doi: 10.7326/M15-3118

Matta, J. A., and Ahern, G. P. (2007). Voltage is a partial activator of rat thermosensitive TRP channels. *J. Physiol.* 585, 469–482. doi: 10.1113/jphysiol.2007.144287

Moazzami, A., Tjen-A-Looi, S. C., Guo, Z.-L., and Longhurst, J. C. (2010). Serotonergic projection from nucleus raphe pallidus to rostral ventrolateral medulla modulates cardiovascular reflex responses during acupuncture. *J. Appl. Physiol.* 108, 1336–1346. doi: 10.1152/japplphysiol.00477.2009

Muehlethaler, M., Gaehwiler, B. H., and Dreifuss, J. J. (1980). V.Enkephalin-induced inhibition of hypothalmaic paraventricular neurons. *Brain Res.* 197, 264–268. doi: 10.1016/0006-8993(80)90457-6

Nakagawa, H., and Hiura, A. (2006). Capsaicin, transient receptor potential (TRP) protein subfamilies and the particular relationship between capsaicin receptors and small primary sensory neurons. *Anat. Sci. Int.* 81, 135–155. doi: 10.1111/j.1447-073X.2006.00141.x

Pan, H., and Chen, S. (2004). Sensing tissue ischemia: another new function for capsaicin receptors? *Circulation* 110, 1826–1831.

Pan, H.-L. (2004). Brain angiotensin II and synaptic transmission. *Neuroscientist* 10, 422–431. doi: 10.1177/1073858404264678

Paxinos, G., and Watson, C. (2009). *The Rat Brain in Stereotaxic Coordinates*. Cambridge, MA: Academic Press.

Pittman, Q. J., Hatton, J. D., and Bloom, F. E. (1980). Morphine and opioid peptides reduce paraventricular neuronal activity: studies on the rat hypothalamic slice preparation. *Proc. Natl. Acad. Sci. U.S.A.* 77, 5527–5531. doi: 10.1073/pnas.77.9.5527

Pyner, S., and Coote, J. H. (1999). Identification of an efferent projection from the paraventricular nucleus of the hypothalamus terminating close to spinally projecting rostral ventrolateral medullary neurons. *Neuroscience* 88, 949–957. doi: 10.1016/S0306-4522(98)00255-3

Sanchez, J. F., Krause, J. E., and Cortright, D. N. (2001). The distribution and regulation of vanilloid receptor VR1 and VR1 5' splice variant RNA expression in rat. *Neuroscience* 107, 373–381. doi: 10.1016/S0306-4522(01)00373-6

Shi, Y., Chen, Y. H., Yin, X. J., Wang, A. Q., Chen, X. K., Lu, J. H., et al. (2015). Electroacupuncture versus moxibustion for irritable bowel syndrome: a randomized, parallel-controlled trial. *Evid. Based Complement. Alternat. Med.* 2015:361786. doi: 10.1155/2015/361786

Su, Y. S., Xin, J. J., Yang, Z. K., He, W., Shi, H., Wang, X. Y., et al. (2015). Effects of different local moxibustion-like stimuli at zusanli (ST36) and zhongwan (CV12) on gastric motility and its underlying receptor mechanism. *Evid. Based Complement. Alternat. Med.* 2015:486963. doi: 10.1155/2015/486963

Su, Y. S., Yang, Z. K., Xin, J. J., Wei, H., Shi, H., Wang, X. Y., et al. (2014). Somatosensory nerve fibers mediated generation of De-qi in manual acupuncture and local moxibustion-like stimuli-modulated gastric motility in rats. *Evid. Based Complement. Alternat. Med.* 2014:673239. doi: 10.1155/2014/673239

Tjen, A. L. S., and Fu, L. W. (2017). Sustained effects of acupuncture in treatment of chronic constipation. *Ann. Palliat. Med.* 6, S124–S127. doi: 10.21037/apm.2017.03.02

Tjen-A-Looi, S. C., Fu, L. W., Guo, Z. L., and Longhurst, J. C. (2018). Modulation of neurally mediated vasodepression and bradycardia by electroacupuncture

through opioids in nucleus tractus solitarius. *Sci. Rep.* 8:1900. doi: 10.1038/s41598-018-19672-9

Tjen-A-Looi, S. C., Guo, C., and Longhurst, J. C. (2013). Paraventricular nucleus contributes to acupuncture modulation of sympathoexcitatory cardiovascular reflexes. *FASEB J.* 27:LB692.

Tjen-A-Looi, S. C., Guo, Z. L., Fu, L. W., and Longhurst, J. C. (2016). Paraventricular nucleus modulates excitatory cardiovascular reflexes during electroacupuncture. *Sci. Rep.* 6:25910. doi: 10.1038/srep25910

Tjen-A-Looi, S. C., Li, P., Li, M., and Longhurst, J. C. (2012). Modulation of cardiopulmonary depressor reflex in nucleus ambiguus by electroacupuncture: roles of opioids and gamma aminobutyric acid. *Am. J. Physiol.* 302, R833–R844. doi: 10.1152/ajpregu.00440.2011

Tjen-A-Looi, S. C., Li, P., and Longhurst, J. C. (2003). Prolonged inhibition of rostral ventral lateral medullary premotor sympathetic neuron by electroacupuncture in cats. *Auton. Neurosci.* 106, 119–131. doi: 10.1016/S1566-0702(03)00076-6

Tjen-A-Looi, S. C., Li, P., and Longhurst, J. C. (2004). Medullary substrate and differential cardiovascular response during stimulation of specific acupoints. *Am. J. Physiol.* 287, R852–R862. doi: 10.1152/ajpregu.00262.2004

Tjen-A-Looi, S. C., Li, P., and Longhurst, J. C. (2006). Midbrain vlPAG inhibits rVLM cardiovascular sympathoexcitatory responses during acupuncture. *Am. J. Physiol.* 290, H2543–H2553

Tjen-A-Looi, S. C., Li, P., and Longhurst, J. C. (2007). Role of medullary GABA, opioids, and nociceptin in prolonged inhibition of cardiovascular sympathoexcitatory reflexes during electroacupuncture in cats. *Am. J. Physiol.* 293, H3627–H3635. doi: 10.1152/ajpheart.00842.2007

Tjen-A-Looi, S. C., Li, P., and Longhurst, J. C. (2009). Processing cardiovascular information in the vlPAG during electroacupuncture in rats: roles of endocannabinoids and GABA. *J. Appl. Physiol.* 106, 1793–1799. doi: 10.1152/japplphysiol.00142.2009

Tominaga, M., Wada, M., and Masu, M. (2001). Potentiation of capsaicin receptor activity by metabotropic ATP receptors as a possible mechanism for ATP-evoked pain and hyperalgesia. *Proc. Natl. Acad. Sci. U.S.A.* 98, 6951–6956. doi: 10.1073/pnas.111025298

Voets, T., Droogmans, G., Wissenbach, U., Janssens, A., Flockerzi, V., Nilius, B., et al. (2004). The principle of temperature-dependent gating in cold- and heat-sensitive TRP channels. *Nature* 430, 748–754. doi: 10.1038/nature02732

Wang, Y. S., Zhang, J. B., Jiang, J. F., and Wang, L. L. (2013). Research on effects of the thermal stimulation by moxibustion at different temperatures on cardiac function in rats and on mast cells in the local site of moxibustion. *Evid. Based Complement. Alternat. Med.* 2013:545707. doi: 10.1155/2013/545707

Xin, J., Su, Y., Yang, Z., He, W., Shi, H., Wang, X., et al. (2016). Distinct roles of ASIC3 and TRPV1 receptors in electroacupuncture-induced segmental and systemic analgesia. *Front. Med.* 10:465–472. doi: 10.1007/s11684-016-0482-7

Xiong, X., Liu, W., Yang, X., Feng, B., and Wang, J. (2014). Moxibustion for essential hypertension. *Complement. Ther. Med.* 22, 187–195. doi: 10.1016/j.ctim.2013.11.005

Xu, B., Zheng, H., and Patel, K. P. (2012). Enhanced activation of RVLM-projecting PVN neurons in rats with chronic heart failure. *Am. J. Physiol. Heart Circ. Physiol.* 302, H1700–H1711. doi: 10.1152/ajpheart.00722.2011

Zhao, J. M., Chen, L., Zhou, C. L., Shi, Y., Li, Y. W., Shang, H. X., et al. (2016). Comparison of electroacupuncture and moxibustion for relieving visceral hypersensitivity in rats with constipation-predominant irritable bowel syndrome. *Evid. Based Complement. Alternat. Med.* 2016:9410505. doi: 10.1155/2016/9410505

Zhou, W., Fu, L. W., Tjen-A-Looi, S. C., Li, P., and Longhurst, J. C. (2005a). Afferent mechanisms underlying stimulation modality-related modulation of acupuncture-related cardiovascular responses. *J. Appl. Physiol.* 98, 872–880.

Zhou, W., Tjen-A-Looi, S., and Longhurst, J. C. (2005b). Brain stem mechanisms underlying acupuncture modality-related modulation of cardiovascular responses in rats. *J. Appl. Physiol.* 99, 851–860.

Conflict of Interest Statement: The authors declare that the research was conducted in the absence of any commercial or financial relationships that could be construed as a potential conflict of interest.

frontiers in Neuroscience

PERSPECTIVE
published: 11 February 2019
doi: 10.3389/fnins.2019.00100

Default Mode Network as a Neural Substrate of Acupuncture: Evidence, Challenges and Strategy

Yuqi Zhang[1], Haolin Zhang[2], Till Nierhaus[3,4], Daniel Pach[5,6], Claudia M. Witt[5,6,7] and Ming Yi[1,8]**

[1] Department of Neurobiology, School of Basic Medical Sciences, Neuroscience Research Institute, Peking University, Beijing, China, [2] Department of Traditional Chinese Medicine, Peking University Third Hospital, Beijing, China, [3] Neurocomputation and Neuroimaging Unit, Department of Education and Psychology, Freie Universität Berlin, Berlin, Germany, [4] Department of Neurology, Max Planck Institute for Human Cognitive and Brain Sciences, Leipzig, Germany, [5] Institute for Social Medicine, Epidemiology, and Health Economics, Charité-Universitätsmedizin Berlin, Corporate Member of Freie Universität Berlin, Humboldt-Universität zu Berlin, and Berlin Institute of Health, Berlin, Germany, [6] Institute for Complementary and Integrative Medicine, University Hospital Zurich, University of Zurich, Zurich, Switzerland, [7] Center for Integrative Medicine, University of Maryland School of Medicine, Baltimore, MD, United States, [8] Key Laboratory for Neuroscience, Ministry of Education, National Health Commission, Peking University, Beijing, China

OPEN ACCESS

Edited by:
Florian Beissner, Hannover Medical School, Germany

Reviewed by:
Norman Waldemar Kettner, Logan College of Chiropractic, United States
Jeungchan Lee, Harvard Medical School, United States

***Correspondence:**
Haolin Zhang
zhanghaolin@bjmu.edu.cn
Ming Yi
mingyi@hsc.pku.edu.cn;
mingyi@bjmu.edu.cn

Specialty section:
This article was submitted to Perception Science, a section of the journal Frontiers in Neuroscience

Received: *11 September 2018*
Accepted: *28 January 2019*
Published: *11 February 2019*

Citation:
Zhang Y, Zhang H, Nierhaus T, Pach D, Witt CM and Yi M (2019) Default Mode Network as a Neural Substrate of Acupuncture: Evidence, Challenges and Strategy. Front. Neurosci. 13:100. doi: 10.3389/fnins.2019.00100

Acupuncture is widely applied all over the world. Although the neurobiological underpinnings of acupuncture still remain unclear, accumulating evidence indicates significant alteration of brain activities in response to acupuncture. In particular, activities of brain regions in the default mode network (DMN) are modulated by acupuncture. DMN is crucial for maintaining physiological homeostasis and its functional architecture becomes disrupted in various disorders. But how acupuncture modulates brain functions and whether such modulation constitutes core mechanisms of acupuncture treatment are far from clear. This *Perspective* integrates recent literature on interactions between acupuncture and functional networks including the DMN, and proposes a back-translational research strategy to elucidate brain mechanisms of acupuncture treatment.

Keywords: acupuncture, default mode network, neuroimaging, pain, fMRI

COMPLEX BRAIN MECHANISMS OF ACUPUNCTURE

Acupuncture, an important component of traditional Chinese medicine, has been practiced in China for more than 3000 years, and is now widely applied all over the world (Zhuang et al., 2013). Studies have shown that for disorders such as chronic pain, the effects of acupuncture cannot be fully attributed to placebo (Vickers et al., 2012, 2018). Neuroimaging studies have revealed significant brain activity changes in response to acupuncture, indicating possible brain contribution to its effects.

Intriguingly, brain responses to acupuncture stimuli encompass a broad network of regions involving not only somatosensory, but affective and cognitive processing. A meta-analysis of brain activities associated with acupuncture stimulation reveals activation in the sensorimotor cortical network, including the insula, thalamus, anterior cingulate cortex (ACC), and primary and secondary somatosensory cortices, and deactivation in the limbic-paralimbic neocortical network, including the medial prefrontal cortex (mPFC), caudate, amygdala, posterior cingulate cortex

(PCC), and parahippocampus (Chae et al., 2013). These findings indicate multi-dimensional brain responses to acupuncture. However, contribution of each dimension to acupuncture effects is poorly defined.

Additional complexity stems from differences between various acupuncture paradigms (Huang et al., 2012). Such variations may stem from (but not restricted to) manual versus electro-acupuncture, electro-acupuncture of different stimulating frequencies and intensities, acupuncture in different points, responders versus non-responders of acupuncture, and acupuncture in healthy versus morbid participants (Han, 2003; Yi et al., 2011; Huang et al., 2012; Xie et al., 2013). Thus, common and specific brain responses need to be clarified between these conditions for delicate mechanistic understanding of acupuncture.

DEFAULT MODE NETWORK AS A NEURAL SUBSTRATE OF ACUPUNCTURE

Default mode network (DMN) is a recently appreciated brain system, which shows strong activity at rest but deactivates upon externally oriented attention (Buckner et al., 2008; Northoff et al., 2010). Resting state functional magnetic resonance imaging has identified key clusters of human DMN including mPFC, ACC, PCC, orbital frontal cortex, lateral temporal cortex, inferior parietal lobe, retrosplenial cortex and precuneus (Buckner et al., 2008). Simultaneous with signal attenuation in the DMN, a significant signal potentiation in the salience network can be observed (Napadow et al., 2009; Nierhaus et al., 2015), with anterior insula initiating dynamic switching between these intrinsic networks (Bai et al., 2009).

We could note that brain regions within the DMN overlap to a large extent with acupuncture-responsive regions (Chae et al., 2013), which leads to the hypothesis that acupuncture exerts effects through its modulation over the DMN (Otti and Noll-Hussong, 2012; Zhao et al., 2014). In addition to local activation/deactivation, the functional connectivity within and across DMN is also modulated by acupuncture (Dhond et al., 2008; Zyloney et al., 2010; Long et al., 2016; Shi et al., 2016). More importantly, acupuncture-induced deactivation of DMN is stronger than sham acupuncture or tactile stimulation, but attenuated or reversed in direction if sharp pain occurs during acupuncture practice (Hui et al., 2010). In addition, increasing the "dose" of acupuncture, by increasing the number of needles or the intensity of needle stimulation, might induce an enhanced modulation of DMN that persisted even after the termination of acupuncture stimulation (Lin et al., 2016).

Disrupted DMN activities have been observed in various diseases including pain (Dhond et al., 2008; Kucyi et al., 2014; Alshelh et al., 2018), autism (Kennedy and Courchesne, 2008), schizophrenia (Bluhm et al., 2009), Alzheimer's disease (Sorg et al., 2007), depression (Liston et al., 2014), attention-deficit/hyperactivity disorder (Norman et al., 2017), insomnia (Yu et al., 2018), multiple sclerosis-related fatigue (Jaeger et al., 2018), and posttraumatic stress disorder (Sripada et al., 2012; Akiki et al., 2018). Chronic low back pain is associated with less connectivity within DMN, mainly in the dorsolateral prefrontal cortex, mPFC, ACC and precuneus (Baliki et al., 2008, 2014; Loggia et al., 2013; Ceko et al., 2015; Jiang et al., 2016; Alshelh et al., 2018). Acupuncture reverses these changes almost to the levels seen in healthy controls, and reductions in clinical pain are correlated with increases in DMN connectivity (Li et al., 2014). Similar results are also reported in chronic sciatica patients (Li et al., 2012). In another study on experimental acute low back pain (Shi et al., 2015), pain state induces higher regional homogeneity values in the limbic system and DMN, and acupuncture yields broad deactivation in DMN, consistent with other research as previously described. Apart from pain, acupuncture has also been evaluated in other disorders. In patients with depression, acupuncture induced wide posterior DMN activation (Quah-Smith et al., 2013) and increased functional connectivity between PCC and bilateral ACC (Deng et al., 2016). In stroke patients, enhanced interregional interaction between ACC and PCC, two key DMN hubs, was observed after acupuncture (Zhang et al., 2014). Finally, acupuncture attenuates impaired DMN connectivity seen in patients with Alzheimer disease (Liang et al., 2014).

If DMN is generally affected by acupuncture, we might observe both common and specific modulation of DMN by stimulation at different acupuncture points. Liu et al. performed electro-acupuncture stimulation at three acupuncture points (GB37, BL60, and KI8) and observed consistently interrupted correlation between PCC and ACC, two key nodes of the DMN (Liu et al., 2009b). However, stimulating these three points produced different correlation strength between other nodes in DMN. In addition, visual cortical regions and mPFC are specifically responsive to the stimulation of GB37, whereas KI8 is more associated with activity changes in insula and hippocampus (Liu et al., 2009a). This modulatory pattern is consistent with clinical practice that GB37 is one of the important acupuncture points for eye diseases whereas KI8 is related to gynecological disorders such as menstrual pain. Claunch et al. (2012) examined the specificity and commonality of the brain response to manual acupuncture at LI4, ST36, and LV3, and found clusters of deactivation in the mPFC, medial parietal and medial temporal lobes showing significant convergence of two or all three of the acupuncture points. For differences, LI4 predominated in the pregenual cingulate and hippocampal formation, ST36 predominated in the subgenual cingulate, and LV3 predominated in the posterior hippocampus and PCC. Similar commonality and specificity of brain responses to different acupuncture points, with DMN regions as crucial hubs, are also reported by a series of studies on PC6, PC7, and GB37 (Bai et al., 2010; Ren et al., 2010; Feng et al., 2011).

A BACK-TRANSLATIONAL STRATEGY FOR FUTURE RESEARCH

Despite these correlative observations, direct evidence to causally validate DMN as a neural substrate of acupuncture is lacking:

the modulation of DMN by acupuncture could only reflect indirect consequences of other more specific therapeutic effects, or even some insignificant by-products of the stimulation. Additional complexity stems from the fact that DMN changes upon acupuncture could be directly driven by somatosensory afference of acupuncture (i.e., stimulation intensity or de-qi sensation), or indirectly caused by affective or cognitive processes related to the therapeutic effect. Caution should be taken to differentiate between these mechanisms using sham acupuncture methodology. Indeed, it remains a tremendous challenge to causally elucidate brain mechanisms of acupuncture. In the first instance, mechanisms of both physiological and pathological brain networks are still under investigation, before we superimpose acupuncture stimulation above them. For example, the molecular and cellular architecture of DMN is far from clear, despite the discovery of DMN-like networks in laboratory animals (Hayden et al., 2009; Popa et al., 2009; Northoff et al., 2010; Lu et al., 2012; Sforazzini et al., 2014) and some pilot mechanistic findings (Nair et al., 2018; Turchi et al., 2018; Yang et al., 2018). Indeed, mechanisms of acupuncture, pain and other neural processes could not be fully clarified without understanding these network substrates, since the same brain region could participate in distinct processes through different microcircuits (Zheng et al., 2017; Jiang et al., 2018). In addition, acupuncture may exert its effects at multiple levels ranging from local stimulation sites to higher centers in the brain. For example, adenosine locally released in acupuncture sites is sufficient to induce analgesia (Goldman et al., 2010; Takano et al., 2012), in which case brain activity changes may only reflect secondary responses of this peripheral mechanism. However, ACC and other brain regions have a crucial role in at least some forms of acupuncture-induced analgesia (Yi et al., 2011). It is challenging to differentiate between causal brain mechanisms of acupuncture stimulation and secondary responses of peripheral effects.

Despite these challenges, novel techniques, especially those targeting neural circuitries, are becoming available to solve the problem. We propose a back-translational strategy involving several key experimental steps toward scientific verification of brain mechanisms of acupuncture, including the possible role of DMN or other functional networks.

First, the architecture of functional neuronal networks requires elucidation at neuronal and molecular levels. Taking the DMN as an example, the concept of default mode stems from neuroimaging studies primarily based on blood oxygen metabolism, which only indirectly reflects neuronal activities. Recent years have witnessed several intriguing studies linking blood oxygen level-dependent signals with electrophysiological measures of neuronal ensembles, especially high frequency neuronal oscillations in the gamma band (Niessing et al., 2005; Scholvinck et al., 2010). Key brain regions in the DMN revealed from neuroimaging studies in humans could first be confirmed with *in vivo* multi-channel electrophysiological recording in freely behaving animal models, taking advantages of accurate evaluation of cross-regional interactions and their behavioral correlates (Li et al., 2017). Neuronal and molecular substrates of these networks could be further examined with pharmacological and genetic techniques. Special attention may focus on activity- and metabolism-associated molecules such as adenosine triphosphate, adenosine and neurosteroids (Goldman et al., 2010; Zhang et al., 2016, 2017).

With the same techniques, the multi-dimensional brain responses of various acupuncture paradigms could be evaluated at both neuronal network and single cell levels. Such "mapping" studies in animals would complement neuroimaging studies in humans, and form the basis for following causal verification. Computational methods including pattern recognition and machine learning would show their strength in differentiating common and specific brain responses between various stimulating paradigms and to isolate key electrophysiological features.

Finally and most importantly, interventional techniques such as opto- and chemo-genetics are required to causally verify the molecular and neuronal mechanisms of functional networks, the overlying acupuncture effects, and the contribution of different dimensions of brain responses to acupuncture effects. Basal forebrain has been suggested to underlie DMN-like activities in rodents (Nair et al., 2018; Turchi et al., 2018), but causal evidence for this hypothesis is still missing. Similarly, causal contribution of brain activity changes in acupuncture is also lacking. These techniques would finally demonstrate causal contribution of DMN activity changes to acupuncture effects.

With this strategy, one might elucidate brain mechanisms of acupuncture in animal models. This knowledge could then be used to improve future acupuncture studies in humans.

AUTHOR CONTRIBUTIONS

MY, DP, and CW designed the perspective. YZ, HZ, TN, and DP reviewed the relevant literature. YZ, HZ, and MY drafted the manuscript. All authors read and confirmed the manuscript.

FUNDING

This work was supported by the National Natural Science Foundation of China (81603446 and 31872774) and Beijing Natural Science Foundation (7174363 and 5182013).

REFERENCES

Akiki, T. J., Averill, C. L., Wrocklage, K. M., Scott, J. C., Averill, L. A., Schweinsburg, B., et al. (2018). Default mode network abnormalities in posttraumatic stress disorder: a novel network-restricted topology approach. *Neuroimage* 176, 489–498. doi: 10.1016/j.neuroimage.2018.05.005

Alshelh, Z., Marciszewski, K. K., Akhter, R., Di Pietro, F., Mills, E. P., Vickers, E. R., et al. (2018). Disruption of default mode network dynamics in acute and chronic pain states. *Neuroimage Clin.* 17, 222–231. doi: 10.1016/j.nicl.2017.10.019

Bai, L., Qin, W., Tian, J., Dong, M., Pan, X., Chen, P., et al. (2009). Acupuncture modulates spontaneous activities in the anticorrelated resting brain networks. *Brain Res.* 1279, 37–49. doi: 10.1016/j.brainres.2009.04.056

Bai, L., Yan, H., Li, L., Qin, W., Chen, P., Liu, P., et al. (2010). Neural specificity of acupuncture stimulation at pericardium 6: evidence from an FMRI study. *J. Magn. Reson. Imaging* 31, 71–77. doi: 10.1002/jmri.22006

Baliki, M. N., Geha, P. Y., Jabakhanji, R., Harden, N., Schnitzer, T. J., and Apkarian, A. V. (2008). A preliminary fMRI study of analgesic treatment in chronic back pain and knee osteoarthritis. *Mol. Pain* 4:47. doi: 10.1186/1744-8069-4-47

Baliki, M. N., Mansour, A. R., Baria, A. T., and Apkarian, A. V. (2014). Functional reorganization of the default mode network across chronic pain conditions. *PLoS One* 9:e106133. doi: 10.1371/journal.pone.0106133

Bluhm, R. L., Miller, J., Lanius, R. A., Osuch, E. A., Boksman, K., Neufeld, R. W., et al. (2009). Retrosplenial cortex connectivity in schizophrenia. *Psychiatry Res.* 174, 17–23. doi: 10.1016/j.pscychresns.2009.03.010

Buckner, R. L., Andrews-Hanna, J. R., and Schacter, D. L. (2008). The brain's default network: anatomy, function, and relevance to disease. *Ann. N. Y. Acad. Sci.* 1124, 1–38. doi: 10.1196/annals.1440.011

Ceko, M., Shir, Y., Ouellet, J. A., Ware, M. A., Stone, L. S., and Seminowicz, D. A. (2015). Partial recovery of abnormal insula and dorsolateral prefrontal connectivity to cognitive networks in chronic low back pain after treatment. *Hum. Brain Mapp.* 36, 2075–2092. doi: 10.1002/hbm.22757

Chae, Y., Chang, D. S., Lee, S. H., Jung, W. M., Lee, I. S., Jackson, S., et al. (2013). Inserting needles into the body: a meta-analysis of brain activity associated with acupuncture needle stimulation. *J. Pain* 14, 215–222. doi: 10.1016/j.jpain.2012.11.011

Claunch, J. D., Chan, S. T., Nixon, E. E., Qiu, W. Q., Sporko, T., Dunn, J. P., et al. (2012). Commonality and specificity of acupuncture action at three acupoints as evidenced by FMRI. *Am. J. Chin. Med.* 40, 695–712. doi: 10.1142/S0192415X12500528

Deng, D., Liao, H., Duan, G., Liu, Y., He, Q., Liu, H., et al. (2016). Modulation of the default mode network in first-episode, drug-naive major depressive disorder via acupuncture at Baihui (GV20) acupoint. *Front. Hum. Neurosci.* 10:230. doi: 10.3389/fnhum.2016.00230

Dhond, R. P., Yeh, C., Park, K., Kettner, N., and Napadow, V. (2008). Acupuncture modulates resting state connectivity in default and sensorimotor brain networks. *Pain* 136, 407–418. doi: 10.1016/j.pain.2008.01.011

Feng, Y., Bai, L., Zhang, W., Ren, Y., Xue, T., Wang, H., et al. (2011). Investigation of acupoint specificity by whole brain functional connectivity analysis from fMRI data. *Conf. Proc. IEEE Eng. Med. Biol. Soc.* 2011, 2784–2787. doi: 10.1109/IEMBS.2011.6090762

Goldman, N., Chen, M., Fujita, T., Xu, Q., Peng, W., Liu, W., et al. (2010). Adenosine A1 receptors mediate local anti-nociceptive effects of acupuncture. *Nat. Neurosci.* 13, 883–888. doi: 10.1038/nn.2562

Han, J. S. (2003). Acupuncture: neuropeptide release produced by electrical stimulation of different frequencies. *Trends Neurosci.* 26, 17–22. doi: 10.1016/S0166-2236(02)00006-1

Hayden, B. Y., Smith, D. V., and Platt, M. L. (2009). Electrophysiological correlates of default-mode processing in macaque posterior cingulate cortex. *Proc. Natl. Acad. Sci. U.S.A.* 106, 5948–5953. doi: 10.1073/pnas.0812035106

Huang, W., Pach, D., Napadow, V., Park, K., Long, X., Neumann, J., et al. (2012). Characterizing acupuncture stimuli using brain imaging with FMRI–a systematic review and meta-analysis of the literature. *PLoS One* 7:e32960. doi: 10.1371/journal.pone.0032960

Hui, K. K., Marina, O., Liu, J., Rosen, B. R., and Kwong, K. K. (2010). Acupuncture, the limbic system, and the anticorrelated networks of the brain. *Auton. Neurosci.* 157, 81–90. doi: 10.1016/j.autneu.2010.03.022

Jaeger, S., Paul, F., Scheel, M., Brandt, A., Heine, J., Pach, D., et al. (2018). Multiple sclerosis-related fatigue: altered resting-state functional connectivity of the ventral striatum and dorsolateral prefrontal cortex. *Mult. Scler.* doi: 10.1177/1352458518758911 [Epub ahead of print].

Jiang, Y., Oathes, D., Hush, J., Darnall, B., Charvat, M., Mackey, S., et al. (2016). Perturbed connectivity of the amygdala and its subregions with the central executive and default mode networks in chronic pain. *Pain* 157, 1970–1978. doi: 10.1097/j.pain.0000000000000606

Jiang, Y. Y., Shao, S., Zhang, Y., Zheng, J., Chen, X., Cui, S., et al. (2018). Neural pathways in medial septal cholinergic modulation of chronic pain: distinct contribution of the anterior cingulate cortex and ventral hippocampus. *Pain* 159, 1550–1561. doi: 10.1097/j.pain.0000000000001240

Kennedy, D. P., and Courchesne, E. (2008). Functional abnormalities of the default network during self- and other-reflection in autism. *Soc. Cogn. Affect. Neurosci.* 3, 177–190. doi: 10.1093/scan/nsn011

Kucyi, A., Moayedi, M., Weissman-Fogel, I., Goldberg, M. B., Freeman, B. V., Tenenbaum, H. C., et al. (2014). Enhanced medial prefrontal-default mode network functional connectivity in chronic pain and its association with pain rumination. *J. Neurosci.* 34, 3969–3975. doi: 10.1523/JNEUROSCI.5055-13.2014

Li, J., Dong, J. C., and Yue, J. J. (2012). Effects of acupuncture on default mode network images of chronic sciatica patients in the resting network state. *Zhongguo Zhong Xi Yi Jie He Za Zhi* 32, 1624–1627.

Li, J., Zhang, J. H., Yi, T., Tang, W. J., Wang, S. W., and Dong, J. C. (2014). Acupuncture treatment of chronic low back pain reverses an abnormal brain default mode network in correlation with clinical pain relief. *Acupunct. Med.* 32, 102–108. doi: 10.1136/acupmed-2013-010423

Li, X., Zhao, Z., Ma, J., Cui, S., Yi, M., Guo, H., et al. (2017). Extracting neural oscillation signatures of laser-induced nociception in pain-related regions in rats. *Front. Neural Circuits* 11:71. doi: 10.3389/fncir.2017.00071

Liang, P., Wang, Z., Qian, T., and Li, K. (2014). Acupuncture stimulation of Taichong (Liv3) and Hegu (LI4) modulates the default mode network activity in Alzheimer's disease. *Am. J. Alzheimers Dis. Other Demen.* 29, 739–748. doi: 10.1177/1533317514536600

Lin, Y. J., Kung, Y. Y., Kuo, W. J., Niddam, D. M., Chou, C. C., Cheng, C. M., et al. (2016). Effect of acupuncture 'dose' on modulation of the default mode network of the brain. *Acupunct. Med.* 34, 425–432. doi: 10.1136/acupmed-2016-011071

Liston, C., Chen, A. C., Zebley, B. D., Drysdale, A. T., Gordon, R., Leuchter, B., et al. (2014). Default mode network mechanisms of transcranial magnetic stimulation in depression. *Biol. Psychiatry* 76, 517–526. doi: 10.1016/j.biopsych.2014.01.023

Liu, P., Qin, W., Zhang, Y., Tian, J., Bai, L., Zhou, G., et al. (2009a). Combining spatial and temporal information to explore function-guide action of acupuncture using fMRI. *J. Magn. Reson. Imaging* 30, 41–46. doi: 10.1002/jmri.21805

Liu, P., Zhang, Y., Zhou, G., Yuan, K., Qin, W., Zhuo, L., et al. (2009b). Partial correlation investigation on the default mode network involved in acupuncture: an fMRI study. *Neurosci. Lett.* 462, 183–187. doi: 10.1016/j.neulet.2009.07.015

Loggia, M. L., Kim, J., Gollub, R. L., Vangel, M. G., Kirsch, I., Kong, J., et al. (2013). Default mode network connectivity encodes clinical pain: an arterial spin labeling study. *Pain* 154, 24–33. doi: 10.1016/j.pain.2012.07.029

Long, X., Huang, W., Napadow, V., Liang, F., Pleger, B., Villringer, A., et al. (2016). Sustained effects of acupuncture stimulation investigated with centrality mapping analysis. *Front. Hum. Neurosci.* 10:510. doi: 10.3389/fnhum.2016.00510

Lu, H., Zou, Q., Gu, H., Raichle, M. E., Stein, E. A., and Yang, Y. (2012). Rat brains also have a default mode network. *Proc. Natl. Acad. Sci. U.S.A.* 109, 3979–3984. doi: 10.1073/pnas.1200506109

Nair, J., Klaassen, A. L., Arato, J., Vyssotski, A. L., Harvey, M., and Rainer, G. (2018). Basal forebrain contributes to default mode network regulation. *Proc. Natl. Acad. Sci. U.S.A.* 115, 1352–1357. doi: 10.1073/pnas.1712431115

Napadow, V., Dhond, R. P., Kim, J., LaCount, L., Vangel, M., Harris, R. E., et al. (2009). Brain encoding of acupuncture sensation–coupling on-line rating with fMRI. *Neuroimage* 47, 1055–1065. doi: 10.1016/j.neuroimage.2009.05.079

Nierhaus, T., Pach, D., Huang, W., Long, X., Napadow, V., Roll, S., et al. (2015). Differential cerebral response to somatosensory stimulation of an acupuncture point vs. two non-acupuncture points measured with EEG and fMRI. *Front. Hum. Neurosci.* 9:74. doi: 10.3389/fnhum.2015.00074

Niessing, J., Ebisch, B., Schmidt, K. E., Niessing, M., Singer, W., and Galuske, R. A. (2005). Hemodynamic signals correlate tightly with synchronized gamma oscillations. *Science* 309, 948–951. doi: 10.1126/science.1110948

Norman, L. J., Carlisi, C. O., Christakou, A., Cubillo, A., Murphy, C. M., Chantiluke, K., et al. (2017). Shared and disorder-specific task-positive and default mode network dysfunctions during sustained attention in paediatric Attention-Deficit/Hyperactivity Disorder and obsessive/compulsive disorder. *Neuroimage Clin.* 15, 181–193. doi: 10.1016/j.nicl.2017.04.013

Northoff, G., Qin, P., and Nakao, T. (2010). Rest-stimulus interaction in the brain: a review. *Trends Neurosci.* 33, 277–284. doi: 10.1016/j.tins.2010.02.006

Otti, A., and Noll-Hussong, M. (2012). Acupuncture-induced pain relief and the human brain's default mode network – an extended view of central effects of acupuncture analgesia. *Forsch Komplementmed.* 19, 197–201. doi: 10.1159/000341928

Popa, D., Popescu, A. T., and Pare, D. (2009). Contrasting activity profile of two distributed cortical networks as a function of attentional demands. *J. Neurosci.* 29, 1191–1201. doi: 10.1523/JNEUROSCI.4867-08.2009

Quah-Smith, I., Suo, C., Williams, M. A., and Sachdev, P. S. (2013). The antidepressant effect of laser acupuncture: a comparison of the resting brain's default mode network in healthy and depressed subjects during functional magnetic resonance imaging. *Med. Acupunct.* 25, 124–133. doi: 10.1089/acu.2012.0901

Ren, Y., Bai, L., Feng, Y., Tian, J., and Li, K. (2010). Investigation of acupoint specificity by functional connectivity analysis based on graph theory. *Neurosci. Lett.* 482, 95–100. doi: 10.1016/j.neulet.2010.06.091

Scholvinck, M. L., Maier, A., Ye, F. Q., Duyn, J. H., and Leopold, D. A. (2010). Neural basis of global resting-state fMRI activity. *Proc. Natl. Acad. Sci. U.S.A.* 107, 10238–10243. doi: 10.1073/pnas.0913110107

Sforazzini, F., Schwarz, A. J., Galbusera, A., Bifone, A., and Gozzi, A. (2014). Distributed BOLD and CBV-weighted resting-state networks in the mouse brain. *Neuroimage* 87, 403–415. doi: 10.1016/j.neuroimage.2013.09.050

Shi, Y., Liu, Z., Zhang, S., Li, Q., Guo, S., Yang, J., et al. (2015). Brain network response to acupuncture stimuli in experimental acute low back pain: an fMRI study. *Evid. Based Complement. Alternat. Med.* 2015:210120. doi: 10.1155/2015/210120

Shi, Y., Zhang, S., Li, Q., Liu, Z., Guo, S., Yang, J., et al. (2016). A study of the brain functional network of Deqi via acupuncturing stimulation at BL40 by rs-fMRI. *Complement. Ther. Med.* 25, 71–77. doi: 10.1016/j.ctim.2016.01.004

Sorg, C., Riedl, V., Muhlau, M., Calhoun, V. D., Eichele, T., Laer, L., et al. (2007). Selective changes of resting-state networks in individuals at risk for Alzheimer's disease. *Proc. Natl. Acad. Sci. U.S.A.* 104, 18760–18765. doi: 10.1073/pnas.0708803104

Sripada, R. K., King, A. P., Welsh, R. C., Garfinkel, S. N., Wang, X., Sripada, C. S., et al. (2012). Neural dysregulation in posttraumatic stress disorder: evidence for disrupted equilibrium between salience and default mode brain networks. *Psychosom. Med.* 74, 904–911. doi: 10.1097/PSY.0b013e318273bf33

Takano, T., Chen, X., Luo, F., Fujita, T., Ren, Z., Goldman, N., et al. (2012). Traditional acupuncture triggers a local increase in adenosine in human subjects. *J. Pain* 13, 1215–1223. doi: 10.1016/j.jpain.2012.09.012

Turchi, J., Chang, C., Ye, F. Q., Russ, B. E., Yu, D. K., Cortes, C. R., et al. (2018). The basal forebrain regulates global resting-state fMRI fluctuations. *Neuron* 97, 940.e4–952.e4. doi: 10.1016/j.neuron.2018.01.032

Vickers, A. J., Cronin, A. M., Maschino, A. C., Lewith, G., MacPherson, H., Foster, N. E., et al. (2012). Acupuncture for chronic pain: individual patient data meta-analysis. *Arch. Intern. Med.* 172, 1444–1453. doi: 10.1001/archinternmed.2012.3654

Vickers, A. J., Vertosick, E. A., Lewith, G., MacPherson, H., Foster, N. E., Sherman, K. J., et al. (2018). Acupuncture for chronic pain: update of an individual patient data meta-analysis. *J. Pain* 19, 455–474. doi: 10.1016/j.jpain.2017.11.005

Xie, D., Liu, Z., Hou, X., Zhang, B., Xiong, J., Yi, M., et al. (2013). Heat sensitisation in suspended moxibustion: features and clinical relevance. *Acupunct. Med.* 31, 422–424. doi: 10.1136/acupmed-2013-010409

Yang, X., Gong, J., Jin, L., Liu, L., Sun, J., and Qin, W. (2018). Effect of catechol-O-methyltransferase Val158Met polymorphism on resting-state brain default mode network after acupuncture stimulation. *Brain Imaging Behav.* 12, 798–805. doi: 10.1007/s11682-017-9735-6

Yi, M., Zhang, H., Lao, L., Xing, G. G., and Wan, Y. (2011). Anterior cingulate cortex is crucial for contra- but not ipsi-lateral electro-acupuncture in the formalin-induced inflammatory pain model of rats. *Mol. Pain* 7:61. doi: 10.1186/1744-8069-7-61

Yu, S., Guo, B., Shen, Z., Wang, Z., Kui, Y., Hu, Y., et al. (2018). The imbalanced anterior and posterior default mode network in the primary insomnia. *J. Psychiatr. Res.* 103, 97–103. doi: 10.1016/j.jpsychires.2018.05.013

Zhang, M., Liu, J., Zhou, M. M., Wu, H., Hou, Y., Li, Y. F., et al. (2016). Elevated neurosteroids in the lateral thalamus relieve neuropathic pain in rats with spared nerve injury. *Neurosci. Bull.* 32, 311–322. doi: 10.1007/s12264-016-0044-7

Zhang, M., Liu, J., Zhou, M. M., Wu, H., Hou, Y., Li, Y. F., et al. (2017). Anxiolytic effects of hippocampal neurosteroids in normal and neuropathic rats with spared nerve injury. *J. Neurochem.* 141, 137–150. doi: 10.1111/jnc.13965

Zhang, Y., Li, K., Ren, Y., Cui, F., Xie, Z., Shin, J. Y., et al. (2014). Acupuncture modulates the functional connectivity of the default mode network in stroke patients. *Evid. Based Complement. Alternat. Med.* 2014:765413. doi: 10.1155/2014/765413

Zhao, L., Liu, J., Zhang, F., Dong, X., Peng, Y., Qin, W., et al. (2014). Effects of long-term acupuncture treatment on resting-state brain activity in migraine patients: a randomized controlled trial on active acupoints and inactive acupoints. *PLoS One* 9:e99538. doi: 10.1371/journal.pone.0099538

Zheng, J., Jiang, Y. Y., Xu, L. C., Ma, L. Y., Liu, F. Y., Cui, S., et al. (2017). Adult hippocampal neurogenesis along the dorsoventral axis contributes differentially to environmental enrichment combined with voluntary exercise in alleviating chronic inflammatory pain in mice. *J. Neurosci.* 37, 4145–4157. doi: 10.1523/JNEUROSCI.3333-16.2017

Zhuang, Y., Xing, J. J., Li, J., Zeng, B. Y., and Liang, F. R. (2013). History of acupuncture research. *Int. Rev. Neurobiol.* 111, 1–23. doi: 10.1016/B978-0-12-411545-3.00001-8

Zyloney, C. E., Jensen, K., Polich, G., Loiotile, R. E., Cheetham, A., LaViolette, P. S., et al. (2010). Imaging the functional connectivity of the periaqueductal gray during genuine and sham electroacupuncture treatment. *Mol. Pain* 6:80. doi: 10.1186/1744-8069-6-80

Conflict of Interest Statement: The authors declare that the research was conducted in the absence of any commercial or financial relationships that could be construed as a potential conflict of interest.

frontiers in Neuroscience

ORIGINAL RESEARCH
published: 12 February 2019
doi: 10.3389/fnins.2019.00074

Expectations of the Physiological Responses Can Change the Somatosensory Experience for Acupuncture Stimulation

*Hyun-Seo Song[1], Won-Mo Jung[1], Ye-Seul Lee[1,2], Seung-Woo Yoo[1] and Younbyoung Chae[1]**

[1] Acupuncture and Meridian Science Research Center, College of Korean Medicine, Kyung Hee University, Seoul, South Korea, [2] Department of Anatomy and Acupoint, College of Korean Medicine, Gachon University, Seongnam, South Korea

Objective: Humans interpret sensory inputs based on actual stimuli and expectations of the stimuli. We investigated whether manipulating information related to the physiological response could change the somatosensory experience of acupuncture.

Methods: Twenty-four participants received tactile stimulations with a von Frey filament on the left arm. Participants were informed that they would receive acupuncture stimulations at different angles while they were presented with changes in their peripheral blood flow (PBF) measured with Laser Doppler perfusion imaging. However, in reality, they were observing premade pseudo-biosignal images (six sessions: one circular, two rectangular elongated, two diagonally elongated, and one cross-fixation [control] shape). After each session, the participants reported the intensity and location of the *de qi* sensations perceived on their arm using a bodily sensation mapping tool. The spatial patterns of the somatic sensations were visualized using statistical parametric mapping. The F1 score was calculated to measure the similarity between the presented pseudo-biosignals and reported *de qi* response images.

Results: The spatial configurations of the presented pseudo-biosignal images and *de qi* response images were similar. The rectangular elongated pseudo-biosignal shape had a significantly higher F1 score compared to the control. All tactile stimulations produced similar levels of enhanced PBF regardless of the pseudo-biosignal shape.

Conclusion: The spatial configurations of somatic sensations changed according to the presented pseudo-biosignal shape, suggesting that expectations of the physiological response to acupuncture stimulation can influence the perceived somatic sensation.

Keywords: acupuncture, biosignal, *de qi*, expectation, psychophysics

OPEN ACCESS

Edited by:
Vitaly Napadow, Harvard Medical School, United States

Reviewed by:
Meryem A. Yucel, Harvard University, United States
Shellie Ann Boudreau, Aalborg University, Denmark

***Correspondence:**
Younbyoung Chae
ybchae@khu.ac.kr

Specialty section:
This article was submitted to Perception Science, a section of the journal Frontiers in Neuroscience

Received: *16 July 2018*
Accepted: *23 January 2019*
Published: *12 February 2019*

Citation:
Song H-S, Jung W-M, Lee Y-S, Yoo S-W and Chae Y (2019) Expectations of the Physiological Responses Can Change the Somatosensory Experience for Acupuncture Stimulation. Front. Neurosci. 13:74. doi: 10.3389/fnins.2019.00074

INTRODUCTION

A fundamental characteristic of acupuncture treatment is the elicitation of unique somatic sensations around points (i.e., *de qi* sensations) stimulated with the insertion of a needle (Chae et al., 2013; Chae and Olausson, 2017). Achieving an appropriate *de qi* sensation is believed to be a key component of acupuncture treatment (Kong et al., 2005; Mao et al., 2007). In a clinical research

data-mining study, 82.1% of studies supported that *de qi* sensations were closely related to clinical efficacy (Pan et al., 2017). *De qi* sensations include a combination of various sensations, such as heaviness, numbness, soreness, distention, and even a spreading sensation far from the stimulus site (MacPherson and Asghar, 2006). Recently, spatial patterns of acupuncture-induced sensations, including sensations propagated along the acupuncture meridians, have been demonstrated based on a geographic information system using a bodily sensation map (BSM) (Beissner and Marzolff, 2012; Jung et al., 2016). The BSM, one of a digital pen-and-paper platform, is useful to measure location and intensity of the bodily sensation (Jung et al., 2017a,c).

Humans perceive somatic sensations by integrating afferent signals and higher cognitive processes. For example, placebo stimulations have been reported to cause considerable and widespread sensations despite a lack of peripheral stimulus (Beissner et al., 2015). Moreover, in a clinical trial using laser acupuncture, remarkable *de qi* sensations were elicited without any cutaneous sensory input (Salih et al., 2010). Furthermore, brain activation associated with acupuncture stimulation was influenced by enhanced bodily awareness and bodily attention around the acupoint (Chae et al., 2015; Jung et al., 2016). In a recent study, expectations of acupuncture stimulation elicited a distinct somatic sensation experience and activation of the salience network in the brain, even without an afferent somatosensory signal (Jung et al., 2018). Together, these results suggest that experiences and expectations prior to tactile stimulation can influence the perception of somatic sensations.

These properties of somatic sensory experience suggest that *de qi* sensation patterns can be influenced by expectations of psychophysiological responses to acupuncture stimulations. In this study, we hypothesized that biosignal information (i.e., peripheral blood flow change) presented as a psychophysiological response to acupuncture would alter the spatial configurations of somatic sensations in response to tactile stimulations. More specifically, since propagated sensations induced by acupuncture were prominently along perpendicular and horizontal lines on the body, it can be assumed that rectangular elongated pseudo-biosignal of acupuncture can efficiently influence on the perceived somatic sensations. When tactile stimulations were applied to the arm, the perceived sensation showed circular-shaped spatial patterns. Thus, it is assumed that there will be no differences in the spatial patterns of the *de qi* sensations between the circular images session and the control session.

To test this hypothesis, we presented participants with different Laser Doppler perfusion images of pseudo-biosignal shapes mimicking changes in peripheral blood flow (PBF) and compared the spatial configurations of the somatic sensations induced by tactile stimulation.

MATERIALS AND METHODS

Subjects

We recruited 24 healthy volunteers via advertisements targeting students of Kyung Hee University and Korea University. None of the participants of this study had any history of cardiac, neurological, psychiatric, or visual disorders. Participants refrained from drinking alcohol or caffeine or from taking any drugs or medications for 12 h before the experiment. All participants received a detailed explanation of the experiment and provided written informed consent. This experiment was conducted in accordance with the Declaration of Helsinki and approved by the Institutional Review Board of Kyung Hee University. All procedures were conducted in a quiet and temperature-controlled room (24 ± 2°C) throughout the experiment.

Experimental Design and Procedure

Each participant was asked to sit in a comfortable position in front of a computer monitor before the experiment. Participants were informed that they would receive acupuncture stimulation at various angles and that they would be presented with changes in their PBF measured using Laser Doppler perfusion imaging. However, in reality, the participants were presented with premade pseudo-biosignal images (one circular, two rectangular elongated, two diagonally elongated, and one cross-fixation [control] shape). A total of six sessions were conducted and all participants were unaware of the procedures. The pseudo-biosignals and control image were presented in a pseudorandom order. The experiment followed a within-subject crossover design, in which the independent variable was the pseudo-biosignal shape. All participants were unaware of the procedures. The pseudo-biosignals were presented in a pseudorandom order.

Each experimental session lasted for 315 s, during which the participants looked at the cross fixation for the preparation period for 60 s and they received tactile stimulation for 15 s. Right after stimulation, participants were presented with the pseudo-biosignal for 120 s. They were required to fix their gaze on the computer monitor to view the change of the pseudo-biosignal immediately following the tactile stimulation. The actual PBF around the stimulation site was measured before and after stimulation. Finally, participants were asked to mark the areas of induced sensation on a BSM for 120 s. A 2-min break was given between sessions to allow the participants to relax (**Figure 1A**).

Basic demographic data were collected from all participants before commencing the experiments. Participants also evaluated the expectancy and fear of the acupuncture treatment using the Acupuncture Expectancy Scale (AES) and Acupuncture Fear Scale (AFS) (Kim et al., 2013, 2014).

Tactile Stimulation

Each participant received a tactile stimulation at the same site of the left arm (TE5 acupoint: on the posterior aspect of the forearm, at the midpoint of the interosseous space between the radius and ulna, 2 B-cun proximal to the dorsal wrist crease). All tactile stimulations were delivered using a 60-g von Frey filament (North Coast Medical Inc., San Jose, CA, United States). Tactile stimulations designed to mimic acupuncture stimulation were given at a frequency of 1 Hz for 15 s. The stimulated sites on the arm were hidden from the participants' sight to make them believe that they were receiving real acupuncture stimulations. All participants were told that they would receive

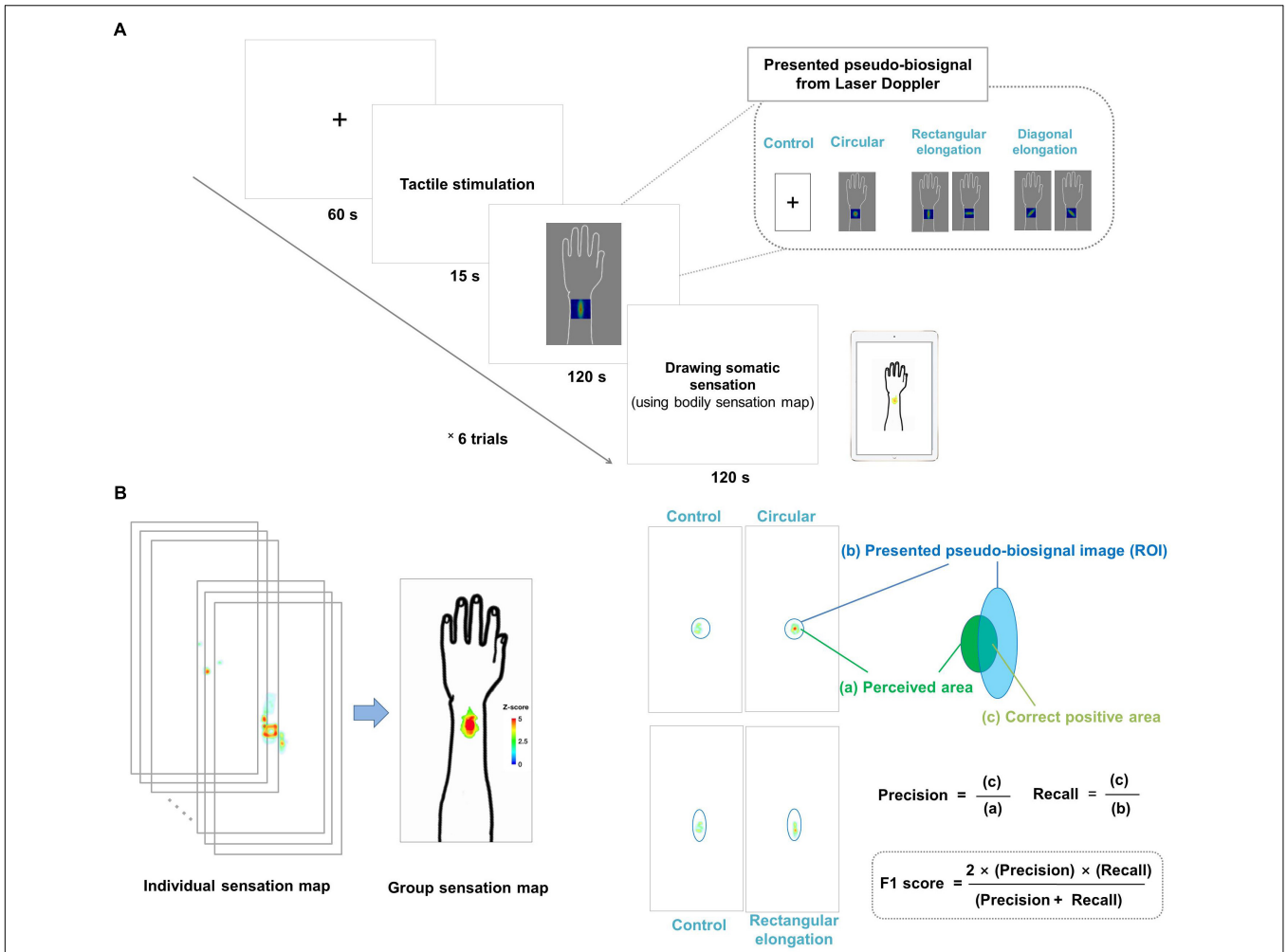

FIGURE 1 | (A) Experimental design. All participants were shown images of four different pseudo-biosignal shapes. Each participant received a tactile stimulation at the same site on the left arm using a von Frey filament. In each session, the participants were asked to report the location and intensity of the resulting sensation on a bodily sensation map tool. **(B)** Data visualization and data analysis. The spatial distributions of the somatic sensations were visualized using the human body template by applying *Z* scores. The F1 score was used to measure the similarity between the presented pseudo-biosignal image and reported somatic sensation area. The F1 score is calculated as (2 × precision × recall)/(precision + recall), where precision is the area of the correct positive results divided by the area of all relevant samples from the perceived *de qi* sensation area (c/a) and recall is the area of correct positive results divided by the area of all positive results from the region of interest of the presented pseudo-biosignal image (c/b).

different acupuncture stimulations at various angles in each session. However, we did not inform the participants which angle of the needle was being inserted. In acupuncture practice, it is common to change the angle of needle insertion according to the site and the disease. Thus, participants might have supposed that various directions of the pseudo-biosignal image are derived from various angle of the needle stimulation.

Measurement of Perceived Tactile Sensations Using the Bodily Sensation Map

Following stimulation, the participants were asked to report the locations and intensity of bodily sensations using the BSM[1]. This tool presents a template of the human body as two-dimensional images, including a lateral view of the left arm. The perceived sensations after each session were recorded in 1,024 × 512 matrices on an iPad (Apple Inc., Cupertino, CA, United States). Participants could express the intensity of the somatic sensation by changing the color of the points on a continuous color map via successive strokes with a touch pen (Adonit Inc., Austin, TX, United States).

Measurement of Peripheral Blood Flow Using Laser Doppler Perfusion Imaging

Measurements of peripheral blood perfusion around the stimulation site were performed using a Laser Doppler perfusion imager (PeriScan PIM 3 System; Perimed AB, Järfälla, Sweden). The left arm of the participants was stabilized with a kapok-filled

[1]http://cmslab.khu.ac.kr/downloads/bsm

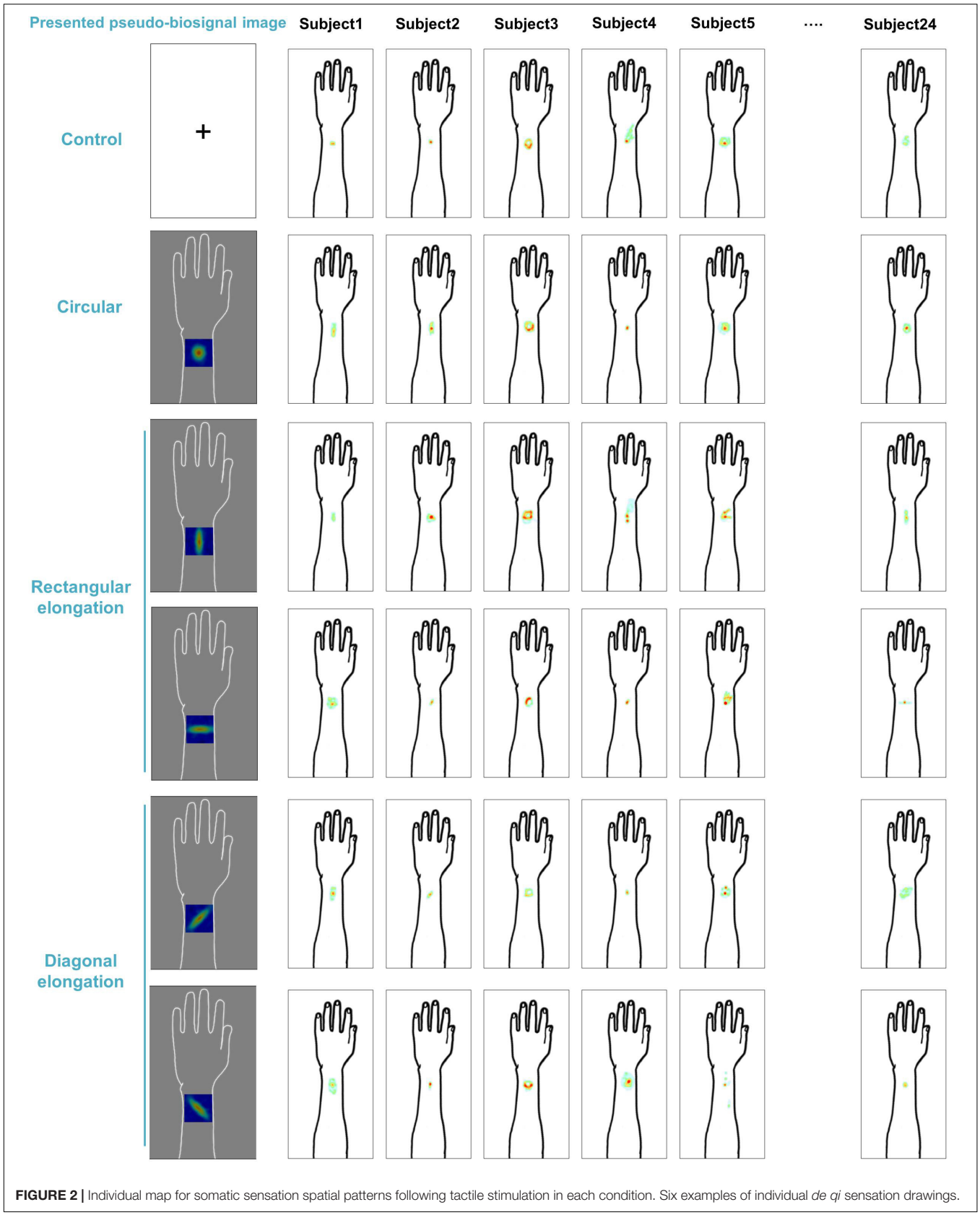

FIGURE 2 | Individual map for somatic sensation spatial patterns following tactile stimulation in each condition. Six examples of individual *de qi* sensation drawings.

vacuum cushion to maintain its position, and measurements were conducted every 10 s for 180 s before and after stimulation. PBF (symbolized as Ri, [i = 1, 2, 3, . . ., 18]) was calculated as the average perfusion value during each 10-s scan in the region of interest (ROI) (a 2 cm × 2 cm square centered on the TE5 acupoint), and the change in PBF was defined as ΔPBF = (Ri − R1)/R1. Each 10 s PBF was subtracted and divided by a baseline (collected over 30 s) in each session, which yielded the change in scores reflecting the increase in PBF from the baseline.

Data Analysis

To determine the spatial patterns of the sensations under each condition, we extracted parametric maps of bodily sensation using the BSM tool. Individual datasets for each subject were normalized within the range of 0–1. The normalized BSMs were subjected to group-level analysis of the statistical parametric maps. The group-level analysis consisted of a random effects analysis using the pixel-wise univariate t-test of individual BSMs for each session (3dttest++, AFNI[2]). False discovery rate (FDR) corrections were carried out to account for false positives due to multiple comparisons (FDR-corrected $p < 0.05$). The resulting t-value maps were transformed into Z scores that reflected significant spatial information of the bodily sensation to tactile stimulation. The information was color-coded based on the Z score.

The regions of color changes for each pseudo-biosignal image were extracted as the ROI of each condition. A larger intersection area and smaller complementary area between the ROI and reported somatic sensation area indicated a greater similarity between them. We used the F1 score to evaluate the similarity between the presented pseudo-biosignal images and reported areas of somatic sensation. The F1 score is generally used as a measure of a test's accuracy in binary classifications (Lipton et al., 2014), and is the harmonic mean of precision and recall, calculated as (2 × precision × recall)/(precision + recall). Here, precision is defined as the area of correct positive results divided by the area of all positive results (from the area of the reported sensation), and recall is the area of correct positive results divided by the area of all relevant samples (from the ROI of the presented pseudo-biosignal image). In this study, precision was the fraction of the intersection area of the reported sensation area and recall was the fraction of the intersection area of the ROI of PBF changes for a given pseudo-biosignal image. The F1 score was calculated for each participant and pseudo-biosignal type (i.e., circular, rectangular elongated, and diagonally elongated shapes) (**Figure 1B**).

[2]http://afni.nimh.nih.gov/afni

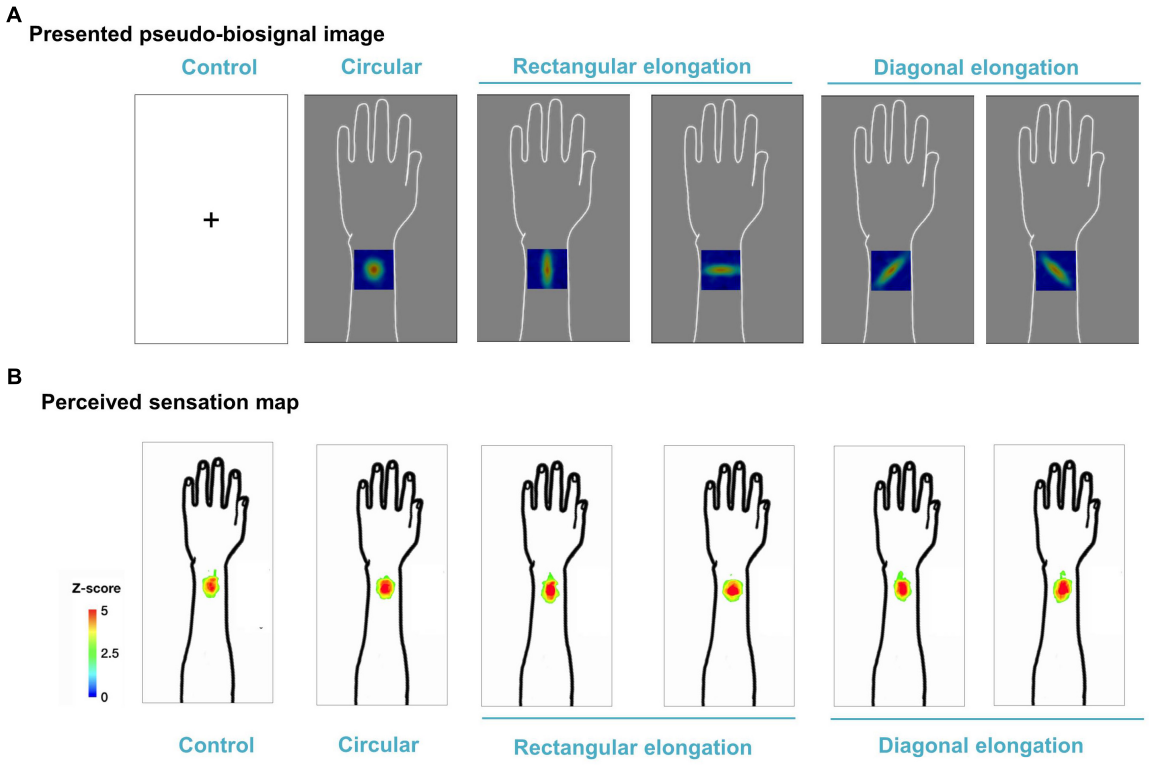

FIGURE 3 | Group map for somatic sensation spatial patterns following tactile stimulation in each condition. **(A)** Presented pseudo-biosignal images (one circular, two rectangular elongated, two diagonally elongated, one cross-fixation [control] shape). **(B)** Group sensation map. The bodily sensation maps were similar to the presented pseudo-biosignal images and *de qi* response images for the rectangular elongated shape. The group-level analysis consisted of a random effects analysis using a pixel-wise univariate t-test of individual sensation maps for each session (FDR-corrected $p < 0.05$). The color coding represents the Z score.

Statistical analyses of the F1 score and PBF data were performed using the R software package[3]. The F1 score for each pseudo-biosignal type was compared to the F1 score extracted from the control session with the same ROI. Paired *t*-test was used to identify significant differences. We conducted repeated measures analysis of variance (ANOVA) to compare the intensities of the change in PBF under each condition over time to determine the effect of time and biosignal type (i.e., the four conditions).

RESULTS

Baseline Characteristics

This study was carried out in 24 right-handed participants (aged 18–37 years; mean = 23.4, standard deviation = 4.0; 13 females). The AES score was 12.6 ± 0.6 and the AFS score was 29.0 ± 2.2.

Effect of Expectation on Tactile Stimulation Sensory Experience

We demonstrated individual spatial patterns of somatic sensation following tactile stimulation in each condition (**Figure 2**). After group level analysis, we found that the spatial configurations of the presented pseudo-biosignal images and the *de qi* response images were similar in the rectangular elongated shape condition, suggesting that presentation with different pseudo-biosignal shapes could influence the spatial configuration of the somatic sensation to the same tactile stimulation (**Figure 3**).

F1 score was used to evaluate the similarity between the presented pseudo-biosignal images and reported areas of somatic sensation. Based on the F1 score, the association between the rectangular elongated pseudo-biosignal image and resulting *de qi* response image exhibited a significant similarity compared to control (0.445 ± 0.039 vs. 0.388 ± 0.043, $t = 2.168$, $p < 0.05$). By contrast, the circular and diagonally elongated pseudo-biosignal images and *de qi* response images did not exhibit any significant similarity (**Figure 4**). These findings suggest that the rectangular elongated pseudo-biosignal image, but not other conditions, can enhance similarity between the pseudo-biosignal images and perceived somatosensation.

Peripheral Blood Flow Response to Tactile Stimulation

All tactile stimulations produced similar levels of enhanced PBF around the acupoint regardless of the pseudo-biosignal shape, and participants exhibited a 40% increase in PBF within 30 s under all conditions (**Figure 5**). Repeated measures ANOVA revealed a significant effect of time [$F_{(3,13)} = 14.877$, $p < 0.001$]; however, the interactive effect of biosignal type × time [$F_{(3,39)} = 0.386$, $p > 1.000$] and biosignal type [$F_{(3,3)} = 0.193$, $p > 0.901$] showed no significant effects.

[3]http://cran.r-project.org

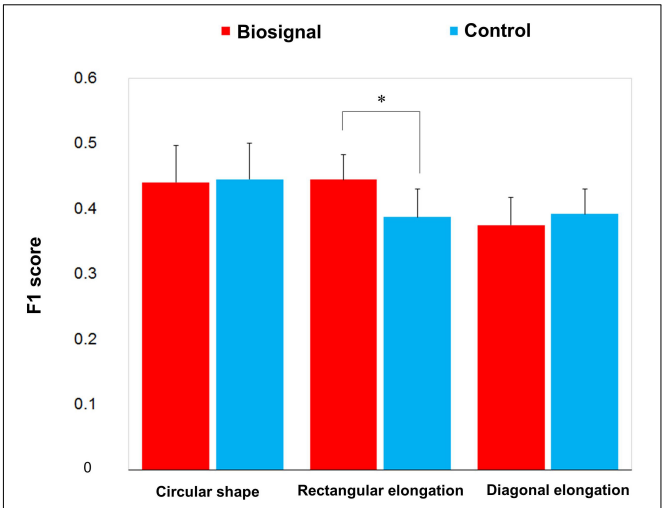

FIGURE 4 | Similarity between the presented biosignal images and *de qi* response images. The F1 score indicates the similarity between the presented pseudo-biosignal image and reported somatic sensation area. Presentation with the rectangular elongated-shaped pseudo-biosignal resulted in a greater similarity between the presented biosignal image and *de qi* response pattern compared to the control. The red bars represent the similarity with the pseudo-biosignal images and the blue bars represent the similarity without presentation of pseudo-biosignal images (control). A paired *t*-test was conducted to identify significant differences between the pseudo-biosignal image and control conditions. *represents $p < 0.05$.

DISCUSSION

The purpose of this study was to determine whether the spatial configurations of *de qi* sensations could be influenced by manipulating the shape of pseudo-biosignal images presented to participants. The results revealed similarities between the spatial configurations of the presented pseudo-biosignal images and somatic sensation response patterns. In particular, presentation with the rectangular elongated pseudo-biosignal resulted in a similar somatic sensation spatial configuration. These findings suggest that biosignal information of psychophysiological responses to acupuncture can change somatic sensation spatial configurations. Overall, this study provides evidence that information from prior experiences and expectations can influence the interpretation of sensory inputs.

Somatic sensations of acupuncture stimulations can be established not only by afferent signals, but also by higher cognitive process, such as expectations. We previously found that expectations of acupuncture stimulations could trigger considerable *de qi* sensations and brain activations in the salience network, even in the absence of actual afferent signals (Jung et al., 2015, 2018). The main finding of the present study is that the spatial configurations of sensory experiences can be altered by biosignal information. To test this, we presented participants with different pseudo-biosignal shapes mimicking Laser Doppler perfusion images to manipulate their expectations of the physiological changes to acupuncture stimulation. Even though we did not explicitly explain the associations between the pseudo-biosignal shapes and *de qi* sensation patterns,

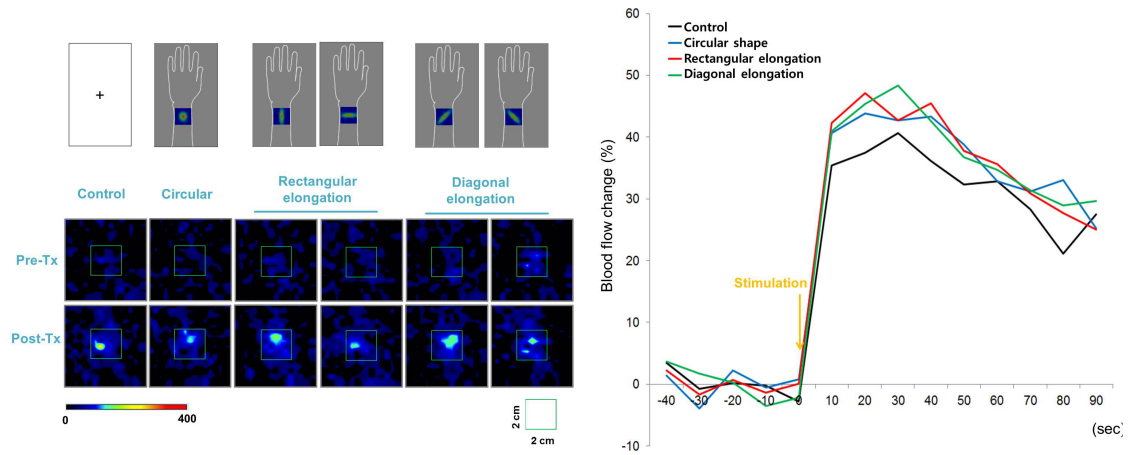

FIGURE 5 | Peripheral blood flow (PBF) response to tactile stimulation. All tactile stimulations produced, similarly, enhanced intensities of PBF around the acupoints across the four pseudo-biosignal shape conditions.

different expectations of physiological changes to acupuncture stimulation successfully induced different somatic sensation spatial configurations. Recent findings in cognitive neuroscience suggest that the brain can actively make inferences based on prior experiences and expectations (Buchel et al., 2014). In other words, information from prior experiences can be used to generate expectations about future perception and interpret sensory inputs (Wiech, 2016). Therefore, we assume that the altered sensory experiences in this experiment might have been derived from the implicit expectation of the association between the physiological response to acupuncture stimulations and the experience of somatic sensations.

When somatic sensations are induced by an acupuncture needle, *de qi* sensations and brain activations to acupuncture stimulation can vary among sessions and participants (Kong et al., 2007; Napadow et al., 2009). Therefore, to control the intensity of the tactile stimulation and induce the same intensity of somatic sensations among tests, we applied a von Frey filament to the TE5 acupoint in the left arm. This method can control for both the tactile stimulation of the cutaneous somatosensory receptor at the acupuncture point and the cognitive processing of participants expecting an acupuncture stimulation (Napadow et al., 2013; Chae et al., 2015). The stimulated sites on the arm were hidden from sight and all participants believed that they received acupuncture stimulations. Moreover, this experiment showed that all tactile stimulations produced, similarly, enhanced PBF around the acupoint regardless of the presented pseudo-biosignal shape, supporting that alterations of spatial patterns to tactile stimulation in rectangular elongated shape condition were not induced by differences in tactile stimulation evoked physiological responses.

The spatial configurations of the presented pseudo-biosignal images and *de qi* response images were similar, especially in the case of the rectangular elongated shape. Meanwhile, the circular pseudo-biosignal shape was created based on preliminary data of the spatial configurations of *de qi* sensations to tactile stimulations. When tactile stimulations were applied to the left arm, the *de qi* sensation elicited circular-shaped spatial configurations around the stimulation site. As expected, there were no differences in the spatial configurations of the *de qi* sensations between the session with the circular pseudo-biosignal image and the control session without pseudo-biosignal images. Meanwhile, the participant somatic sensation pattern responses to tactile stimulation were highly similar to the presented rectangular elongated (but not diagonally elongated) pseudo-biosignal pattern. In this experiment, the participants expected that they would receive acupuncture treatment at various angles. Interestingly, propagated sensations induced by acupuncture have been reported along perpendicular and horizontal lines on the body (Beissner and Marzolff, 2012; Jung et al., 2016). Since diagonal spatial patterns of *de qi* sensations are unusual, the participants may have had weaker expectations of diagonally elongated-shaped response perception patterns.

Perceived sensation to acupuncture stimuli, like other pain perceptions, can be influenced by prior knowledge or expectations (Buchel et al., 2014; Jung et al., 2017b; Ongaro and Kaptchuk, 2019). In this study, we manipulated participants' expectation by using pseudo-biosignal images mimicking the changes in the blood flow during Laser Doppler perfusion imaging. We did not tell them any association between the biosignal from blood flow change and perceive sensations. However, the spatial patterns of *de qi* sensation in response to tactile stimulation were influenced by the information, especially in more plausible response condition. These findings suggest that the implicit expectations from the physiological changes from their own body can have influence on the perception of the tactile stimulation. From this study, the prospective studies include manipulating expectation by alterations of biosignals from the body can be applied to the modulations of other somatosensation areas such as pain control.

In summary, this study reveals that the spatial configurations of *de qi* sensations in response to tactile stimulation can be influenced with visual biosignal information. This suggests that information on physiological responses to acupuncture

stimulations can change participants' expectations of the perception of somatic sensation and interpretation of the stimulations. In future studies, it will be necessary to further clarify the characteristics of the cognitive factors in the perception of acupuncture stimulations.

AUTHOR CONTRIBUTIONS

H-SS, Y-SL, and YC conceived and designed the experiments. H-SS and S-WY performed the trial. H-SS, W-MJ, and YC analyzed the data. H-SS, W-MJ, and YC discussed the data. H-SS and YC wrote the first draft of the paper. H-SS, W-MJ, Y-SL, S-WY, and YC revised the paper and approved the final version.

FUNDING

This research was supported by Basic Science Research Program through the National Research Foundation of Korea (NRF) funded by the Ministry of Science, ICT and Future Planning (No. 2018R1D1A1B07042313).

REFERENCES

Beissner, F., Brunner, F., Fink, M., Meissner, K., Kaptchuk, T. J., and Napadow, V. (2015). Placebo-induced somatic sensations: a multi-modal study of three different placebo interventions. *PLoS One* 10:e0124808. doi: 10.1371/journal.pone.0124808

Beissner, F., and Marzolff, I. (2012). Investigation of acupuncture sensation patterns under sensory deprivation using a geographic information system. *Evid. Based Complement Alternat. Med.* 2012:591304. doi: 10.1155/2012/591304

Buchel, C., Geuter, S., Sprenger, C., and Eippert, F. (2014). Placebo analgesia: a predictive coding perspective. *Neuron* 81, 1223–1239. doi: 10.1016/j.neuron.2014.02.042

Chae, Y., Chang, D. S., Lee, S. H., Jung, W. M., Lee, I. S., Jackson, S., et al. (2013). Inserting needles into the body: a meta-analysis of brain activity associated with acupuncture needle stimulation. *J. Pain* 14, 215–222. doi: 10.1016/j.jpain.2012.11.011

Chae, Y., Lee, I. S., Jung, W. M., Park, K., Park, H. J., and Wallraven, C. (2015). Psychophysical and neurophysiological responses to acupuncture stimulation to incorporated rubber hand. *Neurosci. Lett.* 591, 48–52. doi: 10.1016/j.neulet.2015.02.025

Chae, Y., and Olausson, H. (2017). The role of touch in acupuncture treatment. *Acupunct. Med.* 35, 148–152. doi: 10.1136/acupmed-2016-011178

Jung, W. M., Lee, I. S., Wallraven, C., Ryu, Y. H., Park, H. J., and Chae, Y. (2015). Cortical activation patterns of bodily attention triggered by acupuncture stimulation. *Sci. Rep.* 5:12455. doi: 10.1038/srep12455

Jung, W. M., Lee, S. H., Lee, Y. S., and Chae, Y. (2017a). Exploring spatial patterns of acupoint indications from clinical data: a STROBE-compliant article. *Medicine* 96:e6768. doi: 10.1097/MD.0000000000006768

Jung, W. M., Lee, Y. S., Wallraven, C., and Chae, Y. (2017b). Bayesian prediction of placebo analgesia in an instrumental learning model. *PLoS One* 12:e0172609. doi: 10.1371/journal.pone.0172609

Jung, W. M., Ryu, Y., Lee, Y. S., Wallraven, C., and Chae, Y. (2017c). Role of interoceptive accuracy in topographical changes in emotion-induced bodily sensations. *PLoS One* 12:e0183211. doi: 10.1371/journal.pone.0183211

Jung, W. M., Ryu, Y., Park, H. J., Lee, H., and Chae, Y. (2018). Brain activation during the expectations of sensory experience for cutaneous electrical stimulation. *Neuroimage Clin.* 19, 982–989. doi: 10.1016/j.nicl.2018.06.022

Jung, W. M., Shim, W., Lee, T., Park, H. J., Ryu, Y., Beissner, F., et al. (2016). More than DeQi: spatial patterns of acupuncture-induced bodily sensations. *Front. Neurosci.* 10:462. doi: 10.3389/fnins.2016.00462

Kim, H. S., Kim, Y. J., Lee, H. J., Kim, S. Y., Lee, H., Chang, D. S., et al. (2013). Development and validation of acupuncture fear scale. *Evid. Based Complement Alternat. Med.* 2013:109704. doi: 10.1155/2013/109704

Kim, Y. J., Lee, I. S., Kim, H. S., Lee, H., Park, H. J., Lee, H., et al. (2014). Validation of the korean version of the acupuncture expectancy scale. *Acupunct. Med.* 32, 51–55. doi: 10.1136/acupmed-2013-010412

Kong, J., Fufa, D. T., Gerber, A. J., Rosman, I. S., Vangel, M. G., Gracely, R. H., et al. (2005). Psychophysical outcomes from a randomized pilot study of manual, electro, and sham acupuncture treatment on experimentally induced thermal pain. *J. Pain* 6, 55–64. doi: 10.1016/j.jpain.2004.10.005

Kong, J., Gollub, R. L., Webb, J. M., Kong, J. T., Vangel, M. G., and Kwong, K. (2007). Test-retest study of fMRI signal change evoked by electroacupuncture stimulation. *Neuroimage* 34, 1171–1181. doi: 10.1016/j.neuroimage.2006.10.019

Lipton, Z. C., Elkan, C., and Naryanaswamy, B. (2014). Optimal Thresholding of classifiers to maximize F1 measure. *Mach. Learn. Knowl. Discov. Databases* 8725, 225–239.

MacPherson, H., and Asghar, A. (2006). Acupuncture needle sensations associated with De Qi: a classification based on experts' ratings. *J. Altern. Complement Med.* 12, 633–637. doi: 10.1089/acm.2006.12.633

Mao, J. J., Farrar, J. T., Armstrong, K., Donahue, A., Ngo, J., and Bowman, M. A. (2007). De qi: Chinese acupuncture patients' experiences and beliefs regarding acupuncture needling sensation–an exploratory survey. *Acupunct. Med.* 25, 158–165. doi: 10.1136/aim.25.4.158

Napadow, V., Dhond, R. P., Kim, J., Lacount, L., Vangel, M., Harris, R. E., et al. (2009). Brain encoding of acupuncture sensation–coupling on-line rating with fMRI. *Neuroimage* 47, 1055–1065. doi: 10.1016/j.neuroimage.2009.05.079

Napadow, V., Lee, J., Kim, J., Cina, S., Maeda, Y., Barbieri, R., et al. (2013). Brain correlates of phasic autonomic response to acupuncture stimulation: an event-related fMRI study. *Hum. Brain Mapp.* 34, 2592–2606. doi: 10.1002/hbm.22091

Ongaro, G., and Kaptchuk, T. J. (2019). Symptom perception, placebo effects, and the Bayesian brain. *Pain* 160, 1–4. doi: 10.1097/j.pain.0000000000001367

Pan, Q., Ma, L., Yang, Y., and Zhu, J. (2017). Application of data mining on the relationship between deqi and effect. *Zhongguo Zhen Jiu* 37, 668–672. doi: 10.13703/j.0255-2930.2017.06.026

Salih, N., Baumler, P. I., Simang, M., and Irnich, D. (2010). Deqi sensations without cutaneous sensory input: results of an RCT. *BMC Complement Altern. Med.* 10:81. doi: 10.1186/1472-6882-10-81

Wiech, K. (2016). Deconstructing the sensation of pain: the influence of cognitive processes on pain perception. *Science* 354, 584–587. doi: 10.1126/science.aaf8934

Conflict of Interest Statement: The authors declare that the research was conducted in the absence of any commercial or financial relationships that could be construed as a potential conflict of interest.

The handling Editor is currently editing a Research Topic with one of the authors YC, and confirms the absence of any other collaboration.

frontiers in Human Neuroscience

ORIGINAL RESEARCH
published: 12 February 2019
doi: 10.3389/fnhum.2019.00049

Paired Associative Electroacupuncture and Transcranial Magnetic Stimulation in Humans

*Yi Huang[1], Jui-Cheng Chen[2,3], Chun-Ming Chen[4], Chon-Haw Tsai[2,3] and Ming-Kuei Lu[1,2]**

[1]Graduate Institute of Biomedical Sciences, Medical College, China Medical University, Taichung, Taiwan, [2]Neuroscience Laboratory, Department of Neurology, China Medical University Hospital, Taichung, Taiwan, [3]School of Medicine, Medical College, China Medical University, Taichung, Taiwan, [4]Department of Radiology, China Medical University Hospital, Taichung, Taiwan

Pairing transcutaneous electric nerve stimulation (TENS) and transcranial magnetic stimulation (TMS) with specific stimulus-intervals induces associative motor plasticity at the primary motor cortex (M1). Electroacupuncture (EA) is an established medical technique in the eastern countries. This study investigates whether EA paired with TMS induces distinct M1 motor plasticity. Fifteen healthy, right-handed subjects (aged 23.6 ± 2.0 years, eight women) were studied. Two-hundred and twenty-five pairs of TMS of the left M1 preceded by right EA at acupoint "Neiguan" [Pericardium 6 (PC6), located 2 decimeters proximal from the wrist wrinkle] were respectively applied with the interstimulus interval (ISI) of individual somatosensory evoked potential (SSEP) N20 latency plus 2 ms (N20+2) and minus 5 ms (N20-5) with at least 1-week interval. The paired stimulation was delivered at a rate of 0.25 Hz. Sham TMS with a sham coil was adopted to examine the low-frequency EA influence on M1 in eleven subjects. M1 excitability was assessed by motor-evoked potential (MEP) recruitment curve with five TMS intensity levels, short-interval intracortical inhibition (SICI), intracortical facilitation (ICF) and cerebellar inhibition (CBI) at the abductor pollicis brevis (APB) muscle of the right hand before and after the EA-M1 paired associative stimulation (PAS). In addition, median nerve SSEPs and H-reflex were respectively measured to monitor somatosensory and spinal excitability. The MEP showed significantly facilitated after the sham EA-M1 PAS while tested with 80% of the TMS intensity producing on average 1 mV amplitude (i.e., $MEP_{1\ mV}$) in the resting APB muscle. It was also facilitated while tested with 90% $MEP_{1\ mV}$ irrespective of the stimulation conditions. The SSEP showed a higher amplitude from the real EA-M1 PAS compared to that from the sham EA-M1 PAS. No significant change was found on SICI, ICF, CBI and H-reflex. Findings suggest that repetitive low frequency EA paired with real TMS did not induce spike-timing dependent motor plasticity but EA paired with sham TMS induced specific M1 excitability change. Complex sensory afferents with dispersed time locked to the sensorimotor cortical area could hamper instead of enhancing the induction of the spike-timing dependent plasticity (STDP) in M1.

Keywords: electroacupuncture, motor cortex, motor evoked potential, paired associative stimulation, transcranial magnetic stimulation

OPEN ACCESS

Edited by:
Florian Beissner, Hannover Medical School, Germany

Reviewed by:
Antonio Ivano Triggiani, University of Foggia, Italy
Matt J. N. Brown, California State University, Sacramento, United States

****Correspondence:***
Ming-Kuei Lu
d4297@mail.cmuh.org.tw

Received: *05 November 2018*
Accepted: *29 January 2019*
Published: *12 February 2019*

Citation:
Huang Y, Chen J-C, Chen C-M, Tsai C-H and Lu M-K (2019) Paired Associative Electroacupuncture and Transcranial Magnetic Stimulation in Humans. Front. Hum. Neurosci. 13:49. doi: 10.3389/fnhum.2019.00049

INTRODUCTION

Primary motor cortex (M1) receives multi-direction gated sensory information and executes the final motor command in humans (Cheng et al., 2017; Lei et al., 2018). It plays a key role in motor learning and motor performance. Nowadays there are several non-invasive techniques capable of inducing M1 excitability change, such as fixed-frequency repetitive transcranial magnetic stimulation (rTMS), paired associative stimulation (PAS; Stefan et al., 2000), theta burst stimulation (Huang et al., 2005) and so on (for a review see Quartarone et al., 2006; Huang et al., 2017). The modification of abnormal M1 excitability by these non-invasive brain stimulation techniques has shown possible clinical benefits on neuropathic pain and Parkinson's disease (Lefaucheur et al., 2012; Brys et al., 2016; Goodwill et al., 2017).

PAS is one of the well-known non-invasive brain stimulation techniques with which to investigate Hebbian principles of neural plasticity in humans (Stefan et al., 2000). The most traditional form of PAS consists of repeated pairing of a single electric stimulus at the peripheral median nerve and a TMS pulse on the contralateral M1 with a specific interstimulus interval (ISI) between these two stimuli. It induces aftereffects representing the associative long-term potentiation (LTP)- and depression (LTD)-like phenomenon that bears resemblance to spike-timing dependent plasticity (STDP) as it has been elaborated in animal models (Carson and Kennedy, 2013). An ISI of 25 ms or individual N20 latency plus 2 ms (N20+2) results in arrival of the afferent sensory signal elicited by the peripheral median nerve stimulation before or almost at the same time in M1 when the TMS of the M1 generates actions potentials in excitatory interneurons and corticospinal neurons. The order of the events in M1 is reversed if an ISI of 10 ms or individual N20 latency minus 5 ms (N20-5) is applied (Müller-Dahlhaus et al., 2010). Nevertheless, the PAS effect can be affected by many factors and identifying these factors is a challenge in the current clinical practice (Murase et al., 2015; Huang et al., 2017). Among the factors relevant to the PAS effects, attention and the afferent somatosensory stimulation play an instrumental role in determining the magnitude of the PAS effects (Carson and Kennedy, 2013). In the original PAS protocol, the afferent somatosensory input is mediated through transcutaneous electric nerve stimulation (TENS) at wrist median nerve. The electric stimulation is prone to be adapted for most of the subjects so an additional device for maintaining the subject's attention during the experiment is usually required (Stefan et al., 2004; Lu et al., 2009).

Acupuncture is an ancient medical technique frequently applied for pain control in the eastern countries. Evidences from functional brain imaging have suggested that acupuncture needle stimulation actually modulates specific neural networks in the brain (Hui et al., 2000; Fang et al., 2009), and different acupuncture modalities recruit different brain networks (Jiang et al., 2013). The invention of electric power allows acupuncture delivering a repetitive and constant stimulation at the specific stimulation site which is called "acupoint." Stimulation at different acupoints may have distinct associations with neurocircuits. For example, acupuncture at acupoint "Shenmen; HT7," but not "Neiguan; PC6," improves the ventral tegmental area (VTA)-nucleus accumbens dopaminergic function *via* inhibition of brain-derived neurotrophic factor (BDNF) expression in the VTA (Zhao et al., 2015). Intriguingly, the acupoint "Neiguan; PC6" is approximately located in the same site where median nerve TENS is adopted for PAS. PC6 has been documented with a capacity to change brain activation patterns relevant to attention and improve cognition for stroke patients (Chou et al., 2009; Jung et al., 2015). A study compared the median nerve somatosensory evoked potentials (SSEPs) between TENS, electroacupuncture (EA) and sham stimulation of the specific acupoints (i.e., ST36 and ST37) in the leg (Kang et al., 2015). The results showed that EA, but not TENS nor sham stimulation, alters the mean amplitude of N20 and N30 during and post the stimulation periods (Kang et al., 2015). The findings also suggest a possibility that EA may have different influences on the somatosensory cortex from TENS stimulation. In a recent study, recruitment of additional corticospinal pathway has been achieved by the state-dependent PAS protocol in which sensorimotor event-related desynchronization (ERD) of the β-band was used to trigger peripheral stimulation (Kraus et al., 2018). Gathering evidences raise an issue: whether the peripheral EA stimulation carries a distinct impact on the PAS effect? If the answer is yes, in which level the influence may occur? Since the central mechanism of EA remains not clear, we wondered that EA paired with TMS has a consistent STDP-like effect similar to the traditional PAS. Complex sensory afferents might disrupt instead of enhancing STDP in M1. This study aims to clarify this issue.

MATERIALS AND METHODS

Subjects

In total 15 right-handed (Oldfield, 1971) healthy subjects (23.6 ± 2.0 years, eight women) were recruited in this study. They all received both real and sham stimulation conditions including two different stimulation protocols in each [see "Paired Associative Electroacupuncture and TMS (PAET)" section]. This study was carried out in accordance with the recommendations of the local ethics committee of the China Medical University Hospital with written informed consent from all subjects. All subjects gave written informed consent in accordance with the Declaration of Helsinki. The protocol was approved by the local ethics committee of the China Medical University Hospital (CMUH104-REC2-164). They all received a brain MRI examination to exclude structure lesion.

Procedures

Measurement of Motor Cortical Excitability

TMS was delivered through a focal figure-of-eight stimulating coil (inner diameter of each wing, 70 mm) connected *via* a BiStim module to two Magstim 200 magnetic stimulators (Magstim Co., Carmarthenshire, Wales, UK). The optimal coil position ("hot spot"; $M1_{HAND}$) is determined as the site where TMS at a slightly supra-threshold intensity produced consistently the largest motor-evoked potentials (MEPs) in the right abductor

pollicis brevis (APB). The intensity of TMS adjusted to produce MEPs of on average 1 mV in peak-to-peak amplitude in the resting APB is defined as the $MEP_{1\ mV}$. The individual resting motor threshold (RMT) and active motor threshold (AMT) was determined over the left $M1_{HAND}$. AMT was additionally determined over the inion (inion AMT) prior to the baseline recording. The detailed procedure for determining RMT and AMT has been described elsewhere (Lu et al., 2012).

MEP IO curve is a quantitative measurement for corticospinal excitability. It was measured by stimulation at five intensity levels ranging from two levels below and two levels above $MEP_{1\ mv}$ with a step of 20% $MEP_{1\ mv}$ (i.e., five levels of stimulus intensity). Due to the constraint of the whole experiment time, eight stimuli were recorded at each intensity level. The ISI was determined as 7 s with a 25% variance to limit the anticipation effect.

Short-Interval Intracortical Inhibition (SICI)/Intracortical Facilitation (ICF)

Short-interval intracortical inhibition (SICI) and intracortical facilitation (ICF) were studied using an established paired-pulse TMS protocol (Kujirai et al., 1993; Ziemann et al., 1996). In brief, the two magnetic stimuli were given through the same figure-of-eight stimulating coil over the left $M1_{HAND}$ and the effect of the sub-threshold conditioning stimulus on the test MEP elicited by the subsequent supra-threshold test stimulus (TS) was investigated. SICI was assessed at an ISI of 2.0 ms because at this interval SICI is not contaminated by SICF (Peurala et al., 2008). At the baseline recording, the condition stimulation (CS) intensity was adjusted to produce approximately 50% inhibition in order to provide highest sensitivity for detection of changes in SICI after PAS. The CS intensities usually ranged from 70 to 90% AMT in different individuals (Lu et al., 2012). This CS intensity was kept constant throughout the experiment. ICF was assessed at an ISI of 10 ms (Ziemann et al., 1996). The CS intensities usually ranged from 75 to 95% AMT in different individuals to produce consistent test MEP facilitation (Ziemann et al., 1996; Lu et al., 2012).

Cerebello-Motor Cortical Inhibition (CBI)

Cerebellar inhibition (CBI) was measured with a double-cone coil positioned at the midpoint of the inion and the right incisura mastoidea for CS (Ugawa et al., 1995). 95% AMT_{inion} was adopted for the CS intensity to avoid any corticospinal excitability (Ugawa et al., 1995; Lu et al., 2012). The TS was delivered at left M1 and kept an intensity to elicit an average MEP of ∼0.7 mV while delivered alone. The ISI between CS and TS was 6 ms.

Median Nerve Somatosensory-Evoked Potentials (SSEPs)

The early component of median nerve SSEP (N20-P25) is an index of the somatosensory cortex (S1) excitability. It was recorded while the subjects voluntarily relaxed with eyes closed (Krivanekova et al., 2011). The active electroencephalography electrode was placed at C3', 2 cm posterior to C3 according to the International 10–20 system, corresponding to the putative site of the left S1. The reference electrode was placed on the frontal midline (Fz). The right median nerve was stimulated through a bipolar electrode (cathode proximal) with a constant current square pulse of 0.2 ms duration at rate of 3 Hz (Digitimer DS7A, Digitimer Ltd., UK). Stimulus intensity is adjusted to 110% of twitching threshold in the right thenar muscle. Six-hundred trials were recorded and averaged for offline analysis.

H-Reflex

The H-reflex is an electrical analog of the spinal stretch reflex and an index of spinal excitability. Subjects were positioned in sitting with the elbow at 45° flexion. A stimulus location in the medial bicipital groove was determined where a maximal H-reflex without an M-wave was evoked on the flexor carpi radialis muscle. Stimulation intensity was sequentially increased with a step of 1 mA from a sub-H-reflex threshold intensity to the level when H-reflex amplitude began to decline. The intensity which provokes a maximal H-wave peak-to-peak amplitude (H_{Max}) was determined and used for the following measurement.

Acupuncture

Acupoint "Neiguan" (Pericardium 6; PC6) is located 2 decimeters (i.e., 5.08 cm) proximal from the wrist wrinkle (Chou et al., 2009; **Figure 1**). This location is approximately

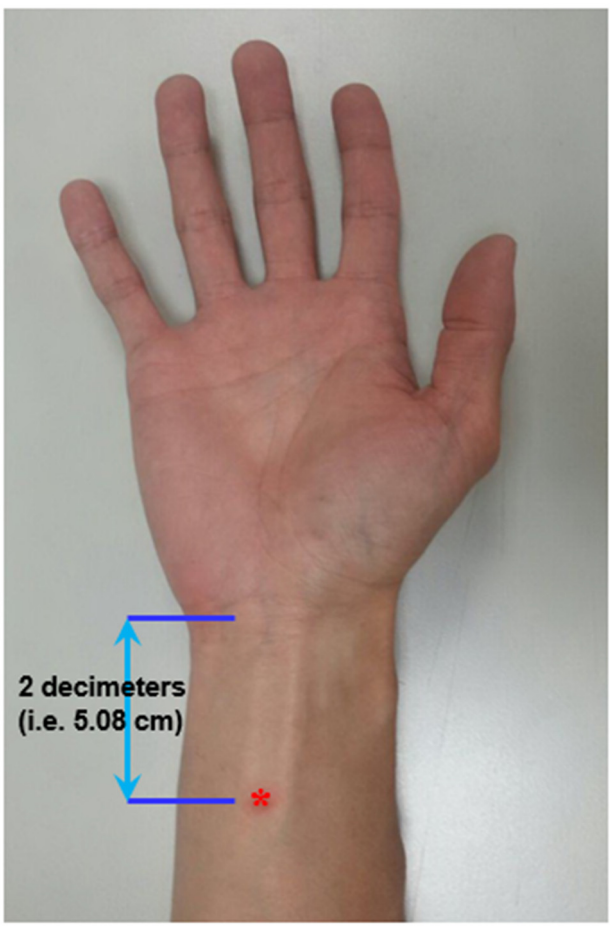

FIGURE 1 | Localization of the acupoint "Neiguan" (Pericardium 6, PC6; *).

the same site where median nerve SSEP is stimulated. Prior to the EA, an acupuncture needle (sterile stainless needle, 0.3 mm diameter, 50 mm length, Yuguang Corporation, Taiwan) was inserted into the right PC6 with a depth of 10 mm. The *de-chi* sensation of the acupuncture is somewhat subjective and difficult to be quantitatively defined. Therefore, it was not essential for subjects to report *de-chi* sensation in this study.

Paired Associative Electroacupuncture and TMS (PAET)

The conventional PAS protocol consists of 225 pairs of a cutaneous electric stimulation of the median nerve at the wrist followed by a single TMS at the contralateral $M1_{HAND}$ (Stefan et al., 2000). The cutaneous nerve stimulation was replaced by the EA at PC6 in the current PAET paradigm. The needle for EA was connected to the stimulator (Digitimer DS7A, Digitimer Ltd., UK) which was triggered by a computer-based interface (Spike2 for Windows, Version 3.05, CED, UK). The stimulus intensity was adjusted to evoke a same level of the right-hand muscle twitching observed during the SSEP recording. There were two intervals between the EA and the TMS, individual N20 latency plus 2 ms (N_{20+2}) and minus 5 ms (N_{20-5}). Based on the STDP principle and the previous evidences, the N_{20+2} interval produces LTP-like and the N_{20-5} interval produces LTD-like plasticity (Ziemann et al., 2004; Müller-Dahlhaus et al., 2010; Lu et al., 2016). The intensity of TMS was adjusted to produce MEPs of on average 1 mV in peak-to-peak amplitude in the resting APB. To carefully examine the effect of the repetitive low-frequency EA stimulation, we designed sham TMS by using a sham TMS coil (Magstim Co., Carmarthenshire, Wales, UK). In total 225 pairs were delivered at a rate of 0.25 Hz (i.e., duration of PAET, 15 min; **Figure 2**).

Statistical Analysis

Repeated measures analyses of variance (rmANOVA) was applied to test the effects of PAET on the five intensity steps of the MEP, SICI, ICF, CBI, SSEP and H-reflex. The within-subject effects were TIME (Pre-PAET vs. Post-PAET), PROTOCOL ($PAET_{N20+2}$ vs. $PAET_{N20-5}$) and CONDITION (Real vs. Sham). Conditional on a significant F value, *post hoc* comparisons were performed using paired-sample t-tests with Bonferroni's correction. Violation of sphericity was checked with Mauchly's test and degrees of freedom were adjusted whenever Mauchly's $W < 0.05$ using the Greenhouse-Geisser correction (SPSS 22.0). Data are reported as means ± SD if not stated otherwise.

RESULTS

All of the subjects were cooperative throughout the experimental procedures. None of them reported any noticeable adverse effects during or after the study.

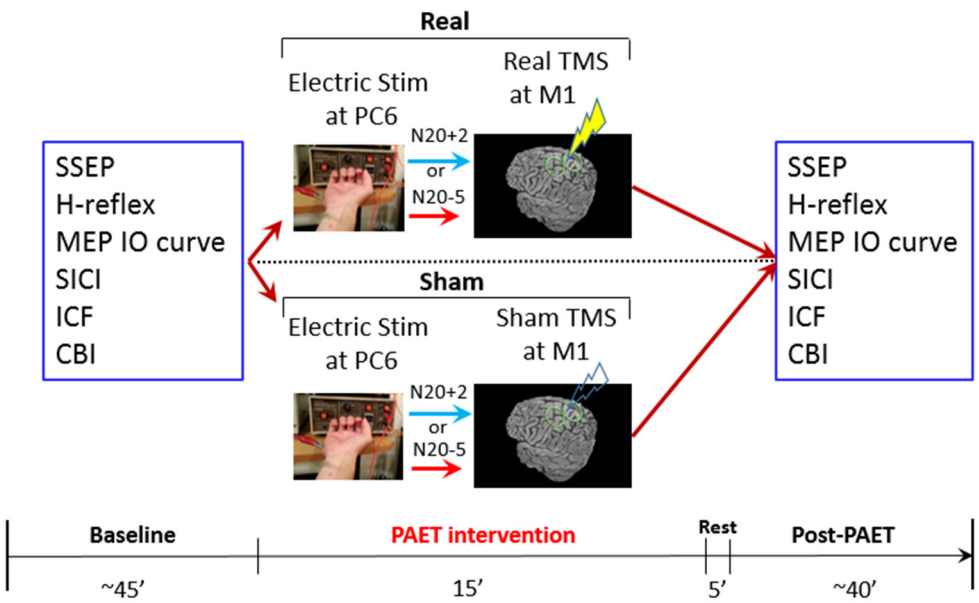

Abbreviations: CBI, cerebellar-motor cortex inhibition; ICF, intracortical facilitation; IO curve, input-output excitability curve; M1, primary motor cortex; MEP, motor-evoked potential; PAET, paired associative electroacupuncture and TMS; PC6, acupoint "Nei-Guan" (Pericardium 6); SICI, short-interval intracortical inhibition; SSEP, somatosensory-evoked potential; TMS, transcranial magnetic stimulation

FIGURE 2 | Experimental design and the time line of the paired associative electroacupuncture and transcranial magnetic stimulation (TMS; PAET) study.

The mean RMT, AMT and inion AMT of the 15 participants were 54 ± 7.9%, 45 ± 7.0% and 39 ± 4.8%, respectively. The mean $MEP_{1\ mv}$ was 65 ± 12.0%. The intensities applied for measuring SICI, ICF and CBI were listed in **Table 1**. We analyzed the data of the 15 subjects for three main effects (i.e., CONDITION, PROTOCOL and TIME). RmANOVA of the MEP amplitude revealed a significant effect of TIME ($F_{(1,14)}$ = 8.8, P = 0.01) and a significant CONDITION × TIME interaction at TMS intensity of 80% $MEP_{1\ mV}$ ($F_{(1,14)}$ = 5.63, P = 0.03), and a significant effect of TIME at TMS intensity of 90% $MEP_{1\ mV}$ ($F_{(1,14)}$ = 12.73, P = 0.003; **Table 2**). RmANOVA of the SICI did not show any significant effect (all $P > 0.08$). A significant PROTOCOL × TIME interaction was found for the analysis of ICF ($F_{(1,14)}$ = 7.46, P = 0.02). A significant main effect of CONDITION was found on SSEP ($F_{(1,14)}$ = 8.97, P = 0.01). RmANOVA of the H_{Max} did not show any significant effect (all $P > 0.3$). The statistical power reaches 0.93 with the effect size of 0.4 for the three-way rmANOVA.

Post hoc comparisons showed a significant MEP amplitude increase after Sham condition at 80% $MEP_{1\ mV}$ (Pre/Post: 0.36 ± 0.16/0.47 ± 0.25 mV, $P < 0.01$ by paired *t*-test; **Figure 3**). At 90% $MEP_{1\ mV}$, the MEP amplitude showed a significant increase after the PAET intervention irrespective of CONDITION and PROTOCOL (Pre/Post: 0.58 ± 0.26/0.77 ± 0.49 mV, $P < 0.01$ by paired *t*-test; **Figure 3**). There was no significant difference from the *post hoc* comparisons on ICF (all $P > 0.05$ by paired *t*-test; **Figure 4**). The *post hoc* comparison of SSEP revealed a significant difference between the real condition and the sham condition (Real/Sham: 1.5 ± 0.8/1.1 ± 0.6 μV, $P < 0.01$ by paired *t*-test; **Figure 4**).

DISCUSSION

PAET Effect on M1 Excitability

The current data support the notion that the PAET intervention may have complex influences on the M1 excitability. While M1 excitability was investigated with a relatively low TMS intensity such as 80% or 90% $MEP_{1\ mV}$, the PAET, particularly the sham PAET, significantly facilitated the MEP amplitude. Following the increase of the TMS test intensity, the aftereffect of PAET was not detectable with the MEP recording.

It has been known that acupuncture has clinical effects on analgesia (Xiang et al., 2017; Pang et al., 2018). The rTMS protocols which facilitate M1 excitability also revealed a benefit response on neuropathic pain (Hosomi et al., 2013; Boyer et al., 2014). Whether the analgesic effect of acupuncture is mediated through a similar mechanism with rTMS remains not clear and

TABLE 1 | The transcranial magnetic stimulation (TMS) intensity* adopted for measuring short-interval intracortical inhibition (SICI), intracortical facilitation (ICF) and cerebello-motor cortical inhibition (CBI).

	SICI	ICF	CBI
Conditioning	43 ± 7	43 ± 7	37 ± 5
Test	68 ± 12	69 ± 12	63 ± 12

**Presented as percentage of maximal stimulator output.*

TABLE 2 | Repeated measures analysis of variance (rmANOVA) of the paired associative electroacupuncture (EA) and TMS (PAET) effect.

		MEP										SICI		ICF		CBI		SSEP		H_{Max}	
		80%		90%		100%		110%		120%											
	d.f.	*F*	*P*	*F*	*P*	*F*	*P*	*F*	*P*	*F*	*P*	*F*	*P*	*F*	*P*	*F*	*P*	*F*	*P*	*F*	*P*
Condition[a]	1, 14	1.96	0.18	1.93	0.19	4.38	0.06	2.15	0.17	1.40	0.26	0.94	0.35	0.04	0.85	2.09	0.17	**8.97**	**0.01***	0.66	0.44
Protocol[b]	1, 14	0.31	0.58	0.82	0.38	0.06	0.81	0.002	0.97	0.99	0.34	0.09	0.77	3.62	0.08	0.96	0.35	0.02	0.88	0.07	0.79
Time[c]	1, 14	**8.80**	**0.01***	**12.73**	**0.003****	0.65	0.44	3.69	0.08	0.59	0.46	3.45	0.09	1.85	0.20	2.61	0.13	2.75	0.12	0.95	0.35
Condition × Protocol	1, 14	0.60	0.45	0.37	0.55	0.14	0.72	0.96	0.34	2.08	0.17	1.33	0.27	0.83	0.38	2.35	0.15	1.92	0.19	0.17	0.69
Condition × Time	1, 14	**5.63**	**0.03***	4.04	0.06	4.09	0.06	2.26	0.16	0.04	0.85	0.007	0.94	0.14	0.72	1.36	0.26	0.01	0.92	0.06	0.81
Protocol × Time	1, 14	0.28	0.61	0.88	0.36	0.46	0.51	0.02	0.90	1.55	0.23	0.29	0.60	**7.46**	**0.02***	0.37	0.55	1.87	0.19	0.30	0.60
Condition × Protocol × Time	1, 14	0.48	0.50	1.47	0.25	0.37	0.55	0.33	0.57	0.25	0.63	1.26	0.28	0.05	0.83	2.43	0.14	0.47	0.51	0.86	0.38

*$P < 0.05$, **$P < 0.01$. [a] 2 levels (Real and Sham). [b] 2 levels (N20+2 and N20-5). [c] 2 levels (pre-PAET and post-PAET). Abbreviations: CBI, cerebellar inhibition; d.f., degrees of freedom; H_{Max}, maximal H-wave peak-to-peak amplitude; ICF, intracortical facilitation; MEP, motor evoked potential; SICI, short-interval intracortical inhibition; SSEP, somatosensory evoked potential.*

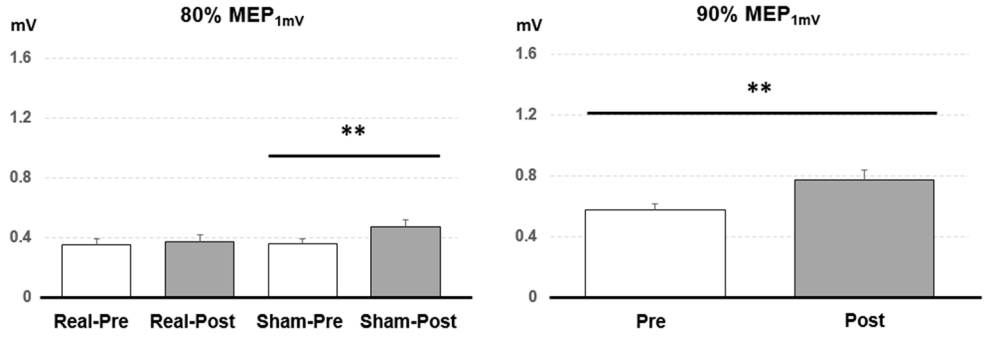

FIGURE 3 | *Post hoc* comparisons of the motor evoked potential (MEP) evoked with different TMS intensities for the 15 subjects. $MEP_{1\ mV}$ means the TMS intensity inducing on average 1 mV MEP amplitude in the resting abductor pollicis brevis (APB) muscle. The MEP amplitude showed a significant facilitation after the sham PAET intervention with 80% $MEP_{1\ mV}$ and the PAET intervention with 90% $MEP_{1\ mV}$. Data are shown by means ± standard errors. $^{**}P < 0.01$ by paired *t*-test with Bonferroni's correction.

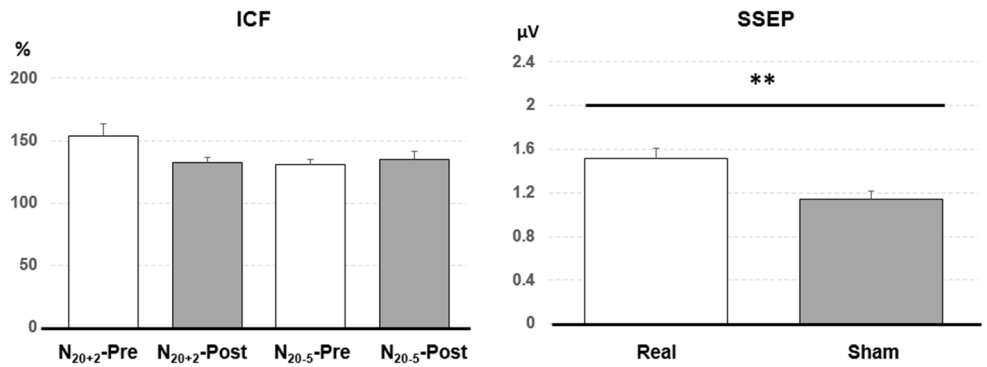

FIGURE 4 | *Post hoc* comparisons of the intracortical facilitation (ICF) and somatosensory evoked potential (SSEP). The ICF comparisons did not show any significant difference. The SSEP amplitude of the real condition was significantly higher than that of the sham condition. Data are shown by means ± standard errors. $^{**}P < 0.01$ by paired *t*-test with Bonferroni's correction.

needs further investigation. Our findings on the sham PAET provided evidence showing that EA may facilitate M1 excitability and the change of the M1 excitability is only detectable with a low to moderate TMS intensity. In addition to EA, the trains of 1 Hz electrical stimulation and 25 Hz repetitive magnetic stimulation on the peripheral nerve also have shown ability to modulate sensorimotor excitability (Kaelin-Lang et al., 2002; Gallasch et al., 2015). Since the low intensity TMS activates interneurons instead of corticospinal neurons (Di Lazzaro and Rothwell, 2014), it is likely that the PAET-induced M1 plasticity is mediated through the interneurons. SICI and ICF are two common parameters representing the function of the interneurons (Chen et al., 1998).

The reason why the sham PAET induced a higher MEP amplitude compared to the real PAET can be explained by the frequency of the repetitive TMS. In this study the real PAET consists of 225 TMS pulses with 0.25 Hz. It has been known that the supra-threshold rTMS of low frequency (i.e., 1 Hz or less) at M1 suppresses corticospinal excitability and reduced MEPs (Chen et al., 1997). It might be achieved by suppressing the amplitude of later I-waves, which have been proposed based on the epidural observation (Di Lazzaro et al., 2008). The reduction of the corticospinal neuronal excitability was supposed to be robust enough to block or erase the EA-induced interneuron plasticity mentioned above.

The current findings suggest that there is no significant role on the protocol difference. That is, we did not find any M1 excitability change following the spike-timing dependent pattern. One of the possible explanations is that EA carries complex sensory modalities including somatosensory, pain and variable attention. These different sensory afferents are actually not homogeneously time-locked to the cortical sensorimotor area. Despite the EA location (i.e., PC6) is very close to that adopted for the traditional PAS, the subtle difference of the location between these two methods could result in different findings. Therefore, it would be difficult to detect typical M1 motor plasticity similar to that induced by the traditional PAS protocols. Another possibility for the absence of a significant spike-timing dependent pattern is probably due to the inter-subjects variability, which has been recognized as a notable issue for the non-invasive brain stimulation protocols including PAS (López-Alonso et al., 2014; Guerra et al., 2017).

SICI/ICF

The current findings on SICI are agree with the previous report which revealed SICI was not consistently affected by the traditional PAS intervention (Russmann et al., 2009). SICI has been found mediated by the $GABA_A$ receptors (Di Lazzaro et al., 2006; Florian et al., 2008). In a recent animal study, EA may increase $GABA_A$ receptors but the influence is only restricted in the spinal cord (Jiang et al., 2018).

The PAS protocol facilitating M1 excitability increases ICF, which suggests that the modification of M1 excitability is contributed from the intracortical excitatory circuits (Pyndt and Ridding, 2004). In the *post hoc* analysis we could not find any significant change following the PAET (**Figure 4**). A further study with more conditioning and test TMS intensities would be helpful to clarify the role of ICF in the M1 excitability change induced by the PAET.

SSEP/H-Reflex

Low frequency (0.05 Hz) EA intervention for 4 months can induce fluctuating cortical plasticity in the somatosensory area, pain-related areas and limbic/paralimbic areas in rats (Wu et al., 2018). In the previous report the amplitude of the median SSEP was found significantly increased by 2 Hz EA at the leg acupoint for 15 min (Kang et al., 2015). However, the SSEP finding in this study did not support the notion that the EA *per se* induce a significant plasticity in the somatosensory area. The main effect of CONDITION instead of TIME from the current rmANOVA analysis suggests that EA paired with real or sham M1 TMS may induce different excitability in the somatosensory area (**Table 2**, **Figure 4**). The finding is consistent with the previous report showing that the traditional PAS consisting of paired median nerve stimulation and TMS at M1 changes SSEP (Murakami et al., 2008). Since the SSEP amplitude may depend on the adopted method (Macerollo et al., 2018), a more sensitive method such as using a non-cephalic reference would be better to measure the excitability change of the somatosensory area in this regard.

H-reflex represents the spinal excitability. Fifty hertz EA can modulate H-reflex response in the experimental rat (Escobar-Corona et al., 2017). The current low frequency (i.e., 0.25 Hz) EA did not significantly alter H-reflex, suggesting that the observed MEP changes are induced in the cortical level, probably the M1 instead of the spinal cord.

There are limitations in this study. As a proof-of-concept study, we merely recruited a limited number of subjects. This inevitably constrained our findings and interpretations. In addition, there was no control condition (e.g., sham or TENS) for the EA stimulation. This also diminishes the significance of the current findings. Nevertheless, the method adopted in this study could shed light on how to combine EA and TMS approaches in the future.

CONCLUSION

Repetitive EA paired with sham TMS at M1 induces specific motor cortical plasticity which could be only detectable with moderate TMS intensities. EA paired with real low-frequency (i.e., 0.25 Hz) rTMS may interrupt instead of enhancing this kind of plasticity. That is, there is no spike-timing dependent character for this plasticity. Complex sensory afferents with dispersed time locked to the sensorimotor cortical area may hamper the induction of the STDP-like plasticity in M1. GABAergic, glutamatergic, cerebellar afferent and spinal excitability respectively examined by SICI, ICF, CBI and H-reflex were not significantly affected.

DATA AVAILABILITY

All datasets generated for this study are included in the manuscript.

AUTHOR CONTRIBUTIONS

YH: subject recruitment, acquisition of data, writing first draft of the manuscript. J-CC: experimental design, critical review of the manuscript, revision of the first draft. C-MC: experimental execution, acquisition of data, review of the manuscript. C-HT: experimental design, critical review of the manuscript, comments on the manuscript. M-KL: study concept and experimental design, data analysis and interpretation, critical revision of the manuscript.

FUNDING

This study is supported in part by grants from the Ministry of Science and Technology (MOST105-2314-B-039-002-MY2 and MOST105-2632-B-039-003) and the Brain Disease Research Center in China Medical University Hospital (DMR-107-190, CRS-106-060), Taichung, Taiwan.

ACKNOWLEDGMENTS

We thank Miss Nai-An Yang for her assistance on data collection.

REFERENCES

Boyer, L., Dousset, A., Roussel, P., Dossetto, N., Cammilleri, S., Piano, V., et al. (2014). rTMS in fibromyalgia: a randomized trial evaluating QoL and its brain metabolic substrate. *Neurology* 82, 1231–1238. doi: 10.1212/WNL.0000000000000280

Brys, M., Fox, M. D., Agarwal, S., Biagioni, M., Dacpano, G., Kumar, P., et al. (2016). Multifocal repetitive TMS for motor and mood symptoms of Parkinson disease: a randomized trial. *Neurology* 87, 1907–1915. doi: 10.1212/wnl.0000000000003279

Carson, R. G., and Kennedy, N. C. (2013). Modulation of human corticospinal excitability by paired associative stimulation. *Front. Hum. Neurosci.* 7:823. doi: 10.3389/fnhum.2013.00823

Chen, R., Classen, J., Gerloff, C., Celnik, P., Wassermann, E. M., Hallett, M., et al. (1997). Depression of motor cortex excitability by low-frequency transcranial magnetic stimulation. *Neurology* 48, 1398–1403. doi: 10.1212/wnl.48.5.1398

Chen, R., Tam, A., Butefisch, C., Corwell, B., Ziemann, U., Rothwell, J. C., et al. (1998). Intracortical inhibition and facilitation in different representations of the human motor cortex. *J. Neurophysiol.* 80, 2870–2881. doi: 10.1152/jn.1998.80.6.2870

Cheng, C. H., Tsai, S. Y., Liu, C. Y., and Niddam, D. M. (2017). Automatic inhibitory function in the human somatosensory and motor cortices: an MEG-MRS study. *Sci. Rep.* 7:4234. doi: 10.1038/s41598-017-04564-1

Chou, P., Chu, H., and Lin, J. G. (2009). Effects of electroacupuncture treatment on impaired cognition and quality of life in Taiwanese stroke patients. *J. Altern. Complement. Med.* 15, 1067–1073.

Di Lazzaro, V., Pilato, F., Dileone, M., Profice, P., Oliviero, A., Mazzone, P., et al. (2008). Low-frequency repetitive transcranial magnetic stimulation suppresses specific excitatory circuits in the human motor cortex. *J. Physiol.* 586, 4481–4487. doi: 10.1113/jphysiol.2008.159558

Di Lazzaro, V., Pilato, F., Dileone, M., Ranieri, F., Ricci, V., Profice, P., et al. (2006). $GABA_A$ receptor subtype specific enhancement of inhibition in human motor cortex. *J. Physiol.* 575, 721–726. doi: 10.1113/jphysiol.2006.114694

Di Lazzaro, V., and Rothwell, J. C. (2014). Corticospinal activity evoked and modulated by non-invasive stimulation of the intact human motor cortex. *J. Physiol.* 592, 4115–4128. doi: 10.1113/jphysiol.2014.274316

Escobar-Corona, C., Torres-Castillo, S., Rodríguez-Torres, E. E., Segura-Alegría, B., Jiménez-Estrada, I., and Quiroz-González, S. (2017). Electroacupuncture improves gait locomotion, H-reflex and ventral root potentials of spinal compression injured rats. *Brain Res. Bull.* 131, 7–17. doi: 10.1016/j.brainresbull.2017.02.008

Fang, J., Jin, Z., Wang, Y., Li, K., Kong, J., Nixon, E. E., et al. (2009). The salient characteristics of the central effects of acupuncture needling: limbic-paralimbic-neocortical network modulation. *Hum. Brain Mapp.* 30, 1196–1206. doi: 10.1002/hbm.20583

Florian, J., Müller-Dahlhaus, M., Liu, Y., and Ziemann, U. (2008). Inhibitory circuits and the nature of their interactions in the human motor cortex a pharmacological TMS study. *J. Physiol.* 586, 495–514. doi: 10.1113/jphysiol.2007.142059

Gallasch, E., Christova, M., Kunz, A., Rafolt, D., and Golaszewski, S. (2015). Modulation of sensorimotor cortex by repetitive peripheral magnetic stimulation. *Front. Hum. Neurosci.* 9:407. doi: 10.3389/fnhum.2015.00407

Goodwill, A. M., Lum, J. A. G., Hendy, A. M., Muthalib, M., Johnson, L., Albein-Urios, N., et al. (2017). Using non-invasive transcranial stimulation to improve motor and cognitive function in Parkinson's disease: a systematic review and meta-analysis. *Sci. Rep.* 7:14840. doi: 10.1038/s41598-017-13260-z

Guerra, A., López-Alonso, V., Cheeran, B., and Suppa, A. (2017). Variability in non-invasive brain stimulation studies: reasons and results. *Neurosci. Lett.* doi: 10.1016/j.neulet.2017.12.058 [Epub ahead of print].

Hosomi, K., Shimokawa, T., Ikoma, K., Nakamura, Y., Sugiyama, K., Ugawa, Y., et al. (2013). Daily repetitive transcranial magnetic stimulation of primary motor cortex for neuropathic pain: a randomized, multicenter, double-blind, crossover, sham-controlled trial. *Pain* 154, 1065–1072. doi: 10.1016/j.pain.2013.03.016

Huang, Y. Z., Edwards, M. J., Rounis, E., Bhatia, K. P., and Rothwell, J. C. (2005). Theta burst stimulation of the human motor cortex. *Neuron* 45, 201–206. doi: 10.1016/j.neuron.2004.12.033

Huang, Y. Z., Lu, M. K., Antal, A., Classen, J., Nitsche, M., Ziemann, U., et al. (2017). Plasticity induced by non-invasive transcranial brain stimulation: a position paper. *Clin. Neurophysiol.* 128, 2318–2329. doi: 10.1016/j.clinph.2017.09.007

Hui, K. K., Liu, J., Makris, N., Gollub, R. L., Chen, A. J., Moore, C. I., et al. (2000). Acupuncture modulates the limbic system and subcortical gray structures of the human brain: evidence from fMRI studies in normal subjects. *Hum. Brain Mapp.* 9, 13–25. doi: 10.1002/(sici)1097-0193(2000)9:1<13::aid-hbm2>3.0.co;2-f

Jiang, S. W., Lin, Y. W., and Hsieh, C. L. (2018). Electroacupuncture at hua tuo jia ji acupoints reduced neuropathic pain and increased $GABA_A$ receptors in rat spinal cord. *Evid. Based Complement. Alternat. Med.* 2018:8041820. doi: 10.1155/2018/8041820

Jiang, Y., Wang, H., Liu, Z., Dong, Y., Dong, Y., Xiang, X., et al. (2013). Manipulation of and sustained effects on the human brain induced by different modalities of acupuncture: an fMRI study. *PLoS One* 8:e66815. doi: 10.1371/journal.pone.0066815

Jung, W. M., Lee, I. S., Wallraven, C., Ryu, Y. H., Park, H. J., and Chae, Y. (2015). Cortical activation patterns of bodily attention triggered by acupuncture stimulation. *Sci. Rep.* 5:12455. doi: 10.1038/srep12455

Kaelin-Lang, A., Luft, A. R., Sawaki, L., Burstein, A. H., Sohn, Y. H., and Cohen, L. G. (2002). Modulation of human corticomotor excitability by somatosensory input. *J. Physiol.* 540, 623–633. doi: 10.1113/jphysiol.2001.012801

Kang, Y. T., Liao, Y. S., and Hsieh, C. L. (2015). Different effects of transcutaneous electric nerve stimulation and electroacupuncture at ST36-ST37 on the cerebral cortex. *Acupunct. Med.* 33, 36–41. doi: 10.1136/acupmed-2014-010650

Kraus, D., Naros, G., Guggenberger, R., Leão, M. T., Ziemann, U., and Gharabaghi, A. (2018). Recruitment of additional corticospinal pathways in the human brain with state-dependent paired associative stimulation. *J. Neurosci.* 38, 1396–1407. doi: 10.1523/JNEUROSCI.2893-17.2017

Krivanekova, L., Lu, M. K., Bliem, B., and Ziemann, U. (2011). Modulation of excitability in human primary somatosensory and motor cortex by paired associative stimulation targeting the primary somatosensory cortex. *Eur. J. Neurosci.* 34, 1292–1300. doi: 10.1111/j.1460-9568.2011.07849.x

Kujirai, T., Caramia, M. D., Rothwell, J. C., Day, B. L., Thompson, P. D., Ferbert, A., et al. (1993). Corticocortical inhibition in human motor cortex. *J. Physiol.* 471, 501–519. doi: 10.1113/jphysiol.1993.sp019912

Lefaucheur, J. P., Ayache, S. S., Sorel, M., Farhat, W. H., Zouari, H. G., Ciampi De Andrade, D., et al. (2012). Analgesic effects of repetitive transcranial magnetic stimulation of the motor cortex in neuropathic pain: influence of theta burst stimulation priming. *Eur. J. Pain* 16, 1403–1413. doi: 10.1002/j.1532-2149.2012.00150.x

Lei, Y., Ozdemir, R. A., and Perez, M. A. (2018). Gating of sensory input at subcortical and cortical levels during grasping in humans. *J. Neurosci.* 38, 7237–7247. doi: 10.1523/JNEUROSCI.0545-18.2018

López-Alonso, V., Cheeran, B., Río-Rodríguez, D., and Fernández-Del-Olmo, M. (2014). Inter-individual variability in response to non-invasive brain stimulation paradigms. *Brain Stimul.* 7, 372–380. doi: 10.1016/j.brs.2014.02.004

Lu, M. K., Bliem, B., Jung, P., Arai, N., Tsai, C. H., and Ziemann, U. (2009). Modulation of preparatory volitional motor cortical activity by paired associative transcranial magnetic stimulation. *Hum. Brain Mapp.* 30, 3645–3656. doi: 10.1002/hbm.20793

Lu, M. K., Chen, C. M., Duann, J. R., Ziemann, U., Chen, J. C., Chiou, S. M., et al. (2016). Investigation of motor cortical plasticity and corticospinal tract diffusion tensor imaging in patients with parkinsons disease and essential tremor. *PLoS One* 11:e0162265. doi: 10.1371/journal.pone.0162265

Lu, M. K., Tsai, C. H., and Ziemann, U. (2012). Cerebellum to motor cortex paired associative stimulation induces bidirectional STDP-like plasticity in human motor cortex. *Front. Hum. Neurosci.* 6:260. doi: 10.3389/fnhum.2012.00260

Macerollo, A., Brown, M. J. N., Kilner, J. M., and Chen, R. (2018). Neurophysiological changes measured using somatosensory evoked potentials. *Trends Neurosci.* 41, 294–310. doi: 10.1016/j.tins.2018.02.007

Müller-Dahlhaus, F., Ziemann, U., and Classen, J. (2010). Plasticity resembling spike-timing dependent synaptic plasticity: the evidence in human cortex. *Front. Synaptic Neurosci.* 2:34. doi: 10.3389/fnsyn.2010.00034

Murakami, T., Sakuma, K., Nomura, T., Uemura, Y., Hashimoto, I., and Nakashima, K. (2008). Changes in somatosensory-evoked potentials and high-frequency oscillations after paired-associative stimulation. *Exp. Brain Res.* 184, 339–347. doi: 10.1007/s00221-007-1103-0

Murase, N., Cengiz, B., and Rothwell, J. C. (2015). Inter-individual variation in the after-effect of paired associative stimulation can be predicted from short-interval intracortical inhibition with the threshold tracking method. *Brain Stimul.* 8, 105–113. doi: 10.1016/j.brs.2014.09.010

Oldfield, R. C. (1971). The assessment and analysis of handedness: the Edinburgh inventory. *Neuropsychologia* 9, 97–113. doi: 10.1016/0028-3932(71)90067-4

Pang, Y., Liu, H., Duan, G., Liao, H., Liu, Y., Feng, Z., et al. (2018). Altered brain regional homogeneity following electro-acupuncture stimulation at sanyinjiao (SP6) in women with premenstrual syndrome. *Front. Hum. Neurosci.* 12:104. doi: 10.3389/fnhum.2018.00104

Peurala, S. H., Müller-Dahlhaus, J. F., Arai, N., and Ziemann, U. (2008). Interference of short-interval intracortical inhibition (SICI) and short-interval intracortical facilitation (SICF). *Clin. Neurophysiol.* 119, 2291–2297. doi: 10.1016/j.clinph.2008.05.031

Pyndt, H. S., and Ridding, M. C. (2004). Modification of the human motor cortex by associative stimulation. *Exp. Brain Res.* 159, 123–128. doi: 10.1007/s00221-004-1943-9

Quartarone, A., Siebner, H. R., and Rothwell, J. C. (2006). Task-specific hand dystonia: can too much plasticity be bad for you? *Trends Neurosci.* 29, 192–199. doi: 10.1016/j.tins.2006.02.007

Russmann, H., Lamy, J. C., Shamim, E. A., Meunier, S., and Hallett, M. (2009). Associative plasticity in intracortical inhibitory circuits in human motor cortex. *Clin. Neurophysiol.* 120, 1204–1212. doi: 10.1016/j.clinph.2009.04.005

Stefan, K., Kunesch, E., Cohen, L. G., Benecke, R., and Classen, J. (2000). Induction of plasticity in the human motor cortex by paired associative stimulation. *Brain* 123, 572–584. doi: 10.1093/brain/123.3.572

Stefan, K., Wycislo, M., and Classen, J. (2004). Modulation of associative human motor cortical plasticity by attention. *J. Neurophysiol.* 92, 66–72. doi: 10.1152/jn.00383.2003

Ugawa, Y., Uesaka, Y., Terao, Y., Hanajima, R., and Kanazawa, I. (1995). Magnetic stimulation over the cerebellum in humans. *Ann. Neurol.* 37, 703–713. doi: 10.1002/ana.410370603

Wu, J. J., Lu, Y. C., Hua, X. Y., Ma, S. J., and Xu, J. G. (2018). A longitudinal mapping study on cortical plasticity of peripheral nerve injury treated by direct anastomosis and electroacupuncture in rats. *World Neurosurg.* 114, e267–e282. doi: 10.1016/j.wneu.2018.02.173

Xiang, A., Cheng, K., Shen, X., Xu, P., and Liu, S. (2017). The immediate analgesic effect of acupuncture for pain: a systematic review and meta-analysis. *Evid. Based Complement. Alternat. Med.* 2017:3837194. doi: 10.1155/2017/3837194

Zhao, Z., Kim, S. C., Zhao, R., Wu, Y., Zhang, J., Liu, H., et al. (2015). The tegmental-accumbal dopaminergic system mediates the anxiolytic effect of acupuncture during ethanol withdrawal. *Neurosci. Lett.* 597, 143–148. doi: 10.1016/j.neulet.2015.04.045

Ziemann, U., Ilic, T. V., Pauli, C., Meintzschel, F., and Ruge, D. (2004). Learning modifies subsequent induction of long-term potentiation-like and long-term depression-like plasticity in human motor cortex. *J. Neurosci.* 24, 1666–1672. doi: 10.1523/JNEUROSCI.5016-03.2004

Ziemann, U., Rothwell, J. C., and Ridding, M. C. (1996). Interaction between intracortical inhibition and facilitation in human motor cortex. *J. Physiol.* 496, 873–881. doi: 10.1113/jphysiol.1996.sp021734

Conflict of Interest Statement: The authors declare that the research was conducted in the absence of any commercial or financial relationships that could be construed as a potential conflict of interest.

frontiers in Neuroscience

ORIGINAL RESEARCH
published: 20 February 2019
doi: 10.3389/fnins.2019.00110

Peripheral Sensory Nerve Tissue but Not Connective Tissue Is Involved in the Action of Acupuncture

*Suchan Chang[1†], O. Sang Kwon[2†], Se Kyun Bang[1], Do-Hee Kim[1], Min Won Baek[1], Yeonhee Ryu[2], Jong Han Bae[3], Yu Fan[1], Soo Min Lee[1], Hyung Kyu Kim[1], Bong Hyo Lee[1], Chae Ha Yang[1] and Hee Young Kim[1,3]**

[1] College of Korean Medicine, Daegu Haany University, Daegu, South Korea, [2] Clinical Medicine Division, Korea Institute of Oriental Medicine, Daejeon, South Korea, [3] Department of Physics, Yeungnam University, Gyeongsan, South Korea

OPEN ACCESS

Edited by:
Florian Beissner, Hannover Medical School, Germany

Reviewed by:
Helene M. Langevin, Brigham and Women's Hospital, Harvard Medical School, United States
Stephanie Tjen-A-Looi, University of California, Irvine, United States

***Correspondence:**
Hee Young Kim
hykim@dhu.ac.kr

† These authors have contributed equally to this work

Specialty section:
This article was submitted to Perception Science, a section of the journal Frontiers in Neuroscience

Received: *03 November 2018*
Accepted: *29 January 2019*
Published: *20 February 2019*

Citation:
Chang S, Kwon OS, Bang SK, Kim D-H, Baek MW, Ryu Y, Bae JH, Fan Y, Lee SM, Kim HK, Lee BH, Yang CH and Kim HY (2019) Peripheral Sensory Nerve Tissue but Not Connective Tissue Is Involved in the Action of Acupuncture. Front. Neurosci. 13:110. doi: 10.3389/fnins.2019.00110

Acupuncture has been used to treat a variety of diseases and symptoms for more than 2,500 years. While a number of studies have shown that nerves are responsible for initiating the effects of acupuncture, several lines of study have emphasized the role of connective tissue in the initiation of acupuncture signals. To determine whether nerves or connective tissue mediate the action of acupuncture, we constructed a robotic acupuncture needle twister that mimicked the twisting of the needle by an acupuncturist, and we examined the role of nerves and connective tissues in the generation of acupuncture effects in rat cocaine-induced locomotion, stress-induced hypertension, and mustard oil-induced visceral pain models. Robotic or manual twisting of acupuncture needles effectively suppressed cocaine-induced hyperactivity, elevated systemic blood pressure or mustard oil-induced visceral pain in rats. These acupuncture effects were completely abolished by injecting bupivacaine, a local anesthetic, into acupoints. However, disruption of connective tissue by injecting type I collagenase into acupoints did not affect these acupuncture effects. Our findings suggest that nerve tissue, but not connective tissue, is responsible for generating the effects of acupuncture.

Keywords: acupuncture, peripheral sensory nerve, connective tissue, robotic acupuncture needle twister, collagenase

INTRODUCTION

Acupuncture has been used to treat various diseases in Asian countries over the last 2,500 years and has been widely practiced in many countries. In 1997, the United States' National Institutes of Health (NIH) reported acupuncture's safety and efficacy for treating a wide range of conditions, including drug abuse, stroke rehabilitation, and headache (Nih Consensus Conference, 1998). In a bibliometric review of the publications on acupuncture research in PubMed over the last 20 years, acupuncture research has increased markedly in the past two decades, with twice the growth rate of overall biomedical research. While pain (approximately 38% of publications) is consistently the most common topic of acupuncture research, the publications of randomized clinical trials have been increasing in numbers at a high rate (Ma et al., 2016). Although these studies have shown acupuncture's effectiveness, the mechanisms by which the acupuncture signals are initiated and conveyed remain contradictory and inconclusive.

Acupuncture is a therapeutic intervention for improving the efficiency of homeostatic mechanisms of the body by stimulating acupoints. There are two leading models of the initiation of acupuncture signals: the neurologic model and the connective tissue model. The neurologic model, which is by far the more widely accepted and studied, posits mediation by the nervous system, with acupuncture signals being initiated by the activation of sensory nerve endings and specific nerve fibers and transmitted to the brain through nervous pathways, resulting in a variety of physiological effects. In support of this view, it was reported that acupuncture produces an antinociceptive effect by releasing adenosine at peripheral nerve terminals in rodents (Goldman et al., 2010). Acupuncture stimulation at acupoints in the wrist, PC5-6, increased Aδ- and C-fiber activity to evoke cardiovascular effects (Zhou et al., 2005). Our previous studies showed that acupuncture at HT7 attenuates drug-induced or drug-seeking behaviors for substances such as cocaine, morphine and ethanol (Yoon et al., 2004, 2010, 2012; Yang et al., 2010). During acupuncture stimulation, peripheral sensory afferents, such as Pacinian and Meissner's corpuscles, are activated, and the afferent signals are transmitted via the A-fibers of the ulnar nerve (Kim et al., 2013) and the somatosensory pathway in the spinal dorsal column (Chang et al., 2017). While cumulative evidence has supported the neurological model, in the last two decades another hypothesis, known as the "connective tissue model," has emerged to address possible roles of connective tissue in the initiation of acupuncture's signals (Langevin and Yandow, 2002; Langevin, 2014). According to this model, twisting or rotation of the acupuncture needle creates winding of connective tissue around the needle and deformation of collagen fibers, which initiates mechanical signals transmitted via the whole-body fascia network, the layers of connective tissue surrounding muscle, organs, and blood vessels. Research groups have proposed that the connective tissue may mediate the effects of manual acupuncture through a number of pathways: transmission of a mechanical signal from the needle to nearby sensory afferent nerves, potential purinergic signaling within connective tissue fibroblasts with local effects on sensory nerves, and direct effects on connective tissue pathology, possibly involving reductions in inflammation and/or fibrosis (Langevin and Yandow, 2002; Langevin et al., 2007; Langevin, 2014; Wu et al., 2015). However, it remains to be established whether connective tissue mediates the therapeutic effects of acupuncture. While these models have been thought to provide plausible explanations for the initiation of acupuncture signals, evidence is currently lacking as to whether these two models work in separate or synergistic ways.

To explore whether acupuncture effects are mediated through nerve or connective tissue, we used our newly constructed robotic needle twister to test the effects of twisting acupuncture in the rat models of cocaine-induced locomotion, immobilization-induced hypertension and mustard oil-induced visceral pain, and explored whether the effects of acupuncture are altered by a blockade of nerves or disruption of connective tissue.

MATERIALS AND METHODS

Animals

Male Sprague-Dawley rats (weight 270–320 g, Daehan Animal, Korea) were used, and each group consisted of 5–8 rats. Animals were housed at a constant humidity (40∼60%) and temperature (22 ± 2°C), with a 12 h/12 h light/dark cycle and allowed free access to food and water until use. All procedures were carried out in accordance with the NIH Guide for Care and Use of Laboratory Animals and approved by the Institutional Animal Care and Use Committee (IACUC) at Daegu Haany University.

Chemicals

Cocaine (15 mg/ml saline, MacFarlan Smith Ltd., UK), mustard oil (30∼50 μl; allyl isothiocyanate, Sigma Aldrich, USA), and bupivacaine (20 μl/loci, 5 mg/ml, Huons Pharm, South Korea; a long-acting local anesthetic) were used. Type I collagenase (20 μl/loci, 5 mg/ml saline, Sigma Aldrich, USA) or together with toluidine blue (20 μl/loci, 1 mg/ml, Sigma Aldrich) was injected. Bupivacaine or type I collagenase was injected into acupuncture points to a depth of 3 mm, perpendicular to the skin surface, by using a syringe with a 32-gauge needle.

Measurement of Rotational Duration and Angle During Manual Needle Twisting

A needle (0.20 mm in diameter, needle length of 30 mm and handle length of 20 mm; Dongbang Medical Co., Korea) with red tape on the shaft was inserted into a Styrofoam board to measure the rotational duration (speed) and angle during manual needle twisting (**Figure 1A**). Acupuncturists ($n = 3$) were asked to twist the handle of the acupuncture needle for at least 20 s and video recorded. This procedure was repeated two times per person. Rotation duration and angle were analyzed using a media player program (Gom Player, Gom and Company, Korea).

A Robotic Acupuncture Needle Twister (RANT) and Acupuncture Treatment

A robotic twister was constructed to mimic a needle twisting technique that is commonly performed by acupuncturists. This device consisted of a handheld needling instrument coupled to a servo motor (ez-SERVO, Fastech, Korea), a personal computer connected with a servomotor controller (ez-SERVO, Fastech, Korea) and a custom-made control software program (LabVIEW, National Instruments, Austin, TX, USA). The rotation shaft of the servo motor was coupled to a needle holder (**Figure 1D**). A rubber grommet was fixed to the needle at a distance of 2 or 3 mm from the tip, as described previously (Kim et al., 2013), to control the depth of acupuncture needle insertion.

In the rat model of cocaine-induced locomotor activity, acupuncture needles (0.10 mm in diameter, needle length of 10 mm and handle length of 10 mm; Dongbang Medical Co., South Korea) were inserted perpendicularly into the HT7 acupoint at a depth of 3 mm, twisted for 20 s with the RANT device, maintained in place for up to 60 s after needle insertion and withdrawn. In the animal model of immobilization-induced hypertension, needles were inserted perpendicularly into the

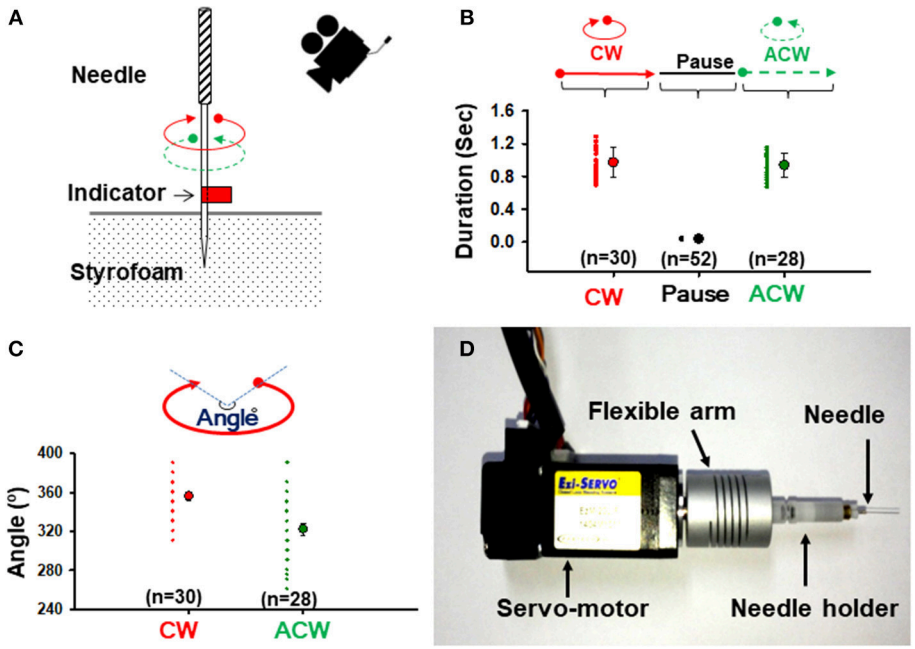

FIGURE 1 | Twisting acupuncture and construction of a robotic acupuncture needle twister (RANT). **(A)** Measurement of rotational durations and angles during manual needle twisting. A needle with a red tape on the shaft was inserted into a Styrofoam board and video-recorded. **(B)** Mean duration of needle rotations. The motions of 30 CW turns, 52 pauses and 28 ACW turns during needle twisting by 3 acupuncturists were analyzed. **(C)** Mean rotation angle of the needle. The motions of 30 CW turns and 28 ACW turns during needle twisting by 3 acupuncturists were analyzed. **(D)** A constructed RANT device. The servo motor in the needling instrument was fitted to a flexible arm fixed with a needle holder and controlled by the control software. CW, clockwise direction; ACW, anticlockwise direction.

PC6 acupoint at a depth of 3 mm, twisted for 10 min with the RANT device and withdrawn. In the rat model for mustard oil-induced visceral pain, acupuncture needles were inserted 2–3 mm deep into BL62-64 and manually twisted for 30 s at 10 min intervals, which was repeated 4 times for a total of 30 min. Type I collagenase or bupivacaine was injected into acupoints 30 min before acupuncture treatments.

Cocaine-Induced Locomotor Activity

Locomotor activity was measured through a video tracking system (EthoVision, Noldus Information Technology BV, Netherlands). Briefly, in a dimly lit room, each animal was placed in a square open field box (40 × 40 × 45 cm) made of black acrylic. Video tracking software (EthoVision 3.1) measured the distance traveled (cm). On the testing day, animals were habituated for at least 60 min. After baseline activity was recorded for 30 min, the animal received an intraperitoneal injection of cocaine (15 mg/kg) and acupuncture treatment and was monitored for up to 60 min after injection. Data are reported as the total distance traveled (cm) in 1 h or the distance traveled (cm) during each 10 min.

Immobilization-Induced Hypertension and Measurement of Blood Pressure

Hypertension was induced by restraining in animals a cone-shaped plastic bag, as described previously (Kim et al., 2017). Systolic blood pressure was measured noninvasively with a tail cuff blood pressure monitor (Model 47, IITC). Briefly, the restrained rats were placed in a chamber kept at 27°C, and an occluding cuff and a pneumatic pulse transducer were positioned on the base of the rat tail. A programmed electrosphygmomanometer (Narco Bio-Systems Inc., USA) was inflated and deflated automatically, and the tail cuff signals from the transducer were automatically collected every 10 min using an IITC apparatus (Model 47, IITC Inc., USA). The mean of the two readings was taken at each blood pressure measurement.

Mustard Oil-Induced Visceral Pain and Measurement of Electromyographic Response to Colorectal Distension

A pair of silver wire electrodes (0.20 mm in diameter, Nilaco, Japan) were inserted into the external oblique abdominis muscle, buried for 10 mm of their length and separated by 10 mm for electromyography (EMG) recording. Colorectal distension (CRD) was applied using an inflatable balloon (3 cm in length, 1 cm in diameter) attached to an intravenous line via a T connector that was connected to a bulb with a valve and a sphygmomanometer. EMG recordings in response to CRD stimulation for 5 s at strengths of 20, 40, 60, and 80 mmHg were carried out. The EMG signal was amplified (×10,000, 300–1,000 Hz; ISO-80, World Precision Instruments, USA), digitized and analyzed with a data acquisition and analysis interface (Micro1401, CED,

UK). After measurement of baseline, for induction of colonic pain, a mustard oil (30∼50 μl; Sigma Aldrich)-soaked Q-tip was inserted into the colon, approximately 5 cm proximal to the anus, kept for 30 min and withdrawn. Acupuncture was then applied, and EMG was recorded up to 30 min after acupuncture treatment.

Measurement of Needle Rotational Force

The rotational force (torque) acting on the needle in the tissue was measured through a custom-made needle force measurement system. The torque sensor was simply constructed by fixing a strain gauge (KFH-C1 Series, OMEGA Engineering, USA) to a plunger of a 50 ml syringe connected to a needle holder (**Figure 4A**) and wired to a Wheatstone bridge. The signals generated from the torque sensor during needle twisting were digitalized using a data acquisition system (DAQ-NI USB-6200, National Instruments, USA) and analyzed with a customized LabVIEW program (National Instruments; **Figure 4B**).

Hematoxylin-Eosin (H&E) Staining and Immunohistochemical Staining of PGP9.5 Expression in the Skin of Type I Collagenase-Treated Rats

At the end of the experiments, the rats were sacrificed under sodium pentobarbital (90 mg/kg, IP) anesthesia. The skin (10 × 10 × 10 mm) over the PC6 acupoints injected with either type I collagenase or bupivacaine was removed and fixed in 4% buffered paraformaldehyde (PFA) for 2 h. The samples were processed, embedded in paraffin wax, and cut into 5-μm-thick serial sections. The skin samples were subjected to H&E staining or immunohistochemistry for PGP9.5. For immunohistochemistry of PGP9.5, the sections were incubated with anti-PGP9.5 mouse monoclonal antibodies (1:1000; Abcam, Cambridge, UK), followed by incubation with a biotinylated donkey anti-mouse Alexa Fluor 488 (1:200; Invitrogen, USA). Images were taken from 4–5 sections from each animal under an epifluorescence microscope (AX70, Olympus, USA) and analyzed with ImageJ software (NIH, USA). A mixture of type I collagenase and toluidine blue (20 μl/locus) was injected into the PC6, HT7, and BL62 acupoints to a depth of 3 mm in a normal rat to further evaluate the extent of the diffusion of type I collagenase after the injection. Thirty minutes after the injection, the tissues were removed, post-fixed, protected with sucrose, and cryosectioned at a thickness of 15 μm. The blue-stained areas were examined under a microscope.

Data Analysis

All data are presented as the mean ± SEM (standard error of the mean) and analyzed by one- or two-way repeated measurement analysis of variance (ANOVA) followed by post hoc testing using Fisher's least significant difference (LSD) method or paired or unpaired *t*-test, where appropriate. Statistical significance was considered at $P < 0.05$.

RESULTS

Construction of a Robotic Acupuncture Needle Twister (RANT) That Mimicked Human Needle Twisting Manipulation

To evaluate the rotational duration (speed) and angle generated during needle twisting, 3 well-trained acupuncturists were asked to manually twist the acupuncture needle (**Figure 1A**), video-recorded and analyzed using media player software. Across 58 instances, the needles were rotated for an average of 0.972 ± 0.034 s ($n = 30$) in a clockwise direction (CW), left stationary for an average of 0.035 ± 0.001 s ($n = 52$) and then rotated for an average of 0.936 ± 0.028 s ($n = 28$) in an anticlockwise direction (ACW) (**Figure 1B**). The angles of rotation were 356° ± 4.37° CW and 322.32° ± 6.19° ACW (**Figure 1C**). However, there were no significant differences in rotation duration or angles between CW and ACW.

To control the rotation speed and angle objectively, a robotic twister was constructed with a servo motor and interfaced with a LabVIEW program written by our laboratory (**Figure 1D**). When the above parameters for the device were set, the robotic twister replicated the motion of human acupuncture needle manipulation (**Supplementary Movie 1**).

Twisting Acupuncture Suppressed Cocaine-Induced Locomotor Activity

To test whether the effect of acupuncture effect is dependent on the needle rotation duration (and speed), we evaluated the effects of needle rotation at various durations on cocaine-enhanced locomotor activity. After baseline recording of locomotor activity for 30 min, rats were given an intraperitoneal (IP) injection of cocaine (15 mg/kg). One minute after injection, acupuncture needles were inserted into the bilateral HT7 and twisted for 20 s at different rotation durations (**Table 1**) using the robotic twister. Control rats received the cocaine injection without acupuncture treatment. An acute cocaine injection rapidly increased locomotor activity, which lasted up to approximately 60 min after injection, with a peak at 10 min (cocaine group in **Figures 2A,B**). Acupuncture applied with the Duration-D3 condition (fastest rotation speed) significantly decreased cocaine-induced locomotion compared to the control group [one-way ANOVA, $F_{(3,21)} = 3.706$; $^{\#}p < 0.05$ vs. Control; **Figures 2C,D**]. However, needle twisting at other durations (Duration-D1 and D2) or needle placement without twisting (**Supplementary Figure 1**) failed to inhibit the cocaine-induced

TABLE 1 | Parameters for various rotational durations by robotic twister.

Group	Clockwise (CW; s)	Pause (s)	Anti-clockwise (ACW; s)	Rotation (°)
Duration D-1	3.80	0.035	3.80	360
Duration D-2	1.90	0.035	1.90	360
Duration D-3	0.95	0.035	0.95	360

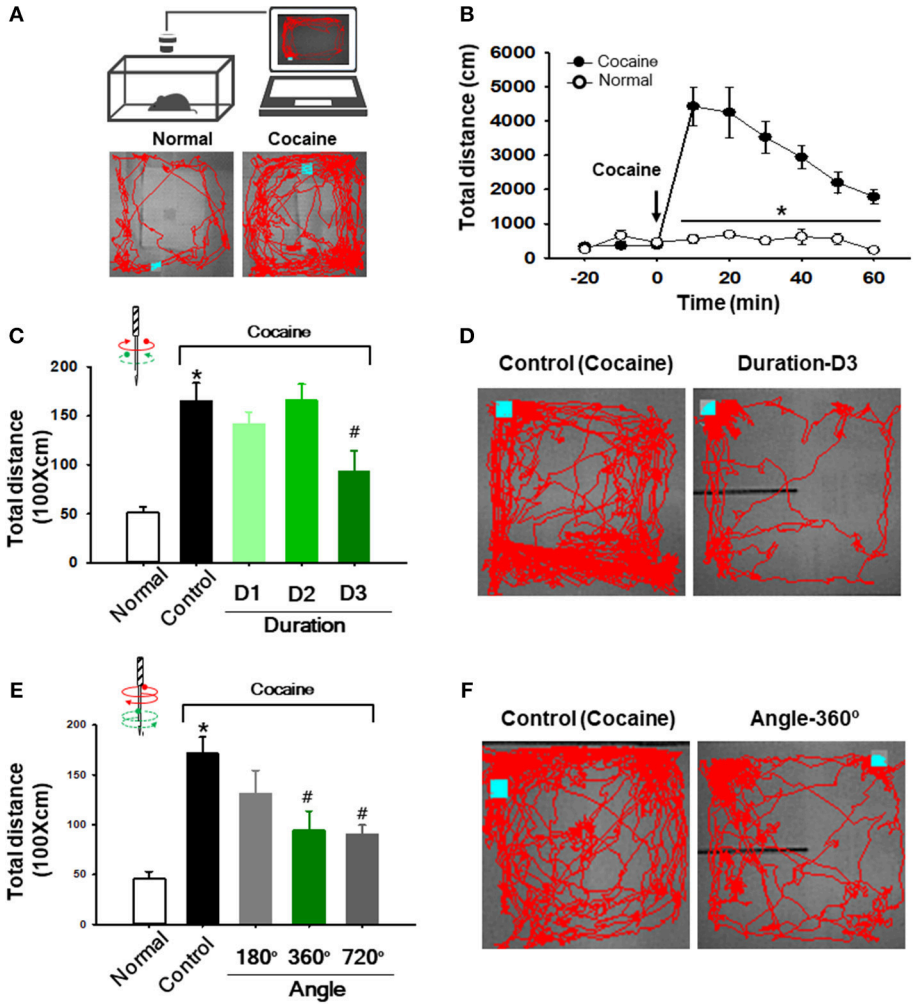

FIGURE 2 | Effect of twisting acupuncture by RANT on cocaine-enhanced locomotor activity. **(A)** Schematic for measurement of locomotor activity (upper) and representative tracings in normal or cocaine-treated rats (lower). **(B)** Enhancement of locomotor activity following intraperitoneal injection of cocaine ($n = 7$) compared to normal rats ($n = 5$). $^{*}p < 0.05$ vs. Normal. **(C,D)** Effect of acupuncture at various rotation durations on cocaine-induced locomotion. Needle twisting at Duration-D3 significantly decreased cocaine-induced locomotion compared to the control group [$^{*}p < 0.05$ vs. Normal; $^{\#}p < 0.05$ vs. Control (cocaine only without acupuncture); Normal, $n = 5$; Control, $n = 7$; Duration-D1, $n = 8$; Duration-D2, $n = 7$; Duration-D3, $n = 6$). **(E,F)** Effect of various needle rotation angles by RANT on cocaine-induced locomotion. Inhibition of cocaine-induced locomotion was found in 360° or 720° rotation angle groups compared to control (cocaine only). ($^{*}p < 0.05$ vs. Normal; $^{\#}p < 0.05$ vs. Control; $n = 6$ per group).

increase in locomotor activity, suggesting that the inhibitory effects were not stimulus-duration dependent. To determine whether the inhibitory effects of twisting acupuncture are dependent on the needle rotation angle, rats ($n = 29$) were randomly divided into the following groups: control and 180°-, 360°-, and 720°-rotation angle groups (**Table 2**). Although acupuncture stimulation tended to decrease the locomotor response to cocaine in an angle-dependent manner, significant inhibitory effects of acupuncture on locomotor activity were found in the 360°- and 720°-rotation angle groups compared to the control [one-way ANOVA, $F_{(3,21)} = 4.998$; $^{\#}p < 0.05$ vs. Control; **Figures 2E,F**]. Because a twisting condition of Duration-D3 produced consistent, reproducible acupuncture effects, the parameter was used in subsequent experiments.

Acupuncture Effects Were Prevented by Blockade of the Nerve but Not Disruption of Connective Tissue

To investigate whether acupuncture effects are mediated via nerve or connective tissue, we injected either bupivacaine (a local anesthetic) or type I collagenase (a proteolytic enzyme) into acupoints 30 min before acupuncture treatment. The experiment was first performed in the rat model of cocaine locomotion. While acupuncture at HT7 attenuated cocaine-induced enhancement of locomotor activity, such effects were inhibited by pretreatment of bupivacaine, but not collagenase, indicating mediation of the afferent nerve [one-way ANOVA, $F_{(3,21)} = 4.998$; $^{*}p < 0.05$ vs. Normal; $^{\#}p < 0.05$ vs. Control; $^{\$}p < 0.05$ vs. BUPIVA+Acup; **Figures 3A–C**]. To further confirm this,

TABLE 2 | Parameters for various rotation angles produced by the robotic twister.

Group	Clockwise (CW; s)	Pause (s)	Anti-clockwise (ACW; s)	Rotation (°)
180°	0.475*	0.035	0.475*	180
360°	0.95*	0.035	0.95*	360
720°	1.90*	0.035	1.90*	720

*Note that rotational speeds (time/turn) were the same in all groups.

we repeated the experiments in the rat models of immobilization-induced hypertension (IMH) or mustard oil-induced visceral pain. For the IMH model, when a rat was placed in an immobilization bag, systolic blood pressure (SBP) gradually increased for the next several hours (Control; **Figures 3D–F**), consistent with our previous study (Kim et al., 2017). Twisting acupuncture at PC6 with the robotic device prevented the development of hypertension compared to the control ($^{*}p < 0.05$ vs. Control; **Figure 3F**). When either bupivacaine or collagenase was injected into PC6 30 min before acupuncture treatment, the acupuncture effects were prevented in bupivacaine-treated rats but not in collagenase-treated rats (**Figures 3E,F**). Unexpectedly, significant differences were observed at the time points of 100–120 min between the control and BUPIVA+Acup groups ($^{\$}p < 0.05$ compared to the control group; **Figure 3F**). Compared to our previous study (Kim et al., 2017), 2 of 5 control rats developed borderline hypertension (140–160 mmHg) and did not reach an SBP of 160–180 mmHg at the end of the 2 h immobilization, which would yield a significant difference at the later time points between the control and Bupiva+Acup groups. In the rat model of mustard oil-induced visceral pain, acupuncture needles were inserted into BL62-64 and manually rotated, and visceral sensitivity was assessed in recording the electromyographic (EMG) responses to graded colorectal distensions (CRD) of 20, 40, 60, and 80 mmHg in conscious rats. A significant increase in the EMG discharges in response to CRDs was observed in mustard oil-treated rats (Control) compared to normal rats (Normal). The elevated EMG responses were attenuated in the rats given acupuncture treatment [one-way ANOVA, 20 mmHg; $F_{(4,30)} = 4.755$; $^{\#}p = 0.025$, 40 mmHg; $F_{(4,30)} = 7.273$; $^{\#}p = 0.003$, 60 mmHg; $F_{(4,30)} = 8.047$; $^{\#}p < 0.001$, 80 mmHg; $F_{(4,30)} = 8.845$; $^{\#}p < 0.001$ vs. Control], which was reversed by pretreatment of bupivacaine [one-way ANOVA, 20 mmHg; $F_{(4,30)} = 4.755$; $p = 0.514$, 40 mmHg; $F_{(4,30)} = 7.273$; $p < 0.001$, 60 mmHg; $F_{(4,30)} = 8.047$; $p = 0.009$, 80 mm Hg; $F_{(4,30)} = 8.845$; $p = 0.002$ vs. Acup]. However, the inhibitory effects of acupuncture on visceral pain were not altered by treatment with collagenase prior to acupuncture treatment (**Figures 3G–I**). This observation indicates the mediating role of afferent nerves in the effects of acupuncture.

Type I Collagenase Disrupted Connective Tissue in Acupoints Without Morphological Changes in the Afferent Nerve

To assess the functional alteration of connective tissue in the acupoints injected with collagenase or bupivacaine, we constructed a torque sensor (**Figures 4A,B**) and measured rotational force (torque) acting on the needle in the tissue. The acupuncture needle inserted into the HT7 acupoint over the wrist was connected to the needle holder of the torque device and manually twisted. The bidirectional needle twisting generated sawtooth waves, with amplitudes in the range of −15 to 15 mN.mm in the untreated normal rats (Normal, **Figure 4C**). While needle rotational force was not changed in bupivacaine-injected acupoints compared to those of normal rats (BUPIVA; **Figures 4E,F**), a significant drop in rotational force was found in collagenase-treated acupoints (COLG; $^{*}p < 0.05$ vs. Normal; **Figures 4D,F**). This observation indicates that type I collagenase eliminated the pulling of collagen fibers created during needle manipulation.

To identify whether collagenase causes morphological damage of connective tissue or peripheral nerve in the acupoints, the skin over acupoints was evaluated through histological or immunohistochemical methods. In H&E staining, the skin treated with collagenase displayed faint staining, with sparse thin collagen bundles and a significantly decreased density of collagen fibers compared to that of normal, untreated rats (**Figures 5A,B**; $^{*}p < 0.05$). On the other hand, in a quantitative immunohistochemical analysis for PGP 9.5, a marker for nerve fibers (Beiswenger et al., 2008), the morphological changes of the peripheral nerve were not observed in collagenase-treated skin compared to the normal group (**Figures 5C,D**). In addition, the histological examination revealed that the type I collagenase that had been injected into the acupoints diffused into the skin, including the epidermis, dermis, and subcutaneous tissues (**Figure 5E**). This suggests that injection of type I collagenase into acupoints disrupted the connectivity of collagen fibers but did not induce morphological damage of peripheral nerves in skin.

DISCUSSION

Using our robotic device that mimicked needle twisting by a human acupuncturist, we demonstrated that twisting acupuncture effectively suppressed cocaine-induced locomotor activity, immobilization-induced hypertension and mustard oil-induced visceral pain, which was completely prevented by blocking afferent nerves with bupivacaine but not by degrading connective tissue with type I collagenase. Furthermore, collagenase destroyed collagen in the skin without damaging the peripheral nerve. Our findings suggest critical mediation of the nerve in producing acupuncture effects. Additionally, modulation of connective tissue does not seem to be sufficiently reliable to serve as the principal explanation for acupuncture effects, at least in the animal models tested.

Acupuncture needles are manually manipulated to obtain therapeutic effects after needle insertion into acupoints (Pomeranz and Berman, 2003). Various manipulation techniques, such as twisting (also known as bidirectional twisting-rotation), vibrating and lifting and thrusting, have been used in clinics. Among them, manual twisting has been popular because it is a simple and effective technique to provoke the needling sensation called *deqi*, which acupuncturists believe to be essential for obtaining effective acupuncture stimulation

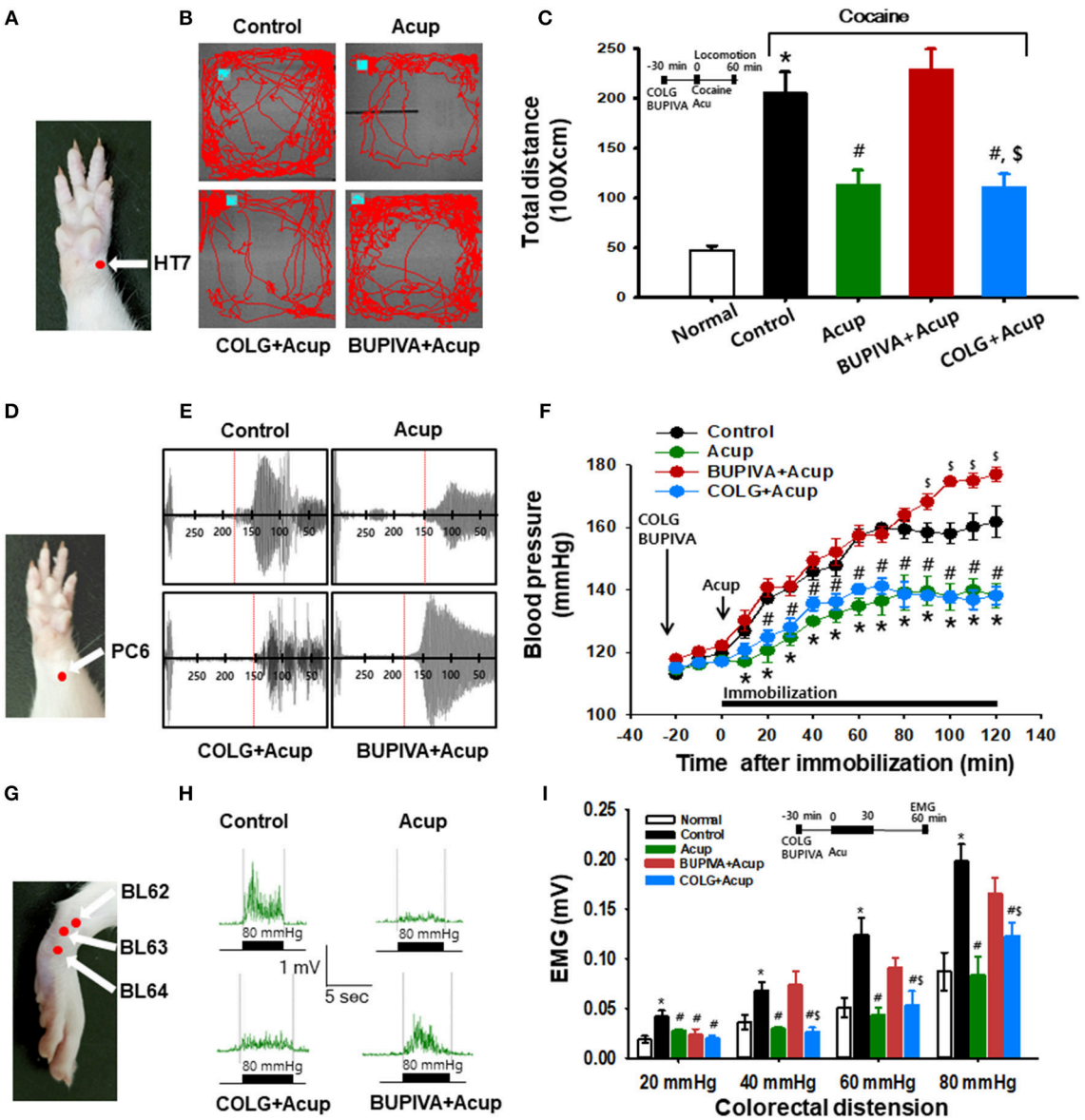

FIGURE 3 | Effect of preinjection of collagenase or bupivacaine into acupoints in various animal models. **(A–C)** Effect of pretreatment of type I collagenase or bupivacaine in HT7 acupoint on cocaine-induced locomotor activity in rats. Inhibition of cocaine-induced locomotion by acupuncture at HT7 (Acup) was prevented by pretreatment of bupivacaine (BUPIVA) into HT7 acupoint **(A)**, but not type I collagenase (COLG; **B,C**). $^{*}p < 0.05$ vs. Normal; $^{\#}p < 0.05$ vs. Control; $^{\$}p < 0.05$ vs. BUPIVA+Acup; $n = 5$ per group. Representative tracings **(B)**. **(D–F)** Effect of pretreatment of type I collagenase or bupivacaine in the PC6 acupoint on immobilization-induced hypertension in rats. Bupivacaine, but not collagenase, inhibited the acupuncture effects of PC6 **(D)** on elevated systolic blood pressure in rats **(E,F)** Representative pulse signals measured from tail **(E)** $^{*}p < 0.05$ vs. Control (immobilization only without acupuncture); $^{\#}p < 0.05$ vs. BUPIVA+Acup; $n = 5$ per group. **(G–I)** Effect of pretreatment of type I collagenase or bupivacaine in acupoints on mustard oil-induced visceral pain in rats. Electromyogram (EMG) in each group was recorded during colorectal distension of 20, 40, 60, and 80 mmHg for approximately 5 s. Normal, normal rats; Control, mustard only without acupuncture; Acup, acupuncture in mustard-treated rats; COLG+Acup, pretreatment of collagenase prior to acupuncture in mustard-treated rats; BUPIVA+Acup, pretreatment of bupivacaine prior to acupuncture in mustard-treated rats. $n = 7$ per group. Acupoints used. **(G)** Representative EMG signals recorded during colorectal distension of 80 mmHg **(H)**. Bupivacaine, but not collagenase, inhibited the acupuncture effects on colorectal distension-induced visceral motor responses in rats **(I)**. $^{*}p < 0.05$ vs. Normal; $^{\#}p < 0.05$ vs. Control; $^{\$}p < 0.05$ vs. BUPIVA+Acup; $n = 7$ per group. Acup, acupuncture; COLG, collagenase; BUPIVA, bupivacaine.

(Pomeranz and Berman, 2003; Stux and Pomeranz, 2012). (Kim G. H. et al., 2010) reported that manual twisting is more effective than the lifting-thrusting technique in producing analgesic effects on formalin-induced pain in rats. We and others have shown that manual twisting of needles applied to HT7 acupoints suppresses addictive behaviors induced by abused drugs, including cocaine, methamphetamine, and ethanol (Yang et al., 2010; Jin et al., 2018; Kim et al., 2018). Moreover,

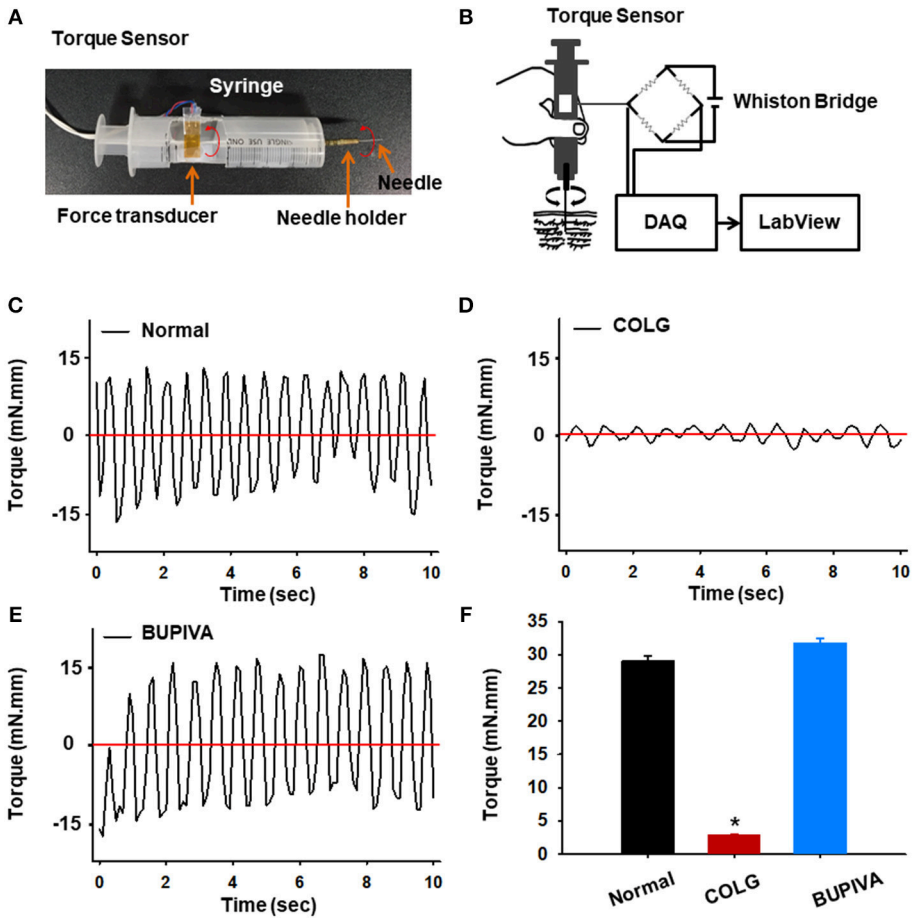

FIGURE 4 | Effect of preinjection of collagenase or bupivacaine into acupoints on rotational force (torque). **(A,B)** A simply constructed torque sensor **(A)** and its electrical circuit **(B)**. **(C–F)** Rotational force recorded during needle twisting in collagenase or bupivacaine-treated acupoints. A significant drop of rotational force was found in collagenase-treated acupoints **(D)** compared to normal **(C)** or bupivacaine-treated **(E)** rats. *$p < 0.05$ vs. Normal; $n = 5$ per group. COLG, collagenase; BUPIVA, bupivacaine.

acupuncture at HT7 attenuates drug-induced dopamine release and metabolic neuronal activity in the nucleus accumbens (Yoon et al., 2004; Jin et al., 2018) through group II metabotropic glutamate receptors (Kim et al., 2018) and modulation of GABA neuron activity in the ventral tegmental area (Yang et al., 2010). While these studies provide evidence that twisting acupuncture needle manipulation produces therapeutic effects, manual acupuncture stimulation could alter its effect by affecting many vagaries, including rotation durations and angles. Unfortunately, few studies have quantified the twisting technique performed by practitioners. Therefore, the present study video-analyzed the motion of needle twisting performed by acupuncturists and found that the duration of needle rotation ranged from 0.75 to 1.21 s (mean value of 0.975 ± 0.073 s) and rotation angles ranged from 325° to 350° (mean value of 340° ± 4.27°). However, considerable variations in both durations and angles were observed within each acupuncturist or across acupuncturists (data not shown). The variations may lead to low reproducibility and high individual variations among practitioners (Napadow et al., 2005; Kim et al., 2013). As our robotic twister has an advantage in controlling rotation duration and angle, it would help solve the control issues of manual needle manipulation.

Researchers have suggested that needle twisting in different stimulation parameters [including durations (or frequency, Hz) and angles, etc.] could produce different physiological responses and therapeutic effects (Kim G. H. et al., 2010; Chang et al., 2017). Hong et al. (2015) showed that the responses of spinal dorsal horn neurons following gastric distension are enhanced by manual acupuncture at 0.5 and 1 Hz, while the dorsal horn neurons are inhibited by manual acupuncture at 2 and 3 Hz. In the present study, the effects of acupuncture were not dependent on the rotation duration or angle when various durations or angles of needle twisting were tested in three different animal models. Similarly, a previous study attempted to determine the analgesic effects of acupuncture in 4 different stimulation conditions (angle and frequency of rotation: 90° + 1 Hz, 90° + 1/4 Hz, 360° + 1 Hz, and 360° + 1/4 Hz)

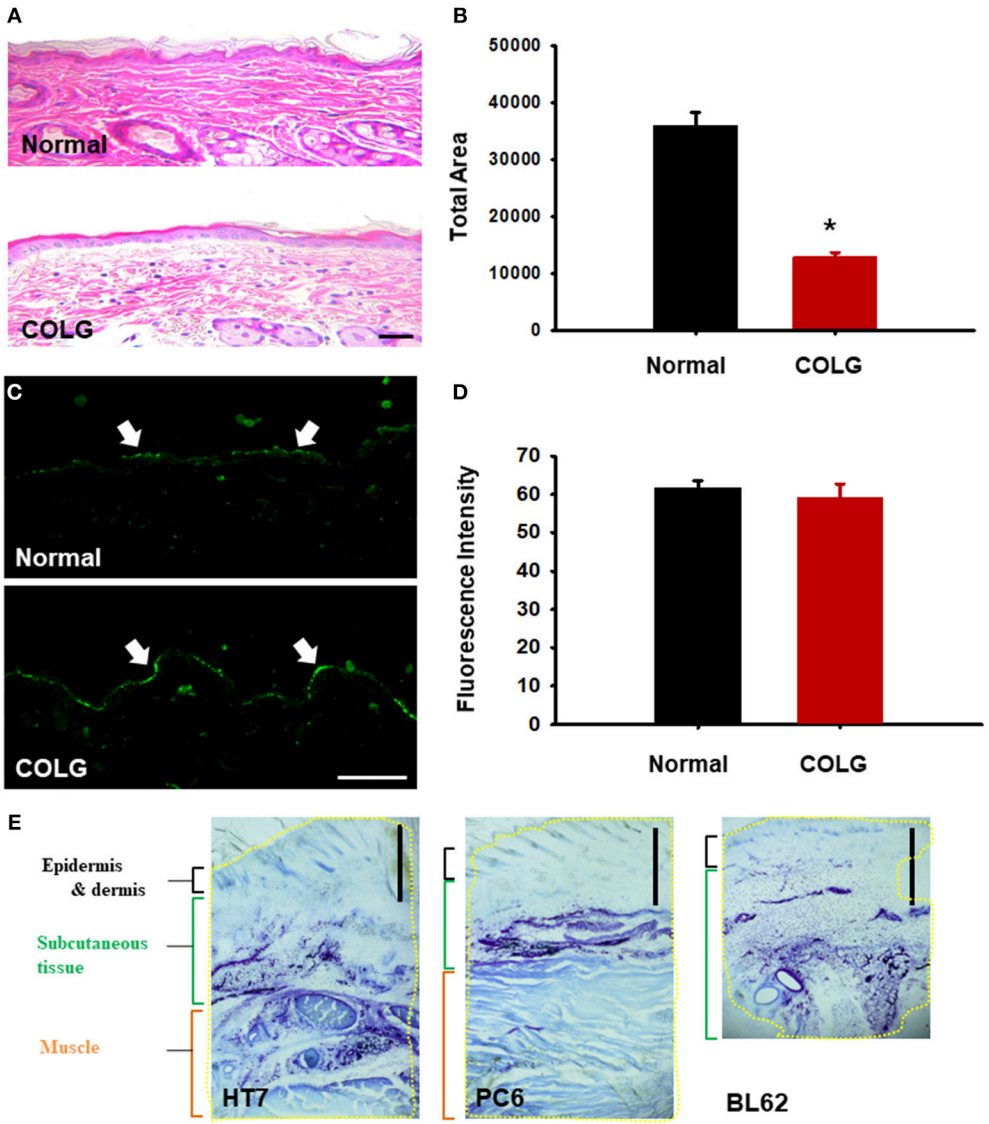

FIGURE 5 | Histological or immunohistochemical examination of collagenase-injected acupoints. **(A,B)** H&E staining of collagenase- or saline-treated acupoints. Quantification of pink-stained area in normal or collagenase-treated skins **(B)**. *$p < 0.05$ vs. Normal; $n = 5$ per group. **(C,D)** Immunohistochemistry for PGP9.5, a neuronal marker, in normal or collagenase-treated acupoints **(C)**. Mean fluorescent intensity in normal or collagenase-treated skins **(D)**. $n = 5$ per group. COLG, collagenase. Bar = 50 μm. **(E)** Diffusion of a mixed solution of toluidine blue dye and type I collagenase injected into acupoints. Yellow line = blue area stained with toluidine blue. Bar = 1 mm.

by using a computer-controlled rotational device in rats. This study showed that only the 90° + 1/4 Hz condition generates a statistically significant effect compared to plain acupuncture (Kim et al., 2006). These findings indicate that there does not appear to be a correlation between rotation durations or angles and the degree of response alteration in the twisting needle manipulation. Rather, acupuncture effects may require specific stimulation parameters, in accordance with what has been found in animal models. Additionally, in accordance with a previous study (Kim et al., 2006), our data showed that simple needle placement did not generate acupuncture effects on cocaine-induced locomotion in rats. It supports the observations that needle manipulations such as rotation and electrical stimulation are needed to achieve the desired effects by activating sensory nerve fibers and cells, in contrast to needle placement (sham acupuncture) (Kim et al., 2006; Guo et al., 2018).

In the present study, injection of a long-lasting local anesthetic bupivacaine into acupoints effectively blocked acupuncture effects in the rat models of cocaine-induced locomotion, hypertension, and mustard oil-induced visceral pain, suggesting that acupuncture signals are conveyed via afferent nerve fibers. These results agree with reports that application of a local anesthetic, 1% lidocaine, to acupoints prior to acupuncture

treatment inhibits antiemetic action by acupuncture at PC6 in patients undergoing gynecological surgery (Dundee and Ghaly, 1991), and that injection of a local anesthetic procaine into ST36 blocks acupuncture analgesia in animal models (Ulett et al., 1998). Additionally, the role of afferent nerve fibers in acupuncture-initiated impulses was supported by several observations (given below). Acupuncture analgesia is reported to be ablated after sectioning nerve innervating acupoints (Noguchi and Hayashi, 1996; Kim H. Y. et al., 2010) and is reproduced by direct stimulation of exposed nerves (Li et al., 1998; Kim H. Y. et al., 2010). Manual and electroacupuncture at PC6-7 acupoints activate Aδ and C fibers to evoke a cardiovascular effect (Zhou et al., 2005), which is eliminated by neonatal capsaicin to block C-fiber afferents (Tjen-a-Looi et al., 2005). The acupoint stimulation activates opioid receptors in the rostral ventrolateral medulla, a central site regulating blood pressure (Sved et al., 2003), and suppresses stimulation-induced hypertension (Tjen-a-Looi et al., 2003; Kim et al., 2017). As shown in our previous study, mechanical stimulation of HT7 acupoints activates peripheral sensory afferents, such as Pacinian and Meissner's corpuscles, which are conveyed via large A-fibers of the ulnar nerve and spinal dorsal column somatosensory pathway. These signals enhance γ-aminobutyric acid (GABA) neuronal activity in the ventral tegmental area (VTA) and suppress extracellular dopamine release in the nucleus accumbens (Jin et al., 2018), resulting in the attenuation of cocaine-induced locomotor activity or cocaine-seeking behaviors (Kim et al., 2013; Chang et al., 2017; Jin et al., 2018). Indeed, the above evidence indicates that acupuncture stimulates afferent nerve fibers which, in turn, send messages to the brain.

An emerging theory proposes a mediating role of connective tissue in the effects of acupuncture, wherein acupuncture transmits signals through the layers of connective tissue surrounding muscle groups, organs, and blood vessels. This theory posits that acupuncture needle manipulation creates winding of connective tissue around the needle, known as "needle grasp," and in turn activates signal pathways by deformation of connective tissue, resulting in therapeutic effects (Langevin and Yandow, 2002; Langevin et al., 2007). Previous studies have also found that needle twisting produces an active cytoskeletal response in a manner dependent on the number of rotations and the angle of the needle (Langevin et al., 2007) This procedure also induces degranulation of the mast cells in the tissues of acupoints through an interaction with the collagen fibers (Zhang et al., 2008; Wu et al., 2015). Although many studies, mostly led by the Langevin research group, have proposed biomechanical actions of connective tissue during acupuncture manipulation (Langevin and Yandow, 2002; Langevin et al., 2007; Langevin, 2014), to date, it has not been determined fully whether the connective tissue is associated with therapeutic effects of acupuncture. In the present study, a peak-to-peak torque value of about 30 mN.mm was generated by twisting a needle inserted into HT7, which was decreased to about 3 mN.mm after injection of type I collagenase, similar to those reported in a previous study (Yu et al., 2009). Thus, an injection of type I collagenase into acupoints disrupted the phenomenon of "needle grasp" by causing connective tissue breakdown. Type I collagenase did not affect the expression of the neuronal marker PGP9.5 in skin, indicating that the afferent nerve in the collagenase-treated skin was intact. Importantly, disruption of connective tissue by type I collagenase failed to block the acupuncture effects generated by needle twisting in the rat models tested. On the other hand, bupivacaine, a long-acting local anesthetic (Rosenberg and Heinonen, 1983), injected into acupoints effectively blocked the acupuncture effects without affecting needle grasp of connective tissue. Taken together, our data suggest that acupuncture may not recruit connective tissue to produce therapeutic effects. In contrast to our results, Yu et al. reported that the destruction of collagen fibers with type I collagenase at ST36 acupoints inhibited the effects of acupuncture on inflammatory pain in rats (Yu et al., 2009). The reason for this discrepancy is not completely understood at present, but a possible explanation is that the acupuncture points chosen in this experiment were located on distal limbs (HT7, PC6, and BL62-64), which contain relatively less subcutaneous tissue, while the experiments in the paper by Yu et al. used ST36, which is a more proximal acupoint enriched in loose connective tissue. Considering that the interaction of the needle with collagen fibers mainly occurs within the loose subcutaneous tissue, but not within the dermis (Langevin and Yandow, 2002), the interaction between the needle and loose connective tissue in proximal acupoints such as ST36 may be greater than the distal acupoints used in the current study. However, our ability to draw conclusions about the importance of afferent nerve fibers in acupuncture-mediated responses, rather than connective tissue, was hampered by the major limitation of the present study, in that 5 points of approximately 360 acupoints were investigated using three animal models. More extensive studies using various animal models and acupoints will be required.

In conclusion, twisting acupuncture produced therapeutic effects in rat cocaine-induced locomotion, hypertension and mustard oil-induced visceral pain models, and these effects were abolished by a blockade of the afferent nerve in the vicinity of acupoints but not by disruption of collagen fibers. Accordingly, it seems reasonable to propose that the effects of acupuncture require mediation by nerve tissue but not connective tissue. This study helps to understand the mechanisms involved in the initiation of acupunctur signals.

AUTHOR CONTRIBUTIONS

HYK and CY designed the experiment. SC, YR, SB, JB, YF, OK, MB, D-HK, SL, HKK, and BL conducted the experiments. HYK was responsible for the overall direction of the project and for edits to the manuscript.

FUNDING

This research was supported by the National Research Foundation of Korea (NRF) grant

funded by the Korean government (MSIT) (No. 2018R1A5A2025272 and 2018R1E1A2A02086499), the KBRI basic research program through the Korea Brain Research Institute funded by the Ministry of Science and ICT (18-BR-03), and the Korea Institute of Oriental Medicine (KIOM) (K18181).

SUPPLEMENTARY MATERIAL

The Supplementary Material for this article can be found online at: https://www.frontiersin.org/articles/10.3389/fnins.2019.00110/full#supplementary-material

Supplementary Movie 1 | Needle twisting by a robotic acupuncture needle twister or an acupuncturist.

REFERENCES

Beiswenger, K. K., Calcutt, N. A., and Mizisin, A. P. (2008). Epidermal nerve fiber quantification in the assessment of diabetic neuropathy. *Acta Histochem.* 110, 351–362. doi: 10.1016/j.acthis.2007.12.004

Chang, S., Ryu, Y., Gwak, Y. S., Kim, N. J., Kim, J. M., Lee, J. Y., et al. (2017). Spinal pathways involved in somatosensory inhibition of the psychomotor actions of cocaine. *Sci. Rep.* 7:5359. doi: 10.1038/s41598-017-05681-7

Dundee, J. W., and Ghaly, G. (1991). Local anesthesia blocks the antiemetic action of P6 acupuncture. *Clin. Pharmacol. Ther.* 50, 78–80. doi: 10.1038/clpt.1991.106

Goldman, N., Chen, M., Fujita, T., Xu, Q., Peng, W., Liu, W., et al. (2010). Adenosine A1 receptors mediate local anti-nociceptive effects of acupuncture. *Nat. Neurosci.* 13, 883–888. doi: 10.1038/nn.2562

Guo, Z.-L., Fu, L.-W., Su, H.-F., Tjen-a-Looi, S. C., and Longhurst, J. C. (2018). Role of TRPV1 in acupuncture modulation of reflex excitatory cardiovascular responses. *Am. J. Physiol. Regulat. Integr. Comparat. Physiol.* 314, R655–R666. doi: 10.1152/ajpregu.00405.2017

Hong, S., Ding, S., Wu, F., Xi, Q., Li, Q., Liu, Y., et al. (2015). Strong manual acupuncture manipulation could better inhibit spike frequency of the dorsal horn neurons in rats with acute visceral nociception. *Evid. Based Complement. Alternat. Med.* 2015:675437. doi: 10.1155/2015/675437

Jin, W., Kim, M. S., Jang, E. Y., Lee, J. Y., Lee, J. G., Kim, H. Y., et al. (2018). Acupuncture reduces relapse to cocaine-seeking behavior via activation of GABA neurons in the ventral tegmental area. *Addict. Biol.* 23, 165–181. doi: 10.1111/adb.12499

Kim, D. H., Ryu, Y., Hahm, D. H., Sohn, B. Y., Shim, I., Kwon, O. S., et al. (2017). Acupuncture points can be identified as cutaneous neurogenic inflammatory spots. *Sci. Rep.* 7:15214. doi: 10.1038/s41598-017-14359-z

Kim, G. H., Yeom, M., Yin, C. S., Lee, H., Shim, I., Hong, M. S., et al. (2010). Acupuncture manipulation enhances anti-nociceptive effect on formalin-induced pain in rats. *Neurol. Res.* 32, 92–95. doi: 10.1179/016164109X12537002794327

Kim, H. Y., Koo, S. T., Kim, J. H., An, K., Chung, K., and Chung, J. M. (2010). Electroacupuncture analgesia in rat ankle sprain pain model: neural mechanisms. *Neurol. Res.* 32, 10–17. doi: 10.1179/016164109X12537002793689

Kim, N. J., Ryu, Y., Lee, B. H., Chang, S., Fan, Y., Gwak, Y. S., et al. (2018). Acupuncture inhibition of methamphetamine-induced behaviors, dopamine release and hyperthermia in the nucleus accumbens: mediation of group II mGluR. *Addict. Biol.* 24, 206–217. doi: 10.1111/adb.12587

Kim, S. A., Lee, B. H., Bae, J. H., Kim, K. J., Steffensen, S. C., Ryu, Y. H., et al. (2013). Peripheral afferent mechanisms underlying acupuncture inhibition of cocaine behavioral effects in rats. *PLoS ONE* 8:e81018. doi: 10.1371/journal.pone.0081018

Kim, S. K., Moon, H. J., Na, H. S., Kim, K. J., Kim, J. H., Park, J. H., et al. (2006). The analgesic effects of automatically controlled rotating acupuncture in rats: mediation by endogenous opioid system. *J. Physiol. Sci.* 56, 259–262. doi: 10.2170/physiolsci.SC002706

Langevin, H. M. (2014). Acupuncture, connective tissue, and peripheral sensory modulation. *Crit. Rev. Eukaryot. Gene Expr.* 24, 249–253. doi: 10.1615/CritRevEukaryotGeneExpr.2014008284

Langevin, H. M., Bouffard, N. A., Churchill, D. L., and Badger, G. J. (2007). Connective tissue fibroblast response to acupuncture: dose-dependent effect of bidirectional needle rotation. *J. Altern. Complement. Med.* 13, 355–360. doi: 10.1089/acm.2007.6351

Langevin, H. M., and Yandow, J. A. (2002). Relationship of acupuncture points and meridians to connective tissue planes. *Anat. Rec.* 269, 257–265. doi: 10.1002/ar.10185

Li, P., Pitsillides, K. F., Rendig, S. V., Pan, H. L., and Longhurst, J. C. (1998). Reversal of reflex-induced myocardial ischemia by median nerve stimulation: a feline model of electroacupuncture. *Circulation* 97, 1186–1194. doi: 10.1161/01.CIR.97.12.1186

Ma, Y., Dong, M., Zhou, K., Mita, C., Liu, J., and Wayne, P. M. (2016). Publication trends in acupuncture research: a 20-year bibliometric analysis based on pubmed. *PLoS ONE* 11:e0168123. doi: 10.1371/journal.pone.0168123

Napadow, V., Makris, N., Liu, J., Kettner, N. W., Kwong, K. K., and Hui, K. K. (2005). Effects of electroacupuncture versus manual acupuncture on the human brain as measured by fMRI. *Hum. Brain Mapp.* 24, 193–205. doi: 10.1002/hbm.20081

Nih Consensus Conference (1998). NIH consensus conference. Acupuncture. *JAMA* 280, 1518–1524.

Noguchi, E., and Hayashi, H. (1996). Increases in gastric acidity in response to electroacupuncture stimulation of the hindlimb of anesthetized rats. *Jpn. J. Physiol.* 46, 53–58. doi: 10.2170/jjphysiol.46.53

Pomeranz, B., and Berman, B. (2003). *Scientific Basis of Acupuncture.* Berlin: Springer.

Rosenberg, P. H., and Heinonen, E. (1983). Differential sensitivity of A and C nerve fibres to long-acting amide local anaesthetics. *Br. J. Anaesth.* 55, 163–167. doi: 10.1093/bja/55.2.163

Stux, G., and Pomeranz, B. (2012). *Acupuncture: Textbook and Atlas.* Berlin: Springer Science and Business Media.

Sved, A. F., Ito, S., and Sved, J. C. (2003). Brainstem mechanisms of hypertension: role of the rostral ventrolateral medulla. *Curr. Hypertens. Rep.* 5, 262–268. doi: 10.1007/s11906-003-0030-0

Tjen-A-Looi, S. C., Fu, L. W., Zhou, W., Syuu, Z., and Longhurst, J. C. (2005). Role of unmyelinated fibers in electroacupuncture cardiovascular responses. *Auton. Neurosci.* 118, 43–50. doi: 10.1016/j.autneu.2004.12.006

Tjen-a-Looi, S. C., Li, P., and Longhurst, J. C. (2003). Prolonged inhibition of rostral ventral lateral medullary premotor sympathetic neurons by electroacupuncture in cats. *Autonomic Neurosci.* 106, 119–131. doi: 10.1016/S1566-0702(03)00076-6

Ulett, G. A., Han, S., and Han, J. S. (1998). Electroacupuncture: mechanisms and clinical application. *Biol. Psychiatry* 44, 129–138. doi: 10.1016/S0006-3223(97)00394-6

Wu, M.-L., Xu, D.-S., Bai, W.-Z., Cui, J.-J., Shu, H.-M., He, W., et al. (2015). Local cutaneous nerve terminal and mast cell responses to manual acupuncture in acupoint LI4 area of the rats. *J. Chem. Neuroanat.* 68, 14–21. doi: 10.1016/j.jchemneu.2015.06.002

Yang, C. H., Yoon, S. S., Hansen, D. M., Wilcox, J. D., Blumell, B. R., Park, J. J., et al. (2010). Acupuncture inhibits GABA neuron activity in the ventral tegmental area and reduces ethanol self-administration. *Alcohol. Clin. Exp. Res.* 34, 2137–2146. doi: 10.1111/j.1530-0277.2010.01310.x

Yoon, S. S., Kim, H., Choi, K. H., Lee, B. H., Lee, Y. K., Lim, S. C., et al. (2010). Acupuncture suppresses morphine self-administration through the GABA receptors. *Brain Res. Bull.* 81, 625–630. doi: 10.1016/j.brainresbull.2009.12.011

Yoon, S. S., Kwon, Y. K., Kim, M. R., Shim, I., Kim, K. J., Lee, M. H., et al. (2004). Acupuncture-mediated inhibition of ethanol-induced dopamine release in the rat nucleus accumbens through the GABAB receptor. *Neurosci. Lett.* 369, 234–238. doi: 10.1016/j.neulet.2004.07.095

Yoon, S. S., Yang, E. J., Lee, B. H., Jang, E. Y., Kim, H. Y., Choi, S. M., et al. (2012). Effects of acupuncture on stress-induced relapse to cocaine-seeking in rats. *Psychopharmacology* 222, 303–311. doi: 10.1007/s00213-012-2683-3

Yu, X., Ding, G., Huang, H., Lin, J., Yao, W., and Zhan, R. (2009). Role of collagen fibers in acupuncture analgesia therapy on rats. *Connect. Tiss. Res.* 50, 110–120. doi: 10.1080/03008200802471856

Zhang, D., Ding, G., Shen, X., Yao, W., Zhang, Z., Zhang, Y., et al. (2008). Role of mast cells in acupuncture effect: a pilot study. *Explore J. Sci. Healing* 4, 170–177. doi: 10.1016/j.explore.2008.02.002

Zhou, W., Fu, L. W., Tjen, A. L. S. C., Li, P., and Longhurst, J. C. (2005). Afferent mechanisms underlying stimulation modality-related modulation of acupuncture-related cardiovascular responses. *J. Appl. Physiol.* 98, 872–880. doi: 10.1152/japplphysiol.01079.2004

Conflict of Interest Statement: The authors declare that the research was conducted in the absence of any commercial or financial relationships that could be construed as a potential conflict of interest.

frontiers in Neuroscience

ORIGINAL RESEARCH
published: 21 February 2019
doi: 10.3389/fnins.2019.00149

Effects of Leg Motor Imagery Combined With Electrical Stimulation on Plasticity of Corticospinal Excitability and Spinal Reciprocal Inhibition

Yoko Takahashi[1,2], Michiyuki Kawakami[1], Tomofumi Yamaguchi[1,3], Yusuke Idogawa[2], Shigeo Tanabe[4], Kunitsugu Kondo[2] and Meigen Liu[1]*

[1] Department of Rehabilitation Medicine, Keio University School of Medicine, Tokyo, Japan, [2] Tokyo Bay Rehabilitation Hospital, Chiba, Japan, [3] Department of Physical Therapy, Yamagata Prefectural University of Health Sciences, Yamagata, Japan, [4] Faculty of Rehabilitation, School of Health Sciences, Fujita Health University, Toyoake, Japan

Motor imagery (MI) combined with electrical stimulation (ES) enhances upper-limb corticospinal excitability. However, its after-effects on both lower limb corticospinal excitability and spinal reciprocal inhibition remain unknown. We aimed to investigate the effects of MI combined with peripheral nerve ES (MI + ES) on the plasticity of lower limb corticospinal excitability and spinal reciprocal inhibition. Seventeen healthy individuals performed the following three tasks on different days, in a random order: (1) MI alone; (2) ES alone; and (3) MI + ES. The MI task consisted of repetitive right ankle dorsiflexion for 20 min. ES was percutaneously applied to the common peroneal nerve at a frequency of 100 Hz and intensity of 120% of the sensory threshold of the tibialis anterior (TA) muscle. We examined changes in motor-evoked potential (MEP) of the TA (task-related muscle) and soleus muscle (SOL; task-unrelated muscle). We also examined disynaptic reciprocal inhibition before, immediately after, and 10, 20, and 30 min after the task. MI + ES significantly increased TA MEPs immediately and 10 min after the task compared with baseline, but did not change the task-unrelated muscle (SOL) MEPs. MI + ES resulted in a significant increase in the magnitude of reciprocal inhibition immediately and 10 min after the task compared with baseline. MI and ES alone did not affect TA MEPs or reciprocal inhibition. MI combined with ES is effective in inducing plastic changes in lower limb corticospinal excitability and reciprocal Ia inhibition.

Keywords: motor imagery, motor-evoked potential, H-reflex, disynaptic reciprocal inhibition, peripheral nerve electrical stimulation

OPEN ACCESS

Edited by:
Younbyoung Chae,
Kyung Hee University, South Korea

Reviewed by:
Kyungmo Park,
Kyung Hee University, South Korea
Junsuk Kim,
Max Planck Institute for Biological Cybernetics, Germany

***Correspondence:**
Michiyuki Kawakami
michiyukikawakami@hotmail.com

Specialty section:
This article was submitted to Perception Science, a section of the journal Frontiers in Neuroscience

Received: *12 October 2018*
Accepted: *08 February 2019*
Published: *21 February 2019*

Citation:
Takahashi Y, Kawakami M, Yamaguchi T, Idogawa Y, Tanabe S, Kondo K and Liu M (2019) Effects of Leg Motor Imagery Combined With Electrical Stimulation on Plasticity of Corticospinal Excitability and Spinal Reciprocal Inhibition. Front. Neurosci. 13:149. doi: 10.3389/fnins.2019.00149

INTRODUCTION

Motor imagery (MI) has been described as a dynamic state during which the representation of a given motor act is internally rehearsed within working memory without any overt motor output (Decety and Grezes, 1999). Brain activation during MI is similar to that observed during motor execution (Jackson et al., 2001; Chen et al., 2016; Sacheli et al., 2017). MI has been shown to increase

corticospinal excitability, the H-reflex, spinal stretch reflex, and reciprocal inhibition (Kiers et al., 1997; Hale et al., 2003; Bakker et al., 2008; Aoyama and Kaneko, 2011; Lebon et al., 2012; Kato and Kanosue, 2017; Ruffino et al., 2017; Kawakami et al., 2018). Mental practice using MI is widely used in sports and rehabilitation (Jackson et al., 2001; de Lange et al., 2008; Malouin and Richards, 2010; Mrachacz-Kersting et al., 2012, 2016; Grospretre et al., 2016; Guerra et al., 2017; Ruffino et al., 2017).

Introducing the plasticity of neural circuits involved in motor activation is important for motor recovery (Stefan et al., 2000; Wolpaw and Tennissen, 2001; Wolpaw, 2007; Di Pino et al., 2014). Previous studies using a paired associative stimulation (PAS) protocol (Stefan et al., 2000; Stinear and Hornby, 2005) have shown that spike-timing-dependent input to the motor cortex and peripheral nerves is important for the induction of plasticity in the motor cortex. Input to the motor cortex and spinal cord is also important for inducing plastic changes in spinal circuits (Wolpaw and Tennissen, 2001; Chen et al., 2016; Yamaguchi et al., 2018). One previous study used MI as the input to the motor cortex and ES as the input to the peripheral nerve (Saito et al., 2013). Indeed, a combination of finger movement MI and ES was shown to increase corticospinal excitability to a greater extent than MI or ES alone (Saito et al., 2013). Finger movement MI during action observation combined with ES for 20 min induced plastic change of corticospinal excitability at the time just after the end of the intervention, but each intervention alone was ineffective (Yasui et al., 2018). In the lower limb, Mrachacz-Kersting et al. (2012) showed that the corticospinal excitability during the application of MI using electroencephalography combined with peripheral nerve ES was greater than that during the period without MI. However, whether these effects remain after the task is currently unknown. Systematic reviews have reported the effects of MI on the upper or lower limb hemiparesis in patients with stroke (Braun et al., 2006; Guerra et al., 2017). The number of studies in the lower limb were less than those in upper limb; therefore, the therapeutic effect has not been established. Basic knowledge on the neurological effects of MI and MI combined with ES are needed to develop therapeutic strategies for lower limb MI.

The neural control of the upper and lower limb is differ depending on the task (Arya and Pandian, 2014). For motor control of the lower limb (such as that required for walking), both spinal and descending neural circuits from the motor cortex are important. Spinal reciprocal inhibition between agonist and antagonist muscles is responsible for the achievement of smooth movements (Crone and Nielsen, 1989; Morita et al., 2001). Reciprocal inhibition of calf muscles is often reduced or facilitated in patients with stroke and spinal cord injury (Crone and Nielsen, 1994; Okuma et al., 2002; Crone et al., 2003). Normalization of the reciprocal inhibition is as important as that of the neural circuits in the brain for motor recovery in the lower limb or for gait rehabilitation (Dietz and Sinkjaer, 2007).

In this study, we aimed to examine the effects of MI combined with ES on the plasticity of both corticospinal excitability and spinal reciprocal inhibition in the lower limb. We hypothesized that MI combined with peripheral nerve electrical stimulation (ES) may be superior in inducing plastic changes in cortical and spinal neural circuits than MI or ES alone.

MATERIALS AND METHODS

The Tokyo Bay Rehabilitation Hospital ethics committee approved the study protocol (approval number: 175-2). All tests were performed at the Tokyo Bay Rehabilitation Hospital. This study was registered in the University Hospital Medical Information Network (UMIN; registration number: 000028087). All participants provided written informed consent prior to enrolment. The procedures complied with the Declaration of Helsinki.

Seventeen healthy adults (mean age: 24.6 ± 2.1 years, seven females) participated in this study. None of the participants had history of neurological disease or was receiving any acute or chronic medications that could affect the central nervous system.

All participants performed the following three tasks, in a random order: (1) MI alone; (2) peripheral nerve ES alone (ES alone); and (3) MI combined with ES (MI + ES; **Figure 1A**). Tasks were performed on different days, and were separated by more than 7 days to minimize carry-over effects. Participants performed each task for 20 min. Motor-evoked potential (MEP) and disynaptic reciprocal inhibition were assessed before, immediately after (post0), and 10 (post10), 20 (post20), and 30 min (post30) after the task.

During the experimental sessions, participants remained seated on a chair with a backrest in a relaxed position with 80° hip flexion, 80° knee flexion, 10° ankle plantar flexion and their feet on the floor (**Figure 1B**).

Task

Motor Imagery

Participants were instructed to imagine dorsiflexion of their right ankle with the help of a video, for 20 min (kinesthetic motor imaging of ankle dorsiflexion). A trial consisted of imagination for 2 s and a rest period of 4 s. The full task consisted of 200 trials that were repeated over a 20 min period. To avoid muscle contraction during the MI, we monitored the electromyographic recording of the tibialis anterior (TA) and soleus (SOL) muscles and provided verbal feedback to avoid muscle contraction when signs of muscle contraction were identified.

Peripheral Nerve Electrical Stimulation

Electrical stimulation was applied to the common peroneal nerve at the fibular head. ES was delivered with a frequency of 100 Hz (pulse width 1 ms) for 2 s at an intensity of 120% of the sensory threshold of the TA at rest without muscle contraction. This stimulus intensity was determined so that MEP can be increased to a level greater than those at rest when combined with MI (Yamaguchi et al., 2012). A trial consisted of stimulation for 2 s and a rest period of 4 s. 200 trials were conducted over 20 min.

Motor Imagery Combined With Electrical Stimulation

MI was applied in the same manner as in the MI alone paradigm. Participants were asked to imagine dorsiflexion of their right

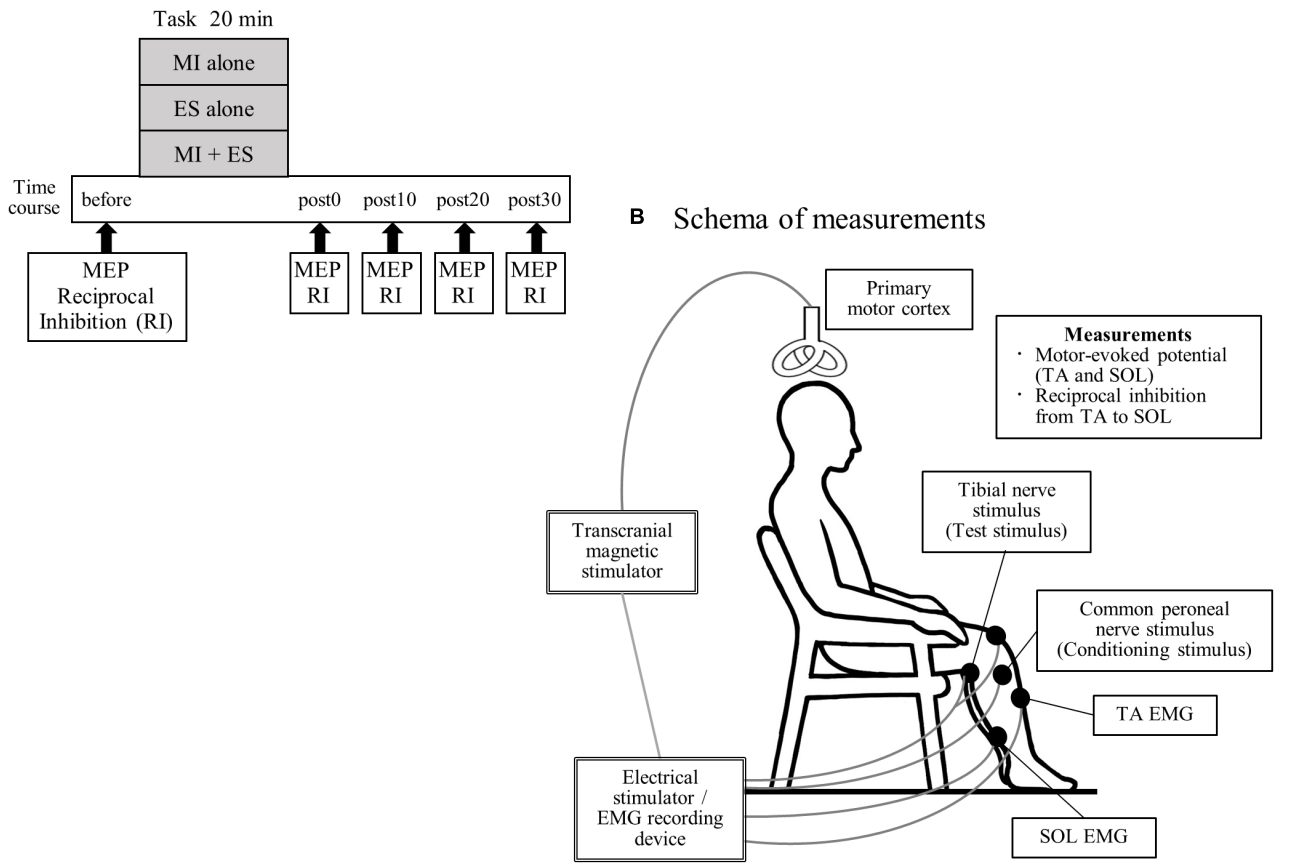

FIGURE 1 | Experimental procedure and schema of measurements. **(A)** Seventeen healthy individuals performed the following three tasks, on separate days in a random order: (1) motor imagery (MI) alone; (2) peripheral nerve electrical stimulation (ES) alone; and (3) MI combined with ES (MI + ES). We measured motor-evoked potentials (MEPs) of the tibialis anterior (TA) and soleus (SOL) muscles and reciprocal inhibition (RI) at baseline (before), immediately after (post0), 10 min after (post10), 20 min after (post20), and 30 min after (post30) the task. **(B)** Participants remained seated on a chair with a backrest, in a relaxed position. During MEP measurement, we stimulated the left primary motor cortex of the leg area using a transcranial magnetic stimulator and recorded electromyography (EMG) of the right TA and SOL. Reciprocal inhibition was assessed using a soleus H-reflex conditioning-test paradigm. The H-reflex in SOL was elicited by stimulating the tibial nerve at the popliteal fossa. A positive stimulation electrode was set above the patella. The conditioning stimulus was applied to the common peroneal nerve below the fibular head.

ankle at the same time that ES was applied. 200 trials were conducted over 20 min.

Assessment

Motor-Evoked Potential

The schema of the experimental measurements is presented in **Figure 1B**. MEPs were assessed using transcranial magnetic stimulation. Since the MI task consisted of ankle dorsiflexion, we selected the TA as a task-related muscle, and the SOL as a task-unrelated muscle. We stimulated the left primary motor cortex using a Magstim 200 magnetic stimulator (The Magstim Company, Whitland, Dyfed, United Kingdom) and a double-cone coil. The stimulation site was selected to coincide with the point where MEP amplitude of the right TA was the largest. The stimulus intensity was defined as 120% of the resting motor threshold of each muscle. The resting motor threshold was defined as the intensity that evoked responses of 100-μV (at 5 of 10) in the TA or SOL muscle at rest. A total of 15 MEPs were recorded for each muscle. Peak-to-peak amplitudes were averaged for each time point.

Reciprocal Inhibition

We measured spinal reciprocal inhibition of the calf muscles, i.e., reciprocal inhibition from the TA to the SOL. Reciprocal inhibition was assessed using a soleus H-reflex conditioning-test paradigm. The H-reflex in the soleus muscle was elicited by stimulating the tibial nerve at the popliteal fossa (1 ms rectangular pulse). A positive (anode) stimulation electrode was set above the patella. Throughout the experiment, the test H-reflex amplitude was maintained at 15–20% of the amplitude of the maximum motor response for the SOL, as previously described (Crone et al., 1990). The conditioning stimulus was delivered to the common peroneal nerve using surface electrodes positioned below the fibular head. The conditioning stimulus intensity was defined

as 1.0 × motor threshold. The motor threshold was defined as the intensity that evoked a response of 100 μV in the TA at rest. The common peroneal nerve-stimulating electrode was carefully positioned to avoid activation of the peroneus muscles, thereby ensuring selective stimulation of the deep branch of the peroneal nerve (Crone et al., 1990). The conditioning stimulus was repeatedly checked during the experiments by monitoring the M wave of the TA. The interval between the conditioning and test stimulus was set at 0, 1, 2, and 3 ms (Fujiwara et al., 2011). The optimal interval to produce disynaptic reciprocal inhibition by stimulating the common peroneal nerve was determined at the beginning of each session and used throughout. Ten conditioned and 10 test H-reflexes were recorded at each time point. Reciprocal inhibition was defined as the mean conditioned H-reflex amplitude/mean test H-reflex amplitude.

Motor Imagery Ability

To assess MI ability, all participants answered the Vividness of Movement Imagery Questionnaire-2 (VMIQ-2, Roberts et al., 2008) at the beginning of the experiment. The VMIQ-2 is one of the most commonly used questionnaires to assess the vividness of MI. This questionnaire is used to determine the level of vividness with which the 12 motor tasks can be imagined from the viewpoint of the following three factors: internal visual imagery, external visual imagery, and kinesthetic imagery. Subjects rate the vividness of their MI on a five-point scale (1 = perfectly vivid and as clear as normal vision, 5 = no image at all). The maximum score is 60 points per factor. A low score indicates greater imagery ability.

Statistical Analysis

We calculated the sample size of the study based on our previous study that examined the after-effects of reciprocal inhibition by ES combined with voluntary contraction (Takahashi et al., 2017). We performed the power analysis based on the following: effect size, 1.39; α error, 0.05; and statistical power, 0.95 using G*Power 3.1.9.2 for Windows (Heinrich Heine University, Dusseldorf, Germany). The power analysis indicated that 12 samples were needed. We recruited 17 participants, which fully satisfied the power sample size requirements.

A two-factor repeated-measures analysis of variance (ANOVA) was used to analyze the main and interaction effects of task (MI alone, ES alone, and MI + ES) and time (before, post0, post10, post20, and post30) on TA MEP amplitudes, test H amplitudes, and reciprocal inhibition. Paired *t*-tests, with Bonferroni correction for multiple comparisons, were performed as post-hoc tests, when a significant result was obtained in the primary analyses. Prior to ANOVA, we confirmed that all TA MEPs and reciprocal inhibition variables were normally distributed using Shapiro–Wilk tests. SOL MEPs were not normally distributed; therefore, we used Wilcoxon signed rank tests to compare SOL MEPs before and at each time point after the task.

To assess the relationship between MI ability and the effects of the MI + ES task, a Spearman's rank correlation coefficient was performed. We compared the correlation between the VMIQ-2 mean score (internal visual imagery, external visual imagery, and kinesthetic imagery) and changes in TA MEPs and reciprocal inhibition after the intervention. Changes in TA MEPs and reciprocal inhibition after the intervention were calculated as the difference between the valuables before and post0.

Statistical analyses were performed using SPSS 24 (IBM Corp., Armonk, NY, United States) for Windows. Results with $p < 0.05$ were considered statistically significant.

RESULTS

MEP Amplitudes

Figure 2 shows the representative change in TA MEPs in one participant. We found a significant main effect of task ($F_{2,32} = 7.733$, $p = 0.002$) and a significant interaction between task (MI alone, ES alone, and MI + ES) and time (before, post0, post10, post20, and post30) ($F_{8,128} = 2.892$, $p = 0.005$) for MEPs of the task-related TA muscle. No significant main effect of time ($F_{4,64} = 0.854$, $p = 0.497$) was observed. *Post hoc* paired *t*-test comparisons revealed that TA MEPs were significantly higher at post0 and post10 after MI + ES than at baseline (post0: $p = 0.009$, post10: $p = 0.009$; **Table 1** and **Figure 3A**). MI alone and ES alone did not produce any significant changes in TA MEPs at any time point. TA MEPs of MI + ES were significantly higher than that of MI alone at post0 ($p = 0.014$). TA MEPs of MI + ES were also significantly higher than that of ES alone at post0 ($p = 0.002$), post10 ($p = 0.004$), post20 ($p = 0.027$), and post30 ($p = 0.011$).

We could only measure SOL MEPs in 12 of the 17 participants. A Wilcoxon signed rank test revealed no significant difference among SOL MEPs at any time point (**Figure 3B**).

Reciprocal Inhibition

No significant main effects of task ($F_{2,32} = 0.339$, $p = 0.715$) or time ($F_{4,64} = 0.971$, $p = 0.43$), and no significant interactions

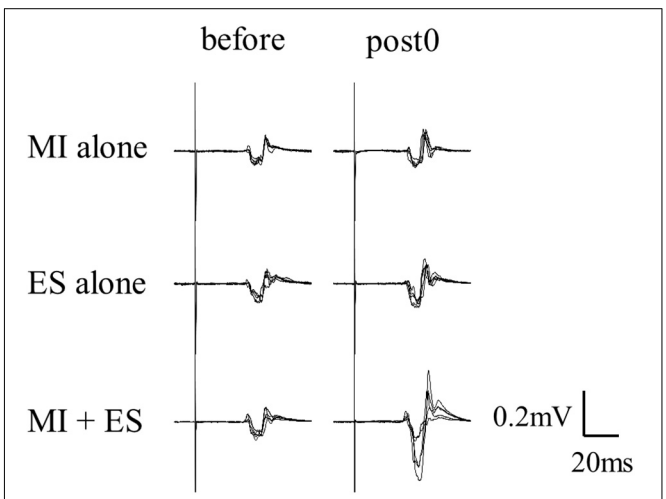

FIGURE 2 | Representative TA MEPs (before and at post0). MI alone and ES alone showed no significant change in TA MEPs at post0 in comparison with baseline. TA MEP of MI combined with ES (MI + ES) at post0 was significantly higher than at baseline.

TABLE 1 | Statistical results of the *post hoc* paired *t*-tests with Bonferroni correction in tibialis anterior motor-evoked potentials.

Comparison with the baseline within task				
Task	***p*-value [95% confidence interval of mean difference]**			
	post0	**post10**	**post20**	**post30**
MI alone	1.0 [−44.3–91.8]	1.0 [−61.1–50.5]	1.0 [−63.9–110.8]	1.0 [−97.1–81.7]
ES alone	1.0 [−75.0–77.6]	1.0 [−65.9–64.2]	1.0 [−81.4–71.9]	1.0 [−68.4–82.1]
MI + ES	0.009** [−117.3–−13.2]	0.009** [−111.6–−12.3]	0.132 [−123.8–9.6]	1.0 [−111.9–35.3]
Comparison of the value among tasks at the same time points				
Task	***p*-value [95% confidence interval of mean difference]**			
	post0	**post10**	**post20**	**post30**
MI alone vs. ES alone	0.819 [−29.1–72.1]	0.245 [−20.6–114.3]	1.0 [−35.9–64.4]	0.213 [−21.7–135.9]
MI alone vs. MI + ES	0.014* [−162.1–−16.3]	0.152 [−128.9–15.1]	0.052 [−0.6–162.2]	0.947 [−48.7–110.3]
ES alone vs. MI + ES	0.002* [−180.4–−41.0]	0.004* [−174.5–−33.1]	0.027* [−180.8–−9.3]	0.011* [−157.2–−18.5]

*MI, motor imagery; ES, electrical stimulation; MI + ES, motor imagery combined with electrical stimulation; **$p < 0.01$, *$p < 0.05$.*

between task and time ($F_{8,128} = 0.909$, $p = 0.511$) were identified for the test H amplitudes.

We found significant main effects of task ($F_{2,32} = 13.764$, $p < 0.001$) and time ($F_{4,64} = 3.384$, $p = 0.014$) for reciprocal inhibition. A significant interaction between task and time was also observed ($F_{8,128} = 13.764$, $p = 0.004$). *Post hoc* paired *t*-test comparisons showed that reciprocal inhibition was significantly higher at post0 and post10 in the MI + ES group than at baseline (post0: $p = 0.003$, post10: $p = 0.032$; **Table 2** and **Figure 3C**). MI alone and ES alone showed no significant changes in reciprocal inhibition in comparison with baseline at any of the time point evaluated. Reciprocal inhibition in MI + ES was significantly higher than in MI alone at post0 ($p = 0.007$), post10 ($p = 0.003$), and post20 ($p = 0.028$). Reciprocal inhibition in MI + ES was also significantly higher than in ES alone at post0 ($p = 0.027$), post10 ($p = 0.035$), post20 ($p = 0.026$), and post30 ($p = 0.04$).

Motor Imagery Ability

The VMIQ-2 mean score was 26.9 ± 8.7 (mean ± SD) for the internal visual imagery subscale, 28.5 ± 11.0 for the external visual imagery subscale, and 26.1 ± 8.4 for the kinesthetic imagery subscale. There were no significant correlations between changes in TA MEPs or reciprocal inhibition after intervention and the VMIQ-2 scores.

DISCUSSION

We found that ankle dorsiflexion MI combined with ES increased task-related muscle (TA) MEPs and reciprocal inhibition from the TA to the SOL. Intervention had no effect on task-unrelated muscle (SOL) MEPs. MI and ES alone produced no effects on TA or SOL MEPs or reciprocal inhibition. Our study provides the first evidence that a combination of MI and ES is effective at inducing plasticity of both lower limb corticospinal excitability and spinal reciprocal inhibition circuits.

Corticospinal Excitability

We found that MI + ES resulted in significantly higher TA MEPs immediately after the task than at baseline. These effects remained for up to 10 min after the task. These results indicate that MI combined with ES can induce plastic changes such as long-term potentiation of the primary motor cortex and/or corticospinal circuits (Huang et al., 2011). Our results align with those previously presented by Khaslavskaia and Sinkjaer (2005), where the authors reported that voluntary dorsiflexion combined with ES of the common peroneal nerve maintained the enhanced corticospinal excitability of the TA for longer than voluntary dorsiflexion or ES alone. The combination of the activities of the somatosensory afferents and intrinsic motor cortical circuits may be important for inducing cortical plasticity (Stefan et al., 2000). It is known that MI alone and ES alone (Bakker et al., 2008; Yamaguchi et al., 2012), and MI using electroencephalography combined with ES (Mrachacz-Kersting et al., 2012) increase the excitability of a region of the primary motor cortex in real time. It is possible that the spike-timing-dependent plasticity resulting from combined inputs may have occurred at a synapse somewhere in corticospinal pathway of the TA (Stefan et al., 2000; Stinear and Hornby, 2005). Few studies have investigated the effects of ES alone on MEPs after intervention. One study indicated that ES applied to the common peroneal nerve for 30 min induced plastic changes in TA MEPs (Khaslavskaia and Sinkjaer, 2005). In another study targeting the upper extremity, ES alone for 14 min did not induce any plastic changes (Taylor et al., 2012). Thus, it is possible that the time-window of stimulation used in our study (20 min) was insufficient to induce plastic changes in the corticospinal excitability of the TA following ES. Kaneko et al. (2014) showed that MEP during ES alone was not higher than at rest. The short-term effect of ES alone on corticospinal excitability may be less than that of MI + ES. Yasui et al. (2018) demonstrated that MI during action observation combined with ES significantly increased MEP by 10 min, however, MI during action observation or ES alone for

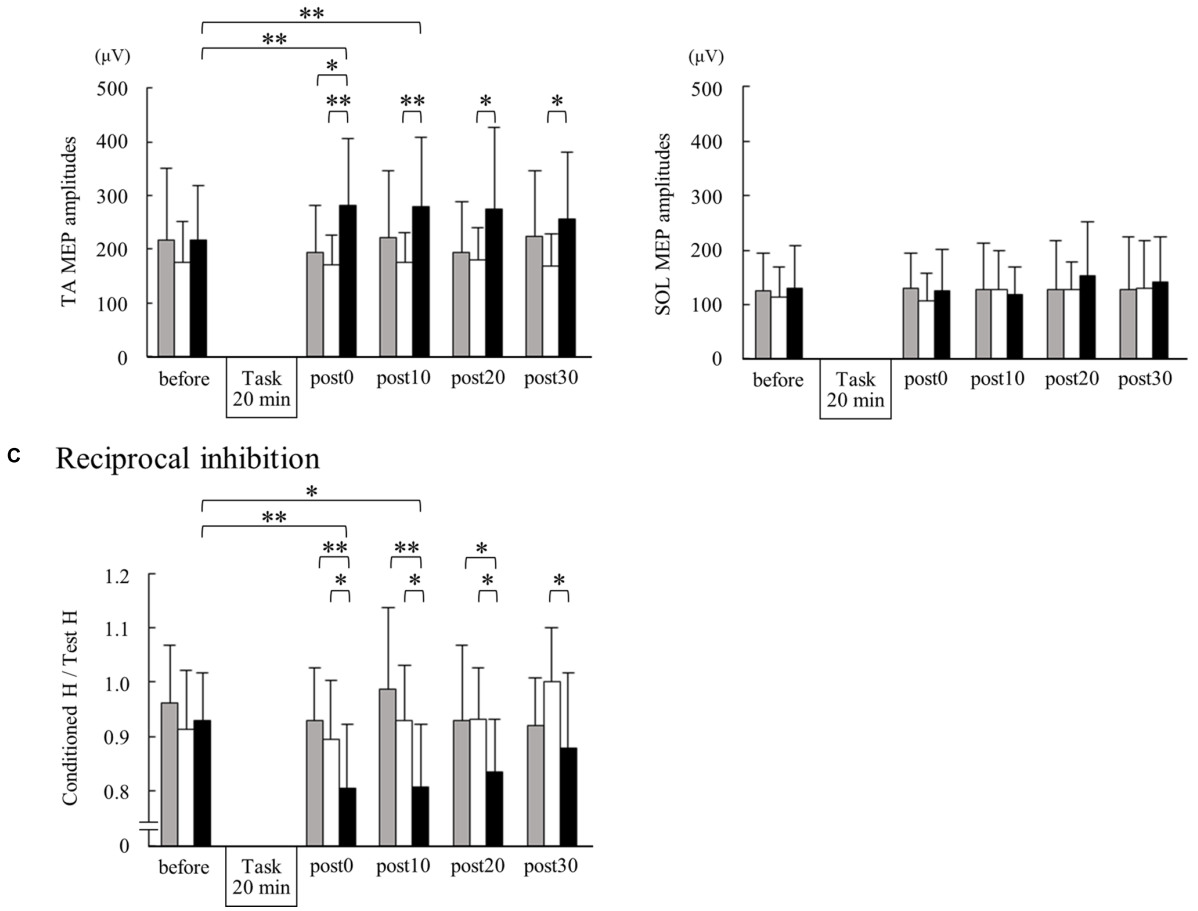

FIGURE 3 | Changes in TA MEPs, soleus (SOL) MEPs, and reciprocal inhibition before and after motor imagery alone, electrical stimulation alone, and motor imagery combined with electrical stimulation. The peak-to-peak amplitudes from 15 TA MEPs **(A)** and 15 SOL MEPs **(B)** measurements acquired at each time point were averaged for each subject. For reciprocal inhibition **(C)**, 10 test and 10 conditioned reflexes were averaged at each time point for each subject. Group means + standard deviations are plotted for each time point; motor imagery alone (gray bar), electrical stimulation alone (white bar), motor imagery combined with electrical stimulation (black bar). Asterisks indicate significant differences as identified by *post hoc* paired *t*-tests (*$p < 0.05$, **$p < 0.01$).

TABLE 2 | Statistical results of the *post hoc* paired *t*-tests with Bonferroni correction in reciprocal inhibition.

Comparison with the baseline within task				
Task	***p*-value [95% confidence interval of mean difference]**			
	post0	**post10**	**post20**	**post30**
MI alone	1.0 [−0.079–0.140]	1.0 [−0.170–0.116]	1.0 [−0.086–0.147]	1.0 [−0.070–0.149]
ES alone	1.0 [−0.068–0.103]	1.0 [−0.103–0.067]	1.0 [−0.135–0.096]	0.364 [−0.213–0.037]
MI + ES	0.003** [0.036–0.209]	0.032* [0.007–0.237]	0.073 [−0.006–0.194]	1.0 [−0.088–0.188]
Comparison of the value among tasks at the same time points				
Task	***p*-value [95% confidence interval of mean difference]**			
	post0	**post10**	**post20**	**post30**
MI alone vs. ES alone	1.0 [−0.068–0.138]	0.624 [−0.059–0.173]	1.0 [−0.094–0.089]	0.062 [−0.163–0.003]
MI alone vs. MI + ES	0.007** [0.032–0.217]	0.003** [0.060–0.302]	0.028* [0.009–0.182]	0.982 [−0.069–0.153]
ES alone vs. MI + ES	0.027* [0.009–0.170]	0.035* [0.008–0.241]	0.026* [0.011–0.185]	0.04* [0.005–0.239]

*MI, motor imagery; ES, electrical stimulation; MI + ES, motor imagery combined with electrical stimulation; **$p < 0.01$, *$p < 0.05$.*

20 min did not increase MEP. The effect of MI alone for 20 min on corticospinal excitability might be insufficient, just as ES alone.

As expected, we could not find any changes in the task-unrelated muscle (SOL) MEPs following any of our tasks. One previous study examining corticospinal excitability during MI showed that MI increased corticospinal excitability in both task-related and task-unrelated muscles (Bakker et al., 2008). Although we cannot completely discard the possibility of an increase in corticospinal excitability for the task-unrelated muscle given the limited amount of data we were able to collect, we hypothesize that combining ES with MI may help to focalize the effects on excitability in the areas of the primary motor cortex or corticospinal tract related to the task-relevant muscle.

Reciprocal Inhibition

We found that MI + ES also significantly increased reciprocal inhibition immediately after the task when compared to the baseline. This effect remained up to 10 min after the task. Spinal Ia inhibitory interneurons projecting to the antagonist (SOL) motor neuron receive convergent inputs from the motor cortex and Ia afferents of the agonist muscle (TA) (Nielsen et al., 1993; Masakado et al., 2001). It has been shown that combining descending inputs coming from the corticospinal tracts during voluntary movements with those coming from Ia afferents during ES induces plastic changes of the Ia inhibitory circuit (Yamaguchi et al., 2013; Takahashi et al., 2017, 2018). This mechanism may underlie the effects on reciprocal inhibition we have reported herein. MI and ES alone did not affect reciprocal inhibition. Long-term interventions that target the upper extremities using MI have been known to induce plasticity of the reciprocal inhibition circuits in patients after stroke (Kawakami et al., 2018). However, the effect of short-time MI on reciprocal inhibition remains unknown. Motor cortex excitability is important for maintaining plastic changes in spinal reciprocal inhibition (Wolpaw and Tennissen, 2001; Chen et al., 2006; Fujiwara et al., 2011; Yamaguchi et al., 2013, 2016). Based on our findings, we suggest that short-term motor descending inputs during MI alone are not sufficient to induce plastic changes of the reciprocal inhibition spinal circuits – and that longer times may be needed for the effects to emerge.

In our study, ES alone also did not change reciprocal inhibition. Perez et al. (2003) showed that ES that mimicked aspects of sensory feedback from muscle spindle during walking was effective in inducing plastic changes in reciprocal inhibition, while ES with constant period parameters was ineffective. In our study, stimulus intensity was lower than that found by Perez et al. (2003). The parameters used for the stimulation may be important determinants of the ES effects on the plasticity of the reciprocal inhibition circuits.

Motor Imagery Ability

Although we first hypothesized that the increase in MEP and reciprocal inhibition after MI + ES would be correlated with an individual's MI ability, we did not find any significant relationship between the effects on TA MEPs or reciprocal inhibition after MI + ES and the VMIQ-2 scores. MI ability, as assessed by the VMIQ-2, and corticospinal excitability during MI have been known to correlate positively, at least when the upper extremities are the targets for the MI intervention (Lebon et al., 2012; Williams et al., 2012). Previous studies have focused on skillful finger movement imagery. To our knowledge, no previous reports have examined the relationship between MI ability and corticospinal excitability during MI, when the lower limb are the targets for the MI intervention. It is possible that the absence of a correlation between MI + ES effects on MEPs and reciprocal inhibition and MI ability in our study derives from the fact that the movement of the lower limb is coarse when compared with that of skillful finger movement. Future studies examining and comparing different movements will be needed to clarify whether this association is found only in some cases.

Comparison With Results in the Upper Limb

The present study showed that MI alone and ES alone did not change MEPs or reciprocal inhibition, and that MI + ES effectively increased TA MEP and reciprocal inhibition. The combined effects found were similar to those from a previous study in the upper limb (Yasui et al., 2018). These results suggest that combining ES with MI rehabilitation in the lower limb might be effective for neuromodulation in patients with central nervous system lesions. For gait rehabilitation in patients with central nervous system lesions, some strategies such as robotic gait training (Cheung et al., 2017; Holanda et al., 2017; Bruni et al., 2018) or body-weight support treadmill gait training (Mehrholz et al., 2017) can be used; however, the therapy for lower limb paralysis itself is limited. Our results, which indicated that MI + ES might be an effective treatment of lower limb paralysis, are of clinical importance.

Clinical Implications

The induction of long-term potentiation in neural circuits is important for motor recovery in patients with central nervous system lesions. Reduced reciprocal inhibition correlates with the development of hyperactive reflexes and spasticity (Crone and Nielsen, 1994; Okuma et al., 2002; Crone et al., 2003). Furthermore, restoring reciprocal inhibition is important to improve the movement of paretic ankles. We suggest that MI + ES is a useful and safe rehabilitation method that can be performed even in patients who are severely paralyzed and have difficulty performing voluntary movements. As a next step, we would like to investigate the effects of MI + ES on reciprocal inhibition in patients with central nervous system lesions.

Limitations

In this study, we measured the effects of MI + ES in healthy subjects. It is necessary to investigate the effects of MI + ES in patients with central nervous system lesions, i.e., those who would be the target of neuromodulation in clinical practice. We could not measure SOL MEPs from all subjects, which limited our power to detect potential effects on the task-unrelated muscle. A similar problems was faced by Bakker et al. (2008), who was unable to reliably record MEPs of the medial gastrocnemius muscle during ankle dorsiflexion MI. Future studies should

consider this limitation when selecting about the MI task and the muscle used to record MEPs.

CONCLUSION

Ankle dorsiflexion MI combined with ES enhanced TA MEPs and reciprocal inhibition; these effects persisted after the task. In addition to other descending modulation methods such as brain stimulation or voluntary muscle contraction, the combination of MI with afferent input stimulation through ES may be effective in inducing plasticity of the corticospinal excitability and spinal reciprocal inhibition circuits.

AUTHOR CONTRIBUTIONS

YT, MK, and TY contributed to the concept, idea, research design, and project management. YT, MK, TY, and ML wrote the manuscript. YT, YI, and KK recruited participants and collected data. YT and YI performed data analysis. MK, TY, and KK provided facilitates and equipment. ST wrote the program for data collection. ML procured funding. YT, MK, TY, KK, and ML provided consultation (including review of manuscript before submission).

FUNDING

This work was partially supported Japan Agency for Medical Research and Development (AMED): Research and Development of Advanced Medical Devices and Systems to Achieve the Future of Medicine-Development of advanced medical equipment-research and development into medical device systems to restore function in patients with motor and sensory paralysis under Grant Number JP18he0402255.

ACKNOWLEDGMENTS

The authors would like to thank Ms. Saeko Kawamoto for her descriptive illustration.

REFERENCES

Aoyama, T., and Kaneko, F. (2011). The effect of motor imagery on gain modulation of the spinal reflex. *Brain Res.* 1372, 41–48. doi: 10.1016/j.brainres.2010.11.023

Arya, K. N., and Pandian, S. (2014). Interlimb neural coupling: implications for poststroke hemiparesis. *Ann. Phys. Rehabil. Med.* 57, 696–713. doi: 10.1016/j.rehab.2014.06.003

Bakker, M., Overeem, S., Snijders, A. H., Borm, G., van Elwijik, G., Toni, I., et al. (2008). Motor imagery of foot dorsiflexion and gait: effects on corticospinal excitability. *Clin. Neurophysiol.* 119, 2519–2527. doi: 10.1016/j.clinph.2008.07.282

Braun, S. M., Beurskens, A. L., Borm, P. J., Schack, T., and Wade, D. T. (2006). The effects of mental practice in stroke rehabilitation: a systematic review. *Arch. Phys. Med. Rehabil.* 87, 842–852. doi: 10.1016/j.apmr.2006.02.034

Bruni, M. F., Melegari, C., De Cola, M. C., Bramanti, A., Bramanti, P., and Calabro, R. S. (2018). What does best evidence tell us about robotic gait rehabilitation in stroke patients: a systematic review and meta-analysis. *J. Clin. Neurosci.* 48, 11–17. doi: 10.1016/j.jocn.2017.10.048

Chen, X., Wan, L., Qin, W., Zheng, W., Qi, Z., Chen, N., et al. (2016). Functional preservation and reorganization of brain during motor imagery in patients with incomplete spinal cord injury: a pilot fMRI study. *Front. Hum. Neurosci.* 10:46. doi: 10.3389/fnhum.2016.00046

Chen, X. Y., Chen, L., Chen, Y., and Wolpaw, J. R. (2006). Operant conditioning of reciprocal inhibition in rat soleus muscle. *J. Neurophysiol.* 96, 2144–2150. doi: 10.1152/jn.00253.2006

Cheung, E. Y. Y., Ng, T. K. W., Yu, K. K. K., Kwan, R. L. C., and Cheing, G. L. Y. (2017). Robot-assisted training for people with spinal cord injury: a meta-analysis. *Arch. Phys. Med. Rehabil.* 98, 2320–2331. doi: 10.1016/j.apmr.2017.05.015

Crone, C., Hultborn, H., Mazieres, L., Morin, C., Nielsen, J., and Pierrot-Deseilligny, E. (1990). Sensitivity of monosynaptic test reflex to facilitation and inhibition as a function of the test reflex size: a study in man and the cat. *Exp. Brain Res.* 81, 35–45. doi: 10.1007/BF00230098

Crone, C., Johnsen, L. L., Biering-Sørensen, F., and Nielsen, B. (2003). Appearance of reciprocal facilitation of ankle extensors from ankle flexors in patients with stroke or spinal cord injury. *Brain* 126, 495–507. doi: 10.1093/brain/awg036

Crone, C., and Nielsen, J. (1989). Spinal mechanisms in man contributing to reciprocal inhibition during voluntary dorsiflexion of the foot. *J. Physiol.* 416, 255–272. doi: 10.1113/jphysiol.1989.sp017759

Crone, C., and Nielsen, J. (1994). Central control disynaptic reciprocal inhibition in humans. *Acta Physiol. Scand.* 152, 351–363. doi: 10.1111/j.1748-1716.1994.tb09817.x

de Lange, F. P., Roelofs, K., and Toni, I. (2008). Motor imagery: a window into the mechanisms and alterations of the motor system. *Cortex* 44, 494–506. doi: 10.1016/j.cortex.2007.09.002

Decety, J., and Grezes, J. (1999). Neural mechanisms subserving the perception of human actions. *Trends Cogn. Sci.* 3, 172–178. doi: 10.1016/S1364-6613(99)01312-1

Di Pino, G., Pellegrino, G., Assenza, G., Capone, F., Ferreri, F., Formica, D., et al. (2014). Modulation of brain plasticity in stroke: a novel model for neurorehabilitation. *Nat. Rev. Neurol.* 10, 597–608. doi: 10.1038/nrneurol.2014.162

Dietz, V., and Sinkjaer, T. (2007). Spastic movement disorder: impaired reflex function and altered muscle mechanics. *Lancet Neurol.* 6, 725–733. doi: 10.1016/S1474-4422(07)70193-X

Fujiwara, T., Tsuji, T., Honaga, K., Hase, K., Ushiba, J., and Liu, M. (2011). Transcranial direct current stimulation modulates the spinal plasticity induced with patterned electrical stimulation. *Clin. Neurophysiol.* 122, 1834–1837. doi: 10.1016/j.clinph.2011.02.002

Grospretre, S., Ruffino, C., and Lebon, F. (2016). Motor imagery and cortico-spinal excitability: a review. *Eur. J. Sport Sci.* 16, 317–324. doi: 10.1080/17461391.2015.1024756

Guerra, Z. F., Lucchetti, A. L. G., and Lucchetti, G. (2017). Motor imagery training after stroke: a systematic review and meta-analysis of randomized controlled trials. *J. Neurol. Phys. Ther.* 41, 205–214. doi: 10.1097/NPT.0000000000000200

Hale, B. S., Raglin, J. S., and Koceja, D. M. (2003). Effect of mental imagery of a motor task on the Hoffman reflex. *Behav. Brain Res.* 142, 81–87. doi: 10.1016/S0166-4328(02)00397-2

Holanda, L. J., Silva, P. M. M., Amorim, T. C., Lacerda, M. O., Simao, C. R., and Morya, E. (2017). Robotic assisted gait as a tool for rehabilitation of individuals with spinal cord injury: a systematic review. *J. Neuroeng. Rehabil.* 14:126. doi: 10.1186/s12984-017-0338-7

Huang, Y. Z., Rothwell, J. C., Chen, R. S., Lu, C. S., and Chuang, W. L. (2011). The theoretical model of theta burst form of repetitive transcranial magnetic stimulation. *Clin. Neurophysiol.* 122, 1011–1018. doi: 10.1016/j.clinph.2010.08.016

Jackson, P. L., Lafleur, M. F., Malouin, F., Richards, C., and Doyon, J. (2001). Potential role of mental practice using motor imagery in neurologic rehabilitation. *Arch. Phys. Med. Rehabil.* 82, 1133–1141. doi: 10.1053/apmr.2001.24286

Kaneko, F., Hayami, T., Aoyama, T., and Kizuka, T. (2014). Motor imagery and electrical stimulation reproduce corticospinal excitability at levels similar to voluntary contraction. *J. Neuroeng. Rehabil.* 11:94. doi: 10.1186/1743-0003-11-94

Kato, K., and Kanosue, K. (2017). Corticospinal excitability for hand muscles during motor imagery of foot changes with imagined force level. *PLoS One* 12:e0185547. doi: 10.1371/journal.pone.0185547

Kawakami, M., Okuyama, K., Takahashi, Y., Hiramoto, M., Nishimura, A., Ushiba, J., et al. (2018). Change in reciprocal inhibition of the forearm with motor imagery among patients with chronic stroke. *Neural Plast.* 2018:3946367. doi: 10.1155/2018/3946367

Khaslavskaia, S., and Sinkjaer, T. (2005). Motor cortex excitability following repetitive electrical stimulation of the common peroneal nerve depends on the voluntary drive. *Exp. Brain Res.* 162, 497–502. doi: 10.1007/s00221-004-2153-1

Kiers, L., Fernando, B., and Tomkins, D. (1997). Facilitatory effect of thinking about movement on magnetic motor-evoked potentials. *Electromyogr. Clin. Neurophysiol.* 105, 262–268. doi: 10.1016/S0921-884X(97)00027-1

Lebon, F., Byblow, W. D., Collet, C., Guillot, A., and Stinear, C. M. (2012). The modulation of motor cortex excitability during motor imagery depends on imagery quality. *Eur. J. Neurosci.* 35, 323–331. doi: 10.1111/j.1460-9568.2011.07938.x

Malouin, F., and Richards, C. L. (2010). Mental practice for relearning locomotor skills. *Phys. Ther.* 90, 240–251. doi: 10.2522/ptj.20090029

Masakado, Y., Muraoka, Y., Tomita, Y., and Chino, N. (2001). The effect of transcranial magnetic stimulation on reciprocal inhibition in the human leg. *Electromyogr. Clin. Neurophysiol.* 41, 429–432.

Mehrholz, J., Thomas, S., and Elsner, B. (2017). Treadmill training and body weight support for walking after stroke. *Cochrane Database Syst. Rev.* 8:CD002840. doi: 10.1002/14651858.CD002840

Morita, H., Crone, C., Chistenhuis, D., Petersen, N. T., and Nielsen, J. B. (2001). Modulation of presynaptic inhibition and disynaptic reciprocal Ia inhibition during voluntary movement in spasticity. *Brain* 124, 826–837. doi: 10.1093/brain/124.4.826

Mrachacz-Kersting, N., Jiang, N., Stevenson, A. J., Niazi, I. K., Kostic, V., Pavlovic, A., et al. (2016). Efficient neuroplasticity induction in chronic stroke patients by an associative brain-computer interface. *J. Neurophysiol.* 115, 1410–1421. doi: 10.1152/jn.00918.2015

Mrachacz-Kersting, N., Kristensen, S. R., Niazi, I. K., and Farina, D. (2012). Precise temporal association between cortical potentials evoked by motor imagination and afference induces cortical plasticity. *J. Physiol.* 590, 1669–1682. doi: 10.1113/jphysiol.2011.222851

Nielsen, J., Petersen, N., Deuschi, G., and Ballegaard, M. (1993). Task-related changes in the effect of magnetic brain stimulation on spinal neurons in man. *J. Physiol.* 471, 223–243. doi: 10.1113/jphysiol.1993.sp019899

Okuma, Y., Mizuno, Y., and Lee, R. G. (2002). Reciprocal Ia inhibition in patients with asymmetric spinal spasticity. *Clin. Neurophysiol.* 113, 292–297. doi: 10.1016/S1388-2457(02)00004-4

Perez, M. A., Field-Fote, E. C., and Floeter, M. K. (2003). Patterned sensory electrical stimulation induces plasticity in reciprocal Ia inhibition in humans. *J. Neurosci.* 23, 2014–2018. doi: 10.1523/JNEUROSCI.23-06-02014.2003

Roberts, R., Callow, N., Hardy, L., Markland, D., and Bringer, J. (2008). Movement imagery ability: development and assessment of a revised version of the vividness of movement imagery questionnaire. *J. Sport Exerc. Psychol.* 30, 200–221. doi: 10.1123/jsep.30.2.200

Ruffino, C., Papaxanthis, C., and Lebon, F. (2017). Neural plasticity during motor learning with motor imagery practice: review and perspectives. *Neuroscience* 341, 61–78. doi: 10.1016/j.neuroscience.2016.11.023

Sacheli, L. M., Zapparoli, L., Santis, C. D., Preti, M., Pelosi, C., Ursino, N., et al. (2017). Mental steps: differential activation of internal pacemakers in motor imagery and in mental imitation of gait. *Hum. Brain Mapp.* 38, 5195–5216. doi: 10.1002/hbm.23725

Saito, K., Yamaguchi, T., Yoshida, N., Tanabe, S., Kondo, K., and Sugawara, K. (2013). Combined effect of motor imagery and peripheral nerve electrical stimulation on the motor cortex. *Exp. Brain Res.* 227, 333–342. doi: 10.1007/s00221-013-3513-5

Stefan, K., Kunesch, E., Cohen, L. G., Benecke, R., and Classen, J. (2000). Induction of plasticity in the human motor cortex by paired associative stimulation. *Brain* 123, 572–584. doi: 10.1093/brain/123.3.572

Stinear, J. W., and Hornby, T. G. (2005). Stimulation-induced changes in lower corticomotor excitability during treadmill walking in humans. *J. Physiol.* 567, 701–711. doi: 10.1113/jphysiol.2005.090654

Takahashi, Y., Fujiwara, T., Yamaguchi, T., Kawakami, M., Mizuno, K., and Liu, M. (2017). The effects of patterned electrical stimulation combined with voluntary contraction on spinal reciprocal inhibition in healthy individuals. *Neuroreport* 28, 434–438. doi: 10.1097/WNR.0000000000000777

Takahashi, Y., Fujiwara, T., Yamaguchi, T., Matsunaga, H., Kawakami, M., Honaga, K., et al. (2018). Voluntary contraction enhances spinal reciprocal inhibition induced by patterned electrical stimulation in patients with stroke. *Restr. Neurol. Neurosci.* 36, 99–105. doi: 10.3233/RNN-170759

Taylor, L., Lewis, G. N., and Taylor, D. (2012). Short-term effects of electrical stimulation and voluntary activity on corticomotor excitability in healthy individuals and people with stroke. *J. Clin. Neurophysiol.* 29, 237–243. doi: 10.1097/WNP.0b013e3182570f17

Williams, J., Pearce, A., Loporto, M., Morris, T., and Holmes, P. (2012). The relationship between corticospinal excitability during motor imagery and motor imagery ability. *Behav. Brain Res.* 226, 369–375. doi: 10.1016/j.bbr.2011.09.014

Wolpaw, J. R. (2007). Spinal cord plasticity in acquisition and maintenance of motor skills. *Acta Physiol.* 189, 155–169. doi: 10.1111/j.1748-1716.2006.01656.x

Wolpaw, J. R., and Tennissen, A. M. (2001). Activity-dependent spinal cord plasticity in health and disease. *Annu. Rev. Neurosci.* 24, 807–843. doi: 10.1146/annurev.neuro.24.1.807

Yamaguchi, T., Fujiwara, T., Lin, S. C., Takahashi, Y., Hatori, K., Liu, M., et al. (2018). Priming with intermittent theta burst transcranial magnetic stimulation promotes spinal plasticity induced by peripheral patterned electrical stimulation. *Front. Neurosci.* 12:508. doi: 10.3389/fnins.2018.00508

Yamaguchi, T., Fujiwara, T., Saito, K., Tanabe, S., Muraoka, Y., Otaka, Y., et al. (2013). The effect of active pedaling combined with electrical stimulation on spinal reciprocal inhibition. *J. Electromyogr. Kinesiol.* 23, 190–194. doi: 10.1016/j.jelekin.2012.08.007

Yamaguchi, T., Fujiwara, T., Tsai, Y. A., Tang, S. C., Kawakami, M., Mizuno, K., et al. (2016). The effects of anodal transcranial direct current stimulation and patterned electrical stimulation on spinal inhibitory interneurons and motor function in patients with spinal cord injury. *Exp. Brain Res.* 234, 1469–1478. doi: 10.1007/s00221-016-4561-4

Yamaguchi, T., Sugawara, K., Tanaka, S., Yoshida, N., Saito, K., Tanabe, S., et al. (2012). Real-time changes in corticospinal excitability during voluntary contraction with concurrent electrical stimulation. *PLoS One* 7:e46122. doi: 10.1371/journal.pone.0046122

Yasui, T., Yamaguchi, T., Tanabe, S., Tatemoto, T., Takahashi, Y., Kondo, K., et al. (2018). Time course changes in corticospinal excitability induced by motor imagery during action observation combined with peripheral nerve electrical stimulation. *Exp. Brain Res.* doi: 10.1007/s00221-018-5454-5 [Epub ahead of print].

Conflict of Interest Statement: The authors declare that the research was conducted in the absence of any commercial or financial relationships that could be construed as a potential conflict of interest.

frontiers in Neuroscience

ORIGINAL RESEARCH
published: 11 March 2019
doi: 10.3389/fnins.2019.00147

Somatosensory Stimulation With XNKQ Acupuncture Modulates Functional Connectivity of Motor Areas

Till Nierhaus[1,2†], Yinghui Chang[3,4†], Bin Liu[3], Xuemin Shi[3], Ming Yi[5,6], Claudia M. Witt[4,7†] and Daniel Pach[4,7*†]*

[1] Neurocomputation and Neuroimaging Unit, Department of Education and Psychology, Freie Universität Berlin, Berlin, Germany, [2] Department of Neurology, Max Planck Institute for Human Cognitive and Brain Sciences, Leipzig, Germany, [3] First Teaching Hospital of Tianjin University of Traditional Chinese Medicine, Tianjin, China, [4] Charité-Universitätsmedizin Berlin, Corporate Member of Freie Universität Berlin, Humboldt-Universität zu Berlin, Berlin Institute of Health, Institute for Social Medicine, Epidemiology and Health Economics, Berlin, Germany, [5] Neuroscience Research Institute and Department of Neurobiology, School of Basic Medical Sciences, Peking University, Beijing, China, [6] Key Laboratory for Neuroscience, Ministry of Education/National Health Commission, Peking University, Beijing, China, [7] Institute for Complementary and Integrative Medicine, University of Zurich and University Hospital Zurich, Zurich, Switzerland

OPEN ACCESS

Edited by:
Florian Beissner,
Hannover Medical School, Germany

Reviewed by:
Yihuai Zou,
Beijing University of Chinese Medicine, China
Ming-Kuei Lu,
China Medical University, Taiwan

***Correspondence:**
Till Nierhaus
till.nierhaus@fu-berlin.de
Daniel Pach
daniel.pach@charite.de

† These authors have contributed equally to this work

Specialty section:
This article was submitted to Perception Science, a section of the journal Frontiers in Neuroscience

Received: *19 November 2018*
Accepted: *08 February 2019*
Published: *11 March 2019*

Citation:
Nierhaus T, Chang Y, Liu B, Shi X, Yi M, Witt CM and Pach D (2019) Somatosensory Stimulation With XNKQ Acupuncture Modulates Functional Connectivity of Motor Areas. Front. Neurosci. 13:147. doi: 10.3389/fnins.2019.00147

Xingnao Kaiqiao (XNKQ) acupuncture is an acupuncture technique used for stroke patients. In 24 healthy volunteers, we applied this complex acupuncture intervention, which consists of a manual needle-stimulation on five acupuncture points (DU26 unilaterally, PC6, and SP6 bilaterally). XNKQ was compared to three control conditions: (1) insertion of needles on the XNKQ acupuncture points without stimulation, (2) manual needle-stimulation on five nearby non-acupuncture points, and (3) insertion of needles on the non-acupuncture points without stimulation. In a within-subject design, we investigated functional connectivity changes in resting-state functional magnetic resonance imaging (fMRI) by means of the data-driven eigenvector centrality (EC) approach. With a 2 × 2 factorial within-subjects design with two-factor stimulation (stimulation vs. non-stimulation) and location (acupuncture points vs. non-acupuncture points), we found decreased EC in the precuneus after needle-stimulation (stimulation<non-stimulation), whereas the factor location showed no statistically significant EC differences. XNKQ acupuncture compared with needle-stimulation on non-acupuncture points showed decreased EC primarily in subcortical structures such as the caudate nucleus, subthalamic nucleus, and red nucleus. *Post-hoc* seed-based analysis revealed that the decrease in EC was mainly driven by reduced temporal correlation to primary sensorimotor cortices. The comparison of XNKQ acupuncture with the other two (non-stimulation) interventions showed no significant differences in EC. Our findings support the importance of the stimulation component of the acupuncture intervention and hint toward the modulation of functional connectivity by XNKQ acupuncture, especially in areas involved in motor function. As a next step, similar mechanisms should be validated in stroke patients suffering from motor deficits.

ClinicalTrials.gov ID: NCT02453906

Keywords: resting-state fMRI, acupuncture, functional connectivity, centrality, stroke, red nucleus, precuneus

BACKGROUND

The acupuncture procedure consists of at least two components: stimulation and point location (Nierhaus et al., 2016; Langevin and Wayne, 2018). According to Chinese Medicine (TCM) theory, different types of stimulation will provide different clinical effects. The stimulation of the needle is mostly accompanied by a needle sensation that is called "deqi" in Chinese Medicine (Kong et al., 2007; Pach et al., 2011). Stimulation that elicited deqi was shown in a PET study to increase blood flow in the hypothalamus, insula, and subcortical structures compared with minimal or non-stimulation after needle insertion (Hsieh et al., 2001). Another study showed that acupuncture impacted selective attention networks, enhancing the efficiency of the alerting and executive control networks, and that acupuncture had a significantly greater effect on the alerting network compared to painful stimulation (Liu et al., 2013). Therefore, the subjective quality and the intensity of the stimulation seem to have an impact on the brain activity changes observed (Hui et al., 2005, 2009; Huang et al., 2012).

The role of location or point specificity in acupuncture is still controversial (Choi et al., 2012; Langevin and Wayne, 2018) and might depend on whether this role is evaluated (i) from the perspective of acupuncture with its concept of meridians and extra points or (ii) from the perspective of modern anatomy and physiology, which can take into account dermal, muscular, and neural components as well as connective tissue and chemical aspects (Nierhaus et al., 2016). In a previous trial of our group, point-specific cerebral responses were shown for one acupuncture point (ST36) in comparison to two control locations (Nierhaus et al., 2015b; Long et al., 2016).

Numerous neuroimaging studies that evaluated the impact of acupuncture on the brain hinted toward specific brain activity and functional connectivity changes due to acupuncture (Dhond et al., 2007; Huang et al., 2012; Chae et al., 2013). Most of these studies either investigate manual acupuncture only on one single point or investigate the effects of electro-acupuncture (Huang et al., 2012). The latter applies an electrical current between acupuncture needles inserted into the skin and is therefore easier to evaluate due to its better potential for blinding, standardization, and easier simultaneous multipoint application. However, in most clinical settings (in China and the West), manual needle-stimulation on multiple acupuncture points is applied.

Xingnao Kaiqiao (XNKQ) acupuncture is a semi-standardized manual acupuncture technique developed in Tianjin, China, by Professor Shi Xuemin using a specific set of acupuncture points and strong needle-stimulation for different neuropathological conditions such as acute and chronic stroke symptoms (Shi, 2013) and multiple sclerosis. In a clinical setting, it was shown that stroke patients suffering from motor deficits react especially well to XNKQ acupuncture (杜蓉 et al., 2015). This suggests an impact of XNKQ on central mechanisms. However, modulation of brain activity following XNKQ acupuncture has not yet been fully investigated.

In the present study, we aimed to evaluate the impact of XNKQ acupuncture (and its components "stimulation" and "point location") on resting-state functional MRI connectivity. For this, we developed a 2 × 2 design that varied the stimulation component (stimulation vs. non-stimulation) and the location component of acupuncture (acupuncture points vs. non-acupuncture points). We applied data-driven eigenvector centrality mapping (ECM) to evaluate functional connectivity differences for the stimulation component (comparison of stimulated and non-stimulated acupuncture conditions) as well as the point location component (comparison of conditions with acupuncture points and non-acupuncture points).

We had assumed that it would be possible to detect a difference between stimulated and non-stimulated acupuncture conditions as well as between acupuncture conditions which used the established acupuncture point location according to Chinese medicine and conditions which used non-acupuncture point locations. Moreover, we hypothesized that XNKQ acupuncture differed from the three control conditions.

MATERIALS AND METHODS

Subjects

We studied 24 healthy volunteers between 18 and 36 years of age (26.1 ± 4.3 years *(SD)*; 12 females). They gave written informed consent to participate in the experiment according to the declaration of Helsinki. The ethics committee of Charité - Universitätsmedizin Berlin approved the study (Ethics No EA1/338/14) and the study was registered (ClinicalTrials.gov NCT02453906).

Prior to participation, all volunteers underwent a clinical neurological examination and they confirmed they were not taking any medications for acute or chronic diseases.

According to the Edinburgh inventory for the assessment of handedness (Oldfield, 1971), all subjects were right-handed [laterality score: 90.1 ± 17.3 (SD) over a range of −100 (fully left-handed) and +100 (fully right-handed)].

Design

In a 2 × 2 factorial within-subject design we evaluated four different interventions in four different sessions (four different days with at least 24 h in between each) in a random order: (a) XNKQ acupuncture as manual needle-stimulation on five acupuncture points (DU26 unilaterally, PC6 and SP6 bilaterally); (b) insertion of needles on the five XNKQ acupuncture points without stimulation; (c) manual needle-stimulation on five nearby non-acupuncture points; and (d) insertion of needles on five non-acupuncture points without stimulation. The intervention had a duration of 5 min and was applied in the MRI scanner room. Resting-state fMRI was acquired before and after each intervention to compare changes (post minus pre) in functional connectivity between interventions. The break between pre- and post-resting state scans was about 10 min. Before informed consent, subjects were informed that they would receive acupuncture with five needles at the lower leg, the forearm, and above the upper lip on four separate days, on 2 days with stimulation of the needle and on the other two without. Subjects were blinded regarding the point specificity (acupuncture points vs. non-acupuncture points).

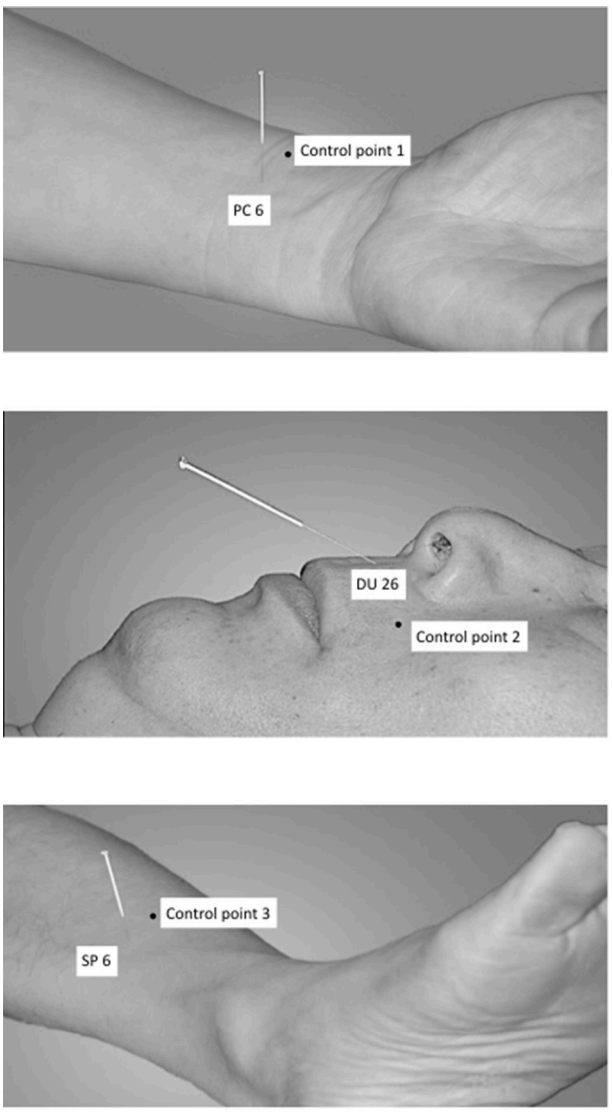

FIGURE 1 | Acupuncture points and respective control points.

Point Locations

The following acupuncture points have been used: PC6 (nei guan, bilateral), DU26 (ren zhong, unilateral), and SP6 (san yin jiao, bilateral) (Shi, 2002, 2013), see **Figure 1**.

DU26 is located at the junction of the upper 1/3 and middle 1/3 of the philtrum. PC6 is located 2 cun above the transverse crease of the wrist, between the tendons of radial wrist flexor and palmaris longus. SP6 is located 3 cun above the tip of the medial malleolus, behind the posterior border of the medial aspect of the tibia (Shi, 2002).

The control points have been used in an earlier study on XNKQ acupuncture (李筱媛 and 李军, 2009) and were chosen after a discussion process with acupuncture experts. They are not located on a meridian or above a main nerve and are within a radius of 2.5 cm of the respective acupuncture point (**Figure 1**). Control point 1 (control of PC 6) is located laterally to PC 6, between the lung meridian of hand-taiyin and the pericardium meridian of hand-jueyin (李筱媛 and 李军, 2009). Control point 2 (control of DU 26) is located on the vertical line of the mouth, left-horizontal to DU26 (李筱媛 and 李军, 2009). Control point 3 (control of SP 6) is located six cun above the tip of the medial malleolus, between the spleen meridian of foot-taiyin and the liver meridian of foot-jueyin. It is three cun above the tip of the medial malleolus, in front of the inner of the tibia, 1.25 cun in front of SP 6 (李筱媛 and 李军, 2009).

Acupuncture Procedures

The acupuncture was performed while the subjects lay in a supine position on the scanner bed by an acupuncturist from Tianjin University of Traditional Chinese Medicine (YC) trained for 12 years and with 8 years of clinical experience. The acupuncturist was trained directly by the developer of the XNKQ acupuncture and had long-time experience in the application of XNKQ acupuncture in patients in China and was also familiar with German study settings. For the acupuncture, sterile, single use, individually wrapped acupuncture needles (0.20 × 30 mm; titanium, DongBang, Acupuncture, Inc., Boryeong, Korea) were used.

For the XNKQ acupuncture PC6 was punctured bilaterally to a depth of 0.5–1.0 cun and stimulated with the reducing method by lifting and thrusting with simultaneous twirling manipulation for 1 min (twirling anticlockwise with the left hand and clockwise with the right hand). After this, DU26 was punctured obliquely toward the nasal septum to a depth of ∼0.3–0.5 cun with bird-pecking needling until the eyes became wet or developed tears. Subsequently, SP6 was punctured on both sides obliquely along with the medial border of the tibia to a depth of ∼0.5–1.0 cun, with lifting and thrusting reinforcing manipulation, thrusts with heavy strength and lifting with gentle strength for 1 min. The needles were removed directly after stimulation [called "quick needles" technique (Shi, 2013)].

Control condition 1 consisted of the insertion of needles on the same five acupuncture points in the same order as used for XNKQ acupuncture (PC6 bilaterally, DU26 unilaterally, SP6 bilaterally), but without needle-stimulation.

Control condition 2 consisted of manual needle-stimulation on the five nearby non-acupuncture points (control point 1 bilaterally, control point 2 unilaterally, control point 3 bilaterally), identically to the XNKQ needle-stimulation.

Control condition 3 consisted of the insertion of needles on the five non-acupuncture points (control point 1 bilaterally, control point 2 unilaterally, control point 3 bilaterally) without manual needle-stimulation.

Needle sensation as a proxy for deqi and pain sensation was measured after each session by the Massachusetts General Hospital Acupuncture Sensation Scale [MASS, (Kong et al., 2007)].

MRI Data Acquisition

Before all measurements, participants were instructed to keep the eyes open and to stay relaxed. Data was acquired using a 3T Tim Trio Siemens MRI System (Siemens Medical, Erlangen, Germany) equipped with a 12-channel head coil. For resting-state fMRI images, we used a T2*-weighted echo planar imaging (EPI) sequence (37 axial slices, in-plane resolution is 3 × 3 mm,

slice thickness = 3 mm, flip angle = 70°, gap = 0.3 mm, repetition time = 2,000 ms, echo time = 30 ms). A structural image was acquired for each participant using a T1-weighted MPRAGE sequence (repetition time = 1,900 ms, inversion time = 900 ms, echo time = 2.52 ms, and flip angle = 9, voxel size 1 × 1 × 1 mm). Subjects' heads were immobilized by cushioned supports, and they wore earplugs to protect against MRI gradient noise throughout the experiment.

Resting-State fMRI Data Analysis

We removed the first ten volumes of each resting-state scan (RS_pre and RS_post for each subject and all four interventions) to account for adaptation of the participant to scanner noise and environment. We performed slice time correction, head motion correction, and spatial normalization to MNI152 space with SPM12 (www.fil.ion.ucl.ac.uk/spm/). The toolbox REST (www.restfmri.net) was used for temporal band-pass filtering (0.01–0.08 Hz). We did not regress out the global mean signal since this step might affect the correlation between time courses (Buckner et al., 2009; Lohmann et al., 2010; Fransson et al., 2011; Taubert et al., 2011). The anatomical T1-images were normalized to MNI152 space and then segmented into gray matter, whiter matter and cerebral spinal fluid (CSF). Average masks were generated for gray matter, white matter, and CSF derived from the segmented T1 images of all subjects. Principal component analysis (CompCor) was done by the DPABI toolbox (toolbox for Data Processing & Analysis of Brain Imaging, http://becs.aalto.fi/~eglerean/bramila.html) within the CSF/white matter mask on the resting-state data (Behzadi et al., 2007). The first five principal components and six head motion parameters were used as nuisance signals to regress out associated variance. We did not apply spatial smoothing before the centrality analysis, as this could generate artificially high correlation coefficients (Zuo et al., 2012).

To compare differences in head motion across resting-state scans, we calculated the frame-wise displacement (FD) using BRAMILA tools (Power et al., 2012) (http://becs.aalto.fi/~eglerean/bramila.html). The average FD for all scans was examined with two two-factorial ANOVAs, including (a) the factors "session" (1–4) and "time" (pre-post) and (b) the factors "condition" and "time."

We used the data-driven ECM approach to characterize whole-brain functional connectivity without prior assumptions (Nierhaus et al., 2015a; Long et al., 2016; Antonenko et al., 2018). This graph theoretical network approach quantifies the correlation of each voxel with all other voxels in the brain, aiming to identify how "central" (or prominent) this region is within the whole-brain network (Lohmann et al., 2010). For each individual resting-state scan, the EC map has been generated within the gray matter mask by using fastECM, which provides a more efficient way to perform the centrality analysis without calculating the voxel-wise correlation matrix (Wink et al., 2012). Z-standard transformation (i.e., for each voxel, subtract the mean value of the whole brain then divide by the standard deviation of the whole brain) and 6 mm FWHM smoothing was performed on the individual ECM maps (Zuo et al., 2012; Yan et al., 2013). To evaluate the impact of the four different acupuncture conditions on EC, we analyzed the difference EC-maps (post minus pre) in a 2 × 2 flexible factorial design [correlated repeated measures (Gläscher and Gitelman, 2008)] with the factors "stimulation" (stimulation vs. non-stimulation of the needles) and "location" (acupuncture points vs. non-acupuncture points) within SPM12 with age, gender, and MASS index as covariate. For statistical analysis, we determined cluster-extent thresholds with Monte Carlo simulation (AlphaSim procedure) as implemented in Neuroelf Version 1.1 (http://neuroelf.net) using a family-wise error (FWE) cluster level correction of pFWE <0.05.

The ECM analysis identifies brain regions with altered overall (whole-brain) connectivity, however it does not show to which specific brain areas the connectivity has changed. A complementary seed-based functional connectivity analysis can be applied to characterize the "origin" of observed EC changes.

The comparison of XNKQ with stimulation on non-acupuncture points revealed EC changes in subthalamic brain regions which are known to be involved in motor control, such as the subthalamic nucleus and red nucleus. In order to show that this result might be connected to cortical motor areas, we have performed a complementary seed-based analysis. As two examples, we chose the red nucleus and subthalamic nucleus as seed regions: For all resting-state scans, we calculated the temporal correlation between the time series of the seed region and all other voxels within the gray matter mask. The difference in the resulting correlation maps were analyzed in a 2 × 2 flexible factorial design with the factors "stimulation" and "location" with age, gender, and MASS index as covariate (similar to the ECM analysis). It should be noted that no formal statistics was applied in this step (double dipping), rather it was used to identify the most affected connections, which contributed most to the statistically significant effect of the ECM analysis. For visualization of the most prominent clusters, we used voxel-wise whole brain FWE correction with peak-level $p < 0.05$.

RESULTS

Head Motion

There was no significant difference in head motion (mean FD) across all resting-state scans (4 pre- and 4 post-acupuncture scans) for either the comparison between the four session or the comparison between the four acupuncture conditions (all $p > 0.46$). Over all 8 scans, the mean FD was 0.14 ± 0.06 mm [mean ± std] and the average percentage of volumes exceeding an FD-threshold of 0.5 mm was 1.9 ± 2.8% [mean ± std].

Needle Stimulation Decreases Eigenvector Centrality in Precuneus

For the factor "stimulation," we found a significant cluster of decreased eigenvector centrality (stimulation < non-stimulation, **Figure 2**) in the parietal lobe mainly including the precuneus (maximum T value −4.01, left hemisphere (LH), MNI-coordinates $X = -3$, $y = -78$, $Z = 54$) and the cuneus (Tmax= −4.68, LH, $X = -6$, $y = -81$, $Z = 42$).

Further evaluation of the four different conditions showed that the decreased eigenvector centrality in the precuneus was driven by the stimulation of non-acupuncture points (non-points with stimulation, npws). It was significant for the stimulation of

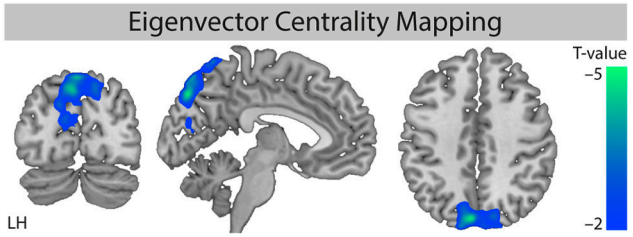

FIGURE 2 | Comparison of ECM values for the factor "stimulation." Whole brain analysis for the contrast [stimulation vs. non-stimulation] shows decreased centrality for the stimulation conditions. Monte Carlo simulation with AlphaSim was used to identify significant clusters at pFWE $<$ 0.05 (family-wise error correction for multiple comparisons). MNI slice coordinates $X = -5$, $Y = -78$, $Z = 42$. LH, left hemisphere.

non-acupuncture points compared to the two non-stimulation conditions (npws vs. points non-stimulation, pns and npws vs. non-points non-stimulation, npns), and it was not significant when XNKQ was compared to the two non-stimulation conditions (XNKQ vs. pns and XNKQ vs. npns). However, the comparison of the two stimulation conditions (XNKQ vs. npws) also showed no significant difference in precuneus.

The factor location showed no statistically significant different eigenvector centrality. Additionally, no effect was found for the comparison of the non-stimulation conditions (pns vs. npns).

XNKQ Modulates Functional Connectivity of Motor Areas

The EC analysis for XNKQ compared with the stimulation of non-acupuncture points (XNKQ vs. npws) showed one significant cluster (mainly subcortical) of decreased centrality (**Figure 3A**). This cluster included subcortical structures such as the caudate (right hemisphere (RH), Tmax = −3.71, MNI-coordinates $X = 12$, $y = 15$, $Z = -3$), the subthalamic nucleus (RH: Tmax = −3.57, $X = 9$, $y = -12$, $Z = -18$), the thalamus (LH: Tmax = −3.48, $X = -6$, $y = -27$, $Z = -3$; RH: Tmax = −3.42, $X = 15$, $y = -24$, $Z = -6$), the lentiform nucleus (RH, Tmax = −3.80, $X = 27$, $y = 3$, $Z = -12$), and the red nucleus (RH, Tmax = −3.13, $X = 9$, $y = -30$, $Z = -18$), as well as the claustrum (RH, Tmax = −5.06, $X = 36$, $y = 0$, $Z = -15$), the anterior cingulate cortex (RH, Tmax = −2.94, $X = 12$, $y = 36$, $Z = 9$), and the cingulate cortex (RH, Tmax = −2.74, $X = 9$, $y = -3$, $Z = 30$). No significant effect was found for XNKQ compared to the two non-stimulation conditions (XNKQ vs. pns and XNKQ vs. npns).

The complementary seed-based functional connectivity analysis revealed that the decreased EC in subthalamic areas was mainly driven by decreased temporal correlation of the respective seed region to primary sensorimotor areas (S1/M1); the red nucleus showed significantly decreased correlation mainly to bilateral S1/M1 (RH: Tmax = −6.00, $X = 42$, $y = -19$, $Z = 55$; LH: Tmax = −6.05, $X = -51$, $y = -22$, $Z = 46$; **Figure 3B**) and the subthalamic nucleus mainly to left S1/M1 (LH: Tmax = −7.04, $X = -39$, $y = -22$, $Z = 49$; **Figure 3C**).

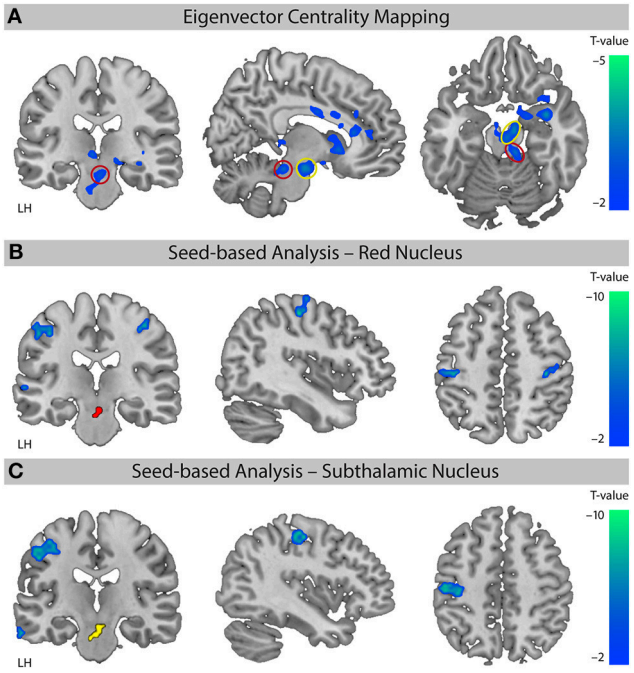

FIGURE 3 | Comparison of the two stimulation conditions. Effect on functional connectivity for the contrast [XNKQ vs. "non-acupuncture point with stimulation" (npws)]. **(A)** Data-driven ECM analysis shows decreased centrality for XNKQ, mainly in subcortical regions. Monte Carlo simulation with AlphaSim was used to identify significant clusters at pFWE $<$ 0.05 (family-wise error (FWE) correction for multiple comparisons). Red circle (Red Nucleus) and yellow circle (Subthalamic Nucleus) indicate areas that were used for seed-based correlation analyses. MNI slice coordinates $X = -8$, $Y = -22$, $Z = -18$. **(B)** Seed-based functional connectivity with seed in Red Nucleus. Whole brain analysis shows for XNKQ decreased temporal correlation of the seed-region (red) with primary sensorimotor areas (voxel-wise FWE correction at pFWE $<$ 0.05). MNI slice coordinates $X = 41$, $Y = -22$, $Z = 51$. **(C)** Seed-based functional connectivity with seed in Subthalamic Nucleus. Whole brain analysis shows for XNKQ decreased temporal correlation of the seed-region (yellow) with left primary sensorimotor areas (voxel-wise FWE correction at pFWE $<$ 0.05). MNI slice coordinates $X = -40$, $Y = -20$, $Z = 48$. LH, left hemisphere.

Needle Sensation

Needle sensation was measured for all four conditions using the MASS index: XNKQ mean 4.17 95%CI[3.34;5.01]; npws 3.44[2.54;4.34]; pns 3.52[2.65;4.39]; and npns 2.29[1.58;3.00]. The statistical analysis showed a significant main effect for both factors (stimulation and location) in our 2 × 2 factorial design (stimulation vs. non-stimulation conditions p=0.030; acupuncture points vs. non-acupuncture points $p = 0.018$). The comparison of the four conditions showed significant differences only for npns comparisons (XNKQ vs. NPNS, $p = 0.001$; NPWS vs. NPNS $p = 0.043$; PNS vs. NPNS $p = 0.028$).

DISCUSSION

To elucidate cerebral effects of manual acupuncture using more than one acupuncture point, we applied XNKQ acupuncture

and three control conditions in a neuroimaging study in healthy subjects. In a 2 × 2 factorial within-subject design, we investigated the impact of the factors stimulation and location, and of XNKQ acupuncture specifically, on resting-state functional connectivity.

While the factor location appears to have no significant effect on centrality, we found decreased eigenvector centrality in the precuneus for the factor stimulation. This result was driven by the stimulation of non-acupuncture points, as the comparison of XNKQ acupuncture with the two non-stimulation interventions showed no significant differences. However, when comparing XNKQ acupuncture with manual needle-stimulation on non-acupuncture points, we found significantly decreased functional connectivity for areas involved in motor function.

Our results support the assumption that (1) needle-stimulation drives the cerebral effects, (2) point location only impacts connectivity when the acupuncture points are stimulated, and (3) XNKQ acupuncture, as a complex form of acupuncture, modulates functional connectivity in motor areas minutes after the acupuncture.

Our study design shows strengths and weaknesses that should be considered when interpreting the results. With our factorial within-subject design including a relatively large number of healthy subjects measured on four separate days, we were able to separate the factors stimulation and location, as well as to reduce variance and carry over effects. The design we chose aimed at a study question relevant for the understanding of clinical acupuncture which primarily uses manual needle-stimulation on more than one point. So far, numerous imaging studies evaluate only one-point acupuncture and/or apply electro-acupuncture (Huang et al., 2012; Chae et al., 2013). Such a setting might be better suited for standardization and blinding options but does not represent clinical acupuncture in usual care settings.

Although in our study design only five locations were acupunctured for a relatively short time interval (hence still does not fully represent the clinical setting), we were able to observe cerebral changes that illustrate the impact of a complex acupuncture, such as XNKQ acupuncture, on the brain. Because the duration of the sustained effect of acupuncture is not known, we do not know whether pausing the intervention for at least 24 h is sufficient to avoid carry-over effects. However, the order of interventions was randomized to minimize the risk of a systematic impact.

We chose a design that can evaluate rapid effects on resting-state functional connectivity, which are observable after the intervention, but not the instant evoked responses of the different acupuncture conditions. This design decision may decrease the sensitivity to identify differences between the conditions. For the evaluation of instant effects, an event-related design with needling during the scanning phase would have been necessary. However, this would be much more difficult to achieve, especially when evaluating manually stimulated acupuncture on multiple acupuncture points.

Although we included a relatively large number of subjects, the sample size might be too low to show robust effects. The level of statistical significance we chose was liberal. For future studies with a similar design, an even larger sample size might be recommended, especially for the evaluation of effects in patients. Based on our findings, it is now possible to evaluate a hypothesis-driven approach, which might create more robust results in contrast to the data-driven approach we chose as the primary analysis.

In our study, we included only healthy subjects for an easy-to-standardize setting to understand the neurophysiology of the different acupuncture conditions. However, usually XNKQ acupuncture is only applied in a clinical setting for patients with neurological deficits such as multiple sclerosis or stroke as part of a multi-component intervention that also includes physiotherapy. Therefore, it is possible that effects in healthy subjects differ from effects expected in patients. However, a study on patients would have created more variance and is more prone to bias, which is not ideal as a first step.

However, only the subjects were blinded for the applied acupuncture conditions as well as the researchers analyzing the data during the first stages of analyses. The acupuncturist applying the manual acupuncture could not be blinded for the different conditions and this might have had an effect on needle-stimulation. However, we measured needle sensation as a proxy for stimulation strength and included it into our statistical model.

The choice of control points for an acupuncture study is very challenging because it is still not clear what constitutes an acupuncture point, and it is difficult to combine the traditional concept of acupuncture with modern anatomy (Nierhaus et al., 2016; Langevin and Wayne, 2018). Therefore, it is possible that the control points chosen for our study were not inert, either from the perspective of acupuncture or from the perspective of anatomy.

To our surprise, we found no significant differences between XNKQ and the two non-stimulated acupuncture conditions. This means that the main effect that we found in precuneus for the factor "stimulation" is driven by the needle-stimulation on non-acupuncture points. However, the comparison within the two stimulated acupuncture conditions (XNKQ vs. stimulation on non-acupuncture points) revealed a significant difference—mainly in subcortical regions—that is not observed in the other comparisons. It seems that the stimulation of acupuncture points (XNKQ) induces subcortical connectivity changes (decreased centrality) that are opposite to the connectivity changes induced by needle-stimulation of "neutral" non-acupuncture points. This result supports the view that both "stimulation" and "point location" contribute to the acupuncture effect.

Other studies have also shown that acupuncture can affect functional connectivity of brain networks such as the default mode network (DMN) or sensorimotor network in pain, stroke, or mental conditions (Dhond et al., 2008; Bai et al., 2009; Hui et al., 2009; Chae et al., 2013; Napadow et al., 2013; Liang et al., 2014; Li et al., 2014; Zhao et al., 2014; Deng et al., 2016). Numerous studies could show that the precuneus (as part of the DMN) is frequently affected by acupuncture (Chae et al., 2013; Nierhaus et al., 2015b). So far, the specific role of the precuneus is not fully understood, however for pain it might be involved in the assessment and integration of pain (Goffaux et al., 2014). The reduced centrality that we found for the precuneus in resting-state after needle-stimulation might hint toward such

cerebral processing induced by the strong and (sometimes) painful stimulation.

Functional connectivity is regularly affected by stroke (Grefkes and Fink, 2011; Rehme and Grefkes, 2013; Baldassarre et al., 2016; Almeida et al., 2017), and brain imaging studies have revealed functional brain reorganization in relation to recovery (Schaechter, 2004; Almeida et al., 2017). In a stroke mouse model, it could be shown that multisensory input can improve functional recovery and resting-state functional connectivity after stroke (Hakon et al., 2018). Acupuncture can be regarded as a complex somatosensory input with needle-stimulation. According to a study by Li et al. both acupuncture and somatosensory stimuli to the contralesional side produce hyperactivation in the ipsilesional primary sensorimotor cortex and SII (Dhond et al., 2007). A study by Schaechter et al. (2007) revealed that after acupuncture intervention (verum or sham), patients exhibited changes in motor cortex activity associated with the stroke-affected hand that were positively correlated with changes in somatosensory-motor function of the affected upper limb. There was a trend toward greater increases in motor cortex activity in patients treated with verum acupuncture than sham acupuncture (Dhond et al., 2007). XNKQ is an acupuncture technique specially designed for different neuropathological conditions such as acute and chronic stroke symptoms (Shi, 2013), and moreover seems to impact on patients suffering from motor deficits. Therefore, our results are well in line with the existing literature and support the assumption that XNKQ affects the motor system.

Our data-driven analysis (ECM) showed that XNKQ acupuncture affects functional connectivity of subcortical areas (e.g., red nucleus or subthalamic nucleus) that are known to be involved in motor function (Milardi et al., 2016). This is supported by our complementary seed-based analysis, which showed reduced functional connectivity between the seed regions and primary sensori-motor areas after XNKQ acupuncture. Maybe this reduced functional connectivity in the motor systems allows for a better reorganization during recovery from motor deficits in stroke. Of course, it needs to be proven if this can be translated to stroke patients.

CONCLUSION

Our findings support the importance of the stimulation component of the acupuncture intervention and hint toward the modulation of functional connectivity by XNKQ acupuncture, especially in areas involved in motor function. As a next step, similar mechanisms should be validated in stroke patients suffering from motor deficits.

DATA AVAILABILITY

The datasets generated for this study are available on request to the corresponding author.

AUTHOR CONTRIBUTIONS

TN, YC, CW, and DP conceived and designed the experiments. TN, YC, BL, and DP performed the trial. TN and DP analyzed the data. TN, DP, YC, and CW wrote the first draft of the paper. TN, YC, BL, XS, MY, CW, and DP discussed the data, revised the paper, and approved the final version.

FUNDING

YC and BL had a scholarship from First Teaching Hospital of Tianjin University of Traditional Chinese Medicine, Tianjin, China.

ACKNOWLEDGMENTS

We thank Christian Kainz for his support during the experiments.

REFERENCES

Almeida, S. R., Vicentini, J., Bonilha, L., De Campos, B. M., Casseb, R. F., and Min, L. L. (2017). Brain connectivity and functional recovery in patients with ischemic stroke. *J. Neuroimaging* 27, 65–70. doi: 10.1111/jon.12362

Antonenko, D., Nierhaus, T., Meinzer, M., Prehn, K., Thielscher, A., Ittermann, B., et al. (2018). Age-dependent effects of brain stimulation on network centrality. *Neuroimage* 176, 71–82. doi: 10.1016/j.neuroimage.2018.04.038

Bai, L., Qin, W., Tian, J., Dong, M., Pan, X., Chen, P., et al. (2009). Acupuncture modulates spontaneous activities in the anticorrelated resting brain networks. *Brain Res.* 1279, 37–49. doi: 10.1016/j.brainres.2009.04.056

Baldassarre, A., Ramsey, L. E., Siegel, J. S., Shulman, G. L., and Corbetta, M. (2016). Brain connectivity and neurological disorders after stroke. *Curr. Opin. Neurol.* 29, 706–713. doi: 10.1097/WCO.0000000000000396

Behzadi, Y., Restom, K., Liau, J., and Liu, T. T. (2007). A component based noise correction method (CompCor) for BOLD and perfusion based fMRI. *Neuroimage* 37, 90–101. doi: 10.1016/j.neuroimage.2007.04.042

Buckner, R. L., Sepulcre, J., Talukdar, T., Krienen, F. M., Liu, H., Hedden, T., et al. (2009). Cortical hubs revealed by intrinsic functional connectivity: mapping, assessment of stability, and relation to Alzheimer's disease. *J. Neurosci.* 29, 1860–1873. doi: 10.1523/JNEUROSCI.5062-08.2009

Chae, Y., Chang, D. S., Lee, S. H., Jung, W. M., Lee, I. S., Jackson, S., et al. (2013). Inserting needles into the body: a meta-analysis of brain activity associated with acupuncture needle stimulation. *J. Pain* 14, 215–222. doi: 10.1016/j.jpain.2012.11.011

Choi, E. M., Jiang, F., and Longhurst, J. C. (2012). Point specificity in acupuncture. *Chin. Med.* 7:4. doi: 10.1186/1749-8546-7-4

Deng, D., Liao, H., Duan, G., Liu, Y., He, Q., Liu, H., et al. (2016). Modulation of the default mode network in first-episode, drug-naive major depressive disorder via acupuncture at Baihui (GV20) acupoint. *Front. Hum. Neurosci.* 10:230. doi: 10.3389/fnhum.2016.00230

Dhond, R. P., Kettner, N., and Napadow, V. (2007). Neuroimaging acupuncture effects in the human brain. *J. Altern Complement. Med.* 13, 603–616. doi: 10.1089/acm.2007.7040

Dhond, R. P., Yeh, C., Park, K., Kettner, N., and Napadow, V. (2008). Acupuncture modulates resting state connectivity in default and sensorimotor brain networks. *Pain* 136, 407–418. doi: 10.1016/j.pain.2008.01.011

Fransson, P., Aden, U., Blennow, M., and Lagercrantz, H. (2011). The functional architecture of the infant brain as revealed by resting-state fMRI. *Cereb. Cortex* 21, 145–154. doi: 10.1093/cercor/bhq071

Gläscher, J., and Gitelman, D. (2008). *Contrast Weights in Flexible Factorial Design With Multiple Groups of Subjects*. Available online at: http://www.sbirc.ed.ac.uk/cyril/download/Contrast_Weighting_Glascher_Gitelman_2008.pdf (Accessed March 23, 2016).

Goffaux, P., Girard-Tremblay, L., Marchand, S., Daigle, K., and Whittingstall, K. (2014). Individual differences in pain sensitivity vary as a function of precuneus reactivity. *Brain Topogr.* 27, 366–374. doi: 10.1007/s10548-013-0291-0

Grefkes, C., and Fink, G. R. (2011). Reorganization of cerebral networks after stroke: new insights from neuroimaging with connectivity approaches. *Brain* 134, 1264–1276. doi: 10.1093/brain/awr033

Hakon, J., Quattromani, M. J., Sjolund, C., Tomasevic, G., Carey, L., Lee, J. M., et al. (2018). Multisensory stimulation improves functional recovery and resting-state functional connectivity in the mouse brain after stroke. *Neuroimage Clin.* 17, 717–730. doi: 10.1016/j.nicl.2017.11.022

Hsieh, J. C., Tu, C. H., Chen, F. P., Chen, M. C., Yeh, T. C., Cheng, H. C., et al. (2001). Activation of the hypothalamus characterizes the acupuncture stimulation at the analgesic point in human: a positron emission tomography study. *Neurosci. Lett.* 307, 105–108. doi: 10.1016/S0304-3940(01)01952-8

Huang, W., Pach, D., Napadow, V., Park, K., Long, X., Neumann, J., et al. (2012). Characterizing acupuncture stimuli using brain imaging with FMRI–a systematic review and meta-analysis of the literature. *PLoS ONE* 7:e32960. doi: 10.1371/journal.pone.0032960

Hui, K. K., Liu, J., Marina, O., Napadow, V., Haselgrove, C., Kwong, K. K., et al. (2005). The integrated response of the human cerebro-cerebellar and limbic systems to acupuncture stimulation at ST 36 as evidenced by fMRI. *Neuroimage* 27, 479–496. doi: 10.1016/j.neuroimage.2005.04.037

Hui, K. K., Marina, O., Claunch, J. D., Nixon, E. E., Fang, J., Liu, J., et al. (2009). Acupuncture mobilizes the brain's default mode and its anti-correlated network in healthy subjects. *Brain Res.* 1287, 84–103. doi: 10.1016/j.brainres.2009.06.061

Kong, J., Gollub, R., Huang, T., Polich, G., Napadow, V., Hui, K., et al. (2007). Acupuncture de qi, from qualitative history to quantitative measurement. *J. Altern. Complement. Med.* 13, 1059–1070. doi: 10.1089/acm.2007.0524

Langevin, H. M., and Wayne, P. M. (2018). What Is the point? The problem with acupuncture research that no one wants to talk about. *J. Altern. Complement. Med.* 24, 200–207. doi: 10.1089/acm.2017.0366

Li, J., Zhang, J. H., Yi, T., Tang, W. J., Wang, S. W., and Dong, J. C. (2014). Acupuncture treatment of chronic low back pain reverses an abnormal brain default mode network in correlation with clinical pain relief. *Acupunct. Med.* 32, 102–108. doi: 10.1136/acupmed-2013-010423

Liang, P., Wang, Z., Qian, T., and Li, K. (2014). Acupuncture stimulation of Taichong (Liv3) and Hegu (LI4) modulates the default mode network activity in Alzheimer's disease. *Am. J. Alzheimers Dis. Other Demen* 29, 739–748. doi: 10.1177/1533317514536600

Liu, G., Ma, H. J., Hu, P. P., Tian, Y. H., Hu, S., Fan, J., et al. (2013). Effects of painful stimulation and acupuncture on attention networks in healthy subjects. *Behav. Brain Funct.* 9:23. doi: 10.1186/1744-9081-9-23

Lohmann, G., Margulies, D. S., Horstmann, A., Pleger, B., Lepsien, J., Goldhahn, D., et al. (2010). Eigenvector centrality mapping for analyzing connectivity patterns in fMRI data of the human brain. *PLoS ONE* 5:e10232. doi: 10.1371/journal.pone.0010232

Long, X., Huang, W., Napadow, V., Liang, F., Pleger, B., Villringer, A., et al. (2016). Sustained effects of acupuncture stimulation investigated with centrality mapping analysis. *Front. Hum. Neurosci.* 10:510. doi: 10.3389/fnhum.2016.00510

Milardi, D., Cacciola, A., Cutroneo, G., Marino, S., Irrera, M., Cacciola, G., et al. (2016). Red nucleus connectivity as revealed by constrained spherical deconvolution tractography. *Neurosci. Lett.* 626, 68–73. doi: 10.1016/j.neulet.2016.05.009

Napadow, V., Lee, J., Kim, J., Cina, S., Maeda, Y., Barbieri, R., et al. (2013). Brain correlates of phasic autonomic response to acupuncture stimulation: an event-related fMRI study. *Hum. Brain Mapp.* 34, 2592–2606. doi: 10.1002/hbm.22091

Nierhaus, T., Forschack, N., Piper, S. K., Holtze, S., Krause, T., Taskin, B., et al. (2015a). Imperceptible somatosensory stimulation alters sensorimotor background rhythm and connectivity. *J. Neurosci.* 35, 5917–5925. doi: 10.1523/JNEUROSCI.3806-14.2015

Nierhaus, T., Pach, D., Huang, W., Long, X., Napadow, V., Roll, S., et al. (2015b). Differential cerebral response to somatosensory stimulation of an acupuncture point vs. two non-acupuncture points measured with EEG and fMRI. *Front. Hum. Neurosci.* 9:74. doi: 10.3389/fnhum.2015.00074

Nierhaus, T., Pach, D., Huang, W., Long, X., Napadow, V., Roll, S., et al. (2016). Difficulties choosing control points in acupuncture research. response: commentary: differential cerebral response, measured with both an EEG and fMRI, to somatosensory stimulation of a single acupuncture point vs. two non-acupuncture points. *Front. Hum. Neurosci.* 10:404. doi: 10.3389/fnhum.2016.00404

Oldfield, R. C. (1971). The assessment and analysis of handedness: the Edinburgh inventory. *Neuropsychologia* 9, 97–113. doi: 10.1016/0028-3932(71)90067-4

Pach, D., Hohmann, C., Ludtke, R., Zimmermann-Viehoff, F., Witt, C. M., and Thiele, C. (2011). German translation of the southampton needle sensation questionnaire: use in an experimental acupuncture study. *Forsch. Komplementarmed. Klass. Naturheilkd.* 18, 321–326. doi: 10.1159/000335241

Power, J. D., Barnes, K. A., Snyder, A. Z., Schlaggar, B. L., and Petersen, S. E. (2012). Spurious but systematic correlations in functional connectivity MRI networks arise from subject motion. *Neuroimage* 59, 2142–2154. doi: 10.1016/j.neuroimage.2011.10.018

Rehme, A. K., and Grefkes, C. (2013). Cerebral network disorders after stroke: evidence from imaging-based connectivity analyses of active and resting brain states in humans. *J. Physiol.* 591, 17–31. doi: 10.1113/jphysiol.2012.243469

Schaechter, J. D. (2004). Motor rehabilitation and brain plasticity after hemiparetic stroke. *Prog. Neurobiol.* 73, 61–72. doi: 10.1016/j.pneurobio.2004.04.001

Schaechter, J. D., Connell, B. D., Stason, W. B., Kaptchuk, T. J., Krebs, D. E., Macklin, E. A., et al. (2007). Correlated change in upper limb function and motor cortex activation after verum and sham acupuncture in patients with chronic stroke. *J. Altern. Complement. Med.* 13, 527–532. doi: 10.1089/acm.2007.6316

Shi, X. (2002). *Science of Acupuncture and Moxibustion.* Beijing: China Press of Traditional Chinese Medicine.

Shi, X. (2013). *Shi Xue-min's Comprehensive Textbook of Acupuncture and Moxibustion*. Beijing: Peoples Medical Pub House.

Taubert, M., Lohmann, G., Margulies, D. S., Villringer, A., and Ragert, P. (2011). Long-term effects of motor training on resting-state networks and underlying brain structure. *Neuroimage* 57, 1492–1498. doi: 10.1016/j.neuroimage.2011.05.078

Wink, A. M., De Munck, J. C., Van Der Werf, Y. D., Van Den Heuvel, O. A., and Barkhof, F. (2012). Fast eigenvector centrality mapping of voxel-wise connectivity in functional magnetic resonance imaging: implementation, validation, and interpretation. *Brain Connect.* 2, 265–274. doi: 10.1089/brain.2012.0087

Yan, C. G., Cheung, B., Kelly, C., Colcombe, S., Craddock, R. C., Di Martino, A., et al. (2013). A comprehensive assessment of regional variation in the impact of head micromovements on functional connectomics. *Neuroimage* 76C, 183–201. doi: 10.1016/j.neuroimage.2013.03.004

Zhao, L., Liu, J., Zhang, F., Dong, X., Peng, Y., Qin, W., et al. (2014). Effects of long-term acupuncture treatment on resting-state brain activity in migraine patients: a randomized controlled trial on active acupoints and inactive acupoints. *PLoS ONE* 9:e99538. doi: 10.1371/journal.pone.0099538

Zuo, X. N., Ehmke, R., Mennes, M., Imperati, D., Castellanos, F. X., Sporns, O., et al. (2012). Network centrality in the human functional connectome. *Cereb. Cortex* 22, 1862–1875. doi: 10.1093/cercor/bhr269

李筱媛, 李军 (LI Xiaoyuan, LI Jun). (2009). "醒脑开窍"针刺法对照非经穴点的设立—经穴特异性临床研究的方法探讨 (Discussion for Non-point Sham Control of Xingnao Kaiqiao Acupuncture). 天津中医药 (Tianjin TCM) 26, 388–390. Retreived from: http://www.tjzhongyiyao.com/tjzyy/ch/index.aspx

杜蓉, 张春红, 张新亚 (Du Rong, Zhang Chunhong, Zhang Xinya). (2015). "醒脑开窍"针刺法治疗中风后痉挛性瘫痪疗效观察 (Therapeutic Observation on Paralysis after Stroke Treated with Xingnao Kaiqiao Needling Terapy). 针灸临床杂志 (Journal of Clinical Acupuncture and Moxibustion). 31, 21–23. Retreived from: http://zjlczz.hljucm.net/ch/index.aspx

Conflict of Interest Statement: The authors declare that the research was conducted in the absence of any commercial or financial relationships that could be construed as a potential conflict of interest.

frontiers in Neuroscience

ORIGINAL RESEARCH
published: 12 March 2019
doi: 10.3389/fnins.2019.00215

Acupuncture for Histamine-Induced Itch: Association With Increased Parasympathetic Tone and Connectivity of Putamen-Midcingulate Cortex

Seorim Min[1,2†], Koh-Woon Kim[3,4†], Won-Mo Jung[1,2], Min-Jung Lee[2], Yu-Kang Kim[1,2], Younbyoung Chae[1,2], Hyangsook Lee[1,2] and Hi-Joon Park[1,2†]*

[1] Department of Science in Korean Medicine, Graduate School, College of Korean Medicine, Kyung Hee University, Seoul, South Korea, [2] Acupuncture and Meridian Science Research Center, Kyung Hee University, Seoul, South Korea, [3] Department of Korean Rehabilitation Medicine, College of Korean Medicine, Kyung Hee University, Seoul, South Korea, [4] East-West Medical Research Institute, Kyung Hee University, Seoul, South Korea

OPEN ACCESS

Edited by:
Florian Beissner, Hannover Medical School, Germany

Reviewed by:
Hee Young Kim, Daegu Haany University, South Korea
Yi-Hung Chen, China Medical University, Taiwan

***Correspondence:**
Hi-Joon Park
acufind@khu.ac.kr

† These authors have contributed equally to this work

Specialty section:
This article was submitted to Perception Science, a section of the journal Frontiers in Neuroscience

Received: *27 July 2018*
Accepted: *25 February 2019*
Published: *12 March 2019*

Citation:
Min S, Kim K-W, Jung W-M, Lee M-J, Kim Y-K, Chae Y, Lee H and Park H-J (2019) Acupuncture for Histamine-Induced Itch: Association With Increased Parasympathetic Tone and Connectivity of Putamen-Midcingulate Cortex. Front. Neurosci. 13:215. doi: 10.3389/fnins.2019.00215

Previous studies have suggested that acupuncture is effective for ameliorating itch intensity. However, factors associated with the antipruritic effects of acupuncture have yet to be clarified. In a randomized, sham-controlled, crossover trial, we investigated the antipruritic effects of acupuncture against histamine-induced itch in healthy volunteers. Autonomic changes using heart rate variability (HRV) and brain connectivity using functional magnetic resonance imaging (fMRI) were also assessed to identify physiological factors associated with the acupuncture response. Acupuncture significantly reduced itch intensity and skin blood perfusion as assessed by laser Doppler perfusion imaging compared to sham control, indicating the antipruritic effects of acupuncture. In responder and non-responder analysis, the power of normalized high frequency (HF norm) was significantly higher, while the power of normalized low frequency (LF norm) and LF/HF ratio were significantly lower in responders compared to non-responders, suggesting the acupuncture response involved parasympathetic activation. In fMRI analysis, the putamen and the posterior part of the midcingulate cortex (pMCC) were positively connected to itch and negatively correlated with itch intensity in responders. These results suggest that parasympathetic activity and functional connectivity of the putamen and pMCC could be associated with antipruritic response to acupuncture.

Keywords: acupuncture, histamine, itch, heart rate variability, functional magnetic resonance imaging, putamen, midcingulate cortex

INTRODUCTION

The sensation of itch, defined as "an unpleasant sensation associated with the desire to scratch," is the most prevalent subjective symptom of inflammatory skin diseases and cause of suffering in many dermatologic and some allergic conditions (Charlesworth and Beltrani, 2002). Itching leads to scratching, consequently interfering with skin barrier function. With the loss of cutaneous integrity

and softening of the skin surface, a vicious cycle of skin damage and inflammation occur. This cycle induces a state of complex dermatitis, creates more itching, resulting in a scratch-itch cycle, and leads to serious quality-of-life problem. Patients with atopic dermatitis (AD) suffer from severe itch, most notably hampering their quality of sleep (Arck and Paus, 2006; Bender et al., 2008).

The autonomic nervous system (ANS) is the primary mechanism for the response to external stimuli. The response results in a fight-or-flight system from the sympathetic nervous system (SNS) or freeze-or-dissociate response from parasympathetic nervous system (PNS). Some studies suggest that the ANS functions in the itch mechanism (Stander and Steinhoff, 2002; Chida et al., 2007; Cicek et al., 2008). A previous study (Kirchner et al., 2002) found that the vagus nerve, which is the main parasympathetic outflow, controls histamine-induced itch, probably by a central mechanism. The brain circuitry involved in the itch sensation is an active topic of study of the peripheral and central sensitization for itch (Desbordes et al., 2015). Itch is usually perceived when inflammatory mediators activate a specific subset of peripheral sensory nerve endings, an activation that is transmitted to the brain via the spinothalamic tract (Andrew and Craig, 2001; Davidson et al., 2007; Napadow et al., 2014).

Many studies have focused on itch itself, but appropriate treatments are far from satisfactory. A systematic review (Yu et al., 2015) suggested that acupuncture is effective for ameliorating itch intensity in itch-related diseases. Topical antihistamines have limited use for acute itch only and have relatively high costs and risks for allergic contact dermatitis sensitization (Callahan and Lio, 2012). A previous study showed that acupuncture has better antipruritic effects than third generation antihistamines (Napadow et al., 2014). Another study comparing acupuncture and second generation antihistamine found that acupuncture demonstrated a greater effect during peak itch intensity, while antihistamine had a stronger effect during lower itch intensity suggesting different mechanisms of action (Pfab et al., 2012a). Acupuncture for experimentally induced itch in healthy participants (Belgrade et al., 1984; Lundeberg et al., 1987; Pfab et al., 2005) and patients with AD (Pfab et al., 2010, 2011, 2012a; Napadow et al., 2014) has a significant antipruritic effect compared to placebo. Possible mechanisms for itch reduction by acupuncture in patients with AD include reduction of *in vitro* allergen-induced basophil activation and modulation of neurotransmitters, peripheral hormone levels, and brain areas that are involved in itch processing (Pfab et al., 2013). Furthermore, acupuncture may reduce itch by creating an inhibitory input called gate-control theory through the response of the sensory nerve with a one-to-one correspondence between dermatomes and spinal segments (Bear et al., 2016). However, factors related to the antipruritic effects of acupuncture remain unclear.

Acupuncture stimulation influences organs and functions including ANS activity (Kawakita et al., 2006) and brain processing (Dhond et al., 2007a,b). Several studies suggest that acupuncture influences ANS functions such as blood pressure, skin conductance, skin temperature, heart rate, and heart rate variability (HRV) (Malliani et al., 1991; Lee et al., 2010; Chung et al., 2014). Studies found that press needle stimulation induces alterations in vagal function (Noda et al., 2015) and acupuncture stimulation at HT7 affects cardiac autonomic neural regulation in healthy individuals, mainly via the PNS (Huang et al., 2015). Acupuncture activates the PNS and default mode network connectivity (Dhond et al., 2008). It induces changes in heart rate and brain stem structures (Beissner et al., 2012).

Using functional magnetic resonance imaging (fMRI), we investigated changes in cerebral perfusion to identify the critical brain areas mediating the antipruritic effect of acupuncture. The fMRI method for imaging brain functions is increasingly used to investigate dynamic brain patterns with acupuncture stimulation (Malliani et al., 1991; Park et al., 2005; Dhond et al., 2007b; Colombo et al., 2015). In clinics, acupuncture treatment typically involves a phase of needle retention following acupuncture insertion and manipulation. Thus, functional connectivity indicating characteristics of acupuncture is better suited for a block design of fMRI analysis. Functional connectivity analysis explores the relationship between neuronal activation patterns that functionally linked, but anatomically separated brain areas (Colombo et al., 2015). The striatum, which consists of the putamen and the caudate, is critical for striato-thalamo-cortical circuits for itch. An fMRI study (Napadow et al., 2014) found itch reduction following acupuncture is associated with reduced activation of the putamen response. Thus, our study chose the putamen as a seed ROI.

Since individually differing responses to acupuncture have been reported and itch is a subjective symptom, an individualistic approach is needed (Park et al., 2005; Chae et al., 2006). Our individualistic approach classified participants into responders and non-responders (Scholz and Woolf, 2002; Woodcock et al., 2007; Schork, 2015). Analysis of the differences between responders and non-responders strengthens therapeutic effects by managing response-related factors (Kim et al., 2007).

The aim of this study was to test the antipruritic effects of acupuncture on experimentally induced itch. Subsequently, we investigated the factors that influenced these effects via ANS response and functional connectivity of the brain by analyzing responder and non-responder groups.

MATERIALS AND METHODS

The study was conducted in two separate steps. *Study 1* was followed by *Study 2*.

Participants

For *Study 1*, 20 healthy participants between 18 and 50 years of age were recruited using an advertisement. Participants with no present history of asthma and AD were screened by telephone. *Study 2* had 15 participants who met the schedule for fMRI scans and retested for MRI compatibility. All participants refrained from alcohol or caffeine for 12 h before experiments. Participants with skin problems on the stimulated site were excluded. Participants had to stop antihistamine medications at least 3 days before the study to avoid potential influence on normal itch perception or flare and wheal response to SPT, nevertheless, in

case of no itch response, the applicable data would be excluded for analysis. Detailed explanations of experimental procedures such as the two conditions and four visits were given. This study was carried out in accordance with the recommendations of the guideline for clinical researches, Kyung Hee University Ethics Committee with written informed consent from all subjects. All subjects gave written informed consent in accordance with the Declaration of Helsinki. The protocol was approved by the Kyung Hee University Ethics Committee (KHSIRB-15-056).

Experimental Design

The study design was a randomized, crossover trial in which each participant served as his or her own control. Participants received acupuncture and placebo stimulation in random order. Session orders were determined with a random number table generated by Excel (Microsoft, Redmond, WA, United States). Each experiment was separated by 7 days and occurred at the same time of the day. Tests were carried out in winter, in January to March 2016, to minimize the influence of environmental allergens.

Study 1 was in a light-conditioned and quiet room. Room temperature was controlled at 23 ± 1°C (mean ± SD). Demographic data including gender, age, height, and weight and psychological factors such as credibility, expectation, and fear of acupuncture and perception of bodily sensation were collected from all participants. After 15 min of resting, participants were seated on a chair throughout and remained comfortable in that position. Baseline skin blood perfusion and HRV measurements were obtained for 5 min and interventions were subsequently performed on the non-dominant side. Skin blood perfusion and HRV were obtained (A1 and A2 phase) for 10 min. After itch induction, HRV, skin blood perfusion and itch intensity were measured for 10 min (H1 and H2 phase). The intervention was removed and skin blood perfusion, HRV, and itch intensity were obtained (H3 and H4 phase) (**Figure 1A**).

For *Study 2*, room temperature was controlled at 11 ± 1°C (mean ± SD). As participants lay in the magnet, they viewed a screen using prism glasses to respond to situations by pressing a button. After 15 min of resting, participants underwent three fMRI scanning sessions. Each session included a 4-min baseline resting state scan, intervention (5 min), and itch resting state scan (0–4, 4–8 min) (**Figure 1B**). The order of acupoints and rest periods within each session were counterbalanced and randomized across participants. Itch was induced as in *Study 1*. The study flow is depicted in **Figure 2**.

Acupuncture and Placebo Control

For *Study 1*, manual acupuncture stimulation was used on the arm and leg of the participant's non-dominant side at LI11 (on the elbow at the midpoint of the end of the transverse cubital crease and lateral epicondyle of the humerus when the elbow is flexed); SP10 (on the medial aspect of the thigh, 6.6 cm above the medio-superior border of the patella, on the bulge of the medial portion of muscle quadriceps femoris when the knee is flexed); PC6 (on the palmar aspect of the forearm, 6.6 cm proximal to the middle point of the carpal fold, on the line connecting PC3 and PC7, between the tendons of muscle palmaris longus and muscle flexor carpi radialis); HT7 (on the wrist, at the ulnar end of the transverse crease, in the depression on the radial side of the tendon of the ulnar flexor muscle); and ST36 (on the anterior aspect of the lower leg, 9.9 cm below ST35, middle finger from the anterior crest of the tibia). Acupoints based on a standard acupuncture textbook, previous study, and clinical experience, are important for treating cutaneous itch. LI11 and SP10 are used frequently to treat itch in clinical and experimental studies (Pfab et al., 2005, 2010, 2011, 2012a). To induce activation of the PNS, HT7 (Huang et al., 2015) and PC6 (Huang et al., 2005; Li et al., 2005) were chosen. ST36 is the most frequently used acupoint for immune regulation and anti-inflammatory effects, and reducing SNS (Michikami et al., 2006). For *Study 2*, due to fMRI system structural problems, LI11 was excluded.

For *Study 1*, sterile stainless steel needles (0.20 mm in diameter, 30 mm in length; Haeng Lim Seo Won, South Korea) were inserted to depth (LI11, 20 mm; SP10, 15 mm; PC6, 15 mm; HT7, 6 mm; ST36, 20 mm) controlled by an empty guide tube and manipulated for 9 s repeated every 5 min over 20 min (**Figure 3A**). For *Study 2*, non-magnetic titanium sterile acupuncture needles (0.20 mm diameter, 40 mm length; DongBang Acupuncture Inc., Boryeong, South Korea) were used. Manipulation techniques were performed as tonifying and reducing, which involved bidirectional rotation (1 Hz). A previous study (Takakura et al., 1995; Min et al., 2015) showed repeated manipulation improves acupuncture effects and traditionally, manual acupuncture uses manipulation to reinforce effects (Kim et al., 2000). The same doctor of Korean medicine with a certified license performed all acupuncture treatments. Prior to baseline, skin was cleaned with alcohol at the acupoint and histamine stimulus locations.

As a placebo control, tactile stimulation was performed by gentle tapping with a size 5.46 von Frey filament (Touch-Test Sensory Evaluator Instructions, North Coast Medical, Inc., CA, United States) every 5 min over 20 min for *Study 1* and over 5 min for *Study 2*. Placebo acupoints were on the arm and leg using the same meridian system, but not acknowledged as acupoints by textbooks. The non-acupoint for LI11 was on the lateral side of the arm at the midpoint of the line connecting LI11 and LI15. The non-acupoint for SP10 was on the medial aspect of the thigh at the midpoint of the line connecting SP10 and SP12. The non-acupoint for PC6 was on the palmar aspect of the forearm at the midpoint of the line connecting PC3 and PC7. The non-acupoint for HT7 was on the palmar aspect of the forearm at the midpoint of the line connecting HT3 and HT7. The non-acupoint for ST36 was on the anterior aspect of the lower leg in the center of the belly of the muscle tibialis anterior. Placebo procedures were carried out as acupuncture procedures. The von Frey filament and acupuncture materials were prepared in advance and placed on a tray and covered so materials could not be seen by participants. Locations of acupoints and non-acupoints were blinded by self-produced blinding box. More detailed procedures according to the Standard for Reporting Interventions in Clinical Trials of Acupuncture (STRICTA) are attached in **Supplementary Appendix 1**.

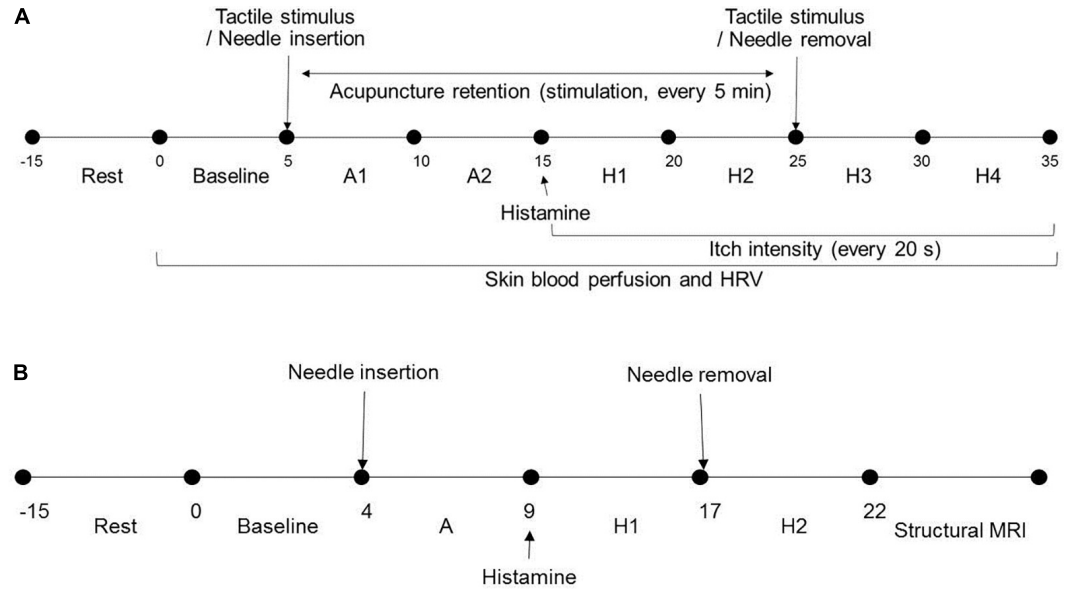

FIGURE 1 | Study design and experimental procedures: **(A)** In *Study 1*, after resting, baseline skin blood perfusion and HRV were obtained for 5 min and intervention was subsequently performed on the non-dominant side. Skin blood perfusion and HRV were obtained (A1 and A2 phase) for 10 min. After itch induction, HRV, skin blood perfusion, and itch intensity were measured for 10 min (H1 and H2 phase). The intervention was removed and skin blood perfusion, HRV, and itch intensity were obtained (H3 and H4 phase). **(B)** In *Study 2*, after 15 min resting, participants underwent three fMRI scanning sessions. Scans for each session were for 4-min baseline resting state, intervention (A, 5 min), and itch resting state (H1, 0–4; H2, 4–8 min). HRV, heart rate variability; s, seconds; min, minutes; fMRI, functional magnetic resonance imaging.

Itch Induction

After acupuncture procedures, 1% histamine (10 mg/ml histamine dihydrochloride, Lofarma, Milan, Italy) was applied to induce itch on the volar aspect of the forearm and medial aspect of the foot of the participant's non-dominant side using SPT. A single drop of histamine in aqueous solution was applied to the skin, followed by puncture with a lancet for SPT as in routine allergy diagnosis. The technique was performed by the same investigator.

Itch Intensity

For *Study 1*, itch intensity was rated at 20-s intervals for 20 min after SPT. Participants were seated with the left arm resting on the cushion of a chair arm and the other hand selecting a number from 0 (no itch) to 10 (worst imaginable itch). One-third of the scale (3.3/10) was the intervention point "scratch threshold," above which the individual felt a strong desire to scratch, which was not allowed. Area under the rating curve above the scratch threshold was calculated as itch intensity multiplied by time (in min). For *Study 2*, participants could view a screen in the scanner through prism glasses in the supine position. Itch intensity was quantitatively expressed in percent of a visual analog scale (VAS) at 4 and 8 min after SPT. Participants reported perceived itch intensity by pressing one of four buttons in an MRI-compatible button box (Current Design^{TM}). Participants were familiarized with the rating procedure, which was a different reporting method than a previous study, with exercises before the fMRI session. This study did not record continuous ratings to minimize other effects.

Skin Blood Perfusion Using Laser Doppler Perfusion Imaging

A PIM3 system (Perimed AB, Järfälla, Sweden) was used to measure skin blood perfusion in this study. The area of interest was 4.5 cm × 4.5 cm at the stimulus site on the non-dominant foot. The distance between the detector and the tissue was fixed to 45 cm with normal resolution. To minimize movement, the foot was fixed with a kapok-filled vacuum cushion. Skin blood perfusion was measured at baseline for 10 min after intervention (A1 and A2 phase), and 20 min post prick testing (H1, H2, H3, and H4 phase) in *Study 1*.

Heart Rate Variability Using MP150

For electrocardiographic recordings, three electrodes were attached to participants' chests. The sampling rate of the electrocardiogram (ECG) was 1000 samples/s and signals were amplified with a BIOPAC (Biopac Systems, Inc., Goleta, CA, United States) ECG100C amplifier. HRV data were calculated from a series of 5-min epochs of ECG signals. Spectral HRV components were evaluated and obtained as absolute values of power (ms^2) based on frequency to one of three bands: very low frequency component (0.00–0.04 Hz), low frequency (LF) component (0.04–0.15 Hz), and high frequency (HF) component (0.15–0.40 Hz). HF and LF components of HRV were conventionally observed in normalized units. HF norm is an indicator of parasympathetic tone and LF norm is a measure of sympathetic regulation (Malliani et al., 1991; Camm et al., 1996). LF/HF ratio, an estimate of the balance between sympathetic

and parasympathetic activities, was calculated from the absolute power of both frequency components.

Blinding

At the end of the study, participants were asked if they believed they received "acupuncture treatment" or "placebo treatment." Bang's blinding index, ranging from −1 to 1, was calculated: 0 was random guessing (50% correct and 50% incorrect); 1 was complete unblinding (all responses correct); and −1 was all responses incorrect (Bang et al., 2010).

Statistical Analysis

Statistical analyses were carried out using SPSS version 22.0 software (IBM SPSS Statistics, IBM Corporation, Armonk, NY, United States). Unless otherwise stated, data are mean values (95% confidence intervals). *P*-values <0.05 were considered statistically significant.

Data on itch intensity, skin blood perfusion, and HRV parameters were divided into 5-min intervals for ease of data management and analysis and changes were calculated using the formula: (change from baseline)/baseline X 100. Measurement times were divided into seven phases: (1) baseline, (2) A1 (0–5 min after acupuncture), (3) A2 (5–10 min after acupuncture), (4) H1 (0–5 min after histamine stimulus), (5) H2 (5–10 min after histamine stimulus), (6) H3 (10–15 min after histamine stimulus), (7) H4 (15–20 min after histamine stimulus). For responder and non-responder analyses, entire samples were separated into responders ($N = 10$) and non-responders ($N = 10$) based on the mean of sum values from arm and foot itch intensity at H1 using peak value.

Analyses were performed after checking all parameters were normally distributed using the Shapiro–Wilk one-sample test. Itch intensities for entire measurements were analyzed by two-way analysis of variance (ANOVA). Effects of time and time × treatment interaction using data divided into 5-min intervals were analyzed by repeated measure ANOVA. If Mauchly's test of sphericity was significant, Greenhouse–Geisser correction for degrees of freedom was used. Differences between acupuncture and placebo conditions were evaluated using a paired sample *t*-test or Wilcoxon signed rank test. Blinding integrity was analyzed using a chi-square test. Differences between responder and non-responder groups were evaluated using independent sample *t*-test or Mann–Whitney test. Correlation analysis used Pearson's correlation for parametric analysis.

fMRI Data Acquisition

Scanning used a 3-axis gradient head coil in a 3 Tesla Siemens MRI scanner with echo planar imaging. Structural scans were acquired using a magnetization prepared rapid gradient echo sequence with TR = 2000 ms, TE = 2.37 ms, flip angle 9°, field of view 240 mm, and slice thickness 1.0 mm. For resting state analysis, 37 slices were acquired with parameters: TR = 2000 ms, TE = 30 ms, flip angle 90°, field of view 240 mm, and slice thickness 4.0 mm, with in-plane spatial resolution at 3 mm × 3 mm × 3 mm.

fMRI Data Preprocessing and Analysis

This study focused only on resting state scans (baseline) before acupuncture and induced 8-min resting state scans (itch).

Preprocessing of resting state images used SPM12 software[1] implemented in a MATLAB suite (Mathworks, Inc., Natick, MA, United States). Preprocessing included slice time correction, head motion correction, coregistration to patients' structural images, segmentation, normalization, linear detrending, and smoothing (FWHM = 8 mm).

Functional connectivity analysis used the CONN toolbox[2] (Whitfield-Gabrieli and Nieto-Castanon, 2012). Time courses from components associated with white matter and cerebrospinal fluid were regressed from whole-brain gray matter activity and 12 motion regressors (6 realignment parameters and first derivatives) were used to control for correlations during movement. Data were filtered between 0.008 and 0.09 Hz and global brain signal was not subtracted.

Functional connectivity analysis used a seed-to-voxel approach. The left putamen was used as a seed. The segmentation mask of the left putamen in the Harvard-Oxford atlas is implemented in the CONN toolbox by default, so connectivity of the putamen with the anatomically defined brain areas was examined. The putamen mask used in our study (center MNI coordinates of $X = 26$, $Y = 3$, $Z = -1$) includes the MNI coordinates ($X = -32$, $Y = -14$, $Z = 6$) where is reported to be significantly correlated with itch rating in a previous study (Napadow et al., 2014). In first-level analysis, we produced a correlation map for each subject by extracting blood-oxygen-level dependent time courses from the putamen seed. Connectivity values between the putamen seed and other brain areas for the baseline and itch sessions (baseline-acupuncture and itch-acupuncture) were extracted for each participant. Furthermore, we performed Pearson correlation to explore the relationship between connectivity values of the putamen to VAS at 8 min, to determine if behavioral measures correlated with connectivity in the acupuncture conditions. Second-level connectivity analysis was performed with a between group factor (responder minus non-responder) and a within-subject factor treatment (itch minus baseline) to identify effects compared to baseline by two-way ANOVA. For all analyses, a threshold of $p < 0.05$, FDR corrected, was used based on the intensity threshold $p < 0.001$.

RESULTS

This study was conducted in two separate steps: *Study 1* was followed by *Study 2*. *Study 1* was 20 healthy participants (10 women, 10 men), mean age 22.5 (95% CI, 21.8–23.2) years, mean height 167.4 cm (95% CI, 163.5–171.3), mean weight 60.8 kg (55.8–65.9), and mean BMI 21.6 (95% CI, 20.3–22.9). From the 20 participants in *Study 1*, 15 (6 women, 9 men) who met the schedule for fMRI scans and retested for MRI compatibility, were mean age 22.8 (95% CI, 22.0–23.5) years, mean height 170.1 cm (95% CI, 166.0–174.1), mean weight 64.1 kg (59.0–69.2), and

[1] http://www.fil.ion.ucl.ac.uk/spm

[2] www.nitrc.org/projects/conn

mean BMI 22.1 (95% CI, 20.7–23.5) and included in *Study 2*. *Study 1* and *Study 2* courses are in **Figure 2**. Participants had more than one experience with acupuncture and no present history of asthma or AD.

Acupuncture vs. Placebo: Antipruritic Effects of Acupuncture

Changes in Itch Intensity

All of the 20 participants reported itch without pain 40 s after SPT. Itch intensities for the entire measurement were significantly lower in the acupuncture condition than the placebo condition for the arm ($p < 0.001$) and foot ($p < 0.001$) by two-way ANOVA (**Figures 3B,C**). Repeated-measure ANOVA showed significant effects on mean itch intensity for time (Greenhouse–Geisser corrected: $F = 70.536$, $p < 0.001$) and time × treatment interaction (Greenhouse–Geisser corrected: $F = 7.486$, $p = 0.002$) on the arm. Repeated-measure ANOVA showed significant effects on mean itch intensity for time (Greenhouse–Geisser corrected: $F = 69.654$, $p < 0.001$) and no significant effects on mean itch time × treatment interaction (Greenhouse–Geisser corrected: $F = 2.150$, $p = 0.120$) on the foot. At H1 and H2 phases, itch intensities were lower in the acupuncture condition (2.1 [95% CI, 1.4–2.7]; 1.3 [95% CI, 0.8–1.8]) compared to the placebo condition (3.8 [95% CI, 2.9–4.6]; 2.5 [95% CI, 1.5–3.5]) ($p < 0.001$ and $p = 0.015$, respectively) on the arm (**Figure 3D**). At H1, H2, and H3 phase, itch intensities were lower in the acupuncture condition (2.5 [95% CI, 1.7–3.4]; 1.6 [95% CI, 1.0–2.3]; 0.8 [95% CI, 0.4–1.2]) compared to the placebo condition (3.4 [95% CI, 2.6–4.1]; 2.6 [95% CI, 1.9–3.4]; 1.7 [95% CI, 1.0–2.3]) ($p = 0.001$, $p = 0.001$, and $p = 0.002$, respectively) on the foot (**Figure 3E**).

Time above scratch threshold was significantly lower in the acupuncture condition (21.7 [95% CI, 5.1–38.3]) than

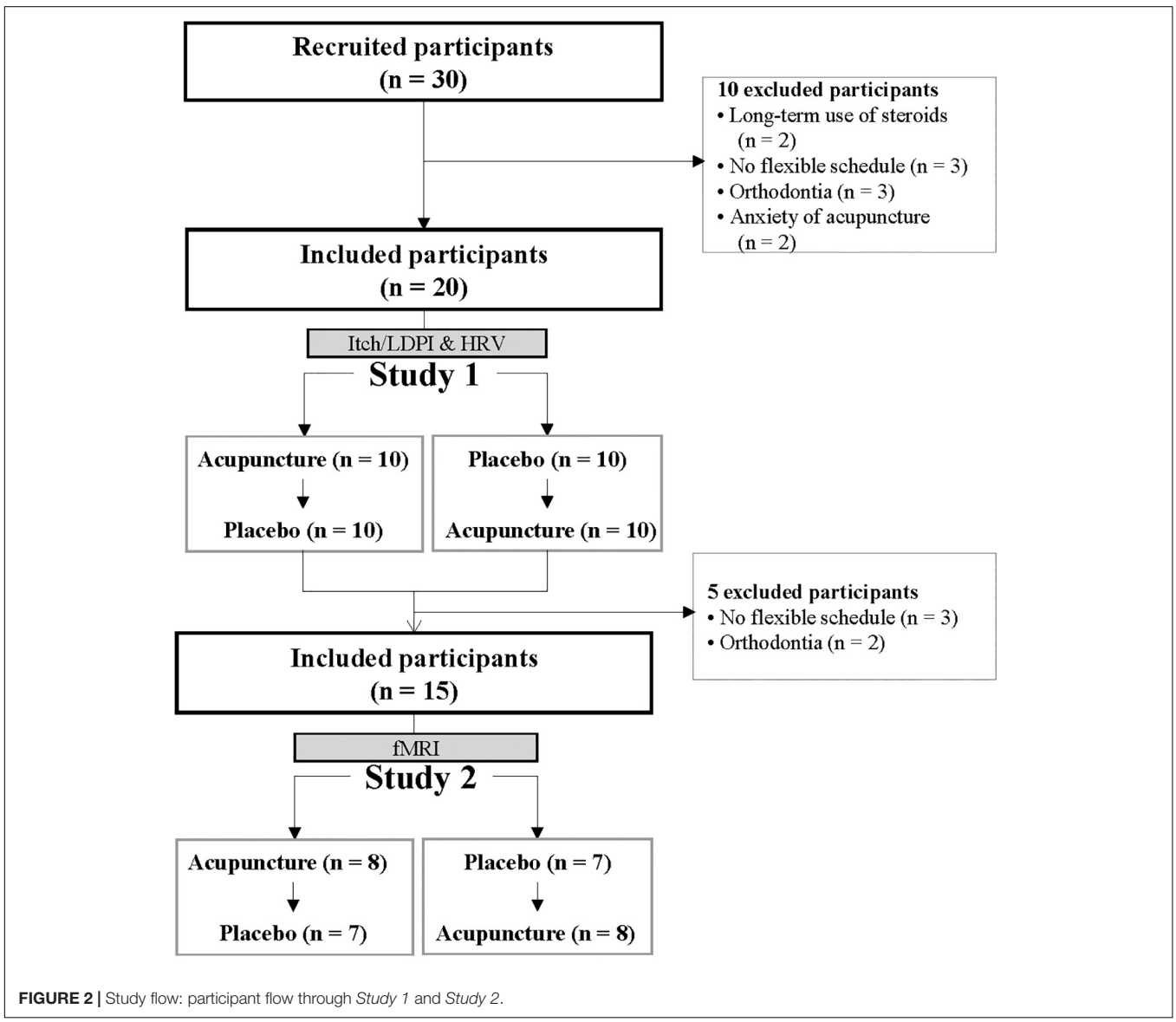

FIGURE 2 | Study flow: participant flow through *Study 1* and *Study 2*.

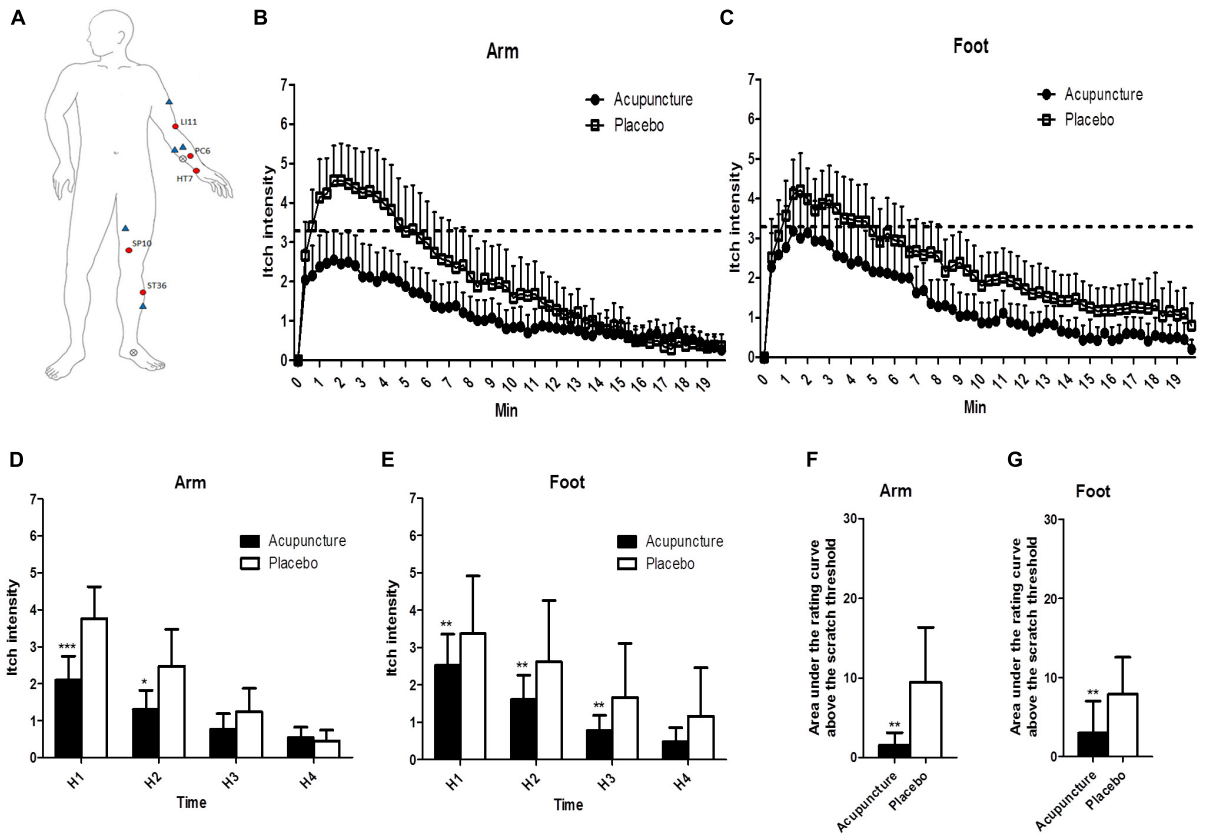

FIGURE 3 | The location of treatments and changes of itch intensity: **(A)** The locations of the acupoints in the acupuncture and the control points and the histamine-stimulated site. Red circles indicate acupoints in the acupuncture group, and blue triangles indicate placebo points. X marks indicate the location of histamine injection. **(B,C)** Itch intensity over time after histamine stimulus in the arm and the foot. The dotted line indicates scratch threshold (3.3/10). Itch intensities for entire measurements were significantly lower in acupuncture compared to the placebo condition for arm ($p < 0.001$) and foot ($p < 0.001$) in two-way ANOVA. **(D,E)** Area under the rating curve above the scratch threshold in the arm and the foot. **(F,G)** Mean of itch intensity by 5-min intervals after histamine stimulus in the arm and the foot. Values are mean (95% CI). *P*-values show results of paired sample *t*-test or Wilcoxon signed rank test for comparison of itch intensity between two conditions at each time point. $^{*}p < 0.05$, $^{**}p < 0.01$, $^{***}p < 0.001$. Relative to histamine stimulus, H1 is 0–5 min, H2 is 5–10 min, H3 is 10–15 min, and H4 is 15–20 min.

the placebo condition (71.4 [95% CI, 31.5–111.2], $p = 0.002$) on the arm. Time above scratch threshold was significantly lower in the acupuncture condition (29.3 [95% CI, 4.6–53.9]) than in the placebo condition (74.3 [95% CI, 33.3–115.3], $p = 0.008$) on the foot. The area under the rating curve above the scratch threshold for itch intensity was significantly lower in the acupuncture condition (94.2 [95% CI, −0.3 to 188.6]) than the placebo condition (568.3 [95% CI, 155.7–980.9], $p = 0.001$) on the arm (**Figure 3F**). The area under the rating curve above the scratch threshold for itch intensity was significantly lower in the acupuncture condition (178.1 [95% CI, −64.3 to 420.5]) than the placebo condition (473.7 [95% CI, 193.2–754.2], $p = 0.008$) on the foot (**Figure 3G**).

Changes in Skin Blood Perfusion

Mean perfusion units in the acupuncture condition were 323.3 (95% CI, 221.1–425.5), 391.5 (95% CI, 223.8–559.2), and 310.2 (95% CI, 166.9–453.6), and in the placebo condition 427.9 (95% CI, 283.6–572.1), 587.1 (95% CI, 419.7–754.4), 455.2 (95% CI, 318.6–591.8) ($p = 0.049$ at H1; $p = 0.021$ at H2; $p = 0.011$ at H3; $p = 0.022$ at H4) (**Figure 4A**). Maximum perfusion units were 642.8 (95% CI, 436.0–849.7) in the acupuncture condition and 840.6 (95% CI, 631.4–1050.0) in the placebo condition, with a significant difference ($p = 0.036$) (**Figure 4B**). Itch intensity was significantly correlated with skin blood perfusion ($r = 0.36$, $p = 0.02$) (**Figure 4C**). Representative images of skin blood perfusion from a participant are in **Figure 4D**.

Changes in Heart Rate Variability

Acupuncture compared to placebo showed no significant change on normalized high frequency (HF norm), normalized low frequency (LF norm), or LF/HF ratio. Participants in the acupuncture condition experienced increased HF norm and decreased LF norm and LF/HF ratio from baseline at H1, while participants in the placebo condition did not.

Assessment of Blinding

Comparisons of blinding rates showed no significant difference between conditions, as assessed by chi-square test with $p = 0.068$.

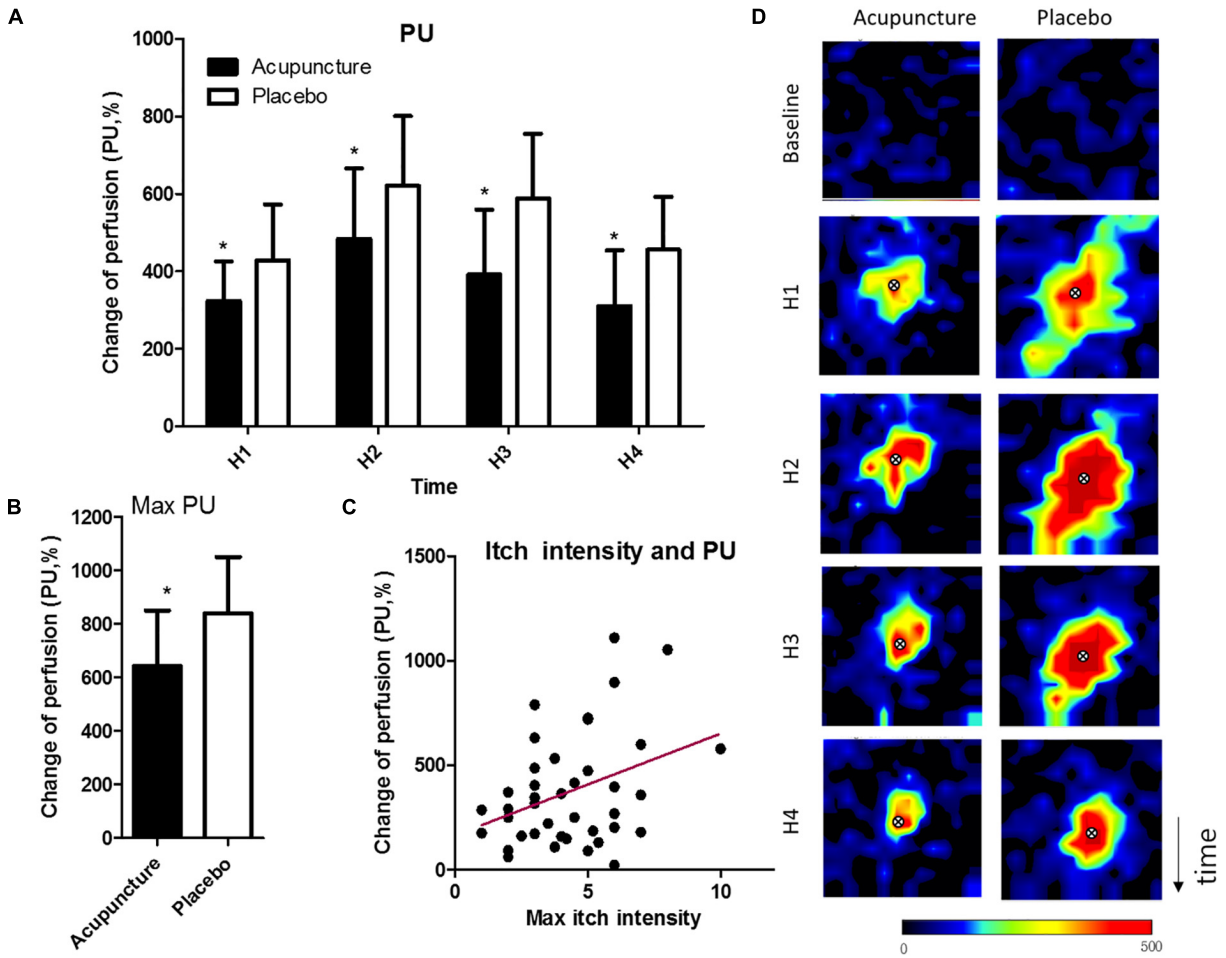

FIGURE 4 | Changes in skin blood perfusion: **(A)** Mean of skin blood perfusion every 5 min after histamine stimulus, **(B)** Maximum skin blood perfusion during the study, **(C)** Correlation of maximum of itch intensity and skin blood perfusion, **(D)** Representative images of skin blood perfusion of a participant. X marks indicate the location of histamine injection. Values are mean (95% CI). *P*-values are for paired sample *t*-tests for comparison of change in skin blood perfusion from baseline between the two conditions. $*p < 0.05$. Perfusion unit ranges from black (lowest value) to red (highest). Relative to histamine stimulus, H1 is 0–5 min, H2 is 5–10 min, H3 is 10–15 min, and H4 is 15–20 20 min. PU, perfusion unit.

Thus, participants could not predict if they received acupuncture or placebo. In the acupuncture condition, 75% of participants correctly guessed the treatment (Bang's blinding index = 0.75 [95% CI, 0.52–0.98]). Placebo treatment had successful blinding (Bang's blinding index = 0 [95% CI, −0.39 to 0.39]).

Seed-Based Functional Connectivity Analysis Using fMRI

Acupuncture stimulation ("itch" minus "baseline") compared to placebo stimulation ("itch" minus "baseline") revealed no significant change in functional connectivity of the putamen.

Responder vs. Non-responder Analysis: Factors Influencing Acupuncture Response

For responder and non-responder analysis, the entire sample was separated into 10 responders and 10 non-responders in *Study 1*. They were based on a mean of the sum values of arm itch intensity and foot itch intensity at H1 in *Study 1* involving peak value in the acupuncture condition. Mean itch intensities at H1 phase in *Study 1* were 2.5 (95% CI, 1.9–3.1) in responders and 6.7 (95% CI, 4.9–8.5) in non-responders for sum values from arm and foot itch intensity in the acupuncture condition.

Baseline data for psychological factors influencing response to acupuncture are in **Figure 5**. Questionnaire results for acupuncture credibility were not significantly different between responder and non-responder groups: values were 17.5 (95% CI, 15.9–19.1) in the responder group and 17.9 (95% CI, 15.9–19.9) in the non-responder group (**Figure 5A**). Acupuncture expectancy for the treatment indicated no significant difference between the responder (13.6 [95% CI, 11.9–15.2]) and non-responder groups (12.6 [95% CI, 9.9–15.3]) (**Figure 5B**). Perception of bodily sensation showed no significant difference between responder and non-responder groups: the value was 39.9 (95% CI, 31.9–47.9) in the responder group and 37.0 (95%

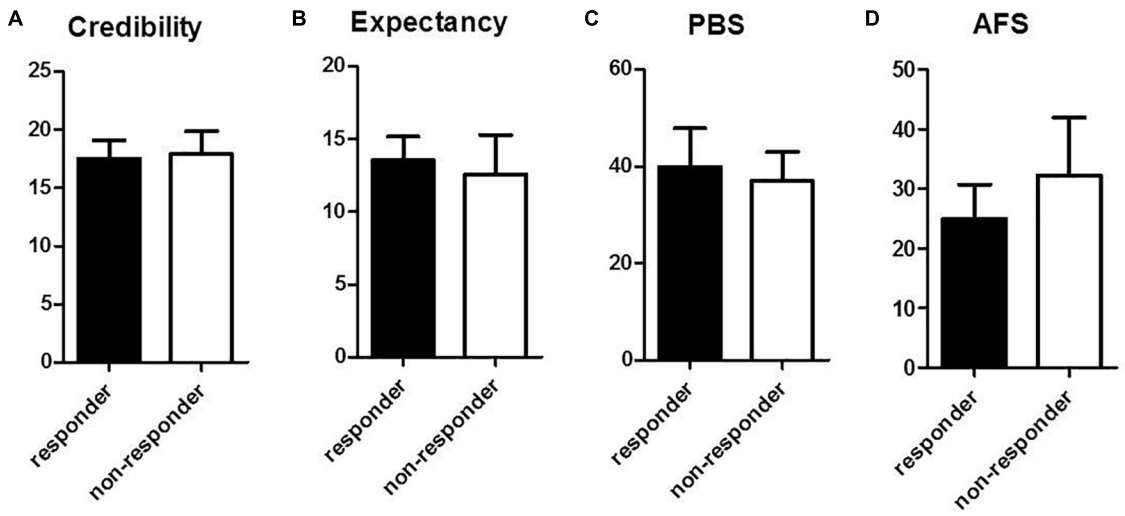

FIGURE 5 | Comparison of psychological factors between responder and non-responder groups at baseline: **(A)** Questionnaire for acupuncture credibility, **(B)** Questionnaire for acupuncture expectancy, **(C)** Perception of bodily sensation, PBS, **(D)** Acupuncture Fear Scale. Values represent mean (95% CI).

CI, 31.0–43.0) in the non-responder group (**Figure 5C**). Fear of acupuncture was not significantly different between responder and non-responder groups. The scale was 25.0 (95% CI, 19.3–30.7) in the responder group and 32.3 (95% CI, 22.6–42.0) in the non-responder group (**Figure 5D**).

Changes in Itch Intensity

In *Study 1*, mean itch intensities at H1 phase were lower in responders (2.5 [95% CI, 1.9–3.1]) compared to non-responders (6.7 [95% CI, 4.9–8.5]) for sum values from arm and foot itch intensity ($p < 0.001$) in the acupuncture condition. In *Study 2*, mean itch intensities at 8 min were lower in responders (2.7 [95% CI, 0.7–4.6]) compared to non-responders (6.0 [95% CI, 4.0–8.1]) for sum values for arm and foot itch intensity ($p = 0.021$) in the acupuncture condition.

Changes in Heart Rate Variability

HF norm in the responder group was 32.9 (95% CI, 3.0–62.9) and 49.5 (95% CI, 8.7–90.3). In the non-responder group, HF norm was −1.0 (95% CI, −11.7 to 9.8) and 0.8 (95% CI, −10.9 to 12.5) at A1 and A2 phase with a significant difference ($p = 0.009$ for A1 and $p = 0.035$ for A2). HF norm in the responder group was 81.2 (95% CI, −22.6 to 184.9) and 34.9 (95% CI, −24.8 to 94.7). HF norm in the non-responder group was −9.9 (95% CI, −17.2 to 2.6) and −22.1 (95% CI, −34.7 to 9.5) after histamine stimulus (H1 and H3 phase) with a significant difference ($p = 0.007$ for H1 and $p = 0.029$ for H3) between responder and non-responders to acupuncture (**Figure 6A**). HF norm values were not significantly different between responders and non-responders for placebo (**Figure 6B**).

LF norm for responders to acupuncture was −16.18 (95% CI, −25.3 to 7.1) for A1 phase, −12.4 (95% CI, −27.7 to 2.9) for H1 and 5.8 (95% CI, −16.4 to 28.0) for H3. LF norm for non-responders was 7.1 (95% CI, −12.1 to 26.3) for A1, 13.8 (95% CI, −2.7 to 30.2) for H1 and 42.9 (95% CI, 10.1–75.7) for H3. Differences were significant ($p = 0.028$, $p = 0.015$, and $p = 0.023$, respectively) (**Figure 6C**). LF norm values were not significantly different between responders and non-responders in the placebo condition (**Figure 6D**).

The LF/HF ratios in responders to acupuncture were −31.8 (95% CI, −46.9 to 16.7) for A1 phase, −29.0 (95% CI, −58.1 to 0.0) for H1 and 11.2 (95% CI, −49.9 to 72.4) for H3. LF/HF ratios for non-responders to acupuncture were 22.8 (95% CI, −19.9 to 65.5) for A1, 29.3 (95% CI, 2.9–55.8) for H1, and 1127 (95% CI, 26.2–199.3) for H3. Differences were significant ($p = 0.019$, $p = 0.003$, and $p = 0.019$, respectively) (**Figure 6E**). HF norm values were not significantly different between responders and non-responders for placebo given (**Figure 6F**).

Seed-Based Functional Connectivity Analysis Using fMRI

Responder ("itch" minus "baseline") compared to non-responder showed significant changes in putamen-posterior part of the midcingulate cortex (pMCC) connectivity (MNI coordinates of the peak voxel: $X = -6$, $Y = 0$, $Z = 40$, cluster p-FDR = 0.043). More positive putamen-pMCC connectivity was observed in the responder group following acupuncture stimulation compared to the non-responder group. Connectivity correlated negatively with itch intensity ($r = -0.573$ $p = 0.032$) (**Figure 7**). Functional connectivity changed significantly from baseline to itch for several of seed regions including basal ganglia (peak p-unc <0.001) (**Table 1**).

DISCUSSION

This study showed that experimentally induced itch and skin blood perfusion that were increased by histamine injection were significantly reduced after acupuncture compared to placebo.

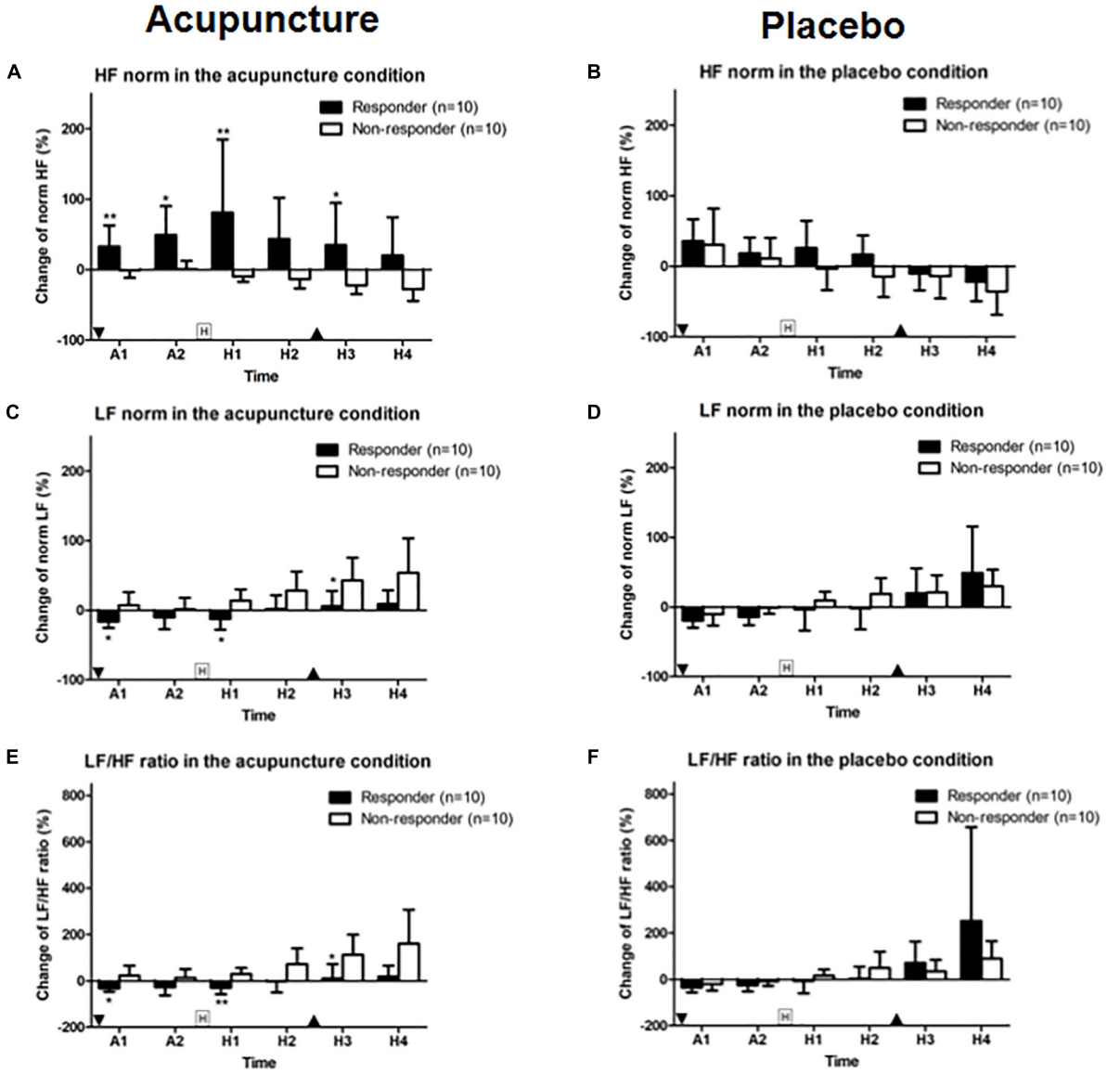

FIGURE 6 | Change in HF and LF norm and LF/HF ratios: **(A,B)** HF norm, **(C,D)** LF norm, and **(E,F)** LF/HF ratio for acupuncture and placebo stimulation between responder and non-responder groups. Values are mean (95% CI). "Squared H" indicates time points for histamine stimulus. "Inverted triangle" indicates time point for insertion of acupuncture and "triangle," removal of acupuncture. *P*-values are for independent sample *t*-tests comparing changes in heart rate variability from baseline between groups. $^{*}p < 0.05$, $^{**}p < 0.01$. A1 is 0–5 min and A2 is 5–10 min after intervention. Relative to histamine stimulus, H1 is 0–5 min, H2 is 5–10 min, H3 is 10–15 min, and H4 is 15–20 min.

Because itch is not a local symptom but a systemic symptom in clinical situations, we induced itch on both the arm and the foot simultaneously. Acupuncture reduced itch in both areas, indicating the systemic antipruritic effects of acupuncture. This study also showed via responder and non-responder analysis that itch intensity reduction was associated with PNS activation and positive functional connectivity of the putamen-pMCC following acupuncture. Psychological factors such as credibility, expectation, and fear of acupuncture and perception of bodily sensation were not related to itch response to acupuncture. To our knowledge, this is the first study to investigate factors related to acupuncture by distinguishing differences between responders and non-responders to itch.

In previous studies, the effects of acupuncture stimulation on histamine-induced itch were observed in healthy participants: Belgrade et al. (1984) and Lundeberg et al. (1987) reported reduced itch intensity using electroacupuncture stimulation during intradermal histamine injection. Pfab et al. (2005) showed significant reduced histamine-induced itch and wheal formation after acupuncture-point treatment compared to placebo-point treatment and no treatment; Kesting et al. (2006) showed ipsilateral acupuncture treatment significantly reduces areas

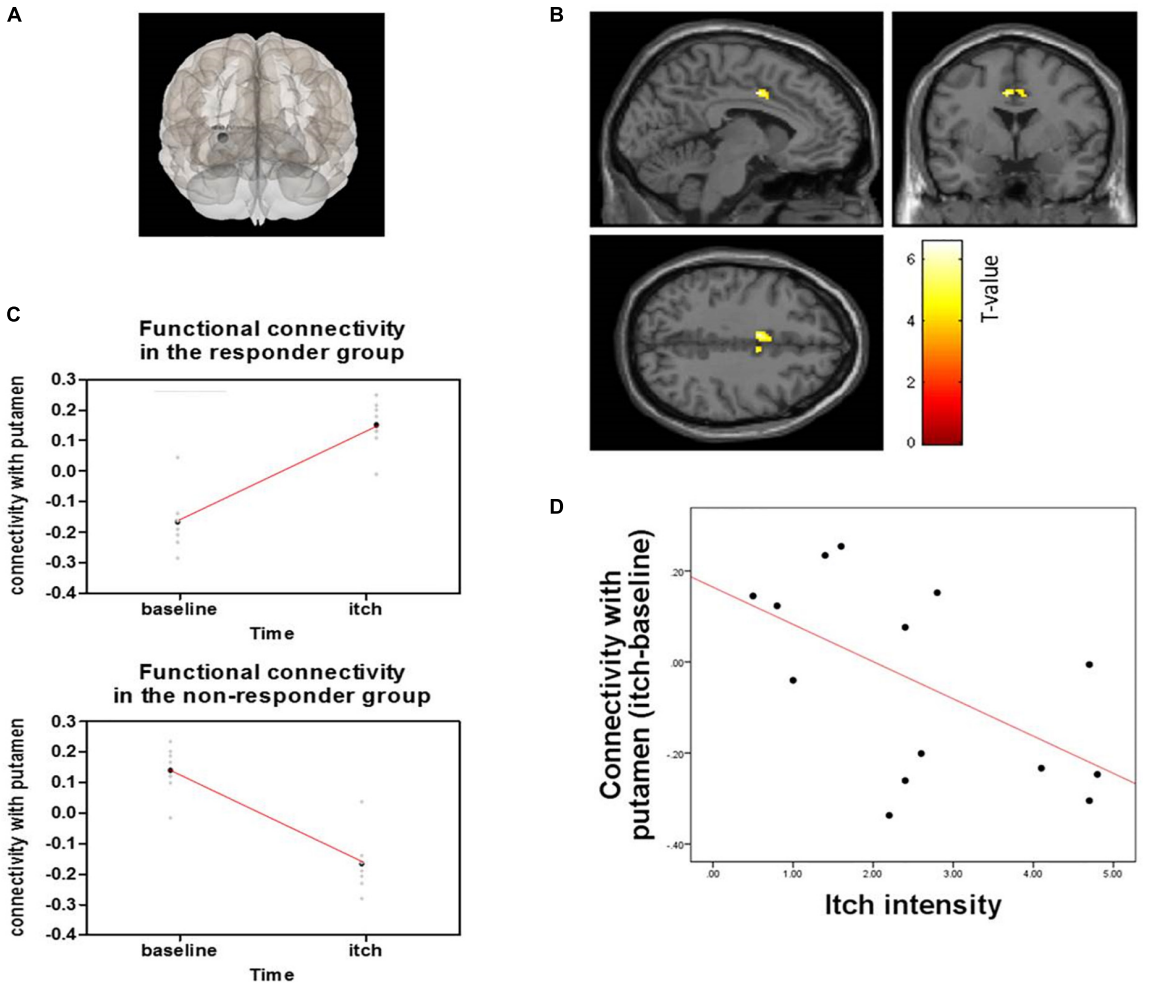

FIGURE 7 | Functional connectivity of the putamen and pMCC and correlation with connectivity and itch intensity for acupuncture treatment between responder and non-responder groups: **(A)** Seed was putamen, **(B)** Seed-based functional connectivity from the putamen, showing a significant cluster in the midcingulate cortex ($X = -6$, $Y = 0$, $Z = 40$), **(C)** Change in functional connectivity from baseline resting state to histamine-induced itch state in responders (top) and non-responders (bottom), **(D)** Graph shows differences in connectivity from baseline to itch as a function of differences in perceived itch intensity from baseline to itch, as reported by participants for each scan session.

of alloknesis (a sensory phenomenon that appears in area surrounding an itching source) after histamine application compared with contralateral and no-acupuncture treatment. Pfab et al. (Pfab et al., 2010, 2012a) showed that patients had significantly reduced type I hypersensitivity itch, which is commonly seen in AD. Acupuncture could therefore be useful for managing itch, urticarial or eczema in patients with AD. Pfab et al. (2011) also showed that itch intensity and basophil activation decreased with acupuncture in patients with AD from IgE-mediated allergy. And as did in the previous study, our study chose a protocol of pretreatment acupuncture and skin prick test (SPT) for histamine, to investigate the preventive antipruritic effects of acupuncture. Because the itch VAS is a subjective outcome, we used the laser Doppler perfusion imaging detecting skin blood perfusion to measure itch objectively.

The ANS innervates almost every part of the body and interacts with the immune system. In particular, the parasympathetic division of the ANS facilitates the immune response (Bear et al., 2016). Recent studies elucidated the role of the ANS in the itch mechanism (Chida et al., 2007; Cicek et al., 2008). In healthy participants, histamine stimulus induces an increase in the SNS from baseline (Tran et al., 2010). Stander and Steinhoff (2002) suggested that ANS dysfunction may contribute to itch in patients with AD. Kirchner et al. (2002) showed that the vagus nerve controls histamine-induced itch. Several studies (Backer et al., 2008) explored the action of acupuncture on the ANS by analyzing changes in HRV. These studies suggest that acupuncture stimulates parasympathetic activity (Kitagawa et al., 2014). In our study, participants in the responder group had an activated PNS and deactivated SNS, but non-responder groups did not. These results imply that an activated PNS might be associated with the antipruritic effect of acupuncture.

The PNS was more highly activated during the first 5 min after acupuncture insertion (A1 phase) in the placebo condition

TABLE 1 | Brain regions showing functional connectivity of basal ganglia.

Seed region	Atlas label	Cluster (x, y, z)	Contrast	Size	Cluster *p*-FDR	Cluster *p*-unc
Putamen (l)	pMCC	(−6, 0, +40)	Positive	88	0.043	0.001
	aPaHC (l)	(−28, +10, +04)	Positive	92	0.036	0.001
Putamen (r)	aPaHC (l)	(+30, −06, −02)	Positive	65	0.040	0.004
Pallidum (l)	SubCalC	(−02, +26, −10)	Positive	84	0.049	0.003
	PaCiG (r)	(+06, +10, +46)	Positive	48	0.049	0.004
	FP (r)	(+42, +36, −16)	Negative	168	0.002	$p < 0.001$

FDR, false discovery rate; unc, uncorrection; l, left; r, right; pMCC, posterior part of the midcingulate cortex; aPaHC, anterior parahippocampal gyrus; SubCalC, subcallosal cortex; PaCiG, paracingulate gyrus; FP, frontal pole.

than in the acupuncture condition. A possible explanation for this phenomenon of slightly higher activation after acupuncture stimulation could be a belief in an acupuncture effect, which was shown in another placebo study (Darragh et al., 2015). A study demonstrated that the needling-specific component (somatosensory needling stimulation) induces sympathetic activation, whereas needling non-specific components (needling credibility by ritual/contextual influence) result in increased parasympathetic activation after acupuncture needling (Lee et al., 2014). This result could also explain the more strongly activated PNS in the placebo condition. In this study, placebo treatment was successfully blinded. A Bang's blinding index of 0 indicated that it might be a credible placebo (Bang et al., 2010). After histamine stimulus, acupuncture resulted in more activation of the PNS than placebo (H1 phase), showing that acupuncture increased parasympathetic activity; however, no significant change was observed in HF norm, LF norm, or LF/HF ratio between the acupuncture and placebo conditions. This result was partially because of high deviations in the HRV of participants, as examined by Kim and Woo (2011) in a normal Korean population. The impact of age, gender, and mean heart rate on short-term HRV measurement might have affected the results (Tsuji et al., 1996; Jensen-Urstad et al., 1997; Agelink et al., 2001; Kuch et al., 2001; Parati and Di Rienzo, 2003).

This study indicated that acupuncture had antipruritic effects via the positive connectivity of putamen and the pMCC. Itch is perceived by activation of inflammatory mediators via the spinothalamic tract to the brain (Davidson et al., 2007), influencing cortical and subcortical structures (Dhand and Aminoff, 2013). The striatum has a prominent function in striato-thalamo-cortical circuits (Koob and Volkow, 2010). The basal ganglia consists of the caudate nucleus, the putamen, the globus pallidus (consisting of an internal segment and an external segment), and the subthalamic nucleus (Bear et al., 2016). The putamen and caudate together are called the striatum, which is the target of cortical input to the basal ganglia. The globus pallidus is the source of output to the thalamus. Previous studies indicate that experimentally induced itch activates a brain network that includes a premotor and supplementary motor area, the thalamus, and the cingulate, insular, inferior parietal, and prefrontal cortices in healthy individuals (Pfab et al., 2012b). Electroacupuncture activates the putamen (Napadow et al., 2005), which is implicated in salience detection, particularly for stimuli such as pain (Downar et al., 2003) and itch. Recent fMRI study of patients with AD (Napadow et al., 2014) showed that acupuncture reduced itch and itch-evoked activation of parts of the putamen, insula, prefrontal, and premotor cortex (Napadow et al., 2014). Among these brain regions, greater reduction in putamen response was associated with greater decrease of itch intensity following acupuncture. The putamen is the region implicating the motivation and habitual behavior underlying the urge to scratch, and thus they suggested that the changes of putamen response are closely correlated with the antipruritic effects of acupuncture (Napadow et al., 2014). Based on this previous finding, we selected the putamen as seed for functional connectivity analysis using fMRI. The cingulate cortex consists of anterior cingulate cortex (ACC), midcingulate cortex (MCC), and posterior cingulate cortex (PCC). Among them, MCC or posterior part of the ACC was activated during itch induction or itch related behaviors (i.e., scratch), and the activation in this regions might be linked with cognition or evaluation of itch (Hsieh et al., 1994; Drzezga et al., 2001; Mochizuki et al., 2003, 2017; Herde et al., 2007; Papoiu et al., 2012). In a previous study, seed-based functional connectivity from the right anterior MCC showed a significant cluster in the right putamen in AD (Desbordes et al., 2015). In contrast, in this study, the significant connectivity of putamen and pMCC was found especially in responder to acupuncture during itch. The primary role of pMCC is reflexive orientation of the body in space to sensory stimuli including noxious ones (Vogt, 2016). Numerous neuroimaging studies have reported the activation of the pMCC during pain processing including the heat pain (Erpelding et al., 2012), short-duration and early noxious stimuli (Peyron et al., 2000; Bentley et al., 2003; Vogt et al., 2003; Frot et al., 2008). The MCC areas are thought to be numerous submodalities of sensory cortical processing (Vogt, 2014) and be involved in premotor planning and in affective-motivational processing in itch (Schneider et al., 2008). The motor-related regions such as the MCC along with the supplementary motor area and reward system including the putamen are associated with the reflexive process of scratching an itch (Mochizuki et al., 2015; Vogt, 2016). Thus, the antipruritic effect of acupuncture may be associated with the pMCC. Identifying negative correlations with clinical outcomes would allow us to understand how the positive connectivity of the putamen and pMCC lead to reduced itch.

Still, our results cannot exclude the possibility of the influence of individual difference of itch perception and responsiveness to histamine apart from the factors related with response to acupuncture. In this protocol of pretreatment acupuncture and SPT for histamine to investigate the preventive antipruritic

effects of acupuncture, as the baseline itch sensation data before acupuncture are not exist, responders and non-responders were determined using absolute values of the itch sensation obtained in the acupuncture condition rather than the optimal way of using subtracted value between baseline and endpoint. And we decided not to use the subtracted value between placebo and acupuncture condition as we thought it was inappropriate for responder analysis of this study based on the clinical perspective. Though we investigated the antipruritic effects of acupuncture against experimentally induced itch in healthy volunteers, we purposed not to distinguish acupuncture-specific factors, but to explore factors contributing the clinical antipruritic effects of acupuncture and we tried to focus on the total effect of acupuncture not excluding placebo factors in responder analysis. However, this might have led to another possible conclusion that responders in this study may be simply less responsive to itch. There are several studies on the individual difference of itch sensitivity in patients with AD or psoriasis which conclude that patients with chronic itch reacted with a higher itch response to histamine, suggesting somatosensory stimuli are processed in line with that patients' main symptom through generic sensitization processes (van Laarhoven et al., 2007, 2013). A seed-based analysis of a previous fMRI study (Desbordes et al., 2015) on evoked itch perception in chronic itch patients revealed decreased functional connectivity from baseline resting state to the evoked-itch state between several itch-related brain regions, particularly the insular and cingulate cortices and basal ganglia, where decreased connectivity was significantly correlated with increased levels of perceived itch. In contrast, evoked itch increased connectivity between key nodes of the frontoparietal control network (superior parietal lobule and dorsolateral prefrontal cortex), where higher increase in connectivity was correlated with a lesser increase in perceived itch, suggesting that greater interaction between nodes of this executive attention network serves to limit itch sensation via enhanced top-down regulation. Although these result cannot be directly applied to our study with healthy participants, individual difference of itch perception can naturally exist among healthy individuals. Further studies on brain regions or network in healthy participants that explain why some subjects perceive less itch are needed. Another fMRI study (Napadow et al., 2015) with AD patients demonstrated that expectations and other psychological factors play a role in modulating itch perception in chronic itch patients. In our study, psychological factors such as credibility, expectation, and fear of acupuncture and perception of bodily sensation were not related to itch response to acupuncture. The level of perceived bodily sensation varies from person to person and might lead to different responses of brain activation. In this study, perception of bodily sensation showed no significant difference between responder and non-responder groups: the value was 39.9 (95% CI, 31.9–47.9) in the responder group and 37.0 (95% CI, 31.0–43.0) in the non-responder group (**Figure 5C**).

In this study, acupuncture response to anti-pruritic effects might be associated with an anti-inflammatory effect mediated by an activated PNS and increased functional connectivity of putamen-pMCC. Acupuncture is thought to multidimensionally modulate anticipatory, somatosensory, and cognitive re-appraisal circuitries. Considering that the putamen and the MCC are related with somatosensory processing (Downar et al., 2003; Almeida et al., 2004; Vogt, 2014), the somatosensory aspect of acupuncture might be important for its antipruritic effects. However, while acupuncture may also have peripheral mechanisms as a counter stimulus (Ward, 1996), in this study, we induced itch on both the arm and the foot simultaneously and acupuncture reduced itch in both areas, suggesting that the systemic antipruritic effects of acupuncture are mediated by multiple central nervous pathways (Davidson and Giesler, 2010). Other studies indicated that antipruritic effects of acupuncture may modulate TRPV1 activation (McDonald et al., 2015, 2016) or endogenous opioid peptides in the central nervous system (Han, 2004; Wang et al., 2005; Dougherty et al., 2008; Guo et al., 2008; Zheng et al., 2008; Pfab et al., 2012a). Han et al. (2008) suggested that the antipruritic effects of acupuncture treatment are mediated by kappa-opioid receptor activation in a rat AD model. In addition to anti-inflammatory effects, the response of the sensory nerve could be a possible explanation for the antipruritic effects of acupuncture.

This study had several limitations that warrant consideration. First, we performed responder and non-responder analysis of itch intensity. Because we did not have a clinical standard due to the experimentally induced itch, entire participants were separated into responders and non-responders based on a mean of the sum values of arm and foot itch intensities. As mentioned above, responders and non-responders were determined using absolute values of the itch sensation obtained in the acupuncture condition, the possibility of the influence of individual difference of itch perception and responsiveness to histamine apart from the factors related with response to acupuncture still remains. Second, our model was not clinical itch symptoms, but experimentally induced itch. Third, this study also had a small sample size. By classifying into responder and non-responder participants, the sample numbers became even smaller considering that recommended sample size for fMRI studies is usually 16 or more. Thus, this study should be regarded as a pilot study requiring further studies with larger sample size and additional normal control group without any interventions to compensate the defect appeared in this pilot study and to induce definite conclusion. Next, according to the Bang's blinding indexes for this study, the experimental condition was unblinded with 75% of correct guessing, while the control condition was completely blinded. Although this result can be interpreted as indicating that tactile stimulation acted as a credible placebo, the greater treatment effect in the experimental condition compared to control condition might have affected the study results (Park et al., 2008). Finally, no differences were seen in the analysis of the acupuncture and placebo conditions using HRV and fMRI data. As an explanation for the HRV results, acupuncture can be divided into needling-specific and non-specific components and it is equally applied to the placebo tactile stimulation (Langevin et al., 2011). Considering that the putamen and the pMCC are somatosensory

processing regions related to afferent pain stimulation (Downar et al., 2003; Almeida et al., 2004; Vogt, 2014), the acupuncture and placebo condition might have had common brain responses.

CONCLUSION

In conclusion, the results suggested that acupuncture treatment was useful against histamine-induced itch. Additionally, an activated PNS and the functional connectivity of putamen-pMCC could be considered factors related to the antipruritic response of acupuncture. Explaining clear mediators of the observed effects is still difficult. Thus, further work on the mechanisms involved in specific regulatory factors is needed. Further study to identify the most important brain region for the antipruritic effects of acupuncture with more participants is warranted. These factors might allow better prediction of the therapeutic effects of acupuncture.

DATA AVAILABILITY

The raw data supporting the conclusions of this manuscript will be made available by the authors, without undue reservation, to any qualified researcher.

AUTHOR CONTRIBUTIONS

SM and K-WK involved in the manuscript preparation. SM and H-JP conceived and designed the experiments. W-MJ, M-JL, and Y-KK made substantial contributions to the study conception and performed the overall experiments. K-WK, YC, and HL provided the critiques and revised the article for important intellectual content. H-JP participated in the critical revision of the manuscript and had the final responsibility for the decision to submit for publication. All authors read and approved the final manuscript.

FUNDING

This research was supported by the National Research Foundation of Korea funded by the Korean Ministry of Science, ICT and Future Planning (NRF-2015M3A9E052338).

SUPPLEMENTARY MATERIAL

The Supplementary Material for this article can be found online at: https://www.frontiersin.org/articles/10.3389/fnins.2019.00215/full#supplementary-material

REFERENCES

Agelink, M. W., Malessa, R., Baumann, B., Majewski, T., Akila, F., Zeit, T., et al. (2001). Standardized tests of heart rate variability: normal ranges obtained from 309 healthy humans, and effects of age, gender, and heart rate. *Clin. Auton. Res.* 11, 99–108. doi: 10.1007/BF02322053

Almeida, T. F., Roizenblatt, S., and Tufik, S. (2004). Afferent pain pathways: a neuroanatomical review. *Brain Res.* 1000, 40–56. doi: 10.1016/j.brainres.2003.10.073

Andrew, D., and Craig, A. D. (2001). Spinothalamic lamina I neurons selectively sensitive to histamine: a central neural pathway for itch. *Nat. Neurosci.* 4, 72–77. doi: 10.1038/82924

Arck, P., and Paus, R. (2006). From the brain-skin connection: the neuroendocrine-immune misalliance of stress and itch. *Neuroimmunomodulation* 13, 347–356. doi: 10.1159/000104863

Backer, M., Grossman, P., Schneider, J., Michalsen, A., Knoblauch, N., Tan, L., et al. (2008). Acupuncture in migraine: investigation of autonomic effects. *Clin. J. Pain* 24, 106–115. doi: 10.1097/AJP.0b013e318159f95e

Bang, H., Flaherty, S. P., Kolahi, J., and Park, J. (2010). Blinding assessment in clinical trials: a review of statistical methods and a proposal of blinding assessment protocol. *Clin. Res. Regul. Aff.* 27, 42–51. doi: 10.3109/10601331003777444

Bear, M. F., Connors, B. W., and Paradiso, M. A. (eds) (2016). *Neuroscience: Exploring the Brain*. Philadelphia, PA: Wolters Kluwer.

Beissner, F., Deichmann, R., Henke, C., and Bar, K. J. (2012). Acupuncture–deep pain with an autonomic dimension? *Neuroimage* 60, 653–660. doi: 10.1016/j.neuroimage.2011.12.045

Belgrade, M. J., Solomon, L. M., and Lichter, E. A. (1984). Effect of acupuncture on experimentally induced itch. *Acta Derm. Venereol.* 64, 129–133.

Bender, B. G., Ballard, R., Canono, B., Murphy, J. R., and Leung, D. Y. (2008). Disease severity, scratching, and sleep quality in patients with atopic dermatitis. *J. Am. Acad Dermatol.* 58, 415–420. doi: 10.1016/j.jaad.2007.10.010

Bentley, D. E., Derbyshire, S. W., Youell, P. D., and Jones, A. K. (2003). Caudal cingulate cortex involvement in pain processing: an inter-individual laser evoked potential source localisation study using realistic head models. *Pain* 102, 265–271. doi: 10.1016/S0304-3959(02)00405-0

Callahan, S. W., and Lio, P. A. (2012). Current therapies and approaches to the treatment of chronic itch. *Dermatology* 17, 29–40.

Camm, A., Malik, M., Bigger, J., Breithardt, G., Cerutti, S., Cohen, R., et al. (1996). Heart rate variability: standards of measurement, physiological interpretation and clinical use. task force of the European society of cardiology and the North American society of pacing and electrophysiology. *Circulation* 93, 1043–1065. doi: 10.1161/01.CIR.93.5.1043

Chae, Y., Park, H. J., Hahm, D. H., Yi, S. H., and Lee, H. (2006). Individual differences of acupuncture analgesia in humans using cDNA microarray. *J. Physiol. Sci.* 56, 425–431. doi: 10.2170/physiolsci.RP010206

Charlesworth, E. N., and Beltrani, V. S. (2002). Pruritic dermatoses: overview of etiology and therapy. *Am. J. Med.* 113(Suppl. 9A), 25S–33S. doi: 10.1016/S0002-9343(02)01434-1

Chida, Y., Steptoe, A., Hirakawa, N., Sudo, N., and Kubo, C. (2007). The effects of psychological intervention on atopic dermatitis. A systematic review and meta-analysis. *Int. Arch. Allergy Immunol.* 144, 1–9. doi: 10.1159/000101940

Chung, J. W., Yan, V. C., and Zhang, H. (2014). Effect of acupuncture on heart rate variability: a systematic review. *Evid. Based Complement. Alternat. Med.* 2014:819871. doi: 10.1155/2014/819871

Cicek, D., Kandi, B., Berilgen, M. S., Bulut, S., Tekatas, A., Dertlioglu, S. B., et al. (2008). Does autonomic dysfunction play a role in atopic dermatitis? *Br. J. Dermatol.* 159, 834–838. doi: 10.1111/j.1365-2133.2008.08756.x

Colombo, B., Rocca, M. A., Messina, R., Guerrieri, S., and Filippi, M. (2015). Resting-state fMRI functional connectivity: a new perspective to evaluate pain modulation in migraine? *Neurol. Sci.* 36(Suppl. 1), 41–45. doi: 10.1007/s10072-015-2145-x

Darragh, M., Vanderboor, T., Booth, R. J., Sollers, J. J. III, and Consedine, N. S. (2015). Placebo 'serotonin' increases heart rate variability in recovery from psychosocial stress. *Physiol. Behav.* 145, 45–49. doi: 10.1016/j.physbeh.2015.03.043

Davidson, S., and Giesler, G. J. (2010). The multiple pathways for itch and their interactions with pain. *Trends Neurosci.* 33, 550–558. doi: 10.1016/j.tins.2010.09.002

Davidson, S., Zhang, X., Yoon, C. H., Khasabov, S. G., Simone, D. A., and Giesler, G. J. Jr. (2007). The itch-producing agents histamine and cowhage activate separate populations of primate spinothalamic tract neurons. *J. Neurosci.* 27, 10007–10014. doi: 10.1523/JNEUROSCI.2862-07.2007

Desbordes, G., Li, A., Loggia, M. L., Kim, J., Schalock, P. C., Lerner, E., et al. (2015). Evoked itch perception is associated with changes in functional brain connectivity. *Neuroimage Clin.* 7, 213–221. doi: 10.1016/j.nicl.2014.12.002

Dhand, A., and Aminoff, M. J. (2013). The neurology of itch. *Brain* 137(Pt 2), 313–322. doi: 10.1093/brain/awt158

Dhond, R. P., Kettner, N., and Napadow, V. (2007a). Do the neural correlates of acupuncture and placebo effects differ? *Pain* 128, 8–12. doi: 10.1016/j.pain.2007.01.001

Dhond, R. P., Kettner, N., and Napadow, V. (2007b). Neuroimaging acupuncture effects in the human brain. *J. Altern. Complement. Med.* 13, 603–616. doi: 10.1089/acm.2007.7040

Dhond, R. P., Yeh, C., Park, K., Kettner, N., and Napadow, V. (2008). Acupuncture modulates resting state connectivity in default and sensorimotor brain networks. *Pain* 136, 407–418. doi: 10.1016/j.pain.2008.01.011

Dougherty, D. D., Kong, J., Webb, M., Bonab, A. A., Fischman, A. J., and Gollub, R. L. (2008). A combined [11C]diprenorphine PET study and fMRI study of acupuncture analgesia. *Behav. Brain Res.* 193, 63–68. doi: 10.1016/j.bbr.2008.04.020

Downar, J., Mikulis, D. J., and Davis, K. D. (2003). Neural correlates of the prolonged salience of painful stimulation. *Neuroimage* 20, 1540–1551. doi: 10.1016/S1053-8119(03)00407-5

Drzezga, A., Darsow, U., Treede, R. D., Siebner, H., Frisch, M., Munz, F., et al. (2001). Central activation by histamine-induced itch: analogies to pain processing: a correlational analysis of O-15 H2O positron emission tomography studies. *Pain* 92, 295–305. doi: 10.1016/S0304-3959(01)00271-8

Erpelding, N., Moayedi, M., and Davis, K. D. (2012). Cortical thickness correlates of pain and temperature sensitivity. *Pain* 153, 1602–1609. doi: 10.1016/j.pain.2012.03.012

Frot, M., Mauguière, F., Magnin, M., and Garcia-Larrea, L. (2008). Parallel procesiing of nociceptive A-delta inputs in SII and midcingulate cortex in humans. *J. Neurosci.* 28, 944–952. doi: 10.1523/JNEUROSCI.2934-07.2008

Guo, Z. L., Moazzami, A. R., Tjen, A. L. S., and Longhurst, J. C. (2008). Responses of opioid and serotonin containing medullary raphe neurons to electroacupuncture. *Brain Res.* 1229, 125–136. doi: 10.1016/j.brainres.2008.07.020

Han, J. B., Kim, C. W., Sun, B., Kim, S. K., Lee, M. G., Park, D. S., et al. (2008). The antipruritic effect of acupuncture on serotonin-evoked itch in rats. *Acupunct. Electrother. Res.* 33, 145–156. doi: 10.3727/036012908803861168

Han, J. S. (2004). Acupuncture and endorphins. *Neurosci. Lett.* 361, 258–261. doi: 10.1016/j.neulet.2003.12.019

Herde, L., Forster, C., Strupf, M., and Handwerker, H. O. (2007). Itch induced by a novel method leads to limbic deactivations a functional MRI study. *J. Neurophysiol.* 98, 2347–2356. doi: 10.1152/jn.00475.2007

Hsieh, J. C., Hägermark, O., Ståhle-Bäckdahl, M., Ericson, K., Eriksson, L., Stone-Elander, S., et al. (1994). Urge to scratch represented in the human cerebral cortex during itch. *J. Neurophysiol.* 72, 3004–3008. doi: 10.1152/jn.1994.72.6.3004

Huang, H., Zhong, Z., Chen, J., Huang, Y., Luo, J., Wu, J., et al. (2015). Effect of acupuncture at HT7 on heart rate variability: an exploratory study. *Acupunct. Med.* 33, 30–35. doi: 10.1136/acupmed-2013-010441

Huang, S.-T., Chen, G.-Y., Lo, H.-M., Lin, J.-G., Lee, Y.-S., and Kuo, C.-D. (2005). Increase in the vagal modulation by acupuncture at neiguan point in the healthy subjects. *Am. J. Chin. Med.* 33, 157–164. doi: 10.1142/S0192415X0500276X

Jensen-Urstad, K., Storck, N., Bouvier, F., Ericson, M., Lindblad, L. E., and Jensen-Urstad, M. (1997). Heart rate variability in healthy subjects is related to age and gender. *Acta Physiol. Scand.* 160, 235–241. doi: 10.1046/j.1365-201X.1997.00142.x

Kawakita, K., Shinbara, H., Imai, K., Fukuda, F., Yano, T., and Kuriyama, K. (2006). How do acupuncture and moxibustion act? - Focusing on the progress in Japanese acupuncture research. *J. Pharmacol. Sci.* 100, 443–459. doi: 10.1254/jphs.CRJ06004X

Kesting, M. R., Thurmuller, P., Holzle, F., Wolff, K. D., Holland-Letz, T., and Stucker, M. (2006). Electrical ear acupuncture reduces histamine-induced itch (alloknesis). *Acta Derm. Venereol.* 86, 399–403. doi: 10.2340/00015555-0115

Kim, G. M., and Woo, J. M. (2011). Determinants for heart rate variability in a normal Korean population. *J. Korean Med. Sci.* 26, 1293–1298. doi: 10.3346/jkms.2011.26.10.1293

Kim, J. H., Min, B. I., Schmidt, D., Lee, H. J., and Park, D. S. (2000). The difference between electroacupuncture only and electroacupuncture with manipulation on analgesia in rats. *Neurosci. Lett.* 279, 149–152. doi: 10.1016/S0304-3940(99)00994-5

Kim, S. K., Moon, H. J., Park, J. H., Lee, G., Shin, M. K., Hong, M. C., et al. (2007). The maintenance of individual differences in the sensitivity of acute and neuropathic pain behaviors to electroacupuncture in rats. *Brain Res. Bull.* 74, 357–360. doi: 10.1016/j.brainresbull.2007.07.006

Kirchner, A., Stefan, H., Schmelz, M., Haslbeck, K. M., and Birklein, F. (2002). Influence of vagus nerve stimulation on histamine-induced itching. *Neurology* 59, 108–112. doi: 10.1212/WNL.59.1.108

Kitagawa, Y., Kimura, K., and Yoshida, S. (2014). Spectral analysis of heart rate variability during trigger point acupuncture. *Acupunct. Med.* 32, 273–278. doi: 10.1136/acupmed-2013-010440

Koob, G. F., and Volkow, N. D. (2010). Neurocircuitry of addiction. *Neuropsychopharmacology* 35, 217–238. doi: 10.1038/npp.2009.110

Kuch, B., Hense, H. W., Sinnreich, R., Kark, J. D., von Eckardstein, A., Sapoznikov, D., et al. (2001). Determinants of short-period heart rate variability in the general population. *Cardiology* 95, 131–138. doi: 10.1159/000047359

Langevin, H. M., Wayne, P. M., Macpherson, H., Schnyer, R., Milley, R. M., Napadow, V., et al. (2011). Paradoxes in acupuncture research: strategies for moving forward. *Evid. Based Complement. Alternat. Med.* 2011:180805. doi: 10.1155/2011/180805

Lee, J., Napadow, V., Kim, J., Lee, S., Choi, W., Kaptchuk, T. J., et al. (2014). Phantom acupuncture: dissociating somatosensory and cognitive/affective components of acupuncture stimulation with a novel form of placebo acupuncture. *PLoS One* 9:e104582. doi: 10.1371/journal.pone.0104582

Lee, S., Lee, M. S., Choi, J. Y., Lee, S. W., Jeong, S. Y., and Ernst, E. (2010). Acupuncture and heart rate variability: a systematic review. *Auton. Neurosci.* 155, 5–13. doi: 10.1016/j.autneu.2010.02.003

Li, Z., Wang, C., Mak, A. F., and Chow, D. H. (2005). Effects of acupuncture on heart rate variability in normal subjects under fatigue and non-fatigue state. *Eur. J. Appl. Physiol.* 94, 633–640. doi: 10.1007/s00421-005-1362-z

Lundeberg, T., Bondesson, L., and Thomas, M. (1987). Effect of acupuncture on experimentally induced itch. *Br. J. Dermatol.* 117, 771–777. doi: 10.1111/j.1365-2133.1987.tb07359.x

Malliani, A., Pagani, M., Lombardi, F., and Cerutti, S. (1991). Cardiovascular neural regulation explored in the frequency domain. *Circulation* 84, 482–492. doi: 10.1161/01.CIR.84.2.482

McDonald, J. L., Cripps, A. W., and Smith, P. K. (2015). Mediators, receptors, and signalling pathways in the anti-inflammatory and antihyperalgesic effects of acupuncture. *Evid. Based Complement. Alternat. Med.* 2015:975632. doi: 10.1155/2015/975632

McDonald, J. L., Smith, P. K., Smith, C. A., Changli Xue, C., Golianu, B., and Cripps, A. W. (2016). Effect of acupuncture on house dust mite specific IgE, substance P, and symptoms in persistent allergic rhinitis. *Ann. Allergy Asthma Immunol.* 116, 497–505. doi: 10.1016/j.anai.2016.04.002

Michikami, D., Kamiya, A., Kawada, T., Inagaki, M., Shishido, T., Yamamoto, K., et al. (2006). Short-term electroacupuncture at Zusanli resets the arterial baroreflex neural arc toward lower sympathetic nerve activity. *Am. J. Physiol. Heart Circ. Physiol.* 291, H318–H326. doi: 10.1152/ajpheart.00975.2005

Min, S., Lee, H., Kim, S. Y., Park, J. Y., Chae, Y., and Park, H. J. (2015). Local changes in microcirculation and the analgesic effects of acupuncture: a laser Doppler perfusion imaging study. *J. Altern. Complement. Med.* 21, 46–52. doi: 10.1089/acm.2013.0442

Mochizuki, H., Papoiu, A. D. P., Nattlemper, L. A., Lin, A. C., Kraft, R. A., Coghill, R. C., et al. (2015). Scratching induces overactivity in motor-related regions and reward system in chronic itch patients. *J. Invest. Dermatol.* 135, 2814–2823. doi: 10.1038/jid.2015.223

Mochizuki, H., Schut, C., Nattkemper, L. A., and Yosipovitch, G. (2017). Brain mechanism of itch in atopic dermatitis and its possible alteration through non-invasive treatments. *Allergol. Int.* 66, 14–21. doi: 10.1016/j.alit.2016.08.013

Mochizuki, H., Tashiro, M., Kano, M., Sakurada, Y., Itoh, M., and Yanai, K. (2003). Imaging of central itch modulation in the human brain using positron emission tomography. *Pain* 105, 339–346. doi: 10.1016/S0304-3959(03)00249-5

Napadow, V., Li, A., Loggia, M. L., Kim, J., Mawla, L., Desbordes, G., et al. (2015). The imagined itch: brain circuitry supporting nocebo-induced itch in atopic dermatitis patients. *Allergy* 70, 1485–1492. doi: 10.1111/all.12727

Napadow, V., Li, A., Loggia, M. L., Kim, J., Schalock, P. C., Lerner, E., et al. (2014). The brain circuitry mediating antipruritic effects of acupuncture. *Cereb. Cortex* 24, 873–882. doi: 10.1093/cercor/bhs363

Napadow, V., Makris, N., Liu, J., Kettner, N. W., Kwong, K. K., and Hui, K. K. (2005). Effects of electroacupuncture versus manual acupuncture on the human brain as measured by fMRI. *Hum. Brain Mapp.* 24, 193–205. doi: 10.1002/hbm.20081

Noda, Y., Izuno, T., Tsuchiya, Y., Hayasaka, S., Matsumoto, K., Murakami, H., et al. (2015). Acupuncture-induced changes of vagal function in patients with depression: a preliminary sham-controlled study with press needles. *Complement. Ther. Clin. Pract.* 21, 193–200. doi: 10.1016/j.ctcp.2015.07.002

Papoiu, A. D., Coghill, R. C., Kraft, R. A., Wang, H., and Yosipovitch, G. (2012). A tale of two itches. Common features and notable differences in brain activation evoked by cowhage and histamine induced itch. *Neuroimage* 59, 3611–3623. doi: 10.1016/j.neuroimage.2011.10.099

Parati, G., and Di Rienzo, M. (2003). Determinants of heart rate and heart rate variability. *J. Hypertens.* 21, 477–480. doi: 10.1097/01.hjh.0000052455.40108.db

Park, H. J., Kim, S. T., Yoon, D. H., Jin, S. H., Lee, S. J., Lee, H. J., et al. (2005). The association between the DRD2 TaqI A polymorphism and smoking cessation in response to acupuncture in Koreans. *J. Altern. Complement. Med.* 11, 401–405. doi: 10.1089/acm.2005.11.401

Park, J., Bang, H., and Canette, I. (2008). Blinding in clinical trials, time to do it better. *Complement. Ther. Med.* 16, 121–123. doi: 10.1016/j.ctim.2008.05.001

Peyron, R., Laurent, B., and García-Larrea, L. (2000). Functional imaging of brain responses to pain. A review and meta-analysis. *Neurophysiol. Clin.* 30, 263–288. doi: 10.1016/S0987-7053(00)00227-6

Pfab, F., Athanasiadis, G. I., Huss-Marp, J., Fuqin, J., Heuser, B., Cifuentes, L., et al. (2011). Effect of acupuncture on allergen-induced basophil activation in patients with atopic eczema:a pilot trial. *J. Altern. Complement. Med.* 17, 309–314. doi: 10.1089/acm.2009.0684

Pfab, F., Hammes, M., Backer, M., Huss-Marp, J., Athanasiadis, G. I., Tolle, T. R., et al. (2005). Preventive effect of acupuncture on histamine-induced itch: a blinded, randomized, placebo-controlled, crossover trial. *J. Allergy Clin. Immunol.* 116, 1386–1388. doi: 10.1016/j.jaci.2005.08.055

Pfab, F., Huss-Marp, J., Gatti, A., Fuqin, J., Athanasiadis, G. I., Irnich, D., et al. (2010). Influence of acupuncture on type I hypersensitivity itch and the wheal and flare response in adults with atopic eczema - a blinded, randomized, placebo-controlled, crossover trial. *Allergy* 65, 903–910. doi: 10.1111/j.1398-9995.2009.02284.x

Pfab, F., Kirchner, M. T., Huss-Marp, J., Schuster, T., Schalock, P. C., Fuqin, J., et al. (2012a). Acupuncture compared with oral antihistamine for type I hypersensitivity itch and skin response in adults with atopic dermatitis: a patient- and examiner-blinded, randomized, placebo-controlled, crossover trial. *Allergy* 67, 566–573. doi: 10.1111/j.1398-9995.2012.02789.x

Pfab, F., Valet, M., Napadow, V., Tolle, T. R., Behrendt, H., Ring, J., et al. (2012b). Itch and the brain. *Chem. Immunol. Allergy* 98, 253–265. doi: 10.1159/000336529

Pfab, F., Schalock, P. C., Napadow, V., Athanasiadis, G. I., Yosipovitch, G., and Ring, J. (2013). Complementary integrative approach for treating pruritus. *Dermatol. Ther.* 26, 149–156. doi: 10.1111/dth.12031

Schneider, G., Ständer, S., Burgmer, M., Driesch, G., Heuft, G., and Weckesser, M. (2008). Significan differences in central imaging of histamine-induced itch between atopic dermatitis and healthy subjects. *Eur. J. Pain* 12, 834–841. doi: 10.1016/j.ejpain.2007.12.003

Scholz, J., and Woolf, C. J. (2002). Can we conquer pain? *Nat. Neurosci.* 5(Suppl.), 1062–1067. doi: 10.1038/nn942

Schork, N. J. (2015). Personalized medicine: time for one-person trials. *Nature* 520, 609–611. doi: 10.1038/520609a

Stander, S., and Steinhoff, M. (2002). Pathophysiology of pruritus in atopic dermatitis: an overview. *Exp. Dermatol.* 11, 12–24. doi: 10.1034/j.1600-0625.2002.110102.x

Takakura, N., Ogawa, H., Iijima, S., Nishimura, K., Kanamaru, A., Sibuya, M., et al. (1995). Effect of acupuncture at the Hoku point on vibration-induced finger flexion reflex in man: comparison between press needle technique, electroacupuncture, and in-situ technique. *Am. J. Chin. Med.* 23, 313–318. doi: 10.1142/S0192415X95000377

Tran, B. W., Papoiu, A. D., Russoniello, C. V., Wang, H., Patel, T. S., Chan, Y. H., et al. (2010). Effect of itch, scratching and mental stress on autonomic nervous system function in atopic dermatitis. *Acta Derm. Venereol.* 90, 354–361. doi: 10.2340/00015555-0890

Tsuji, H., Venditti, F. J. Jr., Manders, E. S., Evans, J. C., Larson, M. G., Feldman, C. L., et al. (1996). Determinants of heart rate variability. *J. Am. Coll. Cardiol.* 28, 1539–1546. doi: 10.1016/S0735-1097(96)00342-7

van Laarhoven, A. I., Kraaimaat, F. W., Wilder-Smith, O. H., van de Kerkhof, P. C., Cats, H., van Riel, P. L., et al. (2007). Generalized and symptom-specific sensitization of chronic itch and pain. *J. Eur. Acad. Dermatol. Venereol.* 21, 1187–1192. doi: 10.1111/j.1468-3083.2007.02215.x

van Laarhoven, A. I., Kraaimaat, F. W., Wilder-Smith, O. H., van Riel, P. L., van de Kerkhof, P. C., and Evers, A. W. (2013). Sensitivity to itch and pain in patients with psoriasis and rheumatoid arthritis. *Exp. Dermatol.* 22, 530–534. doi: 10.1111/exd.12189

Vogt, B. A. (2014). Submodalities of emotion in the context of cingulate subregions. *Cortex* 59, 197–202. doi: 10.1016/j.cortex.2014.04.002

Vogt, B. A. (2016). Midcingulate cortex: structure, connections, homologies, functions and diseases. *J. Chem. Neuroanat.* 74, 28–46. doi: 10.1016/j.jchemneu.2016.01.010

Vogt, B. A., Berger, G. R., and Derbyshire, S. W. (2003). Stuructural and functional dichotomy of human midcingulate cortes. *Eur. J. Neurosci.* 18, 3134–3144. doi: 10.1111/j.1460-9568.2003.03034.x

Wang, Y., Zhang, Y., Wang, W., Cao, Y., and Han, J. S. (2005). Effects of synchronous or asynchronous electroacupuncture stimulation with low versus high frequency on spinal opioid release and tail flick nociception. *Exp. Neurol.* 192, 156–162. doi: 10.1016/j.expneurol.2004.11.003

Ward, A. A. (1996). Spontaneous electrical activity at combined acupuncture and myofascial trigger point sites. *Acupunct. Med.* 14, 75–79. doi: 10.1136/aim.14.2.75

Whitfield-Gabrieli, S., and Nieto-Castanon, A. (2012). *Conn*: a functional connectivity toolbox for correlated and anticorrelated brain networks. *Brain Connect.* 2, 125–141. doi: 10.1089/brain.2012.0073

Woodcock, J., Witter, J., and Dionne, R. A. (2007). Stimulating the development of mechanism-based, individualized pain therapies. *Nat. Rev. Drug Discov.* 6, 703–710. doi: 10.1038/nrd2335

Yu, C., Zhang, P., Lv, Z. T., Li, J. J., Li, H. P., Wu, C. H., et al. (2015). Efficacy of acupuncture in itch: a systematic review and meta-analysis of clinical randomized controlled trials. *Evid. Based Complement. Alternat. Med.* 2015:208690. doi: 10.1155/2015/208690

Zheng, Z., Guo, R. J., Helme, R. D., Muir, A., Da Costa, C., and Xue, C. C. (2008). The effect of electroacupuncture on opioid-like medication consumption by chronic pain patients: a pilot randomized controlled clinical trial. *Eur. J. Pain* 12, 671–676. doi: 10.1016/j.ejpain.2007.10.003

Conflict of Interest Statement: The authors declare that the research was conducted in the absence of any commercial or financial relationships that could be construed as a potential conflict of interest.

The handling Editor is currently organizing a Research Topic with one of the authors YC and confirms the absence of any other collaboration.

frontiers in Cellular Neuroscience

ORIGINAL RESEARCH
published: 26 March 2019
doi: 10.3389/fncel.2019.00075

Thymosin Beta 4 Is Involved in the Development of Electroacupuncture Tolerance

*Juan Wan, Yi Ding, Sha Nan, Qiulin Zhang, Jinrui Sun, Chuanguang Suo and Mingxing Ding**

College of Veterinary Medicine, Huazhong Agricultural University, Wuhan, China

Background: Electroacupuncture (EA) tolerance, a negative therapeutic effect, is a gradual decline in antinociception because of its repeated or prolonged use. This study aims to explore the role of thymosin beta 4 (Tβ4), having neuro-protection properties, in EA tolerance (EAT).

Methods: Rats were treated with EA once daily for eight consecutive days to establish EAT, effect of Tβ4 on the development of EAT was determined through microinjection of Tβ4 antibody and siRNA into the cerebroventricle. The mRNA and protein expression profiles of Tβ4, opioid peptides (enkephalin, dynorphin and endorphin), and anti-opioid peptides (cholecystokinin octapeptide, CCK-8 and orphanin FQ, OFQ), and mu opioid receptor (MOR) and CCK B receptor (CCKBR) in the brain areas (hypothalamus, thalamus, cortex, midbrain and medulla) were characterized after Tβ4 siRNA was administered.

Results: Tβ4 levels were increased at day 1, 4, and 8 and negatively correlated with the changes of tail flick latency in all areas. Tβ4 antibody and siRNA postponed EAT. Tβ4 siRNA caused decreased Tβ4 levels in all areas, which resulted in increased enkephalin, dynorphin, endorphin and MOR levels in most measured areas during repeated EA, but unchanged OFQ, CCK-8, and CCKBR levels in most measured areas. Tβ4 levels were negatively correlated with enkephalin, dynorphin, endorphin, or MOR levels in all areas except medulla, while positively correlated with OFQ and CCK-8 levels in some areas.

Conclusion: These results confirmed Tβ4 facilitates EAT probably through negatively changing endogenous opioid peptides and their receptors and positively influencing anti-opioid peptides in the central nervous system.

Keywords: electroacupuncture tolerance (EAT), opioid peptides, anti-opioid peptides, mu opioid receptor (MOR), CCK B type receptor (CCKBR)

OPEN ACCESS

Edited by:
Yi-Wen Lin,
China Medical University, Taiwan

Reviewed by:
Senthilkumar Rajagopal,
Rayalaseema University, India
Hongwei Dong,
Vanderbilt University Medical Center, United States

***Correspondence:**
Mingxing Ding
dmx@mail.hzau.edu.cn

Received: *10 December 2018*
Accepted: *14 February 2019*
Published: *26 March 2019*

Citation:
Wan J, Ding Y, Nan S, Zhang Q, Sun J, Suo C and Ding M (2019) Thymosin Beta 4 Is Involved in the Development of Electroacupuncture Tolerance. Front. Cell. Neurosci. 13:75. doi: 10.3389/fncel.2019.00075

INTRODUCTION

Electroacupuncture (EA), derived from traditional hand acupuncture, has been widely used for treating various pains with few side effects (Xum et al., 2009; Zeng et al., 2016; Zhao et al., 2017). EA stimulation for a short time (10–40 min) can induce analgesic effect (Ulett et al., 1998; Qiu et al., 2015; Hu et al., 2016). However, prolonged or repeated EA stimulations would attenuate and finally nullify analgesic effect, which is termed "EA tolerance" (EAT) (Han et al., 1979, 1981b).

Because the tolerance to EA results in the decrease or even loss of its treatment effects, it has attracted more attention from practitioners and researchers. To explore EAT mechanism, some studies focus on the roles of analgesic and anti-analgesic neuromodulators in the central nerve system (CNS). It has been verified that EA produces analgesic effect through the release of endogenous opioid peptides (EOP) (Chen and Han, 1992b; Han, 2003). Tang et al. (1979) found repeated EA induced the higher levels of EOP in EAT rats. Further studies demonstrated that EA induced the release of anti-opioid substances including cholecystokinin octapeptide (CCK-8) and orphanin FQ (OFQ) (Bian et al., 1993; Tian et al., 1998) while it provoked the release of opioid peptides. The increase in anti-opioid peptides is believed to be due to the feedback regulation of opioid peptides. Tang et al. (1997) microinjected CCK antisense RNA into the lateral cerebral ventricle of rats to block the CCK gene expression, and found the development of tolerance elicited by prolonged EA stimulation was delayed. Tian and Han (2000) reported that intracerebroventricularly injecting OFQ antibody partially reversed tolerance to chronic EA. These studies indicate that the tipping of the balance to anti-opioid peptides may attenuate EA analgesia and contribute to EAT.

Opioid peptides or anti-opioid peptides exert analgesic or anti-analgesic effect through binding to their corresponding receptors. Therefore, some researchers have paid attention to the roles of these receptors in EAT. Ni et al. (1987) developed EAT and found that the opioid receptors decreased in the brain of rats. Dong et al. (1998) also found the decreased level of opioid receptors in the midbrain and striatum of rats after repeated application of EA. Huang et al. (2007) reported that CCK B type receptor (CCKBR) antagonist (L365, 260) can potentiate EA-induced analgesia and reverse chronic EAT. These findings showed that EAT was related to a change in opioid and anti-opioid receptors levels. However, the specific mechanism deserves further investigation.

Recently, Hu et al. (2018) found thymosin beta 4 (Tβ4) gene differentially expressed in the periaqueductal gray at 4 h in EA-treated goats. Tβ4, a 44-amino acid pleiotropic polypeptide, has important roles in neurobiological processes, including neurogenesis, neuronal developing, metabolism plasticity, and apoptosis (Sun and Kim, 2007; Chopp and Zheng, 2015). Recent studies reported that Tβ4 had a neuro-protective effect (Xiong et al., 2012a,b). EAT induced by prolonged or repeated EA stimulation can be considered as a neuro-protection response. Therefore, there may be a potential association between Tβ4 and EAT, which is worthy being studied.

In the present study, rats were stimulated with EA for 30 min once daily for eight consecutive days to establish EAT. Effect of Tβ4 on the development of EAT was determined through microinjection of Tβ4 antibody and siRNA into the cerebroventricle. The expression profiles of Tβ4, opioid peptides (endorphin, encephalin, and dynorphin), anti-opioid peptides (CCK-8 and OFQ) and related receptors (mu receptor and CCKBR) in the brain were characterized at mRNA and protein levels after Tβ4 siRNA was intracerebroventricularly administered to determine effects of Tβ4 on these proalgesic or analgesic substances and to further explore the role of Tβ4 in EAT.

Abbreviations: CCK-8, Cholecystokinin octapeptide; CCKBR, CCK B type receptor; CNS, Central nerve system; DYN, Dynorphin; EA, Electroacupuncture; EAT, EA tolerance; EOP, Endogenous opioid peptides; ENK, Enkephalin, END, Endorphin; icv, Intracerebroventricular; MOR, Mu opioid receptor; OFQ, Orphanin FQ; PONC, Prepronociceptin; PDYN, Prodynorphin; PENK, Proenkephalin; POMC, Proopiomelanocortin; TFL, Tail flick latency; Tβ4, Thymosin beta 4.

MATERIALS AND METHODS

Animals

The study was conducted under the guidelines approved by Institutional Animal Care and Use Committee of Huazhong Agricultural University, Wuhan, China and adhered to the guidelines of the Committee for Research and Ethical Issues of the International Association for the Study of Pain.

Female Sprague–Dawley rats (No. 42000600024665) weighing 200–220 g were purchased from the laboratory animal center of Huazhong Agricultural University. Rats were housed six per cage with food pellets and water *ad libitum*. One week was allowed for adaptation to the surroundings.

Experiment Design

To explore the dynamic expression of Tβ4 in the brain of rats induced by repeated EA, thirty rats were randomly divided into sham group ($n = 6$) and EA group ($n = 24$). The rats in EA group were treated with EA once per day for 8 days consecutively. The rats in sham group were treated in the same manner as the rats in EA group, but without electricity. The tail-flick latency (TFL) was detected everyday immediately before and after EA, respectively, and the change rates of TFL were calculated. Six rats from EA group at day 0 (before EA), 1, 4, and 8, respectively, were euthanized.

To investigate the effect of Tβ4 neutralizing antibody on the development of EAT. Thirty-six rats were randomly classified into five groups: Sham + PBS (Sh- PBS, $n = 6$), EA + PBS (EA-PBS, $n = 6$), EA + IgG (EA-IgG, $n = 6$), EA + 0.1 μg Tβ4 antibody (EA-0.1 μg Ab, $n = 6$), EA + 1 μg Tβ4 antibody (EA-1 μg Ab, $n = 6$), and EA + 10 μg Tβ4 antibody(EA-10 μg Ab, $n = 6$). The rats in EA-0.1 μg Ab, EA-1 μg Ab, EA-10 μg Ab, or EA-IgG group were intracerebroventricularly injected with 15 μL 0.1 μg, 1 μg, 10 μg Tβ4 neutralizing antibody or isotype IgG, respectively. The rats in Sh-PBS and EA-PBS groups were treated with 15 μL PBS. The rats except those in Sh-PBS group were treated with EA 30 min after intracerebroventricular (icv) injection, for total 8 times. The rats in Sh-PBS group were treated as the same as the rats in EA-PBS group, but without electricity. TFL was examined every day immediately before and after EA, respectively.

To further detect the effect of Tβ4 silencing on the formation of EAT and expression pattern of Tβ4, endorphin (END), encephalin (ENK), dynorphin (DYN), CCK-8, OFQ, MOR, and CCKBR in EA-treated rats, 93 rats were randomly classified into five groups: sham EA (Sh-EA, $n = 18$), EA treatment (EA-tr, $n = 18$), EA treated with lipofection (EA-L, $n = 18$), and EA treated with lipofection mixture with control siRNA (EA-C-si, $n = 18$),

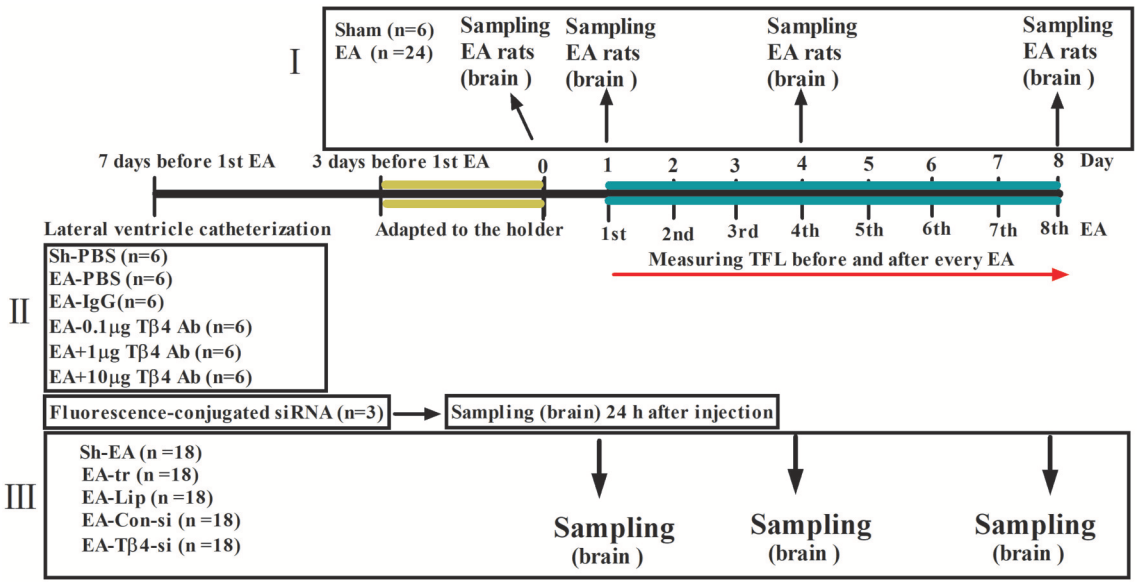

FIGURE 1 | The scheme of experiment. **(I)** The rats in EA group were treated with EA (2/15 Hz, 30 min) once per day for 8 days consecutively. The rats in sham group were treated in the same manner as the rats in EA group, but without electricity. **(II)** The rats in EA-0.1 μg Ab, EA-1 μg Ab, EA-10 μg Ab, or EA-IgG group were intracerebroventricularly injected with 15 μL 0.1 μg, 1 μg, 10 μg Tβ4 neutralizing antibody or isotype IgG, respectively. The rats in Sh-PBS and EA-PBS groups were treated with 15 μL PBS. The rats except those in Sh-PBS group were treated with EA (2/15 Hz, 30 min) 30 min after intracerebroventricular (icv) injection, for total 8 times. The rats in Sh-PBS group were treated as the same as the rats in EA-PBS group, but without electricity. **(III)** The rats in EA-L, EA-C-si, or EA-Tβ4-si group were intracerebroventricularly injected with lipofection, lipofection mixture with control siRNA or Tβ4 siRNA, respectively. The rats except those in Sh-EA group were treated with EA (2/15 Hz, 30 min) at the day after icv injection and thereafter every day, for total 8 times. The rats in Sh-EA group were treated as the same as the rats in EA-tr group, but without electricity. The tail flick latency (TFL) was examined every day immediately before and after EA, respectively. The symbols have the same meanings in **Figures 2**–**5**.

or Tβ4 siRNA (EA-Tβ4-si, $n = 18$). The rats in EA-L, EA-C-si, or EA-Tβ4-si group were intracerebroventricularly injected with lipofection (15 μL), lipofection (10 μL) mixture with control siRNA (5 μL) or Tβ4 siRNA (5 μL), respectively. The rats except those in Sh-EA group were treated with EA at the day after icv injection and thereafter every day, for total 8 times. The rats in Sh-EA group were treated as the same as the rats in EA-tr group, but without electricity. TFL was examined every day immediately before and after EA, respectively. Six rats from each group at day 1, 4, and 8, respectively, were euthanized. Additional three rats were used to verify a fluorescence-conjugated siRNA transfection into the brain at 24 h after icv injection (**Figure 1**).

Intracerebroventricular Injection

The surgery for icv injection was conducted based on a previous method (Cui et al., 2017a). Briefly, rats were anesthetized with sodium pentobarbital (40 mg/kg, Sigma, USA) and then mounted on a stereotaxic apparatus (RWD, Shenzhen, China). Skin over the skull was incised, and a small hole was micro-drilled on the skull 1.5 mm lateral to and 0.8 mm posterior to the bregma. Then, a small cannula was inserted 4.0 mm below the skull surface and placed in the position. All rats were allowed for recovery for 7 days and for adaption to the cylinder for 3 days before the formal experiment. For icv administration, an injection needle was inserted into the cannula to reach the target site. PBS, Tβ4 antibody (Santa Cruz, CA, USA), lipofection (Santa Cruz, CA, USA) or lipofection mixture with control siRNA (Santa Cruz, CA, USA) / Tβ4 siRNA (Santa Cruz, CA, USA) was administered at a rate of 1 μL/15 min. After injection, the needle was kept in place for 5 min to reduce the backflow of the solution. To verify if siRNA could be transfected into brain areas after icv injection, a fluorescence-conjugated siRNA (Santa Cruz, CA, USA) was used in rats (n =3).

Electroacupuncture Application

EA stimulation was conducted at a fixed time of a day (9:00 a.m.), according to the method reported by Cui et al. (2017a). Briefly, each rat was gently placed into a specially designed polyethylene holder, with the hind legs and tail exposed. Before EA, rats were adapted to the holder for 3 days, and the room temperature was controlled at 22 ± 1°C. The skin of the hind legs was sterilized with 75% alcohol. Stainless-steel needles (0.30 mm in diameter, 13 mm in length) were inserted into bilateral Zusanli points (ST36, 4 mm lateral to the anterior tuber point of the tibia, which is marked by a notch, 6–7 mm depth) and Sanyinjiao points (SP6, 3 mm proximal to the medial malleolus at the posterior border of the tibia, 4–5 mm depth). Rats were administered electrical impulses for 30 min with WQ-6F Electronic Acupunctoscope (Beijing Xindonghua Electronic Instrument Co., Ltd., Beijing, China). The stimuli were set as square waves with 2/15 Hz in frequency (dense-and disperse-mode) and 3 mA in amplitude. Throughout the EA, rats were kept in the holder without anesthesia.

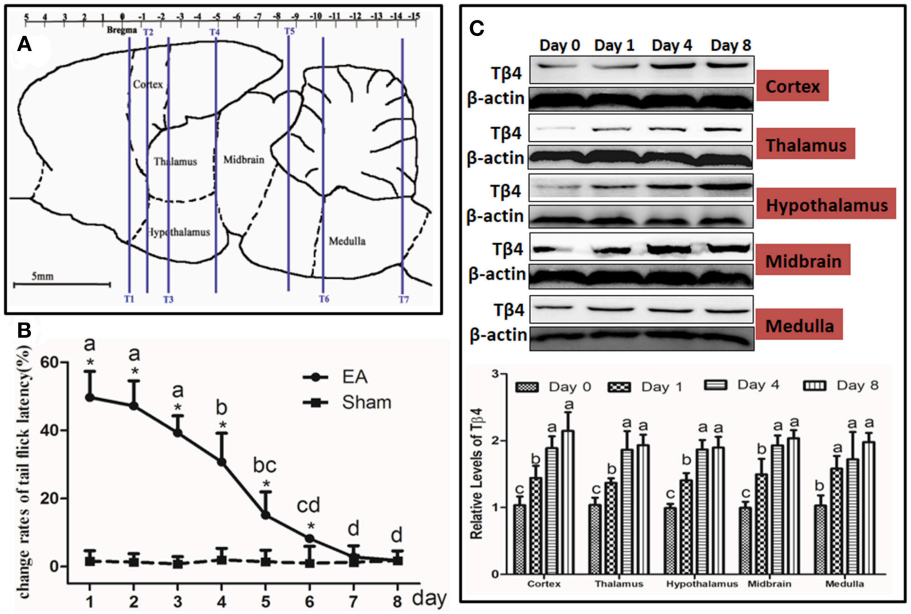

FIGURE 2 | Electroacupuncture (EA)-induced Tβ4 expressions in the brain areas and change rates of tail flick latency. **(A)** Brain areas sampling. The areas to be observed were hypothalamus, thalamus, cortex (sensory region), midbrain and medulla. T1, T2, T3, T4, T5, T6, and T7: marker tubes, show transverse planes at −0.40, −1.30, −2.40, −4.80, −8.60, −10.30, and −14.2 mm rostral to the transverse plane of bregma, respectively. **(B)** Change rates of tail flick latency after repeated EA (Mean ± SD, %, $n = 6$). The significance of differences was calculated by a *t*-test between sham and EA groups or a one-way ANOVA among different time points in EA group followed by Bonferroni's post-test.*$P < 0.05$ compared with sham group. The values with different letters (a–d) within the EA treatment differ. **(C)** The Tβ4 expressions in the brain areas after repeated EA (Mean ± SD, $n = 6$). The values with different letters differ significantly among different time points within the same brain area ($P < 0.05$). One-way ANOVA followed by Bonferroni's post-test.

Measurement of Tail Flick Latency

The nociceptive threshold was assessed using the TFL response elicited by radiant heat with the YLS-12A Tail Flick Analgesia Instrument (ZS Dichuang Science and Technology Development Co., Ltd., Beijing, China). Focused light from a projection bulb was applied to the proximal third of the tail and the TFL was measured. The intensity of the thermal stimulus was adjusted to obtain a basal TFL within the range of 4–6 s. A cutoff limit of 15 s was set to avoid tissue damage. Before EA, the basal TFL was determined by averaging three consecutive measures at 5-min intervals. TFL after EA was measured every 10 min during the 30 min of EA application. The change rate of TFL was taken as EA-induced antinociception and was calculated as the formula: TFL (%) = (TFL after EA–basal TFL)/basal TFL × 100%.

Sample Collection

At day 1, 4, and 8, immediately after TFL measurement, six rats from each group were anesthetized and euthanized by an overdose of sodium pentobarbital and their brains were quickly removed on a DEPC water-treated icebox. According to the atlas of Paxinos and Watson (1986), the hypothalamus, thalamus, cortex (sensory region), midbrain, medulla were taken immediately and stored in liquid nitrogen for western blotting and qPCR detection (**Figure 2A**).

Three rats were euthanized by an overdose of sodium pentobarbital at 24 h after fluorescence-conjugated siRNA injection, and intracardiac perfused ice-cold 4% paraformaldehyde in PBS. The brain was removed, cryoprotected in 30% sucrose in PBS and embedded in TissuTek. Cryostat sections (10 μm) were collected on slides and observed with an OLYMPUS BX51 microscope with fluorescence light.

Western Blotting

Brain sample was weighed, grinded in liquid nitrogen, then protein extracted from the grinded brain tissue using the RIPA buffer according to the manufacturer's instruction (Beyotime Biotech, Nantong, China). The protein concentration was measured with Nano Drop Spectrophotometer (Thermo Fisher Scientific, Inc., USA). Equal amounts of protein sample (40 μg) was loaded in 15% SDS polyacrylamide gel and transferred to a PVDF membrane with the Mini-PROTEIN Tetra Cell (Bio-Rad, CA, USA). The membrane was blocked for 2 h at the room temperature in 5% skimmed milk, and was subsequently immunolabeled overnight at 4°C with rabbit anti-endorphin IgG (1:500, ABclonal, Wuhan, China), rabbit anti-enkephalin IgG (1:500, ABclonal, Wuhan, China), rabbit anti-dynorphin IgG (1:500, ABclonal, Wuhan, China), rabbit anti-CCK-8 IgG (1:500, ABclonal, Wuhan, China), rabbit anti-OFQ IgG (1:500, ABclonal, Wuhan, China), rabbit anti-CCKBR IgG (1:500, ABclonal, Wuhan, China), mouse anti-MOR IgG (1:1,000, Novus, CO, USA), mouse anti-Tβ4 IgG (1:300, Santa Cruze, CA, USA), or rabbit anti-beta-actin (1:2,000, Boster biotech, Wuhan, China), respectively. The membrane was washed and treated with horseradish-peroxidase-conjugated anti-rabbit secondary

TABLE 1 | Primer sequences of opioid- and anti-opioid peptide and related receptor genes.

Name	Accession number	Primer sequence
Tβ4	NM_031136	F:5′-GGCTGAGATCGAGAAATT-3′
		R:5′-CTTTTGAAGGCAGAGGAT-3′
PNOC	U48262	F:5′-GTCCGCTGCTCTTTACCA-3′
		R:5′-TGCTTCTGCTCCACCTCAT-3′
CCK	NM_012829	F:5′-TGTCTGTGCGTGGTGATGG-3′
		R:5′-AGGGAGCTTTGCGGACCTG-3′
CCKBR	NM_013165	F:5′-GCCTAAGAACGGTCACCAACG-3′
		R:5′-GACTGTGCCGAAGATGAATGTG-3′
PENK	NM_017139	F:5′-GTGGAGCCAGAAGAAGAGG-3′
		R:5′-CAGCAGGTCGGAGGAGTT-3′
PDYN	NM_019374	F:5′-CGGAGGAGTGGGAGACAT-3′
		R:5′-TGAGACGCTGGTAAGGAGTT-3′
POMC	NM_139326	F:5′-CCTCCTGCTTCAGACCTCCA-3′
		R:5′-GGCTGTTCATCTCCGTTGC-3′
MOR	NM_013071	F:5′-GCTATCGGGCTCCAAAGAA-3′
		R:5′-GCAGAAGTGCCAGGAAACG-3′
GAPDH	NM_017008	F:5′-GTTCAACGGCACAGTCAA-3′
		R:5′-CTCGCTCCTGGAAGATGG-3′

Tβ4, Thymosin beta 4; POMC, proopiomelanocortin; PENK, proenkephalin; PDYN, prodynorphin; PONC, prepronociceptin; CCK, cholecystokinin ; MOR, mu opioid receptor; and CCKBR, CCK B receptor.

antibody (1:5,000, Boster biotech, Wuhan, China) for 1 h at the room temperature. Visualization of the antigen-antibody complex was conducted with a horseradish peroxidase substrate (Millipore, MA, USA) with the Image Quant LAS 4,000 min CCD camera (GE Healthcare, CHI, USA). The bands were analyzed with Quantity One software (Bio-Rad, CA, USA). Beta-actin was used as the internal control. Values of these substances were represented as the ratio of the optical density of the bands to the density of the related beta-actin band.

RT-PCR

Total RNA was extracted from the each brain area of each group using Trizol reagent (Invitrogen, CA, USA). Subsequently, cDNA was synthesized from 900 ng of total RNA using a First Strand cDNA Synthesis Kit (TOYOBO, Osaka, Japan). The primer sequences of proopiomelanocortin (POMC), proenkephalin (PENK), prodynorphin (PDYN), CCK, prepronociceptin (PONC), Tβ4, MOR, CCKBR, and GAPDH were shown in **Table 1**. RT-PCR was performed with Step One Plus™ Real-Time PCR System (Applied Biosystems, CA, USA) using SYBR Green RT-PCR kit (Takara, Dalian, China). The mRNA of POMC, PDYN, PENK, CCK-8, PONC, Tβ4, MOR, and CCKBR relative to GAPDH mRNA were quantified with the $2^{-\Delta Ct}$ method, where $\Delta Ct = Ct_{\text{target gene}} - Ct_{\text{GAPDH}}$.

Statistical Analysis

All data were expressed as mean ± SD. Statistical analyses were performed with SPSS version 18.0 (SPSS Inc., CHI, USA). Independent *T*-test was used to analyze variables, including Tβ4 and its mRNA levels between EA treatment and sham treatment. One-way ANOVA was used to analyze protein and mRNA levels of opioid and anti-opioid peptides and related receptors among the groups with different treatments. Data including TFL changes after repeated EA were analyzed with repeated ANOVA. Bonferroni post-test was used when significant differences were found. The correlation coefficient (Pearson's) was used to examine the correlations. A difference was considered significant if P was < 0.05.

RESULTS

Repeated EA-Induced Tβ4 Expression and Change Rate of Tail Flick Latency

The TFL was measured every day throughout the experiment (**Figure 2B**). No change ($P > 0.05$) was found in TFL in sham treatment during this trial. EA-induced TFL change rate was 49.6 ± 7.6% at day 1, then declined ($P < 0.001$) to 30.7 ± 8.5% at day 4 and fell ($P < 0.001$) to 1.8 ± 1.2% at day 8, implying EAT formation. TFL change rates in EA treatment were higher ($P < 0.05$) than those in sham treatment at day 1 to 6.

The dynamic expression of Tβ4 induced by repeated EA was determined in cortex, thalamus, hypothalamus, midbrain and medulla at day 0, 1, 4, and 8. EA increased ($P < 0.05$) the expression of Tβ4 in the measured areas at day 1–8 (**Figure 2C**). Statistical analysis showed that TFL change rates had a negative correlation with Tβ4 levels in cortex ($r = -0.774$, $P < 0.001$), in thalamus ($r = -0.689$, $P = 0.002$), in hypothalamus ($r = -0.705$, $P = 0.001$), in midbrain ($r = -0.709$, $P = 0.001$) and in medulla ($r = -0.612$, $P = 0.007$).

The Effect of Intracerebroventricularly Injection of Tβ4 Antibody on Repeated EA-Induced Tail Flick Latency

TFL change rates in Sh-EA and EA-PBS groups showed the same change pattern as those in **Figure 2B**. TFL change rate of EA-treated rats was decreased in a Tβ4-antibody-dose- and time-dependent manner. EA-treated rats with icv injection of Tβ4 antibody showed higher ($P < 0.05$) TFL change rates than rats with PBS or isotype IgG at day 3–7. TFL change rates in 10 μg antibody group were higher ($P < 0.05$) than that in 1 μg or 0.1 μg antibody group at day 4–7 (**Figure 3A**).

The Effect of Tβ4 siRNA on Repeated EA-Induced Tail Flick Latency

To verify siRNA was able to transfect, the fluorescence-conjugated control siRNA was intracerebroventricularly injected, the fluorescence in hypothalamus, thalamus, cortex, midbrain, and medulla was observed at 24 h after injection (**Figure 3B**).

TFL change rates in Sh-EA and EA-tr groups showed the same change pattern as those in **Figure 2B**, and the development of EAT at day 8. TFL change rates in EA-tr, EA-L, and EA-C-si groups were higher ($P < 0.05$) than those in Sh-EA group at day 1–5, but lower ($P < 0.05$) than those in EA-Tβ4-si group at day 3–8. No change was observed in TFLs among EA-tr, EA-L, and EA-C-si groups (**Figure 3C**).

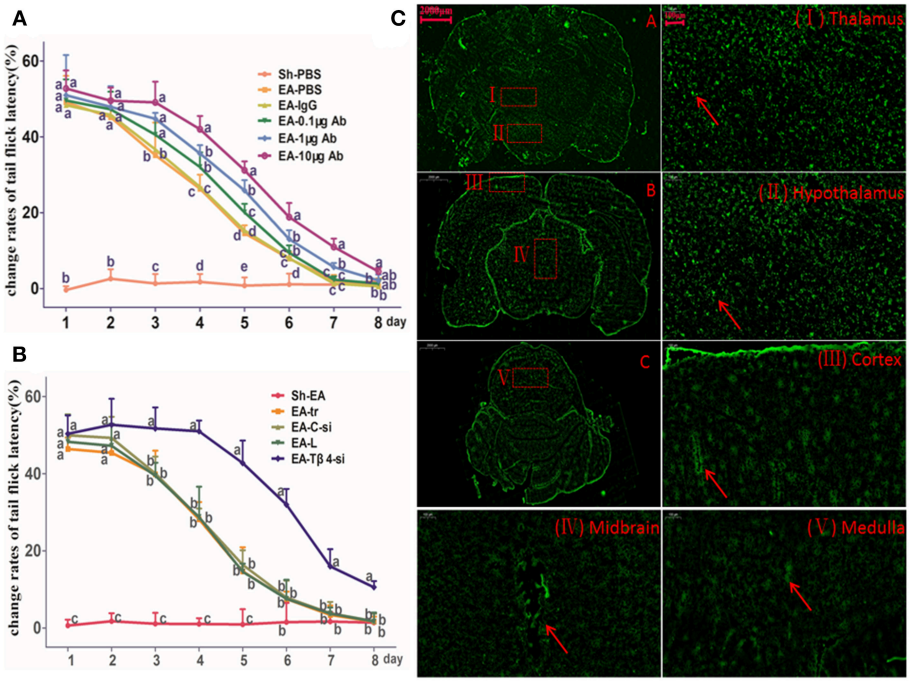

FIGURE 3 | The effect of intracerebroventricularly (icv) injection of Tβ4 antibody or siRNA on electroacupuncture (EA)-induced tail flick latency (TFL). **(A)** The effect of icv injection of Tβ4 antibody on change rates of TFL (mean ± SD, %, $n = 6$). The values with different letters differ significantly in different groups at the same day ($P < 0.05$). One-way ANOVA followed by Bonferroni's post-test. **(B)** The effect of icv injection of Tβ4 siRNA on change rates of TFL (mean ± SD, %, $n = 6$). The values with different letters differ significantly in different groups at the same day ($P < 0.05$). One-way ANOVA followed by Bonferroni's post-test. **(C)** The fluorescence in cortex, thalamus, hypothalamus, mid-brain and medulla. Arrows point to the high fluorescence intensity. Scale bars represent 2,000 μm in picture **(A–C)**, and 100 μm in others.

The Effect of Tβ4 siRNA on Protein Expressions of Opioid- and Anti-opioid Peptides and Related Receptors in the Brain Areas of Rats With Repeated EA

The protein expressions of END, ENK, DYN, CCK-8, OFQ, Tβ4, MOR, and CCKBR were observed in hypothalamus, thalamus, cortex, midbrain and medulla at day 1–8. No difference ($P > 0.05$) was observed in the expressions of these eight substances among EA-tr, EA-L, and EA-C-si groups in the measured areas during the experiment.

The protein levels of those substances in cortex were shown in **Figure 4A**. Compared with sham treatment, EA treatment induced an increase in OFQ, CCK-8, and CCKBR levels (day 4 and 8), and Tβ4, ENK, DYN, and END levels (day 1–8), and MOR level (day 1 and 4). EA-Tβ4 siRNA-treated rats exhibited lower Tβ4 level (day 1–8), but higher levels of CCKBR (day 4), DYN (day 1), ENK, END, and MOR (day 1 and 4) than EA-treated rats. TFL change rates were negatively ($P < 0.05$) correlated with Tβ4, OFQ, CCK-8, or CCKBR levels, but positively ($P < 0.05$) correlated with ENK, DYN, END, or MOR levels. Tβ4 levels were negatively correlated with ENK, DYN, END, or MOR levels (**Figure 4B**).

In thalamus, compared with Sh-EA treated rats, EA-treated rats showed an increase in Tβ4 and OFQ (day 1–8), and CCK-8 and CCKBR (day 4 and 8), and ENK, DYN, END, and MOR (day 1 and 4). Compared with EA-treated rats, **EA**-Tβ4 siRNA-treated rats showed a decrease in Tβ4 (day 1–8), but an increase in OFQ and ENK (day 4 and 8), DYN and MOR (day 1–8), and END (day 4). TFL change rates were negatively ($P < 0.05$) correlated with Tβ4, OFQ, CCK-8, or CCKBR levels, but positively ($P < 0.05$) correlated with ENK, DYN, END, or MOR levels. Tβ4 levels were positively correlated with OFQ levels, but negatively correlated with ENK, DYN, END, END, or MOR levels (**Table 2**).

In hypothalamus, rats in EA-tr group showed an increase in CCK-8 (day 4 and 8), and Tβ4, OFQ, CCKBR, and MOR (day 1–8), and ENK, DYN, and END (day 1 and 4) compared with rats in Sh-EA group. **EA**-Tβ4 siRNA treatment caused a decrease ($P < 0.05$) in Tβ4 (day 1 and 4), but an increase in OFQ, CCK-8, and MOR (day 8), in ENK and DYN (day 4 and 8), and END (day 4) and CCKBR (day 1) Compared with EA treatment. TFL change rates were negatively ($P < 0.05$) correlated with Tβ4, OFQ, or CCK-8 levels, but positively ($P < 0.05$) correlated with ENK, DYN, END, or MOR levels. Tβ4 levels were positively correlated with OFQ or CCK-8 levels, but negatively correlated with ENK, DYN, END, or MOR levels (**Table 2**).

In midbrain, EA treatment caused increased Tβ4, OFQ, CCK-8, CCKBR, ENK, DYN, and END (day 1–8) and MOR levels (day 1 and 4) compared with sham treatment. EA-Tβ4 siRNA treatment induced a decrease in Tβ4 (day 1–8), but an increase in OFQ and CCK-8 (day 1 and 4), ENK, END, and MOR (day 4 and 8), and DYN (day 4) compared with EA treatment.

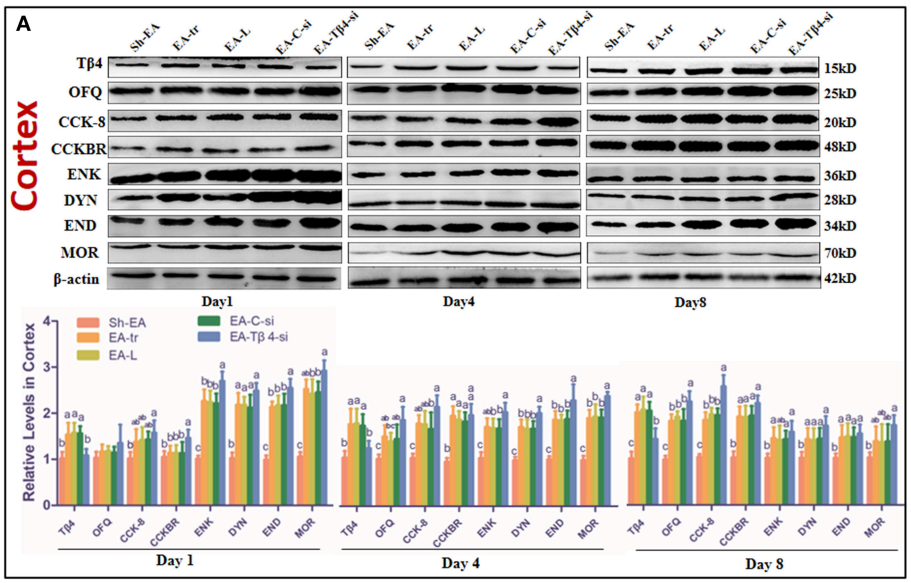

B

Correlation coefficients	Tβ4	OFQ	CCK-8	CCKBR	ENK	DYN	END	MOR
Change rates of tail flick latency (r_{TFL})	-0.55*	-0.638**	-0.715**	-0.624**	0.717**	0.665**	0.83**	0.822**
Tβ4 levels ($r_{Tβ4}$)		0.39	0.527	0.394	-0.691*	-0.587*	-0.612**	-0.566*

FIGURE 4 | (A) The effect of Tβ4 siRNA on the levels of opioid and anti-opioid peptides and their receptors in the cortex of rats with repeated EA on day 1, 4, and 8 (mean ± SD, $n = 6$). The expressions of thymosin beta 4 (Tβ4), orphanin FQ (OFQ), cholecystokinin octapeptide (CCK-8), CCK B receptor (CCKBR), endorphin (END), encephalin (ENK), dynorphin (DYN), and mu opioid receptor (MOR) were observed. The values with different letters (a-c) differ significantly in different groups at the same day ($P < 0.05$). One-way ANOVA followed by Bonferroni's post-test. **(B)** The correlation coefficients between the levels of opioid or anti-opioid peptides or their receptors and the change rates of tail flick latency (TFL) or Tβ4 levels. *$P < 0.05$, **$P < 0.01$. The correlation coefficient was analyzed with Pearson's correlation coefficient.

TFL change rates were negatively ($P < 0.05$) correlated with Tβ4 levels, but positively ($P < 0.05$) correlated with ENK, DYN, END, or MOR levels. Tβ4 levels were positively correlated with CCK-8 levels, but negatively correlated with ENK, DYN, END, or MOR levels (**Table 2**).

In medulla, Tβ4, OFQ, CCK-8, CCKBR, ENK, and DYN levels (day 1–8) and END and MOR levels (day 1 and 4) in EA-tr group were enhanced compared with those in sham group. Rats in EA-Tβ4-si group exhibited a decrease in Tβ4 (day 1–8), but an increase in CCK-8, CCKBR, and ENK (day 4), DYN (day 8), END (day 1 and 4), and MOR (day 4 and 8) compared with rats in EA-tr group. TFL change rates were negatively ($P < 0.05$) correlated with Tβ4, OFQ or CCKBR levels, but positively ($P < 0.05$) correlated with ENK, DYN, END, or MOR levels. Tβ4 levels were positively correlated with OFQ levels, but negatively correlated with ENK, DYN, END, or MOR levels (**Table 2**).

The Effect of Tβ4 siRNA on Gene Expressions of Opioid- and Anti-opioid Peptides and Related Receptors in the Brain Areas of Rats With Repeated EA

PNOC, PENK, POMC, and PDYN are the precursors of OFQ, ENK, END, and DYN, respectively. The mRNA levels of POMC, PENK, PDYN, CCK, Tβ4, MOR, and CCKBR are measured in hypothalamus, thalamus, cortex, midbrain, and medulla at day 1–8 (**Table 3**). No difference ($P > 0.05$) was observed in the expression of these eight genes among EA-tr, EA-L, and EA-C-si groups in the measured areas during the experiment.

In cortex, EA treatment induced an increase in Tβ4, CCK, and MOR mRNAs (day 1–8), PNOC and POMC mRNAs (day 4 and 8), PENK and PDYN mRNAs (day 4), and CCKBR mRNA (day 8) compared with sham treatment. EA-Tβ4 siRNA treatment caused a decrease in Tβ4 mRNA (day 1–8), but an increase PDYN and MOR mRNAs (day 1 and 4) and PENK mRNA (day 4) compared with EA treatment.

In thalamus, compared with rats in Sh-EA group, rats in EA-tr group showed increased Tβ4 and PNOC (day 1–8), CCK (day 4 and 8), and CCKBR, PENK, POMC, and MOR (day 4) mRNAs. Compared with rats in EA-tr group, rats in EA-Tβ4-si group showed decreased Tβ4 mRNA (day 1 and 4), but increased CCK (day 4), POMC (day 4 and 8), and PDYN and MOR (day 1) mRNAs.

In hypothalamus, mRNA levels of Tβ4 (day 1–8), PNOC and CCK (day 4 and 8), CCKBR (day 1 and 8), and PENK, PDYN, POMC, and MOR (day 4) mRNAs in EA-tr group were higher than those in Sh-EA group. EA-Tβ4 siRNA treatment induced a decrease in Tβ4 (day 1), but an increase in PENK (day 1), and PDYN and MOR (day 1 and 4) mRNAs compared with EA treatment.

In midbrain, EA-treated rats exhibited higher Tβ4, PNOC, CCK, CCKBR, PENK, and MOR (day 4 and 8), PDYN (day 1 and

TABLE 2 | The effect of Tβ4 siRNA on protein levels of opioid- and anti-opioid peptides and related receptors.

Areas	Day 1				Day 4				Day 8							Correlation coefficients	
	Sh-EA	EA-tr	EA-L-si	EA-C-si	EA-Tβ4-si	Sh-EA	EA-tr	EA-L-si	EA-C-si	EA-Tβ4-si	Sh-EA	EA-tr	EA-L-si	EA-C-si	EA-Tβ4-si	$r_{(TFL)}$	$r_{(Tβ4)}$
THALAMUS																	
Tβ4	1.01 ± 0.06^{b}	1.5 ± 0.39^{a}	1.52 ± 0.29^{a}	1.53 ± 0.21^{a}	1.24 ± 0.08^{b}	1.04 ± 0.12^{b}	1.83 ± 0.23^{a}	1.81 ± 0.24^{a}	1.78 ± 0.22^{a}	1.25 ± 0.19^{b}	1.04 ± 0.11^{c}	1.94 ± 0.16^{a}	1.97 ± 0.13^{a}	1.94 ± 0.15^{a}	1.51 ± 0.23^{b}	−0.637**	
OFQ	0.99 ± 0.1^{b}	1.58 ± 0.11^{a}	1.52 ± 0.17^{a}	1.56 ± 0.18^{a}	1.6 ± 0.29^{a}	1 ± 0.12^{c}	1.52 ± 0.12^{b}	1.5 ± 0.2^{b}	1.52 ± 0.29^{b}	1.91 ± 0.19^{a}	1.02 ± 0.11^{c}	1.87 ± 0.16^{a}	1.78 ± 0.32^{a}	1.83 ± 0.14^{a}	2.23 ± 0.19^{b}	−0.677**	0.563*
CCK-8	1.05 ± 0.11	1.04 ± 0.17	1.06 ± 0.14	1.03 ± 0.18	1.23 ± 0.22	1.01 ± 0.12^{b}	1.42 ± 0.21^{a}	1.43 ± 0.23^{a}	1.48 ± 0.18^{a}	1.77 ± 0.22^{a}	1.05 ± 0.13^{b}	1.63 ± 0.14^{a}	1.63 ± 0.09^{a}	1.62 ± 0.15^{a}	1.92 ± 0.28^{a}	−0.527*	0.369
CCKBR	0.99 ± 0.09	1.1 ± 0.18	1.12 ± 0.13	1.19 ± 0.08	1.2 ± 0.25	1.01 ± 0.09^{b}	1.8 ± 0.12^{a}	1.84 ± 0.18^{a}	1.72 ± 0.25^{a}	1.74 ± 0.53^{a}	1 ± 0.09^{b}	1.84 ± 0.18^{a}	1.88 ± 0.16^{a}	1.86 ± 0.19^{a}	2.02 ± 0.2^{a}	−0.515*	0.086
ENK	1.01 ± 0.11^{b}	2.01 ± 0.13^{a}	1.97 ± 0.13^{a}	1.99 ± 0.19^{a}	2.25 ± 0.22^{a}	1.01 ± 0.13^{c}	1.53 ± 0.16^{b}	1.52 ± 0.14^{b}	1.48 ± 0.18^{b}	2 ± 0.1^{a}	1.01 ± 0.12^{b}	1.2 ± 0.12^{b}	1.18 ± 0.08^{b}	1.2 ± 0.14^{b}	1.57 ± 0.19^{a}	0.837**	−0.690*
DYN	1 ± 0.11^{c}	2.28 ± 0.23^{b}	2.11 ± 0.15^{b}	2.1 ± 0.16^{b}	2.62 ± 0.24^{a}	1.01 ± 0.14^{c}	1.66 ± 0.24^{b}	1.63 ± 0.19^{b}	1.66 ± 0.21^{b}	2.17 ± 0.19^{a}	1.04 ± 0.11^{b}	1.23 ± 0.14^{b}	1.22 ± 0.12^{b}	1.26 ± 0.13^{b}	1.68 ± 0.21^{a}	0.785**	−0.530*
END	1.03 ± 0.12^{b}	2.55 ± 0.28^{a}	2.58 ± 0.21^{a}	2.55 ± 0.39^{a}	2.86 ± 0.26^{a}	1.07 ± 0.12^{c}	1.72 ± 0.21^{b}	1.68 ± 0.35^{b}	1.68 ± 0.2^{b}	2.21 ± 0.24^{a}	1.02 ± 0.17	1.08 ± 0.27	0.99 ± 0.15	1.01 ± 0.23	1.26 ± 0.28	0.874**	−0.713**
MOR	1.04 ± 0.11^{c}	2.34 ± 0.22^{b}	2.31 ± 0.2^{b}	2.28 ± 0.22^{b}	2.82 ± 0.16^{a}	1 ± 0.11^{c}	1.76 ± 0.16^{b}	1.75 ± 0.15^{b}	1.77 ± 0.19^{b}	2.25 ± 0.17^{a}	1 ± 0.04^{b}	1.28 ± 0.13^{b}	1.24 ± 0.17^{b}	1.21 ± 0.17^{b}	1.9 ± 0.26^{a}	0.668**	−0.537*
HYPOTHALAMUS																	
Tβ4	1.04 ± 0.11^{b}	1.47 ± 0.21^{a}	1.48 ± 0.22^{a}	1.49 ± 0.21^{a}	1.13 ± 0.07^{b}	1.02 ± 0.14^{c}	1.92 ± 0.17^{a}	1.93 ± 0.28^{a}	1.92 ± 0.35^{a}	1.45 ± 0.09^{b}	1.04 ± 0.07^{b}	2.18 ± 0.3^{a}	2.16 ± 0.24^{a}	2.12 ± 0.25^{a}	1.87 ± 0.06^{a}	−0.868**	
OFQ	1 ± 0.13^{b}	1.3 ± 0.08^{a}	1.33 ± 0.09^{a}	1.3 ± 0.11^{a}	1.49 ± 0.17^{a}	1.03 ± 0.14^{b}	1.68 ± 0.3^{a}	1.69 ± 0.2^{a}	1.51 ± 0.13^{a}	1.87 ± 0.27^{a}	0.98 ± 0.08^{c}	1.86 ± 0.12^{b}	1.87 ± 0.09^{b}	1.85 ± 0.11^{b}	2.19 ± 0.28^{a}	−0.65**	0.788**
CCK-8	1.03 ± 0.08^{b}	1.36 ± 0.11^{ab}	1.33 ± 0.28^{ab}	1.33 ± 0.26^{ab}	1.55 ± 0.17^{a}	0.99 ± 0.05^{b}	1.87 ± 0.22^{a}	1.77 ± 0.41^{a}	1.82 ± 0.16^{a}	2.12 ± 0.16^{a}	0.98 ± 0.1^{c}	1.73 ± 0.38^{b}	1.71 ± 0.21^{b}	1.68 ± 0.25^{b}	2.28 ± 0.26^{a}	−0.493*	0.746**
CCKBR	0.98 ± 0.06^{c}	1.42 ± 0.23^{b}	1.44 ± 0.3^{b}	1.4 ± 0.19^{ab}	1.8 ± 0.18^{a}	1.01 ± 0.12^{a}	2 ± 0.24^{a}	2.06 ± 0.31^{a}	1.97 ± 0.32^{a}	2.03 ± 0.4^{a}	1.1 ± 0.18^{b}	1.97 ± 0.4^{a}	1.95 ± 0.31^{a}	2.03 ± 0.23^{a}	2.09 ± 0.21^{a}	−0.263	0.321
ENK	1.03 ± 0.09^{b}	2.64 ± 0.33^{a}	2.76 ± 0.27^{a}	2.77 ± 0.21^{a}	3.12 ± 0.17^{a}	1.03 ± 0.11^{c}	1.6 ± 0.13^{b}	1.57 ± 0.32^{b}	1.57 ± 0.32^{b}	2.01 ± 0.17^{a}	1 ± 0.04^{b}	1.29 ± 0.28^{b}	1.33 ± 0.12^{b}	1.32 ± 0.13^{b}	1.65 ± 0.21^{a}	0.647**	−0.879**
DYN	1.01 ± 0.08^{b}	2.31 ± 0.26^{a}	2.34 ± 0.29^{a}	2.42 ± 0.39^{a}	2.63 ± 0.27^{a}	1.01 ± 0.04^{c}	1.49 ± 0.2^{b}	1.47 ± 0.32^{b}	1.45 ± 0.23^{b}	1.99 ± 0.11^{a}	1.02 ± 0.07^{b}	1.13 ± 0.18^{b}	1.14 ± 0.33^{b}	1.05 ± 0.28^{b}	1.7 ± 0.17^{a}	0.638**	−0.853**
END	1.03 ± 0.09^{b}	2.74 ± 0.28^{a}	2.74 ± 0.23^{a}	2.79 ± 0.17^{a}	3.01 ± 0.34^{a}	1.02 ± 0.07^{c}	1.51 ± 0.27^{b}	1.57 ± 0.21^{b}	1.58 ± 0.26^{b}	2.14 ± 0.11^{a}	1 ± 0.04^{b}	1.31 ± 0.22^{ab}	1.29 ± 0.28^{ab}	1.27 ± 0.23^{ab}	1.56 ± 0.19^{a}	0.757**	−0.912**
MOR	1.04 ± 0.09^{b}	2.73 ± 0.3^{a}	2.74 ± 0.3^{a}	2.83 ± 0.26^{a}	3.2 ± 0.32^{a}	1 ± 0.11^{b}	1.72 ± 0.16^{a}	1.72 ± 0.17^{a}	1.76 ± 0.17^{a}	2.27 ± 0.35^{a}	1 ± 0.04^{c}	1.23 ± 0.19^{b}	1.19 ± 0.23^{b}	1.24 ± 0.19^{b}	1.9 ± 0.23^{a}	0.622**	−0.836**
MIDBRAIN																	
Tβ4	1.01 ± 0.11^{b}	1.48 ± 0.25^{a}	1.51 ± 0.27^{a}	1.48 ± 0.22^{a}	1.06 ± 0.16^{b}	0.98 ± 0.11^{c}	1.95 ± 0.17^{a}	1.98 ± 0.35^{a}	1.95 ± 0.22^{a}	1.44 ± 0.07^{b}	0.98 ± 0.11^{c}	1.99 ± 0.11^{a}	2.07 ± 0.3^{a}	1.97 ± 0.11^{a}	1.51 ± 0.16^{b}	−0.505*	
OFQ	1.02 ± 0.07^{c}	1.41 ± 0.18^{b}	1.46 ± 0.18^{b}	1.45 ± 0.17^{b}	1.86 ± 0.32^{a}	1.01 ± 0.11^{c}	1.53 ± 0.21^{b}	1.54 ± 0.27^{b}	1.59 ± 0.27^{b}	2.06 ± 0.24^{a}	1.03 ± 0.06^{b}	1.72 ± 0.24^{a}	1.78 ± 0.3^{a}	1.77 ± 0.19^{a}	2.04 ± 0.27^{a}	−0.154	0.065
CCK-8	1.04 ± 0.07^{c}	1.52 ± 0.24^{b}	1.53 ± 0.2^{b}	1.57 ± 0.25^{b}	1.98 ± 0.14^{a}	1 ± 0.11^{c}	1.79 ± 0.17^{b}	1.79 ± 0.2^{b}	1.79 ± 0.25^{b}	2.29 ± 0.33^{a}	1.03 ± 0.07^{b}	2.08 ± 0.25^{a}	2.06 ± 0.27^{a}	2.07 ± 0.26^{a}	2.33 ± 0.18^{a}	−0.275	0.518*
CCKBR	1.04 ± 0.07^{b}	1.47 ± 0.29^{a}	1.42 ± 0.25^{ab}	1.45 ± 0.27^{a}	1.53 ± 0.21^{a}	1.06 ± 0.12^{b}	1.42 ± 0.31^{a}	1.42 ± 0.26^{a}	1.47 ± 0.24^{a}	1.83 ± 0.2^{a}	1.01 ± 0.08^{b}	1.9 ± 0.3^{a}	1.93 ± 0.26^{a}	1.92 ± 0.58^{a}	1.97 ± 0.49^{a}	−0.375	0.451
ENK	1.02 ± 0.13^{b}	2.05 ± 0.28^{a}	2.1 ± 0.35^{a}	2.07 ± 0.35^{a}	2.41 ± 0.3^{a}	0.99 ± 0.1^{c}	1.47 ± 0.15^{b}	1.45 ± 0.26^{b}	1.47 ± 0.41^{b}	1.99 ± 0.14^{a}	0.94 ± 0.12^{c}	1.35 ± 0.26^{b}	1.38 ± 0.29^{b}	1.38 ± 0.21^{b}	1.88 ± 0.15^{a}	0.478*	−0.811**
DYN	1.05 ± 0.15^{b}	2.21 ± 0.2^{a}	2.22 ± 0.4^{a}	2.22 ± 0.28^{a}	2.64 ± 0.2^{a}	1 ± 0.09^{c}	1.85 ± 0.23^{b}	1.92 ± 0.24^{b}	1.9 ± 0.22^{b}	2.34 ± 0.25^{a}	1.04 ± 0.12^{b}	1.44 ± 0.27^{a}	1.5 ± 0.27^{a}	1.44 ± 0.36^{a}	1.82 ± 0.16^{a}	0.818**	−0.674**
END	1.05 ± 0.14^{b}	2.13 ± 0.29^{a}	2.11 ± 0.34^{a}	2.18 ± 0.33^{a}	2.51 ± 0.31^{a}	1.02 ± 0.14^{c}	1.85 ± 0.19^{b}	1.87 ± 0.21^{b}	1.89 ± 0.34^{b}	2.34 ± 0.27^{a}	0.96 ± 0.11^{c}	1.41 ± 0.24^{b}	1.48 ± 0.25^{ab}	1.42 ± 0.32^{b}	1.85 ± 0.16^{a}	0.752**	−0.736**
MOR	1.02 ± 0.11^{b}	2.65 ± 0.19^{a}	2.69 ± 0.22^{a}	2.66 ± 0.16^{a}	2.97 ± 0.27^{a}	1.03 ± 0.07^{c}	2.04 ± 0.35^{b}	2 ± 0.29^{b}	2 ± 0.38^{b}	2.66 ± 0.23^{a}	1.02 ± 0.09^{b}	1.39 ± 0.35^{b}	1.42 ± 0.26^{b}	1.41 ± 0.07^{b}	1.89 ± 0.29^{a}	0.857**	−0.607**
MEDULLA																	
Tβ4	1.01 ± 0.12^{b}	1.3 ± 0.17^{a}	1.3 ± 0.2^{a}	1.29 ± 0.28^{a}	0.86 ± 0.16^{b}	1.03 ± 0.14^{b}	1.5 ± 0.21^{a}	1.44 ± 0.2^{a}	1.49 ± 0.28^{a}	1.18 ± 0.22^{b}	1.04 ± 0.14^{c}	1.68 ± 0.33^{a}	1.62 ± 0.21^{ab}	1.67 ± 0.21^{a}	1.25 ± 0.22^{b}	−0.476*	
OFQ	0.99 ± 0.09^{b}	1.49 ± 0.22^{a}	1.48 ± 0.24^{a}	1.46 ± 0.26^{a}	1.47 ± 0.25^{a}	1.05 ± 0.12^{b}	1.68 ± 0.33^{a}	1.7 ± 0.22^{a}	1.71 ± 0.23^{a}	1.99 ± 0.18^{a}	1.02 ± 0.09^{b}	1.98 ± 0.23^{a}	1.94 ± 0.23^{a}	1.92 ± 0.29	2.29 ± 0.25^{a}	−0.625**	0.565*
CCK-8	1.01 ± 0.09^{b}	1.45 ± 0.2^{a}	1.42 ± 0.22^{a}	1.42 ± 0.22^{a}	1.77 ± 0.26^{a}	1.03 ± 0.13^{c}	1.68 ± 0.23^{b}	1.68 ± 0.13^{b}	1.71 ± 0.17^{b}	2.04 ± 0.19^{a}	1.05 ± 0.07^{b}	1.68 ± 0.23^{a}	1.7 ± 0.26^{a}	1.7 ± 0.25^{a}	2.05 ± 0.39^{a}	−0.249	0.215
CCKBR	0.99 ± 0.13^{b}	1.52 ± 0.15^{a}	1.56 ± 0.27^{a}	1.53 ± 0.22^{a}	1.58 ± 0.21^{a}	1.05 ± 0.09^{b}	1.35 ± 0.33^{b}	1.35 ± 0.21^{b}	1.37 ± 0.23^{b}	1.81 ± 0.11^{a}	1.03 ± 0.12^{b}	1.61 ± 0.43^{a}	1.68 ± 0.26^{a}	1.7 ± 0.3^{a}	1.92 ± 0.23^{a}	−0.532*	0.395
ENK	1.01 ± 0.1^{b}	2.08 ± 0.2^{a}	2.12 ± 0.3^{a}	2.11 ± 0.23^{a}	2.3 ± 0.43^{a}	1.04 ± 0.14^{c}	1.72 ± 0.2^{b}	1.74 ± 0.23^{b}	1.77 ± 0.17^{b}	2.4 ± 0.26^{a}	1.02 ± 0.11^{b}	1.47 ± 0.26^{a}	1.44 ± 0.3^{a}	1.52 ± 0.19^{a}	1.74 ± 0.25^{a}	0.698**	−0.178
DYN	1.02 ± 0.07^{b}	2.18 ± 0.28^{a}	2.14 ± 0.3^{a}	2.2 ± 0.25^{a}	2.53 ± 0.34^{a}	1.05 ± 0.11^{b}	1.68 ± 0.33^{a}	1.7 ± 0.23^{a}	1.7 ± 0.28^{a}	2.13 ± 0.37^{a}	1.03 ± 0.07^{c}	1.25 ± 0.3^{b}	1.28 ± 0.26^{b}	1.27 ± 0.22^{b}	1.75 ± 0.26^{a}	0.586*	−0.497*
END	1.04 ± 0.12^{c}	2.02 ± 0.26^{b}	2.09 ± 0.31^{b}	2.11 ± 0.28^{b}	2.68 ± 0.28^{a}	1.03 ± 0.1^{c}	1.69 ± 0.26^{b}	1.71 ± 0.21^{b}	1.7 ± 0.19^{b}	2.09 ± 0.15^{a}	1 ± 0.11	1.22 ± 0.32	1.24 ± 0.2	1.24 ± 0.18	1.44 ± 0.37	0.79**	−0.565*
MOR	1.03 ± 0.09^{b}	2.24 ± 0.38^{a}	2.24 ± 0.26^{a}	2.21 ± 0.21^{a}	2.4 ± 0.3^{a}	1 ± 0.11^{c}	1.84 ± 0.23^{b}	1.84 ± 0.16^{b}	1.85 ± 0.45^{b}	2.35 ± 0.15^{a}	1.02 ± 0.08^{b}	1.22 ± 0.24^{b}	1.25 ± 0.3^{b}	1.27 ± 0.26^{ab}	1.7 ± 0.29^{a}	0.773**	−0.482*

The measured brain areas included hypothalamus, thalamus, midbrain and medulla. The protein levels of Tβ4, thymosin beta 4; OFQ orphanin; CCK-8, cholecystokinin octapeptide; CCKBR, CCK B receptor; END, endorphin; ENK, encephalin; DYN, dynorphin; MOR, mu opioid receptor were measured with western blotting. The rats in EA-L, EA-C-si, or EA-Tβ4-si group were icv injected with lipofection, lipofection mixture with Control siRNA or Tβ4 siRNA, respectively. The rats except those in Sh-EA group were treated with EA (2/15 Hz, 30 min) at the day after icv injection and thereafter every day, for total 8 times. The rats in Sh-EA group were treated as the same as the rats in EA-tr group, but without electricity. The symbols have the same meanings in ***Table 3****. The values with different letters (a-c) differ significantly in different groups at the same day (P < 0.05). One-way ANOVA followed by Bonferroni's post-test. *means the levels of opioid or anti-opioid peptides or their receptors correlate with the change rates of tail flick latency (TFL) or Tβ4 levels at the 0.05 level, and **means at the 0.01 level. The correlation coefficient was analyzed with Pearson's correlation coefficient.*

TABLE 3 | The effect of Tβ4 siRNA on mRNAs of opioid- and anti-opioid peptides and related receptors.

Areas	Day 1					Day 4					Day 8				
	Sh-EA	EA-tr	EA-L-si	EA-C-si	EA-Tβ4-si	Sh-EA	EA-tr	EA-L-si	EA-C-si	EA-Tβ4-si	Sh-EA	EA-tr	EA-L-si	EA-C-si	EA-Tβ4-si
CORTEX															
Tβ4	1.03 ± 0.12^{b}	1.56 ± 0.19^{a}	1.53 ± 0.29^{a}	1.58 ± 0.13^{a}	1.06 ± 0.16^{b}	1.04 ± 0.11^{c}	2.01 ± 0.12^{a}	1.93 ± 0.11^{a}	1.95 ± 0.09^{a}	1.51 ± 0.22^{b}	1.01 ± 0.06^{c}	2.17 ± 0.24^{a}	2.18 ± 0.19^{a}	2.19 ± 0.16^{a}	1.74 ± 0.07^{b}
PNOC	1.02 ± 0.11^{b}	1.44 ± 0.35^{ab}	1.23 ± 0.11^{ab}	1.5 ± 0.35^{ab}	1.8 ± 0.5^{a}	1 ± 0.12^{c}	1.89 ± 0.1^{ab}	1.86 ± 0.11^{ab}	1.84 ± 0.1^{b}	2.05 ± 0.12^{a}	1.05 ± 0.12^{b}	1.88 ± 0.36^{a}	1.72 ± 0.38^{a}	1.82 ± 0.35^{a}	1.86 ± 0.3^{a}
CCK	1 ± 0.11^{b}	1.39 ± 0.14^{a}	1.37 ± 0.16^{a}	1.31 ± 0.24^{ab}	1.58 ± 0.22^{a}	0.99 ± 0.13^{b}	1.73 ± 0.38^{a}	1.71 ± 0.21^{a}	1.68 ± 0.25^{a}	1.97 ± 0.16^{a}	1.05 ± 0.11^{b}	1.81 ± 0.37^{a}	1.8 ± 0.42^{a}	1.73 ± 0.38^{a}	1.91 ± 0.36^{a}
CCKBR	1.04 ± 0.07^{b}	1.36 ± 0.17^{ab}	1.31 ± 0.16^{ab}	1.33 ± 0.24^{ab}	1.39 ± 0.27^{a}	1.01 ± 0.08	1.41 ± 0.3	1.43 ± 0.19	1.43 ± 0.23	1.24 ± 0.39	0.99 ± 0.09^{b}	1.68 ± 0.38^{a}	1.79 ± 0.37^{a}	1.65 ± 0.39^{a}	1.57 ± 0.36^{ab}
PENK	1.01 ± 0.12^{b}	1.33 ± 0.22^{b}	1.34 ± 0.27^{ab}	1.36 ± 0.25^{ab}	1.74 ± 0.25^{a}	0.94 ± 0.12^{c}	1.61 ± 0.2^{b}	1.7 ± 0.17^{b}	1.68 ± 0.23^{b}	2.08 ± 0.2^{a}	1.04 ± 0.14	1.03 ± 0.22	0.95 ± 0.32	1.01 ± 0.36	1.03 ± 0.36
PDYN	1.03 ± 0.07^{b}	1.26 ± 0.22^{b}	1.31 ± 0.31^{b}	1.31 ± 0.12^{b}	1.73 ± 0.31^{a}	1.05 ± 0.11^{c}	1.61 ± 0.24^{b}	1.63 ± 0.14^{b}	1.67 ± 0.22^{b}	2.01 ± 0.14^{a}	1.01 ± 0.14	1.38 ± 0.28	1.35 ± 0.33	1.3 ± 0.31	1.39 ± 0.18
POMC	1.02 ± 0.14	1.08 ± 0.27	0.99 ± 0.15	1.01 ± 0.23	1.26 ± 0.28	1.07 ± 0.12^{b}	1.87 ± 0.24^{a}	1.83 ± 0.16^{a}	1.9 ± 0.33^{a}	2.17 ± 0.15^{a}	1.02 ± 0.17^{b}	1.48 ± 0.27^{a}	1.45 ± 0.26^{a}	1.34 ± 0.23^{ab}	1.69 ± 0.24^{a}
MOR	1 ± 0.1^{c}	1.28 ± 0.13^{ab}	1.24 ± 0.17^{bc}	1.21 ± 0.17^{bc}	1.54 ± 0.21^{a}	1.01 ± 0.12^{c}	1.85 ± 0.08^{b}	1.82 ± 0.22^{b}	1.88 ± 0.15^{b}	2.33 ± 0.16^{a}	1 ± 0.11^{b}	1.63 ± 0.22^{a}	1.67 ± 0.13^{a}	1.64 ± 0.21^{a}	1.97 ± 0.27^{a}
THALAMUS															
Tβ4	1.01 ± 0.11^{c}	1.42 ± 0.18^{a}	1.39 ± 0.24^{a}	1.37 ± 0.19^{ab}	1.08 ± 0.08^{bc}	1.01 ± 0.14^{c}	1.84 ± 0.25^{a}	1.9 ± 0.33^{a}	1.84 ± 0.12^{a}	1.34 ± 0.23^{b}	1.04 ± 0.12^{b}	1.85 ± 0.36^{a}	1.8 ± 0.32^{a}	1.82 ± 0.37^{a}	1.77 ± 0.24^{a}
PNOC	1.03 ± 0.13^{b}	1.46 ± 0.22^{a}	1.48 ± 0.2^{a}	1.48 ± 0.29^{a}	1.78 ± 0.16^{a}	1 ± 0.13^{b}	1.71 ± 0.22^{a}	1.64 ± 0.37^{a}	1.61 ± 0.24^{a}	2.01 ± 0.19^{a}	1.04 ± 0.06^{b}	1.92 ± 0.29^{a}	1.95 ± 0.29^{a}	1.97 ± 0.16^{a}	2.04 ± 0.37^{a}
CCK	1.03 ± 0.08^{b}	1.31 ± 0.25^{ab}	1.37 ± 0.28^{ab}	1.35 ± 0.13^{ab}	1.55 ± 0.17^{a}	0.98 ± 0.1^{c}	1.44 ± 0.15^{b}	1.43 ± 0.25^{b}	1.4 ± 0.16^{b}	1.77 ± 0.22^{a}	1.04 ± 0.11^{b}	1.91 ± 0.18^{a}	1.92 ± 0.12^{a}	1.94 ± 0.17^{a}	1.96 ± 0.3^{a}
CCKBR	1.01 ± 0.12	1.37 ± 0.27	1.36 ± 0.18	1.36 ± 0.24	1.42 ± 0.21	1.01 ± 0.12^{b}	1.31 ± 0.17^{a}	1.33 ± 0.06^{a}	1.32 ± 0.1^{a}	1.58 ± 0.27^{a}	1.05 ± 0.09	1.55 ± 0.42	1.56 ± 0.35	1.46 ± 0.32	1.53 ± 0.25
PENK	1.01 ± 0.1	1.14 ± 0.17	1.13 ± 0.22	1.19 ± 0.33	1.25 ± 0.26	1.04 ± 0.13^{b}	1.64 ± 0.28^{a}	1.55 ± 0.25^{a}	1.54 ± 0.28^{a}	1.84 ± 0.31^{a}	1.03 ± 0.11^{b}	1.48 ± 0.33^{ab}	1.44 ± 0.35^{ab}	1.43 ± 0.27^{ab}	1.63 ± 0.32^{a}
PDYN	1.01 ± 0.08^{b}	1.19 ± 0.09^{b}	1.17 ± 0.13^{b}	1.25 ± 0.14^{b}	1.68 ± 0.21^{a}	1.05 ± 0.15^{b}	1.45 ± 0.24^{ab}	1.37 ± 0.28^{ab}	1.39 ± 0.09^{ab}	1.71 ± 0.37^{a}	1.02 ± 0.07	1.44 ± 0.46	1.42 ± 0.33	1.39 ± 0.38	1.59 ± 0.33
POMC	1.03 ± 0.1^{b}	1.31 ± 0.29^{ab}	1.29 ± 0.22^{ab}	1.26 ± 0.23^{ab}	1.56 ± 0.19^{a}	1.05 ± 0.14^{c}	1.59 ± 0.28^{b}	1.59 ± 0.19^{b}	1.58 ± 0.27^{b}	2.09 ± 0.2^{a}	1 ± 0.11^{b}	1.2 ± 0.16^{b}	1.15 ± 0.22^{b}	1.32 ± 0.23^{ab}	1.55 ± 0.2^{a}
MOR	1.02 ± 0.09^{b}	1.16 ± 0.18^{b}	1.16 ± 0.11^{b}	1.19 ± 0.18^{ab}	1.46 ± 0.22^{a}	1.02 ± 0.08^{b}	1.69 ± 0.28^{a}	1.64 ± 0.23^{a}	1.7 ± 0.22^{a}	1.82 ± 0.4^{a}	1.03 ± 0.09^{b}	1.32 ± 0.2^{ab}	1.29 ± 0.18^{ab}	1.37 ± 0.26^{ab}	1.73 ± 0.42^{a}
HYPOTHALAMUS															
Tβ4	1.02 ± 0.14^{b}	1.48 ± 0.22^{a}	1.51 ± 0.27^{a}	1.48 ± 0.25^{a}	1.16 ± 0.17^{b}	1.02 ± 0.12^{b}	1.67 ± 0.13^{a}	1.62 ± 0.16^{a}	1.64 ± 0.18^{a}	1.24 ± 0.08^{ab}	1.04 ± 0.1^{b}	1.66 ± 0.32^{a}	1.6 ± 0.34^{a}	1.66 ± 0.37^{a}	1.29 ± 0.35^{ab}
PNOC	0.99 ± 0.1^{b}	1.21 ± 0.18^{ab}	1.26 ± 0.11^{ab}	1.17 ± 0.27^{ab}	1.41 ± 0.22^{a}	1.02 ± 0.1^{b}	1.59 ± 0.18^{a}	1.68 ± 0.23^{a}	1.68 ± 0.23^{a}	1.75 ± 0.33^{a}	0.99 ± 0.11^{b}	1.9 ± 0.32^{a}	1.87 ± 0.35^{a}	1.76 ± 0.32^{a}	1.72 ± 0.43^{a}
CCK	1.01 ± 0.09	1.07 ± 0.17	1.07 ± 0.16	1.04 ± 0.14	1.17 ± 0.12	1.05 ± 0.13^{b}	1.47 ± 0.16^{a}	1.46 ± 0.15^{a}	1.52 ± 0.16^{a}	1.61 ± 0.25^{a}	1.04 ± 0.07^{b}	1.69 ± 0.34^{a}	1.65 ± 0.31^{a}	1.61 ± 0.34^{a}	1.66 ± 0.44^{a}
CCKBR	0.96 ± 0.08^{b}	1.32 ± 0.18^{a}	1.38 ± 0.22^{a}	1.35 ± 0.09^{a}	1.53 ± 0.15^{a}	1.01 ± 0.12^{b}	1.34 ± 0.19^{ab}	1.36 ± 0.23^{ab}	1.37 ± 0.35^{ab}	1.51 ± 0.35^{a}	1.01 ± 0.09^{b}	1.66 ± 0.38^{a}	1.67 ± 0.36^{a}	1.61 ± 0.41^{a}	1.64 ± 0.13^{ab}
PENK	1.02 ± 0.13^{b}	1.2 ± 0.12^{b}	1.2 ± 0.12^{b}	1.17 ± 0.1^{b}	1.57 ± 0.19^{a}	1 ± 0.11^{b}	1.37 ± 0.11^{a}	1.37 ± 0.13^{a}	1.37 ± 0.12^{a}	1.49 ± 0.27^{a}	1.01 ± 0.13	1.24 ± 0.2	1.28 ± 0.2	1.22 ± 0.36	1.43 ± 0.26
PDYN	1.02 ± 0.07^{b}	1.14 ± 0.14^{ab}	1.11 ± 0.18^{b}	1.09 ± 0.17^{b}	1.4 ± 0.18^{a}	1.02 ± 0.16^{c}	1.59 ± 0.11^{b}	1.6 ± 0.19^{b}	1.6 ± 0.17^{b}	2.07 ± 0.22^{a}	1.04 ± 0.11	1.49 ± 0.4	1.44 ± 0.43	1.39 ± 0.36	1.62 ± 0.26
POMC	1.04 ± 0.12^{b}	1.19 ± 0.24^{ab}	1.18 ± 0.13^{ab}	1.14 ± 0.22^{b}	1.47 ± 0.19^{a}	0.99 ± 0.12^{b}	1.87 ± 0.24^{a}	1.89 ± 0.19^{a}	1.89 ± 0.18^{a}	2.22 ± 0.22^{a}	1.03 ± 0.12^{b}	1.51 ± 0.2^{ab}	1.46 ± 0.3^{ab}	1.57 ± 0.35^{a}	1.69 ± 0.35^{a}
MOR	1.03 ± 0.11^{b}	1.16 ± 0.21^{b}	1.18 ± 0.12^{b}	1.19 ± 0.14^{b}	1.52 ± 0.25^{a}	1.05 ± 0.12^{c}	1.9 ± 0.16^{b}	1.93 ± 0.29^{b}	1.93 ± 0.16^{b}	2.38 ± 0.09^{a}	1.04 ± 0.11	1.24 ± 0.16	1.42 ± 0.17	1.26 ± 0.24	1.15 ± 0.42
MIDBRAIN															
Tβ4	1.03 ± 0.14^{ab}	1.29 ± 0.21^{ab}	1.29 ± 0.27^{ab}	1.32 ± 0.18^{a}	0.97 ± 0.13^{b}	0.98 ± 0.11^{b}	1.59 ± 0.28^{a}	1.61 ± 0.27^{a}	1.62 ± 0.27^{a}	1.25 ± 0.22^{b}	1.04 ± 0.14^{b}	1.91 ± 0.14^{a}	1.91 ± 0.14^{a}	1.92 ± 0.31^{a}	1.75 ± 0.16^{a}
PNOC	1.02 ± 0.06^{b}	1.12 ± 0.18^{b}	1.1 ± 0.22^{b}	1.15 ± 0.14^{ab}	1.43 ± 0.22^{a}	1.01 ± 0.11^{b}	1.53 ± 0.18^{a}	1.54 ± 0.18^{a}	1.47 ± 0.27^{a}	1.76 ± 0.24^{a}	0.99 ± 0.09^{b}	2.08 ± 0.12^{a}	2.06 ± 0.15^{a}	2.04 ± 0.12^{a}	2.01 ± 0.26^{a}
CCK	1.04 ± 0.06^{b}	1.11 ± 0.2^{b}	1.07 ± 0.21^{b}	1.16 ± 0.08^{ab}	1.48 ± 0.2^{a}	1.01 ± 0.11^{c}	1.69 ± 0.28^{b}	1.73 ± 0.29^{b}	1.78 ± 0.12^{b}	1.97 ± 0.16^{a}	1.03 ± 0.13^{c}	2.02 ± 0.18^{b}	2.2 ± 0.2^{b}	2.08 ± 0.26^{b}	2.18 ± 0.23^{a}
CCKBR	1.06 ± 0.12	1.27 ± 0.4	1.12 ± 0.24	1.19 ± 0.26	1.45 ± 0.24	1 ± 0.09^{b}	1.72 ± 0.26^{a}	1.76 ± 0.21^{a}	1.76 ± 0.29^{a}	1.59 ± 0.41^{a}	1.02 ± 0.1^{c}	1.93 ± 0.24^{a}	1.99 ± 0.23^{a}	2.04 ± 0.11^{a}	1.47 ± 0.19^{b}
PENK	1.02 ± 0.11	1.09 ± 0.21	1.06 ± 0.23	1.02 ± 0.18	1.18 ± 0.18	1.06 ± 0.15^{b}	1.75 ± 0.11^{a}	1.79 ± 0.14^{a}	1.77 ± 0.17^{a}	2.01 ± 0.2^{a}	1.01 ± 0.13^{c}	$1.41 \pm 0.14a^{b}$	1.32 ± 0.15^{b}	1.35 ± 0.21^{b}	1.7 ± 0.2^{a}
PDYN	0.99 ± 0.08^{c}	1.3 ± 0.16^{bc}	1.33 ± 0.2^{b}	1.35 ± 0.1^{b}	1.71 ± 0.32^{a}	1.01 ± 0.12^{c}	1.64 ± 0.26^{b}	1.59 ± 0.2^{b}	1.69 ± 0.3^{b}	2.13 ± 0.37^{a}	1 ± 0.09	1.01 ± 0.14	1.07 ± 0.38	1.19 ± 0.22	1.19 ± 0.37
POMC	1.01 ± 0.07^{b}	1.18 ± 0.33^{ab}	1.24 ± 0.21^{ab}	1.21 ± 0.14^{ab}	1.61 ± 0.36^{a}	1.01 ± 0.11^{b}	1.59 ± 0.32^{a}	1.64 ± 0.13^{a}	1.63 ± 0.36^{a}	2.06 ± 0.37^{a}	1.02 ± 0.07	0.99 ± 0.22	1.07 ± 0.33	1.01 ± 0.24	1.13 ± 0.22
MOR	1 ± 0.04^{b}	1.18 ± 0.14^{b}	1.13 ± 0.22^{b}	1.18 ± 0.22^{b}	1.65 ± 0.25^{a}	1.03 ± 0.07^{c}	1.85 ± 0.2^{b}	1.83 ± 0.25^{b}	1.76 ± 0.16^{b}	2.23 ± 0.2^{a}	1.01 ± 0.08^{c}	1.51 ± 0.24^{b}	1.47 ± 0.21^{b}	1.57 ± 0.18^{b}	1.95 ± 0.22^{a}
MEDULLA															
Tβ4	1.01 ± 0.12	1.25 ± 0.17	1.28 ± 0.35	1.25 ± 0.22	0.95 ± 0.23	1.05 ± 0.15^{b}	1.82 ± 0.17^{a}	1.81 ± 0.23^{a}	1.72 ± 0.28^{a}	1.51 ± 0.16^{a}	0.98 ± 0.11^{c}	2.2 ± 0.18^{a}	2.24 ± 0.28^{a}	2.19 ± 0.26^{a}	1.66 ± 0.26^{b}
PNOC	1.02 ± 0.07	1.06 ± 0.29	1.05 ± 0.18	1.03 ± 0.21	1.1 ± 0.21	0.99 ± 0.08^{b}	1.68 ± 0.28^{a}	1.6 ± 0.39^{a}	1.66 ± 0.14^{a}	1.76 ± 0.43^{a}	1.02 ± 0.09^{b}	1.87 ± 0.11^{a}	1.91 ± 0.13^{a}	1.89 ± 0.17^{a}	2.06 ± 0.24^{a}
CCK	1.05 ± 0.09^{b}	1.18 ± 0.15^{b}	1.21 ± 0.25^{b}	1.22 ± 0.19^{b}	1.57 ± 0.26^{a}	1.03 ± 0.07^{b}	1.8 ± 0.14^{a}	1.79 ± 0.29^{a}	1.78 ± 0.16^{a}	1.97 ± 0.09^{a}	1.02 ± 0.14^{b}	2.06 ± 0.13^{a}	1.93 ± 0.25^{a}	1.95 ± 0.15^{a}	2.16 ± 0.19^{a}
CCKBR	0.98 ± 0.06	1.11 ± 0.2	0.98 ± 0.2	0.98 ± 0.27	1.29 ± 0.22	1.03 ± 0.13^{b}	1.62 ± 0.29^{a}	1.61 ± 0.29^{a}	1.61 ± 0.33^{a}	1.95 ± 0.16^{a}	1.05 ± 0.13^{b}	1.96 ± 0.26^{a}	1.97 ± 0.57^{a}	1.82 ± 0.31^{a}	2.14 ± 0.33^{a}
PENK	1.02 ± 0.09	1.22 ± 0.31	1.19 ± 0.33	1.15 ± 0.36	1.11 ± 0.24	1.01 ± 0.11^{b}	1.54 ± 0.15^{ab}	1.42 ± 0.33^{ab}	1.42 ± 0.34^{ab}	1.82 ± 0.34^{a}	1.01 ± 0.07	1.01 ± 0.2	1.03 ± 0.18	0.96 ± 0.24	1.29 ± 0.27
PDYN	1.02 ± 0.13^{b}	0.99 ± 0.18^{b}	1.09 ± 0.1^{b}	1.06 ± 0.21^{b}	1.42 ± 0.17^{a}	1.04 ± 0.12^{b}	1.39 ± 0.29^{b}	1.38 ± 0.2^{b}	1.41 ± 0.28^{b}	1.86 ± 0.27^{a}	1.03 ± 0.12^{b}	0.97 ± 0.13^{b}	0.97 ± 0.25^{b}	1.04 ± 0.33^{b}	1.42 ± 0.1^{a}
POMC	1.02 ± 0.09^{b}	1.22 ± 0.24^{ab}	1.24 ± 0.34^{ab}	1.28 ± 0.25^{ab}	1.54 ± 0.34^{a}	0.96 ± 0.11^{c}	1.47 ± 0.26^{b}	1.44 ± 0.25^{b}	1.49 ± 0.33^{b}	2.05 ± 0.14^{a}	0.99 ± 0.1	0.97 ± 0.34	0.95 ± 0.24	1.09 ± 0.34	1.36 ± 0.27
MOR	1.02 ± 0.11^{b}	1.44 ± 0.14^{a}	1.45 ± 0.08^{a}	1.44 ± 0.18^{a}	1.55 ± 0.17^{a}	1 ± 0.11^{c}	1.49 ± 0.32^{b}	1.47 ± 0.16^{b}	1.41 ± 0.1^{b}	1.89 ± 0.29^{a}	1.06 ± 0.1^{c}	1.52 ± 0.21^{ab}	1.42 ± 0.32^{bc}	1.45 ± 0.23^{bc}	1.92 ± 0.23^{a}

The measured brain areas included hypothalamus, thalamus, cortex, midbrain and medulla. The mRNA expressions of Tβ4, thymosin beta 4; PONC, prepronociceptin; CCK , cholecystokinin; CCKBR,CCK B receptor; POMC, proopiomelanocortin; PENK , proenkephalin; PDYN , prodynorphin; MOR, mu opioid receptor were measured with qPCR. The values with different letters (a-c) differ significantly in different groups at the same day ($P < 0.05$). One-way ANOVA followed by Bonferroni's post-test.

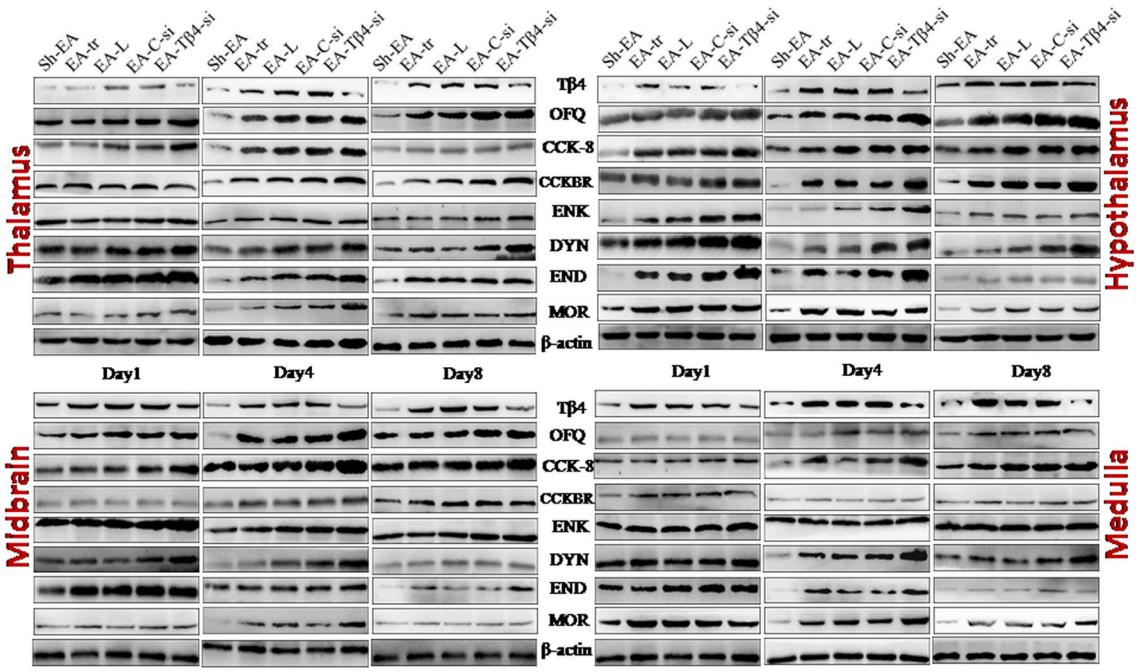

FIGURE 5 | The represented bands of Tβ4, OFQ, CCK-8, CCKBR, ENK, END, DYN, and MOR detected with western blotting in the thalamus, hypothalamus, midbrain and medulla of rats on day 1, 4, and 8.

4), and POMC (day 4) mRNAs than sham-treated rats. EA-Tβ4 siRNA-treated rats showed decreased Tβ4 (day 4), PNOC (day 1), CCK, and PDYN (day 1 and 4), CCKBR and PENK (day 8) and MOR (day 1–8) mRNAs compared with those in EA-treated rats.

In medulla, EA treatment caused an increase in Tβ4, PNOC, CCK and CCKBR mRNAs (day 4 and 8), in POMC mRNA (day 4) and MOR mRNA (day 1 to 4) compared with sham treatment. EA-Tβ4 siRNA treatment induced decreased Tβ4 (day 8), CCK (day 1), PDYN (day 1–8), POMC (day 4), and MOR (day 4 and 8) mRNAs compared with EA treatment.

DISCUSSION

EA has been extensively used for treating various diseases (Liu et al., 2009; Shah et al., 2016; Cui et al., 2017b; Wan et al., 2018), especially pain disorders (Zeng et al., 2016; Hu et al., 2017; Wan et al., 2017). However, it also can provoke EAT, which is a negative effect for its application. Some researchers use different EA modalities to establish EAT. Tian et al. (1998) used 100 Hz EA to stimulate rats for consecutive 6 h, and found that the pain threshold decreased at 1 h (105%) and approximated to the level before EA (25%) at 6 h, suggesting that continuous EA can provoke a rapid EAT. Repeated EA is more commonly used than continuous EA for pain therapy in clinical practice. Cui et al. (2016, 2017a) stimulated rats with 2/15 Hz and 2 Hz EA (30 min/day, total 8 days), and found that the pain thresholds decreased from 59.6 ± 4.6% and 61.4 ± 5.5% at day 1–2.1 ± 4.1% and 1.9 ± 7.4% at day 8, respectively, showing that repeated EA can elicit chronic EAT. Wang et al. (2002) used 2 Hz EA for 30 min every time for total 6 times with different intervals (0, 1, 2, and 3 days, respectively) in rats, and found that EA with the interval of 1 day induced EAT whereas EA with the interval of 3 days produced potent analgesia, showing that EA interval is an important factor influencing the development of EAT. In the present study, 2/15 Hz was used to stimulate rats for 30 min once daily for consecutive 8 day. The TFL change rate was reduced from 47.0 ± 3.4% at day 1 to 1.5 ± 1.5% at day 8, indicating the formation of EAT. The result in our experiment is similar to the report by Cui et al. (2016, 2017a).

Intracerebroventricular injection has been frequently used to study neural substrates in acupuncture analgesia (Tang et al., 1997; Cui et al., 2017a). Icv injection of antibody is a classical method for verifying the function of neural substrates. SiRNA has been shown to be a powerful technology allowing the silencing of mammalian genes with great specificity and potency (Alisky and Davidson, 2004; Aigner, 2006). A number of experiments have demonstrated the potential of appropriately designed siRNAs (Karagiannis and Elosta, 2005). Several formulations, including liposomal and viral vectors, have been shown to be efficacious for delivering siRNAs to local sites of the CNS (Bumcrot et al., 2006). Intracereboventricularly injected siRNA can maintain a longer effect because the cerebrospinal fluid lacks a significant nuclease (Guo et al., 1996). In the present study, strong fluorescence at 24 h after icv injection of the mixture of fluorescence-conjugated siRNA and lipofection was observed in several brain areas, including hypothalamus, thalamus, cortex, midbrain and medulla, which implied that siRNA was successfully transfected into the cells in targeted brain tissues via the cerebrospinal fluid. The dosage (5 μL Tβ4 siRNA mixture with 10 μL lipofection) and a single application of the mixture solution were determined

according to fluorescence intensity in brain areas and the duration of Tβ4 siRNA effect (a lower level of Tβ4 lasted for 8 days), respectively, in our pretest.

Numerous studies confirmed that EOPs in the CNS were main mediators to participate in EA analgesia regulation (Han et al., 1984; Han, 2003). Hence, opioid tolerance may be an important mechanism for EAT. In the present study, EOPs levels in the measured areas were positively correlated with the change rates in TFLs of rats treated with repeated EA.Tβ4 siRNA injection evoked an increase in ENK, DYN and END levels in most measured areas. ENK, DYN, or END level was negatively correlated with Tβ4 levels in the measured areas except in medulla where no correlation was observed between ENK and Tβ4 level. These results obviously displayed that the inhibition of Tβ4 partly reversed the expression of EOPs, hereby delayed the formation of EAT.

It has been found that EA induces the release of anti-opioid peptides (CCK-8 and OFQ) as it increases levels of opioid peptides in the CNS (Bian et al., 1993; Tian et al., 1998). Therefore, the roles of these anti-opioid peptides in EAT have attracted more attention. Han et al. (1985) injected CCK-8 into the cerebroventricle or spinal subarachnoid space in rats, and found that CCK-8 dose-dependently antagonized EA-induced analgesic effect. They also confirmed that icv or intrathecal injection of the antiserum against CCK-8 postponed or reversed the EAT (Han et al., 1986). Microinjection of OFQ into rats' periaqueductal gray remarkably antagonized EA analgesia in a dose-related manner (Zhi-Qi, 2008). Tian et al. (1998) reported that icv injection of OFQ antibody reversed EAT. These studies indicate that endogenous CCK-8 and OFQ participate in the formation of EAT. In this trial, Tβ4 siRNA treatment caused unchanged OFQ and CCK-8 levels in most brain areas except midbrain and hypothalamus. Studies found that the increased CCK-8 and OFQ were along with the increment of EOPs, which is believed to be a negative feedback of the former (Huang et al., 2003; Wang et al., 2006). Therefore, the increase of CCK-8 and OFQ in midbrain and hypothalamus may be also due to negative feedback on increased opioid peptides induced by Tβ4 siRNA.

Since opioid and anti-opioid peptides exert biological functions through their receptors, the roles of opioid and anti-opioid receptors in the development of EAT appeal to researchers. MOR, one of classic opioid receptors with a high affinity for ENK and END, is involved in EA-induced analgesia (Han et al., 1981a; Chen and Han, 1992a; Huang et al., 2000). CCK-8 could interact with CCK receptors (especially CCKBR) in the specific sites of the CNS to interfere with the functions of MOR, resulting in anti-analgesic effect (Wang et al., 1990; Shen et al., 1995; Huang et al., 2007). MOR and CCKBR can be selected as representatives of EOP- and anti-EOP- receptors, respectively. Ni et al. (1987) found that repeated EA resulted in EAT and decreased opioid receptors in rats' brain. Huang et al. (2007) demonstrated that CCKBR antagonist (L365, 260) potentiated 100 Hz EA-induced analgesia and reversed chronic tolerance to 100 Hz EA in mice. These findings demonstrated that MOR and CCKBR were involved in EAT. In the current study, the level of MOR decreased as EA application frequencies increased, which was consistent with the report of Ni et al. (1987). However, Tβ4 siRNA treatments caused increased MOR level; MOR levels were negative correlation with Tβ4 levels in the measured brain areas. Tβ4 siRNA caused CCKBR levels to be unchanged in thalamus and midbrain, and to be increased in cortex, hypothalamus and medulla at some specific time points. However, CCKBR levels were not correlated with Tβ4 levels. These results indicated that Tβ4 facilitated EAT probably via influencing opioid receptors. However, the underlying mechanisms need to be further studied.

Tβ4 is a small molecule polypeptide that widely exists in the CNS. Tβ4 can be released from neurons, but the targets it works on are unclear. Xiong et al. (2012a,b) reported that Tβ4 provided neuro-protection and neuro-restoration in experimental traumatic brain injury. Santra et al. (2012) reported that Tβ4 mediated oligodendrocyte differentiation via the inhibition of p38MAPK and the reduction of phosphorylated JNK accumulation. Jeon et al. (2013) found that Tβ4 facilitated mesenchymal stem cells proliferation through activation of ERK. These studies suggested that Tβ4 exerted neuro-protection via MAPK (ERK1/2, P38, and JNK) signal pathways. (Chen and Sommer, 2009) reported that MAPK signaling pathways were activated in the CNS and the periphery in the chronic morphine tolerance which was reduced by the inhibitors of these pathways. The similarity between EA and morphine tolerance has been demonstrated in a cross-tolerance study (Han et al., 1981b). Cui et al. (2017a) reported that the MAPK signaling pathway was targeted by miRNAs involved in chronic EAT. The previous studies suggest that there is a potential relationship between MAPK signal pathways and chronic EAT (Han et al., 1981b; Cui et al., 2017a). However, whether Tβ4 activates these pathways in chronic EAT needs to be confirmed.

In summary, repeated EA can result in decreased TFL, which is a negative effect of its treatment. Studies have showed that Tβ4 has neuroprotective and neuro-nutritional effects. Repeated EA, as a stimulus, caused increased Tβ4 in brain areas. Tβ4 siRNA icv injection postponed the formation of EAT, reversed decreased opioid- and their receptors induced by EAT in most brain areas. These results confirmed Tβ4 facilitated EAT probably through negatively changing endogenous opioid peptides and their receptors and positively influencing anti-opioid peptides in the CNS. Neuromodulators (opioid peptides and non-opioid peptides) in the CNS are distributed in different regions in which the neurons communicate with each other through neural fibers, and constitute a regulating network. EA induces the release of the neuromodulators in the specific regions, thereby exerts the analgesic modification. In the present study, the expression levels of opioid- and anti-opioid-peptides and their receptors induced by Tβ4 siRNA were fluctuated in some brain areas, indicating the complex regulations of these neuromodulators and brain areas in the formation of EAT. Although the present study exhibited that Tβ4 siRNA delayed the formation of EAT through affecting the expression of opioid peptides, anti-opioid peptides and opioid receptors in a wide range of the brain regions. Since substances are not evenly distributed in the specific pain-regulated nuclei, the brain area sampling may result in their homogenization; it may not accurately reflect their levels in the specific nuclei. It will be more important to investigate the effect of Tβ4 on

neuromodulators in the specific nuclei in the formation of EAT. In addition, the role of Tβ4 in anti-analgesic neural circuits or cellular signaling pathways needs to be further studied. Anyhow, our results provided an important foundation for investigating the molecular mechanisms by which Tβ4 modifies EAT in the future.

AUTHOR CONTRIBUTIONS

MD contributed to the conception and design of the study. JW, YD, QZ, SN, JS, and CS performed animal experiments, collected samples and accomplished the laboratory investigations. YD, JW, and SN performed the acquisition of data. YD, JW, and QZ conducted the data analysis and interpretation of data. WJ drafted the manuscript. MD, YD, and JW revised the manuscript. All authors read and approved the final manuscript.

FUNDING

This study was supported by the National Natural Science Foundation of China (Nos. 31672615 and 31272619).

REFERENCES

Aigner, A. (2006). Gene silencing through RNA interference (RNAi) *in vivo*: strategies based on the direct application of siRNAs. *J. Biotechnol.* 124, 12–25. doi: 10.1016/j.jbiotec.2005.12.003

Alisky, J. M., and Davidson, B. L. (2004). Towards therapy using RNA interference. *Am. J. Pharmacogenom.* 4, 45–51. doi: 10.2165/00129785-200404010-00005

Bian, J. T., Sun, M. Z., and Han, J. S. (1993). Reversal of electroacupuncture tolerance by CCK-8 antiserum: an electrophysiological study on pain-related neurons in nucleus parafascicularis of the rat. *Int. J. Neurosci.* 72:15. doi: 10.3109/00207459308991620

Bumcrot, D., Manoharan, M., Koteliansky, V., and Sah, D. W. (2006). RNAi therapeutics: a potential new class of pharmaceutical drugs. *Nat. Chem. Biol.* 2:711. doi: 10.1038/nchembio839

Chen, X., and Han, J. (1992a). All three types of opioid receptors in the spinal cord are important for 2/15 Hz electroacupuncture analgesia. *Eur. J. Pharmacol.* 211, 203–210. doi: 10.1016/0014-2999(92)90530-H

Chen, X. H., and Han, J. S. (1992b). Analgesia induced by electroacupuncture of different frequencies is mediated by different types of opioid receptors: another cross-tolerance study. *Behav. Brain Res.* 47, 143–149. doi: 10.1016/S0166-4328(05)80120-2

Chen, Y., and Sommer, C. (2009). The role of mitogen-activated protein kinase (MAPK) in morphine tolerance and dependence. *Mol. Neurobiol.* 40, 101–107. doi: 10.1007/s12035-009-8074-z

Chopp, M., and Zheng, G. Z. (2015). Thymosin β4 as a restorative/regenerative therapy for neurological injury and neurodegenerative diseases. *Exp. Opin. Biol. Ther.* 15(Suppl. 1):1–4. doi: 10.1517/14712598.2015.1005596

Cui, L., Ding, Y., Feng, Y., Chen, S., Xu, Y., Li, M., et al. (2017a). MiRNAs are involved in chronic electroacupuncture tolerance in the rat hypothalamus. *Mol. Neurobiol.* 54, 1429–1439. doi: 10.1007/s12035-016-9759-8

Cui, L., Yi, D., Jie, Z., Yan, F., Meng, L., and Ding, M. (2016). Spinal glutamate transporters are involved in the development of electroacupuncture tolerance. *Int. J. Mol. Sci.* 17:357. doi: 10.3390/ijms17030357

Cui, L. Y., Guo, N. N., Li, Y. L., Li, M., and Ding, M. X. (2017b). Analgesic and physiological effect of electroacupuncture combined with epidural lidocaine in goats. *Vet. Anaesthes. Analgesia* 44, 959–967. doi: 10.1016/j.vaa.2016.10.003

Dong, Y. N., Mao, M. H., Wang, X. M., and Han, J. S. (1998). [Changes in the binding characteristics of central kappa-opioid receptor during the development of 100 Hz electroacupuncture (EA) tolerance in rats]. *Sheng LI Xue Bao* 50, 663–670.

Guo, H. F., Tian, J., Wang, X., Fang, Y., Hou, Y., and Han, J. (1996). Brain substrates activated by electroacupuncture (EA) of different frequencies (II): role of Fos/Jun proteins in EA-induced transcription of preproenkephalin and preprodynorphin genes. *Brain Res. Mol. Brain Res.* 43:167. doi: 10.1016/S0169-328X(96)00171-4

Han, J., Jian, T., Huang, B., Liang, X., and Zhang, N. (1979). Acupuncture tolerance in rats: anti-opiate substrates implicated. *Endogen. Exogen. Opiate Agonists Antagon.* 92, 205–208.

Han, J. S. (2003). Acupuncture: neuropeptide release produced by electrical stimulation of different frequencies. *Trends Neurosci.* 26, 17–22. doi: 10.1016/S0166-2236(02)00006-1

Han, J. S., Ding, X., and Fan, S. (1986). Cholecystokinin octapeptide (CCK-8): antagonism to electroacupuncture analgesia and a possible role in electroacupuncture tolerance. *Pain* 27, 101–115. doi: 10.1016/0304-3959(86)90227-7

Han, J. S., Ding, X. Z., and Fan, S. G. (1985). Is cholecystokinin octapeptide (CCK-8) a candidate for endogenous anti-opioid substrates? *Neuropeptides* 5, 399–402. doi: 10.1016/0143-4179(85)90038-1

Han, J. S., Li, S. J., and Tang, J. (1981b). Tolerance to electroacupuncture and its cross tolerance to morphine. *Neuropharmacology* 20, 593–596. doi: 10.1016/0028-3908(81)90213-6

Han, J. S., Xie, G., Zhou, Z., Folkesson, R., and Terenius, L. (1981a). Enkephalin and beta-endorphin as mediators of electro-acupuncture analgesia in rabbits: an antiserum microinjection study. *Adv. Biochem. Psychopharmacol.* 33, 369–377.

Han, J. S., Xie, G. X., Ding, X. Z., and Fan, S. G. (1984). High and low frequency electroacupuncture analgesia are mediated by different opioid peptides. *Pain* 18, S369–S369. doi: 10.1016/0304-3959(84)90676-6

Hu, M., Zhou, F., Liu, J., Ding, Y., Zhong, J., and Ding, M. (2017). Electroacupuncture inhibits the activation of p38MAPK in the central descending facilitatory pathway in rats with inflammatory pain. *Evid. Based Compl. Altern. Med.* 2017, 1–10. doi: 10.1155/2017/7531060

Hu, M. L., Qiu, Z. Y., Kuang, H., and Ding, M. X. (2016). Analgesic neural circuits are activated by electroacupuncture at two sets of acupoints. *Evid. Based Compl. Altern. Med.* 2016:3840202. doi: 10.1155/2016/3840202

Hu, M. L., Zhu, H. M., Zhang, Q. L., Liu, J. J., Ding, Y., Zhong, J. M., et al. (2018). Exploring the mechanisms of electroacupuncture-induced analgesia through RNA sequencing of the periaqueductal gray. *Int. J. Mol. Sci.* 19:E2. doi: 10.3390/ijms19010002

Huang, C., Hu, Z-P., Jiang, S-Z., Li, H-T., Han, J-S., and Wan, Y. (2007). CCKB receptor antagonist L365,260 potentiates the efficacy to and reverses chronic tolerance to electroacupuncture-induced analgesia in mice. *Brain Res. Bull.* 71, 447–451. doi: 10.1016/j.brainresbull.2006.11.008

Huang, C., Long, H., Shi, Y. S., Han, J. S., and Wan, Y. (2003). Nocistatin potentiates electroacupuncture antinociceptive effects and reverses chronic tolerance to electroacupuncture in mice. *Neurosci. Lett.* 350, 93–96. doi: 10.1016/S0304-3940(03)00863-2

Huang, C., Wang, Y., Chang, J-K., and Han, J-S. (2000). Endomorphin and μ-opioid receptors in mouse brain mediate the analgesic effect induced by 2 Hz but not 100 Hz electroacupuncture stimulation. *Neurosci. Lett.* 294, 159–162. doi: 10.1016/S0304-3940(00)01572-X

Jeon, B-J., Yang, Y., Kyung, S. S., Yang, H-M., Cho, D., and Ik, B. S. (2013). Thymosin beta-4 promotes mesenchymal stem cell proliferation via an interleukin-8-dependent mechanism. *Exp. Cell Res.* 319, 2526–2534. doi: 10.1016/j.yexcr.2013.04.014

Karagiannis, T. C., and Elosta, A. (2005). RNA interference and potential therapeutic applications of short interfering RNAs. *Cancer Gene Ther.* 12, 787–795. doi: 10.1038/sj.cgt.7700857

Liu, D., Zhou, Z., Ding, Y., Chen, J., Hu, C., Chen, X., et al. (2009). Physiologic effects of electroacupuncture combined with intramuscular administration of xylazine to provide analgesia in goats. *Am. J. Vet. Res.* 70, 1326–1332. doi: 10.2460/ajvr.70.11.1326

Ni, L., Lv, Z., An, L., and Liu, D. (1987). The changes of opiate receptor binding in the rat brain under electroacupuncture tolerance conditions. *Acupunct. Res.* 12:222.

Paxinos, G., and Watson, C. (1986). *The Rat Brain in Stereotaxic Coordinates*. San Diego, CA: Elsevier Academic Press.

Qiu, Z. Y., Ding, Y., Cui, L. Y., Hu, M. L., and Ding, M. X. (2015). The expression patterns of c-Fos and c-jun induced by different frequencies of electroacupuncture in the brain. *Evid. Based Compl. Alternat. Med.* 2015:343682. doi: 10.1155/2015/343682

Santra, M., Chopp, M., Zhang, Z. G., Lu, M., Santra, S., Nalani, A., et al. (2012). Thymosin beta 4 mediates oligodendrocyte differentiation by upregulating p38 MAPK. *Glia* 60, 1826–1838. doi: 10.1002/glia.22400

Shah, Z., Hu, M. L., Qiu, Z. Y., Zhou, F. Y., Zeng, J., Wan, J., et al. (2016). Physiologic and biochemical effects of electroacupuncture combined with intramuscular administration of dexmedetomidine to provide analgesia in goats. *Am. J. Vet. Res.* 77:252. doi: 10.2460/ajvr.77.3.252

Shen, S., Tian, J., and Han, J. (1995). Electroacupuncture-induced release of cholecystokinin octapeptide mediated by spinal m-and k-opioid receptors. *Chin. Sci. Bull.* 40, 1291–1295.

Sun, W., and Kim, H. (2007). Neurotrophic roles of the beta-thymosins in the development and regeneration of the nervous system. *Ann. N. Y. Acad. Sci.* 1112, 210–218. doi: 10.1196/annals.1415.013

Tang, J., Liang, X., Zhang, W., and Han, J. (1979). The tolerance to elecetroacupuncture and its cross tolerance to morphine on rats [J]. *Beijing Med. J.* 1, 34–37.

Tang, N. M., Dong, H. W., Wang, X. M., Tsui, Z. C., and Han, J. S. (1997). Cholecystokinin antisense RNA increases the analgesic effect induced by electroacupuncture or low dose morphine: conversion of low responder rats into high responders. *Pain* 71, 71–80. doi: 10.1016/S0304-3959(97)03341-1

Tian, J. H., and Han, J. S. (2000). Functional studies using antibodies against orphanin FQ/nociceptin. *Peptides* 21, 1047–1050. doi: 10.1016/S0196-9781(00)00242-4

Tian, J. H., Zhang, W., Fang, Y., Xu, W., Grandy, D. K., and Han, J. S. (1998). Endogenous orphanin FQ: evidence for a role in the modulation of electroacupuncture analgesia and the development of tolerance to analgesia produced by morphine and electroacupuncture. *Br. J. Pharmacol.* 124, 21–26. doi: 10.1038/sj.bjp.0701788

Ulett, G. A., Han, S., and Han, J. S. (1998). Electroacupuncture: mechanisms and clinical application. *Biol. Psychiatry* 44, 129–138. doi: 10.1016/S0006-3223(97)00394-6

Wan, J., Ding, Y., Tahir, A. H., Shah, M. K., Janyaro, H., Li, X., et al. (2017). Electroacupuncture attenuates visceral hypersensitivity by inhibiting JAK2/STAT3 signaling pathway in the descending pain modulation system. *Front. Neurosci.* 11:644. doi: 10.3389/fnins.2017.00644

Wan, J., Qiu, Z., Ding, Y., Nan, S., and Ding, M-X. (2018). The expressing patterns of opioid peptides, anti-opioid peptides and their receptors in the central nerve system are involved in electroacupuncture tolerance. *Front. Neurosci.* 12:902. doi: 10.3389/fnins.2018.00902

Wang, H. C., Wan, Y., Yao, L., and Han, J. S. (2002). Comparison of the therapeutic effects of electroacupuncture with different interval for treatment of chronic neuropathic pain in rats. *Acupuncture Res.* 2, 112–118. doi: 10.3969/j.issn.1000-0607.2002.02.007

Wang, J. Q., Fibuch, E. E., Sakurada, S., and Han, J. S. (2006). "CHAPTER 187 – anti-opioid peptides," in *Handbook of Biologically Active Peptides*, ed A. J. Kastin (Burlington, MA: Academic Press), 1345–1350.

Wang, X-J., Wang, X-H., and Han, J-S. (1990). Cholecystokinin octapeptide antagonized opioid analgesia mediated by μ-and κ-but not δ-receptors in the spinal cord of the rat. *Brain Res.* 523, 5–10. doi: 10.1016/0006-8993(90)91629-U

Xiong, Y., Mahmood, A., Meng, Y., Zhang, Y., Zhang, Z. G., Morris, D. C., et al. (2012a). Neuroprotective and neurorestorative effects of thymosin β4 treatment following experimental traumatic brain injury. *Ann. N. Y. Acad. Sci.* 1270, 51–58. doi: 10.1111/j.1749-6632.2012.06683.x

Xiong, Y., Zhang, Y., Mahmood, A., Meng, Y., Zhang, Z. G., Morris, D. C., et al. (2012b). Neuroprotective and neurorestorative effects of thymosin β4 treatment initiated 6 hours after traumatic brain injury in rats. *J. Neurosurg.* 116, 1081–1092. doi: 10.3171/2012.1.JNS111729

Xum G, Y., Winston, J. H., Chen, J. D. (2009). Electroacupuncture attenuates visceral hyperalgesia and inhibits the enhanced excitability of colon specific sensory neurons in a rat model of irritable bowel syndrome. *Neurogastroenterol. Motility*. 21, 1302–e1125. doi: 10.1111/j.1365-2982.2009.01354.x

Zeng, J., Cui, L. Y., Feng, Y., and Ding, M. X. (2016). Electroacupuncture relieves neuropathic pain via upregulation of glutamate transporters in the spinal cord of rats. *Neurosci. Lett.* 620, 38–42. doi: 10.1016/j.neulet.2016.03.041

Zhao, L., Chen, J., Li, Y., Sun, X., Chang, X., Zheng, H., et al. (2017). The long-term effect of acupuncture for migraine prophylaxis: a randomized clinical trial. *JAMA Inter. Med.* 177, 508–515. doi: 10.1001/jamainternmed.2016.9378

Zhi-Qi, Z. (2008). Neural mechanism underlying acupuncture analgesia. *Progr. Neurobiol.* 85, 355–375. doi: 10.1016/j.pneurobio.2008.05.004

Conflict of Interest Statement: The authors declare that the research was conducted in the absence of any commercial or financial relationships that could be construed as a potential conflict of interest.

frontiers in Neuroscience

ORIGINAL RESEARCH
published: 05 April 2019
doi: 10.3389/fnins.2019.00314

Transcriptome Analysis on Maternal Separation Rats With Depression-Related Manifestations Ameliorated by Electroacupuncture

Yuanjia Zheng[1†], Jiang He[1†], Lili Guo[1], Lin Yao[1,2], Xiaorong Zheng[1], Zhihua Yang[1], Yucen Xia[1], Xiaoli Wu[1], Yang Su[1], Nenggui Xu[1] and Yongjun Chen[1,3]**

[1] South China Research Center for Acupuncture and Moxibustion, Medical College of Acu-Moxi and Rehabilitation, Guangzhou University of Chinese Medicine, Guangzhou, China, [2] School of Pharmaceutical Sciences, Guangzhou University of Chinese Medicine, Guangzhou, China, [3] Center for Brain Science and Brain-Inspired Intelligence, Guangdong-Hong Kong-Macao Greater Bay Area, Guangzhou, China

OPEN ACCESS

Edited by:
Yi-Wen Lin,
China Medical University, Taiwan

Reviewed by:
Sin-Jhong Cheng,
Academia Sinica, Taiwan
Dongwoon Han,
Hanyang University, South Korea

***Correspondence:**
Nenggui Xu
ngxu8018@163.com
Yongjun Chen
chyj417@126.com

[†] *These authors have contributed equally to this work*

Specialty section:
This article was submitted to Perception Science, a section of the journal Frontiers in Neuroscience

Received: *15 November 2018*
Accepted: *19 March 2019*
Published: *05 April 2019*

Citation:
Zheng Y, He J, Guo L, Yao L, Zheng X, Yang Z, Xia Y, Wu X, Su Y, Xu N and Chen Y (2019) Transcriptome Analysis on Maternal Separation Rats With Depression-Related Manifestations Ameliorated by Electroacupuncture. Front. Neurosci. 13:314. doi: 10.3389/fnins.2019.00314

Maternal separation (MS), a stressful event in early life, has been linked to neuropsychiatric disorders later in life, especially depression. In this study we investigated whether treatment with electroacupuncture (EA) could ameliorate depression-related manifestations in adult animals that had adverse early life experiences. We demonstrated depression-like behavior deficiencies in a sucrose preference test and a forced swimming test in a rat model with neonatal MS. Repeated EA treatment at the acupoints Baihui (GV20) and Yintang (GV29) during adulthood was shown to be remarkably attenuated above behavioral deficits. Using unbiased genome-wide RNA sequencing to investigate alterations in the transcriptome of the prefrontal cortex (PFC), we explored the altered gene sets involved in circadian rhythm and neurotransmitter transporter activity in MS rats, and their expression tended to be reversed after EA treatment. In addition, we analyzed the interaction network of differentiated lncRNA– or circRNA–miRNA–mRNA by using the principle of competitive endogenous RNA (ceRNA). These results suggest that EA at GV20 and GV29 ameliorates depression-related manifestations by regulating the expression of multiple genes.

Keywords: electroacupuncture, transcriptome, prefrontal cortex, maternal separation, depression

INTRODUCTION

The mother–child relationship has been reshaped by rapid societal changes. Mother-newborn separation shortly after birth, for example, has become routine following hospital births (Csaszar-Nagy and Bokkon, 2018). In the past 30 years, the phenomenon of rural children living apart from their parents, who work in cities, has become so widespread that as many as 37.7% of children in China are affected (Wang, 2015). A growing body of literature indicates that adverse early life experience is significantly associated with susceptibility to stress-related psychopathologies such as depression (Gibb et al., 2007) and anxiety (Coplan et al., 2014; Ishikawa et al., 2015)

disorders. Similarly, parental loss due to sudden death increases the vulnerability of children to depression (Brent et al., 2009). Although the molecular basis has not been fully elucidated, neonatal maternal separation (MS), an early-life adverse event, can have long-lasting effects on neural development and increases risk of adult psychopathology in human adults (Hanson et al., 2012).

Depression is a common mental disorder worldwide, with over 322 million people being diagnosed with it every year. As the leading cause of disability worldwide (Cai et al., 2015) participants with depression had greatly higher total healthcare costs than those without ($20,046 vs. $11,956; $p < 0.01$) in previous study (Unutzer et al., 2009). The selective serotonin reuptake inhibitors (SSRIs) and serotonin and noradrenaline reuptake inhibitors (SNRIs) that are currently the first-line treatment options for major depressive disorder (MDD) (Dale et al., 2015) usually require 4–6 weeks, and sometimes longer, to be effective (Liu et al., 2015). The side effects of their long-term use include sleep disturbance (Roohi-Azizi et al., 2018) and non-response to other classes of antidepressants (Li Q. et al., 2013). To induce a depression-like phenotype for investigating the antidepressant effects of the drugs, various rodent models were used, such as being exposed to chronic unpredictable mild stress, learned helplessness, chronic social defeat stress and so on (Cao et al., 2013; Alboni et al., 2017; Post and Warden, 2018). Adverse experience in early life is associated with stress-related psychopathologies, and previous studies have shown neonatal rats or mice exposed to MS were displayed depression-like behavior in adulthood (Vetulani, 2013; Sadeghi et al., 2016; Tchenio et al., 2017).

Acupuncture as a well-known useful treatment for depression has been proven. For example, acupuncture (electro- and manual) may moderately reduce the severity of depression by the end of treatment (SMD −0.66, 95% CI −1.06 to −0.25, five trials) in total 488 participants (Smith et al., 2010). According to a report from the Department of Veterans' Affairs from Washington, DC, United States, depression is one of the nine clinical indications relevant to mental health for acupuncture (Hempel et al., 2014). However, the molecular mechanisms through which electroacupuncture (EA) modulates depressive behaviors are largely uncharacterized. Rat is an organism that provides a model with clinically relevant phenotypes for exploring new therapeutics (Jacob and Kwitek, 2002) and for studying the mechanism of acupuncture (Kou et al., 2017; Zhang Z.Y. et al., 2018). Furthermore, as acupuncture or EA can ameliorate depressive-like behaviors, a rat model of depression is a tool that has been widely used to investigate the antidepressant effects of acupuncture (Lu et al., 2016, 2017; Jiang et al., 2017). "Baihui" (GV 20) – "Yintang" (GV 29) are considered to be the optimized acupoint modules for mental illness (Duan et al., 2009a, 2014; Jiang et al., 2017), and our previous study indicates that EA at GV 20–GV 29 acupoints ameliorates cognitive deficits and improves hippocampal synaptic plasticity in adult rats with neonatal MS (Guo et al., 2018).

To investigate whether acupuncture can alleviate psychopathology in adults with stress-related adverse early life experiences, as well as to detail the mechanism by which acupuncture might regulate gene expression, we generated rat neonatal MS models and applied EA treatment at the GV20 and GV29 acupoints. Additionally, to explore experimentally the mechanisms involved with MS-induced depression, unbiased RNA sequencing (RNA-Seq) was used to identify rat genome-wide alterations in the prefrontal cortex (PFC) after MS and EA treatments. Furthermore, analysis of the interaction network of differentiated long non-coding RNA (lncRNA)- or circular RNA (circRNA)-miRNA-mRNA was performed using the principle of competitive endogenous RNA (ceRNA). Our study is the first to provide new information on the mechanism underlying anti-depressive effects of EA in adult rats with neonatal MS experience.

MATERIALS AND METHODS

Experimental Animals

Male and nulliparous female Wistar rats of 180∼220 g were obtained from the Guangdong Medical Laboratory Animal Center. Animals were housed in the standard cages in controlled temperatures (20–22°C) and a 12-h light–dark cycle room. Food and water were available *ad libitum*. Animals entered the study at 8 weeks of age following a week-long acclimatization period and were mated at a 2:1 ratio of male to female rats. The female rats were raised alone once found to be pregnant. Wistar dams were assigned partly to control groups, with most to the molding groups. For each litter, the day of birth was named as postnatal day 0 (PND0) and the day after PND0 was the first day of molding, which was set as PND1. The experimental procedure was approved by the Animals Care and Use Committee of Guangzhou University of Traditional Chinese Medicine.

Maternal Separation Model

From PND1 to PND21, MS that kept the mothers from their filial generation of molding groups into another cage for 4 h (9:00–13:00) was conducted every day. The mothers and litters in control groups were under no disturbance until weaning. All pups were weaned at PND21 and the males were housed four or five per cage until adult age, and the females were eliminated. The experimental procedure was approved by the Animals Care and Use Committee of Guangzhou University of Traditional Chinese Medicine. All efforts were made to minimize the animals' suffering and to reduce the number of animals used for experiments.

Animal Groups

Vehi, MS+Vehi, and MS+Flu

To determine whether the MS model induced depression in adulthood, at PND60, the litters belonging to healthy reservation groups were assigned to Vehicle group (Vehi), and the molding rats were assigned randomly into two groups: vehicle group (MS+Vehi) and Fluoxetine group (MS+Flu).

Cont, MS, EA, and Sham-EA

To examine whether the EA stimulation had effect on MS rats, in another trial, at the PND60, the litters belonging to

healthy reservation groups were assigned to control group (Cont), and the molding rats were assigned randomly into three groups: maternal separation group (MS), MS with electro-acupuncture treatment group (EA) and MS with sham EA treatment group (Sham-EA).

Treatment

All the treatments were performed from PND61 to PND81 every other day.

EA Stimulation

Using isoflurane (RWD, Shenzhen, China), the EA rats were positioned in the induction case with an anesthetized concentration of 5% for the initial 5 min for deep anesthetized condition, and then they were moved to the EA operating platform with a 2% concentration for the middle 10 min, decreasing to 1.5% for the last 5 min. Disposable acupuncture needles as previous reported (Guo et al., 2018) were inserted to the acupoints of GV20 and GV29. The Master-8 Stimulator (Master-8, AMPI, Israel) was connected to deliver electrical current to the needles. We set the output parameters as follows: holding the frequency constant at 2 Hz and intensities at 2 mA, for 15 min. EA stimulation was administered every other day for 15 min starting at 8:30 a.m. Rats in the Sham-EA group were anesthetized with isoflurane as the EA group. The difference was rats in the Sham-EA group received no electrical stimulation; a disposable acupuncture needle was attached to the surface near GV20 and GV29 but apart from any other known acupoints. The Cont rats and MS rats only received anesthetization conduction.

Fluoxetine Administration

The MS+Flu group were given injections of fluoxetine (10 mg kg^{-1}, i.p.) while rats in the Vehi group and the MS+Vehi group received injections of an equal volume of saline (i.p.) from PND61 to PND81.

Behavioral Tests

Body Weight Measurement

The body weights of rats in each group were measured every week during this period at 9 a.m. by balances (MS3002ts/00, Mettler Toledo).

Sucrose Preference Test (SPT)

In training days, each rat was exposure to two bottles of 1% sucrose solution for 24 h in the first day, and two bottles of tap water in the second day. In the third day, the bottles and food were withdrawn to make the rats hungry and thirsty. On the test day, bottle A contained 1% sucrose solution, and bottle B contained water. The fluid that was consumed from each bottle was measured after 24 h. The sucrose preference of each rat was calculated as $100 \times [VolA/(VolA + VolB)]$, and the total fluid intake was calculated as VolA + VolB.

Forced Swimming Test (FST)

The FST was performed in a clear glass cylinder (height 45 cm, diameter 20 cm), which was filled to 30 cm with water (22–25°C). The test lasted for 5 min. The duration of immobility was recorded by JLBehv-FSR-4 (Shanghai Jiliang Software Technology Co., Ltd.).

Elevated-Plus-Maze Test (EPMT)

The elevated-plus-maze test consisted of two opposing open arms (50 cm × 15 cm) and two opposing enclosed arms (30 cm × 50 cm × 15 cm) that were connected by a central platform (15 cm × 15 cm), forming the shape of a plus sign. All of the measurements were taken in a dimly lit experimental room, in which the rats where acclimatized for at least 30 min before testing. The times that were spent in the open arms and the enclosed arms were recorded over a 10 min test period. The maze was cleaned with a solution of 20% ethanol in water between the sessions.

Open Field Test (OFT)

The open field presented an open box structure (80 cm × 80 cm × 40 cm) with a black square at the bottom. A camera device was installed directly above the central area of the open field. Before the experiment, the rats were conditioned for 60 min in advance in the test room. Uniform light and a quiet environment throughout the test were ensured. The rats were gently lowered into the central part of the square and allowed to move freely in the open field for 10 min. Its total distance and the time in the central area were recorded. The area was cleaned with 20% alcohol between the sessions. Only after the alcohol smell dissipated and the bottom of the box was without obvious signs of moisture were the rats tested.

Light-Dark Box Test

The test was carried out in a soundproof box with a light box (25 cm × 25 cm × 40 cm) and a dark box (25 cm × 25 cm × 40 cm). The dividing wall was inserted with an opening hole (8 cm × 7.5 cm) to allow the animal's free movement from one compartment to another. The illumination was above the light box. The animal was released into the center of the light compartment (facing away from the opening) and was allowed to explore the area for 10 min. Distance traveled and time spent in different compartments were recorded by JLBehv-FSR-4 (Shanghai Jiliang Software Technology Co., Ltd.). The box was cleaned with a solution of 20% ethanol in water between the sessions.

Radioimmunoassay

The reagent kits of corticosteroid (CORT) and adrenocorticotropic hormone (ACTH) for measurement of amounts were purchased from IZOTOP Institute of Isotopes Ltd. and Beijing North Biotechnology Research Institute, respectively. All determination procedures were according to the manufacturers' instructions.

Tissue Extraction and RNA Sequencing

Three samples per group (Cont, MS, and EA group) were sent for RNA sequencing. Rats were anesthetized with isoflurane (RWD, Shenzhen, China). The induced anesthesia concentration was 5% to perform tissue extraction. PFC was removed quickly and then put in liquid nitrogen for quick freezing.

Then the PFC was stored at −80°C until tissue processing. Total RNA was extracted by Trizol reagent (Invitrogen) from tissue. RNA samples were prepared by using rRNA Depletion Kit (NEBNext®). The DNA libraries were applied to cluster generation and sequencing using cBot Operation for HD V2.5 Reagent and HiSeq X Operation for HD v2.5 reagent_v1.3 (Illumina). Sequencing was performed using Hiseq X ten (Illumina, United States). The raw data were deposited onto NCBI's Read Gene Expression Omnibus (GEO) database and the accession number is GSE124387. RPKM (Reads Per kb per Million reads) was used to calculate gene expression from RNA-Seq data, which can eliminate the influence of gene length and sequencing amount for calculating gene expression. If multiple transcripts exist in a gene, we select the longest one to calculate sequencing depth and expression.

Data Analysis

Statistical Analyses

All of the results are expressed as the means ± SEM. The statistical analyses were performed using SPSS 17.0 software. Potential differences between the mean values were evaluated using two-way or one-way analysis of variance (ANOVA) followed by the least significant difference (LSD) test for *post hoc* comparisons when equal variances were assumed. Non-parametric Kruskal–Wallis test was used to compare differences through groups when there was heterogeneity of variance. The significance level for all of the tests was set at $p < 0.05$.

Computational Analysis for RNA-Seq Data

Reads were filtered for quality by Fast-QC program and mapped to the rat genome (NCBI assembly Rnor_6.0) by the Hisat2 program. EB-Seq algorithm (Leng et al., 2013) was applied to filter the differentially expressed genes after the significant analysis and false discovery rate (FDR) analysis under the following criteria: fold change >1.5 or <0.667; FDR <0.05. According to the NCBI Gene Ontology database, GO analysis was performed by using Fisher's exact test. It classifies the GO terms, and the FDR was calculated to correct the *p*-value. We utilized Miranda (Picao-Osorio et al., 2015) and RNAhybrid (Rehmsmeier et al., 2004) as the tools for predicting differentially expressed miRNA targets on circRNA, lncRNA, and mRNA.

For Series Cluster analysis, the raw expression values were converted into log2 ratio. Using a strategy for clustering short time-series gene expression data, we defined some unique profiles. Significant profiles have higher probability than expected by Fisher's exact test and multiple comparison test (Ramoni et al., 2002). The following expression tendencies are what we had interest in: the genes decreased in MS rats compared to control rats but increase in EA rats contrasted with MS rats (decrease-increase type); the genes increased in MS rats compared to control rats but decreased in EA rats in contrast to MS rats (increase-decrease type). Based on that, the expression of mRNA and circRNA as well as mRNA and lncRNA satisfying this relationship are positively correlated; series cluster analysis is performed to identify a set of unique expression tendencies.

RESULTS

Neonatal MS Induced Depression-Like Behavioral Deficits in Adults

To confirm whether neonatal MS affects the onset of affective disorders in adults, we replicated the MS model to monitor depression- and anxiety-related behaviors in Wistar rats (**Figure 1A**). Before the beginning of the behavior test, body weight was measured every week. We found that the weight of rats with MS (MS+Vehi) increased slightly in adulthood compared with control (Vehi) and MS rats with Fluoxetine treatment (MS+Flu) (**Figure 1B**). In tests for depression-like behaviors, we applied SPT and FST, two well-known tests for detecting anhedonia and despair symptoms of depression disorder (Tye et al., 2013; Liu et al., 2018; Ji et al., 2019). Rats in the MS+Vehi group showed a significantly reduced sucrose consumption rate in SPT and increased duration of immobility in FST compared to Vehi. The administration of Fluoxetine restored sucrose consumption and immobility behavior deficits in both instances (**Figures 1C,D**). We next performed the EPM task, a well-established test of anxiety-like behavior (Walf and Frye, 2007). We found that rats from the three groups spent similar amounts of time in open arms (**Figure 1E**). To further detect whether MS rats have anxiety-like behaviors, the OFT and light/dark box test were performed (Bourin and Hascoet, 2003). There was no difference between the control and MS rats on the total distance, time in center in OFT, and time in light in light/dark box test (**Supplementary Figure S1**). Together, these results suggested that the MS model rat in the current study was successfully replicated for depression, but not anxiety.

EA Induced Antidepressant-Like Effects

To assess the effect of EA treatment on depression-like behavioral deficits in adult rats that suffered from MS, rats were tested for sucrose consumption in SPT and the total duration of immobility in FST (**Figure 2A**). Rats in the MS and the Sham-EA groups exhibited a decreased rate of sucrose consumption compared to controls (**Figure 2B**). However, the level of sucrose consumption in the MS+EA group was similar to the control group ($p > 0.05$), suggesting the anhedonia was attenuated after the EA treatment. Similarly, rats in the MS and Sham-EA groups showed increased immobility time compared to controls in FST. However, EA treatment dramatically decreased the total duration of immobility in rats with neonatal MS (**Figure 2C**). These results suggested that MS-induced depression-like behavior deficits were ameliorated after EA treatment.

To further demonstrate that EA could attenuate depression-like impairment in rats with neonatal MS, we measured the plasma ACTH and CORT levels, which is a biological indicator of depression and in part explains the relationship between hypothalamic-pituitary-adrenal (HPA) axis regulation and MS-induced depression (Mirescu et al., 2004; van der Doelen et al., 2014; Gururajan et al., 2016; Salvat-Pujol et al., 2017). Rats in the MS and Sham-EA groups showed dramatically increased plasma ACTH and CORT levels, which were significantly decreased by EA treatment (**Figures 2D,E**). These results indicated that

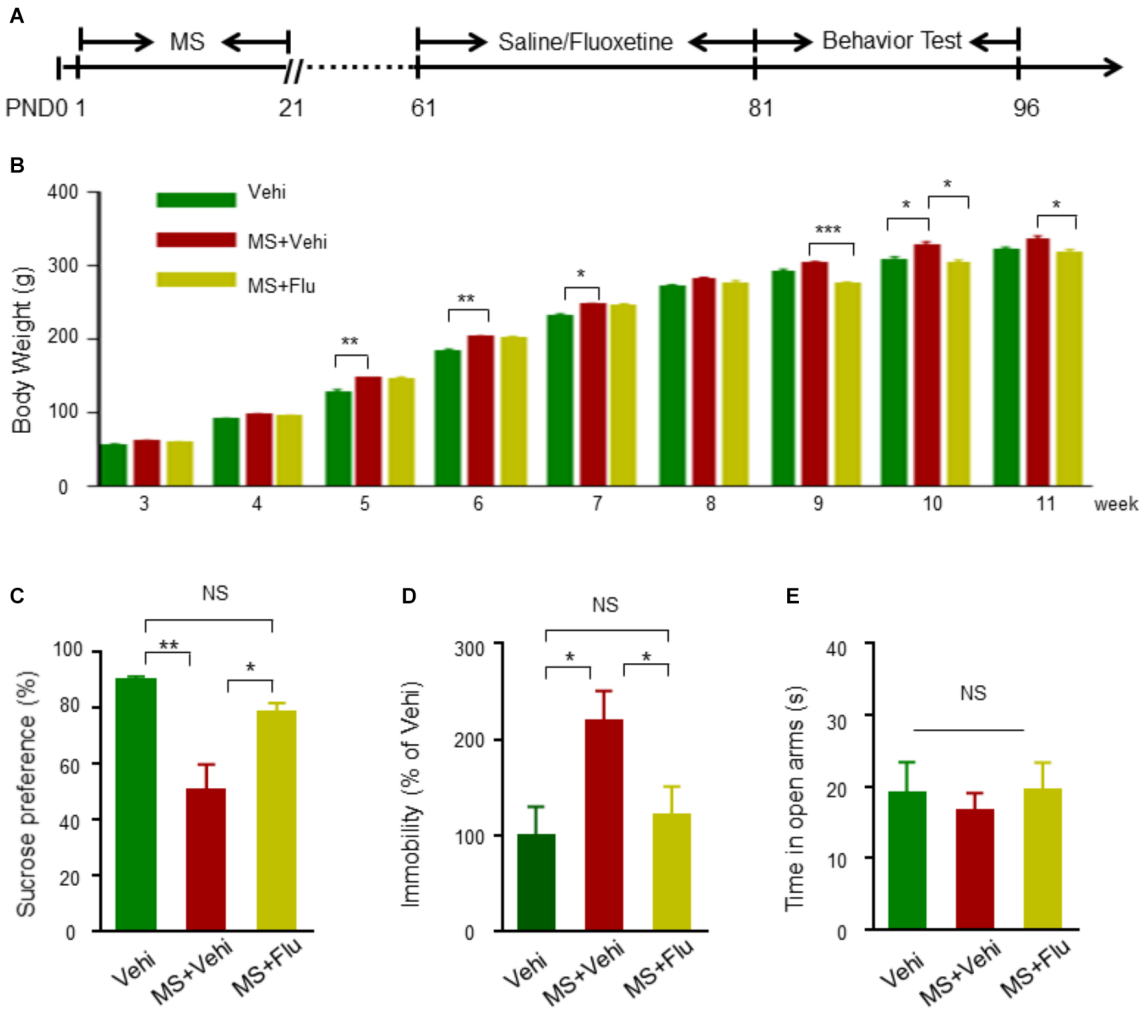

FIGURE 1 | Neonatal MS induced depression-like behavioral deficits in adult Wistar rats. **(A)** The experimental schedule of MS, Fluoxetine administration, and behavioral test. Fluoxetine 10 mg kg^{-1} i.p. administration when rats were 8 weeks old before behavioral assessment at 11 weeks old. **(B)** Animals in all subgroups were weighted on the 3rd, 4th, 5th, 6th, 7th, 8th, 9th, 10th, and 11th postnatal weeks (n = 11 rats per group). **(C)** Reduced sucrose preference rate by rats with MS in SPT test compared to Vehi group rats, and the reduction was diminished after Fluoxetine administration (n = 11 rats per group, $F_{(2,30)}$ = 30.82, one way-ANOVA). **(D)** Elevated immobility time in rats with MS+Vehi compared to Vehi rats and the elevation was ameliorated by Fluoxetine administration (n = 11 rats per group, $F_{(2,30)}$ = 0.037, one way-ANOVA). **(E)** There was no difference on time in open arms in EMP test (n = 10–11 rats per group, $F_{(2,28)}$ = 1.086, one way-ANOVA). Data are expressed as the means ± SEM. $^{*}p < 0.05$, $^{**}p < 0.01$, $^{***}p < 0.001$. NS, not significant.

repeated EA intervention induced antidepressant-like effects in rats with neonatal MS.

RNA-Seq of PFC Transcriptome

We further investigated the possible mechanisms after confirming the anti-depressive effects of EA on rats with neonatal MS. RNA was extracted from the PFC, a brain area which is highly associated with the onset of depression (Kumar et al., 2015; Seo et al., 2017), in control, MS and EA therapy rats. After depletion of rRNA, unbiased deep sequencing was performed to an average depth of ∼89 million reads per sample in the three groups. Approximately 68 million reads mapped to unique locations on the NCBI assembly Rnor_6.0 reference genome (**Supplementary Table S1**).

Identification of Differentially Expressed Genes Under EA Treatment in PFC of Rats With Neonatal MS

To determine the regulation of mRNA expression, we performed an unsupervised clustering analysis of the significantly regulated genes in the PFC (**Figure 3A**). The EBseq algorithm was applied to filter the differentially expressed genes after the significant and FDR analyses (fold change >1.5 or <0.667; FDR <0.05). Forty-eight genes were significantly and differentially expressed in MS rats relative to control rats, with 39 upregulated genes and 9 downregulated genes. Thirty-nine genes in the EA rats relative to the MS rats show differential expression, with 21 genes upregulated and 18 genes downregulated (**Supplementary Table S2**). Venn analysis was additionally applied to learn

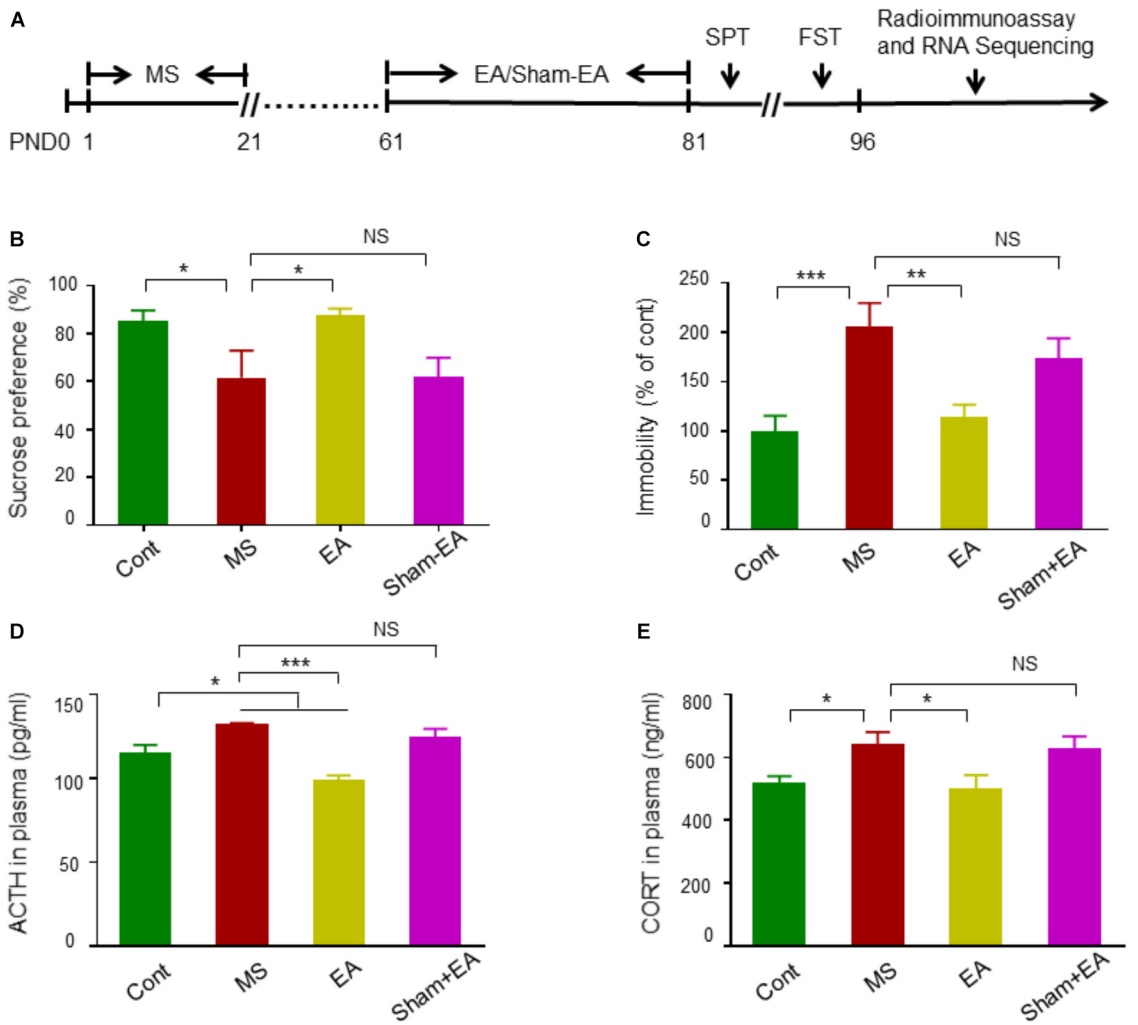

FIGURE 2 | Electroacupuncture (EA) ameliorated depression-like behavioral deficits in rats exposed to neonatal MS. **(A)** The experimental schedule of MS, EA, or Sham-EA treatment, behavior tests and radioimmunoassay. **(B,C)** EA at GV20 and GV29 on rats with neonatal MS significantly elevated sucrose preference rate and reduced immobile rate in rats with neonatal MS (n = 10–13 rats per group, $F_{(3,44)}$ = 7.949, non-parametric Kruskal–Wallis; $F_{(3,44)}$ = 1.109, one way-ANOVA). **(D,E)** Radioimmunoassay of ACTH and CORT levels in plasma (n = 8–10 rats per groups, $F_{(3,32)}$ = 2.884, one way-ANOVA; $F_{(3,36)}$ = 0.793, one way-ANOVA). Data are expressed as the means ± SEM. $^{*}p < 0.05$, $^{**}p < 0.01$, $^{***}p < 0.001$. NS, not significant.

the possible marker that participates in the exertion of acupuncture's antidepressant effect. We found three of them (*Ucp3*, *Cplx3*, *Dbp*) can be reversed by EA treatment in the nine downregulated genes following MS. Similarly, EA treatment reversed 2 (*LOC102555167*, *Syt6*) of the 39 upregulated genes following MS (**Figures 3B,C**).

To show the possible cellular functions linked to differentially expressed genes, we used Gene Ontology (GO) enrichment analysis for the differentially expressed genes across three domains, including molecular functions (MF), cellular components (CC), and biological processes (BP) (**Table 1**). The genes that differentially decreased in the MS group but tended to be reversed after EA treatment were involved in synaptic vesicle exocytosis, circadian rhythm, syntaxin binding and synapse, and so on. Upregulated gene sets in the MS rats and reversed in the EA group were involved in mitochondrial transport, oxidative phosphorylation uncoupler activity, etc.

Long non-coding RNA is a type of RNA molecule that is more than 200 bp in length and has no protein coding ability. Using the same method as above, we found 11 genes increased significantly in the MS rats relative and 4 genes decreased relative to controls. Thirty-one genes increased in the EA rats relative to the MS rats while one gene decreased. Venn analysis shows that 1 gene co-occurred in two comparison groups: Rps2-ps2 (**Figure 4** and **Supplementary Table S2**).

Circular RNA is a new class of RNA that differs from traditional linear RNA. It has a closed loop structure and is abundantly present in the eukaryotic transcriptome. CircRNAs were predicted by finding reads that cover both exons, but the direction is opposite to linear RNA. Twenty genes increased

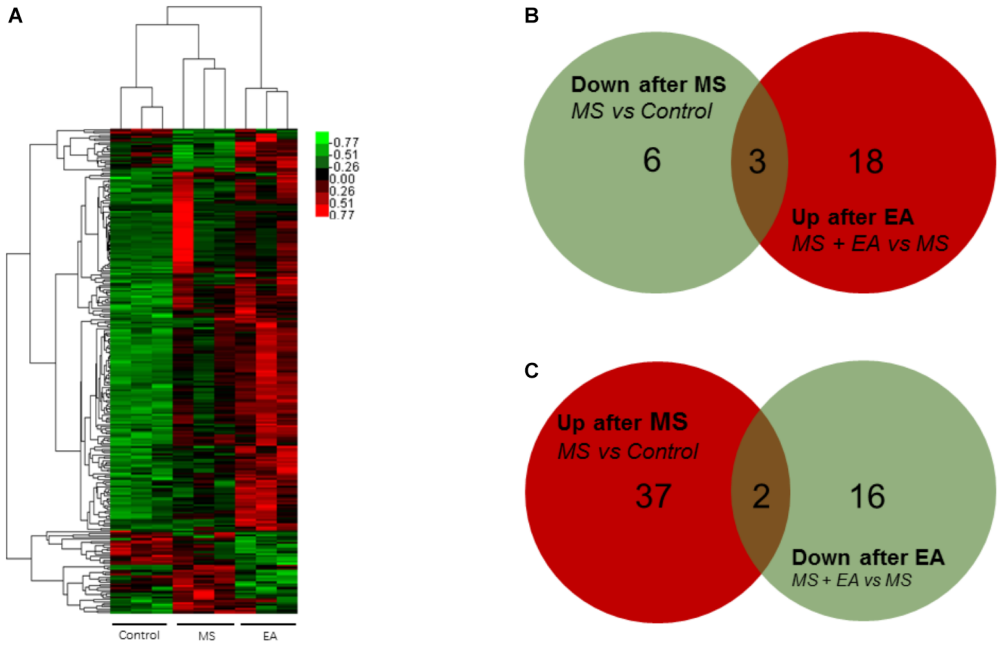

FIGURE 3 | Differential mRNA expression in the prefrontal cortex of Cont, MS, and MS+EA in adult rats. **(A)** Heatmap of differentially expressed genes between Cont, MS, and MS+EA samples ($p < 0.05$) with green and red spectrum colors indicating downregulated and upregulated expression, respectively. **(B,C)** Venn diagrams show overlaps of differentially expressed genes between experimental groups. Three genes decreased in MS group but increased in EA group. Two genes increased expression in MS group but decreased in EA group.

TABLE 1 | The significant GO terms downregulated in MS but upregulated in EA or upregulated in MS but downregulated in EA ($p < 0.05$).

Domain	GO terms	
	Down-regulated in MS and Up-regulated in EA	**Up-regulated in MS and Down-regulated in EA**
BP:	Synaptic vesicle exocytosis	Response to superoxide
	Acrosomal vesicle exocytosis	Response to steroid hormone
	Regulation of neurotransmitter secretion	Mitochondrial transport
	Acrosome reaction	Response to glucocorticoid
	Insulin secretion	Cellular response to hormone stimulus
	Neurotransmitter transport	Response to activity
	Circadian rhythm	
	Rhythmic process	
MF:	Syntaxin binding	Hydrogen ion transmembrane transporter activity
	Calcium-dependent protein binding	Oxidative phosphorylation uncoupler activity
	Calcium-dependent phospholipid binding	
	Clathrin binding	
	SNARE binding	
	Neurotransmitter transporter activity	
	RNA polymerase II regulatory region sequence-specific DNA binding	
CC:	Nucleus	Mitochondrial membrane
	Synapse	
	Extrinsic component of membrane	
	Synaptic vesicle membrane	
	Perinuclear endoplasmic reticulum	

significantly in the MS rats relative to control rats and 17 genes decreased. Eighteen genes increased in the EA rats relative to the MS rats while 28 genes decreased. Venn Analysis shows that expression of two genes increased in the MS group but decreased in the EA group, while one gene decreased in the MS group but increased in the EA group. According to the position of the gene

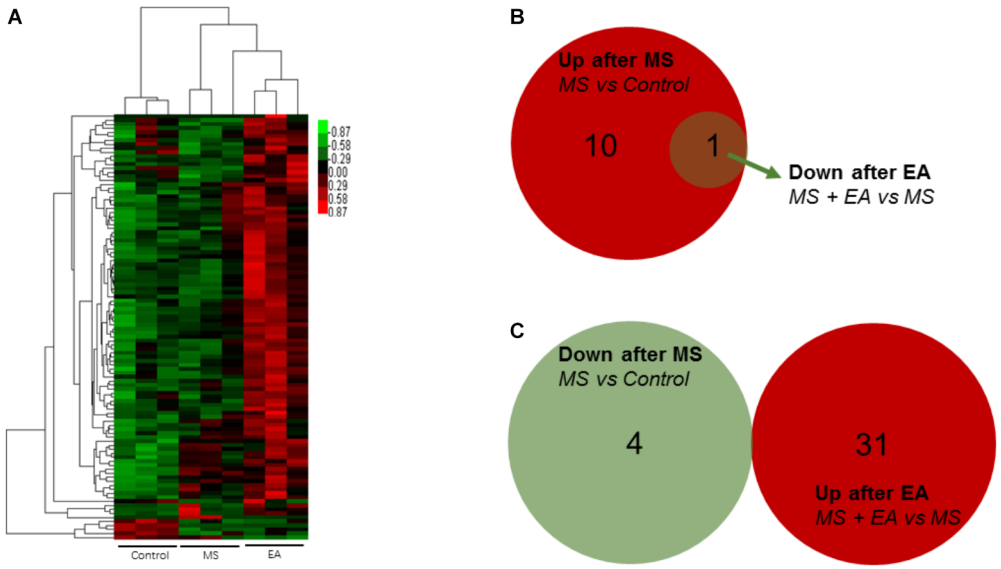

FIGURE 4 | Differential lncRNA expression in the prefrontal cortex of Cont, MS, and MS+EA in adult rats. **(A)** Heatmap of differentially expressed lncRNAs between Cont, MS, and MS+EA samples ($p < 0.05$) with green and red spectrum colors indicating downregulated and upregulated expression, respectively. **(B,C)** Venn diagrams show overlaps of differentially expressed lncRNAs between experimental groups. One gene increased expression in MS group but decreased in EA group. No genes decreased expression in MS group but increased in EA group.

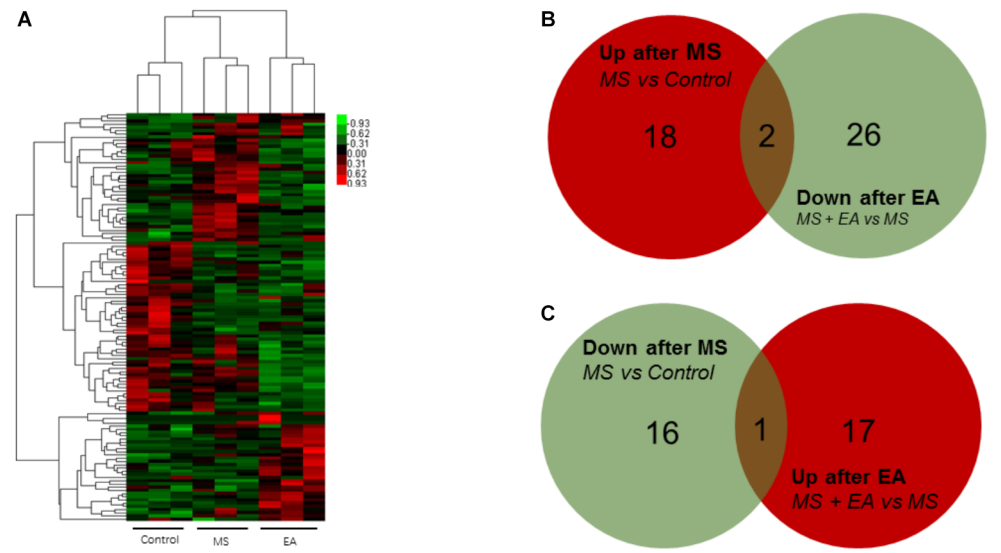

FIGURE 5 | Differential circRNA expression in the prefrontal cortex of Cont, MS, and MS+EA in adult rats. **(A)** Heatmap of differentially expressed circRNAs between Cont, MS, and MS+EA samples ($p < 0.05$) with green and red spectrum colors indicating downregulated and upregulated expression, respectively. **(B,C)** Venn diagrams show overlaps of differentially expressed circRNAs between experimental groups. Two genes increased expression in MS group but decreased in EA group. One gene decreased expression in MS group but increased in EA group.

loop, these three genes were derived from *LOC102555866*, *Npepo*, *Cdh12* (**Figure 5** and **Supplementary Table S2**).

MicroRNA (miRNAs) is a short-chain RNA about 22 nt in length that can reverse the expression of the target gene by inhibiting its translation or degrading it. Competitively binding miRNAs to regulate the expression of target genes is called competitive endogenous RNA (ceRNA). To explore the relationship between mRNA expression and its regulation, co-expression analysis of lncRNA/circRNA, miRNA and mRNA was carried out using the principle of ceRNA. First, the Miranda and the RNAhybrid algorithms were used to predict the target miRNAs for the circRNA, lncRNA, and mRNA, respectively. The combination of the two algorithms was used as the final result (**Supplementary Table S3**). Then,

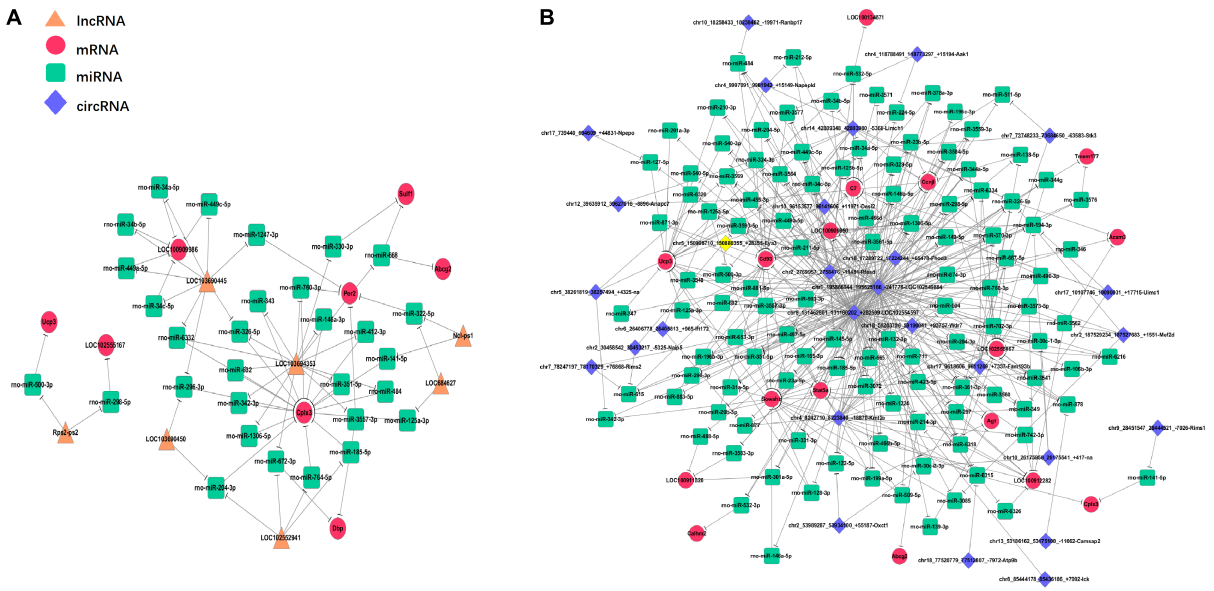

FIGURE 6 | Interaction network of differentiated lncRNA–miRNA–mRNA and circRNA–miRNA–mRNA in the prefrontal cortex of Cont, MS, and MS+EA in adult rats. Diamond, round rectangle, ellipse, and triangle represent circRNA, miRNA, mRNA, and lncRNA, respectively. The genes shown in this figure are the same that belong to the increase-decrease type/decrease-increase type. **(A)** In the lncRNA–miRNA–mRNA predicted interaction network, 30 miRNAs are predicted to be possible target genes for regulating them. **(B)** In the circRNA–miRNA–mRNA predicted interaction network, 116 miRNAs are predicted.

the genes with the same expression trend (both belong to decrease/increase – increase/decrease type) of lncRNA/circRNA and mRNA were extracted, and the lncRNA/circRNA, miRNA, and mRNA were combined to form an interaction network after Series Cluster analysis (**Supplementary Table S3**). In the lncRNA-miRNA-mRNA predicted interaction network, seven lncRNAs and eight mRNAs had the same expression trend (belonging to the increase-decrease type/decrease-increase type). Thirty miRNAs were predicted to be possible target genes for regulation (**Figure 6A**). In the circRNA-miRNA-mRNA predicted interaction network, 28 circRNAs and 17 mRNAs had the same trend. One hundred sixteen miRNAs were predicted to be potential target genes to regulate these circRNA and mRNA changes (**Figure 6B**).

DISCUSSION

Maternal separation rats exhibited a significantly lower preference for sucrose and higher immobility time (**Figures 1C,D**), but these behaviors were reversed in the fluoxetine injection group, suggesting MS is a stable and reliable means to model depression-like behaviors. These results are consistent with previous studies that showed chronic stress in early life could induce depressive-like behaviors in adults rats or mice (Arborelius et al., 2004; Vetulani, 2013; Masrour et al., 2018; Ruiz et al., 2018). However, some animal studies have shown that neonatal MS induced anxiety-like behaviors (Banqueri et al., 2017; Auth et al., 2018). Contrastingly, our result in the EPM task, OFT and Light-dark box test showed that rats with neonatal MS spent similar amounts of time in the open arms, center area, and light box, respectively, compared to controls (**Figure 1E** and **Supplementary Figure S1**). This difference may be due to a variation of species of animals (rats vs. mice), the MS protocol (longer vs. shorter duration of separation), and the different postnatal periods (PDN1-21 vs. PDN2-15) of MS (Auth et al., 2018). Meanwhile, the difference of housing conditions during the separation period (staying in home cage under 20–22°C vs. being kept in a new cage under 30°C) may also contribute to the variation of behavior phenotypes in adult MS (Banqueri et al., 2017). In addition, we found that the weight of rats with MS increased slightly in adulthood compared to control mice, which is consistent with previous studies (Macri et al., 2008; Yoo et al., 2013; Gonzalez-Pardo et al., 2019). However, other studies show normal body weight or reduced weight of MS rats in adulthood (Ryu et al., 2009; Paternain et al., 2016). Therefore, the relationship between body weight, located environment and MS-induced behavior deficits of animals still needs to be further studied.

Acupuncture (electro- and manual) is a treatment generally recommended for mental illnesses, including depression (Smith et al., 2010; Hempel et al., 2014). Recently, EA at the GV20 and GV29 acupoints has been reported to alleviate depression-related symptoms in model rats induced by chronic unpredictable mild stress (Duan et al., 2009b). Our results are in line with this finding, showing that EA significantly enhanced the sucrose uptake rate in the SPT and decreased the immobility duration in the FST, enabling the most characteristic presentations of depression to be reversed (Han et al., 2015). In addition, early-life stress influenced mature adults with sustained hyper-activation of the HPA axis (Maniam et al., 2014). Consistent with this conclusion, we found rats with MS induced a higher level of ACTH and

CORT in their plasma compared to healthy rats (**Figures 2D,E**), which may in part reveal the potential relationship between early life adverse stress and depression in adulthood (Choi et al., 2018; Frost et al., 2018). Notably, the EA treatment can reverse the increased concentration of ACTH and CORT in rats with MS (**Figures 2D,E**), which is compatible with other studies showing that EA regulates the function of the HPA axis to treat depression (Tanahashi et al., 2016). Together, these results further confirmed that EA is an effective therapy for depression induced by neonatal MS.

Little is known of the mechanism of depression caused by MS, and the mechanism of anti-depression after EA. To the best of our knowledge, this was the first study to show EA has anti-depressive effects in a depression rat model induced by early MS. We detected the PFC genome-wide transcriptome of male rats suffering from MS to reveal the antidepressant effects of EA at the molecular level. Previous studies found EA can alter gene expression in a chronic unpredictable mild stress-induced rat model for mRNA or miRNA by using microarray or RNA-sequencing (Duan et al., 2014, 2016). However, instead of constructing the cDNA libraries by extracting poly-A (Wang et al., 2017), we constructed them after rRNA depletion to obtain data at a larger scale. Sequencing depth involves mRNA (**Figure 3**), lncRNA (**Figure 4**), and circRNA (**Figure 5**), which allowed us to detect differences in gene expression at the transcriptome level and predict the regulatory mechanisms that may mediate changes to their expression by ceRNA (**Figure 6**). These results suggest more comprehensive perspectives to explore the antidepressant mechanisms of acupuncture.

By GO enrichment analysis, we found altered gene sets are involved in circadian rhythm (**Table 1**), which is in accordance with other studies. From the dataset of transcripts from postmortem brains, it has been observed that >100 transcripts exhibited rhythmicity across six brain regions, including the dorsolateral PFC, while rhythmicity was much weaker in these brain areas of patients with MDD compared to those with no history of psychiatric disorders. Correspondingly, the canonical clock genes, including *Arntl*, *Per2-3*, and *Dbp* found in subject transcripts were observed in our analysis (Li J.Z. et al., 2013; Bunney et al., 2015). Furthermore, the clock genes (*Arntl*, *Per2-3*) of animals suffering from chronic mild stress (CMS) were strongly expressed in the PFC, but did not follow a circadian rhythm. The other study also found a reduction of the BMAL1 protein (*Arntl*) in the PFC of CMS rats (Calabrese et al., 2016; Christiansen et al., 2016). Consistent with our conclusions, one previous study reported EA can ameliorate the bowel dysfunction in spinal cord injury rats, and increase *Per2* expression (Cheng et al., 2016). Another reported that EA has regulatory effects on the circadian rhythm of temperature in CMS rats (Yao et al., 2014).

Additionally, we found the altered genes enrich in the neurotransmitter transporter activity, syntaxin binding, synaptic vesicle membrane. The genes corresponding to the GO terms are *Cplx3* and *Syt6*. *Cplx3* (complexin 3) is a subunit of the presynaptic protein that affects synaptic transmission. Previous studies indicated that *Cplx3* can affect the neurotransmitter release process by modulating exocytosis (Vaithianathan et al., 2015; Mortensen et al., 2016). Also, activity-dependent BDNF release via endocytic pathways can be regulated by syt6 and complexin (Wong et al., 2015), which is closely linked to depression (Gururajan et al., 2016). Thus, the above altered expression of the syntaxin binding may provide a means to investigate EA anti-depression effects.

Some previous studies suggested lncRNAs with mouse depression models may relate to depression pathologies (Bond et al., 2009; Huang et al., 2017). Furthermore, a study on peripheral blood profiling also found the expression of certain lncRNAs was changed in patients with MDD (Liu et al., 2014). In CMS mice, total saponins from the leaves of Panax notoginseng inhibited depression by regulating circRNA expression (Zhang H. et al., 2018). In the peripheral blood mononuclear cells of MDD patients, hsa_circRNA_103636 was significantly altered, suggesting that circRNA may be a potential novel biomarker (Cui et al., 2016). This suggests that lncRNA and circRNA play a non-negligible role in the mechanisms of pathological depression.

There are many examples of using transcriptome data analysis to investigate the mechanism of acupuncture without co-expression analysis, which could lead to the limitation of unclear and false positives targets (Fu et al., 2014; Hansen et al., 2014; Wang et al., 2015). Using ceRNA, we narrowed the targets of mRNA from 31 to 17 genes with a circRNA_miRNA_mRNA network, and narrowed the targets of mRNA from 31 to 8 genes with a lncRNA_miRNA_mRNA network (**Figure 6**), pointing the way for further studies to verify the genes and describe their function.

CONCLUSION

In summary, our investigation indicates that attenuated neonatal MS induced depression-related manifestation by repeated EA treatment at the acupoints GV20 and GV29 during adulthood. Furthermore, we explored the altered gene sets involved in circadian rhythm and neurotransmitter transporter activity in MS rats through unbiased genome-wide RNA sequencing to investigate alterations in the transcriptome of the PFC.

ETHICS STATEMENT

The experimental procedure was approved by the Animals Care and Use Committee of Guangzhou University of Traditional Chinese Medicine.

AUTHOR CONTRIBUTIONS

YC and NX designed the experiments. YZ and JH conducted the EA treatment and data analysis. ZY, XZ,

and YS conducted the behavioral tests. YC and LG performed the radioimmunoassay analysis. YZ, JH, and YC wrote the manuscript. LY, XW, and YX helped revise the manuscript. All authors read and approved the final manuscript.

FUNDING

This work was supported by the National Natural Science Foundation of China (31571041 and 3160060271); Guangdong Province Universities and Colleges Pearl River Scholar Funded Scheme (2016); Scientific Research and Innovation Team Program of Guangzhou University of Chinese Medicine (2017KYTD03); the Innovation Team Program of Guangdong Provincial Department of Education (2017KCXTD006); and Science and Technology Program of Guangdong (2018B030334001).

SUPPLEMENTARY MATERIAL

The Supplementary Material for this article can be found online at: https://www.frontiersin.org/articles/10.3389/fnins.2019.00314/full#supplementary-material

FIGURE S1 | Results of OFT and light/dark box test between Cont and MS group. **(A,D)** Track graphs show the moving trail of Cont and MS rats in OFT and light/dark box test. **(B,C)** In the OFT, there was no difference in the total distance and time in center between two groups [n = 10–11 rats per groups, $F(1,19) = 1.348$, Student's t-test; $F(1,19) = 0.932$, Student's t-test]. **(E,F)** There was no difference in the total distance and time in light among control and MS rats in light/dark box test (n = 10–11 rats per groups, $F(1,19) = 0.619$, Student's t-test; $F(1,19) = 1.335$, Student's t-test).

TABLE S1 | Statistical results by sequence quality control and the mapping rate by comparing with reference genes.

TABLE S2 | Differentially expressed mRNA/lncRNA/circRNA in rats.

TABLE S3 | Detail of the lncRNA/circRNA-miRNA-mRNA predicted interaction network.

REFERENCES

Alboni, S., van Dijk, R. M., Poggini, S., Milior, G., Perrotta, M., Drenth, T., et al. (2017). Fluoxetine effects on molecular, cellular and behavioral endophenotypes of depression are driven by the living environment. *Mol. Psychiatry* 22, 552–561. doi: 10.1038/mp.2015.142

Arborelius, L., Hawks, B. W., Owens, M. J., Plotsky, P. M., and Nemeroff, C. B. (2004). Increased responsiveness of presumed 5-HT cells to citalopram in adult rats subjected to prolonged maternal separation relative to brief separation. *Psychopharmacology* 176, 248–255. doi: 10.1007/s00213-004-1883-x

Auth, C. S., Weidner, M. T., Popp, S., Strekalova, T., Schmitt-Bohrer, A. G., van den Hove, D., et al. (2018). Differential anxiety-related behaviours and brain activation in Tph2-deficient female mice exposed to adverse early environment. *Eur. Neuropsychopharmacol.* 28, 1270–1283. doi: 10.1016/j.euroneuro.2018.07.103

Banqueri, M., Mendez, M., and Arias, J. L. (2017). Behavioral effects in adolescence and early adulthood in two length models of maternal separation in male rats. *Behav. Brain Res.* 324, 77–86. doi: 10.1016/j.bbr.2017.02.006

Bond, A. M., Vangompel, M. J., Sametsky, E. A., Clark, M. F., Savage, J. C., Disterhoft, J. F., et al. (2009). Balanced gene regulation by an embryonic brain ncRNA is critical for adult hippocampal GABA circuitry. *Nat. Neurosci.* 12, 1020–1027. doi: 10.1038/nn.2371

Bourin, M., and Hascoet, M. (2003). The mouse light/dark box test. *Eur. J. Pharmacol.* 463, 55–65. doi: 10.1016/S0014-2999(03)01274-3

Brent, D., Melhem, N., Donohoe, M. B., and Walker, M. (2009). The incidence and course of depression in bereaved youth 21 months after the loss of a parent to suicide, accident, or sudden natural death. *Am. J. Psychiatry* 166, 786–794. doi: 10.1176/appi.ajp.2009.08081244

Bunney, B. G., Li, J. Z., Walsh, D. M., Stein, R., Vawter, M. P., Cartagena, P., et al. (2015). Circadian dysregulation of clock genes: clues to rapid treatments in major depressive disorder. *Mol. Psychiatry* 20, 48–55. doi: 10.1038/mp.2014.138

Cai, N., Bigdeli, T., Kretzschmar, W., Li, Y., Liang, J., Song, L., et al. (2015). Sparse whole-genome sequencing identifies two loci for major depressive disorder. *Nature* 523, 588–591. doi: 10.1038/nature14659

Calabrese, F., Savino, E., Papp, M., Molteni, R., and Riva, M. A. (2016). Chronic mild stress-induced alterations of clock gene expression in rat prefrontal cortex: modulatory effects of prolonged lurasidone treatment. *Pharmacol. Res.* 104, 140–150. doi: 10.1016/j.phrs.2015.12.023

Cao, X., Li, L. P., Wang, Q., Wu, Q., Hu, H. H., Zhang, M., et al. (2013). Astrocyte-derived ATP modulates depressive-like behaviors. *Nat. Med.* 19, 773–777. doi: 10.1038/nm.3162

Cheng, J., Wang, X., Guo, J., Yang, Y., Zhang, W., Xie, B., et al. (2016). Effects of electroacupuncture on the daily rhythmicity of intestinal movement and circadian rhythmicity of colonic Per2 expression in rats with spinal cord injury. *BioMed Res. Int.* 2016:9860281. doi: 10.1155/2016/9860281

Choi, K. W., Na, E. J., Fava, M., Mischoulon, D., Cho, H., and Jeon, H. J. (2018). Increased adrenocorticotropic hormone (ACTH) levels predict severity of depression after six months of follow-up in outpatients with major depressive disorder. *Psychiatry Res.* 270, 246–252. doi: 10.1016/j.psychres.2018.09.047

Christiansen, S. L., Bouzinova, E. V., Fahrenkrug, J., and Wiborg, O. (2016). Altered expression pattern of clock genes in a rat model of depression. *Int. J. Neuropsychopharmacol.* 19:pyw061. doi: 10.1093/ijnp/pyw061

Coplan, J. D., Fulton, S. L., Reiner, W., Jackowski, A., Panthangi, V., Perera, T. D., et al. (2014). Elevated cerebrospinal fluid 5-hydroxyindoleacetic acid in macaques following early life stress and inverse association with hippocampal volume: preliminary implications for serotonin-related function in mood and anxiety disorders. *Front. Behav. Neurosci.* 8:440. doi: 10.3389/fnbeh.2014.00440

Csaszar-Nagy, N., and Bokkon, I. (2018). Mother-newborn separation at birth in hospitals: a possible risk for neurodevelopmental disorders? *Neurosci. Biobehav. Rev.* 84, 337–351. doi: 10.1016/j.neubiorev.2017.08.013

Cui, X., Niu, W., Kong, L., He, M., Jiang, K., Chen, S., et al. (2016). hsa_circRNA_103636: potential novel diagnostic and therapeutic biomarker in Major depressive disorder. *Biomark. Med.* 10, 943–952. doi: 10.2217/bmm-2016-0130

Dale, E., Bang-Andersen, B., and Sanchez, C. (2015). Emerging mechanisms and treatments for depression beyond SSRIs and SNRIs. *Biochem. Pharmacol.* 95, 81–97. doi: 10.1016/j.bcp.2015.03.011

Duan, D., Yang, X., Ya, T., and Chen, L. (2014). Hippocampal gene expression in a rat model of depression after electroacupuncture at the Baihui and Yintang acupoints. *Neural Regen. Res.* 9, 76–83. doi: 10.4103/1673-5374.125333

Duan, D. M., Dong, X., Tu, Y., and Liu, P. (2016). A microarray study of chronic unpredictable mild stress rat blood serum with electro-acupuncture intervention. *Neurosci. Lett.* 627, 160–167. doi: 10.1016/j.neulet.2016.05.054

Duan, D. M., Tu, Y., Chen, L. P., and Wu, Z. J. (2009a). Efficacy evaluation for depression with somatic symptoms treated by electroacupuncture combined with Fluoxetine. *J. Tradit. Chin. Med.* 29, 167–173.

Duan, D. M., Tu, Y., Chen, L. P., and Wu, Z. J. (2009b). Study on electroacupuncture treatment of depression by magnetic resonance imaging. *Zhongguo Zhen Jiu* 29, 139–144.

Frost, C. P., Meyerand, M. E., Birn, R. M., Hoks, R. M., Walsh, E. C., and Abercrombie, H. C. (2018). Childhood emotional abuse moderates associations among corticomotor white matter structure and stress neuromodulators in

women with and without depression. *Front. Neurosci.* 12:256. doi: 10.3389/fnins.2018.00256

Fu, S. P., He, S. Y., Xu, B., Hu, C. J., Lu, S. F., Shen, W. X., et al. (2014). Acupuncture promotes angiogenesis after myocardial ischemia through H3K9 acetylation regulation at VEGF gene. *PLoS One* 9:e94604. doi: 10.1371/journal.pone.0094604

Gibb, B. E., Chelminski, I., and Zimmerman, M. (2007). Childhood emotional, physical, and sexual abuse, and diagnoses of depressive and anxiety disorders in adult psychiatric outpatients. *Depress. Anxiety* 24, 256–263. doi: 10.1002/da.20238

Gonzalez-Pardo, H., Arias, J. L., Vallejo, G., and Conejo, N. M. (2019). Influence of environmental enrichment on the volume of brain regions sensitive to early life stress by maternal separation in rats. *Psicothema* 31, 46–52. doi: 10.7334/psicothema2018.290

Guo, L., Liang, X., Liang, Z., Liu, X., He, J., Zheng, Y., et al. (2018). Electroacupuncture ameliorates cognitive deficit and improves hippocampal synaptic plasticity in adult rat with neonatal maternal separation. *Evid. Based Complement. Alternat. Med.* 2018:2468105. doi: 10.1155/2018/2468105

Gururajan, A., Clarke, G., Dinan, T. G., and Cryan, J. F. (2016). Molecular biomarkers of depression. *Neurosci. Biobehav. Rev.* 64, 101–133. doi: 10.1016/j.neubiorev.2016.02.011

Han, X., Shao, W., Liu, Z., Fan, S., Yu, J., Chen, J., et al. (2015). iTRAQ-based quantitative analysis of hippocampal postsynaptic density-associated proteins in a rat chronic mild stress model of depression. *Neuroscience* 298, 220–292. doi: 10.1016/j.neuroscience.2015.04.006

Hansen, K. F., Sakamoto, K., Pelz, C., Impey, S., and Obrietan, K. (2014). Profiling status epilepticus-induced changes in hippocampal RNA expression using high-throughput RNA sequencing. *Sci. Rep.* 4:6930. doi: 10.1038/srep06930

Hanson, J. L., Chung, M. K., Avants, B. B., Rudolph, K. D., Shirtcliff, E. A., Gee, J. C., et al. (2012). Structural variations in prefrontal cortex mediate the relationship between early childhood stress and spatial working memory. *J. Neurosci.* 32, 7917–7925. doi: 10.1523/JNEUROSCI.0307-12.2012

Hempel, S., Taylor, S. L., Solloway, M. R., Miake-Lye, I. M., Beroes, J. M., Shanman, R., et al. (2014). *Evidence Map of Acupuncture*. Washington, DC: Department of Veterans Affairs.

Huang, X., Luo, Y. L., Mao, Y. S., and Ji, J. L. (2017). The link between long noncoding RNAs and depression. *Prog. Neuropsychopharmacol. Biol. Psychiatry* 73, 73–78. doi: 10.1016/j.pnpbp.2016.06.004

Ishikawa, J., Nishimura, R., and Ishikawa, A. (2015). Early-life stress induces anxiety-like behaviors and activity imbalances in the medial prefrontal cortex and amygdala in adult rats. *Eur. J. Neurosci.* 41, 442–453. doi: 10.1111/ejn.12825

Jacob, H. J., and Kwitek, A. E. (2002). Rat genetics: attaching physiology and pharmacology to the genome. *Nat. Rev. Genet.* 3, 33–42. doi: 10.1038/nrg702

Ji, M. J., Zhang, X. Y., Chen, Z., Wang, J. J., and Zhu, J. N. (2019). Orexin prevents depressive-like behavior by promoting stress resilience. *Mol. Psychiatry* 24, 282–293. doi: 10.1038/s41380-018-0127-0

Jiang, H., Zhang, X., Wang, Y., Zhang, H., Li, J., Yang, X., et al. (2017). Mechanisms underlying the antidepressant response of acupuncture via PKA/CREB signaling pathway. *Neural Plast.* 2017:4135164. doi: 10.1155/2017/4135164

Kou, R. Z., Chen, H., Yu, M. L., Xu, T. C., Fu, S. P., and Lu, S. F. (2017). Acupuncture for behavioral changes of experimental depressive disorder: a systematic review and meta-analysis. *Sci. Rep.* 7:9669. doi: 10.1038/s41598-017-09712-1

Kumar, P., Slavich, G. M., Berghorst, L. H., Treadway, M. T., Brooks, N. H., Dutra, S. J., et al. (2015). Perceived life stress exposure modulates reward-related medial prefrontal cortex responses to acute stress in depression. *J. Affect. Disord.* 180, 104–111. doi: 10.1016/j.jad.2015.03.035

Leng, N., Dawson, J. A., Thomson, J. A., Ruotti, V., Rissman, A. I., Smits, B. M., et al. (2013). EBSeq: an empirical Bayes hierarchical model for inference in RNA-seq experiments. *Bioinformatics* 29, 1035–1043. doi: 10.1093/bioinformatics/btt087

Li, J. Z., Bunney, B. G., Meng, F., Hagenauer, M. H., Walsh, D. M., Vawter, M. P., et al. (2013). Circadian patterns of gene expression in the human brain and disruption in major depressive disorder. *Proc. Natl. Acad. Sci. U.S.A.* 110, 9950–9955. doi: 10.1073/pnas.1305814110

Li, Q., Sullivan, N. R., McAllister, C. E., Van de Kar, L. D., and Muma, N. A. (2013). Estradiol accelerates the effects of fluoxetine on serotonin 1A receptor signaling. *Psychoneuroendocrino* 38, 1145–1157. doi: 10.1016/j.psyneuen.2012.11.005

Liu, M. Y., Yin, C. Y., Zhu, L. J., Zhu, X. H., Xu, C., Luo, C. X., et al. (2018). Sucrose preference test for measurement of stress-induced anhedonia in mice. *Nat. Protoc.* 13, 1686–1698. doi: 10.1038/s41596-018-0011-z

Liu, Y., Feng, H., Mo, Y., Gao, J., Mao, H., Song, M., et al. (2015). Effect of soothing-liver and nourishing-heart acupuncture on early selective serotonin reuptake inhibitor treatment onset for depressive disorder and related indicators of neuroimmunology: a randomized controlled clinical trial. *J. Tradit. Chin. Med.* 35, 507–513. doi: 10.1016/S0254-6272(15)30132-1

Liu, Z., Li, X., Sun, N., Xu, Y., Meng, Y., Yang, C., et al. (2014). Microarray profiling and co-expression network analysis of circulating lncRNAs and mRNAs associated with major depressive disorder. *PLoS One* 9:e93388. doi: 10.1371/journal.pone.0093388

Lu, J., Shao, R. H., Hu, L., Tu, Y., and Guo, J. Y. (2016). Potential antiinflammatory effects of acupuncture in a chronic stress model of depression in rats. *Neurosci. Lett.* 618, 31–38. doi: 10.1016/j.neulet.2016.02.040

Lu, J., Shao, R. H., Jin, S. Y., Hu, L., Tu, Y., and Guo, J. Y. (2017). Acupuncture ameliorates inflammatory response in a chronic unpredictable stress rat model of depression. *Brain Res. Bull.* 128, 106–112. doi: 10.1016/j.brainresbull.2016.11.010

Macri, S., Chiarotti, F., and Wurbel, H. (2008). Maternal separation and maternal care act independently on the development of HPA responses in male rats. *Behav. Brain Res.* 191, 227–234. doi: 10.1016/j.bbr.2008.03.031

Maniam, J., Antoniadis, C., and Morris, M. J. (2014). Early-life stress, HPA axis adaptation, and mechanisms contributing to later health outcomes. *Front. Endocrinol.* 5:73. doi: 10.3389/fendo.2014.00073

Masrour, F. F., Peeri, M., Azarbayjani, M. A., and Hosseini, M. J. (2018). Voluntary exercise during adolescence mitigated negative the effects of maternal separation stress on the depressive-like behaviors of adult male rats: role of NMDA receptors. *Neurochem. Res.* 43, 1067–1074. doi: 10.1007/s11064-018-2519-6

Mirescu, C., Peters, J. D., and Gould, E. (2004). Early life experience alters response of adult neurogenesis to stress. *Nat. Neurosci.* 7, 841–846. doi: 10.1038/nn1290

Mortensen, L. S., Park, S., Ke, J. B., Cooper, B. H., Zhang, L., Imig, C., et al. (2016). Complexin 3 increases the fidelity of signaling in a retinal circuit by regulating exocytosis at ribbon synapses. *Cell Rep.* 15, 2239–2250. doi: 10.1016/j.celrep.2016.05.012

Paternain, L., Martisova, E., Campion, J., Martinez, J. A., Ramirez, M. J., and Milagro, F. I. (2016). Methyl donor supplementation in rats reverses the deleterious effect of maternal separation on depression-like behaviour. *Behav. Brain Res.* 299, 51–58. doi: 10.1016/j.bbr.2015.11.031

Picao-Osorio, J., Johnston, J., Landgraf, M., Berni, J., and Alonso, C. R. (2015). MicroRNA-encoded behavior in *Drosophila*. *Science* 350, 815–820. doi: 10.1126/science.aad0217

Post, R. J., and Warden, M. R. (2018). Depression: the search for separable behaviors and circuits. *Curr. Opin. Neurobiol.* 49, 192–200. doi: 10.1016/j.conb.2018.02.018

Ramoni, M. F., Sebastiani, P., and Kohane, I. S. (2002). Cluster analysis of gene expression dynamics. *Proc. Natl. Acad. Sci. U.S.A.* 99, 9121–9126. doi: 10.1073/pnas.132656399

Rehmsmeier, M., Steffen, P., Hochsmann, M., and Giegerich, R. (2004). Fast and effective prediction of microRNA/target duplexes. *RNA* 10, 1507–1517. doi: 10.1261/rna.5248604

Roohi-Azizi, M., Torkaman-Boutorabi, A., Akhondzadeh, S., Nejatisafa, A. A., Sadat-Shirazi, M. S., and Zarrindast, M. R. (2018). Influence of citicoline on citalopram-induced antidepressant activity in depressive-like symptoms in male mice. *Physiol. Behav.* 195, 151–157. doi: 10.1016/j.physbeh.2018.08.002

Ruiz, R., Roque, A., Pineda, E., Licona-Limon, P., Jose, V. J., and Lajud, N. (2018). Early life stress accelerates age-induced effects on neurogenesis, depression, and metabolic risk. *Psychoneuroendocrino* 96, 203–211. doi: 10.1016/j.psyneuen.2018.07.012

Ryu, V., Yoo, S. B., Kang, D. W., Lee, J. H., and Jahng, J. W. (2009). Post-weaning isolation promotes food intake and body weight gain in rats that experienced neonatal maternal separation. *Brain Res.* 1295, 127–134. doi: 10.1016/j.brainres.2009.08.006

Sadeghi, M., Peeri, M., and Hosseini, M. J. (2016). Adolescent voluntary exercise attenuated hippocampal innate immunity responses and depressive-like

behaviors following maternal separation stress in male rats. *Physiol. Behav.* 163, 177–183. doi: 10.1016/j.physbeh.2016.05.017

Salvat-Pujol, N., Labad, J., Urretavizcaya, M., de Arriba-Arnau, A., Segalas, C., Real, E., et al. (2017). Hypothalamic-pituitary-adrenal axis activity and cognition in major depression: the role of remission status. *Psychoneuroendocrino* 76, 38–48. doi: 10.1016/j.psyneuen.2016.11.007

Seo, J. S., Wei, J., Qin, L., Kim, Y., Yan, Z., and Greengard, P. (2017). Cellular and molecular basis for stress-induced depression. *Mol. Psychiatry* 22, 1440–1447. doi: 10.1038/mp.2016.118

Smith, C. A., Hay, P. P., and Macpherson, H. (2010). Acupuncture for depression. *Cochrane Database Syst. Rev.* 65:CD004046. doi: 10.1002/14651858.CD004046.pub3

Tanahashi, N., Takagi, K., Amagasu, N., Wang, G., Mizuno, K., Kawanoguchi, J., et al. (2016). Effect of acupuncture stimulation on rats with depression induced by water-immersion stress. *Neurosci. Lett.* 618, 99–103. doi: 10.1016/j.neulet.2016.02.051

Tchenio, A., Lecca, S., Valentinova, K., and Mameli, M. (2017). Limiting habenular hyperactivity ameliorates maternal separation-driven depressive-like symptoms. *Nat. Commun.* 8:1135. doi: 10.1038/s41467-017-01192-1

Tye, K. M., Mirzabekov, J. J., Warden, M. R., Ferenczi, E. A., Tsai, H. C., Finkelstein, J., et al. (2013). Dopamine neurons modulate neural encoding and expression of depression-related behaviour. *Nature* 493, 537–541. doi: 10.1038/nature11740

Unutzer, J., Schoenbaum, M., Katon, W. J., Fan, M. Y., Pincus, H. A., Hogan, D., et al. (2009). Healthcare costs associated with depression in medically Ill fee-for-service medicare participants. *J. Am. Geriatr. Soc.* 57, 506–510. doi: 10.1111/j.1532-5415.2008.02134.x

Vaithianathan, T., Henry, D., Akmentin, W., and Matthews, G. (2015). Functional roles of complexin in neurotransmitter release at ribbon synapses of mouse retinal bipolar neurons. *J. Neurosci.* 35, 4065–4070. doi: 10.1523/JNEUROSCI.2703-14.2015

van der Doelen, R. H., Deschamps, W., D'Annibale, C., Peeters, D., Wevers, R. A., Zelena, D., et al. (2014). Early life adversity and serotonin transporter gene variation interact at the level of the adrenal gland to affect the adult hypothalamo-pituitary-adrenal axis. *Transl. Psychiatry* 4:e409. doi: 10.1038/tp.2014.57

Vetulani, J. (2013). Early maternal separation: a rodent model of depression and a prevailing human condition. *Pharmacol. Rep.* 65, 1451–1461. doi: 10.1016/S1734-1140(13)71505-6

Walf, A. A., and Frye, C. A. (2007). The use of the elevated plus maze as an assay of anxiety-related behavior in rodents. *Nat. Protoc.* 2, 322–328. doi: 10.1038/nprot.2007.44

Wang, J. Y., Li, H., Ma, C. M., Wang, J. L., Lai, X. S., and Zhou, S. F. (2015). MicroRNA profiling response to acupuncture therapy in spontaneously hypertensive rats. *Evid. Based Complement. Alternat. Med.* 2015:204367. doi: 10.1155/2015/204367

Wang, M. (2015). Research into media exposure behaviors of left-behind children in rural areas from the perspective of media as substitutes. *High. Educ. Soc.* 5, 24–28. doi: 10.3968/6886

Wang, Y., Jiang, H., Meng, H., Lu, J., Li, J., Zhang, X., et al. (2017). Genome-wide transcriptome analysis of hippocampus in rats indicated that TLR/NLR signaling pathway was involved in the pathogenisis of depressive disorder induced by chronic restraint stress. *Brain Res. Bull.* 134, 195–204. doi: 10.1016/j.brainresbull.2017.07.021

Wong, Y. H., Lee, C. M., Xie, W., Cui, B., and Poo, M. M. (2015). Activity-dependent BDNF release via endocytic pathways is regulated by synaptotagmin-6 and complexin. *Proc. Natl. Acad. Sci. U.S.A.* 112, E4475–E4484. doi: 10.1073/pnas.1511830112

Yao, H. J., Song, H. T., Mo, Y. P., Zhang, T. T., Han, X. B., and Li, Z. G. (2014). Effects of electroacupuncture on circadian rhythm of temperature and melatonin in depression rats model induced by chronic stress. *Zhongguo Zhen Jiu* 34, 685–689.

Yoo, S. B., Kim, B. T., Kim, J. Y., Ryu, V., Kang, D. W., Lee, J. H., et al. (2013). Adolescence fluoxetine increases serotonergic activity in the raphe-hippocampus axis and improves depression-like behaviors in female rats that experienced neonatal maternal separation. *Psychoneuroendocrino* 38, 777–788. doi: 10.1016/j.psyneuen.2012.08.013

Zhang, H., Chen, Z., Zhong, Z., Gong, W., and Li, J. (2018). Total saponins from the leaves of Panax notoginseng inhibit depression on mouse chronic unpredictable mild stress model by regulating circRNA expression. *Brain Behav.* 8:e01127. doi: 10.1002/brb3.1127

Zhang, Z. Y., Liu, Z., Deng, H. H., and Chen, Q. (2018). Effects of acupuncture on vascular dementia (VD) animal models: a systematic review and meta-analysis. *BMC Complement. Altern. Med.* 18:302. doi: 10.1186/s12906-018-2345-z

Conflict of Interest Statement: The authors declare that the research was conducted in the absence of any commercial or financial relationships that could be construed as a potential conflict of interest.

frontiers in Neuroscience

ORIGINAL RESEARCH
published: 20 June 2019
doi: 10.3389/fnins.2019.00652

Augmented Mechanical Forces of the Surface-Modified Nanoporous Acupuncture Needles Elicit Enhanced Analgesic Effects

Sun-Jeong Bae[1,2], Junsik Lim[1,3], Sangmin Lee[1,4], Hansaem Choi[5], Jae-Hwan Jang[1,6], Yu-Kang Kim[1,2,6], Ju-Young Oh[1,2,6], Jeong Hun Park[6], Hyuk-Sang Jung[2], Younbyung Chae[1,2,6], Su-Il In[5] and Hi-Joon Park[1,2,6]**

[1] Acupuncture and Meridian Science Research Center, Kyung Hee University, Seoul, South Korea, [2] College of Korean Medicine, Kyung Hee University, Seoul, South Korea, [3] College of Korean Medicine, Semyung University, Jecheon, South Korea, [4] College of Korean Medicine, Dongguk University, Goyang, South Korea, [5] Department of Energy Science and Engineering, DGIST, Daegu, South Korea, [6] Graduate School of Korean Medicine, Kyung Hee University, Seoul, South Korea

OPEN ACCESS

Edited by:
Florian Beissner,
Hannover Medical School, Germany

Reviewed by:
Jui-Hung Hung,
China Medical University Hospital, Taiwan
Karen M. von Deneen,
Xidian University, China

***Correspondence:**
Su-Il In
insuil@dgist.ac.kr
Hi-Joon Park
acufind@khu.ac.kr

Specialty section:
This article was submitted to Perception Science, a section of the journal Frontiers in Neuroscience

Received: *11 December 2018*
Accepted: *06 June 2019*
Published: *20 June 2019*

Citation:
Bae S-J, Lim J, Lee S, Choi H, Jang J-H, Kim Y-K, Oh J-Y, Park JH, Jung H-S, Chae Y, In S-I and Park H-J (2019) Augmented Mechanical Forces of the Surface-Modified Nanoporous Acupuncture Needles Elicit Enhanced Analgesic Effects. Front. Neurosci. 13:652. doi: 10.3389/fnins.2019.00652

Over the past several decades, clinical studies have shown significant analgesic effects of acupuncture. The efficacy of acupuncture treatment has improved with the recent development of nanoporous needles (PN), which are produced by modifying the needle surface using nanotechnology. Herein, we showed that PN at acupoint ST36 produces prolonged analgesic effects in an inflammatory pain model; the analgesic effects of PN acupuncture were sustained over 2 h, while those using a conventional needle (CN) lasted only 30 min. In addition, the PN showed greater therapeutic effects than CN after 10 acupuncture treatments once per day for 10 days. We explored how the porous surface of the PN contributes to changes in local tissue, which may in turn result in enhanced analgesic effects. We showed that the PN has greater rotational torque and pulling force than the CN, particularly at acupoints ST36 and LI11, situated on thick muscle layers. Additionally, in *ex vivo* experiments, the PN showed greater winding of subcutaneous connective tissues and muscle layers. Our results suggest that local mechanical forces are augmented by the PN and its nanoporous surface, contributing to the enhanced and prolonged analgesic effects of PN acupuncture.

Keywords: acupuncture analgesia, nanoporous needle, muscle, connective tissue, torque, complete Freund's adjuvant

INTRODUCTION

Acupuncture treatment has been used as a therapeutic modality in East Asia since 6000 BC, starting with a sharpened stone and progressing to stainless steel needles (White and Ernst, 2004; Wang et al., 2008). Acupuncture is of continuing global interest; the World Health Organization stated that acupuncture can be used to treat 63 diseases. Controlled clinical studies have shown its effectiveness in treating 28 diseases, including depression, nausea, vomiting, insomnia, and

pain (Lao, 1996; Leake and Broderick, 1999). Among these conditions, treating pain is one of the most common uses of acupuncture therapy (Wang et al., 2008; Han, 2011; Vickers et al., 2012; Lee et al., 2013), particularly for treating lower back pain (Gunn et al., 1980; Macdonald et al., 1983; Manheimer et al., 2005; Lee et al., 2013) and osteoarthritis (Casimiro et al., 2005; Kwon et al., 2006).

Acupuncture is the practice of inserting needles into specific areas of the body surface, called acupoints, by penetrating the epidermis, dermis, subcutaneous layer, and/or muscle (Kimura et al., 1992; Park et al., 2011; Zhang et al., 2015). To enhance its therapeutic effect, acupuncture is often accompanied by manipulation of the needle involving rotation, vibration, and in-and-out movements (Stux et al., 2003; Meridians and Acupoints Compilation Committee of Korean Oriental Medical Colleges, 2015). Although details of the underlying mechanisms remain unclear, the impact of acupuncture is believed to involve various molecules [e.g., adenosine (Fredholm, 2007; Goldman et al., 2010), pERK (Park et al., 2014), and/or TRPV1 (Abraham et al., 2011; Wu et al., 2014; Liao et al., 2017)] and structures [e.g., subcutaneous connective tissue (Shen et al., 1973; Langevin et al., 2001b, 2002; Zhao, 2008), muscle (Shen et al., 1973), nerve (Kim et al., 2013), vessels (Huang T. et al., 2013), fibroblasts (Langevin et al., 2007, 2011), mast cells (Zhang et al., 2007; Fung, 2009), and/or keratinocytes (Geoffrey, 2009; Park et al., 2014)] near the acupoints, resulting in reconstitution and activation of various signals (Lin and Chen, 2008; Zhao, 2008; Park et al., 2014; Shu et al., 2016).

Because local changes induced by needle insertion and/or manipulation initiate the therapeutic effects of acupuncture, we hypothesized that potentiating the intensity of acupuncture stimulation could enhance its therapeutic efficacy. Thus, we developed a novel acupuncture needle, the micro/nanoporous acupuncture needle (PN). Unlike the smooth surface of a conventional acupuncture needle (CN), the PN surface has micro/nano-sized holes that provide a 20-fold increase in surface area. Previous studies have explored the properties of the PN surface produced using electrochemical techniques (Lee et al., 2017). Acupuncture using the PN showed a greater therapeutic effect than did the CN in an addiction model (In et al., 2016) and a colorectal cancer model (Lee et al., 2017). Other than the electrical conductivity (Not understood; how is porosity related to electrical conductivity?), the micro/nanoporous surface of PN has different physical characteristics that affect the therapeutic efficacy of acupuncture treatment. However, no studies have explored the physical impact of PN acupuncture, including the pullout force, mechanical load, and structural deformation induced by surface modification of local tissues during PN acupuncture.

In this report, we (i) analyzed various aspects of PNs and CNs on four different acupoints by measuring the pullout force and rotational torque using an Acusensor; (ii) compared the morphological deformation of local tissues induced by PN and CN acupuncture; and (iii) investigated changes in therapeutic effects induced by PN acupuncture by assessing the analgesic effects in an inflammatory pain model.

MATERIALS AND METHODS

Experimental Animals

All experiments were performed using male C57BL/6 mice aged 7–10 weeks (Samtaco, Seoul, Korea). The mice were housed under 12-h light–dark cycle conditions with continuous access to chow and water. The mice were acclimated to the housing facility for 1 week before the experiments. All experiments were approved by the Dongguk University Animal Care Committee for Animal Welfare, and were performed according to the guidelines of the National Institutes of Health and the Korean Academy of Medical Sciences (IACUC-2017-022-1).

Preparation of the PNs

To manufacture the PNs, conventional stainless steel acupuncture needles (8-mm length and 0.30-mm diameter; Dong Bang Acupuncture Inc., Boryeoung, South Korea) were anodized. First, the needles were washed sequentially with acetone, ethanol, and deionized (DI) water. Then, the stainless steel needles were anodized using a two-electrode cell. The cell was composed of a needle for the working electrode, carbon paper (2 cm × 0.5 cm × 0.042 cm carbon and fuel cell; CNL Technology, Suwon, South Korea) for the counter electrode, electrolytes with 0.2 wt.% NH_4F (98%; American Chemical Society reagent, Alfa Aesar; Thermo Fisher Scientific, Waltham, MA, United States), and 2.0 vol% DI water in ethylene glycol. The needles were anodized for 30 min with 20 V (Paulose et al., 2006). Then, the anodized needles were rinsed with acetone, ethanol, and DI water, and dried in a nitrogen gas stream.

Characterization of the PNs

The morphology of the needle surface was evaluated using a high-resolution scanning electron microscope (S-4800; Hitachi, Tokyo, Japan) operated at 3 kV. EIS measurements were obtained using a Biologics SAS (Model VSP-1158; Biologics, Cary, NC, United States) three-electrode workstation with a platinum wire as the counter electrode, Ag/AgCl electrode as the reference electrode and the needles as the working electrodes. The system was operated using EC Lab software in the frequency range of 100 kHz to 200 MHz. The electrolyte consisted of a saline solution (0.9 g NaCl in 100 mL DI water) purchased from JW-Pharma (Seoul, South Korea) and was used without further modifications.

Measurements of the Rotational Torque and Pulling Force

Mice were anesthetized by intraperitoneal (i.p.) injection of Zoletil/Rompun and acupuncture needles (CN and PN, 8 mm in length, 0.18 mm in diameter; Dongbang Co., South Korea) were inserted to a depth of 3 mm at the ST36, LI11, ST25 and BL23 acupoints; **Figure 2b** shows the acupoints used in this study. Acupuncture using CNs and PNs was performed as follows: (1) without manipulation, or (2) with manipulation (consisting of clockwise rotations of 360°/s for nine spins). Pulling and rotational forces of the acupuncture needling were measured using the Acusensor (Stromatec, Inc., Burlington, VT, United States) motion sensor system (**Figure 2a**). The vertical

force acting on the needle to resist its insertion and pulling, and the rotational force acting on the needle to resist its rotation, were measured using a motion sensor. The data of each acupoint were analyzed respectively. And overall values were also calculated using average data.

Histochemical Staining of Abdominal Tissues

Sampling

We performed histochemical analyses of the abdominal tissues around the needle. The large surface area and lack of bones in the abdominal tissues allowed for rapid histological analyses of acupuncture treatment (Langevin et al., 2001a). Mice were anesthetized by Zoletil/Rompun (i.p.). The CNs and PNs (or NN) were inserted on both sides of the abdomen in a random order. Then, the needles were manipulated by nine unilateral spins, with one spin consisting of a clockwise rotation of 360°. For all insertions, the needle depth was held constant at 3 mm, with the needle penetrating the entire abdominal wall, and the track was labeled with tissue-marking dye (Davidson Marking System, Bradley Products, Inc., Bloomington, MN, United States). After the manipulation, the mice were sacrificed without removing the needle, and the whole body was immersion-fixed in 10% formalin for 48 h. Then, the abdominal tissues were excised, including the epidermis to the abdominal muscle layer and the needle, and fixed again in 10% formalin overnight.

Histological Analysis

The needles were removed after paraffinization of the samples and before paraffin embedding. Tissue blocks were cut parallel to the needle axis at 8-μm thickness using a manual rotary microtome (Shandon Finesse 325; Thermo Fisher Scientific Inc.). Every fifth slide with a needle track label was stained with hematoxylin (Merck Co., Darmstadt, Germany) and eosin (Sigma–Aldrich Co., St. Louis, MO, United States), or Masson trichrome-counterstained with aniline blue (Masson Trichrome Stain Kit, Nova Ultra^{TM}; IHC World, Ellicott City, MD, United States), which stains collagen as blue and muscle as red. Then, the thicknesses of the epidermis, dermis, subcutaneous, and abdominal muscle layers along the needle track were measured using a light microscopy (BX51, Olympus, Japan), with the subcutaneous layer divided into adipose tissue, cutaneous muscle, and subcutaneous connective tissue.

Behavioral Experiments

Experimental Groups and Acupuncture Treatment

Acupuncture was performed at the ST36 (Joksamli or Zusanli) acupoint, located 3–4 mm below and 1–2 mm lateral to the midline of the knee (Lim, 2010) (**Figure 2b**). ST36 is one of the most effective points in East Asian medicine and its anti-nociceptive effects in rodent CFA models of chronic pain are well-established (Goldman et al., 2010; Wu et al., 2014; Lu et al., 2016).

The mice were divided into five treatment groups: treatment with CFA only (CFA), treatment with CFA and non-invasive acupuncture (NN) needling at the ST36 acupoint (CFA+NN), treatment with CFA and CN at the ST36 acupoint (CFA+CN), treatment with CFA and PN at the ST36 acupoint (CFA+PN), and control (CON) (n = 7–8 in each group).

The mice in the CFA+CN and CFA+PN groups were immobilized by hand, and the needles were inserted to a depth of 3 mm at the bilateral acupoints. Then, the acupuncture needles were turned at a rate of two spins/s bidirectionally (one spin consisted of clockwise rotation of 180° and a counterclockwise rotation of 180°) for 30 s. The needles were removed immediately after manipulation. To create a blunt non-invasive acupuncture needle, the sharp end of the acupuncture needle was snipped. The mice in the CFA+NN group were pressed with 50 mN of force non-invasively, and no manipulation was done for 30 s. The mice in the CON and CFA groups were also immobilized by hand for 1 min to ensure an equal amount of stress among the acupuncture groups. The treatments began at 4 days after CFA injection once per day for 10 days. **Figures 7A,B** shows the schedule of the acupuncture treatments and behavioral experiments.

CFA-Induced Mouse Pain Model

CFA oil suspension was diluted 1:1 with saline and used to induce chronic inflammation. The mice were anesthetized with ether before the injection. The mice in the CFA, CFA+NN, CFA+CN, and CFA+PN groups received a subcutaneous injection of 100 μL CFA emulsion solution into the plantar of both hind paws, and the mice in the CON group received identical injections with equal amounts of saline. CFA-treated mice developed signs of inflammation that were prominent at 4 days after the injection.

Mechanical Threshold Assessment

Mechanical allodynia was assessed by testing the withdrawal response to von Frey filaments. Before the baseline test, the mice were habituated in 8 × 10 × 10 cm acrylic boxes with gridded floors, daily for 1 h for 2 days. Mechanical thresholds were assessed before CFA injection, as well as and after acupuncture treatment (**Figure 7A**). Prior to each test, the mice were habituated again for 1 h. The mechanical allodynia of the hind paws was assessed using an electronic von Frey filament (**Figure 7B**). The filament was applied to the plantar surface of the hind paw with 0.6 g of force for 1 s. All mice underwent 10 applications on both hind paws, with a 5 s interval between each application. Frequency was defined according to positive responses from 10 applications. The assessor was blinded to the group assignment, and an experienced investigator who was completely blinded counted the withdrawal frequencies.

To observe the short-term changes of allodynia induced by acupuncture, tests were performed before an acupuncture treatment and every 30 min for 2 h after the treatment (0, 30, 60, 90 and 120 min after acupuncture treatment). We tested these short-term effects only after the 1st and the 8th acupuncture treatment, to minimize the stress. And to test the long-term changes, we tested mechanical allodynia on the 1st, 3rd, 7th, and 10th day of acupuncture treatment (**Figure 7A**).

Statistical Analyses

GraphPad Prism 7 software (GraphPad Software Inc., La Jolla, CA, United States) was used for the statistical analyses. All data

are expressed as means and standard error of the mean (SEM). Statistical analyses were performed using one-way analysis of variance (ANOVA), two-way ANOVA or repeated measures of ANOVA, where appropriate. The Bonferroni *post hoc* test was followed. In all analyses, $p < 0.05$ was considered to indicate significant differences.

RESULTS

Physical Properties of PNs

Figures 1a–d shows field emission scanning electron microscopy (FE-SEM) images of stainless steel CNs compared with PNs, fabricated by anodizing CNs using an electrolyte of 0.2 wt.% NH_4F and 2 vol.% DI water in ethylene glycol at room temperature for 30 min at 20 V (Paulose et al., 2006). Initially, the CN had a smooth surface (**Figure 1a**); after anodization, the needle showed a micro-nanoscale porous surface topology with a high surface area (**Figure 1b**). High-resolution images of the PN showed uniform formation of conical-shaped pores (**Figure 1c**); a cross-sectional image of the porous topology is shown in **Figure 1d**.

Electrochemical impedance spectroscopy (EIS), a powerful technique for characterizing surfaces (Ehsani et al., 2014), was used to investigate CNs and PNs. **Figure 1e** shows the fitted Nyquist plots corresponding to the EIS results for CNs and PNs immersed in saline solution. The Nyquist plots for both needles show similar shapes, indicating that saline had no effect on the needle surface. Depressed semicircles are formed due to the combination of the charge transfer resistance (R_{CT}) and the constant phase element of the working electrode (acupuncture needles) and the electrolyte interface (Ehsani et al., 2013). A reasonable decrease was observed in the semicircle diameter in the PNs, indicative of a significant decrease in R_{CT}.

Measurements of Rotational Torque and Pullout Force at Four Representative Acupoints

The rotational torque and pullout force of PNs and CNs were measured using the Acusensor motion sensor system (**Figure 2a**). Four representative acupoints at the mouse hindlimb (ST36), forelimb (LI11), abdomen (ST25), and back (BL23) (**Figure 2b**) were used to identify and compare mechanical loads between PN and CN at each acupoint.

The rotational torque was measured during nine rotations at each acupoint (**Figures 3A–D**). The torque induced by PN and CN was enhanced as the number of rotations was increased in both PN and CN groups, and the rate of increase was much higher in the PN than in the CN group. Especially, the PN group showed significantly higher torque than the CN group when acupuncture was administered to ST36 ($P < 0.05$ at both the 6th and 8th rotation) and to ST25 ($P < 0.05$ at the 8th rotation).

The pullout force was measured after nine rotations of the needles (**Figures 3E–H**). These rotations induced trends of increased pullout force compared to no rotations for both the PN and CN groups; the increase was significant at acupoint ST36 (only PN: $P < 0.001$), LI11 (CN: $p < 0.05$, PN: $P < 0.001$), ST25 (only PN: $P < 0.05$), and BL23 (only PN: $P < 0.01$). As shown in **Figures 3E–H**, compared with the CN group, the PN group showed significantly higher pullout force at ST36 ($P < 0.001$) and LI11 ($P < 0.01$). No increase in pullout force was found for either needle group when the needle was inserted without rotation.

To explore differences in mechanical load between PNs and CNs on local tissues, we calculated the overall pulling force and rotational torque by averaging data of each location (**Figure 4**). The results showed that the overall rotational torque of the PN group increased to a more significant degree than did that of the CN group ($P < 0.01$, $P < 0.001$, $P < 0.01$, and $P < 0.001$ at the 5th, 7th, 8th, and 9th rotations, respectively; **Figure 4A**). The overall

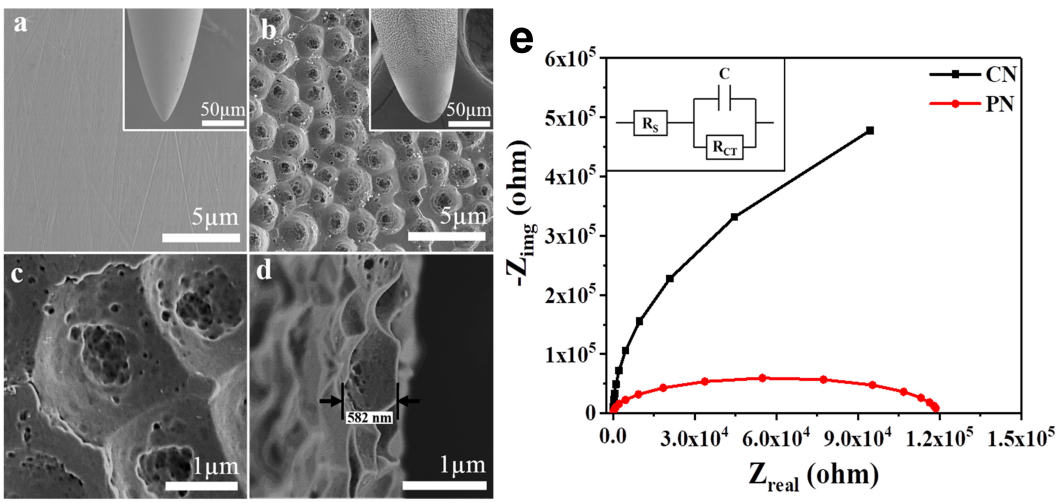

FIGURE 1 | Surfaces of the conventional needle (CN) **(a)** and micro-nanoporous needle (PN) **(b)**. High-resolution image of the PN acupuncture needle **(c)** and cross-sectional image of the PN anodized needle **(d)**. Electrochemical impedance spectra (EIS) with fitted Nyquist plots corresponding to the CN and PN **(e)**. The inset shows equivalent circuits for EIS measurements, where RS = solution resistance, RCT = charge transfer resistance, and C = double layer capacitance.

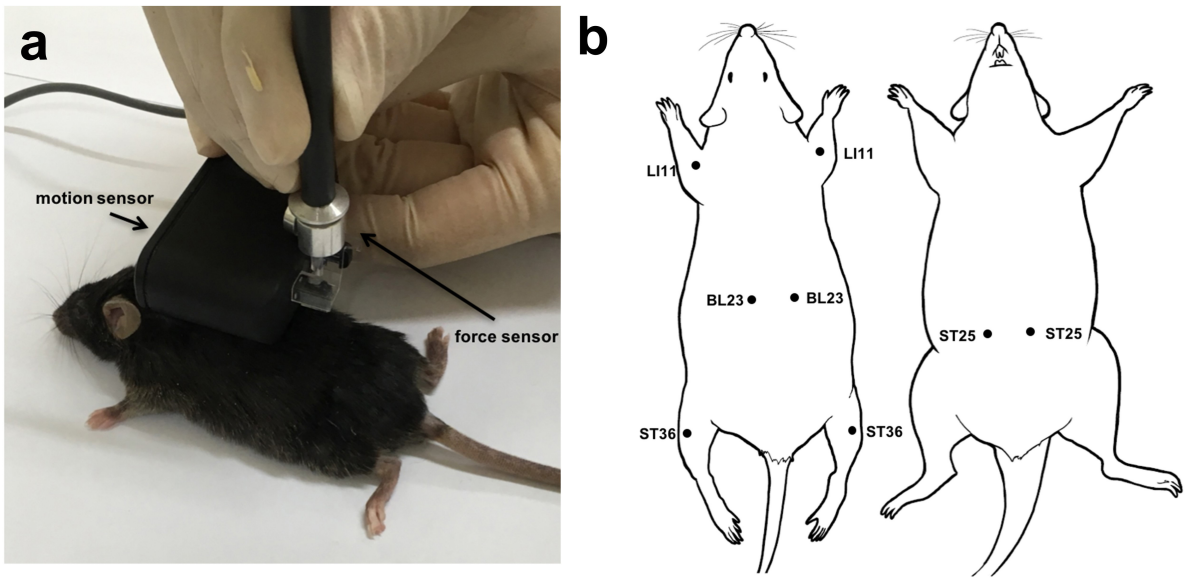

FIGURE 2 | Image of acupuncture needling using the Acusensor **(a)**. Acupoints used in this study **(b)**.

pulling force of the PN group was significantly higher than that of the CN group ($P < 0.01$, **Figure 4A**).

Histological Analysis in Local Tissues After Acupuncture

Histological analysis using hematoxylin and eosin staining (**Figures 5a,c,e**) or Masson's trichrome staining (**Figures 5b,d,f**) was performed to investigate acupuncture-induced morphological changes in local tissues, including the epidermis, dermis, subcutaneous tissue (adipose, cutaneous muscle, and subcutaneous connective tissue), and muscle layers. Masson's trichrome staining of the samples revealed that collagen-containing layers such as dermis, adipose, and subcutaneous connective tissue were stained blue; the epidermis, cutaneous muscle, and abdominal muscle were stained red. The measured thicknesses of the layers are shown in **Figure 6**.

Histological analysis showed that the thickness of subcutaneous layers increased after rotating CNs and PNs. In the adipose layer, both CNs and PNs increased the thickness, but only PNs showed a significant change compared to the CON group (CON: 69.4 ± 10.3 μm; CN: 173.6 ± 42.1 μm; PN: 218.5 ± 28.1 μm, $P < 0.05$ CON vs. PN). In the cutaneous muscle layer, both CNs and PNs increased the thickness, but only PNs induced a significant difference compared to the CON group (CON: 42.9 ± 4.3 μm; CN: 64.2 ± 7.0 μm; PN: 78.1 ± 4.1 μm, $P < 0.01$ vs. CON). In subcutaneous connective tissue, both CNs and PNs induced significantly greater thickness compared to the CON group (CON: 58.0 ± 11.7 μm; CN: 259.2 ± 77.0 μm; PN: 339.2 ± 53.3 μm, all $P < 0.05$ vs. CON); there was no difference between CNs and PNs (**Figures 5**, **6**). Masson's trichrome staining showed a whorl pattern in collagen fibers in subcutaneous connective tissues in the CN and PN groups (**Figures 5b,d,f**).

Based on muscle layer analysis, morphological changes in muscle thickness were only significant with PNs: the thickness using PNs (942.7 ± 44.8 μm) was significantly greater than that using CNs (665.4 ± 122.0 μm, PN vs. CN: $P < 0.01$) and that for the CON group (524.7 ± 38.3 μm, PN vs. CON: $P < 0.001$, **Figures 5**, **6**). Masson's trichrome staining analyses showed significant whorl patterns in muscles layers in the PN group (**Figures 5b,d,f**).

No morphological changes in the dermis and epidermis were observed in either group.

Effects of PN Acupuncture on the Mechanical Pain Threshold in Complete Freund's Adjuvant (CFA)-Induced Inflammatory Pain Model

We investigated the short-term and long-term analgesic effects of CN and PN acupuncture in a CFA-induced inflammatory pain model. Acupuncture was performed at acupoint ST36 (**Figure 2b**), and mechanical allodynia was measured using Von Frey filaments (**Figure 7B**). The baseline mechanical threshold before CFA injection was similar across all groups. Acupuncture treatments with CN and PN started 4 days after CFA injection, when the pain reached a stable level.

At the 1st acupuncture treatment, both CN and PN attenuated mechanical allodynia at 30–60 min post-acupuncture; however, only the PN group (5.9 ± 0.4) showed a significant difference compared to the CFA group (7.8 ± 0.4, $P < 0.001$) at 30 min post-acupuncture. Moreover, allodynia scores of the PN group were significantly lower than those of the CN group (7.0 ± 0.3, $P < 0.05$) at the same time point. At 120 min after treatment, mechanical allodynia in both the CN (7.69 ± 0.2) and PN (7.57 ± 0.3) groups returned to the pre-treatment values (**Figure 7A**).

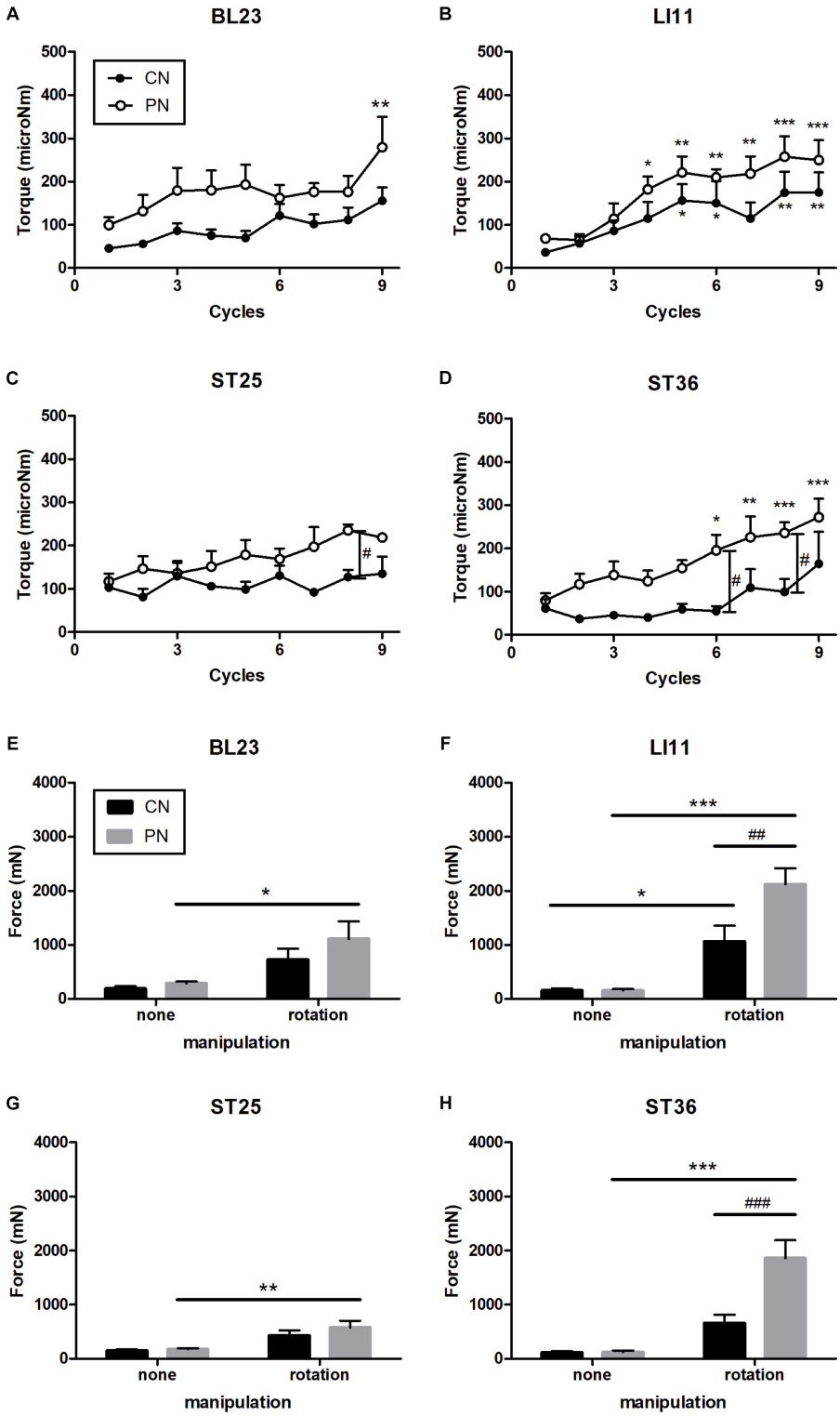

FIGURE 3 | Measurement of rotational torque at acupoints ST36 **(A)**, LI11 **(B)**, ST25 **(C)**, and BL23 **(D)**. Measurement of pulling force at ST36 **(E)**, LI11 **(F)**, ST25 **(G)**, and BL23 **(H)**. Rotation of the PN significantly increased the pulling force. At ST36, the pulling force of the PN with rotation was significantly higher than the CN with rotation. With increased numbers of rotation cycles, the torque in the PN and CN increased. In addition, PN had significantly stronger torque than did CN at ST25 and ST36 ($^{*}P < 0.05$, $^{**}P < 0.01$, $^{***}P < 0.001$, compared to the no-manipulation group; at the 1st cycle: $^{\#}P < 0.05$, $^{\#\#}P < 0.01$, $^{\#\#\#}P < 0.001$, CN vs. PN; Two-way repeated-measures ANOVA **(A–D)** and two-way ANOVA **(E–H)** followed by the Bonferroni test; each $n = 4–9$). Error bars indicate the standard error of the mean (SEM).

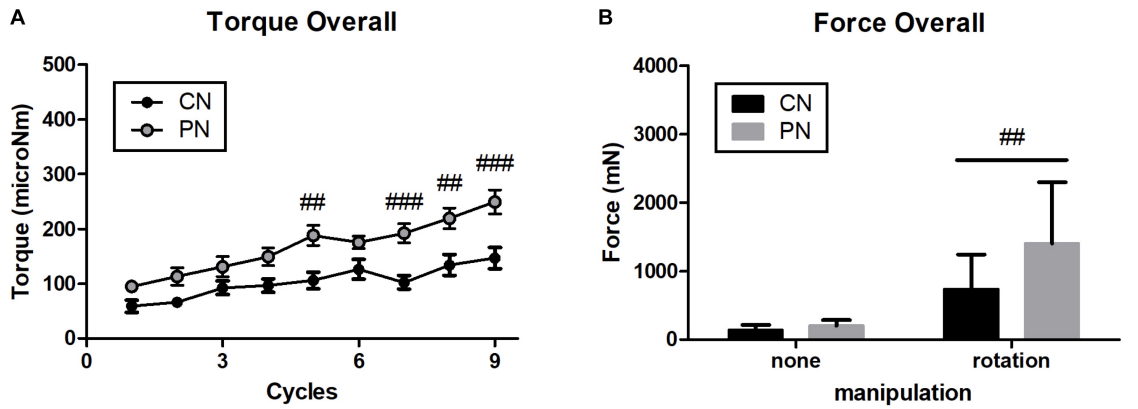

FIGURE 4 | Overall value of rotational torque **(A)** and pulling force **(B)**. PNs had significantly stronger pulling force and rotational torque than CNs ($^{\#\#}P < 0.01$, $^{\#\#\#}P < 0.001$, CN vs. PN; two-way ANOVA followed by the Bonferroni test; each $n = 16$). Error bars indicate the SEM.

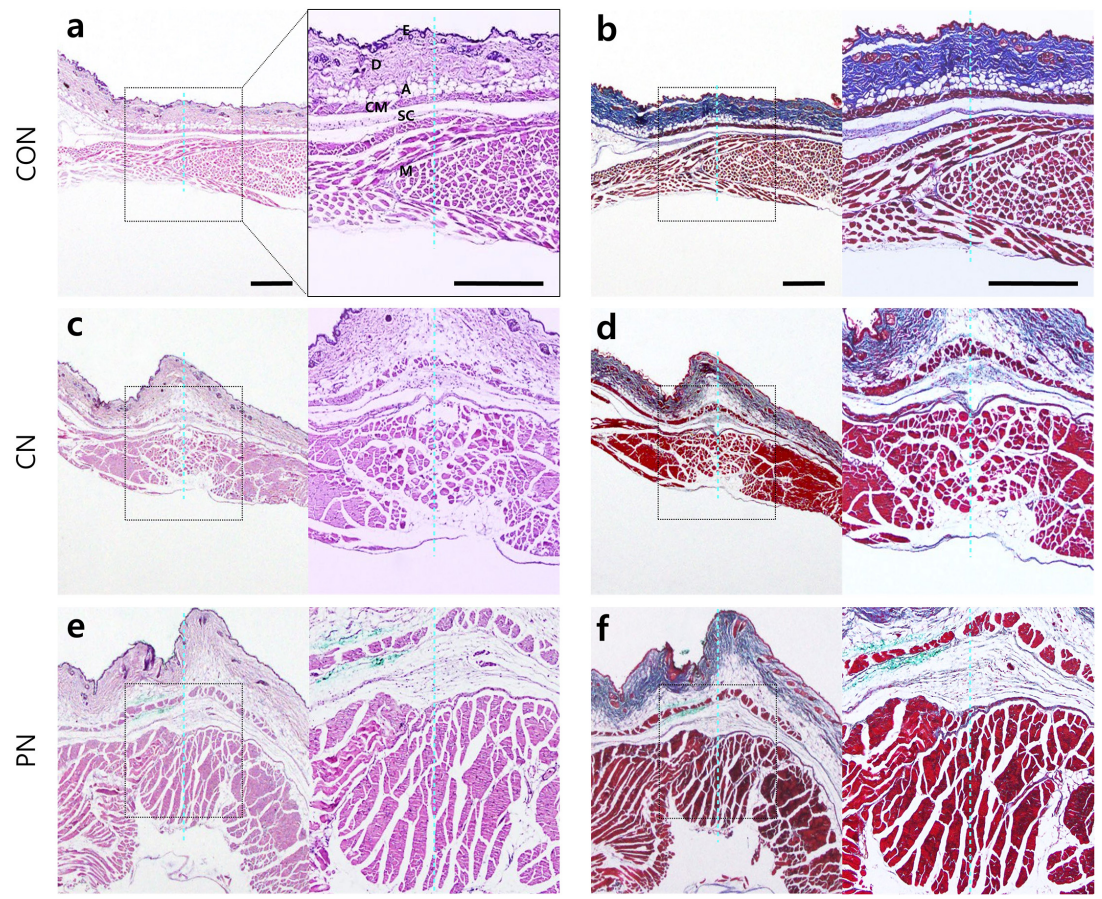

FIGURE 5 | Histological images in abdominal wall tissues. Control [CON **(a,b)**, CN **(c,d)**, and PN **(e,f)**]. Histological analyses were performed after nine acupuncture rotations. The adjacent sections from the same tissues were stained with hematoxylin and eosin (H&E) **(a,c,e)** or Masson's trichrome counterstained with aniline blue **(b,d,f)**. The histological layer includes the epidermis (E), dermis (D), adipose (A), cutaneous muscle (CM), subcutaneous connective tissue (SC), and abdominal muscle (M). The dotted blue line indicates the inserted trace of acupuncture needle. Scale bar, 500 μm.

After the 7th acupuncture treatment, the short-term effects of PN and CN acupuncture were tested again using the same protocol. As previously shown (Zhao, 2008; Goldman et al., 2010), the most effective time for CN acupuncture was 30 min after acupuncture (4.4 ± 0.6, $P < 0.001$ vs. CFA group), with the effect returning to baseline after 90 min. In contrast, in the PN group,

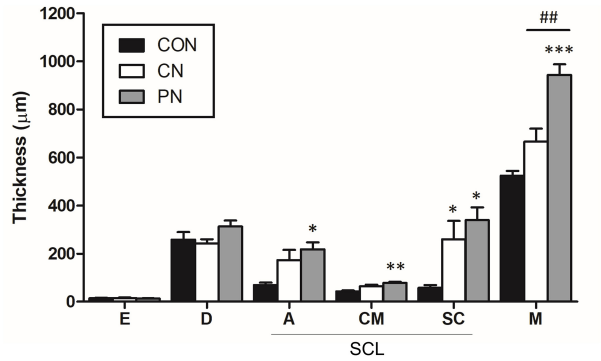

FIGURE 6 | Thickness of each layer in the abdominal wall. The thickness of each tissue layer was measured at the epidermis (E), dermis (D), adipose (A), cutaneous muscle (CM), subcutaneous connective tissue (SC), and abdominal muscle (M). SCL represents the subcutaneous layer. $^{*}P < 0.05$, $^{***}P < 0.001$, compared to the CON group; one-way ANOVA followed by the Bonferroni test; each $n = 4$–5. Error bars indicate the SEM.

the level of mechanical allodynia decreased gradually until 90 min after acupuncture (4.0 ± 0.3, $P < 0.001$ vs. CFA group), and the decrease continued until 120 min after acupuncture.

A comparison of the pain levels of those in the PN group with that of those in the CN group showed that the PN group exhibited significantly less pain than did the CN group at 90 and 120 min after acupuncture (both $P < 0.001$, **Figure 7B**).

In addition to the short-term analgesic effect, we observed long-term therapeutic effects measured 24 h after each acupuncture treatment. Throughout 10 acupuncture treatments (once per day for 10 days), both the PN and CN groups showed gradual alleviation of mechanical allodynia (PN vs. CFA, $P < 0.01$ after the 1st acupuncture session; CN vs. CFA, $P < 0.05$ after the 2nd acupuncture session). The difference between the PN and CN groups gradually increased as the number of treatments increased; the anti-allodynic effect of PN (4.5 ± 0.4) was significantly greater than that of CN (5.8 ± 0.4) after 10 acupuncture sessions (measured 1 day after the 10th acupuncture treatment, $P < 0.05$, **Figure 8**).

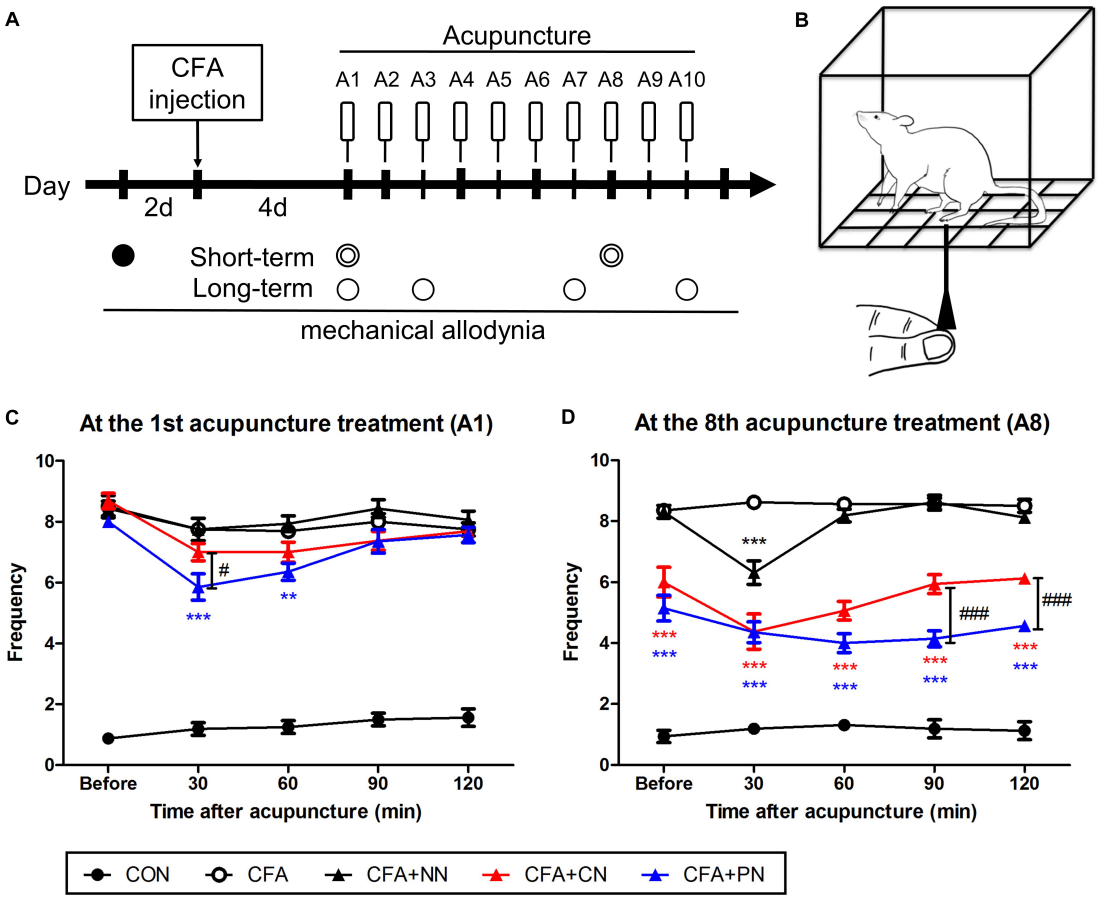

FIGURE 7 | The short-term effects of porous and conventional acupuncture needles in the CFA-induced inflammatory pain model. Timeline of the mechanical threshold assessment in the complete Freund's adjuvant (CFA)-induced pain model **(A)** Starting 4 days after CFA treatment, acupuncture treatment was administered once per day for 10 days (A1–A10, total 10 times). The Von Frey test was conducted as follows: at 2 days before CFA injection (●, baseline); at 30, 60, 90, and 120 min after acupuncture treatment (◎); and at 1 day after acupuncture (○). Schematic diagram of the von Frey test **(B)**. The analgesic effect of acupuncture under the CFA-induced inflammatory pain model was assessed after the 1st **(C)** and 7th **(D)** acupuncture treatments ($^{**}P < 0.01$, $^{***}P < 0.001$, compared to the CFA; $^{\#}P < 0.05$, $^{\#\#\#}P < 0.001$, CN vs. PN; two-way repeated measures ANOVA followed by the Bonferroni test; each $n = 7$–8) **(C,D)**. Error bars indicate the SEM.

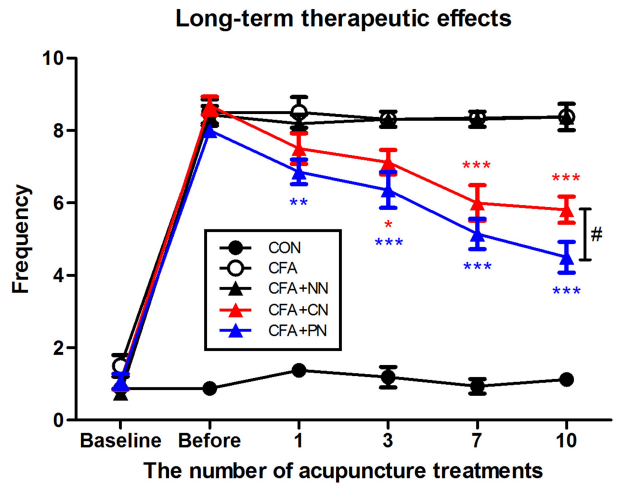

FIGURE 8 | Therapeutic effects of porous and conventional acupuncture needles in the CFA-induced inflammatory pain model. The paw withdrawal frequency of each mouse was measured 24 h after acupuncture treatments. The PN group showed a greater therapeutic effect than the CN group (*$P < 0.05$, **$P < 0.01$, ***$P < 0.001$, compared to the CFA group; #$P < 0.05$, CN vs. PN; two-way repeated measures ANOVA followed by the Bonferroni test; each $n = 7$–8). Error bars indicate the SEM.

DISCUSSION

Although PNs have been developed and applied for improving acupuncture treatment efficacy (In et al., 2016; Lee et al., 2017; Sorcar et al., 2018), no study has explored their analgesic effect, mechanical load, or influence on tissues. Therefore, we investigated the local impact and morphological changes caused by PN acupuncture and measured the difference in analgesic effects between PN and CN acupuncture. The results are summarized as follows: (1) PN induced larger mechanical load than CN; (2) likewise, the PN treatment tended to produce greater morphological changes in muscle layer thickness around the needle track than the CN treatment; and (3) in the CFA inflammatory pain mouse model, PN acupuncture at ST36 resulted in a longer duration of analgesic effect and longer-term treatment efficacy compared with CN acupuncture.

The different impact of PN on local tissues compared with that of CN is likely due to the high surface area of the needle. In et al. reported that the surface area of a PN is 20× greater than that of a CN of the same diameter (In et al., 2016). FE-SEM images confirm the presence of micro-nano porosity on the PN surface. This porosity significantly increases the PNs contact with the surrounding environment; the smaller R_{CT} of EIS implies a greater surface area (Ehsani et al., 2013, 2014). The larger surface area enhances the manipulation-induced frictional force between the needle and adjacent tissues, in turn enhancing the needle-grasp force (Kwon et al., 2017). PNs showed greater deformation of tissues (subcutaneous and muscle layers) around the needle and higher needle-grasp compared to CNs, as measured by the pulling force and torque on four different acupoints.

Histological examination of mouse abdominal tissues indicated that PN acupuncture significantly thickened the subcutaneous connective tissues and muscle layer, resulting in thicker layers than those induced by CN acupuncture, especially in the muscle. Subcutaneous connective tissue and muscle are the two main components of needle grasp, facilitating the therapeutic effect (Shen et al., 1973; Langevin et al., 2002; Zhao, 2008). Rotational manipulation of the acupuncture needle facilitates the gathering of collagen fibers of connective tissues around the needle (Langevin et al., 2006), transmitting mechanical stimulation to the surrounding cells and activating a cellular response in the fibroblasts of connective tissues (Burridge et al., 1988; Banes et al., 1995). Muscle contraction is also believed to induce needle grasp, and its polymodal-type receptor in deep tissue is associated with needle grasp and therapeutic effects (Shen et al., 1973; Lin et al., 1979). Furthermore, other tissue layers (e.g., the epidermis and dermis) may play a role in the effects of acupuncture (Langevin et al., 2007, 1; Abraham et al., 2011; Park et al., 2014); however, morphological changes were minimal in this study.

The exact mechanism through which PNs exert a greater effect cannot be determined based on morphological observation. However, our results are consistent with previous reports suggesting that a greater dose of acupuncture stimulation leads to greater changes at the molecular level, increasing signal transduction and thus exerting an enhanced effect (Goldman et al., 2010; Zylka, 2010; Abraham et al., 2011; Park et al., 2014; Wu et al., 2014). This newly developed PN acupuncture method results in greater stimulation of tissues around the needle track and enhances spinal dorsal horn neuronal activity by acupuncture stimulation in rats (In et al., 2016). Several studies have shown that PNs enhance the therapeutic effect of acupuncture (In et al., 2016; Lee et al., 2017; Sorcar et al., 2018); however, this study is the first to describe the analgesic effect of PNs, the most representative effect of acupuncture.

This study showed that the short-term analgesic effect of PN acupuncture at ST36 was greater than that of CN acupuncture in the CFA-induced pain mouse model. PN acupuncture showed greater immediate (30 min after treatment) and prolonged (90–120 min after treatment) analgesic effects. Our results are in agreement with studies showing higher efficacy and greater therapeutic effects of PN acupuncture in an addiction model (In et al., 2016) and a colorectal cancer model (Lee et al., 2017) compared with CN acupuncture.

Morphologically, CN acupuncture needle rotations induce collagen winding in subcutaneous connective tissues with no structural changes in the muscle layers (Langevin et al., 2001a). In contrast, PN acupuncture resulted in winding of both muscle and subcutaneous connective tissues. The difference in needle grasp between the PN and CN was noticeable at ST36 and LI11. Anatomically, ST36 and LI11 are situated on thicker muscle layers (i.e., the tibialis anterior muscle for ST36 and extensor carpi radialis longus muscle for LI11) compared to ST25 and BL23. In the upper skin layer, the collagen fibers are relatively small, and only needle tracks can be observed rather than tissue twirling; thus, morphological changes appear to be relatively minimal. However, the lower degree of morphological change

does not indicate that there are no biological changes associated with the therapeutic effects of acupuncture. Park et al. reported that acupuncture manipulation increased the expression level of pERK in keratinocytes of the epidermis, which may be associated with the analgesic effects of acupuncture. Further studies should be performed simultaneously considering both morphological and molecular changes. Although our results do not preclude the participation of other layers in the acupuncture effects, this study supports that muscle layers may play an important role in the improvements induced by PNs. Taken together, these findings suggest that both subcutaneous connective tissue and muscle contribute to the effects of acupuncture; however, the enhanced therapeutic effects by PNs may be associated with the effects on muscle layers.

Changes in subcutaneous connective tissue in the CN group were less marked than those reported previously (Li et al., 2005; Langevin et al., 2011; Huang C.-P. et al., 2013; Lu et al., 2016). This difference is likely due to the less marked manipulation in the present versus previous studies (Langevin et al., 2002, 2007) because a smaller manipulation using PNs was sufficient to produce an effective change similar to that reported previously (Kwon et al., 2017).

Our study has several limitations. First, to perform the experiments more precisely, sample size calculation is recommended based on a previous study (Festing and Wilkinson, 2007; Kar and Ramalingam, 2013). Since no previous studies have evaluated the analgesic effects of PN and CN, we could not calculate the sample size for this experiment. For subsequent large-scale studies of CN and PN groups, the sample size was calculated using G*Power (G*Power 3.1.9.2 for Windows 10, Faul et al., 2007)[1]. The measurement of mechanical pain in the CN and PN groups was used as ground data. The sample size was calculated using the independent *t*-test with an α-level of 0.05 and power of 80%. The number calculated was 10 per group, with an effect size d:1.219424, critical *t*: 1.7340636, Df: 18, non-centrality parameter δ:2.7267150, and actual power: 0.8357533. Next, our results did not reveal whether the PN had better effects than the CN at the other acupoints (excluding ST36). Therefore, further studies are required to compare the effects of the two types of needles using clinically relevant disease models with each acupoint. For example, the effects of ST25 can be tested in a visceral pain or colitis model (Shi et al., 2011; Zhu L. et al., 2018; Zhu X. et al., 2018; Ji et al., 2019). Differences in structural changes according to the modified needle surfaces may be associated with greater analgesic efficacy, but the detailed mechanisms should be explored. In addition, further experiments are required to characterize the enhanced analgesic effect of PN and its detailed mechanism in humans.

Overall, this study is the first to report that the PN, with its large surface area, shows a greater needle grasping power than the CN, thus producing greater morphological changes in subcutaneous and muscle tissues. More importantly, we showed that this treatment increases the analgesic effects with prolonged time. This study suggests that the PN is an effective tool for improving acupuncture efficacy in clinical medicine.

[1] http://www.gpower.hhu.de

ETHICS STATEMENT

All experiments were approved by the Dongguk University Animal Care Committee for Animal Welfare, and were performed according to the guidelines of the National Institutes of Health and the Korean Academy of Medical Sciences (IACUC-2017-022-1).

AUTHOR CONTRIBUTIONS

JP, S-JB, JL, and SL conceived and designed the study. S-II, J-HJ, S-JB, JL, SL, and YC developed the methodology. SB, JL, SL, Y-KK, and HC acquired the data. S-JB, JL, SL, H-SJ, and J-YO analyzed and interpreted the data. SB, JL, SL, H-JP, and S-II wrote, reviewed, and revised the manuscript. H-JP, S-II, and JP administrated the technical or material support. H-JP supervised the study. S-JB, JL, and SL drew the **Figures 2**, **7**. All authors had input into the manuscript and have approved the manuscript for publication.

FUNDING

This work was supported by grants from the National Research Foundation of Korea funded by the Korean Government (2017R1A2B4009963) and the Korea Institute of Oriental Medicine (Grant K18182) to H-JP, and by grants of the Korea Health Technology R&D Project through the Korea Health Industry Development Institute (KHIDI), funded by the Ministry of Health and Welfare (HI19C0506) to S-II.

REFERENCES

Abraham, T. S., Chen, M. L., and Ma, S. X. (2011). TRPV1 expression in acupuncture points: response to electroacupuncture stimulation. *J. Chem. Neuroanat.* 41, 129–136. doi: 10.1016/j.jchemneu.2011.01.001

Banes, A. J., Tsuzaki, M., Yamamoto, J., Brigman, B., Fischer, T., Brown, T., et al. (1995). Mechanoreception at the cellular level: the detection, interpretation, and diversity of responses to mechanical signals. *Biochem. Cell Biol.* 73, 349–365. doi: 10.1139/o95-043

Burridge, K., Fath, K., Kelly, T., Nuckolls, G., and Turner, C. (1988). Focal adhesions: transmembrane junctions between the extracellular matrix and the cytoskeleton. *Annu. Rev. Cell Biol.* 4, 487–525. doi: 10.1146/annurev.cb.04.110188.002415

Casimiro, L., Barnsley, L., Brosseau, L., Milne, S., Welch, V., Tugwell, P., et al. (2005). Acupuncture and electroacupuncture for the treatment of rheumatoid arthritis. *Cochrane Database Syst. Rev.* 19:CD003788. doi: 10.1002/14651858.CD003788.pub2

Ehsani, A., Jaleh, B., and Nasrollahzadeh, M. (2014). Electrochemical properties and electrocatalytic activity of conducting polymer/copper nanoparticles supported on reduced graphene oxide composite. *J. Power Sources* 257, 300–307. doi: 10.1016/j.jpowsour.2014.02.010

Ehsani, A., Mahjani, M. G., Bordbar, M., and Adeli, S. (2013). Electrochemical study of anomalous diffusion and fractal dimension in poly ortho aminophenol

electroactive film: comparative study. *J. Electroanal. Chem.* 710, 29–35. doi: 10.1016/j.jelechem.2013.01.008

Faul, F., Erdfelder, E., Lang, A.-G., and Buchner, A. (2007). G*Power 3: a flexible statistical power analysis program for the social, behavioral, and biomedical sciences. *Behav. Res. Methods* 39, 175–191. doi: 10.3758/BF03193146

Festing, S., and Wilkinson, R. (2007). The ethics of animal research. Talking point on the use of animals in scientific research. *EMBO Rep.* 8, 526–530. doi: 10.1038/sj.embor.7400993

Fredholm, B. B. (2007). Adenosine, an endogenous distress signal, modulates tissue damage and repair. *Cell Death Differ.* 14, 1315–1323. doi: 10.1038/sj.cdd.4402132

Fung, P. C. W. (2009). Probing the mystery of Chinese medicine meridian channels with special emphasis on the connective tissue interstitial fluid system, mechanotransduction, cells durotaxis and mast cell degranulation. *Chin. Med.* 4:10. doi: 10.1186/1749-8546-4-10

Geoffrey, B. (2009). Acupuncture: a novel hypothesis for the involvement of purinergic signalling. *Med. Hypotheses* 73, 470–472. doi: 10.1016/j.mehy.2009.05.031

Goldman, N., Chen, M., Fujita, T., Xu, Q., Peng, W., Liu, W., et al. (2010). Adenosine A1 receptors mediate local anti-nociceptive effects of acupuncture. *Nat. Neurosci.* 13, 883–888. doi: 10.1038/nn.2562

Gunn, C. C., Milbrandt, W. E., Little, A. S., and Mason, K. E. (1980). Dry needling of muscle motor points for chronic low-back pain: a randomized clinical trial with long-term follow-up. *Spine* 5, 279–291.

Han, J. S. (2011). Acupuncture analgesia: areas of consensus and controversy. *Pain* 152, S41–S48. doi: 10.1016/j.pain.2010.10.012

Huang, C.-P., Chen, H.-N., Su, H.-L., Hsieh, C.-L., Chen, W.-H., Lai, Z.-R., et al. (2013). Electroacupuncture reduces carrageenan- and CFA-induced inflammatory pain accompanied by changing the expression of Nav1.7 and Nav1.8, rather than Nav1.9, in mice dorsal root ganglia. *Evid. Based Compliment. Alernat. Med.* 2013:312184. doi: 10.1155/2013/312184

Huang, T., Yang, L., Jia, S., Mu, X., Wu, M., Ye, H., et al. (2013). Capillary blood flow in patients with dysmenorrhea treated with acupuncture. *J. Trad. Chin. Med.* 33, 757–760. doi: 10.1016/S0254-6272(14)60008-X

In, S., Gwak, Y. S., Kim, H. R., Razzaq, A., Lee, K.-S., Kim, H. Y., et al. (2016). Hierarchical micro/nano-porous acupuncture needles offering enhanced therapeutic properties. *Sci. Rep.* 6:34061. doi: 10.1038/srep34061

Ji, M. X., Guo, M. W., Gao, Y. S., Lan, Y., Wang, S., Wang, Y. F., et al. (2019). Comparison of effects of electroacupuncture at "Tianshu" (ST25) and "Dachangshu" (BL25) on intestinal sensitivity and expression of muscarinic M3R and 5-HT3AR in irritable bowel syndrome rats. *Zhen Ci Yan Jiu* 44, 264–269. doi: 10.13702/j.1000-0607.180764

Kar, S. S., and Ramalingam, A. (2013). Is 30 the magic number? Issues in sample size estimation. *Nat. J. Commun. Med.* 4, 175–179.

Kim, S. A., Lee, B. H., Bae, J. H., Kim, K. J., Steffensen, S. C., Ryu, Y.-H., et al. (2013). Peripheral afferent mechanisms underlying acupuncture inhibition of cocaine behavioral effects in rats. *PLoS One* 8:e81018. doi: 10.1371/journal.pone.0081018

Kimura, M., Tohya, K., Kuroiwa, K., Oda, H., Gorawski, E. C., Zhong, X. H., et al. (1992). Electron microscopical and immunohistochemical studies on the induction of "Qi" employing needling manipulation. *Am. J. Chin. Med.* 20, 25–35. doi: 10.1142/S0192415X92000047

Kwon, S., Lee, Y., Park, H.-J., and Hahm, D.-H. (2017). Coarse needle surface potentiates analgesic effect elicited by acupuncture with twirling manipulation in rats with nociceptive pain. *BMC Complement. Altern. Med.* 17:1. doi: 10.1186/s12906-016-1505-2

Kwon, Y. D., Pittler, M. H., and Ernst, E. (2006). Acupuncture for peripheral joint osteoarthritis: a systematic review and meta-analysis. *Rheumatology* 45, 1331–1337. doi: 10.1093/rheumatology/kel207

Langevin, H. M., Bouffard, N. A., Badger, G. J., Churchill, D. L., and Howe, A. K. (2006). Subcutaneous tissue fibroblast cytoskeletal remodeling induced by acupuncture: evidence for a mechanotransduction-based mechanism. *J. Cell. Physiol.* 207, 767–774. doi: 10.1002/jcp.20623

Langevin, H. M., Bouffard, N. A., Churchill, D. L., and Badger, G. J. (2007). Connective tissue fibroblast response to acupuncture: dose-dependent effect of bidirectional needle rotation. *J. Altern. Complement. Med.* 13, 355–360. doi: 10.1089/acm.2007.6351

Langevin, H. M., Bouffard, N. A., Fox, J. R., Palmer, B. M., Wu, J., Iatridis, J. C., et al. (2011). Fibroblast cytoskeletal remodeling contributes to connective tissue tension. *J. Cell. Physiol.* 226, 1166–1175. doi: 10.1002/jcp.22442

Langevin, H. M., Churchill, D. L., and Cipolla, M. J. (2001a). Mechanical signaling through connective tissue: a mechanism for the therapeutic effect of acupuncture. *FASEB J.* 15, 2275–2282. doi: 10.1096/fj.01-0015hyp

Langevin, H. M., Churchill, D. L., Fox, J. R., Badger, G. J., Garra, B. S., and Krag, M. H. (2001b). Biomechanical response to acupuncture needling in humans. *J. Appl. Physiol.* 91, 2471–2478. doi: 10.1152/jappl.2001.91.6.2471

Langevin, H. M., Churchill, D. L., Wu, J., Badger, G. J., Yandow, J. A., Fox, J. R., et al. (2002). Evidence of connective tissue involvement in acupuncture. *FASEB J.* 16, 872–874. doi: 10.1096/fj.01-0925fje

Lao, L. (1996). Acupuncture techniques and devices. *J. Altern. Complement. Med.* 2, 23–25. doi: 10.1089/acm.1996.2.23

Leake, R., and Broderick, J. E. (1999). Treatment efficacy of acupuncture: a review of the research literature. *Integr. Med.* 1, 107–115. doi: 10.1016/S1096-2190(98)00033-X

Lee, B. R., Kim, H.-R., Choi, E.-S., Cho, J.-H., Kim, N.-J., Kim, J.-H., et al. (2017). Enhanced therapeutic treatment of colorectal cancer using surface-modified nanoporous acupuncture needles. *Sci. Rep.* 7:12900. doi: 10.1038/s41598-017-11213-0

Lee, J. H., Choi, T. Y., Lee, M. S., Lee, H., Shin, B. C., and Lee, H. (2013). Acupuncture for acute low back pain: a systematic review. *Clin. J. Pain* 29, 172–185. doi: 10.1097/AJP.0b013e31824909f9

Li, W. M., Cui, K. M., Li, N., Gu, Q. B., Schwarz, W., Ding, G. H., et al. (2005). Analgesic effect of electroacupuncture on complete Freund's adjuvant-induced inflammatory pain in mice: a model of antipain treatment by acupuncture in mice. *Jpn. J. Physiol.* 55, 339–344. doi: 10.2170/jjphysiol.RP001505

Liao, H. Y., Hsieh, C. L., Huang, C. P., and Lin, Y. W. (2017). Electroacupuncture attenuates CFA-induced inflammatory pain by suppressing Nav1.8 through S100B, TRPV1, opioid and adenosine pathways in mice. *Sci. Rep.* 7:42531. doi: 10.1038/srep42531

Lim, S. (2010). WHO standard acupuncture point locations. *Evid. Based Complement. Alternat. Med.* 7, 167–168. doi: 10.1093/ecam/nep006

Lin, J. G., and Chen, W. L. (2008). Acupuncture analgesia: a review of its mechanisms of actions. *Am. J. Chin. Med.* 36, 635–645.

Lin, M. T., Liu, G. G., Soong, J. J., Chern, Y. F., and Wu, K. M. (1979). Effects of stimulation of acupuncture loci Ta-Chuei (Go-14), Nei-Kuan (EH-6) and Tsu-San-Li (St-36) on thermoregulatory function of normal adults. *Am. J. Chin. Med.* 7, 324–332.

Lu, K. W., Hsu, C. K., Hsieh, C. L., Yang, J., and Lin, Y. W. (2016). Probing the effects and mechanisms of electroacupuncture at ipsilateral or contralateral ST36–ST37 acupoints on CFA-induced inflammatory pain. *Sci. Rep.* 6:22123. doi: 10.1038/srep22123

Macdonald, A. J., Macrae, K. D., Master, B. R., and Rubin, A. P. (1983). Superficial acupuncture in the relief of chronic low back pain. *Ann. R. Coll. Surg. Engl.* 65, 44–46.

Manheimer, E., White, A., Berman, B., Forys, K., and Ernst, E. (2005). Meta-analysis: acupuncture for low back pain. *Ann. Intern. Med.* 142, 651–653. doi: 10.7326/0003-4819-142-8-200504190-00014

Meridians and Acupoints Compilation Committee of Korean Oriental Medical Colleges (2015). *Principles of Meridians & Acupoints: a Guidebook for College Students*. Daejeon: Jongnyeonamu Publishing Co.

Park, J. J., Akazawa, M., Ahn, J., Beckman-Harned, S., Lin, F. C., Lee, K., et al. (2011). Acupuncture sensation during ultrasound guided acupuncture needling. *Acupunct. Med.* 29, 257–265. doi: 10.1136/aim.2010.003616

Park, J. Y., Park, J., Jeon, S., Doo, A. R., Kim, S. N., Lee, H., et al. (2014). From peripheral to central: the role of ERK signaling pathway in acupuncture analgesia. *J. Pain* 15, 535–549. doi: 10.1016/j.jpain.2014.01.498

Paulose, M., Shankar, K., Yoriya, S., Prakasam, H. E., Varghese, O. K., Mor, G. K., et al. (2006). Anodic growth of highly ordered TiO 2 nanotube arrays to 134 μm in length. *J. Phys. Chem. B* 110, 16179–16184. doi: 10.1021/jp064020k

Shen, E., Wu, W. Y., Du, H. J., Wei, J. Y., and Zhu, D. X. (1973). Electromyographic activity produced locally by acupuncture manipulation. *Chin. Med. J.* 9, 532–535.

Shi, Y., Qi, L., Wang, J., Xu, M. S., Zhang, D., and Wu, L. Y. (2011). Moxibustion activates mast cell degranulation at the ST25 in rats with colitis. *World J. Gastroenterol.* 17, 3733–3738. doi: 10.3748/wjg.v17.i32.3733

Shu, Q., Chen, L., He, W., Zhou, H., and Liang, F. (2016). A review of inflammatory signaling pathway regulated by acupuncture. *World J. Acupunct. Moxibust.* 26, 63–69. doi: 10.1016/S1003-5257(17)30013-2

Sorcar, S., Grimes, C. A., and In, S. I. (2018). The Biocompatibility of nanoporous acupuncture needles. *J. Acupunct. Meridian Stud.* 11, 107–115. doi: 10.1016/j.jams.2018.03.004

Stux, G., Berman, B., and Pomeranz, B. (2003). *Basics of Acupuncture*, 5th Edn. Berlin: Springer.

Vickers, A. J., Cronin, A. M., Maschino, A. C., Lewith, G., MacPherson, H., Foster, N. E., et al. (2012). Acupuncture for chronic pain: individual patient data meta-analysis. *Arch. Intern. Med.* 172, 1444–1453. doi: 10.1001/archinternmed.2012.3654

Wang, S. M., Kain, Z. N., and White, P. (2008). Acupuncture analgesia: I. The scientific basis. *Anesth. Analg.* 106, 602–610. doi: 10.1213/01.ane.0000277493.42335.7b

White, A., and Ernst, E. (2004). A brief history of acupuncture. *Rheumatology* 43, 662–663. doi: 10.1093/rheumatology/keg005

Wu, S. Y., Chen, W. H., Hsieh, C. L., and Lin, Y. W. (2014). Abundant expression and functional participation of TRPV1 at Zusanli acupoint (ST36) in mice: mechanosensitive TRPV1 as an "acupuncture-responding channel. *BMC Complement. Alternat. Med.* 14:96. doi: 10.1186/1472-6882-14-96

Zhang, D., Ding, G. H., Shen, X. Y., Yao, W., Zhang, Z. Y., Zhang, Y. Q., et al. (2007). Influence of mast cell function on the analgesic effect of acupuncture of "Zusanli" (ST 36) in rats. *Zhen Ci Yan Jiu* 32, 147–152.

Zhang, X., Park, H. J., and Lee, H. (2015). Do acupuncture needle size and needling depth matter? A laser Doppler imaging study. *Integr. Med. Res.* 4, 66–67. doi: 10.1016/j.imr.2015.04.075

Zhao, Z. Q. (2008). Neural mechanism underlying acupuncture analgesia. *Prog. Neurobiol.* 85, 355–375. doi: 10.1016/j.pneurobio.2008.05.004

Zhu, L., Ma, Y., Ye, S., and Shu, Z. (2018). Acupuncture for diarrhoea-predominant irritable bowel syndrome: a network meta-analysis. *Evid. Based Complement. Alternat. Med.* 2018, 1–12. doi: 10.1155/2018/2890465

Zhu, X., Liu, Z., Qin, Y., Niu, W., Wang, Q., Li, L., et al. (2018). Analgesic effects of electroacupuncture at St25 and Cv12 in a rat model of postinflammatory irritable bowel syndrome visceral pain. *Acupunct. Med.* 36, 240–246. doi: 10.1136/acupmed-2016-011320

Zylka, M. J. (2010). Needling adenosine receptors for pain relief. *Nat. Neurosci.* 13, 783–784. doi: 10.1038/nn0710-783

Conflict of Interest Statement: The authors declare that the research was conducted in the absence of any commercial or financial relationships that could be construed as a potential conflict of interest.

The handling Editor is currently organizing a Research Topic with one of the authors, YC, and confirms the absence of any other collaboration.

frontiers in Psychology

ORIGINAL RESEARCH
published: 05 July 2019
doi: 10.3389/fpsyg.2019.01353

Effects of Acupuncture on Chronic Stress-Induced Depression-Like Behavior and Its Central Neural Mechanism

Min-Ju Lee[1†], Jae-Sang Ryu[1†], Seul-Ki Won[1], Uk Namgung[1], Jeeyoun Jung[2], So-Min Lee[2] and Ji-Yeun Park[1]*

[1]Department of Korean Medicine, College of Korean Medicine, Daejeon University, Daejeon, South Korea, [2]Clinical Medicine Division, Korea Institute of Oriental Medicine, Daejeon, South Korea

Depression is a serious psychiatric disorder with an enormous socioeconomic burden, and it is commonly comorbid with pain, chronic fatigue, or other inflammatory diseases. Recent studies have shown that acupuncture is an effective therapeutic method for reducing depressive symptoms; however, the underlying mechanism remains unknown. In this study, we investigated the effects of acupuncture on chronic stress-induced depression-like behavior and its central neural mechanisms in the brain. We induced chronic restraint stress (CRS) in male C57BL/6 mice for 14 or 28 consecutive days. Acupuncture treatment was performed at KI10·LR8·LU8·LR4 or control points for 7 or 14 days. Depression-like behavior was assessed with the open field test. Then, brain neural activity involving c-Fos and serotonin-related mechanisms *via* the 5-HT1A and 5-HT1B receptors were investigated. Acupuncture treatment at KI10·LR8·LU8·LR4 points rescued the depressive-like behavior, while control points (LU8·LR4·HT8·LR2) and non-acupoints on the hips did not. Brain neural activity was changed in the hippocampus, cingulate cortex, motor cortex, insular cortex, thalamus, and the hypothalamus after acupuncture treatment. Acupuncture treatment increased expression of 5-HT1A receptor in the cortex, hippocampus, thalamus, and the hypothalamus, and of 5-HT1B in the cortex and thalamus. In conclusion, acupuncture treatment at KI10·LR8·LU8·LR4 was effective in alleviating the depressive-like behavior in mice, and this therapeutic effect was produced through central brain neural activity and serotonin receptor modulation.

Keywords: acupuncture, brain neural activity, chronic restraint stress, depressive-like behavior, serotonin receptor modulation

OPEN ACCESS

Edited by:
Yi-Wen Lin,
China Medical University, Taiwan

Reviewed by:
Dae Hahm,
Kyung Hee University, South Korea
Xinjing Yang,
The University of Hong Kong, Hong Kong

***Correspondence:**
Ji-Yeun Park
jypark@dju.kr

†These authors have contributed equally to this work

Specialty section:
This article was submitted to Health Psychology, a section of the journal Frontiers in Psychology

Received: *14 December 2018*
Accepted: *24 May 2019*
Published: *05 July 2019*

Citation:
Lee M-J, Ryu J-S, Won S-K, Namgung U, Jung J, Lee S-M and Park J-Y (2019) Effects of Acupuncture on Chronic Stress-Induced Depression-Like Behavior and Its Central Neural Mechanism. Front. Psychol. 10:1353. doi: 10.3389/fpsyg.2019.01353

INTRODUCTION

Depression is a common mood disorder, which has a high mortality and recurrence rate (Reddy, 2010). According to a previous study, about 10% of the world's population has major depressive disorder (Riolo et al., 2005), and continued depression can lead to suicide, sleep disorders, anorexia, anxiety, and gangrene (Hammen, 2005). Depression is not only a serious disease *per se* but also has a major impact on the occurrence of other conditions, such as

pain (Bair et al., 2003; Goldenberg, 2010), chronic fatigue syndrome (Bram et al., 2018), neurodegenerative disease (Modrego and Ferrández, 2004), and inflammatory diseases (Baerwald et al., 2019). The etiology of depression involves genetic, environmental, socioeconomic, and stress-related factors (Dunn et al., 2015). As stress is emerging as a major cause of depression (Yang et al., 2015), there is an interest in developing treatment methods for depression and elucidating the pathological and neurobiological mechanism of stress-induced depression. However, much of the fundamental mechanisms of stress-induced depression have yet to be elucidated.

Although the cause of depression remains unclear, the brain is known to play a fundamental role in the mechanism of depression (Leuchter et al., 1997). Changes in brain neural circuits or a chemical imbalance in the brain are involved in the onset of depression (Palazidou, 2012). Recent brain imaging studies have identified that several brain regions (Pandya et al., 2012), such as the hippocampus, amygdala, and anterior cingulate cortex are involved in depression (Drevets et al., 2008; Eisch and Petrik, 2012). Hippocampal neurons have bilateral connections to the amygdala, and relay the signals to several brain areas (Fried et al., 1997; McEwen et al., 2016). It also receives synaptic inputs through the cingulate cortex. Hippocampal activity is affected by a stressed state and is involved in stress-induced depression (Krugers et al., 2010; Kim et al., 2015). Since hippocampal neurons can be altered by serotonergic and adrenergic inputs, as well as by the corticotropin-releasing hormone, many antidepressants are aimed at blocking or modulating serotonin or serotonin receptors (Kohler et al., 2016).

The serotonergic system is one of the major neurotransmitter systems involved in depression. Monoaminergic neurotransmission imbalance is causally related to the clinical features of depression, and depletion of monoamines such as serotonin (5-hydroxytryptamine, 5-HT) in the brain is a widely accepted hypothesis in the field of depression (Rot et al., 2009). Conventional antidepressants that improve 5-HT transmission or inhibit 5-HT reuptake, such as selective serotonin-reuptake inhibitors (SSRIs), are the most commonly used pharmacotherapy (Gijsman et al., 2004; Holtzheimer and Nemeroff, 2006). However, the efficacy of these drug in some patients remains controversial (Torrens et al., 2005; Papakostas et al., 2008), and they also induce side effects, such as a lack of concentration, gastrointestinal disorder, recurrence of depression, and involve the inconvenience of long-term administration (Penn and Tracy, 2012). Therefore, various alternative therapies for depression are sought.

Acupuncture has been used to treat various disorders, including pain (Vickers et al., 2012; Park et al., 2014), neurodegenerative disease (Cho et al., 2012; Park et al., 2017a), and psychological disorders, such as depression and stress-induced symptoms (Mukaino et al., 2005; Leo and Ligot, 2007), with a very rare occurrence of adverse events. Previous studies have reported that acupuncture is an effective therapeutic approach for improving symptoms of depression (Pilkington, 2010; Zhang et al., 2010; Qu et al., 2013; Chan et al., 2015; Li et al., 2018) by regulating the mTOR signal (Oh et al., 2018), glial glutamate transporter (Luo et al., 2017), neuropeptide Y (Eshkevari et al., 2012), and ERK-CREB pathways in the brain (Lu et al., 2013), as well as the expression of hippocampal brain-derived neurotrophic factor (Yun et al., 2002). However, the biological basis of its efficacy remains largely unknown. Most *in vivo* acupuncture studies aimed at elucidating the effect and the fundamental mechanism underlying acupuncture effects have used a single acupoint for therapy. ST36 has been most commonly used, while some studies used PC6, GB20, and EX-HN3 (Yun et al., 2002; Eshkevari et al., 2012; Lu et al., 2013, 2016). In the clinic, however, practitioners generally use a combination of acupoints, selected on the basis of traditional Korean or Chinese medical theory. Therefore, it is necessary to select acupuncture combinations that are frequently used in clinics when conducting efficacy evaluation and mechanistic studies.

In this study, we investigated the effect of acupuncture treatment consisting of a combination of specific acupoints (KI10·LR8·LU8·LR4) in a mouse model of chronic stress-induced depressive-like behavior. We also analyzed neural activation and the changes in 5-HT receptor expression in various brain regions, to elucidate the central neural mechanism of this acupuncture treatment.

MATERIALS AND METHODS

Animals

Male C57BL/6 mice (age: 6–7 weeks old; weight: 20–25 g) were used in this study (Daehan Biolink, Eum-seong, Korea). Mice were acclimated for at least 1 week before the experiments and maintained with a 12-h light/dark cycle with free access to water and food. The animals were randomly divided, and five mice were placed in each cage (room temperature 25°C and humidity of 55%) in a clean room. Their weight was monitored every 2 days (**Supplementary Figure S1**). This study was carried out in accordance with recommendations in the guidelines for the Care and Use of Laboratory Animals of the National Institutes of Health. All experimental protocols used in this study were approved by the Institutional Animal Care and Use Committee (IACUC) at Daejeon University (approval no. DJUARB2016-40).

Chronic Restraint Stress

All mice were exposed to chronic restraint stress (CRS). CRS was induced by placing mice individually into a 50-ml Falcon tube and the tubes were slightly tilted for 6 h per day (10:00–16:00), for 14 or 28 consecutive days to induce depressive-like behavior. Mice subjected to CRS could not access water and food during the CRS but could freely access water and food at the end of it.

Behavioral Test

Mice were challenged in the open-field test (OFT) before and after the repeated restraint stress procedure to measure depressive-like behavior (**Figure 1A**). Mice were stabilized in the test room for more than 1 h prior to behavioral testing. Then, they were placed in a box (30 cm × 30 cm × 30 cm) which

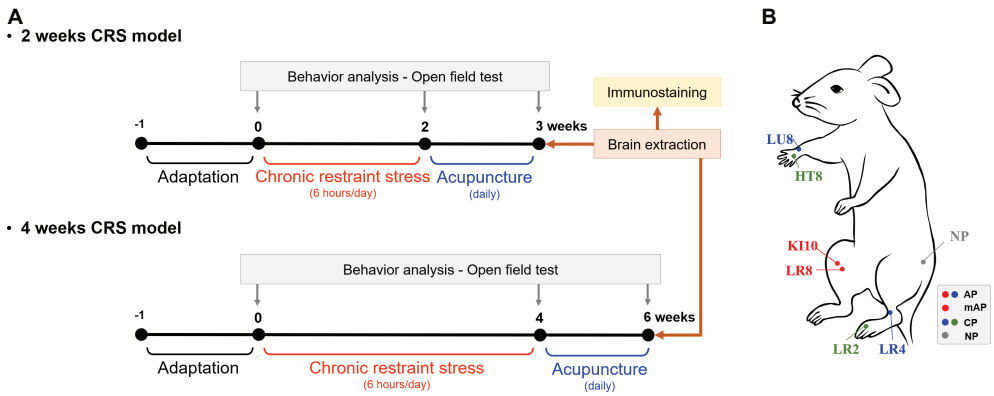

FIGURE 1 | Experimental schedule and acupuncture treatment. **(A)** Two or 4 weeks of chronic restraint stress (CRS) was used to induce depressive-like behavior. Mice were treated with acupuncture for 7 or 14 consecutive days, respectively, and the open field test was performed to observe behavior patterns. **(B)** Location of the acupuncture points used in this study. AP, KI10·LR8·LU8·LR4; mAP, KI10·LR8; CP, LU8·LR4·HT8·LR2; NP, non-acupoints on the hips.

was made of white plastic and the total distance and number of zone transitions measured for a period of 10 min using a video camera system to track movement (SMART 3.0; Panlab S. L., Barcelona, Spain). The tracking images showed that the mice had locomotor activity and explorational ability. All the tests were performed between 10:00 am and 12:00 pm.

Acupuncture Treatments

After CRS inducing, mice were randomly assigned to each group (n = 5–8 per group) according to the acupuncture treatment performed: CRS without acupuncture (CRS group), at the acupuncture points (KI10·LR8·LU8·LR4; AP group), at modified-acupuncture points (KI10·LR8; mAP group), at control points (LU8·LR4·HT8·LR2; CP group), or at non-acupoints (on the hips, located midway between the coccyx and hip joints; NP group) for 7 or 14 consecutive days. For acupuncture treatment, mice were slightly immobilized by fixing their neck. Then, acupuncture needles (0.18 mm in diameter and 8 mm in length; Dong-Bang Acupuncture Inc., Boryung, Korea) were inserted bilaterally at the appropriate positions according to group assignment. Needles were turned at a rate of two spins per second for 30 s, and then immediately removed (Yin et al., 2008). The CRS group was immobilized for the same amount of time to induce an equal amount of stress.

The location of each acupoint is as follows:

KI10 is located on the posteromedial aspect of the knee, just lateral to the semitendinosus tendon, in the popliteal crease. LR8 is located on the medial aspect of the knee, in the depression medial to the tendons of the semitendinosus and the semimembranosus muscles, at the medial end of the popliteal crease. LU8 is located on the anterolateral aspect of the forearm, between the radial styloid process and the radial artery, 1 cun superior to the palmar wrist crease. LR4 is located on the anteromedial aspect of the ankle, in the depression medial to the tibialis anterior tendon, anterior to the medial malleolus. HT8 is located on the palm of the hand, in the depression between the fourth and fifth metacarpal bones, proximal to the fifth metacarpophalangeal joint. LR2 is located on the dorsum of the foot, between the first and second toes, proximal to the web margin, at the border between the red and white flesh (**Figure 1B**; WHO, 2008; Yin et al., 2008).

Brain Tissue Section Preparation

On the last day of the experiment, mice were anesthetized with an intraperitoneal injection of zoletil (30 mg/kg) and xylazine (10 mg/kg). Mice were transcardially perfused with 0.05 M phosphate-buffered saline (PBS) buffer followed by 4% paraformaldehyde (PFA). Their brains were removed, post-fixed overnight in cold 4% PFA, and then cryo-protected in a gradient of 10–30% sucrose solution until the brain sank. Brain tissues were subsequently cut into 40-μm-thick sections using a cryostat at −20°C (Leica Microsystems, Wetzlar, Germany), on the coronal plane, and sections were prepared in free-floating sections.

Immunohistochemistry

Tissue sections were incubated in 1% H_2O_2 to reduce endogenous peroxidase activity, followed by incubation in 1% bovine serum albumin for 1 h at room temperature. Tissue sections were incubated with primary antibodies at 4°C overnight. The details of the primary antibodies were as follows: c-Fos monoclonal antibody (1:150, Santa Cruz, Dallas, TX, USA), 5-HT1A (1:100, Novus Biologicals, Centennial, CO, USA), and 5-HT1B (1:100, Abcam, Cambridge, UK). Thereafter, tissues were incubated with secondary antibodies at room temperature for 2 h; these included biotinylated goat anti-rabbit IgG (H + L) or anti-mouse IgG (H + L) (Vector Laboratories, Burlingame, CA, USA). After washing in PBS, tissue sections were incubated with ABC reagent (Vector Laboratories), with 0.02% diaminobenzidine and 0.003% hydrogen peroxide in 1 M Tris-buffered saline (pH 7.5). The tissues were then dehydrated by immersion in a gradient of 70–100% ethyl alcohol, followed by 100% xylene, before being mounted with Permount solution. Photographs of the stained brain sections were obtained under a microscope (Nikon, Minato, Japan).

The number of c-Fos positive cells on 30 brain regions of the cortex, cerebral nuclei, hippocampus, thalamus, hypothalamus, and midbrain, and the 5-HT1A- and 5-HT1B receptor-positive cells in 25 brain regions of the cortex, hippocampus, thalamus, and hypothalamus were manually counted, within a square of 32 μm × 32 μm. The mean values for the left and right regions were calculated and used for analysis. When the area was wider than the 32 μm × 32 μm square, three regions were randomly selected, and the average value was obtained. All measurements were randomly confirmed. All the brain regions assessed, and their abbreviations are shown in **Table 1**.

Immunoblotting Assay

Proteins were extracted from the brain tissues using RIPA buffer containing a protease and phosphatase inhibitor. The protein amount was measured by a BCA protein assay kit (Thermo Fisher Scientific). Protein lysates (10 μg) were loaded into a 10% SDS-polyacrylamide gel electrophoresis (PAGE) and transferred on polyvinylidene difluoride (PVDF) membranes. Membranes were incubated overnight at 4°C with primary antibodies of c-Fos (1:1,000, Santa Cruz). The secondary antibodies of anti-mouse IgG HRP (1:5,000, Sigma-Aldrich) and anti-rabbit IgG HRP (1:5,000, Sigma-Aldrich) were used. The bands were detected with an ECL western blotting substrate kit (1:1 solution, GE Health Care). All the results were normalized to the respective GAPDH.

TABLE 1 | Brain region and its abbreviation used in this study.

Region	Abbreviation
Cortex	
Cingulate cortex, area 1	CC-1
Cingulate cortex, area 2	CC-2
Primary motor cortex	MC-1
Secondary motor cortex	MC-2
Primary somatosensory cortex	SC-1
Secondary somatosensory cortex	SC-2
Agranular insular cortex, ventral part	IC-AIV
Insular cortex, dorsal part	IC-AID
Granular insular cortex	IC-Gi
Dysgranular insular cortex	IC-Di
Piriform cortex	Pir
Cerebral nuclei	
Caudate putamen (striatum) – dorsal medial	ST-DM
Caudate putamen (striatum) – dorsal lateral	ST-DL
Caudate putamen (striatum) – ventral medial	ST-VL
Hippocampus	
Field CA1 of hippocampus	HIP-CA1
Field CA2 of hippocampus	HIP-CA2
Field CA3 of hippocampus	HIP-CA3
Dentate gyrus	HIP-DG
Thalamus	
Paraventricular thalamic nucleus	TH-PV
Central medial thalamic nucleus	TH-CM
Mediodorsal thalamic nucleus	TH-MD
Ventral posterior thalamic nucleus	TH-VP
Hypothalamus	
Paraventricular hypothalamic nucleus	HyTH-PVN
Arcuate hypothalamic nucleus	HyTH-ARC
Ventromedial hypothalamic nucleus	HyTH-VM
Dorsomedial hypothalamic nucleus	HyTH-DM
Lateral hypothalamic area	HyTH-LH
Posterior hypothalamic area	HyTH-PH
Midbrain	
Dorsomedial periaqueductal gray	PAG-DM
Lateral periaqueductal gray	PAG-L

Statistical Analyses

All data are expressed as mean ± standard error (SEM). The statistical data were analyzed by two-way ANOVA followed by Bonferroni post-tests or one-way ANOVA, followed by Newman-Keul's post-tests using GraphPad Prism 5.0 (GraphPad Software Inc., CA, USA). The significance was set at $p < 0.05$ for all experiments.

RESULTS

AP Acupuncture Treatment Improves CRS-Induced Depressive-Like Behavior

To investigate the anti-depressive effect of acupuncture treatment, we established a murine model of depressive-like behavior by 2 or 4 weeks of CRS. Then, acupuncture treatment, consisting of a specific combination of acupoints (KI10·LR8·LU8·LR4) was performed for 1 week (on the 2-week CRS model) or 2 weeks (on the 4-week CRS model). In the 2-week CRS model, CRS significantly decreased the total distance traveled and the zone transition number, as compared to the NOR mice ($p < 0.001$). Acupuncture treatment at the KI10·LR8·LU8·LR4 points significantly restored the total distance and the zone transition number as compared to the CRS group ($p < 0.001$). However, acupuncture treatment at the non-acupoints (NP group) did not have this rescue effect (**Figures 2A–C**). In the 4-week CRS model, acupuncture treatment at KI10·LR8·LU8·LR4 significantly rescued the decreased total distance as compared to the CRS and NP group ($p < 0.05$) (**Figures 2D–F**).

Effects of Acupuncture Treatment at AP and mAP Points on 2 Weeks CRS-Induced Depressive-Like Behavior

Since AP treatment involved a combination of four acupoints and NP involved a single point, there was a possibility that the effect of AP treatment was more pronounced than NP treatment due to the intensity of the stimulation. Thus, we validated the therapeutic effect of AP in comparison to other combinations of four acupoints (CP; LU8·LR4·HT8·LR2). We found that AP treatment significantly rescued the decreased total distance ($p < 0.001$); the total distance traversed was significantly higher in the AP group than in the CP and NP groups (both $p < 0.001$). There was a similar trend in the zone transition number, but it did not reach statistical significance (**Figures 3A,B**).

Since acupuncture treatment at the AP (KI10·LR8·LU8·LR4) improved depression, while that at the CP (LU8·LR4·HT8·LR2) did not, we hypothesized that among the four acupoints in AP, KI10 and LR8 (mAP) were the major points involved in the therapeutic effect. As expected, the mAP group showed a significant improvement in depressive-like behavior ($p < 0.01$), similar to the AP group, and the AP while the mAP groups were significantly higher in both total travel

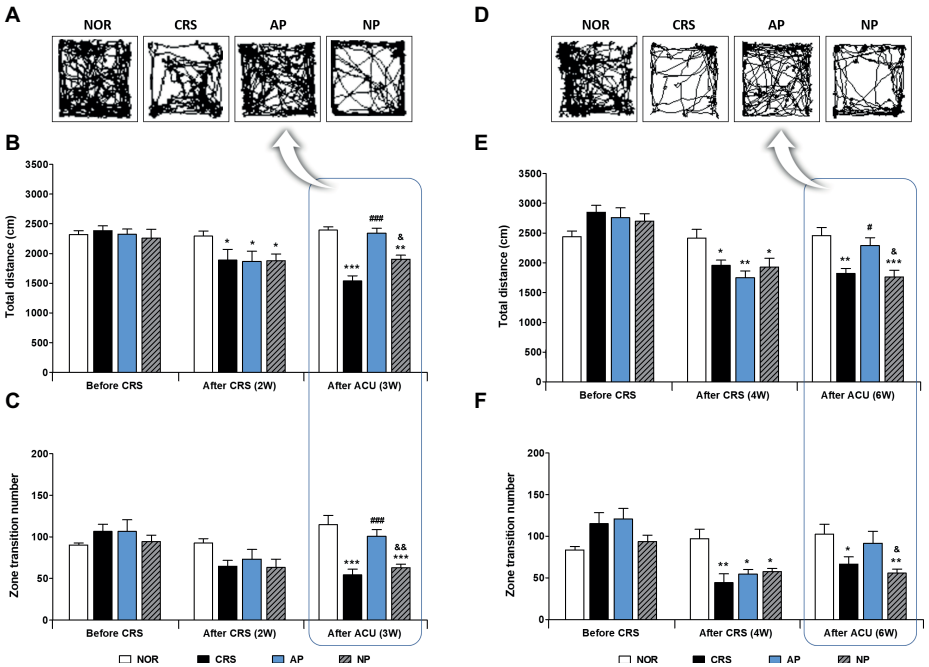

FIGURE 2 | Acupuncture treatment at the AP (KI10·LR8·LU8·LR4) can reverse chronic restraint stress (CRS)-induced depressive-like behavior, as compared to non-acupoint treatment. Acupuncture treatment at KI10·LR8·LU8·LR4 significantly reversed the decrease in the total distance and the number of zone transitions caused by CRS (AP vs. CRS and non-acupoint treatment group) in both the 2-week **(A–C)** and 4-week CRS models **(D–F)**. NOR, normal; AP, CRS and acupuncture treatment at KI10·LR8·LU8·LR4; NP, CRS and acupuncture treatment at non-acupoints on the hips. $^{*}p < 0.05$, $^{**}p < 0.01$, $^{***}p < 0.001$ vs. NOR. $^{\#}p < 0.05$, $^{\#\#\#}p < 0.001$ vs. CRS. $^{\&}p < 0.05$, $^{\&\&}p < 0.01$ vs. AP. Two-way ANOVA followed by the Bonferroni test. Error bars indicate SEM.

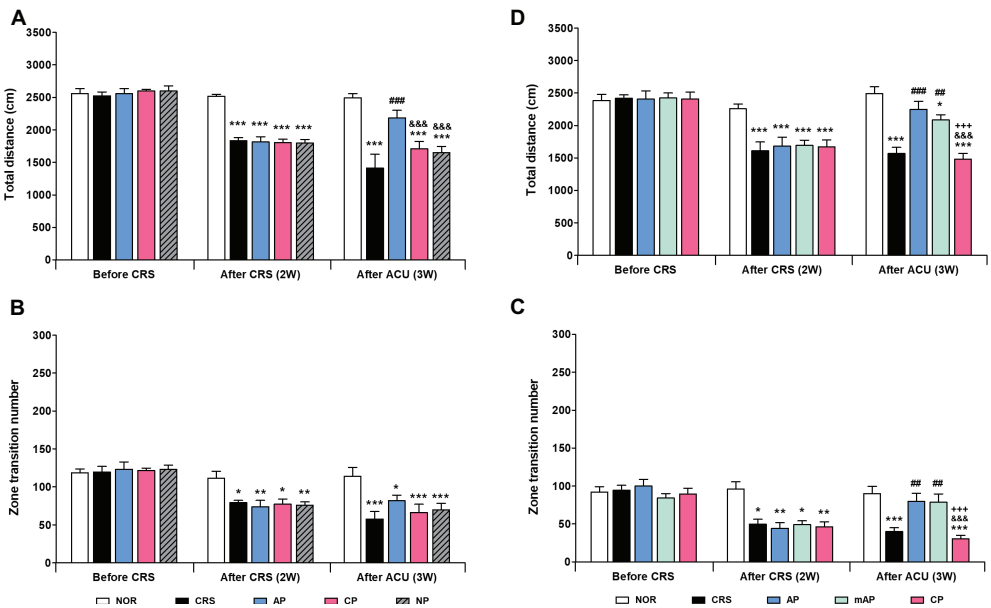

FIGURE 3 | Acupuncture treatment at AP (KI10·LR8·LU8·LR4) and mAP (KI10·LR8) can reverse chronic restraint stress (CRS)-induced depressive-like behavior. **(A,B)** Acupuncture treatment at AP (KI10·LR8·LU8·LR4) significantly reversed the decrease in the total distance and the number of zone transitions caused by CRS (AP vs. CRS, CP, and NP treatment groups). Acupuncture treatment at AP and mAP significantly reversed the decrease in the total distance and the number of zone transitions compared to the CRS and CP treatment groups **(C,D)**. NOR, normal; AP, CRS and acupuncture treatment at KI10·LR8·LU8·LR4; mAP, CRS and acupuncture treatment at KI10·LR8; CP, CRS and acupuncture treatment at LU8·LR4·HT8·LR2; NP, CRS and acupuncture treatment at non-acupoints on the hips. $^{*}p < 0.05$, $^{**}p < 0.01$, $^{***}p < 0.001$ vs. NOR. $^{\#\#}p < 0.01$, $^{\#\#\#}p < 0.001$ vs. CRS. $^{\&\&\&}p < 0.001$ vs. AP. $^{+++}p < 0.001$ vs. mAP. Two-way ANOVA followed by the Bonferroni test. Error bars indicate SEM.

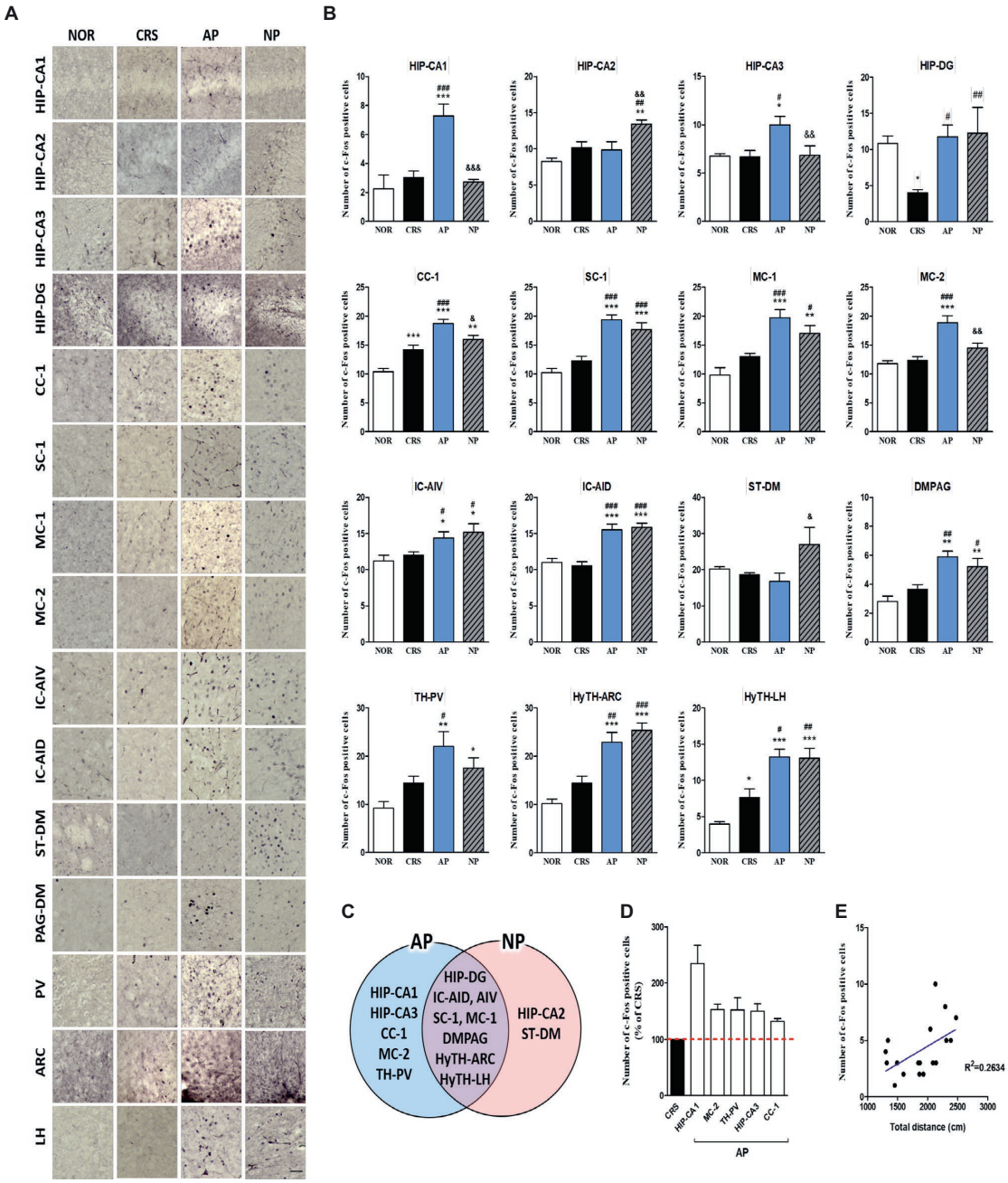

FIGURE 4 | Acupuncture treatment at AP (KI10·LR8·LU8·LR4) causes changes in c-Fos expression in the brain in a 2-week CRS murine model. **(A,B)** Acupuncture treatment at AP (KI10·LR8·LU8·LR4) significantly increased c-Fos activation in specific regions of the cortex, cerebral nuclei, hippocampus, thalamus, hypothalamus, and midbrain. **(C)** Schematic Venn diagram representing the brain areas activated only by AP, only by NP, or by both stimuli. **(D)** Number of c-Fos-positive cells in brain regions changed only by acupuncture treatment (% of CRS group value). **(E)** Correlation between the c-Fos expression of HIP-CA1 and behavioral patterns in CRS, AP and NP group. NOR, normal; AP, CRS and acupuncture treatment at KI10·LR8·LU8·LR4; NP, CRS and acupuncture treatment at non-acupoints on the hips. $^{*}p < 0.05$, $^{**}p < 0.01$, $^{***}p < 0.001$ vs. NOR. $^{\#}p < 0.05$, $^{\#\#}p < 0.01$, $^{\#\#\#}p < 0.001$ vs. CRS. $^{\&}p < 0.05$, $^{\&\&}p < 0.01$, $^{\&\&\&}p < 0.001$ vs. AP. One-way ANOVA followed by the Newman-Keuls test. Error bars indicate SEM.

distance and zone transition number than that of the CP group (both $p < 0.001$) (**Figures 3C, D**). This indicated that KI10·LR8·LU8·LR4, but particularly at KI10 and LR8, are the acupuncture points involved in the improvement of symptoms of depression.

Acupuncture Treatment at AP Induces Brain Neural Activity in the CRS Model

To investigate the therapeutic mechanism of acupuncture, we analyzed how brain neural activity changed after acupuncture treatment. We used activation of the immediate early gene

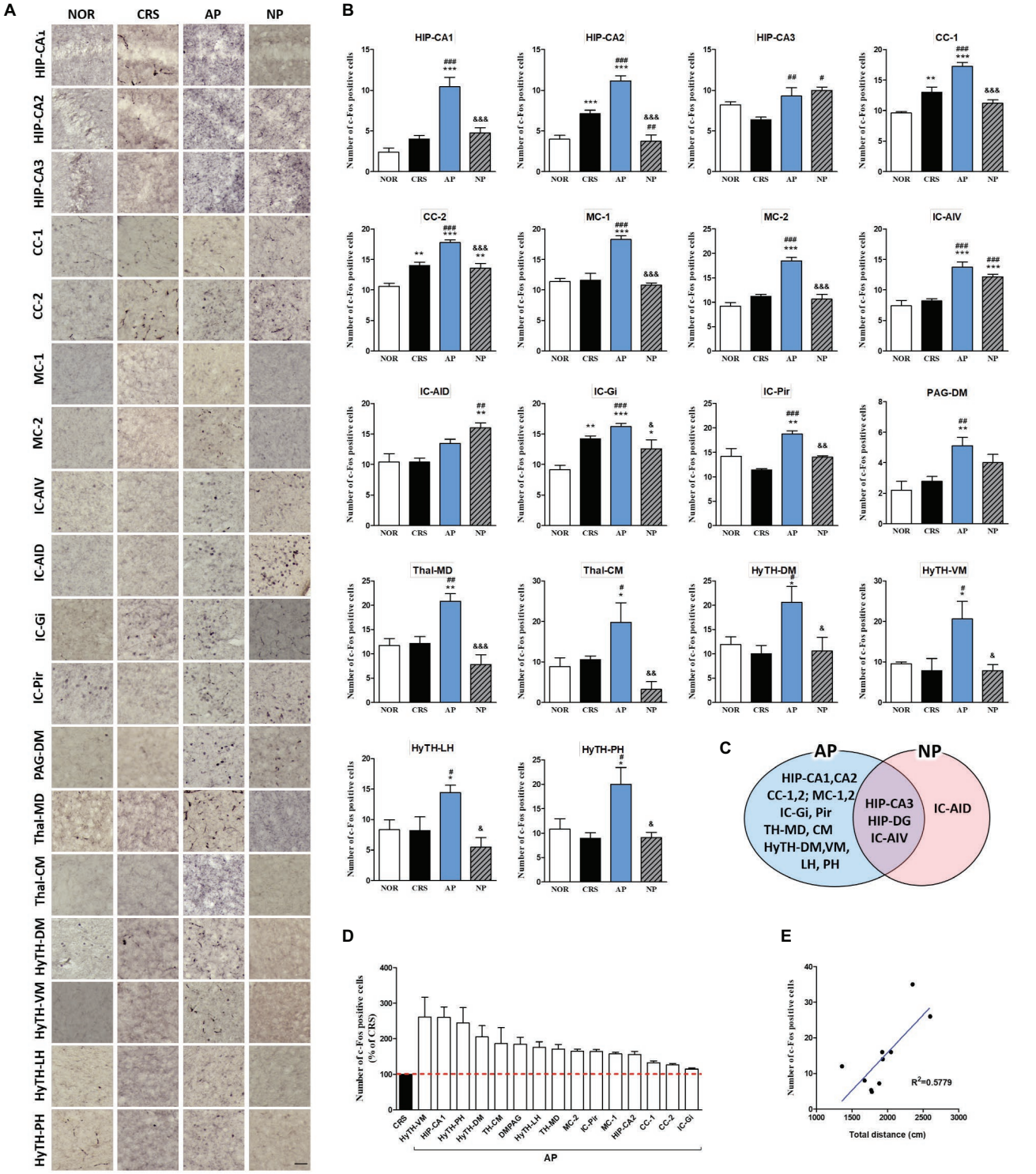

FIGURE 5 | Acupuncture treatment at AP (KI10·LR8·LU8·LR4) causes changes in c-Fos expression in the brains of 4-week CRS model mice. **(A,B)** Acupuncture treatment at AP (KI10·LR8·LU8·LR4) significantly increased c-Fos activation in specific regions of the cortex, hippocampus, thalamus, and hypothalamus. **(C)** Schematic Venn diagram represents brain areas activated only by AP, only by NP, or by both stimuli. **(D)** Number of c-Fos-positive cells in brain regions changed only by acupuncture treatment (% of CRS group value). **(E)** Correlation between the c-Fos expression of HyTH-VM and behavioral patterns in CRS, AP, and NP groups. NOR, normal; AP, CRS and acupuncture treatment at KI10·LR8·LU8·LR4; NP, CRS and acupuncture treatment at non-acupoints on the hips. $^{*}p < 0.05$, $^{**}p < 0.01$, $^{***}p < 0.001$ vs. NOR. $^{\#}p < 0.05$, $^{\#\#}p < 0.01$, $^{\#\#\#}p < 0.001$ vs. CRS. $^{\&}p < 0.05$, $^{\&\&}p < 0.01$, $^{\&\&\&}p < 0.001$ vs. AP. One-way ANOVA followed by the Newman-Keuls test. Error bars indicate SEM.

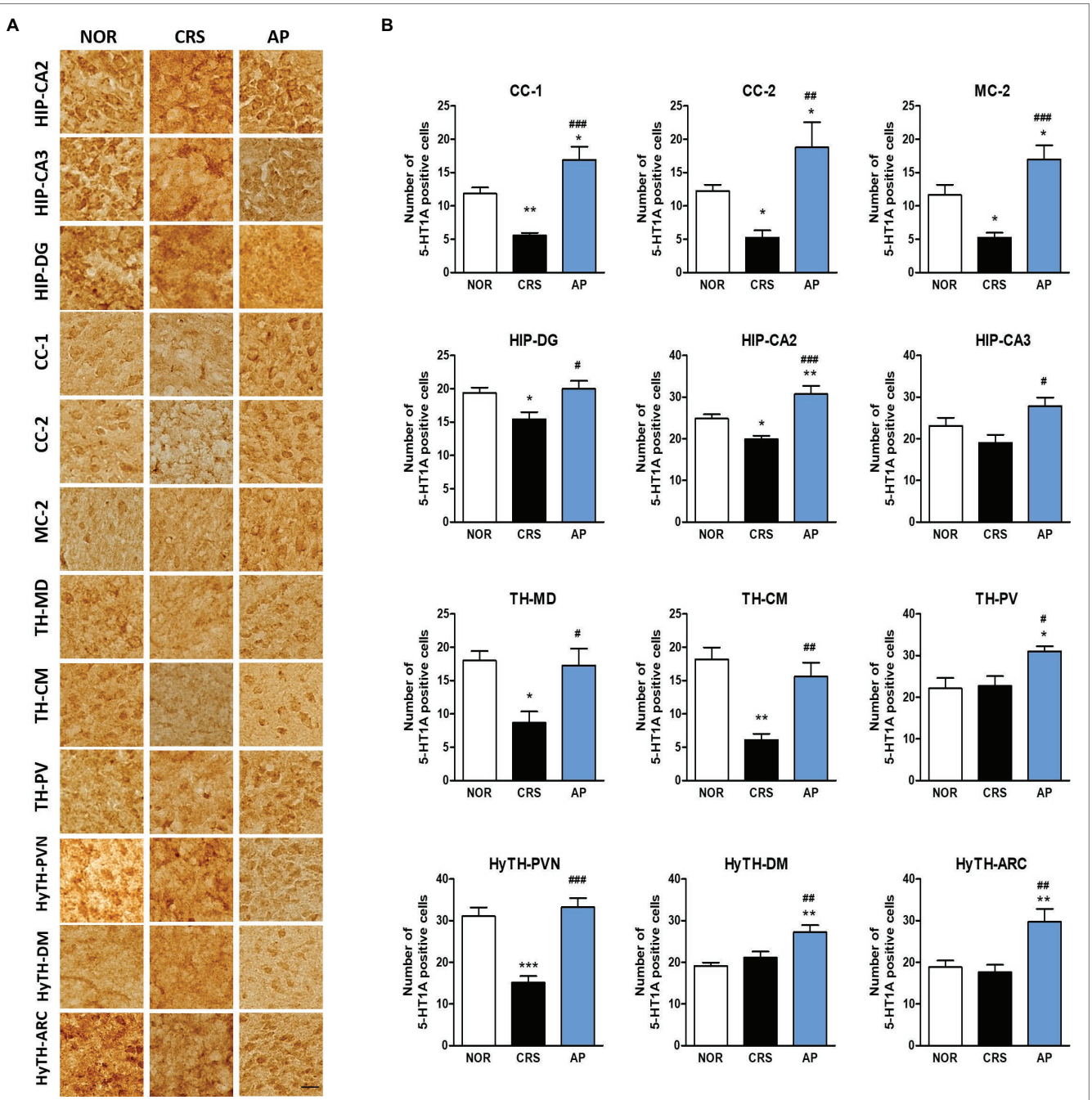

FIGURE 6 | Acupuncture treatment at AP (KI10·LR8·LU8·LR4) changes 5-HT1A receptor expression in the cortex, hippocampus, thalamus, and hypothalamus. **(A,B)** Acupuncture treatment at AP (KI10·LR8·LU8·LR4) significantly increased 5-HT1A expression in the cortex, hippocampus, thalamus, and hypothalamus as compared to the CRS group. NOR, normal; AP, CRS and acupuncture treatment at KI10·LR8·LU8·LR4; NP, CRS and acupuncture treatment at non-acupoints on the hips. $^{*}p < 0.05$, $^{**}p < 0.01$, $^{***}p < 0.001$ vs. NOR. $^{\#}p < 0.05$, $^{\#\#}p < 0.01$, $^{\#\#\#}p < 0.001$ vs. CRS. One-way ANOVA followed by the Newman-Keuls test. Error bars indicate SEM.

c-Fos as a marker of neuronal activity, according to previous studies (Chen et al., 2013; Wheeler et al., 2013). c-Fos activation was slightly lower in the hippocampus and hypothalamus of the 2-week CRS group, and AP increased the c-Fos activation in the hippocampus, thalamus, hypothalamus, and anterior cingulate cortex, as compared to the CRS group, but the difference was not statistically significant (**Supplementary Figures S2A–D**).

For more detailed observations, we observed c-Fos activity by subdividing the cortex, cerebral nuclei, hippocampus,

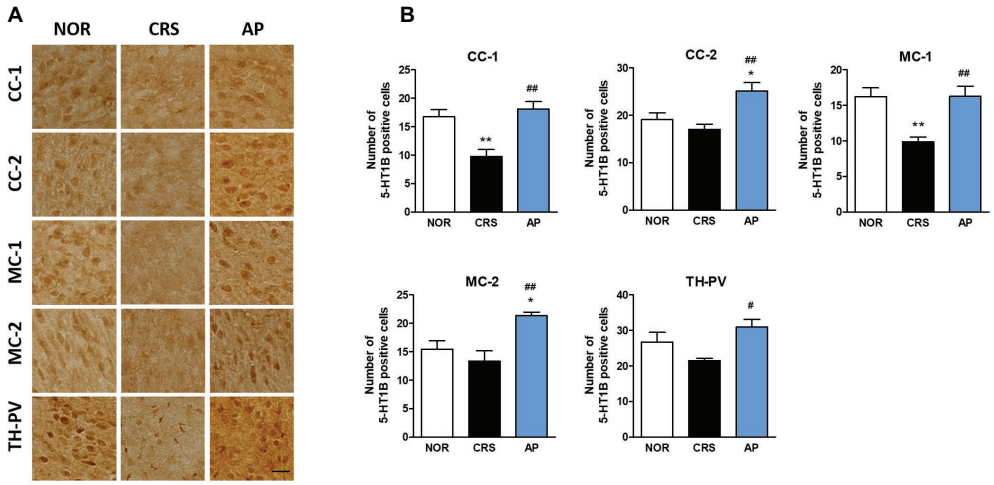

FIGURE 7 | Acupuncture treatment at AP (KI10·LR8·LU8·LR4) changes 5-HT1B receptor expression in the cortex, hippocampus, thalamus, and hypothalamus. **(A,B)** Acupuncture treatment at AP (KI10·LR8·LU8·LR4) significantly increased 5-HT1B receptor expression in the cortex and thalamus as compared to the CRS group. NOR, normal; AP, CRS and acupuncture treatment at KI10·LR8·LU8·LR4; NP, CRS and acupuncture treatment at non-acupoints on the hips. $^{*}p < 0.05$, $^{**}p < 0.01$ vs. NOR. $^{\#}p < 0.05$, $^{\#\#}p < 0.01$ vs. CRS. One-way ANOVA followed by the Newman-Keuls test. Error bars indicate SEM.

thalamus, hypothalamus, and the midbrain regions into a total of 30 regions. We observed significant changes in 15 of the 30 regions in the 2-week CRS model. c-Fos activation in the CA1 and CA3 of the hippocampus (HIP-CA1, HIP-CA3), cingulate cortex area 1 (CC-1), secondary motor cortex (MC-2), and paraventricular thalamic nucleus (TH-PV) was significantly increased after AP, but no other treatment. c-Fos activation in the dentate gyrus (HIP-DG), dorsal part of the insular cortex (IC-AID), ventral part of the insular cortex (IC-AIV), primary somatosensory cortex (SC-1), primary motor cortex (MC-1), arcuate nucleus of the hypothalamus (HyTH-ARC), lateral hypothalamic area (HyTH-LH), and dorsomedial periaqueductal gray (PAG-DM) was increased by both of AP and NP treatment. c-Fos activation in HIP-CA2 and the dorsomedial part of the striatum (ST-DM) was increased only after NP treatment (**Figures 4A–C**). Among the brain regions changed by AP, CA1 demonstrated the greatest change in comparison to the CRS group (**Figure 4D**). In the CRS, AP, and NP groups, c-Fos expression in CA1 showed a positive correlation with the results of the total distance travelled in the open field test ($p < 0.05$) (**Figure 4E**).

In the 4-week CRS model, c-Fos activation in the HIP-CA1, HIP-CA2, CC-1, cingulate cortex area 2 (CC-2), MC-1, MC-2, granular insular cortex (IC-Gi), piriform cortex (Pir), PAG-DM, mediodorsal thalamic nucleus (TH-MD), central medial thalamic nucleus (TH-CM), dorsomedial hypothalamic nucleus (HyTH-DM), ventromedial hypothalamic nucleus (HyTH-VM), HyTH-LH, and posterior hypothalamic area (HyTH-PH) was significantly increased only after AP treatment. c-Fos activation in the HIP-CA3 and IC-AIV was increased by both AP and NP treatment. c-Fos activation in the IC-AID was increased only after NP treatment (**Figures 5A–C**). Among the brain regions changed by AP treatment, HyTH-VM demonstrated the most change as compared to the CRS group (**Figure 5D**). In the CRS, AP, and NP groups, c-Fos expression in the HyTH-VM showed a positive correlation with the total distance travelled in the open field test ($p < 0.01$) (**Figure 5E**).

These results indicated that the cortex, hippocampus, thalamus, and the hypothalamus, which were the only regions changed by AP treatment, were the main regions mediating the therapeutic effect of acupuncture treatment.

Regulation of 5-HT1A and 5-HT1B Receptors by AP Treatment

We further investigated whether acupuncture treatment at KI10·LR8·LU8·LR4 affected the expression of serotonin receptors. We analyzed the activation of 5-HT1A and 5-HT1B receptors in 25 brain regions of the cortex, hippocampus, thalamus, and the hypothalamus, which were identified as the main regions involved in mediating the effect of acupuncture on c-Fos expression. CRS significantly decreased 5-HT1A receptor activation in the CC-1, CC-2, MC-2, HIP-DG, HIP-CA2, TH-MD, TH-CM, and paraventricular hypothalamic nucleus (HyTH-PVN) as compared to the NOR group. Acupuncture treatment at KI10·LR8·LU8·LR4 significantly increased 5-HT1A receptor activation in the CC-1, CC-2, MC-2, HIP-DG, HIP-CA2, HIP-CA3, TH-MD, TH-CM, TH-PV, HyTH-PVN, HyTH-DM, and HyTH-ARC as compared to the CRS group (**Figures 6A,B**).

CRS significantly decreased 5-HT1B receptor activation in the CC-1 and MC-1 compared to the NOR group. AP treatment significantly increased 5-HT1B receptor activation in the CC-1, CC-2, MC-1, MC-2, and TH-PV as compared to the CRS group (**Figures 7A,B**).

These results indicate that the effect of acupuncture treatment was mediated *via* central brain neural activity and modulation of serotonin receptors.

DISCUSSION

To the best of our knowledge, this study is the first to identify the effect of acupoint combination of KI10·LR8·LU8·LR4 in chronic stress-induced depressive-like behavior and its neural mechanism. In this study, we found that acupuncture treatment at KI10·LR8·LU8·LR4 was effective in improving CRS-induced depressive-like behavior, and that among these four acupoints, KI10 and LR8 were the major acupoints effective in the treatment of depressive-like symptoms. Moreover, we also found that this behavioral improvement was mediated by brain neuronal activity involving the modulation of serotonin receptor expression in specific brain regions.

Sa-am acupuncture is a unique Korean traditional acupuncture method developed by Sa-am in the seventeenth century A.D. and most widely adopted by Korean medical doctors in the clinic (Han et al., 2005). Sa-am acupuncture uses *five-transporting points* according to the principle of tonification and sedation. The combination of KI10·LR8·LU8·LR4, called Liver-tonification, has been reported as the most commonly used acupoint combination in Sa-am acupuncture (Yoon et al., 2018), and is used to treat a variety of pain and psychological conditions, such as depression (Kim, 2006; Yoon et al., 2018). However, despite being widely used clinically, few studies have reported the effect of the KI10·LR8·LU8·LR4 acupoint combination, and no animal studies to date have identified its therapeutic effects and underlying biological mechanisms.

In our study, we found that the acupuncture treatment at KI10·LR8·LU8·LR4 significantly improved depressive-like behavior in mice, as compared to non-acupoint treatment on the hips and at control points (LU8·LR4·HT8·LR2). The LU8·LR4·HT8·LR2 combination has been reported to be effective in reducing anxiety (Kim, 1998, 2006; Yoon et al., 2018), which shows a different pathological phenotype to that of depression. This combination also involves four acupoints and can thus exert the same amount of stimulation as the AP combination. Therefore, the difference in effectiveness between the two groups is not due to the amount of stimulation, but due to specific acupoints. We demonstrated that KI10·LR8·LU8·LR4, and particularly KI10 and LR8, play a pivotal role in improving depressive-like behavior. In order to establish a more precise basis in future, it will be necessary to study the therapeutic efficacy of each acupuncture point specifically and define the related mechanism.

To elucidate the therapeutic mechanisms of depression, researchers have focused on the brain, which controls all sensory and behavioral modulations (MacPherson et al., 2016). Since previous studies have reported that hippocampal atrophy occurs with depression (Bremner et al., 2000), and that the hippocampus plays an important role in the pathophysiology of major depressive disorder (Campbell and MacQueen, 2004), the hippocampus has been studied as a major component in the mechanism involved in the treatment of depression. Recently, research has shown that not only the hippocampus but also the prefrontal cortex, thalamus, and hypothalamus are closely related to depression (Pang et al., 2015; Treadway et al., 2015; Kasahara et al., 2016). Stress response is mainly mediated by the hypothalamic-pituitary-adrenal (HPA) axis, and the hypothalamus is a key brain region that has various functions in modulating the endocrine and autonomic nervous systems. The anterior cingulate cortex, amygdala, and hippocampus are anatomically linked to the hypothalamus and midbrain, and interconnected with the prefrontal-limbic network that is strongly related to depressive disorders (Bao et al., 2008; Bennett, 2011).

Previous studies indicated that acupuncture modulates activity within specific brain areas, including the somatosensory-motor cortices, limbic system, basal ganglia and brain stem (Chae et al., 2009; Huang et al., 2011) in healthy subjects. These brain responses reflect acupuncture stimuli-related brain regions. In particular, acupuncture treatment has been reported to cause therapeutic effects by activation of neurons in brain regions such as the somatosensory and motor cortex, prefrontal cortex, cingulate cortex, insular cortex, limbic area, and the hypothalamus (Park et al., 2017a,b). Based on this preliminary report, we found that the therapeutic effect of acupuncture is exerted by a combination of acupuncture stimulated brain regions and disease-related brain regions. Therefore, we broadly selected brain regions that are related to acupuncture stimuli and depression, and then analyzed neural activation in each brain region to identify the acupuncture mechanism by assessing central neural activity. We noted changes in neuronal activity in 15 (2-week CRS model) and 18 (4-week CRS model) of the 30 brain regions. The altered brain area could be divided into the area changed only by AP treatment (at KI10·LR8·LU8·LR4), the area changed only by NP treatment (non-acupoints on the hip), and the area changed by both AP and NP stimulation. The effects of acupuncture therapy included the specific effects of acupuncture as well as nonspecific effects (placebo effect) of acupuncture. Therefore, the brain areas changed by non-acupoint stimulation is thought to be related to the nonspecific effect of acupuncture treatment, and the brain areas changed only by AP treatment (HIP-CA1, HIP-CA3, CC-1, MC-2, and TH-PV in the 2-week CRS model; HIP-CA1, HIP-CA2, CC-1, CC-2, MC-1, MC-2, IC-Gi, IC-Pir, TH-MD, TH-CM, HyTH-DM, HyTH-VM, HyTH-LH, and HyTH-PH in the 4-week CRS model), are considered to be the main brain areas representing the specific effects of acupuncture.

From these results, we could identify that the hippocampus, cingulate cortex, motor cortex, and the thalamus function as important brain regions that exert acupuncture effects. The thalamus acts as a hub that relays information between different subcortical brain areas and the cerebral cortex. It receives sensory signals and sends them to the cortical area (Hwang et al., 2017). The cingulate cortex receives inputs from the thalamus and the neocortex, and projects them to the other brain regions. It integrates the limbic system, which is involved in emotional changes, learning, and memory (Hayden and Platt, 2010). These brain regions are related to both acupuncture signaling transduction and modulating depression. Changes in the motor cortex may be particularly associated with the behavioral improvement of mice.

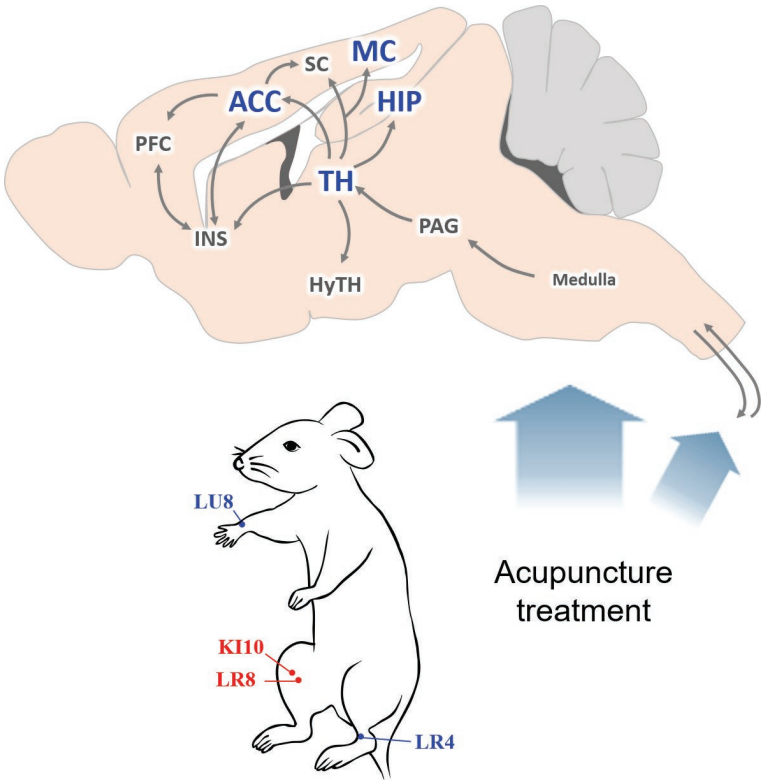

FIGURE 8 | Schematic diagram of the neural mechanism by which acupuncture at AP (KI10·LR8·LU8·LR4) affects depressive-like behavior. A proposed central neural mechanism by which effects of acupuncture needling are exerted. Acupuncture-induced signaling are received by the peripheral nerve endings and are then transmitted to the afferent sensory nervous tract. Brain regions, such as the thalamus, hippocampus, motor cortex, and anterior cingulate cortex are involved in acupuncture-mediated central signals. ACC, anterior cingulate cortex; HIP, hippocampus; HyTH, hypothalamus; INS, insular cortex; MC, motor cortex; PAG, periaqueductal gray; PFC, prefrontal cortex; SC, somatosensory cortex; TH, thalamus.

The neuronal activity in the brain regions associated with the specific effects of acupuncture was prominently increased in the 4-week model as compared to the 2-week model, suggesting that, the longer the treatment period of acupuncture, the more prominent the specific rather than the nonspecific effect was. Moreover, the insular cortex, PAG, and hypothalamic brain areas with increased c-Fos in the 4-week model may be associated with long-term therapeutic effects of acupuncture.

For further mechanistic studies, we observed the expression of serotonin receptors in the core brain regions associated with acupuncture treatment effects. Among the serotonin receptors, 5-HT1A and 5-HT1B receptors have been extensively studied (Savitz et al., 2009). Increased 5-HT1A receptor expression is known to be associated with an improvement in both depressive and anxiety behaviors, while the 5-HT1B receptor plays a role in regulating impulsive behavior, reward, and depression (Heisler et al., 1998; Parks et al., 1998; Knobelman et al., 2001; Parsons et al., 2001). We found that AP treatment increased 5-HT1A receptor expression in the hippocampus, cingulate cortex, motor cortex, thalamus, and the hypothalamus, and 5-HT1B receptor expression in the cingulate cortex, motor cortex, and the thalamus.

Based on our results, we hypothesize that a central neural mechanism underlies the effect of KI10·LR8·LU8·LR4 acupuncture treatment (**Figure 8**). Acupuncture stimulation at KI10·LR8·LU8·LR4 is likely received by peripheral nerve endings, which is then transmitted to the afferent sensory nervous tract. These mechanical signals from the spinal cord might be transmitted to the thalamus, then to the cingulate cortex, somatosensory/motor cortex, insular cortex, and the hippocampus. The thalamus transmits signals to the hypothalamic area, which are then relayed back to the pons and medulla, activating the descending neuronal pathway that provokes the acupuncture effect.

Thus, we found that signal transmission in the brain of a depressive mouse model differed, depending on the acupuncture points used, and the effect of acupuncture correlated with the expression of serotonergic receptors. Although depression studies have mainly focused on the hippocampus, further studies of the prefrontal cortex, thalamus, and hypothalamus are needed. In addition, an analysis of correlations of proteins such as CREB, ERK, and BDNF, in addition to serotonin, is necessary to elucidate the mechanism underlying acupuncture therapeutic effects.

Acupuncture treatment at KI10·LR8·LU8·LR4 was effective in alleviating depressive-like behavior in mice. This therapeutic

effect was produced by the modulation of central neural activity and 5-HT1A/B receptor expression in various brain regions of the hippocampus, cortex, thalamus, and the hypothalamus. In future, the effect of the acupoint combination KI10·LR8·LU8·LR4 needs to be clarified in various diseases, and its neurobiological mechanism of acupuncture requires further elucidation to improve our knowledge of the fundamental mechanism.

ETHICS STATEMENT

This study was carried out in accordance with recommendations in the guidelines for the Care and Use of Laboratory Animals of the National Institutes of Health. All experimental protocols used in this study were approved by the Institutional Animal Care and Use Committee (IACUC) at Daejeon University (approval no. DJUARB2016-40).

AUTHOR CONTRIBUTIONS

M-JL performed immunostaining, data analysis and drafted the manuscript. J-SR performed animal behavioral tests, immunostaining and data analysis. S-KW performed animal behavioral tests and western blotting. JJ, S-ML, and UN contributed to the conception of the work and assisted with protocol development. J-YP designed the study, coordinated the acquisition of all study data, interpretation of results and writing of the article. All co-authors were involved in critical revision of initial drafts.

FUNDING

This research was supported by the Korea Institute of Oriental Medicine (K17860) and the Basic Science Research Program through the National Research Foundation of Korea (NRF) funded by the Ministry of Science, ICT & Future Planning (NRF-2018R1C1B3004424 and NRF-2018R1A 6A1A03025221).

ACKNOWLEDGMENTS

The authors would like to thank Mr. Se-gun Kim and Ms. Geun-Hyang Eom for their help with the animal experiment and all the present and past members of the labs for support and insightful discussions.

SUPPLEMENTARY MATERIAL

The Supplementary Material for this article can be found online at: https://www.frontiersin.org/articles/10.3389/fpsyg.2019.01353/full#supplementary-material

REFERENCES

Baerwald, C., Manger, B., and Hueber, A. (2019). Depression as comorbidity of rheumatoid arthritis. *Z. Rheumatol.* 78, 243–248. doi: 10.1007/s00393-018-0568-5

Bair, M. J., Robinson, R. L., Katon, W., and Kroenke, K. (2003). Depression and pain comorbidity: a literature review. *Arch. Intern. Med.* 163, 2433–2445. doi: 10.1001/archinte.163.20.2433

Bao, A. M., Meynen, G., and Swaab, D. (2008). The stress system in depression and neurodegeneration: focus on the human hypothalamus. *Brain Res. Rev.* 57, 531–553. doi: 10.1016/j.brainresrev.2007.04.005

Bennett, M. (2011). The prefrontal–limbic network in depression: modulation by hypothalamus, basal ganglia and midbrain. *Prog. Neurobiol.* 93, 468–487. doi: 10.1016/j.pneurobio.2011.01.006

Bram, A. D., Gottschalk, K. A., and Leeds, W. M. (2018). Emotional regulation in women with chronic fatigue syndrome and depression: internal representations and adaptive defenses. *J. Am. Psychoanal. Assoc.* 66, 701–741. doi: 10.1177/0003065118798043

Bremner, J. D., Narayan, M., Anderson, E. R., Staib, L. H., Miller, H. L., and Charney, D. S. (2000). Hippocampal volume reduction in major depression. *Am. J. Psychiatry* 157, 115–118. doi: 10.1176/ajp.157.1.115

Campbell, S., and MacQueen, G. (2004). The role of the hippocampus in the pathophysiology of major depression. *J. Psychiatry Neurosci.* 29, 417–426.

Chae, Y., Lee, H., Kim, H., Kim, C. H., Chang, D. I., Kim, K. M., et al. (2009). Parsing brain activity associated with acupuncture treatment in Parkinson's diseases. *Mov. Disord.* 24, 1794–1802. doi: 10.1002/mds.22673

Chan, Y. Y., Lo, W. Y., Yang, S. N., Chen, Y. H., and Lin, J. G. (2015). The benefit of combined acupuncture and antidepressant medication for depression: a systematic review and meta-analysis. *J. Affect. Disord.* 176, 106–117. doi: 10.1016/j.jad.2015.01.048

Chen, C.-Y., Chern, R.-S., Liao, M.-H., Chang, Y.-H., Hsu, J. Y., and Chien, C.-H. (2013). The possible neuronal mechanism of acupuncture: morphological evidence of the neuronal connection between groin A-shi point and uterus. *Evid. Based Complement. Alternat. Med.* 2013:429186. doi: 10.1155/2013/821813

Cho, S. Y., Shim, S. R., Rhee, H. Y., Park, H. J., Jung, W. S., Moon, S. K., et al. (2012). Effectiveness of acupuncture and bee venom acupuncture in idiopathic Parkinson's disease. *Parkinsonism Relat. Disord.* 18, 948–952. doi: 10.1016/j.parkreldis.2012.04.030

Drevets, W. C., Savitz, J., and Trimble, M. (2008). The subgenual anterior cingulate cortex in mood disorders. *CNS Spectr.* 13, 663–681. doi: 10.1017/S1092852900013754

Dunn, E. C., Brown, R. C., Dai, Y., Rosand, J., Nugent, N. R., Amstadter, A. B., et al. (2015). Genetic determinants of depression: recent findings and future directions. *Harv. Rev. Psychiatry* 23, 1–18. doi: 10.1097/HRP.0000000000000054

Eisch, A. J., and Petrik, D. (2012). Depression and hippocampal neurogenesis: a road to remission? *Science* 338, 72–75. doi: 10.1126/science.1222941

Eshkevari, L., Egan, R., Phillips, D., Tilan, J., Carney, E., Azzam, N., et al. (2012). Acupuncture at ST36 prevents chronic stress-induced increases in neuropeptide Y in rat. *Exp. Biol. Med.* 237, 18–23. doi: 10.1258/ebm.2011.011224

Fried, I., MacDonald, K. A., and Wilson, C. L. (1997). Single neuron activity in human hippocampus and amygdala during recognition of faces and objects. *Neuron* 18, 753–765. doi: 10.1016/S0896-6273(00)80315-3

Gijsman, H. J., Geddes, J. R., Rendell, J. M., Nolen, W. A., and Goodwin, G. M. (2004). Antidepressants for bipolar depression: a systematic review of randomized, controlled trials. *Am. J. Psychiatry* 161, 1537–1547. doi: 10.1176/appi.ajp.161.9.1537

Goldenberg, D. L. (2010). Pain/depression dyad: a key to a better understanding and treatment of functional somatic syndromes. *Am. J. Med.* 123, 675–682. doi: 10.1016/j.amjmed.2010.01.014

Hammen, C. (2005). Stress and depression. *Annu. Rev. Clin. Psychol.* 1, 293–319. doi: 10.1146/annurev.clinpsy.1.102803.143938

Han, C., Park, J., and Ahn, S. (2005). A survey about the recognition regarding the Korean acupuncture method and research direction. *J. Kor. Med. Hist.* 18, 89–101.

Hayden, B. Y., and Platt, M. L. (2010). Neurons in anterior cingulate cortex multiplex information about reward and action. *J. Neurosci.* 30, 3339–3346. doi: 10.1523/JNEUROSCI.4874-09.2010

Heisler, L. K., Chu, H. M., Brennan, T. J., Danao, J. A., Bajwa, P., Parsons, L. H., et al. (1998). Elevated anxiety and antidepressant-like responses in serotonin 5-HT1A receptor mutant mice. *Proc. Natl. Acad. Sci. USA* 95, 15049–15054.

Holtzheimer, P. E. 3rd, and Nemeroff, C. B. (2006). Advances in the treatment of depression. *NeuroRx* 3, 42–56. doi: 10.1016/j.nurx.2005.12.007

Huang, Y., Xiao, H., Chen, J., Qu, S., Zheng, Y., Lu, Y., et al. (2011). Needling at the Waiguan (SJ5) in healthy limbs deactivated functional brain areas in ischemic stroke patients: a functional magnetic resonance imaging study. *Neural Regen. Res.* 6, 2829–2833. doi: 10.3969/j.issn.1673-5374.2011.36.005

Hwang, K., Bertolero, M. A., Liu, W. B., and D'esposito, M. (2017). The human thalamus is an integrative hub for functional brain networks. *J. Neurosci.* 37, 5594–5607. doi: 10.1523/JNEUROSCI.0067-17.2017

Kasahara, T., Takata, A., Kato, T. M., Kubota-Sakashita, M., Sawada, T., Kakita, A., et al. (2016). Depression-like episodes in mice harboring mtDNA deletions in paraventricular thalamus. *Mol. Psychiatry* 21, 39–48. doi: 10.1038/mp.2015.156

Kim, D. (1998). *(Kyo Kam) Sa-Ahm's acupuncture method*. (Busan: Sogang).

Kim, G. (2006). *Essays for Sa-am acupuncture therapy*. (Daejeon: Chorakdang).

Kim, E. J., Pellman, B., and Kim, J. J. (2015). Stress effects on the hippocampus: a critical review. *Learn. Mem.* 22, 411–416. doi: 10.1101/lm.037291.114

Knobelman, D. A., Hen, R., and Lucki, I. (2001). Genetic regulation of extracellular serotonin by 5-hydroxytryptamine(1A) and 5-hydroxytryptamine(1B) autoreceptors in different brain regions of the mouse. *J. Pharmacol. Exp. Ther.* 298, 1083–1091.

Kohler, S., Cierpinsky, K., Kronenberg, G., and Adli, M. (2016). The serotonergic system in the neurobiology of depression: relevance for novel antidepressants. *J. Psychopharmacol.* 30, 13–22. doi: 10.1177/0269881115609072

Krugers, H. J., Lucassen, P. J., Karst, H., and Joels, M. (2010). Chronic stress effects on hippocampal structure and synaptic function: relevance for depression and normalization by anti-glucocorticoid treatment. *Front. Synaptic Neurosci.* 2:24. doi: 10.3389/fnsyn.2010.00024

Leo, R. J., and Ligot, J. S. A. Jr. (2007). A systematic review of randomized controlled trials of acupuncture in the treatment of depression. *J. Affect. Disord.* 97, 13–22. doi: 10.1016/j.jad.2006.06.012

Leuchter, A. F., Cook, I. A., Uijtdehaage, S., Dunkin, J., Lufkin, R. B., Anderson-Hanley, C., et al. (1997). Brain structure and function and the outcomes of treatment for depression. *J. Clin. Psychiatry* 58, 22–31.

Li, S., Zhong, W., Peng, W., and Jiang, G. (2018). Effectiveness of acupuncture in postpartum depression: a systematic review and meta-analysis. *Acupunct. Med.* 36, 295–301. doi: 10.1136/acupmed-2017-011530

Lu, J., Liang, J., Wang, J. R., Hu, L., Tu, Y., and Guo, J. Y. (2013). Acupuncture activates ERK-CREB pathway in rats exposed to chronic unpredictable mild stress. *Evid. Based Complement. Alternat. Med.* 2013:469765. doi: 10.1155/2013/469765

Lu, J., Shao, R.-H., Hu, L., Tu, Y., and Guo, J.-Y. (2016). Potential antiinflammatory effects of acupuncture in a chronic stress model of depression in rats. *Neurosci. Lett.* 618, 31–38. doi: 10.1016/j.neulet.2016.02.040

Luo, D., Ma, R., Wu, Y., Zhang, X., Liu, Y., Wang, L., et al. (2017). Mechanism underlying acupuncture-ameliorated depressive behaviors by enhancing glial glutamate transporter in chronic unpredictable mild stress (CUMS) rats. *Med. Sci. Monit.* 23, 3080–3087. doi: 10.12659/MSM.902549

MacPherson, H., Hammerschlag, R., Coeytaux, R. R., Davis, R. T., Harris, R. E., Kong, J.-T., et al. (2016). Unanticipated insights into biomedicine from the study of acupuncture. *J. Altern. Complement. Med.* 22, 101–107. doi: 10.1089/acm.2015.0184

McEwen, B. S., Nasca, C., and Gray, J. D. (2016). Stress effects on neuronal structure: hippocampus, amygdala, and prefrontal cortex. *Neuropsychopharmacology* 41, 3–23. doi: 10.1038/npp.2015.171

Modrego, P. J., and Ferrández, J. (2004). Depression in patients with mild cognitive impairment increases the risk of developing dementia of Alzheimer type: a prospective cohort study. *Arch. Neurol.* 61, 1290–1293. doi: 10.1001/archneur.61.8.1290

Mukaino, Y., Park, J., White, A., and Ernst, E. (2005). The effectiveness of acupuncture for depression – a systematic review of randomised controlled trials. *Acupunct. Med.* 23, 70–76. doi: 10.1136/aim.23.2.70

Oh, J. Y., Kim, Y. K., Kim, S. N., Lee, B., Jang, J. H., Kwon, S., et al. (2018). Acupuncture modulates stress response by the mTOR signaling pathway in a rat post-traumatic stress disorder model. *Sci. Rep.* 8:11864. doi: 10.1038/s41598-018-30337-5

Palazidou, E. (2012). The neurobiology of depression. *Br. Med. Bull.* 101, 127–145. doi: 10.1093/bmb/lds004

Pandya, M., Altinay, M., Malone, D. A. Jr., and Anand, A. (2012). Where in the brain is depression? *Curr. Psychiatry Rep.* 14, 634–642. doi: 10.1007/s11920-012-0322-7

Pang, C., Cao, L., Wu, F., Wang, L., Wang, G., Yu, Y., et al. (2015). The effect of trans-resveratrol on post-stroke depression via regulation of hypothalamus–pituitary–adrenal axis. *Neuropharmacology* 97, 447–456. doi: 10.1016/j.neuropharm.2015.04.017

Papakostas, G. I., Fava, M., and Thase, M. E. (2008). Treatment of SSRI-resistant depression: a meta-analysis comparing within-versus across-class switches. *Biol. Psychiatry* 63, 699–704. doi: 10.1016/j.biopsych.2007.08.010

Park, J. Y., Kim, Y. K., Kim, S. Y., Lee, H., Choi, C. J., Chae, Y., et al. (2017b). Acupuncture modulates brain neural activity in patients: a systematic review and meta-analysis. *Orient. Pharm. Exp. Med.* 17, 111–126. doi: 10.1007/s13596-017-0266-x

Park, J. Y., Kim, S. N., Yoo, J., Jang, J., Lee, A., Oh, J. Y., et al. (2017a). Novel neuroprotective effects of melanin-concentrating hormone in Parkinson's disease. *Mol. Neurobiol.* 54, 7706–7721. doi: 10.1007/s12035-016-0258-8

Park, J. Y., Park, J. J., Jeon, S., Doo, A. R., Kim, S. N., Lee, H., et al. (2014). From peripheral to central: the role of ERK signaling pathway in acupuncture analgesia. *J. Pain* 15, 535–549. doi: 10.1016/j.jpain.2014.01.498

Parks, C. L., Robinson, P. S., Sibille, E., Shenk, T., and Toth, M. (1998). Increased anxiety of mice lacking the serotonin1A receptor. *Proc. Natl. Acad. Sci. USA* 95, 10734–10739.

Parsons, L. H., Kerr, T. M., and Tecott, L. H. (2001). 5-HT(1A) receptor mutant mice exhibit enhanced tonic, stress-induced and fluoxetine-induced serotonergic neurotransmission. *J. Neurochem.* 77, 607–617. doi: 10.1046/j.1471-4159.2001.00254.x

Penn, E., and Tracy, D. K. (2012). The drugs don't work? Antidepressants and the current and future pharmacological management of depression. *Ther. Adv. Psychopharmacol.* 2, 179–188. doi: 10.1177/2045125312445469

Pilkington, K. (2010). Anxiety, depression and acupuncture: a review of the clinical research. *Auton. Neurosci.* 157, 91–95. doi: 10.1016/j.autneu.2010.04.002

Qu, S. S., Huang, Y., Zhang, Z. J., Chen, J. Q., Lin, R. Y., Wang, C. Q., et al. (2013). A 6-week randomized controlled trial with 4-week follow-up of acupuncture combined with paroxetine in patients with major depressive disorder. *J. Psychiatr. Res.* 47, 726–732. doi: 10.1016/j.jpsychires.2013.02.004

Reddy, M. S. (2010). Depression: the disorder and the burden. *Indian J. Psychol. Med.* 32, 1–2. doi: 10.4103/0253-7176.70510

Riolo, S. A., Nguyen, T. A., Greden, J. F., and King, C. A. (2005). Prevalence of depression by race/ethnicity: findings from the National Health and Nutrition Examination Survey III. *Am. J. Public Health* 95, 998–1000. doi: 10.2105/AJPH.2004.047225

Rot, M. A. H., Mathew, S. J., and Charney, D. S. (2009). Neurobiological mechanisms in major depressive disorder. *CMAJ* 180, 305–313. doi: 10.1503/cmaj.080697

Savitz, J., Lucki, I., and Drevets, W. C. (2009). 5-HT(1A) receptor function in major depressive disorder. *Prog. Neurobiol.* 88, 17–31. doi: 10.1016/j.pneurobio.2009.01.009

Torrens, M., Fonseca, F., Mateu, G., and Farré, M. (2005). Efficacy of antidepressants in substance use disorders with and without comorbid depression: a systematic review and meta-analysis. *Drug Alcohol Depend.* 78, 1–22. doi: 10.1016/j.drugalcdep.2004.09.004

Treadway, M. T., Waskom, M. L., Dillon, D. G., Holmes, A. J., Park, M. T. M., Chakravarty, M. M., et al. (2015). Illness progression, recent stress, and morphometry of hippocampal subfields and medial prefrontal cortex in major depression. *Biol. Psychiatry* 77, 285–294. doi: 10.1016/j.biopsych.2014.06.018

Vickers, A. J., Cronin, A. M., Maschino, A. C., Lewith, G., MacPherson, H., Foster, N. E., et al. (2012). Acupuncture for chronic pain: individual patient data meta-analysis. *Arch. Intern. Med.* 172, 1444–1453. doi: 10.1001/archinternmed.2012.3654

Wheeler, A. L., Teixeira, C. M., Wang, A. H., Xiong, X., Kovacevic, N., Lerch, J. P., et al. (2013). Identification of a functional connectome for long-term fear memory in mice. *PLoS Comput. Biol.* 9:e1002853. doi: 10.1371/journal.pcbi.1002853

WHO, R. O. f. t. W. P. (2008). *WHO Standard Acupuncture Point Locations in the Western Pacific Region*. Manila: World Health Organization, Western Pacific Region.

Yang, L., Zhao, Y., Wang, Y., Liu, L., Zhang, X., Li, B., et al. (2015). The effects of psychological stress on depression. *Curr. Neuropharmacol.* 13, 494–504. doi: 10.2174/1570159X1304150831150507

Yin, C. S., Jeong, H. S., Park, H. J., Baik, Y., Yoon, M. H., Choi, C. B., et al. (2008). A proposed transpositional acupoint system in a mouse and rat model. *Res. Vet. Sci.* 84, 159–165. doi: 10.1016/j.rvsc.2007.04.004

Yoon, M. J., Kim, S. Y., and Park, J. Y. (2018). Recent study trends of the liver-tonification and liver-sedation of Saam acupuncture. *Kor. J. Acupunct.* 35, 1–17. doi: 10.14406/acu.2018.004

Yun, S. J., Park, H. J., Yeom, M. J., Hahm, D. H., Lee, H. J., and Lee, E. H. (2002). Effect of electroacupuncture on the stress-induced changes in brain-derived neurotrophic factor expression in rat hippocampus. *Neurosci. Lett.* 318, 85–88. doi: 10.1016/S0304-3940(01)02492-2

Zhang, Z. J., Chen, H. Y., Yip, K. C., Ng, R., and Wong, V. T. (2010). The effectiveness and safety of acupuncture therapy in depressive disorders: systematic review and meta-analysis. *J. Affect. Disord.* 124, 9–21. doi: 10.1016/j.jad.2009.07.005

Conflict of Interest Statement: The authors declare that the research was conducted in the absence of any commercial or financial relationships that could be construed as a potential conflict of interest.

frontiers in Neuroscience

ORIGINAL RESEARCH
published: 11 July 2019
doi: 10.3389/fnins.2019.00498

High Temporal Summation of Pain Predicts Immediate Analgesic Effect of Acupuncture in Chronic Pain Patients—A Prospective Cohort Study

Petra Iris Baeumler[1], Peter Conzen[2] and Dominik Irnich[1]*

[1] Multidisciplinary Pain Center, Department of Anaesthesiology, University Hospital Ludwig-Maximilians-University, Munich, Germany, [2] Department of Anaesthesiology, University Hospital Ludwig-Maximilians-University, Munich, Germany

OPEN ACCESS

Edited by:
Younbyoung Chae,
Kyung Hee University, South Korea

Reviewed by:
Kyungmo Park,
Kyung Hee University, South Korea
In-Seon Lee,
National Center for Complementary and Integrative Health (NCCIH), United States

****Correspondence:***
Petra Iris Baeumler
petra.baeumler@med.uni-muenchen.de

Specialty section:
This article was submitted to Perception Science, a section of the journal Frontiers in Neuroscience

Received: *14 December 2018*
Accepted: *30 April 2019*
Published: *11 July 2019*

Citation:
Baeumler PI, Conzen P and Irnich D (2019) High Temporal Summation of Pain Predicts Immediate Analgesic Effect of Acupuncture in Chronic Pain Patients—A Prospective Cohort Study. Front. Neurosci. 13:498. doi: 10.3389/fnins.2019.00498

Objectives: This prospective cohort study explored whether two distinguished sensory parameters predicted acupuncture effects in chronic pain patients; namely high temporal summation of pain (TS) indicating spinal synaptic facilitation as well as a low vibration detection threshold (VDT) indicating a loss of Aβ-fiber function.

Methods: Pinprick induced TS and VDT were assessed by standardized, validated methods at the most painful body site and a pain free control site in 100 chronic pain patients receiving six acupuncture sessions as part of an interdisciplinary multimodal pain treatment (IMPT). Immediate change in pain intensity after the first acupuncture session (first treatment on the first day of IMPT) was assessed by the verbal rating scale (VRS, 0–100). After 4 weeks of treatment, patients indicated in a questionnaire whether acupuncture had relieved pain immediately and whether it had contributed to overall pain reduction and well-being after IMPT.

Results: Logistic regression analysis revealed an association between high TS at the control site and a reduction in pain intensity of at least 30% (VRS) after the first acupuncture (OR [95%-CI] 4.3 [1.6–11.8]). Questionnaire ratings of immediate pain relief after acupuncture were associated with high TS at the control site (OR [95%-CI] 3.8 [1.4–10.2] any pain relief, OR [95%-CI] 5.5 [1.7–17.1] over 50% pain reduction) and at the pain site (OR [95%-CI] 3.2 [1.2–8.9] any pain relief). Appraisals of the contribution of acupuncture to overall pain reduction and well-being after IMPT were not associated with TS. The VDT was not associated with any outcome.

Conclusion: This explorative study provides first-time evidence that high TS, especially at a pain free control site, but not VDT, might predict immediate analgesic response to acupuncture in chronic pain patients. Thus, highly centrally sensitized chronic pain patients might respond particularly well to acupuncture.

Keywords: quantitative sensory testing, wind-up ratio, vibration detection threshold, responder, sensitization

INTRODUCTION

In the management of chronic pain it is crucial to identify effective treatments in order to minimize the patient's risk of further chronification and to reduce health care costs (Main et al., 2008; Institute of Medicine, 2011). Acupuncture has been shown to be effective in treating chronic pain conditions (MacPherson et al., 2017; Vickers et al., 2018) with responder rates of 50% (Vickers and Linde, 2014), but little is known about predictors of treatment response. The effectiveness of acupuncture is thought to be based among other mechanisms on its potential to reduce central sensitization processes that sustain chronic pain states. This involves a reduction of spinal synaptic facilitation and reestablishment of endogenous pain control (Zhao, 2008; Zhang et al., 2014) up to demodulation of maladaptive functional brain neuroplasticity (Maeda et al., 2017). Thus, it stands to reason that chronic pain patients exhibiting strong central sensitization might respond particularly well to acupuncture.

Quantitative sensory testing has proven to permit conclusions about sensitization mechanisms contributing to chronic pain (Arendt-Nielsen, 2015) and standardized methods have been developed. Those suggested by the German Research Network for Neuropathic Pain (DFNS) are easily applied in clinical practice (Rolke et al., 2006), show good test-retest and interobserver reliability (Geber et al., 2011) and come with the advantage of established reference values (Rolke et al., 2006).

Increased temporal summation of pain (TS) is a sensory sign observed in various chronic pain conditions (Eide et al., 1994; Nikolajsen et al., 1996; Pud et al., 1998; Graven-Nielsen et al., 2000; Staud et al., 2001; List et al., 2008; Edwards et al., 2011; Gerhardt et al., 2015) and considered to reflect advanced spinal synaptic facilitation. TS describes the rise in pain intensity during repetitive nociceptive stimulation and is regarded as the physiological correlate of wind-up (Eide, 2000). This phenomenon is caused by a rapid facilitation of synaptic transmission between nociceptive afferents and spinal projection neurons during repetitive C- and Aδ-fiber activation (Mendell, 1966; Clarke et al., 2002). If spinal synaptic strength is permanently augmented through long-term potentiation (LTP) in chronic pain states, TS was observed to be elevated (Herrero et al., 2000). Furthermore, high TS was found to be associated with further signs of central sensitization such as hyperalgesia (Rabey et al., 2015), number of pain sites (Gerhardt et al., 2015; Vaegter and Graven-Nielsen, 2016) and impaired endogenous pain control (Staud et al., 2001; Lev et al., 2010; Daenen et al., 2014). Thus, the first hypothesis addressed in this study is that high TS is associated with the response to acupuncture in chronic pain patients.

Additionally, considering that acupuncture effects rely on sensory input elicited by the needle stimulus, it can be proposed that patients exhibiting a loss of function of sensory afferents might respond less to acupuncture. In this regard we obtained hints from a previous study in which acupuncture effects on sensory thresholds were assessed by QST in healthy volunteers. This study provided first-time conclusive support for the importance of segmental inhibition for the analgesic effect of electroacupuncture (Baeumler et al., 2015). In contrast, effects of manual acupuncture varied largely. A sub-analysis revealed a particularly poor vibration detection threshold (VDT), indicating a loss of Aβ-fiber function, in volunteers who did not experience a change in heat or pressure pain thresholds in the segment of needle placement after manual acupuncture (Baeumler et al., 2014). Segmental inhibition describes the reduction of nociceptive transmission in the spinal dorsal root through homosegmental A-fiber activation via inhibitory interneurons (Sandkuhler, 1996; Melin et al., 2013). While Aβ-fiber activation seems mainly responsible for an immediate but transient analgesic effect, low intensity Aδ-fiber activation can induce long-term depression of synapses between primary nociceptors and spinal projection neurons (Sandkühler, 2000). In line with these mechanisms as crucial components of the analgesic effects of acupuncture and other naturopathic stimulation therapies (White et al., 2011; Musial et al., 2013) segmental needling represents an integral part of acupuncture practice (Wancura-Kampik, 2012). Thus, the second hypothesis tested in this study is that a loss in vibration detection might be associated with a poor response to acupuncture in chronic pain patients.

In this study, we explored the association of TS and the VDT, as evaluated by DFNS standards, with the immediate analgesic response to acupuncture and with the subjective evaluation of acupuncture effects after a whole treatment in chronic pain patients undergoing multimodal pain therapy.

MATERIALS AND METHODS

Study Design

In this prospective cohort study TS and VDT were assessed as predictors for the analgesic effect of acupuncture. The study population consisted of chronic pain patients who received six to eight acupuncture treatments in the course of a 4-week interdisciplinary multimodal pain treatment (IMPT). Acupuncture was applied as the first treatment modality on the first day; meaning that effects of other therapies were excluded. The percentage change in pain intensity after this first acupuncture treatment was evaluated by the verbal rating scale (VRS). In addition, the subjectively perceived immediate pain relief experienced through acupuncture and its contribution to the overall pain reduction as well as to the general well-being during the whole 4-week treatment period was assessed by a patient questionnaire.

TS and VDT were evaluated at the most painful site (PS) and a pain free control site (CS) before the first acupuncture treatment and were analyzed as predictors for the acupuncture effect. TS and VDT were also assessed at the last day of IMPT and are not subject of this publication.

Study Setting

Recruitment of study participants was performed among chronic pain patients undergoing a multimodal pain treatment program, the Munich Outpatient Program in Complementary and Alternative Medicine (MOCAM) at the Multidisciplinary Pain Center at the Department of Anesthesiology, University Hospital of the Ludwig-Maximilians University of Munich,

Germany. The MOCAM follows the national criteria for IMPT, combining education, physical exercises, relaxation and cognitive behavioral therapy. MOCAM also integrates complementary methods of Traditional Chinese Medicine (acupuncture, qigong) and classical naturopathy (poultices and packs). It is carried out in an outpatient setting. Recruitment period of this study was from 2013, 3rd June to 2015, 23rd February. Data acquisition was completed on 2015, 20th March.

Patients

Inclusion criteria were age between 18 and 75 years, chronic pain condition (>3 months), command of the German language and written informed consent. General exclusion criteria were malignant, neurodegenerative or chronic inflammatory diseases. Patients suffering from pain in the hands were also excluded, because the dorsum of the dominant hand served as a pain free control site. Patients who had received less than six acupuncture treatments in the course of the MOCAM were retrospectively excluded. Patients were informed about conduct and purpose of the study in oral and written form after the introductory seminar of 75 min on the first day of the multimodal pain treatment program. Inclusion was performed after the subsequent coffee break in case that written informed consent was obtained.

Acupuncture

The schedule of the MOCAM stipulates that participating chronic pain patients receive eight acupuncture treatments during the 4-week multimodal pain program. Study documentation included the number of treatments that were actually received. For the course of this study acupuncture was scheduled on the first treatment day as the first intervention. Acupuncture in the MOCAM is exclusively performed by experienced medical acupuncturists with at least 200 h of acupuncture training (A-Diploma of the German Medical Acupuncture Association, *DÄGfA*). Treatments are usually performed in a group setting and point localization, needling depth as well as type and strength of needle stimulation are chosen individually. The individual treatment regimens integrate elements of TCM based acupuncture and western acupuncture techniques. Treatments rely on a differentiation of symptoms according to ba gang as well as on differential point selection according to zang-fu in case of internal diseases or according the theory of qi, blood and fluids. In addition, treatment included meridian orientated choice of points according to the site of pain as well as microsystem and trigger points. Five to ten needles are inserted per treatment. Needling depth is on average 0.5–1 cm and needle stimulation is performed by up and down movement as well as twisting of the needle. Acupuncturists attempt to elicit deqi, but this is not mandatory. Electrical or laser stimulation devices are available, but were not used in any of the patients included in this study. With the needles in place patients relax for 20–40 min.

Outcome Parameters

Acupuncture Responder Based on the Reduction in Pain Intensity After the First Acupuncture Treatment

The pain intensity directly before and after the first acupuncture treatment on the first treatment day of the multimodal pain program was evaluated by the verbal rating scale (VRS, 0 = "no pain," 100 = "worst pain imaginable"). According to recommendations of the US Initiative on Methods, Measurement, and Pain Assessment in Clinical Trials (IMMPACT) (Dworkin et al., 2005) two definitions for clinically relevant pain relief were applied; reduction in pain scores >30 and >50%. A reduction of pain scores of more than 30% has been shown to represent a clinically meaningful pain relief independent from baseline pain (Farrar et al., 2001). Accordingly, percent change in pain intensity was calculated as (VRSpost – VRSpre)/VRSpre *100 to classify patients as acupuncture responders and non-responders. Patients with a reduction in pain intensity of over 30% after the first acupuncture treatment are referred to as Resp30 and those with a reduction in pain intensity of over 50% are referred to as Resp50.

Patient Questionnaire on Acupuncture Effects

After the closing seminar on the last day of the multimodal pain treatment program patients were asked to fill in a questionnaire in order to assess the subjective perception of their response to acupuncture. Patients who were not able to attend this post-treatment visit were offered a separate study visit within the next days, at most 2 weeks later. The questionnaire was designed for the purpose of this study in order to assess the patients' subjective appraisal of immediate pain relief achieved through acupuncture, its contribution to the overall pain reduction during the 4 weeks of treatments as well as its contribution to general well-being. Questionnaire items translated into English read as follows:

1. Did you once experience an immediate pain relief after acupuncture treatments? *Yes/No*
2. If yes, by how much was your pain relieved? *By more than 50%?/By less than 50%?*
3. Do you have the impression that your overall pain relief is related to acupuncture? *Yes/No*
4. If yes, by how much was your pain relieved? *By more than 50%?/By less than 50%?*
5. Do you have the impression that acupuncture contributed to your general wellbeing? *Yes/No*
6. How many acupuncture treatments did you receive? *Free text*

Predictor Assessment

Assessments of TS and VDT were performed by two examiners (PB and a study nurse) during the waiting time before the first acupuncture treatment on the first day of the multimodal pain treatment program. Both sensory signs were determined at the most painful body site (PS) and at the dorsum of the dominant hand, which served as a pain free control site (CS). In headache cases, the temple was classified as the pain site. Measurements were performed according to the protocol for quantitative sensory testing (QST) designed by the German Research Network on Neuropathic Pain (DFNS) (Rolke et al., 2006). According to DFNS reference data, a certain value range at the bottom of the TS scale and at the top of the VDT scale can be regarded as not aberrant. Just exceedingly high TS indicates advanced spinal synaptic facilitation and low VDT a loss of Aβ-fiber function. Thus from a physiological point of view, the postulated relationship between the probability to respond to

acupuncture and these sensory parameters is most likely not linear. This was accounted for by categorizing TS and VDT values in the statistical analysis (see section Data Analysis).

Temporal Summation of Pain

As a measure for TS, the pin-prick evoked wind-up ratio (WUR) was applied. The WUR represents the quotient of the pain intensity evoked by 10 pin-prick stimuli and the pain intensity evoked by one single pin-prick stimulus. For all measurements a pin-prick of 256 mN (*MRC Systems GmbH-Medizintechnische Systeme, Heidelberg, Germany*) was used. Patients were asked to rate the pin-prick evoked pain intensity on the VRS (0–100). First, the researcher applied a single pin-prick stimulus followed by a series of 10 pin-prick stimuli applied with a frequency of 1 Hz within an area of 1 cm^2. WUR assessments were repeated three times per measurement site at intervals of at least 15 s. The WUR was calculated by division of the arithmetic mean of the three VRS ratings of the 10 stimuli by the arithmetic mean of the three VRS ratings of the single stimuli. This is indicated by the denotation [VRS-ratio], since the wind-up ratio is a dimensionless quantity.

Vibration Detection Threshold

The VDT was evaluated by the Rydel-Seiffer tuning fork (*Aesculap AG, B.Braun Melsungen AG, Melsungen, Germany*) which allows the application of vibration stimuli of 64 Hz. The continuously decreasing vibration amplitude can be read from a gauged scale ranging from 0 to 8 with an accuracy of 0.5 points. Patients were asked to notify the examiner as soon as their sensation of vibration stopped, and the corresponding amplitude was recorded. The final VDT value also represents the arithmetic mean of three measurements.

Assessment of Patient Characteristics

Sociodemographic and pain diagnostic data were extracted from the patients' medical records. These data included age in years, sex, right-handedness, pain relevant, and psychological diagnoses according to ICD-10 coding, stage of chronicity according to the Mainz-Pain Staging System (MPSS, 1–3), previous surgery (yes/no) and use of analgesics (yes /no; if yes, class of drugs was recorded). Pain duration in months, the most painful body site as well as the average and maximum pain intensity (VRS, 0-100) were assessed during the first study visit on the first treatment day.

Sample Size Estimation

Sample size estimation was performed on the basis of reference data for the WUR provided by the DFNS which suppose a log-normal data-distribution (Rolke et al., 2006). Given a target difference of 0.4 of WUR raw-values (0.15 in log-values), a standard deviation (SD) of 0.234 in log-values, an α-error of 5% and a power of 80%, the total sample size was estimated as 78 patients. In addition, a correction for an unequal responder/non-responder ratio of 33 to 66% and a drop-out rate of 15% resulted in a final sample size of 101 patients (calculations according to Altman, 1991).

Data Analysis

Data analysis was exploratory and performed in IBM SPSS Statistics for Windows (Version 22.0. Armonk, NY: IBM Corp) as well as in R version 3.5.2 (R Development Core Team, 2008). Categorical study variables are described as absolute and relative frequencies. Assumption of normal distribution of metric study variables was estimated by Shapiro-Wilk test. Besides age all metric study variables (pain intensity measures, pain duration, WUR and VDT) were not normally nor log-normally distributed. Descriptive statistics are therefore given as median with interquartile range (IQR) for the remaining metric variables.

A responder analysis was carried out to evaluate whether the predictors were associated with clinically relevant treatment response. As described above, percent changes in VRS sores were categorized ($\geq$30 and $\geq$50%) to represent responders and non-responders. As recommended for analyses of pain data (Farrar et al., 2006), cumulative proportion of responder analysis graphs are used to illustrate that cut-off selection did not bias results. That this constitutes the best strategy to present our data is based on two main considerations. First, neither raw post-treatment scores nor raw change scores nor percent change scores provide an unbiased estimate of treatment effects (Vickers, 2001). Second, regression analyses with adjustment for baseline scores is not recommended in observational studies, in particular if covariates are likely to be related to baseline scores (Cribbie and Jamieson, 2000; Cole et al., 2010).

Logistic regression was used to assess confounder adjusted associations between the dichotomous outcome parameters representing acupuncture effects (dependent variables) and the VDT as well as the WUR at the control site and at the pain site (independent variables). Based on the neurophysiological considerations introduced above, VDT and WUR data were categorized before application as independent variables in the logistic regression models. We pragmatically chose the 33%-percentile for the VDT and the 66%-percentile for the WUR as cut-off values in order to identify patients with the highest WUR and lowest VDT. These cut-off values were verified by visual inspection of scatter plots of predictors against percent change in pain intensity (**Figure 2**) and ROC-analyses.

Assessed confounders included age, gender, pain duration, pain related surgery before participation in the multimodal pain treatment and intake of analgesics. First, the crude associations of acupuncture effects and patient characteristics were assessed in an exploratory analysis. Subgroups formed according to the different dichotomous outcome variables were compared for metric variables by Mann-Whitney-U test and for categorical variables by Fisher test. Subsequently, final logistic regression models were identified by automated covariate selection using the R-function *bestglm* (McLeod and Changjiang, 2018). Model fit was evaluated by Omnibus test and goodness of fit by Hosmer-Lemeshow test. Odds-ratios (OR) with 95% confidence intervals (95% CI), the Nagelkerke's pseudo R^2 (R^2) as well as correctly specified cases (sensitivity & specificity) were used to describe the predictive value of the VDT and the WUR at the control site and at the pain site. Collinearity was assessed by the variation inflation factor (VIF). Effect modification was assessed by introduction of interaction terms in the final models. For additional graphical

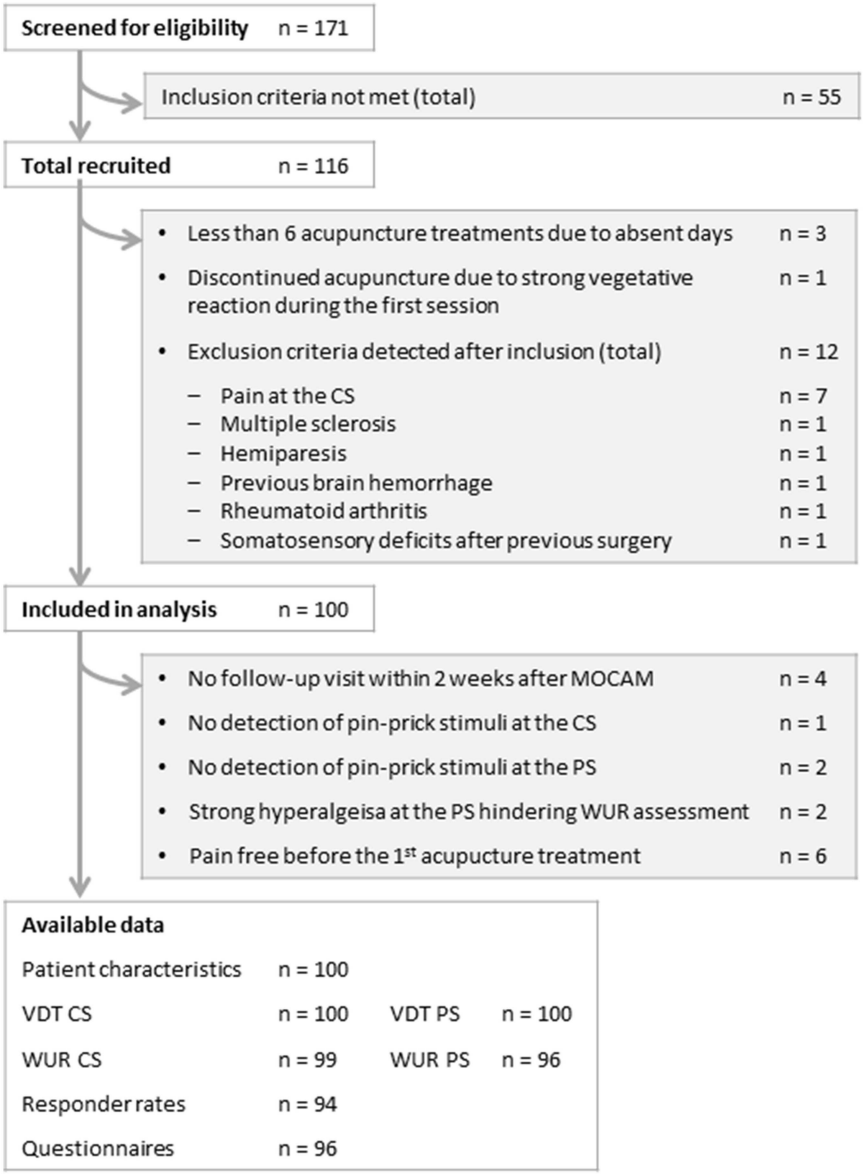

FIGURE 1 | Study flow-chart. MOCAM, Munich Outpatient Program in Complementary and Alternative Medicine; VDT, vibration detection threshold; WUR, wind-up ratio; CS, control site; PS, pain site.

illustration (e.g., cumulative response curves), identified metric confounders were categorized with cut-off values identified by the receiver operating characteristic (ROC-) analysis.

RESULTS

Patient Characteristics

Of 171 screened patients 116 met the inclusion criteria and gave written informed consent. Of these 16 were excluded from the analysis. A late detection of exclusion criteria accounted for exclusion in 12 cases. Three patients had received less than six acupuncture treatments during the multimodal treatment program for organizational reasons, and one patient discontinued the acupuncture treatment after experiencing a strong vegetative reaction during the first session. Four patients did not attend the follow-up visits for personal reasons (**Figure 1**).

Patient characteristics of the 100 patients available for analysis are displayed in **Table 1**. Overall, patients were middle-aged, mainly females, right-handed, with a long history of chronic pain and relevant pain intensity. Most patients (n = 77) were diagnosed with persistent pain with somatic and psychological factors (F45.41). The second most frequent diagnosis (n = 64) was myofascial pain (M79.1-) followed by dorsopathies (M40–54, $n = 42$). Migraine or other headache syndromes (G43.- or G44.-) were present in 21, arthropathies (M00–25) in 18 and disorder of the trigeminal nerve (G50.-) in 12 patients. The most frequent mental and behavioral diagnoses were mood or affective

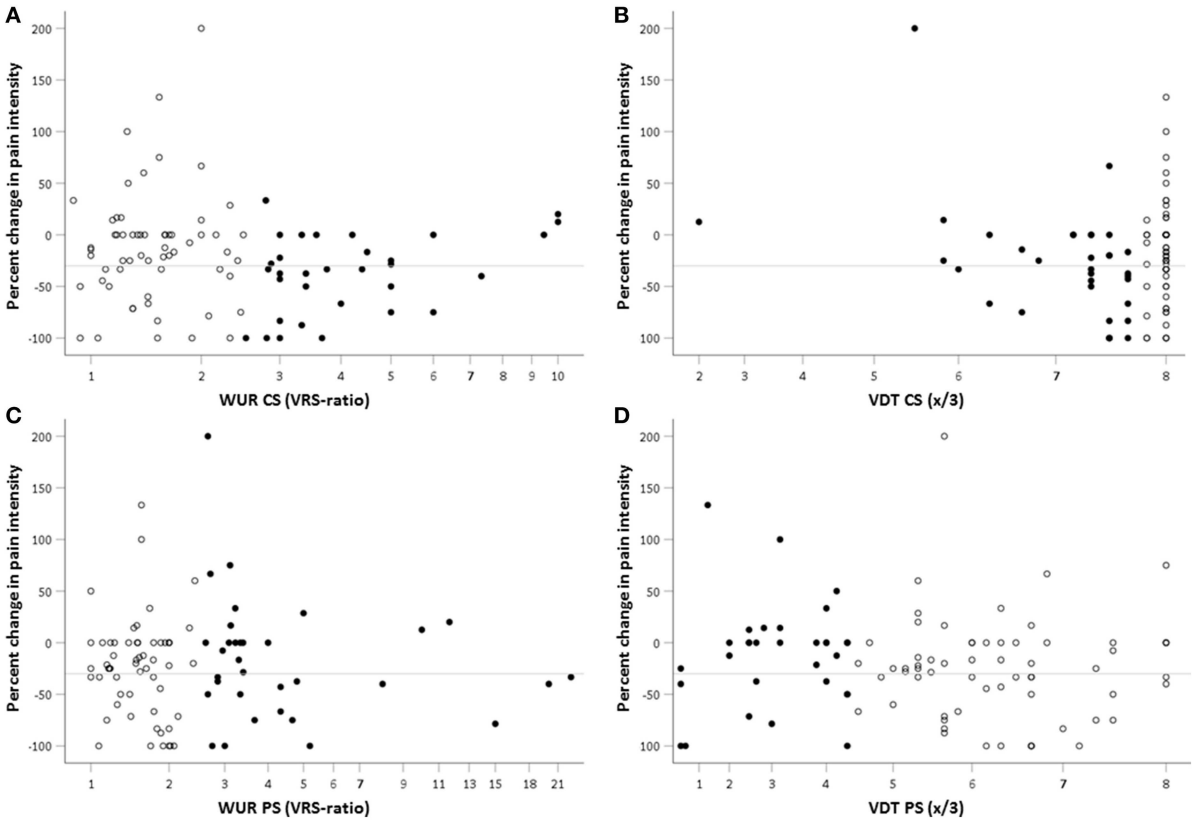

FIGURE 2 | Scatterplot of percent change in pain intensity after the first acupuncture treatment against WUR and VDT at the PS and CS. Percent change in pain intensity as evaluated by the verbal rating scale (VRS) was calculated as (VRSpost – VRSpre)/VRSpre *100. Accordingly, negative values represent a pain relief. The reference line indicates a 30% reduction in pain intensity as the cut-off for clinically relevant pain relief. WUR, wind-up ratio [ratio of the pain intensities evoked by one and by 10 pin-prick stimuli of 256 mN as evaluated by the verbal rating scale (0–100)]; VDT, vibration detection threshold; CS, control site; PS, pain site; filled points, **(A,B)** subjects with high TS (WUR > 2.5 VRS-ratio) as identified by the 66%-percentile **(C)** low VDT at the CS (≤7.7/8) **(D)** low VDT at the PS (≤4.3/8) as identified by the 33%- percentile; empty points, subjects with low TS or high VDT, respectively.

disorder (F30–39) present in 34 patients. The most frequently reported area of the main pain problem was the lower back (25%) followed by the neck and cervical-spine area (22%), the shoulder-arm region (10%), the head (9%) and the area of the thoracic spine (8%).

Descriptive Analysis of Acupuncture Effects, TS and the VDT

Pain intensity as evaluated by the VRS (0–100) was significantly reduced after the first acupuncture treatment when compared to baseline (median (IQR) 30 (10–50) vs 45 (30–60), $p < 0.001$).

Six patients had no pain on the first day of MOCAM and were therefore excluded from responder rate calculations. Of those suffering from pain on the first day of the multimodal pain treatment, 38 (40.4%) experienced a pain reduction of at least 30% ($Resp_{30}$) and 25 (26.6%) of at least 50% ($Resp_{50}$) after the first acupuncture treatment as evaluated by the VRS (0–100).

Thirty seven patients (38.5%) reported that they had experienced an immediate pain relief through acupuncture in the questionnaire filled in after the end of the 4 weeks of treatment. Twenty-four patients (25%) affirmed that acupuncture had reduced their pain immediately by over 50%. Subjective rating of the contribution of acupuncture to the overall pain relief over the whole 4-week treatment period was positive in 52 cases (54.7%). Seventeen patients (17.9%) perceived acupuncture to be responsible for an overall pain relief of over 50%. Seventy-five patients (80.6%) experienced a beneficial effect of acupuncture on general well-being.

TS was similar at the control site and at the pain site with a median WUR (IQR) of 1.9 (1.3–3.0) and 2.0 (1.5–3.1), respectively. Insensitivity to pin-prick stimuli (VRS rating of 1 stimulus with 0) leading to missing values of the WUR were observed in one patient at the control site and in two patients at the pain site. In two patients TS assessments at the pain site could not be performed due to strong hyperalgesia.

Median VDT at the control site was 8.0 with an IQR of 7.0–8.0 indicating a ceiling effect (accumulation of scores at the upper limit of the 8-point scale). At the pain site median VDT was 5.4 (IQR 4.0–6.6).

TABLE 1 | Patient characteristics ($n = 100$).

Sociodemographic and clinical characteristics			Diagnoses established during an interdisciplinary pain assessment	ICD-10	*n*
Age [a], mdn (IQR)		50 (43–56)	Persistent pain with somatic and mental factors	F45.41	77
Female/male, *n*		83/17	Migraine and other headache syndromes	G43.-/ G44.-	21
Right handed, *n*		98	Disorders of trigeminal nerve	G50.-	4
Pain duration [m], mdn (IQR)		66 (22–187)	Mononeuropathies of upper limb	G56.-	2
Pain intensity VRS (0–100) mdn (IQR)	Maximum	80 (61–90)	Tinnitus	H93.1	1
	Average	50 (40–60)	Disorders of circulatory system	I73.9/ I80.28	2
	Current	45 (30–60)	Temporomandibular joint disorders	K07.6	5
Chronicity	1	7	Arthropathies	M00-25	18
MPSS, *n*	2	38	Polymyalgia rheumatica	M35.3	1
	3	55	Deforming dorsopathies	M40–43	3
Previous surgery because of chronic pain, *n*		29	Spondylopathies	M45–49	2
Main pain area, *n*	Lower back	25	Other dorsopathies	M50-54	37
	Neck/cervical-spine area	22	Shoulder lesions	M75.-	7
	Thoracic spine-area	8	Enthesopathies of lower limb, excluding foot	M76.-	5
	Headache	9	Other enthesopathies	M77.-	5
	Jaw	7	Myalgia, myofascial pain syndromes	M79.1-	64
	Shoulder/arm	10	Pain in limb	M79.6-	1
	Hip	5	Fibromyalgia	M79.70	8
	Knee, lower extremity	6	Osteoporosis without pathological fracture	M81.-	2
	Foot	6	Osteomyelitis	M86.-	1
	Abdomen	2	Other biomechanical lesions	M99.8-	7
Pain medication, *n*	Non-opioid analgesics (NSAID/ Pyrazolone/Paracetamole)	68	Other congenital deformities of feet	Q66.8	1
			Symptoms and signs abdomen/urinary system	R10.1/ R39.8	2
	Weak opioids	12	Pain, unspecified	R52.9	1
	Antidepressants	23	Fracture of thoracic vertebra	S22.0	1
	Anticonvulsants	9	Presence of other functional implants	Z96.-	2
	Triptans	6	Mental and behavioral disorders due to	F10 - F19	7
	Muscle relaxants	2	psychoactive substance use		
	Disease-modifying	1	Mood [affective] disorders	F30 - F39	34
	antirheumatic drugs		Neurotic, stress-related and somatoform disorders	F40 - F48	22
	Phytopharmaceuticals	4	Behavioral syndromes associated with	F50 - F59	12
	No analgesics	15	physiological disturbances and physical factors		

n, absolute frequency corresponding to relative frequencies since the total number of patients was 100; a, years; m, months; mdn, median; IQR, interquartile range; VRS, verbal rating scale; MPSS, Mainz Pain Staging System; ICD-10, 10th revision of the International Statistical Classification of Diseases and Related Health Problems.

Crude Association of TS and the VDT With Acupuncture Effects

Comparisons of TS and the VDT at the control site and at the pain site were performed between patient subgroups formed according to the different dichotomous outcome variables: reduction of the pain intensity as evaluated by the VRS after the first acupuncture treatment over 30% ($Resp_{30}$) or 50% ($Resp_{50}$), subjective perception of acupuncture effects as assessed by the questionnaire—immediate pain relief, immediate pain relief of over 50%, contribution to overall pain relief after 4 weeks of treatment, overall pain relief over 50% and contribution to overall well-being (**Table 2**). TS at the control site was significantly higher in patients who reported an immediate pain relief through acupuncture in the questionnaire than in those who did not experience an immediate analgesic acupuncture effect (median WUR (IQR) 2.4 (1.5–3–6) vs. 1.6 (1.3–2.8); $p = 0.050$). Patients who had reported an immediate pain relief of over 50% were even more demarked form the remaining patients in terms of a higher TS at the control site (median WUR (IQR) 2.5 (1.6–4.4) vs. 1.6 (1.3–2.9); $p = 0.029$). In addition, there was a trend toward higher TS at the pain site in patients with an immediate reduction in their pain intensity after the first acupuncture treatment of more than 50% ($Resp_{50}$) as evaluated by the VRS ($p = 0.085$). Conversely, patients with and without acupuncture effects differed neither with regard to the VDT at the control site nor with regard to the VDT at the pain site ($p > 0.05$).

Plotting percent change in pain intensity against the predictor variables showed a non-linear relationship between the WUR

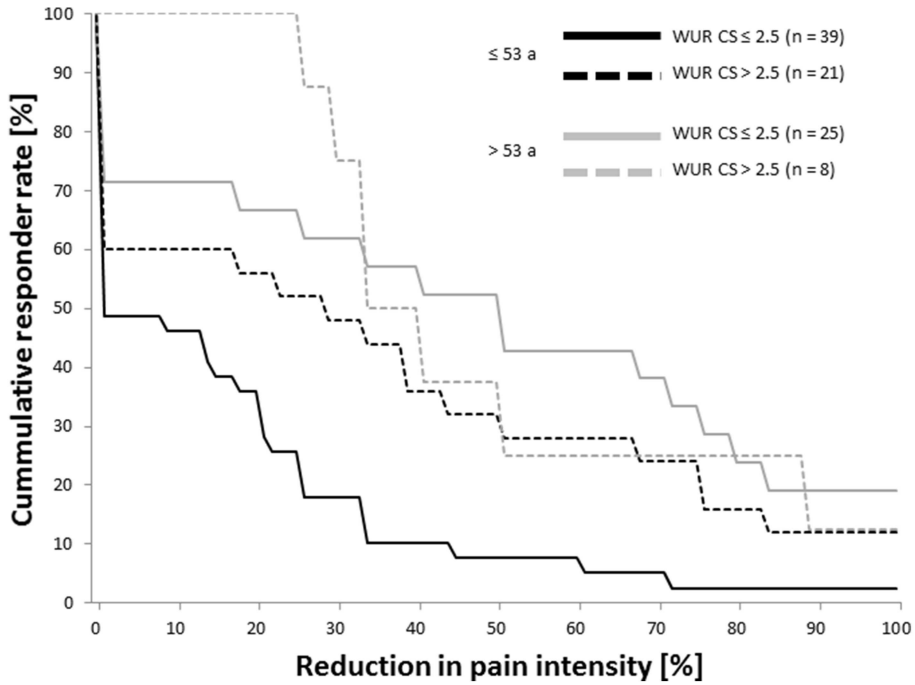

FIGURE 3 | Cumulative response functions in patients with high and low TS at the control site by age-group. Reduction in pain intensity was evaluated by the verbal rating scale (0–100) before and after the first acupuncture treatment. The age cut-off of 53 years was estimated by a receiver operating characteristic analysis. TS, temporal summation of pain; WUR, wind-up ratio [ratio of the pain intensities evoked by one and by ten pin-prick stimuli of 256 mN as evaluated by the verbal rating scale (0–100)]; CS, control site; a, years.

and the immediate reduction in pain intensity after acupuncture. The density of data points representing no or only poor acupuncture response decreases in the value range between 2 and 3 of the WUR at the control site (**Figure 2A**). A similar but less pronounced association was seen for TS at the pain site (**Figure 2B**). In contrast, visual inspection does not suggest an association between percent change in pain intensity and the VDT at the pain site or at the control site (**Figures 2C,D**).

Comparisons of frequencies of low VDT and high TS between patient subgroups with and without acupuncture effects (**Table 3**) support observations from **Figure 2**. High TS (WUR > 2.5) at the control site was more frequent in patients with a reduction in pain intensity of at least 30% ($Resp_{30}$) as evaluated by the VRS than in patients not responding to the first treatment (OR 2.6 [1.1–6.4]; $p = 0$ 0.045). The proportion of patients with high TS at the control site was also larger among those who subjectively rated the immediate pain relief through acupuncture as positive (OR 2.6 [1.1–6.3]; $p = 0.043$) or even over 50% (OR 2.8 [1.1–7.5]; $p = 0.043$). High TS at the pain site was merely associated with the report of an immediate pain relief through acupuncture of over 50% in the questionnaire (OR 3.4 [1.3–9.1]; $p = 0.021$). In addition, a ROC-analysis confirmed the WUR cut-off of 2.5 for all outcomes. Both a low VDT at the control site (≤7.7) and a low VDT at the pain site (≤4.3) were equally frequent in patients with and without acupuncture effects.

Associations Between Acupuncture Effects and Patient Characteristics

Acupuncture effects were similarly distributed between men and women. There was only a trend toward a more frequent perception of an immediate pain relief of over 50% through acupuncture in females (OR 6.6 [0.8–52.5]; $p = 0.062$). All 24 patients who had reported an immediate pain relief through acupuncture of over 50% in the questionnaire took analgesics, while 20.8% (15 out of 72) of patients who experienced less or no immediate pain relief after one of the acupuncture sessions were not on pain medication ($p = 0.019$). Patients of chronicity stage 2 and 3 as defined by the MPSS rated the contribution of acupuncture to their general wellbeing more frequently as positive than patients of chronicity stage 1 (OR 7.7 [1.3–45.4]; $p = 0.031$ and OR 6.4 [1.2–33.5]; $p = 0.036$, respectively). Furthermore, older age was associated with immediate analgesic response to acupuncture. Patients with immediate, clinically relevant reductions in VRS pain scores were older than patients without such response ($Resp_{30}$: mean (SD) 51.7 (9.4) vs. 46.4 (10.8) years, $p = 0.005$; $Resp_{50}$: (52.8 (9.6) vs. 47.0 (10.6) years, $p = 0.006$). The subjective experience of an immediate pain relief through acupuncture of over 50% was also associated with older age (53.3 (8.4) vs. 46.3 (11.3) years; $p = 0.010$). A similar age trend was also observed between patient subgroups formed according to whether an immediate pain relief was experienced at all (50.8 (11.2). vs 46.3 (10.7) years; $p = 0.063$) (**Table 4**).

TABLE 2 | TS and VDT in patients with and without acupuncture effect.

		$Resp_{30}$			$Resp_{50}$		
		Yes	**No**	***p*-value**	**Yes**	**No**	***p*-value**
VDT CS	*n*	38	56		25	69	
(x/8)	mdn [IQR]	7.8 [7.5–8.0]	8 [7.5–8.0]	0.346	7.8 [7.5–8.0]	8.0 (7.5–8.0)	0.61
VDT PS	*n*	38	56		25	69	
(x/8)	mdn [IQR]	5.9 [4.3–6.7]	5.3 [3.9–6.3]	0.135	5.7 [4.3–6.7]	5.3 (4.0–6.4)	0.353
WUR CS	n	38	55		25	68	
(VRS-ratio)	mdn [IQR]	2.4 [1.4–3.4]	1.7 [1.3–2.8]	0.189	2.3 [1.4–3.4]	1.7 (1.3–3.0)	0.553
WUR PS	*n*	37	53		25	65	
(VRS-ratio)	mdn [IQR]	2.0 [1.6–4.0]	1.8 [1.5–3.0]	0.124	2.0 [1.6–3.2]	1.9 (1.5–3.1)	0.479
		Subjective immediate pain relief			**Subjective immediate pain relief >50%**		
		Yes	**No**	**p-value**	**Yes**	**No**	***p*-value**
VDT CS	n	37	59		24	72	
(x/8)	mdn [IQR]	8.0 [7.6–8.0]	8.0 [7.5–8.0]	0.452	8.0 [7.7–8.0]	8.0 (7.5–8.0)	0.345
VDT PS	*n*	37	59		24	72	
(x/8)	mdn [IQR]	5.7 [4.6–6.7]	5.3 [4.0–6.5]	0.265	5.7 [4.4–7.0]	5.3 (4.2–6.5)	0.367
WUR CS	*n*	36	59		23	72	
(VRS-ratio)	mdn [IQR]	2.4 [1.5–3.6]	1.6 [1.3–2.8]	0.050*	2.5 [1.6–4.4]	1.6 (1.3–2.9)	0.029*
WUR PS	*n*	36	56		23	69	
(VRS-ratio)	mdn [IQR]	2.3 [1.6–3.3]	1.9 [1.5–2.6]	0.13	2.8 [1.6–3.4]	1.9 (1.5–2.7)	0.085
		Subjective overall pain relief			**Subjective overall pain relief >50%**		
		Yes	**No**	***p*-value**	**Yes**	**No**	***p*-value**
VDT CS	*n*	52	43		17	78	
(x/8)	mdn [IQR]	8.0 [7.5–8.0]	8.0 [7.7–8.0]	0.373	8.0 [7.4–8.0]	8.0 (7.5–8.0)	0.953
VDT PS	*n*	52	43		17	78	
(x/8)	mdn [IQR]	5.5 [4.0–6.6]	5.7 [4.5–6.7]	0.381	4.7 [4.0–6.3]	5.7 (4.3–6.7)	0.319
WUR CS	*n*	51	43		16	78	
(VRS-ratio)	mdn [IQR]	1.7 [1.3–3.0]	2.0 [1.3–2.8]	0.381	1.7 [1.6–3.0]	1.9 (1.3–3.0)	0.856
WUR PS	*n*	50	42		17	75	
(VRS-ratio)	mdn [IQR]	2.0 [1.5–2.8]	2.0 [1.4–3.2]	0.931	2.0 [1.5–2.7]	2.0 (1.5–3.1)	0.629
		Contribution to general well-being					
		Yes	**No**	***p*-value**			
VDT CS	*n*	75	18				
(x/8)	mdn [IQR]	8.0 [7.5–8.0]	8.0 [7.6–8.0]	0.901			
VDT PS	*n*	75	18				
(x/8)	mdn [IQR]	5.7 [4.2–6.7]	5.3 [4.0–6.6]	0.942			
WUR CS	n	74	18				
(VRS - ratio)	mdn [IQR]	1.7 [1.3–3.0]	2.2 [1.4–3.1]	0.598			
WUR PS	*n*	71	18				
(VRS-ratio)	mdn [IQR]	2.0 [1.5–3.0]	2.3 [1.5–3.4]	0.314			

*$Resp_{30/50}$, Acupuncture responders defined according to a reduction in pain intensity after the first acupuncture treatment of at least 30 and 50%, respectively; VDT, vibration detection threshold; x/8, score out of eight on the Rydel-Seiffer tuning fork; WUR, wind-up ratio; VRS-ratio, ratio of the pain intensities evoked by one and by ten pin-prick stimuli of 256 mN as evaluated by the verbal rating scale (0–100); CS, control site; PS, pain site; n, case number; mdn, median; IQR, interquartile range; *statistically significant at an α-error of 5% according to Mann-Whitney-U test.*

Adjusted Analysis of the Association Between TS and the VDT With Acupuncture Effects

Logistic regression confirmed the positive association of high TS at the control site as well as at the pain site with an immediate reduction in pain after acupuncture and identified age as a relevant confounder (Model 1–4; **Table 5**). Age-adjusted ORs were larger than crude ORs (**Table 4**). All models showed a good model fit (Omnibus test $p < 0.01$ and H-L test > 0.07). There was no collinearity between explanatory variables (VIF < 1.1). Explained variance according to Nagelkerkes R^2 was between 18 and 25%. As identified by automated covariate

TABLE 3 | Crude association between acupuncture effects and high TS and low VDT.

		$Resp_{30}$				$Resp_{50}$			
		Yes	**No**	**OR [95% CI]**	***p*-value**	**Yes**	**No**	**OR [95% CI]**	***p*-value**
VDT control site (x/8)	>7.7	21	39	ref		15	45	ref	
	≤7.7	17	17	1.9 [0.8–4.4]	0.191	10	24	1.3 [0.5–3.2]	0.637
VDT pain site (x/8)	>4.3	28	35	ref		18	45	ref	
	≤4.3	10	21	0.6 [0.2–1.5]	0.275	7	24	0.7 [0.3–2.0]	0.625
WUR control site (VRS-ratio)	≤2.5	20	41	ref		14	47	ref	
	>2.5	18	14	2.6 [1.1–6.4]	0.045*	11	21	1.8 [0.7–4.5]	0.325
WUR pain site (VRS-ratio)	≤2.5	21	36	ref		16	41	ref	
	>2.5	16	17	1.6 [0.7–3.8]	0.374	9	24	1.0 [0.4–2.5]	1.000
		Subjective immediate pain relief				**Subjective immediate pain relief >50%**			
		Yes	**No**	**OR [95% CI]**	***p*-value**	**Yes**	**No**	**OR [95% CI]**	***p*-value**
VDT control site (x/8)	>7.7	24	38	ref		17	45	ref	
	≤7.7	13	21	1.0 [0.4–2.3]	1.000	7	27	0.7 [0.3–1.9]	0.623
VDT pain site (x/8)	>4.3	29	37	ref		18	48	ref	
	≤4.3	8	22	0.5 [0.2–1.2]	0.120	6	24	0.7 [0.2–1.9]	0.612
WUR control site (VRS-ratio)	≤2.5	19	44	ref		11	52	ref	
	>2.5	17	15	2.6 [1.1–6.3]	0.043*	12	20	2.8 [1.1–7.5]	0.043*
WUR pain site (VRS-ratio)	≤2.5	19	41	ref		10	50	ref	
	>2.5	17	15	2.4 [1.0–5.9]	0.072	13	19	3.4 [1.3–9.1]	0.021*
		Subjective overall pain relief				**Subjective overall pain relief >50%**			
		Yes	**No**	**OR [95% CI]**	***p*-value**	**Yes**	**No**	**OR [95% CI]**	***p*-value**
VDT control site (x/8)	>7.7	32	30	ref		11	51	ref	
	≤7.7	20	13	1.4 [0.6–3.4]	0.517	6	27	1.0 [0.3–3.1]	1.000
VDT pain site (x/8)	>4.3	32	33	ref		9	56	ref	
	≤4.3	20	10	2.1 [0.8–5.1]	0.127	8	22	2.3 [0.8–6.6]	0.155
WUR control site (VRS-ratio)	≤2.5	32	30	ref		10	52	ref	
	>2.5	19	13	1.4 [0.6–3.2]	0.518	6	26	1.2 [0.4–3.7]	0.777
WUR pain site (VRS-ratio)	≤2.5	35	24	ref		12	48		
	>2.5	15	17	0.6 [0.3–1.4]	0.380	5	27	0.7 [0.2–2.3]	0.780
		Contribution to general well-being							
		Yes	**No**	**OR [95% CI]**	***p*-value**				
VDT control site (x/8)	>7.7	49	12	ref					
	≤7.7	26	6	1.1 [0.4–3.2]	1.000				
VDT pain site (x/8)	>4.3	52	13	ref					
	≤4.3	23	5	1.2 [0.4–3.6]	1.000				
WUR control site (VRS-ratio)	≤2.5	48	13	ref					
	>2.5	26	5	1.4 [0.5–4.4]	0.782				
WUR pain site (VRS-ratio)	≤2.5	47	11	ref					
	>2.5	24	7	0.8 [0.3–2.3]	0.783				

*$Resp_{30/50}$, Acupuncture responders defined according to a reduction in pain intensity after the first acupuncture treatment of at least 30 or 50%, respectively; VDT, vibration detection threshold; x/8, score out of eight on the Rydel-Seiffer tuning fork; WUR, wind-up ratio; VRS-ratio, ratio of the pain intensities evoked by one and by ten pin-prick stimuli of 256 mN as evaluated by the verbal rating scale (0–100); CS, control site; PS, pain site; OR, odds ratio; 95% CI, 95% confidence interval; *statistically significant at an α-level of 5% according to Fisher test.*

selection, age was the only additional significant explanatory variable. Effect modification by any patient characteristic was not observed. Specificity of prediction (80–94%) was usually larger than sensitivity (13–55%).

Model 1 describes the association between a high TS at the control site and the outcome $Resp_{30}$. It indicates that patients with a high TS (WUR > 2.5) at the control site had a 4.0 (95% CI [1.6–11.8]; $p = 0.005$) times higher chance that their pain intensity was reduced by at least 30% after the first acupuncture treatment. With each year of age the chance to belong to the $Resp_{30}$-subgroup increased by 8% (95% CI [2–13%]; $p = 0.004$). The model correctly classified 55% of responders and 80% of non-responders.

TABLE 4 | Crude associations between acupuncture effects and patient characteristics.

		$Resp_{30}$				$Resp_{50}$			
		Yes	**No**	**OR [95% CI]**	***p*-value**	**Yes**	**No**	**OR [95% CI]**	***p*-value**
Gender	Male	3	11	ref		1	13	ref	
	Female	35	45	2.9 [0.7–11.0]	0.147	24	56	5.6 [0.7–45.0]	0.103
Chronicity MPSS	1	0	5	ref		0	5	ref	
	2	14	20	-	0.139	7	27	-	0.563
	3	24	31	-	0.077	18	37	-	0.310
Surgery	No	28	39	ref		17	50	ref	
	Yes	10	17	0.8 [0.3–2.1]	0.817	8	19	1.2 [0.5–3.3]	0.797
Use of analgesics	No	2	10	ref		1	11		
	Yes	36	46	3.9 [0.8–19.0]	0.114	24	58	4.6 [0.6–37.2]	0.172
Pain duration [m]	mdn (IQR)	48 (16–166)	116 (26–219)		0,119	53 (14–145)	82 (24–218)		0,176
Age [a]	mdn (IQR)	53 (46–59)	49 (42–51)		0.005*	55 (48–61)	49 (42–52)		0.006*
		Subjective immediate pain relief				**Subjective immediate pain relief >50%**			
		Yes	**No**	**OR [95% CI]**	***p*-value**	**Yes**	**No**	**OR [95% CI]**	***p*-value**
Gender	Male	5	12	ref		1	16	ref	
	Female	32	47	1.6 [0.5–5.1]	0.584	23	56	6.6 [0.8–52.5]	0.062
Chronicity MPSS	1	2	5	ref		1	6	ref	
	2	12	23	1.3 [0.2–7.8]	1.000	10	25	2.4 [0.3–22.6]	0.654
	3	23	31	1.9 [0.3–10.4]	0.690	13	41	1.9 [0.2–17.3]	1.000
Surgery	No	25	42	ref		16	51	ref	
	Yes	12	17	1.2 [0.5–2.9]	0.820	8	21	1.2 [0.5–3.3]	0.798
Use of analgesics	No	4	11	ref		0	15	ref	
	Yes	33	48	1.9 [0.6–6.5]	0.393	24	57	-	0.019*
Pain duration [m]	mdn (IQR)	85 (21–217)	49 (21–166)		0.372	65 (17–219)	66 (21–182)		0.889
Age [a]	mdn (IQR)	51 (46–59)	50 (42–52)		0.063	55 (47–60)	50 (41–52)		0.010*
		Subjective overall pain relief				**Subjective overall pain relief >50%**			
		Yes	**No**	**OR [95% CI]**	***p*-value**	**Yes**	**No**	**OR [95% CI]**	***p*-value**
Gender	Male	10	7	ref		2	15	ref	
	Female	42	36	0.8 [0.3–2.4]	0.792	15	63	1.8 [0.4–8.7]	0.729
Chronicity MPSS	1	4	3	ref		2	5	ref	
	2	15	19	0.6 [0.1–3.1]	0.685	3	31	0.2 [0.0–1.8]	0.196
	3	33	21	1.2 [0.2–5.8]	1.000	12	42	0.7 [0.1–4.2]	0.655
Surgery	No	37	29	ref		13	53	ref	
	Yes	15	14	0.8 [0.3–2.0]	0.823	4	25	0.7 [0.2–2.2]	0.573
Use of analgesics	No	8	7	ref		3	12	ref	
	Yes	44	36	1.1 [0.4–3.2]	1.000	14	66	0.8 [0.2–3.4]	0.728
Pain duration [m]	mdn (IQR)	87 (18–229)	49 (21–166)		0.267	123 (15–272)	63 (21–173)		0.344
Age [a]	mdn (IQR)	50 (43–55)	51 (43–57)		0.837	49 (45–57)	51 (43–56)		0.973
		Contribution to general well-being							
		Yes	**No**	**OR [95% CI]**	***p*-value**				
Gender	Male	12	5	ref					
	Female	63	13	2.0 [0.6–6.7]	0.308				
Chronicity MPSS	1	3	4	ref					
	2	29	5	7.7 [1.3–45.5]	0.031*				
	3	43	9	6.4 [1.2–33.5]	0.036*				
Surgery	No	53	12	ref					
	Yes	22	6	0.8 [0.3–2.5]	0.778				
Use of analgesics	No	10	5	ref					
	Yes	65	13	2.5 [0.7–8.5]	0.158				

(Continued)

TABLE 4 | Continued

		Contribution to general well-being			
		Yes	**No**	**OR [95% CI]**	***p*-value**
Pain duration [m]	mdn (IQR)	66 (21–182)	19 (59–202)		0.911
Age [a]	mdn (IQR)	50 (41–52)	49 (34–54)		0.549

*$Resp_{30/50}$, Acupuncture responders defined according to a reduction in pain intensity after the first acupuncture treatment of at least 30 or 50%, respectively; MPSS, Mainz Pain Staging System; m, months; a, years; ref, reference category; mdn, median; IQR, interquartile range; OR, odds ratio; 95% CI, 95% confidence interval; *statistically significant at an α-level of 5% according to Fisher test for dichotomous variables and according to Mann-Whitney-U test for continuous variables.*

TABLE 5 | Logistic regression models of age-adjusted associations between immediate analgesic acupuncture effects and high TS.

Dependent variable		**Model 1**	**Model 2**	**Model 3**	**Dependent variable**		**Model 4**
		$Resp_{30}$	**Subjective immediate pain relief**	**Subjective immediate pain relief >50%**			**Subjective immediate pain relief >50%**
Model fit criteria					**Model fit criteria**		
WUR control site >2.5 (VRS-ratio)	OR [95%-KI]	4.3 [1.6–11.8]	3.8 [1.4–10.2]	5.5 [1.7–17.1]	WUR pain site >2.5 (VRS-ratio)	OR [95%-KI]	3.2 [1.2–8.9]
	p-value	0.005*	0.007*	0.003*		*p-value*	0.024*
Age [a]	OR [95%-KI]	1.08 [1.0–1.1]	1.06 [1.0–1.1]	1.11 [1.0–1.2]	Age [a]	OR [95%-KI]	1.07 [1.0–1.1]
	p-value	0.004*	0.014*	0.002*		*p-value*	0.026*
Constant	OR	0.01	0.02	0.00	Constant	OR	0.01
	p-value	0.001*	0.003*	< 0.001*		*p-value*	0.002*
Omnibus test	*p-value*	0.001*	0.003*	< 0.001*	Omnibus test	*p-value*	0.002*
H-L test	*p-value*	0.407	0.311	0.169	H-L test	*p-value*	0.076
Nagelkerkes R^2		0.199	0.157	0.251	Nagelkerkes R^2		0.183
VIF		1.056	1.056	1.056	VIF		1.034
Correctly classified cases [%]	Yes	55.3	36.1	26.1	Correctly classified cases [%]	Yes	13.0
	No	80.0	86.4	94.4		No	94.2
	Total	69.9	67.4	77.9		Total	73.9

*$Resp_{30}$, Acupuncture responders defined according to a reduction in pain intensity after the first acupuncture treatment of at least 30%; WUR, wind-up ratio; VRS-ratio, ratio of the pain intensities evoked by one and by ten pin-prick stimuli of 256 mN as evaluated by the verbal rating scale (0–100); CS, control site; PS, pain site; a, years; OR, odds ratio; 95% CI, 95% confidence interval; H-L test, Hosmer-Lemeshow test; VIF, variation inflation factor; *statistically significant at an α-level of 5%.*

There was no significant association between a reduction in pain intensity after the first acupuncture treatment of over 50% ($Resp_{50}$) and a high TS (WUR > 2.5). However, when subgrouping patients according to an age cut-off identified by a ROC-analysis (53 years), the cumulative response function (**Figure 3**) shows a trend toward higher frequencies of responders among those with a WUR over 2.5 irrespective of the responder definition. Responder rates in the subgroup of patients over 53 years of age displaying a high WUR are only based on eight cases.

Model 2 indicates that the subjective experience of an immediate pain relief through acupuncture was reported with a 3.8 (95% CI [1.4–10.2%]; $p = 0.007$) times higher odds in patients with a high TS (WUR > 2.5) at the control site. With every year of age the likelihood of such positive appraisal of the immediate analgesic effect of acupuncture increased by 6% (95% CI [1–11%]; $p = 0.014$). Specificity was slightly higher (86%) and sensitivity lower (36%) than in model 2.

The association between a subjective immediate pain relief of over 50% after one of the acupuncture sessions with a high TS at the control site is described by model 3. Patients with a WUR of over 2.5 at the control site were 5.5 (95% CI [1.7–17.1]; $p = 0.003$) times more likely to report such strong immediate analgesic response. The influence of age was larger when compared to the other final models (OR 1.11 [1.04–1.189]; $p < 0.001$). With 78% the percentage of correctly classified cases was also high when compared to the other models. Specificity was 94%, while sensitivity was lower than in the other models (26%).

According to model 4, a high TS (WUR > 2.5) at the pain site increased the chance to experience an immediate pain relief of over 50% after one of the acupuncture treatments by 3.2 (95% CI [1.2–8.9]; $p = 0.024$) times. The odds was further increased by 7% (95% CI [1–14%]; $p = 0.026$) with every year of age. As in model 3, specificity was as high as 94% while the sensitivity of 13% was the lowest among all models.

DISCUSSION

To our knowledge, this is the first study evaluating temporal summation of pain (TS) and the vibration detection threshold (VDT) as predictors for acupuncture effects. The results support the hypothesis that high TS might predict response to acupuncture in chronic pain patients with regard to immediate effects. The presumed association of vibration detection with acupuncture effects was not ascertained.

Association of High Temporal Summation of Pain With Acupuncture Effects

A WUR over 2.5 indicating elevated TS at a pain-free control site and at the most painful body site increased the likelihood to experience immediate analgesic effects through acupuncture by three to five times. This suggests that in chronic pain patients in whom spinal synaptic transmission is facilitated acupuncture may be particularly effective for immediate pain relief. This appears plausible considering that immediate analgesic acupuncture effects are mainly mediated by bottom-up and top-down mechanisms which reduce spinal transmission (Zhao, 2008; Zhang et al., 2014). These include the activation of the descending inhibitory pain control, segmental inhibition, a reduction of spinal pronociceptive peptides and local modulation of primary afferents mediated by purinergic signaling.

Increased TS has been shown to be associated with the efficacy of drugs i.e., Ketamin (Lavand'homme and Roelant, 2009), Pregabalin (Olesen et al., 2013) and Oxycodon (Eisenberg et al., 2010). It is argued that this fact relates to the ability of these substances to reduce spinal synaptic fascilitation (Yarnitsky, 2015). According to numerous animal experiments (mostly conducted in rats), the same can be assumed for acupuncture (Zhang et al., 2014). In particular, electroacupuncture was found to mediate its analgesic effect in different animal pain models (cancer pain, muscle pain and inflammatory pain) through reducing spinal substance P concentration (SP) (Lee et al., 2009; Hsieh et al., 2014) and counteracting the upregulation of the neurokinin receptor 1 (NK1) (Zhang et al., 2005) as well as SP-NK1 downstream targets such as phosphatidylinositol 3-kinase and Akt (Kim et al., 2012). Additionally, reduced hyperalgesia after electroacupuncture was associated with lower upregulation of NGF in a diabetes model (Manni et al., 2011) and decreased NMDA receptor phosphorylation (Tian et al., 2008) as well as lower density of the NMDA subunit (NR2B) in a model of irritable bowel syndrome (Liu et al., 2016). Further acupuncture mechanisms counteracting spinal synaptic facilitation seem to include inhibition of glia cell activation (Lin et al., 2016). In line with this, electroacupuncture reduced spinal concentrations of interleukin-1β in a bone-cancer model (Zhang et al., 2007) and of nitric oxide in a neuropathic pain model (Cha et al., 2010).

Investigations of acupuncture effects on TS in humans that would provide further evidence of its spinal anti-fascilitatory effects are sparse. According to one trial electroacupuncture, but not manual acupuncture decreased TS in healthy volunteers (Zheng et al., 2010), while four studies, two also in healthy volunteers (Lang et al., 2010; Baeumler et al., 2015), one in whip-lash patients (Tobbackx et al., 2013) and one recent trial in patients with chronic low back pain (Leite et al., 2018) found neither electroacupuncture nor manual acupuncture to affect TS. Two main legitimate objections have been raised regarding these conflicting results (Kong et al., 2013). First, except for one trial, effects of a single acupuncture treatment were assessed. However, a clinically relevant reduction of spinal synaptic facilitation would rather be expected after a series of acupuncture sessions. Second, wind-up in healthy volunteers is already low and, thus, may hardly be affected by regulatory interventions such as acupuncture. In addition, methodological differences between studies such as the nociceptive stimulus used to elicit TS and the use of absolute pain scores elicited by repetitive stimuli instead of the ratio between single and repetitive stimuli accounting for overall pain sensitivity may give rise to further source of bias.

High TS at the control site was positively associated with reduced pain intensity after the first acupuncture treatment as indicated by both logistic regression and by the cumulative response function. Additionally, high TS at the control site was associated with subjective pain relief as evaluated by the questionnaire. In contrast, the association of high TS at the most painful body site was only associated with the subjective experience of an immediate pain relief of over 50%. This indicates that propagated synaptic facilitation throughout the spinal cord, e.g., through volume transmission (Zieglgänsberger, 2009), as a sign of advanced central sensitization is more important for the prediction of immediate analgesic acupuncture effects than primary synaptic facilitation. External validity of these results can be assumed high, since no specific selection criteria were applied. The cut-off definition for a high TS as a WUR of over 2.5 applied in our study may also be useful in future trials, as it was confirmed by an ROC-analysis and it matches the population mean established in healthy controls which appears constant over various body sites (Rolke et al., 2006; Puta et al., 2013; Pfau et al., 2014).

Few studies had previously assessed sensory signs as evaluated by QST as predictors for the analgesic effect of acupuncture. Two trials from the same research group identified a low pressure pain threshold at the thumbnail to predict a good response to sham-acupuncture (needling at non-acupuncture points or non-penetrating sham) in fibromyalgia (Harte et al., 2013; Zucker et al., 2017). In their second trial (Zucker et al., 2017), conversely, a low pressure pain threshold predicted a non-response verum acupuncture and strong needle sensations even caused an increase in clinical pain. In addition, a low electrical pain threshold in a pain-free body site has also been found to be lower in electroacupuncture non-responders than responders among patients suffering from painful burn scars (Cuignet et al., 2015). Authors discuss that the strength of needle stimulation needs to be adapted to the patients' sensitivity in order to maximize treatment effects and to avoid unfavorable outcomes. As treatments in our trial were individually tailored, it can be assumed that bias caused by needle stimulation exceeding the patients' comfort zone was minimal.

We found no association of TS with the patients' subjective appraisal of the contribution of acupuncture to overall pain relief during the 4-week multimodal pain treatment program.

However, it needs to be emphasized that our study was not designed to confirm predictors for pain reduction after a series of acupuncture treatments. The appraisal of the contribution of acupuncture to overall pain reduction is likely to be affected by treatment success of the whole multimodal pain program involving a variety of therapy modalities. Therefore, the prediction of the long-term effects of acupuncture by TS and other somatosensory thresholds remain subject of further investigations.

Confounding by Age

Age confounded the association of high TS at the control site with the immediate analgesic acupuncture effect and age-adjusted ORs were larger than crude OR. Collinearity was ruled out according to the VIF of the respective logistic regression models. Thus, one can conclude that older age was positively associated with response to acupuncture and marginally more frequent in patients with high TS at the control site. The latter is in line with previous findings indicating that age does not substantially influence heat evoked TS in fibromyalgia patients (Staud et al., 2008) and pressure evoked TS in patients suffering from knee osteoarthritis (Petersen et al., 2017). In contrast, the relation of age with TS remains elusive in healthy adults in which heat evoked TS was found to be positively associated with age (Edwards and Fillingim, 2001) while pin-prick evoked TS seems age-independent (Magerl et al., 2010).

It can only be speculated why the chance to experience an immediate analgesic effect through acupuncture increased by 6–10% with every year of age. We are only aware of previous studies that assessed the influence of age on long-term pain relief achieved by acupuncture. A reanalysis of the large German acupuncture trials revealed that pain reduction after a series of verum- as well as after a series of sham-acupuncture was weakly associated with younger age (Witt et al., 2011). A more recent qualitative patient assessment of acupuncture effects revealed no association with age (Cramer et al., 2015). Our finding of a more pronounced immediate acupuncture effect in older patients might be explained by the fact that sensory stimulation, such as applied during needling, might have stronger impact on older patients. Sensory perception is known to decrease with age (Magerl et al., 2010), but was shown to be more efficiently modulated by conditioning stimuli in older than in younger subjects (Naugle et al., 2015).

No Association Between Vibration Detection Threshold and Acupuncture Effects

The hypothesis that poor Aβ-fiber function indicated by a loss in vibration detection would predict a poor acupuncture response was not confirmed. However, the large variance in VDT data particularly at the pain sites hampers interpretability of this finding. It is known that the VDT varies largely between body sites (Rolke et al., 2006). Our results once again suggest that a meaningful interpretation of the VDT in clinical practice would require reference values for a large variety of body sites. These are not yet established. To fully reject or approve our hypothesis, patient populations with consistent pain sites might be assessed. It should be considered that supra-spinal and local acupuncture mechanisms might compensate the lack of segmental inhibition related to poor Aβ-fiber function. Consequently, poor VDT might still be associated with immediate analgesic effects of a purely segmental needling regimen. An association between long-term acupuncture effects and the VDT in turn appears unlikely, as segmental effects inducing long-term depression of spinal synaptic pain transmission rely on the activation of Aδ- rather than Aβ-fibers. Furthermore, a loss of mechanical detection that has been described in several also non-neuropathic chronic pain conditions (Geber et al., 2008; Westermann et al., 2011; Puta et al., 2013) might not necessarily be caused by a loss in Aβ-fiber function but rather by a presynaptic inhibition linked to the constant nociceptive input (Janig and Zimmermann, 1971). If the latter hypothesis proves true, a reduced activation of the nociceptive system after a successful acupuncture treatment would also be reflected by an increased ability to detect mechanical stimuli. Future studies on the effectiveness of acupuncture in neuropathic pain conditions might explore this hypothesis.

LIMITATIONS

A source of bias in this study is that recruitment and data collection were integrated into the course of a multimodal pain treatment program. Thus, overall treatment satisfaction might have influenced patients' rating of acupuncture effects. Social desirability bias (Furnham, 1986) might have been caused by the fact that baseline and follow-up examinations were performed by the same examiner. However, evaluations of the reduction in pain intensity after the first acupuncture treatment were free from such bias, as acupuncture was always applied as the first treatment modality on the first day of the multimodal pain program. Furthermore, patients took their usual pain medication. However, it seem unlikely that the intake of analgesics has affected the results. First, short-term drug level changes were avoided as stable pain medication intake is a precondition to take part in the multimodal pain treatment program performed at the study center. Second, the use of analgesics was neither a confounder nor an effect modifier for the associations under investigation, nor was it confirmed to be an independent predictor for pain relief after acupuncture in the multivariate analysis. Additionally, excluding patients on pain medication would have rendered our sample not representative for the average population of chronic pain patients that an acupuncturist encounters in daily clinical practice.

Additionally, it is known that multiple testing might lead to false inferences in observational studies, as they require adjustment for various covariates which automatically increases the number of hypotheses tested (Patel and Ioannidis, 2014; Gruber and Tchetgen, 2016). Consensus on strategies for a meaningful p-value adjustment has not been found. However, Bonferroni correction of each predictor hypothesis test for the four outcome parameters (VRS pain score, subjective immediate and overall pain relief and effect on wellbeing) would results a

critical p-value of 0.0125. Under this assumption, associations between the WUR at the control site but not the pain site would remain statistically significant; supporting the notion that WUR in a pain free control site is a more promising predictor for response to acupuncture. It is argued that hypothesis driven analyses are best to omit bias arising from multiple testing. The design of this study is based on hypotheses driven by clinical and neurophysiological considerations and previous observations. Nevertheless, statistical analyses were performed in an exploratory manner to optimally explain variation in the data. Thus, these results require replication by future confirmatory research and validation of the proposed predictor models in an independent population.

Perspectives

Our results are an important step toward an individualized pain therapy in regard to non-pharmacological treatments based on sensory profiles. Expenditure of resources to explore TS in chronic pain patients as a predictor also for long-term acupuncture effects is now justified. In addition, further research is needed to explore whether effectiveness of acupuncture in certain pain conditions such as neuropathic pain, low back pain etc. can be predicted by strong signs of central sensitization. Another sensory sign of interest in this regard might be the conditioned pain modulation (CPM) indicating descending pain control. Acupuncture has been shown to activate descending pain control mechanisms, but it has not yet been investigated whether CPM predicts acupuncture effects, or whether a lack in CPM can be reestablished by continuous acupuncture treatment.

CONCLUSION

Strong central sensitization reflected by high TS, in particular at pain free control sites, seems to predict the immediate analgesic response to acupuncture. Clinically spoken, acupuncture could be especially effective in highly sensitized chronic pain patients.

ETHICS STATEMENT

Study conduct was in accordance with the Declaration of Helsinki formulated by the World Medical Association [updated version, Seoul (The World Medical Association, 2008)] and was approved by the ethics committee of the Medical Faculty of the Ludwig-Maximilians University of Munich. Written informed consent was obtained from all participants. Withdrawal from study procedures was open to participants at any time. In case of withdrawal all data recorded in the course of the study were deleted. Data handling was performed in pseudonymous form and followed the German data-protection act.

AUTHOR CONTRIBUTIONS

PB, DI, and PC conceptualized the study design, contributed to interpretation of the results and drafted the manuscript. PB was in charge of patient recruitment, data-acquisition, and data-analysis.

ACKNOWLEDGMENTS

We thank the acupuncturists of the MOCAM (Mrs. Gesa Harreus MD, Mrs. Barbara Jopen-Wolff MD, Mrs. Maria Durand MD, Mrs. Franziska Portzky MD and Mr. Christoph Colling MD) for making it possible to conduct the study during their daily clinical practice. We also thank Mrs. Adelheid Wanninger for her support in data-acquisition as well as Mrs. Erika Weber and Mrs. Christina Deisenrieder for their organizational support.

REFERENCES

Altman, D. G. (1991). *Practical Statistic for Medical Research*. London: Chapman and Hall.

Arendt-Nielsen, L. (2015). "Central sensitization in humans assessment and pharmacology," in *Pain Control*, ed H. G. Schaible (Berlin; Heidelberg: Springer-Verlag), 79–102.

Baeumler, P., Benedikt, F., Bader, J., Fleckenstein, J., and Irnich, D. (2014). "Acupuncture induced changes of the pressure pain threshold are mediated by segmental inhibition? A randomized controlled trial," *Poster at the International Scientific Acupuncture and Meridian Symposium (ISAMS)* (Tokyo).

Baeumler, P. I., Fleckenstein, J., Benedikt, F., Bader, J., and Irnich, D. (2015). Acupuncture-induced changes of pressure pain threshold are mediated by segmental inhibition – a randomized controlled trial. *Pain* 156, 2245–2255. doi: 10.1097/j.pain.0000000000000283

Cha, M. H., Bai, S. J., Lee, K. H., Cho, Z. H., Kim, Y. B., Lee, H. J., et al. (2010). Acute electroacupuncture inhibits nitric oxide synthase expression in the spinal cord of neuropathic rats. *Neurol. Res.* 32, 96–100. doi: 10.1179/016164109X12537002794363

Clarke, R. W., Eves, S., Harris, J., Peachey, J. E., and Stuart, E. (2002). Interactions between cutaneous afferent inputs to a withdrawal reflex in the decerebrated rabbit and their control by descending and segmental systems. *Neuroscience* 112, 555–571. doi: 10.1016/S0306-4522(02)00093-3

Cole, S. R., Platt, R. W., Schisterman, E. F., Chu, H., Westreich, D., Richardson, D., et al. (2010). Illustrating bias due to conditioning on a collider. *Int. J. Epidemiol.* 39, 417–20. doi: 10.1093/ije/dyp334

Cramer, H., Chung, V. C., Lauche, R., Zhang, Y., Zhang, A., Langhorst, J., et al. (2015). Characteristics of acupuncture users among internal medicine patients in Germany. *Complement. Ther. Med.* 23, 423–429. doi: 10.1016/j.ctim.2015.04.009

Cribbie, R., and Jamieson, J. (2000). Structural equation models and the regression bias for measuring correlated of change *Edu. Psychol. Meas.* 60, 893–9007. doi: 10.1177/00131640021970970

Cuignet, O., Pirlot, A., Ortiz, S., and Rose, T. (2015). The effects of electroacupuncture on analgesia and peripheral sensory thresholds in patients with burn scar pain. *Burns* 41, 1298–1305. doi: 10.1016/j.burns.2015.03.002

Daenen, L., Nijs, J., Cras, P., Wouters, K., and Roussel, N. (2014). Changes in pain modulation occur soon after whiplash trauma but are not related to altered perception of distorted visual feedback. *Pain Practice* 14, 588–598. doi: 10.1111/papr.12113

Dworkin, R. H., Turk, D. C., Farrar, J. T., Haythornthwaite, J. A., Jensen, M. P., Katz, N. P., et al. (2005). Core outcome measures for chronic pain clinical trials: IMMPACT recommendations. *Pain* 113, 9–19. doi: 10.1016/j.pain.2004.09.012

Edwards, R. R., and Fillingim, R. B. (2001). Effects of age on temporal summation and habituation of thermal pain: clinical relevance in healthy older and younger adults. *J. Pain: Off. J. Am. Pain Soc.* 2, 307–317. doi: 10.1054/jpai.2001.25525

Edwards, R. R., Quartana, P. J., Allen, R. P., Greenbaum, S., Earley, C. J., and Smith, M. T. (2011). Alterations in pain responses in treated and untreated patients with restless legs syndrome: associations with sleep disruption. *Sleep Med.* 12, 603–609. doi: 10.1016/j.sleep.2010.09.018

Eide, P. K. (2000). Wind-up and the NMDA receptor complex from a clinical perspective. *Europ. J. Pain* 4, 5–15. doi: 10.1053/eujp.1999.0154

Eide, P. K., Jorum, E., Stubhaug, A., Bremnes, J., and Breivik, H. (1994). Relief of post-herpetic neuralgia with the N-methyl-D-aspartic acid receptor antagonist ketamine: a double-blind, cross-over comparison with morphine and placebo. *Pain* 58, 347–354. doi: 10.1016/0304-3959(94)90129-5

Eisenberg, E., Midbari, A., Haddad, M., and Pud, D. (2010). Predicting the analgesic effect to oxycodone by static and dynamic quantitative sensory testing in healthy subjects. *Pain* 151, 104–109. doi: 10.1016/j.pain.2010.06.025

Farrar, J. T., Dworkin, R. H., and Max, M. B. (2006). Use of the cumulative proportion of responders analysis graph to present pain data over a range of cut-off points: making clinical trial data more understandable. *J. Pain Symptom Manage.* 31, 369–77. doi: 10.1016/j.jpainsymman.2005.08.018

Farrar, J. T., Young, J. P. Jr., LaMoreaux, L., Werth, J. L., and Poole, R. M. (2001). Clinical importance of changes in chronic pain intensity measured on an 11-point numerical pain rating scale. *Pain* 94, 149–158. doi: 10.1016/S0304-3959(01)00349-9

Furnham, A. (1986). Response bias, social desirability and dissimulation. *Pers. Individ. Dif.* 7, 385–400. doi: 10.1016/0191-8869(86)90014-0

Geber, C., Klein, T., Azad, S., Birklein, F., Gierthmuhlen, J., Huge, V., et al. (2011). Test-retest and interobserver reliability of quantitative sensory testing according to the protocol of the German Research Network on Neuropathic Pain (DFNS): a multi-centre study. *Pain* 152, 548–556. doi: 10.1016/j.pain.2010.11.013

Geber, C., Magerl, W., Fondel, R., Fechir, M., Rolke, R., Vogt, T., et al. (2008). Numbness in clinical and experimental pain—a cross-sectional study exploring the mechanisms of reduced tactile function. *Pain* 139, 73–81. doi: 10.1016/j.pain.2008.03.006

Gerhardt, A., Eich, W., Janke, S., Leisner, S., Treede, R. D., and Tesarz, J. (2015). Chronic widespread back pain is distinct from chronic local back pain: evidence from quantitative sensory testing, pain drawings, and psychometrics. *Clin. J. Pain* 32, 568–579. doi: 10.1097/AJP.0000000000000300

Graven-Nielsen, T., Aspegren Kendall, S., Henriksson, K. G., Bengtsson, M., Sorensen, J., Johnson, A., et al. (2000). Ketamine reduces muscle pain, temporal summation, and referred pain in fibromyalgia patients. *Pain* 85, 483–491. doi: 10.1016/S0304-3959(99)00308-5

Gruber, S., and Tchetgen, E. (2016). Limitations of empirical calibration of p-values using observational data. *Stat. Med.* 35, 3869–3882. doi: 10.1002/sim.6936

Harte, S. E., Clauw, D. J., Napadow, V., and Harris, R. E. (2013). Pressure pain sensitivity and insular combined glutamate and glutamine (Glx) are associated with subsequent clinical response to sham but not traditional acupuncture in patients who have chronic pain. *Med. Acupunct.* 25, 154–160. doi: 10.1089/acu.2013.0965

Herrero, J. F., Laird, J. M., and Lopez-Garcia, J. A. (2000). Wind-up of spinal cord neurones and pain sensation: much ado about something? *Prog. Neurobiol.* 61, 169–203. doi: 10.1016/S0301-0082(99)00051-9

Hsieh, Y. L., Yang, C. C., Liu, S. Y., Chou, L. W., and Hong, C. Z. (2014). Remote dose-dependent effects of dry needling at distant myofascial trigger spots of rabbit skeletal muscles on reduction of substance P levels of proximal muscle and spinal cords. *BioMed Res. Int.* 2014:982121. doi: 10.1155/2014/982121

Institute of Medicine (2011). *Relieving Pain in America - A Blueprint for Transforming Prevention, Care, Education, and Research.* Washington, DC: National Academies Press.

Janig, W., and Zimmermann, M. (1971). Presynaptic depolarization of myelinated afferent fibres evoked by stimulation of cutaneous C fibres. *J. Physiol.* 214, 29–50. doi: 10.1113/jphysiol.1971.sp009417

Kim, H. N., Kim, Y. R., Jang, J. Y., Shin, H. K., and Choi, B. T. (2012). Electroacupuncture inhibits phosphorylation of spinal phosphatidylinositol 3-kinase/Akt in a carrageenan-induced inflammatory rat model. *Brain Res. Bull.* 87, 199–204. doi: 10.1016/j.brainresbull.2011.11.010

Kong, J. T., Schnyer, R. N., Johnson, K. A., and Mackey, S. (2013). Understanding central mechanisms of acupuncture analgesia using dynamic quantitative sensory testing: a review. *Evid. Based Compl. Altern. Med.* 2013:187182. doi: 10.1155/2013/187182

Lang, P. M., Stoer, J., Schober, G. M., Audette, J. F., and Irnich, D. (2010). Bilateral acupuncture analgesia observed by quantitative sensory testing in healthy volunteers. *Anesth. Analg.* 110, 1448–1456. doi: 10.1213/ANE.0b013e3181d3e7ef

Lavand'homme, P., and Roelant, F. (2009). Effect of a low dose of ketamine on postoperative pain after elective cesarean delivery according to the presence of a preoperative temporal summation. *SOAP Abstract A*258.

Lee, H. J., Lee, J. H., Lee, E. O., Lee, H. J., Kim, K. H., Lee, K. S., et al. (2009). Substance P, and beta endorphin mediate electroacupuncture induced analgesic activity in mouse cancer pain model. *Acupuncture Electro–Therap. Res.* 34, 27–40. doi: 10.3727/036012909803861095

Leite, P. M. S., Mendonca, A. R. C., Maciel, L. Y. S., Poderoso-Neto, M. L., Araujo, C. C. A., Gois, H. C. J., et al. Does Electroacupuncture Treatment Reduce Pain and Change Quantitative Sensory Testing Responses in Patients with Chronic Nonspecific Low Back Pain? A Randomized Controlled Clinical Trial. *Evid. Based Complement. Alternative Med.* (2018) 2018:8586746. doi: 10.1155/2018/8586746

Lev, R., Granovsky, Y., and Yarnitsky, D. (2010). Orbitofrontal disinhibition of pain in migraine with aura: an interictal EEG-mapping study. *Cephalalgia: Int. J. Headache* 30, 910–918. doi: 10.1177/0333102409357249

Lin, J. G., Lee, Y. C., Tseng, C. H., Chen, D. Y., Shih, C. Y., MacDonald, I., et al. (2016). Electroacupuncture inhibits pruritogen-induced spinal microglial activation in mice. *Brain Res.* 1649, 23–9. doi: 10.1016/j.brainres.2016.07.007

List, T., Leijon, G., and Svensson, P. (2008). Somatosensory abnormalities in atypical odontalgia: a case–control study. *Pain* 139, 333–341. doi: 10.1016/j.pain.2008.05.002

Liu, H., Zhang, Y., Qi, D., and Li, W. (2016). Downregulation of the spinal NMDA receptor NR2B subunit during electro-acupuncture relief of chronic visceral hyperalgesia. *J.Physiol. Sci.* 67, 197–206. doi: 10.1007/s12576-016-0456-1

MacPherson, H., Vertosick, E. A., Foster, N. E., Lewith, G., Linde, K., Sherman, K. J., et al. (2017). The persistence of the effects of acupuncture after a course of treatment: a meta-analysis of patients with chronic pain. *Pain* 158, 784–793. doi: 10.1097/j.pain.0000000000000747

Maeda, Y., Kim, H., Kettner, N., Kim, J., Cina, S., Malatesta, C., et al. (2017). Rewiring the primary somatosensory cortex in carpal tunnel syndrome with acupuncture. *Brain: J. Neurol.* 140, 914–927. doi: 10.1093/brain/awx015

Magerl, W., Krumova, E. K., Baron, R., Tolle, T., Treede, R. D., and Maier, C. (2010). Reference data for quantitative sensory testing (QST): refined stratification for age and a novel method for statistical comparison of group data. *Pain* 151, 598–605. doi: 10.1016/j.pain.2010.07.026

Main, C. J., Sullivan, M. J. L., and Watson, P. W. (2008). *Pain Management: Practical Applications of the Biopsychosocial Perspective in clinical and Occupational Settings*. Edinburgh; London; New York, NY; Oxford; Philadelphia, PA; St. Louis, MO; Sydney, NSW; Toronto, ON: Churchill Livingstone - Elsevier.

Manni, L., Florenzano, F., and Aloe, L. (2011). Electroacupuncture counteracts the development of thermal hyperalgesia and the alteration of nerve growth factor and sensory neuromodulators induced by streptozotocin in adult rats. *Diabetologia* 54, 1900–1908. doi: 10.1007/s00125-011-2117-5

McLeod, A. I., and Changjiang, X. (2018). *Best Subset, G.* L. M., and Regression Utilities. Available online at: https://cran.r-project.org/web/packages/bestglm/bestglm.pdf

Melin, C., Jacquot, F., Dallel, R., and Artola, A. (2013). Segmental disinhibition suppresses C-fiber inputs to the rat superficial medullary dorsal horn via the activation of GABAB receptors. *Eur. J. Neurosci.* 37, 417–428. doi: 10.1111/ejn.12048

Mendell, L. M. (1966). Physiological properties of unmyelinated fiber projection to the spinal cord. *Exp. Neurol.* 16, 316–332. doi: 10.1016/0014-4886(66)90068-9

Musial, F., Spohn, D., and Rolke, R. (2013). Naturopathic reflex therapies for the treatment of chronic back and neck pain - Part 1: Neurobiological foundations. *Forsch. Komplementmed.* 20, 219–224. doi: 10.1159/000353392

Naugle, K. M., Cruz-Almeida, Y., Vierck, C. J., Mauderli, A. P., and Riley, J. L. III. (2015). Age-related differences in conditioned pain modulation of sensitizing

and desensitizing trends during response dependent stimulation. *Behav. Brain Res.* 289:61–68. doi: 10.1016/j.bbr.2015.04.014

Nikolajsen, L., Hansen, C. L., Nielsen, J., Keller, J., Arendt-Nielsen, L., and Jensen, T. S. (1996). The effect of ketamine on phantom pain: a central neuropathic disorder maintained by peripheral input. *Pain* 67, 69–77. doi: 10.1016/0304-3959(96)03080-1

Olesen, S. S., Graversen, C., Bouwense, S. A., van Goor, H., Wilder-Smith, O. H., and Drewes, A. M. (2013). Quantitative sensory testing predicts pregabalin efficacy in painful chronic pancreatitis. *PLoS ONE* 8:e57963. doi: 10.1371/journal.pone.0057963

Patel, C. J., and Ioannidis, J. P. (2014). Placing epidemiological results in the context of multiplicity and typical correlations of exposures. *J. Epidemiol. Comm. Health* 68, 1096–1100. doi: 10.1136/jech-2014-204195

Petersen, K. K., Arendt-Nielsen, L., Finocchietti, S., Hirata, R. P., Simonsen, O., Laursen, M. B., et al. (2017). Age interactions on pain sensitization in patients with severe knee osteoarthritis and controls. *Clin. J. Pain* 33, 1081–1087. doi: 10.1097/AJP.0000000000000495

Pfau, D. B., Krumova, E. K., Treede, R. D., Baron, R., Toelle, T., Birklein, F., et al. (2014). Quantitative sensory testing in the German Research Network on Neuropathic Pain (DFNS): reference data for the trunk and application in patients with chronic postherpetic neuralgia. *Pain* 155, 1002–1015. doi: 10.1016/j.pain.2014.02.004

Pud, D., Eisenberg, E., Spitzer, A., Adler, R., Fried, G., and Yarnitsky, D. (1998). The NMDA receptor antagonist amantadine reduces surgical neuropathic pain in cancer patients: a double blind, randomized, placebo controlled trial. *Pain* 75, 349–354. doi: 10.1016/S0304-3959(98)00014-1

Puta, C., Schulz, B., Schoeler, S., Magerl, W., Gabriel, B., Gabriel, H. H., et al. (2013). Somatosensory abnormalities for painful and innocuous stimuli at the back and at a site distinct from the region of pain in chronic back pain patients. *PLoS ONE* 8:e58885. doi: 10.1371/journal.pone.0058885

R Development Core Team (2008). *R: A Language and Environment for Statistical Computing. Vienna.* Available online at: http://wwwR-projectorg

Rabey, M., Slater, H., O'Sullivan, P., Beales, D., and Smith, A. (2015). Somatosensory nociceptive characteristics differentiate subgroups in people with chronic low back pain: a cluster analysis. *Pain* 156, 1874–1884. doi: 10.1097/j.pain.0000000000000244

Rolke, R., Baron, R., Maier, C., Tolle, T. R., Treede, R. D., Beyer, A., et al. (2006). Quantitative sensory testing in the German Research Network on Neuropathic Pain (DFNS): standardized protocol and reference values. *Pain* 123, 231–243. doi: 10.1016/j.pain.2006.01.041

Sandkuhler, J. (1996). The organization and function of endogenous antinociceptive systems. *Prog. Neurobiol.* 50, 49–81. doi: 10.1016/0301-0082(96)00031-7

Sandkühler, J. (2000). "Long-Lasting Analgesia following TENS and acupuncture: spinal mechanisms beyond gate control," in *9th World Congress on Pain - Progess in Pain Research and Mnagement – Wien* (Seattle:IASP Press).

Staud, R., Bovee, C. E., Robinson, M. E., and Price, D. D. (2008). Cutaneous C-fiber pain abnormalities of fibromyalgia patients are specifically related to temporal summation. *Pain* 139, 315–323. doi: 10.1016/j.pain.2008.04.024

Staud, R., Vierck, C. J., Cannon, R. L., Mauderli, A. P., and Price, D. D. (2001). Abnormal sensitization and temporal summation of second pain (wind-up) in patients with fibromyalgia syndrome. *Pain* 91, 165–175. doi: 10.1016/S0304-3959(00)00432-2

The World Medical Association (2008). *Declaration of Helsinki-Updated Version. Seoul.* Available online at: https://www.wma.net/what-we-do/medical-ethics/declaration-of-helsinki/doh-oct2008/

Tian, S. L., Wang, X. Y., and Ding, G. H. (2008). Repeated electro-acupuncture attenuates chronic visceral hypersensitivity and spinal cord NMDA receptor phosphorylation in a rat irritable bowel syndrome model. *Life Sci.* 83, 356–363. doi: 10.1016/j.lfs.2008.06.027

Tobbackx, Y., Meeus, M., Wauters, L., De Vilder, P., Roose, J., Verhaeghe, T., et al. (2013). Does acupuncture activate endogenous analgesia in chronic whiplash-associated disorders? randomized crossover trial. *Eur. J. Pain* 17, 279–289. doi: 10.1002/j.1532-2149.2012.00215.x

Vaegter, H. B., and Graven-Nielsen, T. (2016). Pain modulatory phenotypes differentiate subgroups with different clinical and experimental pain sensitivity. *Pain* 157, 1480–1488. doi: 10.1097/j.pain.0000000000000543

Vickers, A. J. (2001). The use of percentage change from baseline as an outcome in a controlled trial is statistically inefficient: a simulation study. *BMC Med. Res. Methodol.* 1:6. doi: 10.1186/1471-2288-1-6

Vickers, A. J., and Linde, K. (2014). Acupuncture for chronic pain. *JAMA* 311, 955–956. doi: 10.1001/jama.2013.285478

Vickers, A. J., Vertosick, E. A., Lewith, G., MacPherson, H., Foster, N. E., Sherman, K. J., et al. (2018). Acupuncture for chronic pain: update of an individual patient data meta-analysis. *J. Pain* 19, 455–474. doi: 10.1016/j.jpain.2017.11.005

Wancura-Kampik, I. (2012). *Segmental Anatomy: The Key to Mastering Acupuncture, Neural Therapy and Manual Therapy*. Munich: Elsevier GmbH, Urban and Fischer Verlag, Lektorat Komplementäre und Integrative Medizin .

Westermann, A., Ronnau, A. K., Krumova, E., Regeniter, S., Schwenkreis, P., Rolke, R., et al. (2011). Pain-associated mild sensory deficits without hyperalgesia in chronic non-neuropathic pain. *Clin. J. Pain* 27, 782–789. doi: 10.1097/AJP.0b013e31821d8fce

White, A., Cummings, M., and Filshie, J. (2011). *An Introduction to Western Medical Acupuncture* (Edinburgh: Churchill Livingstone–Elsevier), 240.

Witt, C. M., Schutzler, L., Ludtke, R., Wegscheider, K., and Willich, S. N. (2011). Patient characteristics and variation in treatment outcomes: which patients benefit most from acupuncture for chronic pain? *Clin. J. Pain* 27, 550–555. doi: 10.1097/AJP.0b013e31820dfbf5

Yarnitsky, D. (2015). Role of endogenous pain modulation in chronic pain mechanisms and treatment. *Pain* 156, 24–31. doi: 10.1097/01.j.pain.0000460343.46847.58

Zhang, R., Lao, L., Ren, K., and Berman, B. M. (2014). Mechanisms of acupuncture-electroacupuncture on persistent pain. *Anesthesiology* 120, 482–503. doi: 10.1097/ALN.0000000000000101

Zhang, R. X., Li, A., Liu, B., Wang, L., Ren, K., Qiao, J. T., et al. (2007). Electroacupuncture attenuates bone cancer pain and inhibits spinal interleukin-1 beta expression in a rat model. *Anesth. Analg.* 105, 1482–1488. doi: 10.1213/01.ane.0000284705.34629.c5

Zhang, R. X., Liu, B., Qiao, J. T., Wang, L., Ren, K., Berman, B. M., et al. (2005). Electroacupuncture suppresses spinal expression of neurokinin-1 receptors induced by persistent inflammation in rats. *Neurosci. Lett.* 384, 339–343. doi: 10.1016/j.neulet.2005.05.001

Zhao, Z. Q. (2008). Neural mechanism underlying acupuncture analgesia. *Prog. Neurobiol.* 85, 355–375. doi: 10.1016/j.pneurobio.2008.05.004

Zheng, Z., Feng, S. J., Costa, C., Li, C. G., Lu, D., and Xue, C. C. (2010). Acupuncture analgesia for temporal summation of experimental pain: a randomised controlled study. *Euro. J. Pain* 14, 725–731. doi: 10.1016/j.ejpain.2009.11.006

Zieglgänsberger, W. (2009). "Neuropeptides: electrophysiology," *in Encyclopedia of Neuroscience,* eds L. R. Squire (Oxford: Academic Press), 885–90. doi: 10.1016/B978-008045046-9.01456-X

Zucker, N. A., Tsodikov, A., Mist, S. D., Cina, S., Napadow, V., and Harris, R. E. (2017). Evoked pressure pain sensitivity is associated with differential analgesic response to verum and sham acupuncture in fibromyalgia. *Pain Med.* 18, 1582–1592. doi: 10.1093/pm/pnx001

Conflict of Interest Statement: PB was presented with the Young Scientists Award (sponsored by 3B-Scientific) for an oral presentation of the results presented in this manuscript at the congress of the International Council for Acupuncture and Related Techniques (ICMART) in June 2017. PB and DI receive honorarium and travel costs from non-profit academic organizations, physician chambers and universities for teaching and lecturing.

The remaining author declares that the research was conducted in the absence of any commercial or financial relationships that could be construed as a potential conflict of interest.

frontiers in Neuroscience

BRIEF RESEARCH REPORT
published: 29 August 2019
doi: 10.3389/fnins.2019.00928

Involvement of the Cuneate Nucleus in the Acupuncture Inhibition of Drug-Seeking Behaviors

Suchan Chang[1†], Yeonhee Ryu[2†], Yu Fan[1], Se Kyun Bang[2,3], Nam Jun Kim[1], Jin Gyeom Lee[1], Jin Mook Kim[1], Bong Hyo Lee[1], Chae Ha Yang[1] and Hee Young Kim[1]*

[1] College of Korean Medicine, Daegu Haany University, Daegu, South Korea, [2] Korean Medicine Fundamental Research Division, Korea Institute of Oriental Medicine, Daejeon, South Korea, [3] Korean Convergence Medicine, University of Science and Technology, Daejeon, South Korea

Our previous studies have shown that acupuncture suppresses addictive behaviors induced by drugs of abuse, including cocaine, morphine and ethanol, by modulating GABA neurons in the ventral tegmental area (VTA) and dopamine (DA) release in the nucleus accumbens (NAc). The mechanisms by which the peripheral signals generated by acupoint stimulation are transmitted to brain reward systems are largely unexplored. The present study aims to investigate the role of spinal dorsal column (DC) somatosensory pathways in the acupuncture inhibition of drug addictive behaviors. Thus, we tested whether acupuncture at *Shenmen* (HT7) points reduces drug-seeking behaviors in rats self-administering morphine or ethanol and whether such effects are inhibited by the disruption of the cuneate nucleus (CN). The stimulation of HT7 suppressed morphine and ethanol self-administration, which were completely abolished by surgical lesioning of the CN. In *in vivo* extracellular recordings, single-unit activity of the CN was evoked during acupuncture stimulation. The results suggest that acupuncture suppresses morphine- and ethanol-seeking behaviors through the modulation of the CN, second-order neurons of the DC somatosensory pathway.

Keywords: acupuncture, dorsal column pathway, cuneate nucleus, morphine, ethanol, self-administration

OPEN ACCESS

Edited by:
Yi-Wen Lin,
China Medical University, Taiwan

Reviewed by:
Antonio Luchicchi,
VU University Medical Center Amsterdam, Netherlands
Eric Andrew Engleman,
Indiana University Bloomington, United States
Sheketha R. Hauser,
Indiana University Bloomington, United States

****Correspondence:***
Hee Young Kim
hykim@dhu.ac.kr;
vet202001@gmail.com

† These authors have contributed equally to this work

Specialty section:
This article was submitted to Perception Science, a section of the journal Frontiers in Neuroscience

Received: *10 November 2018*
Accepted: *19 August 2019*
Published: *29 August 2019*

Citation:
Chang S, Ryu Y, Fan Y, Bang SK, Kim NJ, Lee JG, Kim JM, Lee BH, Yang CH and Kim HY (2019) Involvement of the Cuneate Nucleus in the Acupuncture Inhibition of Drug-Seeking Behaviors. Front. Neurosci. 13:928. doi: 10.3389/fnins.2019.00928

INTRODUCTION

Over the last three decades, there has been an increasing interest in the treatment of substance abuse by acupuncture (Cui et al., 2013). We and others have demonstrated that acupuncture attenuates drug-seeking behaviors and relapse through the modulation of the mesolimbic dopamine (DA) system in animals and humans (Yoon et al., 2004, 2010, 2012; Yang et al., 2010). While the fundamental relationship between somatic input signals induced by acupuncture and brain reward systems are not largely understood, our previous studies have suggested peripheral and spinal mechanisms underlying the inhibitory effects of acupuncture on acute cocaine-induced locomotor activity. Our previous studies have shown that acupuncture at *Shenmen* (HT7) points activates peripheral sensory afferents and that acupuncture-initiated impulses in turn activate large A-fibers within the ulnar nerve trunk, resulting in the inhibition of acute cocaine-induced locomotion (Kim et al., 2013). Furthermore, our recent study revealed that the modulation of the dorsal column (DC) somatosensory pathway by acupuncture signals that stimulate HT7 suppresses cocaine-induced locomotor activity, an effect that is abolished by lesioning of the DC pathway including cuneate nucleus (CN, second order neurons of DC), but not to the spinothalamic tract (Chang et al., 2017). Acupuncture can suppress acute cocaine-induced locomotion through the spinal DC pathway

(Kim et al., 2013; Chang et al., 2017). However, there is no direct evidence that acupuncture signals conveyed by the spinal DC pathway attenuate the reinforcing effects of drugs of abuse. Therefore, the present study extended prior work by testing the effects of acupuncture on drug-taking behaviors in rats self-administering morphine or ethanol. A role for the CN in the effects of acupuncture is also explored.

MATERIALS AND METHODS

Subjects

Male Sprague-Dawley rats (n = 64; Daehan Animal, Korea) weighing 250–280 g at the beginning of the experiment were housed singly on a 12-hr light and dark cycle with free access to food and water. All procedures were approved by the Institutional Animal Care and Use Committee at Daegu Haany University and conducted in accordance with the National Institutes of Health guidelines for the care and use of laboratory animals (National Research Council, 2010).

Acupuncture Treatment

Acupuncture was performed as described elsewhere (Kim et al., 2013). Briefly, while an assistant lightly restrained the rat, a needle (0.10 mm thick, 10 mm long; Dongbang Medical, South Korea) was bilaterally (except during the CN recordings) inserted 3 mm deep into the HT7 or LI5 acupoint, located on the transverse crease of the wrist of the forepaw, and stimulated for 20 sec (10 s for *in vivo* extracellular recordings) in duration and 1.3 m/sec^2 in intensity by using a mechanical acupuncture instrument (MAI) that was developed by our laboratory (Kim et al., 2013; **Figure 1A**). The needle was maintained in place for up to 1 min after insertion and then withdrawn. The rats received acupuncture treatment only once.

Cocaine-Induced Locomotor Activity

Locomotor activity was measured as previously described (Kim et al., 2013; Chang et al., 2017). Briefly, each animal was placed in an open field box and monitored with an image analysis system. After recording baseline activity for 30 min, the animal was given an intraperitoneal injection of cocaine (15 mg/kg) alone or in combination with acupuncture at HT7 or LI5 and monitored for up to 60 min after injection. The distance traveled was analyzed. The data are expressed as a percentage of the baseline activity.

In vivo Extracellular Recording of the Cuneate Nucleus

Extracellular single-unit recordings of the CN were performed in 11 rats as previously described (Qin et al., 2010). In brief, under isoflurane anesthesia, a carbon-filament glass microelectrode (0.4–1.2 MΩ, Carbostar-1, Kation Scientific, United States) was stereotaxically inserted in the CN (0–0.8 mm deep from the dorsal surface of medulla, 1 mm caudal to the obex and 1–2 mm lateral from the midline) (Paxinos and Watson, 1998). Single-unit activity from the discharges was isolated, recorded and analyzed via a CED 1401 Micro3 device and Spike2 software (Cambridge Electronic Design, Cambridge, United Kingdom). After the basal single-unit neuronal activity of the CN neurons was recorded for 20 s prior to stimulation, we monitored single-unit activity following mechanical stimulation (10-sec duration) induced by brushing the receptive area, pressure stimulation (10-sec duration) and pinch stimulation (10-sec duration). The phenotypes of the cuneate neurons were classified according to previous studies (Qin et al., 2010) as follows: high-threshold (HT), wide-dynamic-range (WDR), and low-threshold (LT). The rats were then given MAI acupuncture at unilateral HT7 for 10 s, and the mean values of the firing rates in the 20 s before, 10 s during and 10 s after acupuncture were compared.

Surgical Transection of the Cuneate Nucleus

Bilateral lesions of the CN were made as described elsewhere (McKenna and Whishaw, 1999; Wang and Thompson, 2008) with slight modifications. The animal was placed in a stereotaxic frame with its head tilted forward, the obex was exposed surgically and the CN was macerated along its length with a fine forcep under a microscope. Sham lesions were made using the same procedure (incision of skin, muscle and occipital bone) except the lesion was not created in CN. For histological confirmation of the lesions, all animals were sacrificed at the end of experiment and the brain stems, including the CN, were removed, postfixed in 4% paraformaldehyde and cryoprotected in 30% sucrose. The tissue was then cryosectioned into 30 μm-thick sections and stained with toluidine blue. Only the rats with confirmed CN lesions were included in the data analysis.

Morphine Self-Administration Procedure

Morphine self-administration was carried out in operant chambers (MED Associates Inc., Georgia, VT, United States) equipped with two response levers as described previously (Yoon et al., 2010). Briefly, a total of five rats were allowed to press a lever for the self-administration of morphine (0.5 mg/kg in 0.1 ml over 5 s, time-out period of 10 s) on a fixed ratio 1 (FR1) schedule in daily 1-h sessions for 6 days a week. Responding to the active lever caused 5 s of illumination of the cue light and 15 s of extinction of the house light. After the establishment of the baseline (defined as a mean value in three consecutive lever responses that varied less than 20%), the rats underwent procedures as shown in **Figures 2A,E**. The groups were assigned as follows; Con (control manipulation without the insertion of needles), HT7 (HT7 acupuncture), CN X+HT7 (HT7 acupuncture in CN lesioned rats) and Sham+HT7 (sham lesion and HT7 acupuncture).

Ethanol Self-Administration Procedure

Another set of animals were trained to self-administer ethanol orally in operant chambers using a modified sucrose-fading procedure as previously described (Yang et al., 2010). In brief, rats were initially allowed to press a lever to receive a sucrose solution (20% w/v) on an FR1 schedule to facilitate the acquisition of ethanol self-administration. Following the establishment of a stable response, the sucrose concentration was gradually

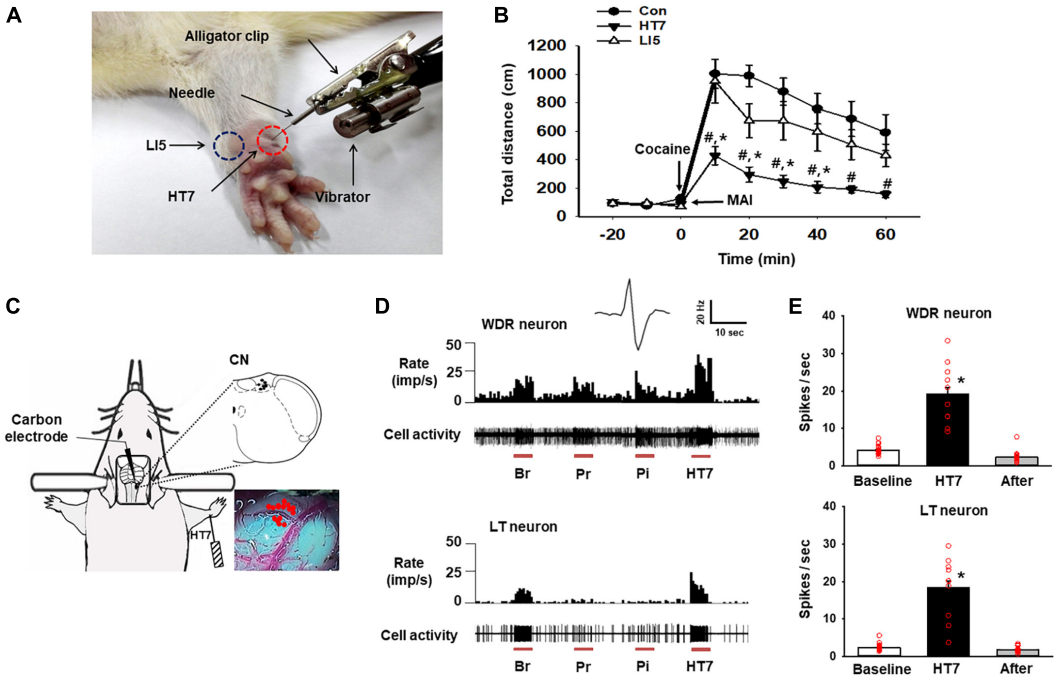

FIGURE 1 | Activation of the cuneate nucleus by mechanical acupuncture at HT7. **(A)** Acupuncture treatment at HT7 (red circle) or LI5 (blue circle) was performed by using our MAI. A bar-type cell phone motor was attached to an alligator clip to generate mechanical vibration of the needle. The intensity, frequency and operation time were controlled by a motor controller. **(B)** The effect of MAI acupuncture at HT7 or LI5 on cocaine-induced locomotor activity. Con, cocaine only (n = 6); HT7, acupuncture at HT7 after cocaine injection (n = 6); LI5, acupuncture at LI5 after cocaine injection (n = 6). #$p < 0.05$ vs. Con, *$p < 0.05$ vs. LI5 by two-way repeated ANOVA, Tukey's *post hoc* test, interaction $F = 2.647$, $p = 0.011$; normality test (Shapiro–Wilk) passed, $P = 0.747$. **(C)** A schematic drawing of the *in vivo* extracellular recordings of the CN (cuneate nucleus). **(D)** The neuronal activity of wide-dynamic-range (WDR) and low-threshold (LT) neurons in response to brush (Br), light pressure (Pr) and pinch (Pi) mechanical stimulation of the somatic field and acupuncture stimulation at HT7 (HT7). **(E)** The mean firing rates of WDR neurons (upper panel), (n = 12, *$p < 0.05$ vs. Baseline by one-way repeated ANOVA, Tukey's *post hoc* test, $F(2,38) = 74.171$, $p < 0.001$; normality test (Shapiro–Wilk) passed, $P = 0.727$) and LT neurons (lower panel), (n = 15, *$p < 0.05$ vs. Baseline by one-way repeated ANOVA, Tukey's *post hoc* test, $F(2,38) = 76.851$, $p < 0.001$, normality test (Shapiro–Wilk) passed, $P = 0.317$) over 10 s before (Baseline), during (HT7), and after (After) acupuncture at HT7.

decreased to 0%, and the ethanol concentration was raised to 10%. After acquiring stable self-administration baselines (with the total varying less than 20% from the average of three consecutive sessions), the rats were exposed to acupuncture and CN lesioning using the same experimental procedure as described above. The groups were assigned as follows; Con (control manipulation), HT7 (HT7 acupuncture), and CN X+HT7 (HT7 acupuncture in CN lesioned rats).

Data Analysis

Statistical analysis was carried out using SigmaStat 3.5 software (Systat Software Inc., United States). All data are presented as the mean ± SEM (standard error of the mean) and were analyzed by one or two-way repeated measures analysis of variance (ANOVA) followed by *post hoc* testing using the Tukey method. Statistical significance was considered at $p < 0.05$.

RESULTS

The systemic injection of cocaine increased locomotor activity, and the effect lasted for approximately 60 min from the peak magnitude at 10 min. Acupuncture at HT7, but not at LI5, attenuated the cocaine-induced enhancement of locomotor activity (**Figures 1A,B**). Thus, HT7 was used as the verum acupoint in the following experiments.

In total, 27 neurons in the CN were isolated and examined for responses to somatic stimuli. The activity of WDR neurons (n = 12 cells) in the CN increased during brushing (Br), light pressure (Pr) and noxious pinch (Pi) stimulation of the somatic field. LT neurons (n = 15 cells) were activated by hair movement or light pressure but not by noxious pinch (**Figures 1C,D**). However, we did not record any HT neurons. The WDR and LT neurons exhibited spontaneous basal firing rates of 4.16 ± 0.27 Hz and 2.44 ± 0.21 Hz, respectively. When an acupuncture needle was inserted into the HT7 acupoint and stimulated for 10 s with the MAI (**Figure 1A**), the firing rates of WDR and LT neurons increased to 19.21 ± 1.76 Hz and 18.42 ± 1.79 Hz, respectively, and they quickly returned to baseline levels after the termination of stimulation ($p < 0.05$, **Figures 1D,E**), indicating the excitation of the CN during acupuncture at HT7.

Next, to determine whether acupuncture suppresses morphine-seeking behaviors via the modulation of the CN, rats were divided into four groups: control manipulation (Con, n = 5), acupuncture treatment (HT7, n = 5), CN

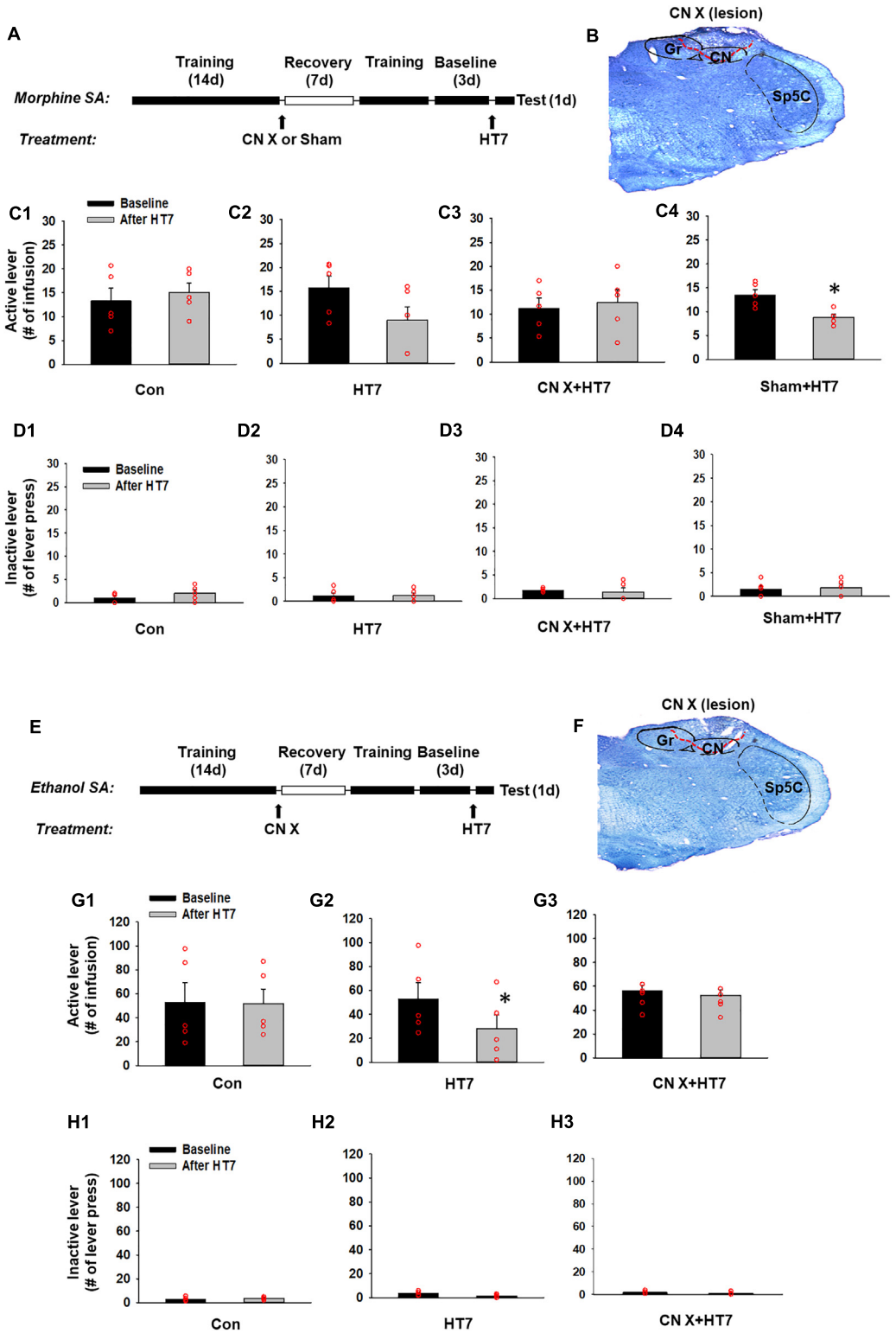

FIGURE 2 | Effect of cuneate nucleus (CN) lesions on the inhibition of morphine or ethanol self-administration behaviors by acupuncture at HT7. **(A–D)** The effect of CN lesions on the inhibition of morphine self-administration behaviors by acupuncture at HT7. A schematic of the procedure of the morphine self-administration experiment **(A)**. While sham operation without HT7 acupuncture did not affect the number of active lever presses (Con) **(C1)**, the active lever response in the HT7-treated group was significantly reduced after HT7 stimulation compared to baseline (HT7; paired *t*-test, $*p = 0.008$ vs. Baseline) **(C2)**. These acupuncture effects were ablated in the rats with CN injury (CN X+HT7) **(C3)**. HT7 acupuncture significantly reduced morphine intake in sham group, compared to baseline

(Continued)

FIGURE 2 | Continued
(Sham+HT7; paired *t*-test, $^*p = 0.017$ vs. Baseline) **(C4)**. There were no differences in the number of inactive lever presses among the groups or before and after HT7 **(D1–D4)**. A representative toluidine blue-stained image of a CN lesion **(B)**. **(E–H)** The effect of cuneate nucleus (CN) lesions on the inhibition of ethanol self-administration behaviors by acupuncture at HT7. A schematic of the procedure of the ethanol self-administration experiment **(E)**. The sham operation without HT7 acupuncture did not affect the number of active lever presses (Con) **(G1)**. The numbers of active lever presses in the HT7-treated group was significantly reduced after HT7 stimulation compared to baseline (HT7; paired *t*-test, $^*p = 0.042$ vs. Baseline) **(G2)**. This effect was not seen in the rats with CN injury (CN X+HT7; **G3**). There were no differences in the number of inactive lever presses among the groups or before and after HT7 **(H1–H3)**. A representative toluidine blue-stained images of a CN lesion **(F)**.

sham lesion/acupuncture treatment (Sham, $n = 5$), and CN lesion/acupuncture treatment (CN X+HT7, $n = 5$). The effect of acupuncture at HT7 with or without surgical lesioning of the CN was compared in the rats self-administering morphine. While control manipulation without acupuncture did not affect morphine self-administration (Con group in **Figure 2C1**), acupuncture at HT7 reduced the number of active lever presses (9.00 ± 2.76), but not inactive lever presses (**Figures 2D1–D4**), compared to baseline (15.80 ± 2.39) (paired *t*-test, $p = 0.008$; HT7 group in **Figure 2C2**). On the other hand, in the animals given bilateral CN lesions (**Figure 2B**), the inhibitory effects of acupuncture on morphine self-administration behaviors were attenuated compared to the corresponding baseline levels (CN X+HT7 group in **Figure 2C3**), whileas the group with the sham surgery (same surgery except CN lesion) showed inhibitory effects of acupuncture on morphine intake (Sham+HT7; $P = 0.017$, paired *t*-test; **Figure 2C4**).

The experiment was repeated in the rats self-administering ethanol. The rats were divided into three groups: control manipulation (Con, $n = 5$), acupuncture treatment (HT7, $n = 5$) and CN lesion/acupuncture treatment (CN X+HT7, $n = 5$; **Figure 2F**). While control manipulation without acupuncture did not affect morphine self-administration (Con group in **Figure 2G1**), Acupuncture stimulation of HT7 significantly suppressed active lever responses (28.00 ± 11.96), but not inactive lever responses (**Figures 2H1–H3**), compared to baseline (52.80 ± 13.50) (paired *t*-test, $p = 0.04$; HT7 group in **Figure 2G2**). This effect was abolished by the surgical dissection of the bilateral CN before acupuncture at HT7 (CN X+HT7 group in **Figure 2G3**). These results suggest that the CN is modulated during the acupuncture inhibition of the reinforcing effects of drugs.

DISCUSSION

We have shown that acupuncture at HT7 can suppress selectively morphine and ethanol self-administration, but not general consummatory behaviors, through GABA receptors in the ventral tegmental area (VTA) and DA release in the nucleus accumbens (NAc) induced by drugs of abuse (Kim et al., 2005; Yang et al., 2010; Yoon et al., 2010). Consistent with our previous studies, the present study showed that acupuncture at HT7 attenuated morphine and ethanol self-administration behaviors. Most importantly, the inhibition of drug-taking behaviors by acupuncture at HT7 was inhibited by the surgical lesioning of the CN, suggesting the involvement of sensory inputs to the CN in the effects of acupuncture. Previously, we reported that the dorsal column-medial lemniscus (DC-ML) pathway is involved in the inhibitory effects of acupuncture at HT7 on cocaine-induced locomotor activity (Chang et al., 2017). Mechanical stimulation of an acupuncture needle inserted into the HT7 acupoint attenuates cocaine-induced locomotor activity via A-fiber modulation of the ulnar nerve (Kim et al., 2013), which is reversed by surgical lesioning of the CN (Chang et al., 2017) and second-order neurons of the DC-ML pathway. The CN has also been reported to be anatomically connected to certain acupuncture points on the forelimb. For example, a neuronal tracing study revealed that, when cholera toxin subunit B, a retrograde tracer, is injected into the PC8 acupoint, which is approximately 5 mm from HT7 in rats, transganglionically labeled axonal terminals are found mainly in the CN and the medial part of the deep laminae of the spinal dorsal horn (Cui et al., 2013), suggesting that the CN can be excited by the stimulation of acupoints on the forelimb in rats. This finding was further confirmed by our previous and present data showing that the mechanical stimulation of HT7 activates both LT (A-fibers) and HT afferent fibers (Aδ and C fibers) (Kim et al., 2013) and excites WDR (responsive to both low- and high-threshold stimuli) and LT (responsive to LT stimuli) neurons in the CN during *in vivo* extracellular recordings. Moreover, the present study showed that reduction of morphine- or ethanol-seeking behaviors by acupuncture at HT7 was ablated by surgical CN lesioning. This finding suggests the involvement of CN neurons in the effects of acupuncture on the reinforcing effects of drugs of abuse. However, one of the limitations of this study is that the electrophysiological recordings of WDR and LT neurons were conducted in anesthetized rats, whereas the behavioral studies were carried out in freely moving rats. It is possible that the state of the rats during the electrophysiological recordings may not accurately reflect the state of the rats during behavioral testing.

While the CN may be particularly important for the acupuncture inhibition of drug-taking behaviors, the exact mechanism by which afferent inputs from the CN function in the mesolimbic DA system to influence addictive behaviors remains elusive, but some evidence suggests that the mechanism is dependent on the lateral habenula (LHb). Our recent study revealed that acupuncture at HT7 activates LHb neurons that project to the VTA and that the electrolytic lesioning of the LHb reduces acupuncture inhibition of cocaine-induced locomotion (Chang et al., 2017). The LHb is known to convey inhibitory reward signals to the VTA that inhibit DA release in the NAc (Velasquez et al., 2014). Thus, the results suggest that the effects of acupuncture on morphine- and ethanol-seeking behaviors might

result from the activation of CN inputs to the LHb-VTA/RMTg pathway via direct or indirect projections. Although the LHb is thought to be sensitive to somatosensory inputs (Benabid and Jeaugey, 1989; Gao et al., 1996), it is not known yet how these inputs enter the LHb. It has been shown that the LHb receives input from various structures, such as the lateral hypothalamus, entopeduncular nucleus and prefrontal cortex (Shelton et al., 2012). As none of these structures provide direct sensory inputs (projections) to the LHb, neural connections that conduct impulses from the CN to the LHb may require multisynaptic pathways. Determining the specific neural circuits between the CN and LHb that are involved in the acupuncture-mediated inhibition of drug-taking behaviors will require additional study.

In conclusion, the results suggest that the CN is involved in the effects of acupuncture on drug-seeking behaviors in rats.

ETHICS STATEMENT

Male Sprague-Dawley rats (Daehan Animal, Korea) weighing 250–280 g at the beginning of the experiment, were housed on a 12 h light and dark cycle and freely accessed to food and water. All procedures were approved by the Institutional Animal Care and Use Committee at the Daegu Haany University and conducted in accordance with the National Institutes of Health guidelines for the care and use of laboratory animals.

AUTHOR CONTRIBUTIONS

HK and CY designed the experiments. SC, YR, SB, YF, NK, JL, JK, and BL conducted the experiments. HK was responsible for the overall direction of the project and for edits to the manuscript.

FUNDING

This research was supported by a National Research Foundation of Korea (NRF) grant funded by the Korean Government (MSIT) (Nos. 2018R1A5A2025272 and 2018R1E1A2A02086499), the KBRI basic research program through the Korea Brain Research Institute funded by the Ministry of Science and the ICT (19-BR-03-01), and the Korea Institute of Oriental Medicine (KIOM; KSN 1812181).

REFERENCES

Benabid, A. L., and Jeaugey, L. (1989). Cells of the rat lateral habenula respond to high-threshold somatosensory inputs. *Neurosci. Lett.* 96, 289–294. doi: 10.1016/0304-3940(89)90393-5

Chang, S., Ryu, Y., Gwak, Y. S., Kim, N. J., Kim, J. M., Lee, J. Y., et al. (2017). Spinal pathways involved in somatosensory inhibition of the psychomotor actions of cocaine. *Sci. Rep.* 7:5359. doi: 10.1038/s41598-017-05681-5687

Cui, J. J., Ha, L. J., Zhu, X. L., Shi, H., Wang, F. C., Jing, X. H., et al. (2013). Neuroanatomical basis for acupuncture point PC8 in the rat: neural tracing study with cholera toxin subunit B. *Acupunct. Med.* 31, 389–394. doi: 10.1136/acupmed-2013-010400

Gao, D. M., Hoffman, D., and Benabid, A. L. (1996). Simultaneous recording of spontaneous activities and nociceptive responses from neurons in the pars compacta of substantia nigra and in the lateral habenula. *Eur. J. Neurosci.* 8, 1474–1478. doi: 10.1111/j.1460-9568.1996.tb01609.x

Kim, M. R., Kim, S. J., Lyu, Y. S., Kim, S. H., keun Lee, Y., Kim, T. H., et al. (2005).). Effect of acupuncture on behavioral hyperactivity and dopamine release in the nucleus accumbens in rats sensitized to morphine. *Neurosci. lett.* 387, 17–21. doi: 10.1016/j.neulet.2005.07.007

Kim, S. A., Lee, B. H., Bae, J. H., Kim, K. J., Steffensen, S. C., Ryu, Y. H., et al. (2013). Peripheral afferent mechanisms underlying acupuncture inhibition of cocaine behavioral effects in rats. *PLoS One* 8:e81018. doi: 10.1371/journal.pone.0081018

McKenna, J. E., and Whishaw, I. Q. (1999). Complete compensation in skilled reaching success with associated impairments in limb synergies, after dorsal column lesion in the rat. *J. Neurosci.* 19, 1885–1894. doi: 10.1523/jneurosci.19-05-01885.1999

National Research Council (2010). *Guide for the Care and use of Laboratory Animals*. Washington, DC: National Academies Press.

Paxinos, G., and Watson, C. (1998). *The Rat Brain in Stereotaxic Coordinates*. San Diego: Academic Press.

Qin, C., Goodman, M. D., Little, J. M., Farber, J. P., and Foreman, R. D. (2010). Comparison of activity characteristics of the cuneate nucleus and thoracic spinal neurons receiving noxious cardiac and/or somatic inputs in rats. *Brain Res.* 1346, 102–111. doi: 10.1016/j.brainres.2010.05.081

Shelton, L., Pendse, G., Maleki, N., Moulton, E. A., Lebel, A., Becerra, L., et al. (2012). Mapping pain activation and connectivity of the human habenula. *J. Neurophysiol.* 107, 2633–2648. doi: 10.1152/jn.00012.2012

Velasquez, K. M., Molfese, D. L., and Salas, R. (2014). The role of the habenula in drug addiction. *Front. Hum. Neurosci.* 8:174. doi: 10.3389/fnhum.2014.00174

Wang, G., and Thompson, S. M. (2008). Maladaptive homeostatic plasticity in a rodent model of central pain syndrome: thalamic hyperexci after spinothalamic tract lesions. *J. Neurosci.* 28, 11959–11969. doi: 10.1523/JNEUROSCI.3296-08.2008

Yang, C. H., Yoon, S. S., Hansen, D. M., Wilcox, J. D., Blumell, B. R., Park, J. J., et al. (2010). Acupuncture inhibits GABA neuron activity in the ventral tegmental area and reduces ethanol self-administration. *Alcohol. Clin. Exp. Res.* 34, 2137–2146. doi: 10.1111/j.1530-0277.2010.01310.x

Yoon, S. S., Kim, H., Choi, K.-H., Lee, B. H., Lee, Y. K., Lim, S. C., et al. (2010). Acupuncture suppresses morphine self-administration through the GABA receptors. *Brain Res. Bull.* 81, 625–630. doi: 10.1016/j.brainresbull.2009.12.011

Yoon, S. S., Kwon, Y. K., Kim, M. R., Shim, I., Kim, K. J., Lee, M. H., et al. (2004). Acupuncture-mediated inhibition of ethanol-induced dopamine release in the rat nucleus accumbens through the GABA B receptor. *Neurosci. Lett.* 369, 234–238. doi: 10.1016/j.neulet.2004.07.095

Yoon, S. S., Yang, E. J., Lee, B. H., Jang, E. Y., Kim, H. Y., Choi, S.-M., et al. (2012). Effects of acupuncture on stress-induced relapse to cocaine-seeking in rats. *Psychopharmacology* 222, 303–311. doi: 10.1007/s00213-012-2683-3

Conflict of Interest Statement: The authors declare that the research was conducted in the absence of any commercial or financial relationships that could be construed as a potential conflict of interest.

frontiers in Neuroscience

ORIGINAL RESEARCH
published: 04 October 2019
doi: 10.3389/fnins.2019.01062

Differential Influence of Acupuncture Somatosensory and Cognitive/ Affective Components on Functional Brain Connectivity and Pain Reduction During Low Back Pain State

*Jeungchan Lee[1], Seulgi Eun[2], Jieun Kim[3], Jun-Hwan Lee[3] and Kyungmo Park[2]**

[1] Athinoula A. Martinos Center for Biomedical Imaging, Department of Radiology, Massachusetts General Hospital, Boston, MA, United States, [2] Department of Biomedical Engineering, Kyung Hee University, Yongin, South Korea, [3] Clinical Research Division, Korea Institute of Oriental Medicine, Daejeon, South Korea

OPEN ACCESS

Edited by:
Yi-Wen Lin,
China Medical University, Taiwan

Reviewed by:
James Liao,
China Medical University, Taiwan
In-Seon Lee,
National Center for Complementary and Integrative Health (NCCIH), United States

***Correspondence:**
Kyungmo Park
saenim@khu.ac.kr

Specialty section:
This article was submitted to Perception Science, a section of the journal Frontiers in Neuroscience

Received: *14 November 2018*
Accepted: *20 September 2019*
Published: *04 October 2019*

Citation:
Lee J, Eun S, Kim J, Lee J-H and Park K (2019) Differential Influence of Acupuncture Somatosensory and Cognitive/ Affective Components on Functional Brain Connectivity and Pain Reduction During Low Back Pain State. Front. Neurosci. 13:1062. doi: 10.3389/fnins.2019.01062

The underlying mechanism of pain reduction by acupuncture is still unclear, because acupuncture treatment involves multidimensional factors. In this study, we investigated the differential influence of acupuncture components on brain functional connectivity and on pain reduction. We used a specific form of sham acupuncture (phantom acupuncture; PHNT), which only has a needling-credibility (a belief that they were treated with real acupuncture needles), while real acupuncture (REAL) has a somatosensory needling stimulation, as well as a needling-credibility. Forty-three patients with low back pain were randomized into the REAL group (n = 25) and the PHNT group (n = 18). They underwent two pain steady-state fMRI runs implemented by a low back extension (LBE) pain model (lifting the low back using air-cuff inflation) before and after REAL or PHNT stimulation. Subjective pain ratings, perceived throughout the LBE runs due to the posture, were reported (LBEpain). The regions of interest (ROI) were (1) the main nodes of the default mode network (DMN) – the medial prefrontal cortex (mPFC), posterior cingulate cortex (PCC), (2) the main nodes of the salience network (SN) – the anterior/posterior insular cortices (a/pINS), and (3) the low back-specific region of sensorimotor network (SMN), $S1_{back}$. Significant reductions in LBEpain were observed in both groups (REAL = −1.02 ± 1.53, PHNT = −1.26 ± 2.20). In REAL group, decreased LBEpain was positively correlated with decreased functional connectivity between the mPFC and pINS (r = 0.58, $P < 0.05$). Reduced LBEpain in PHNT was negatively correlated with increased PCC–aINS connectivity (r = −0.48, $P < 0.05$) and tended toward positive correlation with decreased $S1_{back}$–pINS connectivity (r = 0.44, P = 0.07). Our findings might suggest different brain mechanisms of observed pain reduction; REAL seems to involve detachment of the self from the sensory aspect of pain, while PHNT does to shift attention to self and disengages physical pain processing hubs. This exploratory study proposes a sham methodology to dissociate the influence

of different acupuncture components in acupuncture research. Further studies need to be followed with more elaborated hypothesis, study design, and analysis considering various cognitive/affective factors for better understanding of brain mechanisms of pain reduction regarding the different acupuncture aspects.

Keywords: functional connectivity, default mode network, sensorimotor network, salience network, somatosensory afference, needling credibility

INTRODUCTION

Acupuncture treatment, sham as well as real, is known to modulate pain, but the underlying brain mechanism is not clear, probably because multidimensional factors are involved (Kaptchuk, 2011), and it is not easy to dissociated them from each other. To provide a standard for investigation into the acupuncture mechanism, acupuncture components have been defined as needling-specific (e.g., somatosensory needling, which is exclusive to acupuncture needling such as insertion and manipulation), specific non-needling (e.g., theory-based diagnosis and palpation, which has been considered to be related to treatment efficacy), and non-specific [e.g., needling credibility (patients' belief that they were treated with real acupuncture needles) and visual feedback (observation of treatment procedure), which is not exclusively driven by or related to needling itself] components (Langevin et al., 2011). However, it has not yet been possible to differentiate needling-specific from non-specific components, because tactile (touch) stimulation cannot be excluded as a factor in the proposed sham acupunctures (Lee et al., 2014; Makary et al., 2018). Thus, to differentiate acupuncture needling-specific (somatosensory needling) from non-specific components (needling credibility and visual feedback) (Langevin et al., 2011), phantom acupuncture (PHNT), which can produce non-specific effects without the acupuncture-specific components, has been devised to contrast with real acupuncture (REAL) (Lee et al., 2014; Makary et al., 2018). The comparison between real and PHNT stimulation has shown that somatosensory needling stimulation (acupuncture needling-specific components) produces sympathetic activation (e.g., greater skin conductance response) as well as greater acupuncture-related sensations (overall acupuncture sensation measured as Mass Index (Kong et al., 2007), soreness, tingling, and sharp pain) than other non-specific components (Lee et al., 2014). The posterior insular (pINS) and anterior cingulate cortices (ACC), which process ascending somatosensory and pain signals, showed acupuncture needling-specific brain responses in our previous study (Makary et al., 2018). Conversely, needling credibility has been shown to induce parasympathetic activation (decreased heart rate and pupil size responses), as well as vicarious acupuncture (*deqi*) sensations (deep pressure, heaviness, fullness, and numbness) (Lee et al., 2014). These vicarious sensations have been linked to increased brain response in the primary and secondary somatosensory cortices (S1 and S2) (Kerr et al., 2011; Beissner et al., 2015; Makary et al., 2018), and the evoked sensations may result from a top-down mechanism related to sensory imagery (Beissner et al., 2015) and attention toward stimulated body parts (Kerr et al., 2011). The previous study also showed that vicarious brain response (e.g., S1) and acupuncture sensations play an important role in creating and enhancing needling credibility in PHNT (Makary et al., 2018). Patients' needling credibility was developed by the instruction that they would receive REAL stimulation and by the visual feedback being stimulated. Vicarious acupuncture (*deqi*) sensations induced by the visual feedback of acupuncture stimulation, mediated by the involvement of expectation (Song et al., 2019), mirror neuron system, or mirror-touch synesthesia (Beissner et al., 2015), seemed to bolster the needling expectancy and credibility.

Functional connectivity analysis has been used to investigate interactions between brain regions to better understand chronic pain mechanisms. Various clinical outcomes have been reported to be correlated with the functional connectivity within or between subregions in the default mode network (DMN), sensorimotor network (SMN), and salience network (SN). The strength of functional connectivity (between the DMN and SMN, as well as within DMN subregions) has been shown to be significantly correlated with the reported pain intensity in patients with chronic back pain (Hemington et al., 2018). In patients with chronic pelvic pain, functional connectivity between the anterior insular cortex (aINS; a subregion of the SN) and medial prefrontal cortex (mPFC; a subregion of the DMN) was positively correlated with the levels of anxiety, depression, and pain (As-Sanie et al., 2016). In patients with fibromyalgia, decreased DMN–insula connectivity was significantly positively correlated with decreased pain after acupuncture stimulation (Napadow et al., 2012). Functional connectivity between the insula and the somatotopic region of the leg in the S1 has been correlated with pain sensitivity in healthy controls (Kim et al., 2013) and with pain intensity in fibromyalgia patients (Kim et al., 2015).

Our previous study mainly focused on the brain responses to REAL and PHNT, as well as their neural correlates with clinical LBP levels (Makary et al., 2018). In this functional MRI (fMRI) study, however, the low back extension (LBE) pain model was used to evoke normalized back pain levels across patients, and functional connectivity analysis was performed to investigate the brain mechanism of pain modulation after REAL and PHNT. This allowed us to dissociate acupuncture-needling specific and non-specific components experimentally, as well as to understand the functional brain mechanisms of the short-term pain modulation in different brain hubs. In other words, the REAL was designed to encompass not only all of physical components of acupuncture stimulation (e.g., palpation, needle insertion, manipulation technique) as well as psychological

components (e.g., needling credibility), while the PHNT was designed as a control in that this only has psychological components without any physical components. Thus, the aim of this study was to investigate the association between the physical components of acupuncture (controlled by the influence of psychological components) and brain functional connectivity.

MATERIALS AND METHODS

This study protocol was approved by the Institutional Review Board of the Kyung Hee University (KHNMC-OH-IRB 2010-013), and all participants provided written informed consent in accordance with the Declaration of Helsinki. This study is registered at the clinical research information service (CRIS)[1] (registration number: KCT0002253).

Participants

Fifty-six patients with non-specific low back pain (LBP; 31 men, age = 38.4 ± 12.7 years old, mean ± SD) were enrolled in this study. All patients completed prescreening for MRI eligibility and were included if they reported LBP of greater than four on a visual analog scale (VAS; 0 = no pain, 10 = most pain imaginable) when their low back was lifted (4–7 cm) in the supine position (for more on the LBE pain model, see below). Patients were excluded if they met the following exclusion criteria: (1) LBP greater than four during baseline, (2) severe pain other than LBP (e.g., neck pain) at scan, (3) severe radicular pain extending into lower leg, (4) psychiatric or cardiovascular disorders, (5) accident- or surgery-related back pain, (6) back pain from metastatic cancer, vertebral fracture, spinal infection, inflammatory spondylitis etc., (7) taking medication for pain management (e.g., corticosteroid, narcotics, muscle relaxants, and any herbal medicine), (8) receiving acupuncture treatment for back or neck pain within a month, and (9) participating any previous acupuncture studies.

Experimental Paradigm

The 56 enrolled non-specific LBP patients were randomized into either the REAL (n = 33) or PHNT (n = 23) group. Patients in both groups completed four fMRI runs: a resting-state run (REST, 6 min), an acupuncture stimulation run (REAL or SHAM, 7 min), and two continuous pain runs using the LBE pain model (6 min before and after the acupuncture stimulation run; these were named the LBEpre and LBEpost runs; **Figure 1A**). The perceived pain ratings throughout the LBE runs (LBEpain) were collected and its change (i.e., LBEpost – LBEpre) was analyzed as the main outcome measure in this study (**Figure 1A**).

All the setup equipment needed for the REAL and PHNT runs (MR-compatible acupuncture needles, camera, beam projector, screen, visual barrier, and blanket) was prepared before the MRI session (Makary et al., 2018). An MR-compatible cuff bladder was also placed on the MRI scanner bed for the two LBE runs (LBEpre and LBEpost), under the most painful area of the patients' low back.

[1]http://cris.nih.go.kr/

Before the LBEpre run, the cuff pressure for stimulation was calibrated in each individual patient. Air pressure was slowly applied to the cuff bladder until patients reported the target pain rating (4/10 on a 11-point VAS; 0 = no pain, 10 = most pain imaginable). In this way, we tried to standardize the intensity of induced LBP across all patients (**Figure 1B**). During this procedure, all patients confirmed that the exacerbated pain was due to their change in posture (extended back angle) rather than the force of the pressure. This information was recorded to ensure that the induced pain was not influenced by differing pain thresholds stimulating different layers of the body (e.g., skin, soft tissue, dura, disk, and deep muscle). During the LBEpre run, patients were asked to stay still with their eyes open, staring at crosshairs on a screen while the individually calibrated pressure was applied. They were also instructed to focus on the perceived LBP intensity and sensations. After the run, to prevent additional pain, the air pressure was cautiously removed so that the cuff bladder deflated slowly.

During the setup procedure for the REAL and PHNT runs, a video recording the patient body was projected onto the screen in real time to consolidate the video-body link between the patient's own body and the displayed video. This visual feedback process was designed to initiate/boost needling credibility. Patients randomized into the REAL group were told that they would be stimulated with acupuncture needles (i.e., instruction) and received four real acupuncture needles (diameter = 0.3 mm, length = 30 mm; DongBang Co., Seongnam, South Korea): bilateral SP13, left SP11, and left ST36. Before the REAL run started, the needles were inserted at acupoints (which were chosen by a licensed and experienced acupuncturist based on their clinical effectiveness and easy access during the fMRI scanning) for clinical relevance and manipulated using the traditional technique by an acupuncturist to induce acupuncture (*deqi*) sensations. During the REAL run, the acupuncturist, who were trained for the stimulation paradigm, stimulated each needle in a random order [i.e., somatosensory needling afference; depth = 2–3 cm, 2 s per stimulation at 1 Hz rotation (±180°), five stimulations per acupoint, inter-stimulation interval = 7.9 ± 1.7 s], and the procedure was video-recorded and simultaneously played on the screen (i.e., visual feedback).

Before the PHNT run started, patients in PHNT group were also told that they would be stimulated with acupuncture needles (i.e., the same instruction given to REAL group) and after the video-body link was built by visual feedback procedure, the acupuncturist mimicked the needling ritual (i.e., insertion and manipulation) without actual needles. Patients in PHNT group were told that the needles had been inserted, as in the REAL run. The acupuncturist then pretended to stimulate the needles according to the stimulation paradigm while the previously recorded video from the other patient (in the REAL group, with real needles) was displayed on the screen during the PHNT run (i.e., visual feedback). Thus, the procedure was designed to build needling credibility based on the previous video-body link (during setup) and visual feedback (during the run). Importantly, this was carried out without any somatosensory needling afference.

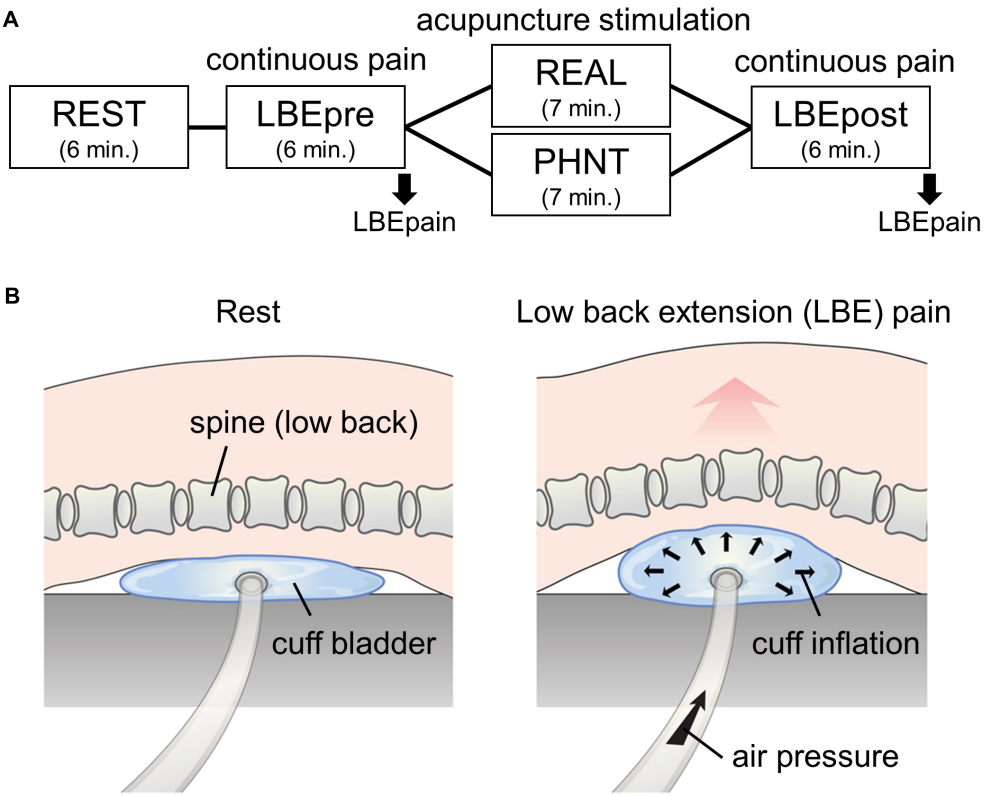

FIGURE 1 | Experimental paradigm. **(A)** fMRI scanning protocol: 6-min resting state (REST) and continuous pain (LBEpre and LBEpost) runs with real (REAL) and phantom (PHNT) acupuncture stimulation. Pain model-induced low back pain (LBEpain) was recorded at the end of the scan. **(B)** Low back extension (LBE) pain model used in continuous pain runs.

For the LBEpost run, patients were stimulated with the same air pressure intensity with that was used in the LBEpre run. Subjective pain ratings (LBEpain, 0-10 VAS), as perceived throughout the LBE runs, were reported at the end of each scan, and the changes in LBEpain between LBEpost and LBEpre were calculated as the primary clinical outcome for pain reduction in REAL and PHNT (**Figure 1A**).

At the end of the experiment, patients' needling credibility during REAL or PHNT runs was assessed retrospectively through an in-depth interview whether they believed that they had experienced REAL stimulation during the acupuncture stimulation run. If patients reported that they had any doubt or strong belief during the run that the stimulation was not happened to them actually (for example, due to no needling sensations), they were classified as non-credible patient group (i.e., without needling credibility) and removed from the analysis. Thus, our study simply hypothesized that REAL has somatosensory tactile stimulation, visual feedback, and needling credibility, whereas PHNT has only visual feedback and needling credibility.

MRI Data Acquisition

MRI data were collected using a 3T Philips Achieva MRI scanner (Philips Medical Systems, Netherlands) with an 8-channel head coil at the Kyung Hee University Hospital, Gangdong. For anatomical localization of the results, structural T1-weighted images were collected using an MP-RAGE pulse sequence [repetition time (TR) = 9886 ms, echo time (TE) = 4.59 ms, flip angle = 8°, field of view (FOV) = 256 × 256 mm, voxel size = 1 × 1 × 1 mm], and functional images were acquired for 6 min using a T2*-weighted echo planar imaging pulse sequence (TR = 2000 ms, TE = 35 ms, flip angle = 90°, FOV = 230 × 230 mm, voxel size = 2.875 × 2.875 × 4 mm, 34 interleaved axial slices) during the REST and LBE runs (LBEpre and LBEpost) for functional connectivity analysis. During fMRI, physiological data (electrocardiogram and respiration signal) were collected using a data acquisition system (PowerLab ML800; ADInstruments, Inc., Australia) to calibrate cardiorespiratory artifacts (Glover et al., 2000).

Data Processing and Analysis

Collected MRI data were processed using conventional analysis software, such as the Functional Magnetic Resonance Imaging of the Brain (FMRIB), Software Library (FSL)[2], Analysis of Functional NeuroImages (AFNI)[3], and FreeSurfer[4]. The fMRI

[2]https://fsl.fmrib.ox.ac.uk/fsl/fslwiki/

[3]https://afni.nimh.nih.gov/

[4]https://surfer.nmr.mgh.harvard.edu/fswiki

data were corrected for cardiorespiratory artifacts (3dretroicor, AFNI) (Glover et al., 2000), and for head motion (MCFLIRT, FSL; ICA-AROMA). They were also preprocessed for skull stripping (BET, FSL), spatial smoothing (Gaussian kernel, full width at half maximum = 6 mm; fslmaths, FSL) and temporal filtering (high-pass cut-off frequency = 0.006 Hz; 3dBandpass, AFNI). Individual structural and functional data were aligned first (bbregister, FreeSurfer). They were then co-registered to the standard Montreal Neurological Institute (MNI) space (FNIRT, FSL) to allow dual-regression independent component analysis (ICA) (Filippini et al., 2009) and seed-voxel connectivity analysis.

In the dual-regression ICA, all fMRI data from the REST, LBEpre, and LBEpost runs were temporally concatenated and then fed into the group ICA (MELODIC, FSL). The group ICs of the DMN, SMN, and SN were selected based on the spatial templates of the resting state networks (Beckmann et al., 2005). ROIs in the DMN (posterior cingulate cortex, PCC; mPFC) and SN (anterior and middle cingulate cortices, aINS and pINS) were decided based on the group map of REST run to ensure they were independent of influence from the pain model and acupuncture stimulation. ROIs in the aINS and pINS were combined bilaterally. The ROI in the SMN was located in the bilateral low back region of the primary somatosensory cortex ($S1_{back}$; MNI $X = \pm 18$ mm, $Y = -38$ mm, $Z = 72$ mm) (**Table 1**) based on a localization run in an independent LBP study (Lee et al., 2018a) that investigated low back-specific functional connectivity. The average time-series brain activities (sphere mask, radius = 4 mm) were extracted from each of the ROIs, and the correlation coefficients (Pearson's r) of cross-correlation between the ROIs were converted into z scores using Fisher z-transformation. The changes in within- and between-network connectivity (LBEpost vs. LBEpre) after REAL and PHNT runs, as well as their association with changes in LBEpain (primary clinical outcome), were calculated (Hemington et al., 2018). Significance was defined at P-values <0.05.

RESULTS

Of the 56 enrolled LBP patients (33 in the REAL group and 23 in the PHNT group), 43 were included in this analysis (25 in the REAL group, 38.4 ± 13.2 years old, mean ± SD, 13 men; 18 in the PHNT group, 38.3 ± 13.0 years old, 8 men; P for age [REAL vs. PHNT] = 0.98). Eight patients were excluded from the REAL group: four due to incomplete scanning, three due to uncorrectable distortions, and one due to excessive head motion (>2 mm). Five were excluded from the PHNT group: four due to the absence of needling credibility (patients reported that the acupuncture procedure did not happen to them, and no acupuncture stimulation was delivered because they did not feel any sensation during the PHNT run) and one due to excessive head motion (>2 mm) (**Figure 2**).

Decreased Pain Model-Induced Pain Intensity (LBEpain) After the REAL and PHNT Stimulation

While the applied air pressure for pain model was individually calibrated and applied with the same intensity in LBEpre and LBEpost [REAL: 118.4 ± 72.4 mmHg, PHNT: 94.4 ± 57.2 mmHg; P (REAL vs. PHNT) = 0.25], the PHNT group reported significantly greater LBEpain than the REAL group during the LBEpre run [REAL: 4.74 ± 1.00/10, PHNT: 5.54 ± 0.83; P (REAL vs. PHNT) = 0.01], and the reported pain was significantly greater than the target value (4/10) in both groups [P (REAL) < 0.005, P (PHNT) < 0.001]. None of the patients reported any pain during the REST run.

Importantly, however, the subjective pain (LBEpain) which patients felt during the continuous pain runs, as measured using the VAS, was significantly reduced after both REAL and PHNT runs [Δ = LBEpain(LBEpost) – LBEpain(LBEpre); ΔREAL: −1.02 ± 1.53, P < 0.005; ΔPHNT: −1.26 ± 2.20, P < 0.01; P (ΔREAL vs. ΔPHNT) = 0.67] (**Figure 3**).

TABLE 1 | Locations of regions of interest in functional connectivity analysis.

Network	ROI	Side	MNI coordinates (mm)		
			X	Y	Z
DMN	mPFC	R	2	64	−8
	PCC	L	−6	−40	24
SMN	$S1_{back}$	R/L	±18	−38	72
	dACC/aMCC	R	4	24	26
SN	aINS	R	38	10	4
		L	−36	12	2
	pINS	R	46	−4	2
		L	−42	−16	−2

ROI, region of interest; MNI, Montreal Neurological Institute; DMN, default mode network; SMN, sensorimotor network; SN, salience network; mPFC, medial prefrontal cortex; PCC, posterior cingulate cortex; $S1_{back}$, low back region in primary somatosensory cortex; dACC, dorsal anterior cingulate cortex; aMCC, anterior middle cingulate cortex; aINS, anterior insular cortex; pINS, posterior insular cortex; R, right hemisphere; L, left hemisphere.

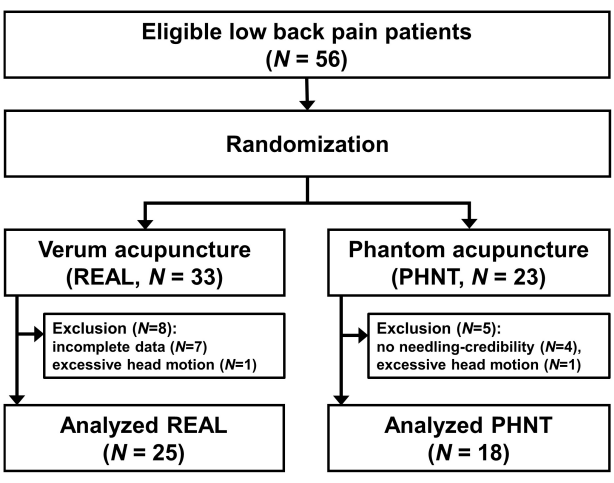

FIGURE 2 | Flow chart for enrollment, randomization, exclusion, and analysis.

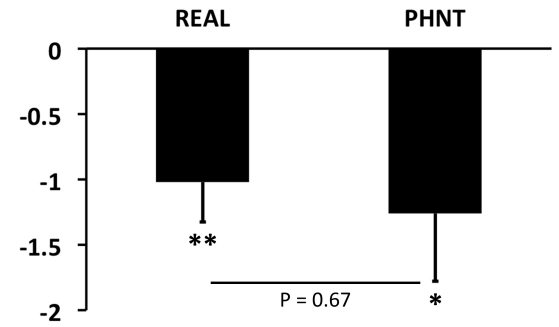

FIGURE 3 | Changes in LBEpain during continuous pain runs. Real (REAL) and phantom (PHNT) acupuncture stimulation showed significant short-term pain-relieving effects ($P < 0.01$ and 0.05, respectively) without any difference between groups ($P = 0.67$). N.B., bar plots show mean ± SEM. $^{*}P < 0.05$; $^{**}P < 0.01$.

In spite of the randomization of the groups, the LBEpain in LBEpre was significantly different in the REAL and PHNT. Thus, for the analysis of brain correlates, we investigated how the LBEpain reduction was correlated with the change of functional connectivity (LBEpost vs. LBEpre).

Changes in Functional Connectivity and Its Association With Clinical Outcome

Twenty-five ICs were derived from the dual-regression group ICA, and the ICs in the DMN, SN, and SMN were identified. The ROIs were then decided in the submodules of each network (**Table 1** and **Supplementary Figure S1**). The DMN mainly comprised the PCC, inferior parietal lobule, and the mPFC. The ROIs in the PCC and mPFC were localized in DMN. The SMN encompassed the pre- and post-central gyri, including the predefined $S1_{back}$ ROI. The SN consisted of the dorsal anterior and anterior middle cingulate cortices, as well as the supplementary motor area, ventrolateral prefrontal cortex, and the aINS and pINS on both sides. The pINS is the main subregion of the SMN, as reported in a previous study involving 1000 healthy controls (Yeo et al., 2011). However, in the present study involving patients with LBP, a substantial portion of the pINS was intrinsically connected with the SN (**Supplementary Figure S1**).

While no significant differences in functional connectivity were found between the LBEpre and LBEpost runs, we found that the REAL group showed significantly positive correlation ($r = 0.58$, $P < 0.01$) between the reduction in LBEpain and the change of functional connectivity between the nodes of the DMN (mPFC) and SN (pINS) (**Figure 4**).

In the PHNT group, the change in LBEpain was negatively correlated with the change of DMN–SN connectivity (PCC–aINS, $r = -0.48$, $P < 0.05$), and it showed a trending positive correlation with the change of SMN–SN functional connectivity ($S1_{back}$-pINS, $r = 0.44$, $P = 0.07$) (**Figure 4**).

Interestingly, there was no significant difference between the REAL and PHNT groups in terms of changes in functional brain connectivity (LBEpost – LBEpre) as well as any other significant correlations between the reduction in LBEpain and the change of functional connectivity between the nodes of the DMN, SN, and SMN.

DISCUSSION

In the present study, we investigated the differential influence of needling-specific and non-specific components in acupuncture treatment using REAL and PHNT, whereby REAL induced needling credibility by combining somatosensory needling afference and visual feedback from the video, while PHNT did so through visual feedback only. The LBE pain model was used to modulate and standardize the patients' back pain levels, while functional connectivity analysis was performed to investigate the brain mechanism of the short-term pain modulation effects of REAL and PHNT. We found that the LBE pain model significantly increased clinical pain levels (LBEpain) in patients with back pain, and that this elevated LBEpain was reduced after both REAL and PHNT stimuli, indicating that both methods shared a common, short-term, pain-relieving effect. However, the corresponding brain mechanisms for pain reduction differed from each other. Somatosensory afference seemed to play an important role in pain modulation in REAL, because the physical-pain processing area (pINS) was engaged during corresponding functional connectivity alteration. In PHNT, a cognitive/affective factor (needling credibility and anticipation) seemed to be involved in the relevant connectivity changes, namely the salience-processing area (aINS). These results allowed us to identify short-term brain connectivity changes related to acupuncture-specific or non-specific effects on back pain intensity (LBEpain).

Clinical Pain Reduction in REAL: Detachment of Self From Pain

In REAL, greater LBEpain reduction was associated with decreased connectivity between the mPFC and pINS. Meta-analysis of acupuncture stimulation has shown significant deactivation in the mPFC and PCC, indicating that these areas modulate pain by shifting the focus between internal physical/mental states and external stimulation (Chae et al., 2013). Deactivation in the DMN subregion has also been observed both during real and sham acupuncture stimulation (Jung et al., 2015; Makary et al., 2018; Zhang et al., 2019). Previous studies have shown that the mPFC plays an important role in self-referential processing, which is critical for physical signal regulation, including pain (Stankewitz et al., 2018). Such processing includes both positive and negative self-appraisal (Dixon et al., 2017), as well as self-rumination and pain catastrophizing (Lee et al., 2018b). This consistent deactivation in the mPFC was interpreted as an attentional shift from self-referential to external-focused attention for a better understanding of given events and stimulations. The pINS shows stimulation-specific responses to the physical aspects of pain, representing bottom-up processing of sensory information. Thus, activity in the pINS has been considered

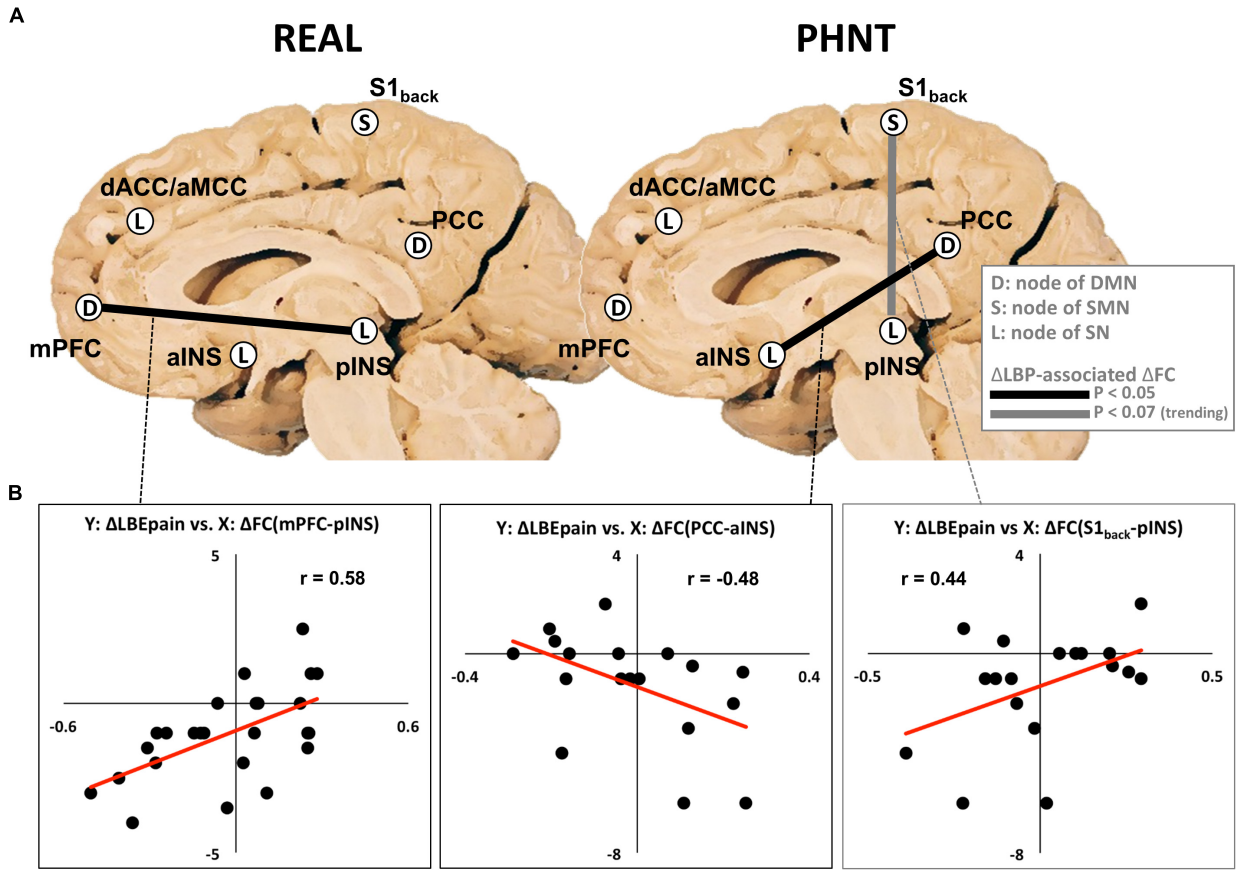

FIGURE 4 | Relationship between changes in functional connectivity and changes in LBEpain (LBEpost vs. LBEpre) after real (REAL) and phantom (PHNT) acupuncture stimulation. **(A)** Functional connectivity changes (mPFC–pINS in REAL, PCC–aINS, and $S1_{back}$–pINS in PHNT) associated with decreased LBEpain. Increased functional connectivities (dACC–MCC and aINS–pINS) were found in PHNT. **(B)** Correlation between changes in LBEpain (*Y*-axis) and functional connectivity (*X*-axis). DMN, default mode network; SMN, sensorimotor network; SN, salience network; FC, functional connectivity; LBP, low back pain; mPFC, medial prefrontal cortex; PCC, posterior cingulate cortex; $S1_{back}$, low back region in primary somatosensory cortex; dACC, dorsal anterior cingulate cortex; aMCC, anterior middle cingulate cortex; aINS, anterior insular cortex; pINS, posterior insular cortex; *Y*, *Y*-axis; *X*, *X*-axis.

a proxy of somatosensory (Christopher et al., 2014), pain (Morel et al., 2013), pain ratings (Segerdahl et al., 2015), and cortical amplification (Lee et al., 2017) processing. It is likely for this reason that activation in the pINS has been reported in most acupuncture neuroimaging studies (Chae et al., 2013). Indeed, it has recently been closely linked to the needling-specific component of acupuncture (somatosensory afference and corresponding arousal) (Jung et al., 2015; Makary et al., 2018). Interestingly, the pINS has been reported to be the main subregion of the SMN in healthy controls (Yeo et al., 2011), because it is significantly engaged in the physical aspects of pain and sensory processing. However, in the present study, a significant portion of the pINS was a part of the SN, rather than the SMN. The physical aspect of back pain, including painful sensations, seemed to capture the patients' attention, at least during the scan runs, in contrast to the healthy controls. This speculation should be further investigated.

Interestingly, the association between DMN and INS functional connectivity and clinical pain levels has been reported in other studies. For example, in patients with fibromyalgia, reduced clinical pain has been associated with reduced DMN–INS connectivity, and the same connectivity has been suggested as a possible marker for chronic pain (Napadow et al., 2012). In patients with low back pain, DMN–pINS connectivity, as well as changes thereof, has been shown to be significantly correlated with baseline (and increased) clinical pain (Loggia et al., 2013). The same relationship has also been reported in patients with LBP, complex regional pain syndrome, and knee osteoarthritis (Stankewitz et al., 2018). Thus, it has been speculated that a greater awareness of pain and the stronger incorporation of pain within the self (increased DMN–INS connectivity) can predict higher pain ratings (Napadow et al., 2012; Loggia et al., 2013). In other words, patients detach themselves from the pain, they report lower levels.

Our findings in REAL are in line with previous studies. Thus, we speculated that detachment of self from the physical aspects of pain contributes to the reduction in back pain (LBEpain) after REAL. As somatosensory tactile input is a predominant factor in creating sensory perception (e.g., reported strong acupuncture

sensations), we speculated that the influence of somatosensory afference may play a crucial role in the relationship between changes in functional connectivity and low back pain.

Clinical Pain Reduction in PHNT: Endorsement of Self and Disengagement in Pain Processing

In PHNT, we found that the increase in functional connectivity between PCC and aINS was associated with reduced LBEpain. The PCC is the main node of the DMN (Zhang et al., 2019), which is associated with self-reflection (Vogt and Laureys, 2005), internally directed cognition (Leech and Sharp, 2014), bodily attention (Jung et al., 2015), and self-referential pain catastrophizing (Lee et al., 2018b). In many acupuncture studies, consistent deactivation in the PCC has been reported in both real and sham acupuncture stimulation (Huang et al., 2012; Chae et al., 2013; Makary et al., 2018). The aINS, as part of the SN, is a key region in directing cognitive process (Christopher et al., 2014), transient attention (Cauda et al., 2012), significance of stimulus (Christopher et al., 2014), and empathy with perceptive-taking (Nieuwenhuys, 2012; Christopher et al., 2014), as well as in the integration of anticipation and sensory inputs (Jung et al., 2015), cognitive and affective processing of pain (Morel et al., 2013; Kuehn et al., 2016; Stankewitz et al., 2018), and self-awareness of physical condition (Stankewitz et al., 2018). In our previous study, increased activity in the aINS and decreased activity in the PCC were observed during both REAL and PHNT, and aINS activity was positively correlated with changes in low back pain (Makary et al., 2018). Thus, neither region is specific to the physical aspects of stimulation, but rather to the cognitive/emotional aspects of it – the PCC to self-referential processing and endorsement of self, and the aINS to processing of the salient/emotional aspects of pain events.

We observed a different pattern during PHNT than during REAL. Specifically, the aINS, which is the center of cognitive/emotional pain processing, as well as salience, plays an important role in pain reduction during PHNT, whereas the pINS, which is the center for physical pain processing does so during REAL. In PHNT, needling credibility can be consolidated by visual information and feedback from acupuncture stimulation, without somatosensory tactile inputs. This needling credibility might be built as a result of an internal decision-making process against incongruent visual and tactile information (i.e., between visual information which shows stimulation ritual and no/less sensations felt in their body) (see section "Empirical Account for Needling Credibility," **Figure 5**). In addition, vicarious sensations might be a result of shift the focus (the aINS) from the physical aspects of pain to the self (the PCC) as they believed they were actually stimulated with needles. Thus, this attentional shift from external pain to the self (increased PCC–aINS connectivity) might be related to LBEpain reduction in PHNT. We speculated that engagement of emotional regulation and subsequent disengagement between pain processing regions may contribute to the improvement in symptoms when there is a cognitive/affective component induced by needling credibility, not by needling (placebo effect).

Interestingly, the decreased level of functional connectivity between the $S1_{back}$ and pINS, which was transited from SMN to SN, tended toward correlation with the reduction in LBEpain (P = 0.07) in PHNT. A functional connection between the pINS and S1 has been reported, and it may result in precise perception and awareness of pain (Christopher et al., 2014). In one study involving healthy controls, S1–pINS connectivity that was somatotopically specific to the leg was negatively correlated with pain sensitivity when cuff stimuli were applied to the leg (Kim et al., 2013), and the S1 has shown significantly stronger pain-specific functional connectivity to the pINS (Peltz et al., 2011). S1–aINS connectivity has been reported to be significantly correlated with clinical pain in fibromyalgia, suggesting that synchronization between pain-processing regions influences exacerbated pain states (Kim et al., 2015). Thus, our results might suggest that bottom-up nociceptive sensory information is delivered to the corresponding S1 subregion ($S1_{back}$), as well as to the physical pain-processing area (pINS), and desynchronization between these two regions may ameliorate back pain (LBEpain) in PHNT. Further study, however, should be followed to investigate this speculation.

Empirical Account for Needling Credibility

Our experimental paradigm was designed to build and enhance needling credibility by an interaction between somatosensory needling afference from needling, visual feedback from the video, and instruction from the acupuncturist. Different combinations of components have been defined and used to model REAL and PHNT conditions and to explain the influence of each component experimentally (**Figure 5A**). In the first PHNT acupuncture experiment (Lee et al., 2014), 20 healthy participants received both REAL and PHNT stimulation in a counterbalanced design. After an in-depth interview with all subjects, eleven subjects of 20 were found to have needling credibility during the experiment and nine were not. Interestingly, some of the subjects believed they were actually stimulated with REAL during PHNT stimulation; some reported retrospectively that they thought the acupuncture stimulation was applied with new and advanced techniques so that they didn't feel much sensations, and some actually reported vicarious sensations. This phenomenon–reporting sensations in observing other's stimulation–has been reported and discussed as results of expectation (Song et al., 2019), sensory mirror system or mirror-touch synesthesia (Beissner et al., 2015; Makary et al., 2018), or body-ownership (Botvinick and Cohen, 1998). This implies that instruction to the subjects and visual feedback are also important factors to create those sensations, where the contribution of needling credibility to vicarious sensation is not significant (i.e., not all subjects with needling credibility reported vicarious sensations). However, four subjects who didn't believe that they were stimulated emphasized synchronization problem between the visual feedback from the video and the actual movement of an acupuncturist. Other five answered that they did not feel any sensation at the stimulation site or surrounding body region during PHNT stimulation, thus they thought the stimulation was not actually applied to

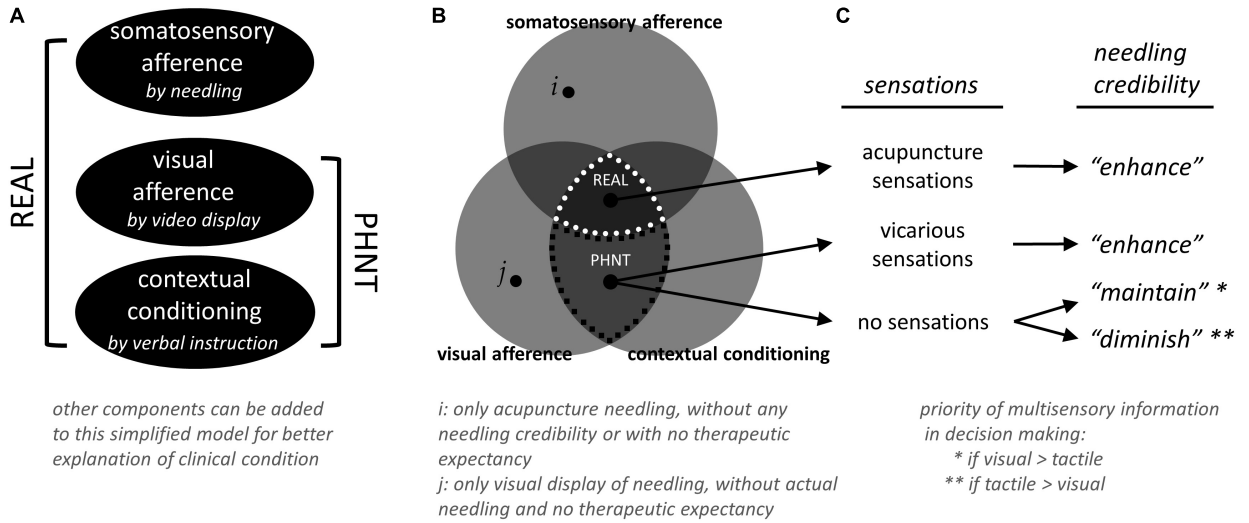

FIGURE 5 | Simplified model for real (REAL) and phantom (PHNT) acupuncture, and needling credibility. **(A)** Different combinations of components have been defined and used to model REAL and PHNT conditions and to explain the influence of each component experimentally. For better explanation and understanding of clinical condition, other components can be added to this simplified model. **(B)** Other than REAL and PHNT conditions (defined by somatosensory afference, visual afference, and contextual conditioning), several other tests can be done with different combination of components. For example, conditions with only acupuncture needling (*i*, without any needling credibility/therapeutic expectancy and visual display of needling) and with only visual display of needling (*j*, without actual needling and needling credibility/therapeutic expectancy) can be tested. Rest of those regions were not tested in this study (based on our experience, visual afference and contextual conditioning themselves might be able to "*initiate*" the needling credibility, but it was not explicitly tested in this study). **(C)** Needling credibility was influenced by a relationship between visual and tactile afferences from video and needling, respectively, contextual conditioning from treatment instruction, and belief of treatment from the in-depth interview with subjects.

them. In the second study (Makary et al., 2018), four LBP patients were excluded from the analysis as they reported the absence of needling credibility during the PHNT run. The major reason was no acupuncture sensations during the stimulation period, too. This shows that the existence of acupuncture sensations is an important factor for needling credibility. Rest of the patients, who believed that they were actually stimulated with needles, reported vicarious sensations or did believe even without any sensations from the stimulation. Thus, once the sensations (either actual or vicarious) were perceived, subjects tend to believe that they were actually stimulated with needles. If there were no sensations felt from the stimulation (while the instruction was given for needling), their needling credibility seemed to rely on the individually different weighting/priority of multisensory information in decision making (i.e., shift attention to self). This gives clue to estimate who will be likely to have needling credibility and who would not in the PHNT stimulation paradigm.

Taken together, (1) instructions from acupuncturist that they would be stimulated with real acupuncture needles and (2) visual feedback that is a simultaneous display of acupuncture stimulation (i.e., observation of treatment procedure with REAL) contributes to induce vicarious sensations and to *initiate* needling credibility (even without actual needling). (3) Actual or vicarious acupuncture sensations play an important role in *enhancing* needling credibility. (4) If tactile/acupuncture sensations are not congruent with visual feedback (for example, when they are observing the treatment procedure but do not feel any sensation from it), individual priority of multisensory information might affect maintaining the needling credibility or diminishing/eliminating of it (**Figures 5B,C**). Further studies should be done to confirm this hypothesis with several experimental conditions: (1) for better explanation and understanding of clinical condition, other components can be added to our model (**Figure 5A**), (2) conditions with only acupuncture needling (without any needling credibility/therapeutic expectancy and visual display of needling) and with only visual display of needling (without actual needling and needling credibility/therapeutic expectancy) (**Figure 5B**, i and j, respectively), (3) with controlling the influence of instructions (Cheon et al., 2018), (4) with different contents of provided visual information (i.e., treatment-relevant or not-relevant, or incongruent with actual stimulation), and (5) with different extents to which patients pay attention to the given visual or perceived sensations.

Limitations

Several limitations in the present study must be noted. Firstly, we had no untreated control group in which to investigate the effect of elapsed time (e.g., habituation or sensitization to our pain model), nor did we include a healthy control group to identify patient-specific brain responses (e.g., the involvement of the pINS in SN and connectivity changes to the pain model). Secondly, the number of subjects who experienced no needling credibility was too small (n = 4) to dissociate the effect of needing credibility from the effect of visual feedback in PHNT. As most of the patients who received PHNT believed that they had been treated with REAL and reported vicarious acupuncture

(*deqi*) sensations, a separate group with enough number of the subject must be included in future studies to explicitly exclude needling credibility during REAL/PHNT session to investigate the influence of needling credibility. Thus, several experimental conditions (with and without somatosensory needling, needling credibility, instruction, and visual feedback etc.) with a sufficient number of the subject are needed to investigate the analgesic effects of somatosensory and cognitive/affective components on back pain. For example, shallow (minimal acupuncture or tactile stimulation) acupuncture to investigate the influence of the amount of somatosensory afference, acupuncture methodology (manual- vs. electrical-acupuncture stimulation), acupoint specificity (by comparing sham points and acupoints), and no/irrelevant display to patients to inquire into the influence of the visual feedback can be used. Thirdly, along with the limitation of experimental conditions, several cognitive/affective factors were not considered in this analysis. Thus, for better understanding future study should also investigate factors which are clinically relevant and influential: doctor–patient relationship (rapport), previous acupuncture experience and its efficacy, expectancy of acupuncture efficacy, accuracy and consistency of sensation reporting, degree of sleepiness/awakeness/engagement during the experiment, and eagerness to be cured. Specific non-needling factors (i.e., acupuncture theory-based factors such as diagnosis and palpation) were not considered in this study. Fourthly, the acupoints were decided for the general purpose of back pain reduction and were not individualized to maximize its efficacy. Further study needs to be done with a set of individualized acupoints to further understand the influence of different aspects of acupuncture. Lastly, randomization should have performed more accurately and systematically. Unbalanced number of patients were allocated for REAL (n = 33) and PHNT (n = 23). Also, the significantly different baseline (LBEpre) pain scores made it difficult to investigate its direct comparison between groups, and thus the analysis of this study was limited to the changes in pain scores.

Conclusion

In the present study, we found significant back pain reduction and corresponding changes in functional connectivity after REAL and PHNT. It suggests that the involvement of different brain regions is related to improved symptoms, for example by detaching self (DMN) from the sensory aspect of pain (pINS) in REAL, by shifting attention (aINS) to self (DMN), and by disengaging between physical pain processing hubs (e.g., pINS and $S1_{back}$ region) in PHNT. We also speculated the relationship between visual and tactile information from video and needling, respectively, contextual conditioning from treatment instruction, and belief of treatment. This experimental paradigm might provide an appropriate sham methodology to dissociate the influence of different acupuncture components in acupuncture study, and the findings might help to understand corresponding brain mechanisms of acupuncture analgesia.

ETHICS STATEMENT

This study protocol was approved by the Institutional Review Board of the Kyung Hee University (KHNMC-OH-IRB 2010-013), and all participants provided written informed consent in accordance with the Declaration of Helsinki. This study is registered at the clinical research information service (CRIS; http://cris.nih.go.kr/) (registration number: KCT0002253).

AUTHOR CONTRIBUTIONS

JL, JK, and KP contributed to the conception and design of the study. JL, SE, J-HL, and KP conducted the experiment and collected the data. JL and SE performed the statistical analysis. JL, SE, and KP interpreted the results and wrote the manuscript. All authors contributed to the manuscript version, read, and approved the submitted version.

FUNDING

This study was supported by grant from the Korea Institute of Oriental Medicine (K18052).

SUPPLEMENTARY MATERIAL

The Supplementary Material for this article can be found online at: https://www.frontiersin.org/articles/10.3389/fnins.2019.01062/full#supplementary-material

REFERENCES

As-Sanie, S., Kim, J., Schmidt-Wilcke, T., Sundgren, P. C., Clauw, D. J., Napadow, V., et al. (2016). Functional connectivity is associated with altered brain chemistry in women with endometriosis-associated chronic pelvic pain. *J. Pain* 17, 1–13. doi: 10.1016/j.jpain.2015.09.008

Beckmann, C. F., DeLuca, M., Devlin, J. T., and Smith, S. M. (2005). Investigations into resting-state connectivity using independent component analysis. *Philos Trans. R. Soc. Lond. B Biol. Sci.* 360, 1001–1013. doi: 10.1098/rstb.2005.1634

Beissner, F., Brunner, F., Fink, M., Meissner, K., Kaptchuk, T. J., and Napadow, V. (2015). Placebo-induced somatic sensations: a multi-modal study of three different placebo interventions. *PLoS One* 10:e0124808. doi: 10.1371/journal.pone.0124808

Botvinick, M., and Cohen, J. (1998). Rubber hands 'feel' touch that eyes see. *Nature* 391:756. doi: 10.1038/35784

Cauda, F., Torta, D. M., Sacco, K., Geda, E., D'Agata, F., Costa, T., et al. (2012). Shared "core" areas between the pain and other task-related networks. *PLoS One* 7:e41929. doi: 10.1371/journal.pone.0041929

Chae, Y., Chang, D. S., Lee, S. H., Jung, W. M., Lee, I. S., Jackson, S., et al. (2013). Inserting needles into the body: a meta-analysis of brain activity associated with acupuncture needle stimulation. *J. Pain* 14, 215–222. doi: 10.1016/j.jpain.2012.11.011

Cheon, S., Park, H. J., Chae, Y., and Lee, H. (2018). Does different information disclosure on placebo control affect blinding and trial outcomes? a case study of participant information leaflets of randomized placebo-controlled trials of acupuncture. *BMC Med. Res. Methodol.* 18:13. doi: 10.1186/s12874-018-0474-471

Christopher, L., Koshimori, Y., Lang, A. E., Criaud, M., and Strafella, A. P. (2014). Uncovering the role of the insula in non-motor symptoms of Parkinson's disease. *Brain* 137(Pt 8), 2143–2154. doi: 10.1093/brain/awu084

Dixon, M. L., Thiruchselvam, R., Todd, R., and Christoff, K. (2017). Emotion and the prefrontal cortex: an integrative review. *Psychol. Bull.* 143, 1033–1081. doi: 10.1037/bul0000096

Filippini, N., MacIntosh, B. J., Hough, M. G., Goodwin, G. M., Frisoni, G. B., Smith, S. M., et al. (2009). Distinct patterns of brain activity in young carriers of the APOE-epsilon4 allele. *Proc. Natl. Acad. Sci. U.S.A.* 106, 7209–7214. doi: 10.1073/pnas.0811879106

Glover, G. H., Li, T. Q., and Ress, D. (2000). Image-based method for retrospective correction of physiological motion effects in fMRI: RETROICOR. *Magn. Reson Med.* 44, 162–167. doi: 10.1002/1522-2594(200007)44:1<162::aid-mrm23>3.3.co;2-5

Hemington, K. S., Rogachov, A., Cheng, J. C., Bosma, R. L., Kim, J. A., Osborne, N. R., et al. (2018). Patients with chronic pain exhibit a complex relationship triad between pain, resilience, and within- and cross-network functional connectivity of the default mode network. *Pain* 159, 1621–1630. doi: 10.1097/j.pain.0000000000001252

Huang, W., Pach, D., Napadow, V., Park, K., Long, X., Neumann, J., et al. (2012). Characterizing acupuncture stimuli using brain imaging with FMRI–a systematic review and meta-analysis of the literature. *PLoS One* 7:e32960. doi: 10.1371/journal.pone.0032960

Jung, W. M., Lee, I. S., Wallraven, C., Ryu, Y. H., Park, H. J., and Chae, Y. (2015). Cortical activation patterns of bodily attention triggered by acupuncture stimulation. *Sci. Rep.* 5:12455. doi: 10.1038/srep12455

Kaptchuk, T. J. (2011). Placebo studies and ritual theory: a comparative analysis of navajo, acupuncture and biomedical healing. *Philos Trans. R. Soc. Lond. B Biol. Sci.* 366, 1849–1858. doi: 10.1098/rstb.2010.0385

Kerr, C. E., Shaw, J. R., Conboy, L. A., Kelley, J. M., Jacobson, E., and Kaptchuk, T. J. (2011). Placebo acupuncture as a form of ritual touch healing: a neurophenomenological model. *Conscious Cogn.* 20, 784–791. doi: 10.1016/j.concog.2010.12.009

Kim, J., Loggia, M. L., Cahalan, C. M., Harris, R. E., Beissner, F. D. P. N., Garcia, R. G., et al. (2015). The somatosensory link in fibromyalgia: functional connectivity of the primary somatosensory cortex is altered by sustained pain and is associated with clinical/autonomic dysfunction. *Arth. Rheumatol.* 67, 1395–1405. doi: 10.1002/art.39043

Kim, J., Loggia, M. L., Edwards, R. R., Wasan, A. D., Gollub, R. L., and Napadow, V. (2013). Sustained deep-tissue pain alters functional brain connectivity. *Pain* 154, 1343–1351. doi: 10.1016/j.pain.2013.04.016

Kong, J., Gollub, R., Huang, T., Polich, G., Napadow, V., Hui, K., et al. (2007). Acupuncture de qi, from qualitative history to quantitative measurement. *J. Altern Complement. Med.* 13, 1059–1070. doi: 10.1089/acm.2007.0524

Kuehn, E., Mueller, K., Lohmann, G., and Schuetz-Bosbach, S. (2016).). Interoceptive awareness changes the posterior insula functional connectivity profile. *Brain Struct. Funct.* 221, 1555–1571. doi: 10.1007/s00429-015-0989-988

Langevin, H. M., Wayne, P. M., Macpherson, H., Schnyer, R., Milley, R. M., Napadow, V., et al. (2011). Paradoxes in acupuncture research: strategies for moving forward. *Evid Based Complement Alternat Med.* 2011:180805. doi: 10.1155/2011/180805

Lee, J., Lin, R. L., Garcia, R. G., Kim, J., Kim, H., Loggia, M. L., et al. (2017). Reduced insula habituation associated with amplification of trigeminal brainstem input in migraine. *Cephalalgia* 37, 1026–1038. doi: 10.1177/0333102416665223

Lee, J., Mawla, I., Kim, J., Loggia, M. L., Ortiz, A., Jung, C., et al. (2018a). Machine learning-based prediction of clinical pain using multimodal neuroimaging and autonomic metrics. *Pain* 160, 550–560. doi: 10.1097/j.pain.0000000000001417

Lee, J., Protsenko, E., Lazaridou, A., Franceschelli, O., Ellingsen, D. M., Mawla, I., et al. (2018b). Encoding of self-referential pain catastrophizing in posterior cingulate cortex in fibromyalgia. *Arth. Rheumatol.* 70, 1308–1318. doi: 10.1002/art.40507

Lee, J., Napadow, V., Kim, J., Lee, S., Choi, W., Kaptchuk, T. J., et al. (2014). Phantom acupuncture: dissociating somatosensory and cognitive/affective components of acupuncture stimulation with a novel form of placebo acupuncture. *PLoS One* 9:e104582. doi: 10.1371/journal.pone.0104582

Leech, R., and Sharp, D. J. (2014). The role of the posterior cingulate cortex in cognition and disease. *Brain* 137(Pt 1), 12–32. doi: 10.1093/brain/awt162

Loggia, M. L., Kim, J., Gollub, R. L., Vangel, M. G., Kirsch, I., Kong, J., et al. (2013). Default mode network connectivity encodes clinical pain: an arterial spin labeling study. *Pain* 154, 24–33. doi: 10.1016/j.pain.2012.07.029

Makary, M. M., Lee, J., Lee, E., Eun, S., Kim, J., Jahng, G. H., et al. (2018). Phantom acupuncture induces placebo credibility and vicarious sensations: a parallel fmri study of low back pain patients. *Sci. Rep.* 8:930. doi: 10.1038/s41598-017-18870-18871

Morel, A., Gallay, M. N., Baechler, A., Wyss, M., and Gallay, D. S. (2013). The human insula: architectonic organization and postmortem MRI registration. *Neuroscience* 236, 117–135. doi: 10.1016/j.neuroscience.2012.12.076

Napadow, V., Kim, J., Clauw, D. J., and Harris, R. E. (2012). Decreased intrinsic brain connectivity is associated with reduced clinical pain in fibromyalgia. *Arth. Rheum* 64, 2398–2403. doi: 10.1002/art.34412

Nieuwenhuys, R. (2012). The insular cortex: a review. *Prog. Brain Res.* 195, 123–163. doi: 10.1016/b978-0-444-53860-4.00007-6

Peltz, E., Seifert, F., DeCol, R., Dorfler, A., Schwab, S., and Maihofner, C. (2011). Functional connectivity of the human insular cortex during noxious and innocuous thermal stimulation. *Neuroimage* 54, 1324–1335. doi: 10.1016/j.neuroimage.2010.09.012

Segerdahl, A. R., Mezue, M., Okell, T. W., Farrar, J. T., and Tracey, I. (2015). The dorsal posterior insula subserves a fundamental role in human pain. *Nat. Neurosci.* 18, 499–500. doi: 10.1038/nn.3969

Song, H.-S., Jung, W.-M., Lee, Y.-S., Yoo, S.-W., and Chae, Y. (2019). Expectations of the physiological responses can change the somatosensory experience for acupuncture stimulation. *Front. Neurosci.* 13:74. doi: 10.3389/fnins.2019.00074

Stankewitz, A., Sorg, C., von Kalckreuth, A., Schulz, E., Valet, M., Neufang, S., et al. (2018). Fronto-insular connectivity during pain distraction is impaired in patients with somatoform pain. *J. Neuroimag.* 28, 621–628. doi: 10.1111/jon.12547

Vogt, B. A., and Laureys, S. (2005). Posterior cingulate, precuneal and retrosplenial cortices: cytology and components of the neural network correlates of consciousness. *Prog. Brain Res.* 150, 205–217. doi: 10.1016/s0079-6123(05)50015-50013

Yeo, B. T., Krienen, F. M., Sepulcre, J., Sabuncu, M. R., Lashkari, D., Hollinshead, M., et al. (2011). The organization of the human cerebral cortex estimated by intrinsic functional connectivity. *J. Neurophysiol.* 106, 1125–1165. doi: 10.1152/jn.00338.2011

Zhang, Y., Zhang, H., Nierhaus, T., Pach, D., Witt, C. M., and Yi, M. (2019). Default mode network as a neural substrate of acupuncture: evidence, challenges and strategy. *Front. Neurosci.* 13:100. doi: 10.3389/fnins.2019.00100

Conflict of Interest: The authors declare that the research was conducted in the absence of any commercial or financial relationships that could be construed as a potential conflict of interest.

frontiers in Neuroscience

REVIEW
published: 17 October 2019
doi: 10.3389/fnins.2019.01110

Acupuncture for the Treatment of Pain – A Mega-Placebo?

*Frauke Musial**

Department of Community Medicine, National Research Center in Complementary and Alternative Medicine, NAFKAM, Faculty of Health Science, UiT – The Arctic University of Norway, Tromsø, Norway

Several control conditions, such as penetrating sham acupuncture and non-penetrating placebo needles, have been used in clinical trials on acupuncture effects in chronic pain syndromes. All these control conditions are surprisingly effective with regard to their analgesic properties. These findings have fostered a discussion as to whether acupuncture is merely a placebo. Meta-analyses on the clinical effectiveness of placebo revealed that placebo interventions in general have minor, clinically important effects. Only in trials on pain and nausea, including acupuncture studies, did placebo effects vary from negligible to clinically important. At the same time, individual patient meta-analyses confirm that acupuncture is effective for the treatment of chronic pain, including small but statistically significant differences between acupuncture and sham acupuncture. All acupuncture control conditions induce *de qi*, a distinct stimulation associated with pain and needling which has been shown to be a nociceptive/pain stimulus. Acupuncture therefore probably activates the pain matrix in the brain in a bottom-up fashion via the spino-thalamic tract. Central nervous system effects of acupuncture can be modulated through expectations, which are believed to be a central component of the placebo response. However, further investigation is required to determine how strong the influence of placebo on the attenuation of activity in the pain matrix really is. A meta-analysis of individual participant functional magnetic imaging data reveals only weak effects of placebo on the activity of the pain network. The clinical acupuncture setting is comprised of a combination of a distinct neurophysiological stimulus, the needling stimulus/experience, and a complex treatment situation. A broader definition of placebo, such as that proposed by Howick (2017) acknowledges a role for expectation, treatment context, emotions, learning, and other contextual variables of a treatment situation. The inclusion of particular treatment feature as a definitional element permits a contextual definition of placebo, which in turn can be helpful in constructing future clinical trials on acupuncture.

Keywords: acupuncture, sham acupuncture, placebo needles, pain, placebo, expectation, pain matrix

OPEN ACCESS

Edited by:
Florian Beissner,
Hannover Medical School, Germany

Reviewed by:
Karin Meissner,
Hochschule Coburg, Germany
Paul Enck,
University of Tübingen, Germany

***Correspondence:**
Frauke Musial
frauke.musial@uit.no

Specialty section:
This article was submitted to Perception Science, a section of the journal Frontiers in Neuroscience

Received: *14 December 2018*
Accepted: *01 October 2019*
Published: *17 October 2019*

Citation:
Musial F (2019) Acupuncture for the Treatment of Pain – A Mega-Placebo? Front. Neurosci. 13:1110. doi: 10.3389/fnins.2019.01110

THE EFFECTS OF ACUPUNCTURE AND PLACEBO IN CLINICAL PAIN STUDIES

Clinical Acupuncture Studies on Chronic Pain Conditions

In clinical acupuncture studies on pain, acupuncture control conditions (often called sham acupuncture) show strong clinical effects. The three most frequently applied acupuncture control conditions are: (i) points that differ from the acupuncture points are needled; (ii) true acupuncture points are needled, but only very gently, and with very thin needles (minimal acupuncture) and

(iii) so-called placebo needles that do not penetrate the skin are used (for further discussion see paragraph "Needling associated procedures as sham acupuncture conditions in clinical trials").

In many of these clinical pain studies on acupuncture, acupuncture control conditions are more effective than standard medical care. In the German Acupuncture Randomized Trials (ART) studies, for example, in which true acupuncture was compared with minimal acupuncture and waiting list control, both true and minimal acupuncture were superior to being on a waiting list for the diagnosis of migraine, tension headache, or chronic back pain (Linde et al., 2005; Melchart et al., 2005; Brinkhaus et al., 2006). The only exception was knee arthritis, where only true acupuncture brought significant relief (Witt et al., 2005).

The German Acupuncture trials (GERAC studies) followed a slightly different design by comparing true acupuncture with minimal-acupuncture and standard medical care (Molsberger et al., 2006a,b). The results were similar: The treatment effect of acupuncture or minimal acupuncture was significantly superior to standard medical care and the effect was strong with no significant differences between the acupuncture conditions (Haake et al., 2007). The close similarity between true acupuncture, sham- and minimal acupuncture has raised the question as to whether the actual procedure of acupuncture is a placebo. Nonetheless, one of the consequences of these trials, which were funded by German health insurance companies, was that acupuncture is now recognized for by many German health insurance companies as a viable treatment for several conditions.

One of the most central questions in clinical studies is, however, whether and how the treatment which is to be tested compares to the available gold standard. A systematic review (Linde et al., 2009) consisting of twenty-two trials with a total of 4,419 patients came to the conclusion that acupuncture is not only at least as effective for migraine prophylaxis as prophylactic drug treatment but that it also has less side effects. Once again, no difference was established between true acupuncture and sham acupuncture procedures. In a systematic review on acupuncture treatment for tension type headache (Linde et al., 2009), the trials included were more heterogeneous (11 trials with 2,317 patients) with regard to the control conditions while the results were less homogeneous. The authors nonetheless came to the conclusion that acupuncture constitutes a valuable non-pharmacological treatment alternative.

Unlike the results from the large clinical acupuncture studies on pain syndromes, several brain-imaging studies in defined patient populations revealed relatively clear therapeutic acupuncture effects. For example, acupuncture therapeutic brain imaging studies in neuropathic pain (carpal tunnel syndrome) (Maeda et al., 2013, 2017) showed distinct true acupuncture-related neuroplasticity in the somatosensory cortex. This neuroplasticity is specifically related to increased neural functionality in the periphery (median nerve function) as well as to symptom improvement. One particularity of these two studies may be partly due to the use of electro acupuncture which constitutes a somewhat powerful acupuncture treatment.

In conclusion, the fact that sham acupuncture was equally effective as true acupuncture in almost all of the clinical trials on acupuncture has fostered a discussion as to whether acupuncture constitutes a particularly effective placebo, or whether sham acupuncture is an inadequate control.

How Powerful Is Placebo? Meta-Analyses on Clinical Placebo Effects

At the same time, the placebo effect, and in particular its potential clinical relevance was under discussion. While basic scientists claimed that a strong placebo effect existed (Benedetti et al., 2005), the authors of the first major Cochrane review on the topic (Hrobjartsson and Gotzsche, 2003), concluded that there was no evidence to suggest that placebo interventions have clinically important effects in general. Moreover, in the only clinical condition in which a significant placebo effect could be detected, i.e., pain, the result was restricted to subjective continuous outcomes, and could not be clearly distinguished from bias (Hrobjartsson and Gotzsche, 2003). The authors came to the same conclusion after incorporating new evidence and trials (Hrobjartsson and Gotzsche, 2004a,b). Despite extending the search to more clinical conditions, the conclusion that placebo interventions in general have no important clinical effects still prevailed (Hrobjartsson and Gotzsche, 2010).

However, on the basis of the new data material, the authors qualified their conclusion as follows: "in certain settings placebo interventions can influence patient-reported outcomes, especially pain and nausea, though it is difficult to distinguish patient-reported effects of placebo from biased reporting. The effect on pain varied, even among trials with low risk of bias, from negligible to clinically important. Variations in the effect of placebo were partly explained by variations in how trials were conducted and how patients were informed" (Hrobjartsson and Gotzsche, 2010). It is important to bear in mind that, since these meta-analyses contained acupuncture trials, in particular with regard to pain, they included and calculated sham- acupuncture conditions as placebo interventions. As discussed later in more detail, non-pharmacological placebos such as sham acupuncture as well as sham surgery maybe clinically more effective than oral pharmacological placebos (Meissner et al., 2013). This has certainly been the case in trials on migraine prophylaxis using network meta-analysis. The interpretation that the effect of non-pharmacological placebos is similar to pharmacological placebos may, therefore, be misleading and may undermine the effectiveness of the verum condition, here true acupuncture.

Consequently, the discussion on the relevance of placebo in general – and its role for acupuncture in particular – was intense and at times heated (Hrobjartsson and Gotzsche, 2006). Nonetheless, even a meta-analysis on acupuncture treatment for pain which included a systematic review of randomized clinical trials with true acupuncture, sham acupuncture, and no acupuncture groups did not reach any conclusion (Madsen et al., 2009). The aim was to explore the analgesic effect of acupuncture and sham acupuncture and to ascertain whether the type of the placebo acupuncture applied is associated with the estimated effect of acupuncture. Only three-armed randomized clinical trials consisting of a true acupuncture,

a sham acupuncture (or other similar controls), and a non-acupuncture group were included. However, this did not alter the results and conclusion: "A small analgesic effect of acupuncture was found, which seems to lack clinical relevance and cannot be clearly distinguished from bias. Whether needling at acupuncture points, or at any site, reduces pain independently of the psychological impact of the treatment ritual is unclear" (Madsen et al., 2009). The general conclusion from meta-analytic approaches to placebo is therefore that placebo effects are small, usually not clinically significant, and that the acupuncture effects in pain trials are inconsistent, dependent on study design and outcome, and very probably the result of bias.

Sham Acupuncture: A Particularly Powerful Placebo?

While several meta-analyses on acupuncture pain trials did not differ, a meta-analyses technique combining individual patient data (Vickers et al., 2010) came to a completely different conclusion. The first individual patient data meta-analyses, using data from 29 of 31 eligible RCTs, with a total of 17,922 patients, established that acupuncture is effective for the treatment of chronic pain (Vickers et al., 2012). Furthermore, they noted small, but statistically significant differences between true- and sham acupuncture. The authors state that "these differences are relatively modest, suggesting that factors in addition to the specific effects of needling are important contributors to the therapeutic effects of acupuncture." An update confirms the results and conclusion (Vickers et al., 2017) and a further detailed analysis of the data set suggests that the clinical benefit persists over time (MacPherson et al., 2017).

The interpretation that acupuncture in general is a particularly powerful placebo is predominantly due to the strong effects of sham acupuncture conditions as control conditions in clinical trials. Nonetheless, with regard to the question as to the clinical relevance of these effects, the comparison of true acupuncture/sham acupuncture conditions to other control conditions, in particular no-treatment controls or routine care controls, is relevant.

In their meta-analysis over 37 trials involving 5,754 patients Linde et al. (2010a) concluded that sham acupuncture conditions have much greater non-specific effects than placebo interventions. This meta-analysis also focused on three-armed trials, including non-acupuncture control groups. Unlike Madsen et al. (2009) the authors distinguished sham acupuncture conditions from inert placebo conditions in the discussion and raised the question as to whether sham acupuncture conditions differ from other placebos in that the former induce particularly large unspecific effects. Such an interpretation would have substantial methodological consequences for the design of clinical trials. The authors also raised the issue as to how such a finding should be evaluated in the light of the clinical relevance of sham acupuncture (Linde et al., 2010a,b). The same issue was raised by Moffet (2009) who, in his systematic review, also deemed sham acupuncture conditions to be as clinically relevant as true acupuncture conditions.

To answer the question as to whether sham acupuncture interventions are generally more clinically effective than other placebos (Linde et al., 2010b), reanalyzed the data from the Cochrane review of Hrobjartsson and Gotzsche (2010) on placebo effects in all clinical conditions. They concluded, with all due caution given the heterogeneity of the included trials, that sham acupuncture conditions are in fact associated with stronger non-specific effects than other physical and pharmacological placebos. As already mentioned above, the phenomenon that sham acupuncture conditions are more clinically effective than, for example, oral placebos, was confirmed by Meissner et al. (2013) in their elegant systematic review on the differential effectiveness of different placebo treatments in trials on migraine prophylaxis. This network meta-analysis revealed that both sham acupuncture and sham-surgery were clinically more effective than oral pharmacological placebos.

Penetrating sham acupuncture has been criticized on account of the fact that it may actually constitute a less effective form of acupuncture treatment. Therefore, non-penetrating devices which mimic the acupuncture procedure but which do not actually penetrate the skin have been developed (Streitberger and Kleinhenz, 1998; Park et al., 2002). Nonetheless, a systematic review by Zhang et al. (2015) reveals precisely the same effect for non-penetrating needles as for other sham acupuncture procedures. They conclude that neither the Streitberger nor the Park device is an inert control intervention. Moreover, sixteen studies recorded adverse events in true and sham acupuncture alike.

Nonetheless, while focusing on the issue of sham acupuncture conditions, it should be borne in mind that acupuncture has also been shown to be clinically more effective than for example non-steroidal anti-inflammatory drugs (NASIDs). In a study on chronic back pain patients, Toroski et al. (2018) ascertained that electro-acupuncture treatment was clinically effective and, moreover, more cost effective than treatment with non-steroidal anti-inflammatory drugs.

In summary, it is generally accepted that acupuncture is clinically effective in treating chronic pain states. There is a significant, but rather small difference between acupuncture and sham acupuncture. At the same time, sham acupuncture conditions appear to be more effective than other physical and pharmacological placebos.

NEEDLING-ASSOCIATED PROCEDURES SUCH AS SHAM ACUPUNCTURE CONDITIONS IN CLINICAL TRIALS

Three frequently employed control strategies are generally defined as sham acupuncture. Two of these methods penetrate the skin: (i) other points than acupuncture points, are needled. This type of control procedure is used to investigate the site (or point)-specific effects of acupuncture (Moore and McQuay, 2005); (ii) applying minimal acupuncture; true acupuncture points are needled, but only very gently and with extremely thin needles. This procedure, which is used for mode-specific control

of acupuncture effects, should enable the physician to define the appropriate "dose" of peripheral sensory stimulation (Backer et al., 2002). A combination of these two strategies is sometimes used. A third procedure utilizes devices with non-penetrating devices similar to the so-called "Streitberger needle" or the "Park-Sham" device. These procedures are similar in that they have the appearance of an acupuncture needle but do not penetrate the skin (Streitberger and Kleinhenz, 1998; Park et al., 2002; Chae et al., 2018). These devices are often called "placebo needles."

On the basis of the findings that sham acupuncture conditions appear to be more effective than other physical and pharmacological placebos, the issue has been raised as to whether sham acupuncture is physiologically active and, as such, not acceptable as a placebo control (Birch, 2006; Langevin et al., 2006, 2011; Lundeberg et al., 2008, 2011; Lund et al., 2009), Moreover, the choice of appropriate control conditions in clinical acupuncture trials on chronic pain syndromes poses a particular challenge, given that it is not possible to blind the acupuncturist. Double blinding is therefore essentially impossible which, in turn, substantially increases the risk of bias. In their recent review Chae et al. (2018) not only discuss the problems associated with non-penetrating sham acupuncture devices but also focus on the methodological challenges associated with trial design while introducing possible solutions with their benefits and shortcomings.

Several of the physiological mechanisms identified by Chae et al. (2018) are liable to account for some of the effects of placebo needles and cover the physiological effects of penetrating sham acupuncture: tactile stimulation is believed to be specific to the intervention and divided into the sensory discriminative and affective social component of the procedure. Some of the particularities of all forms of acupuncture/sham acupuncture/minimal acupuncture is the impossibility of blinding, possibly resulting in greater expectation-related placebo effects than when using a placebo pill. Nonetheless, expectation is also a neurophysiological effect which originates in the brain and which thus exerts its effect top-down.

POSSIBLE NEUROBIOLOGICAL MECHANISMS OF ACUPUNCTURE AND SHAM ACUPUNCTURE

C-Fiber Touch as Potential Mediator for the Affective-Social Dimension of Acupuncture

C-fiber touch (CT's) are tactile low threshold mechanosensitive fibers which are sensitive to gentle touch and which form a second touch system, with pleasant touch as a modality. They are assumed to represent the positive hedonic aspects of gentle touch (McGlone et al., 2007, 2014; Abraira and Ginty, 2013; Musial and Weiss, 2014). Thanks to animal experiments, this system has been known for quite some time and its role for humans has already been acknowledged. In humans, this system has been proposed to represent the neurobiological substrate, inducing feelings of calm and well-being related to gentle touch (McGlone et al., 2007, 2014; Abraira and Ginty, 2013; Musial and Weiss, 2014).

The particular role of touch for humans is not new to us, even though the particular C-fiber touch system has not yet been fully described for humans. For example, holding hands reduces the neural response to threat in an fMRI paradigm, even if the person holding the hand is a complete stranger (Coan et al., 2006). As Chae et al. (2018) point out, touch is a central factor in many medical procedures and an integral factor in all acupuncture conditions, regardless of whether or not the device penetrates the skin.

The touch component *per se* therefore constitutes a distinct neurobiological pathway, uncommon in all non-touch placebos such as a placebo pill. Moreover, it is represented by a specific pathway where the origin of stimulation is generated in the periphery of the body and travels in a bottom-up fashion to the brain. From here, it exerts a complex affective-emotional reaction (McGlone et al., 2007, 2014; Abraira and Ginty, 2013; Musial and Weiss, 2014). At the same time, this pathway is common to all acupuncture control conditions, thereby threatening the validity of virtually all of these conditions (Campbell, 2006; Lund et al., 2009).

De qi and the Sensory-Discriminative Aspects of Acupuncture

Inserting a needle and penetrating the skin is a stimulus of vital importance. Such a procedure will stimulate pain pathways and signal information of an injury, and is therefore recognized by the brain as a potential threat to the body's integrity. It therefore comes as no surprise that acupuncture procedures induce the strong and distinct activation of pain-related areas in the brain (Zhao, 2008; Chae et al., 2013). According to Zhao "Acupuncture analgesia is manifested only when the intricate feeling (soreness, numbness, heaviness, and distension) of acupuncture in patients occurs following acupuncture manipulation" (Zhao, 2008). This sensation, known as *de qi,* is believed to be fundamental to the therapeutic outcome of acupuncture (Choi et al., 2013; Chae et al., 2018).

To date, several studies have shown that even non-penetrating placebo needle procedures induce *de qi* sensations that are indistinguishable from the effect of real acupuncture needles (Chae, 2017; Chae et al., 2018). Taken together, these findings indicate that even non-penetrating acupuncture placebos are capable of stimulating sensory-discriminative pathways, including pain sensation. The current evidence therefore suggests that acupuncture – or indeed any other kind of needling procedure – constitutes a nociceptive and/or pain signal: Acupuncture (e.g., ST 36) activates pain-related brain structures (Biella et al., 2001; Pariente et al., 2005; Beissner et al., 2012; Theysohn et al., 2014); for overview and discussion see Wang et al. (2008), Zhao (2008), and the activation is dependent on the needling sensation (Beissner et al., 2012). Moreover, a meta-analysis across 28 fMRI studies of acupuncture needling showed an activation of the pain matrix (sensorimotor cortical network, including the insula, thalamus, and anterior cingulate cortex (ACC), as well as both the primary and secondary somatosensory cortices) (Chae et al., 2013). In summary, there is ample evidence

that acupuncture *per se* constitutes a nociceptive/pain stimulus which influences brain networks in a bottom-up fashion.

Under the premise that the therapeutic acupuncture effects are at least partly mediated through the pain pathway of the sensory-discriminative system, the processing of nociceptive signals in the spinal cord must be taken into account to explain the effect of needling and its related *de qi* sensation. A needling stimulus in a painful situation, be it clinically manifested such as in a pain syndrome or experimentally induced in the laboratory, is liable to excite two mechanisms on the level of the spinal cord: segmental (gate-control) (Mayer et al., 2000; Irnich and Beyer, 2002; Stux et al., 2003) and spino-medullary (diffuse noxious inhibitory control, DNIC) (Le Bars et al., 1989; Le Bars, 2002; Le Bars and Willer, 2002, 2007; Le Bars and Cadden, 2007) processes.

While gate control is, neurophysiologically speaking, somewhat short-lived (Fields et al., 2005), DNIC is a strong long-term effect, inasmuch as it persists for several minutes after its induction. Such a response is typical of neuroplastic changes (Le Bars and Willer, 2002, 2007). DNIC characterizes an intrinsic mechanism for inhibiting pain that becomes activated when an additional nociceptive stimulus is applied to a region far removed (heterotopic) from the initial region receiving nociceptive stimulation (Le Bars et al., 1989; Le Bars, 2002; Le Bars and Willer, 2002; Le Bars and Cadden, 2007; Le Bars and Willer, 2007). This phenomenon is often classified under the superordinate concept of "counter irritation" (Le Bars et al., 1989) and is mediated via a spino-medullary loop (Le Bars, 2002; Le Bars and Willer, 2007).

In humans, experimental paradigms which test the effect of additional pain stimuli on an already existing experimental pain stimulus, and which are thus homologous to DNIC are often called "heterotopic noxious conditioning stimulations (HNCS)" (Sprenger et al., 2011) or "conditioned pain modulation (CPM)" (Bjorkedal and Flaten, 2012). Sprenger et al. (2011) used a tonic cold pressor task and phasic additional pain stimulation in an fMRI paradigm and noticed a clear HNCS effect with marked endogenous analgesia. This outcome was accompanied by reduced activity in classical pain-related brain structures and the recruitment of an opiate-dependent, descending pain control system (naloxone blockade). In women Bjorkedal and Flaten (2012) were able to show that a CPM response can be reduced by expectations.

Acupuncture has been shown to exhibit rather strong effects in an HCNS/CPM design (Choi et al., 2011a,b; Musial et al., 2012). Moreover, acupuncture decreased somatosensory-evoked potential amplitude to noxious stimuli in anesthetized volunteers in an HCNS/CPM design (Meissner et al., 2004), thus showing clear acupuncture effects in unconscious humans. This is an interesting observation, given that all cortical effects such as expectations, suggestions, beliefs etc, can be excluded as confounding factors in subjects under deep anesthesia. Further evidence from fMRI studies shows less brain activity in somatosensory areas in response to pain following acupuncture stimulation (modulation of cold pain: (Zhang et al., 2003) and electrical pain: (Theysohn et al., 2014).

In conclusion, acupuncture therapeutic effects are seen to be related to the *de qi* sensation, which is characterized as a pain-related sensation. There is evidence that acupuncture and related conditions act via a pain signal elicited in the periphery and traveling bottom-up to the brain. These peripheral nociceptive signals may undergo modulation via spinal and spino-medullary mechanisms. Since virtually all placebo/sham acupuncture procedures are known to induce *de qi* ensations that are indistinguishable from real acupuncture, it should be borne in mind that this pain-related, somatosensory-discriminative mechanism akin to acupuncture is common to all true acupuncture/sham acupuncture/minimal acupuncture, and placebo acupuncture conditions.

Enhanced Expectation as a Mediator for the Strong Effects of "Sham"- and Placebo Acupuncture Conditions?

Despite various creative approaches such as the above discussed non-penetrating placebo needles (Streitberger and Kleinhenz, 1998; Park et al., 2002; Chae et al., 2018), an adequate experimental control of acupuncture for the treatment of chronic pain is scarcely possible, particularly since the acupuncturist cannot be blinded. One of the characteristics of all acupuncture and related procedures is, therefore, the impossibility of blinding, which can lead to greater expectation-related placebo effects than with other placebos (for overview and discussion see Chae (2017), Chae et al. (2018).

Expectation is a key mediator of the placebo response (Kirsch, 1999; Enck et al., 2008; Colloca and Miller, 2011a,b) and its relevance for the clinical effectiveness has already been well documented [(Moffet, 2009; Linde et al., 2010a; Chae et al., 2018)]. Interestingly enough, while it is widely accepted within placebo research that enhancing the placebo effect during drug treatment is desirable (Enck et al., 2013; Evers et al., 2018), the possibility that expectation – and thus placebo – may play a role in clinical acupuncture effects has been held against acupuncture as a treatment, in particular in public discourse. The argument is that acupuncture may merely represent a "placebo" without so-called "specific effects." This is contradictory in view of the fact that, physiologically speaking, the expectancy-mediated placebo effect *per se* has meanwhile been reasonably well defined and represents a rather distinct neurophysiological mechanism (Enck et al., 2008; Wager and Atlas, 2015; Geuter et al., 2017; Schafer et al., 2018).

The individual placebo response has been under close scrutiny ever since the 1990s (Benedetti et al., 1995; Benedetti, 1996; Amanzio and Benedetti, 1999; Benedetti et al., 2005). In an experimental pain-tolerance setting, Benedetti et al., showed how conditioning and expectation processes both play a role in placebo analgesia. The expectation-induced placebo response can be completely blocked by the opioid antagonist naloxone (Benedetti, 1996), whereas the conditioning-dependent placebo response can be blocked by naloxone only when conditioning was carried out with an opioid (Amanzio and Benedetti, 1999). Thus, expectation-dependent placebo responses are, in principle, mediated by the

endogenous opioid system, whereas conditioning-dependent placebo effects depend on the particular subsystem that had been conditioned. The opioid-dependent mechanism of expectation-induced placebo analgesia is also supported by neurophysiological imaging studies in man, showing that an opioid-dependent cortical network becomes activated during a placebo response (Petrovic et al., 2002; Zubieta et al., 2005). Acupuncture analgesia is similar to the expectation-dependent placebo effect in that it too can be blocked by naloxone, i.e., it is also opioid-dependent [for an overview, see (Mayer et al., 2000)].

ACUPUNCTURE, PLACEBO, AND THE PAIN MATRIX

Data from imaging studies have confirmed that not only expectation but also learning and context factors play a role in placebo effects [for overview and discussion see Enck et al. (2008), Wager and Atlas (2015), Geuter et al. (2017), Schafer et al. (2018)]. Moreover, context and social factors are welcome modulators for expectation and associative learning. Most of these models are based on results from pain studies.

With regard to the placebo response, the ventromedial prefrontal cortex (vmPFC), the dorsolateral prefrontal cortex (dlPFC), the lateral orbitofrontal cortex (lOFC), nucleus accumbens, insula, amygdala, hypothalamus, and periaqueductal gray are generally regarded as crucial (Wager and Atlas, 2015; Geuter et al., 2017; Schafer et al., 2018). All these areas increase activity in response to placebo manipulations related to pain stimulation (Wager and Atlas, 2015), albeit the periaqueductal gray (PAG) and the dorsal anterior cingulate cortex (dACC) respond in a more differentiated fashion, and appear to have a modulatory function within the placebo network (Wager and Atlas, 2015). The vmPFC seemingly plays a particularly essential role in the mediation of expectation (Geuter et al., 2017). Thus, the vmPFC represents the part of the placebo brain network that connects situational factors to neurophysiological responses (Geuter et al., 2017).

At the same time, the placebo network appears to be independent from the pain network, even though some structures, primarily the PAG and the dACC, seem to have a modulatory function in both networks (Wager and Atlas, 2015; Geuter et al., 2017). This conceptualization fits well with a number of experimental findings, indicating that the perception of pain is also dependent on the context (Keltner et al., 2006). In one fMRI study, for instance (Koyama et al., 2005) were able to show that, to a great extent, the expectation of one particular stimulus intensity determined its cortical representation, regardless of whether or not it was anticipated to be painful. As the magnitude of the expected pain increased, activation increased simultaneously in the thalamus, insula, prefrontal cortex, and ACC. Pain-intensity-related brain activation was identified in a widely distributed set of brain regions and overlapped partially with expectation-related activation in other regions, including the anterior insula and ACC (Koyama et al., 2005).

Thus, the evidence available with regard to placebo effects on pain in experimental human and animal studies suggests that placebo effects are mediated by a network of brain structures that differ from the pain network. However, the placebo network influences and modulates the pain network, relying on several factors such as context, learning and prior experiences, instructions, etc. These factors probably influence the placebo network by way of expectations. Expectations are fundamental inasmuch as they may signal reward (e.g., reduced pain). Anticipated reward will activate the reward system in the brain, a system that involves the nucleus accumbens, the amygdala, the ventral tegmental area, and the orbitofrontal cortex (Enck et al., 2008). The neurotransmitters of this system are dopamine and opioid peptides, and this network is usually investigated with regard to drug dependencies and reinforcement. In summary, instructions, suggestions, and other types of social information can have powerful effects on pain and these changes are mediated by top-down control via the involvement of prefrontal regions, particularly the dorsolateral and ventromedial prefrontal cortex (Koban et al., 2017).

As already elucidated, current evidence suggests that any kind of needling procedure constitutes a nociceptive and/or pain signal (Biella et al., 2001; Pariente et al., 2005; Beissner et al., 2012; Theysohn et al., 2014); for overview and discussion see Wang et al. (2008), Zhao (2008), Beissner et al. (2012), and that acupuncture needling (a meta-analysis across 28 fMRI studies) induces an activation of the pain matrix (sensorimotor cortical network, including the insula, thalamus, anterior cingulate cortex, and both primary and secondary somatosensory cortices) (Chae et al., 2013). Moreover, data from healthy humans subjects in response to needling of commonly used acupuncture points for the treatment of pain syndromes (manual acupuncture at LI4, ST36) revealed a partial overlap with the pain matrix as well as a deactivation of a limbic-paralimbic-neocortical network (Hui et al., 2009; Claunch et al., 2012). This limbic deactivation is correlated to the psychophysical response modulating the bottom-up nociceptive signal. It therefore modulates brain networks in response to acupuncture stimulation. Assuming that acupuncture is a pain stimulus that travels bottom-up and activates the pain networks, it must also be assumed that expectations, instructions, emotions, and other context factors modulate acupuncture effects.

In an elegant study Lee et al. (2015) modulated and manipulated an acupuncture stimulus by instruction. One group was told that the needling was part of an acupuncture treatment, whereas the other group was informed about the needle insertion only, and that this might be a painful intervention. In addition to their acupuncture stimulation, all participants received the same sensory stimuli which included a pain stimulus. The brain activation in response to the pain stimulus in parts of the pain network was significantly lower in those participants who had been informed that the needle insertion was part of an acupuncture treatment. At the same time, the needling within a therapeutic context activated reward circuits in the brain and modulated the pain matrix.

The results from brain imaging studies emanating from placebo research as well as the results of Chae et al. (2013) and

Lee et al. (2015) suggest that: (i) the pain matrix and the placebo network are primarily independent brain networks; (ii) the pain matrix and the placebo network interact and the placebo-induced modulation of the pain-matrix is mediated by expectation; (iii) acupuncture activates the pain matrix and is a nociceptive/pain stimulus, and (iv) acupuncture as a nociceptive/pain stimulus is modulated by placebo effects, in particular expectation.

Nonetheless, how powerful the modulation of the pain-matrix through placebo effects actually is remains to be elucidated. A meta-analysis of individual participant functional magnetic resonance imaging data combined the results of 603 healthy individuals from 20 studies and investigated the effects of placebo intervention on the pain matrix (Zunhammer et al., 2018). The analysis revealed rather moderate analgesic effects on subjective pain reports and only a very small effect of the placebo condition on the pain matrix. The authors concluded that placebo treatments affect pain through brain mechanisms (top down) and that these influences are largely independent from the bottom-up effects of nociceptive processing.

IS ACUPUNCTURE A MEGA-PLACEBO? ON THE RELATIVITY OF PLACEBO

In particular the neurobiological developments in the understanding of the mechanisms of the placebo response have confirmed that the concept placebo encompasses a wide variety of modalities such as emotions, instructions, suggestions, and other types of social information mediated by alterations in prefrontal brain areas (Koban et al., 2017). These factors are often described as the "unspecific" effects of a particular treatment setting, indicating that the treatment effects are mainly psychological in nature and independent from the treatment provided.

To date, the concept of specificity at brain level, which is reminiscent of the historic theory of phrenology, may be questioned. Defined brain areas, such as the PAG or the dACC play a role in a number of brain functions. This fact tallies well with the concept that brain functions are performed by the activity of neural networks. The concept of neural networks also explains why the perception of pain is context-dependent (Koyama et al., 2005; Keltner et al., 2006); a finding that is relevant for the explanation of pain-related placebo effects.

Howick (2017) proposes a broader definition of placebo which goes beyond the claim that a placebo should consist of an inert "intervention simulation." His modified version of Grünbaum's definition of placebo emphasizes the role of expectations, and thus includes emotions, learning, and other contextual variables. Moreover, his definition assigns a special role to the peculiarities of a treatment situation, including special treatment features, and thus partly allows for a contextual definition of placebo. However, it is worth bearing in mind that Grünbaum's original article (Grunbaum, 1986), which relates to placebo effects in psychiatry and psychotherapy, remains somewhat controversial (Enck and Zipfel, 2019). To what extent this concept can be applied to other non-pharmacological treatments such as acupuncture – which is in many ways more "physical" than psychotherapy – may not be entirely consensual in the field of placebo research.

Nonetheless, Howick's interpretation of Grünbaum's definition (Grunbaum, 1986) provides an opening for the role of treatment theory and thus calls for a broadening of the definition of placebo beyond the role of expectation. In his paper, Howick (2017) uses the acupuncture/sham acupuncture/placebo needle discussion as a case study to illustrate that treatment theory is fundamental to the definition of a placebo condition and that it does not suffice to control exclusively for expectation. In his example, point specificity as treatment theory will lead to an acupuncture-related placebo concept which interprets needling at non-acupuncture points as "placebogenic" [page 1371, Howick (2017)]. In his case study on acupuncture, he argues that independent evidence supports the assumption that the placebo needle itself (Streitberger needle) cannot be a true placebo. He pinpoints that the core challenge in the interpretation of the clinically effective control procedures for the acupuncture treatment of pain states is the lack of an accepted therapeutic theory for acupuncture.

Howick's broadened concept of placebo not only allows for the defined use of placebo controls beyond the pharmacological context but also includes also non-pharmacological interventions. Nonetheless, as he demonstrates in his acupuncture case study, his definition demands and includes a defined therapeutic theory. With regard to many interventions out of the spectrum of complementary and alternative medicine, this may still constitute a challenge, such as in the case of acupuncture. Further clinical studies addressing treatment theory of acupuncture as well as the placebo/expectation issue are therefore required.

The field of placebo research has accepted that placebo might not be as distinctively defined as it is necessary for conducting a clinical trial in the non-pharmacological arena. Placebo effects are viewed as positive and useful factors of a treatment, particularly in clinical practice, and are considered to be a part of *every* regular treatment (Evers et al., 2018). With this definition, the debate as to what extent a treatment is dependent on placebo becomes less pungent and the focus is relocated to the most important question, namely to: what helps patients, what relieves their pain, and how can they be treated most effectively. This pragmatic approach aims to maximize all the positive factors of a treatment that can be recruited while minimizing risk and negative effects, including nocebo (Evers et al., 2018).

AUTHOR CONTRIBUTIONS

The author confirms being the sole contributor of this work and has approved it for publication.

FUNDING

The publication charges for this article were funded by a grant from the publication fund of UiT – The Arctic University of Norway.

REFERENCES

Abraira, V. E., and Ginty, D. D. (2013). The sensory neurons of touch. *Neuron* 79, 618–639. doi: 10.1016/j.neuron.2013.07.051

Amanzio, M., and Benedetti, F. (1999). Neuropharmacological dissection of placebo analgesia: expectation-activated opioid systems versus conditioning-activated specific subsystems. *J. Neurosci.* 19, 484–494. doi: 10.1523/jneurosci.19-01-00484.1999

Backer, M., Hammes, M. G., Valet, M., Deppe, M., Conrad, B., Tolle, T. R., et al. (2002). Different modes of manual acupuncture stimulation differentially modulate cerebral blood flow velocity, arterial blood pressure and heart rate in human subjects. *Neurosci. Lett.* 333, 203–206. doi: 10.1016/s0304-3940(02)01109-6

Beissner, F., Deichmann, R., Henke, C., and Bar, K. J. (2012). Acupuncture–deep pain with an autonomic dimension? *Neuroimage* 60, 653–660. doi: 10.1016/j.neuroimage.2011.12.045

Benedetti, F. (1996). The opposite effects of the opiate antagonist naloxone and the cholecystokinin antagonist proglumide on placebo analgesia. *Pain* 64, 535–543. doi: 10.1016/0304-3959(95)00179-4

Benedetti, F., Amanzio, M., and Maggi, G. (1995). Potentiation of placebo analgesia by proglumide. *Lancet* 346:1231. doi: 10.1016/s0140-6736(95)92938-x

Benedetti, F., Mayberg, H. S., Wager, T. D., Stohler, C. S., and Zubieta, J. K. (2005). Neurobiological mechanisms of the placebo effect. *J. Neurosci.* 25, 10390–10402. doi: 10.1523/jneurosci.3458-05.2005

Biella, G., Sotgiu, M. L., Pellegata, G., Paulesu, E., Castiglioni, I., and Fazio, F. (2001). Acupuncture produces central activations in pain regions. *Neuroimage* 14(1 Pt 1), 60–66. doi: 10.1006/nimg.2001.0798

Birch, S. (2006). A review and analysis of placebo treatments, placebo effects, and placebo controls in trials of medical procedures when sham is not inert. *J. Altern. Comp. Med.* 12, 303–310. doi: 10.1089/acm.2006.12.303

Bjorkedal, E., and Flaten, M. A. (2012). Expectations of increased and decreased pain explain the effect of conditioned pain modulation in females. *J. Pain Res.* 5, 289–300. doi: 10.2147/JPR.S33559

Brinkhaus, B., Witt, C. M., Jena, S., Linde, K., Streng, A., Wagenpfeil, S., et al. (2006). Acupuncture in patients with chronic low back pain: a randomized controlled trial. *Arch. Intern. Med.* 166, 450–457.

Campbell, A. (2006). Role of C tactile fibres in touch and emotion–clinical and research relevance to acupuncture. *Acupunct. Med.* 24, 169–171. doi: 10.1136/aim.24.4.169

Chae, Y. (2017). The dilemma of placebo needles in acupuncture research. *Acupunct. Med.* 35, 382–383.

Chae, Y., Chang, D. S., Lee, S. H., Jung, W. M., Lee, I. S., Jackson, S., et al. (2013). Inserting needles into the body: a meta-analysis of brain activity associated with acupuncture needle stimulation. *J. Pain* 14, 215–222. doi: 10.1016/j.jpain.2012.11.011

Chae, Y., Lee, Y.-S., and Enck, P. (2018). How placebo needles differ from placebo pills? *Front. Psychiatry* 9:243. doi: 10.3389/fpsyt.2018.00243

Choi, K. E., Musial, F., Amthor, N., Rampp, T., Saha, F. J., Michalsen, A., et al. (2011a). Isolated and combined effects of electroacupuncture and meditation in reducing experimentally induced ischemic pain: a pilot study. *Evid Based Comp. Alternat Med.* 2011:9. doi: 10.1155/2011/950795

Choi, K. E., Rampp, T., Saha, F. J., Dobos, G. J., and Musial, F. (2011b). Pain modulation by meditation and electroacupuncture in experimental submaximum effort tourniquet technique (SETT). *Explore* 7, 239–245. doi: 10.1016/j.explore.2011.04.004

Choi, Y. J., Lee, J. E., Moon, W. K., and Cho, S. H. (2013). Does the effect of acupuncture depend on needling sensation and manipulation? *Comp. Ther. Med.* 21, 207–214. doi: 10.1016/j.ctim.2012.12.009

Claunch, J. D., Chan, S. T., Nixon, E. E., Qiu, W. Q., Sporko, T., Dunn, J. P., et al. (2012). Commonality and specificity of acupuncture action at three acupoints as evidenced by FMRI. *Am. J. Chin. Med.* 40, 695–712.

Coan, J. A., Schaefer, H. S., and Davidson, R. J. (2006). Lending a hand: social regulation of the neural response to threat. *Psychol. Sci.* 17, 1032–1039. doi: 10.1111/j.1467-9280.2006.01832.x

Colloca, L., and Miller, F. G. (2011a). How placebo responses are formed: a learning perspective. *Philos. Trans. R. Soc. Lond. B Biol. Sci.* 366, 1859–1869. doi: 10.1098/rstb.2010.0398

Colloca, L., and Miller, F. G. (2011b). Role of expectations in health. *Curr. Opin. Psychiatry* 24, 149–155.

Enck, P., Benedetti, F., and Schedlowski, M. (2008). New insights into the placebo and nocebo responses. *Neuron* 59, 195–206. doi: 10.1016/j.neuron.2008.06.030

Enck, P., Bingel, U., Schedlowski, M., and Rief, W. (2013). The placebo response in medicine: minimize, maximize or personalize? *Nat. Rev. Drug Discov.* 12, 191–204. doi: 10.1038/nrd3923

Enck, P., and Zipfel, S. (2019). Placebo effects in psychotherapy: a framework. *Front. Psychiatry* 10:456. doi: 10.3389/fpsyt.2019.00456

Evers, A. W. M., Colloca, L., Blease, C., Annoni, M., Atlas, L. Y., Benedetti, F., et al. (2018). Implications of placebo and nocebo effects for clinical practice: expert consensus. *Psychother. Psychosom.* 87, 204–210. doi: 10.1159/000490354

Fields, H. L., Basbaum, A. I., and Heinricher, M. M. (2005). "Central nervous system mechanisms of pain modulation," in *Wall and Melzack's Textbook of Pain*, eds S. B. McMahon, and M. Koltzenburg (London: Elsevier Churchill Livingstone), 125–142. doi: 10.1016/b0-443-07287-6/50012-6

Geuter, S., Koban, L., and Wager, T. D. (2017). The cognitive neuroscience of placebo effects: concepts, predictions, and physiology. *Annu. Rev. Neurosci.* 40, 167–188. doi: 10.1146/annurev-neuro-072116-031132

Grunbaum, A. (1986). The placebo concept in medicine and psychiatry. *Psychol. Med.* 16, 19–38. doi: 10.1017/s0033291700002506

Haake, M., Muller, H. H., Schade-Brittinger, C., Basler, H. D., Schafer, H., Maier, C., et al. (2007). German acupuncture trials (GERAC) for chronic low back pain: randomized, multicenter, blinded, parallel-group trial with 3 groups. *Arch. Intern. Med.* 167, 1892–1898.

Howick, J. (2017). The relativity of "placebos": defending a modified version of grünbaum's definition. *Synthese* 194, 1363–1396. doi: 10.1007/s11229-015-1001-0

Hrobjartsson, A., and Gotzsche, P. C. (2003). Placebo treatment versus no treatment. *Cochrane Database Syst. Rev.* CD003974.

Hrobjartsson, A., and Gotzsche, P. C. (2004a). Is the placebo powerless? update of a systematic review with 52 new randomized trials comparing placebo with no treatment. *J. Intern. Med.* 256, 91–100. doi: 10.1111/j.1365-2796.2004.01355.x

Hrobjartsson, A., and Gotzsche, P. C. (2004b). Placebo interventions for all clinical conditions. *Cochrane Database Syst. Rev.* 20:CD003974.

Hrobjartsson, A., and Gotzsche, P. C. (2006). Unsubstantiated claims of large effects of placebo on pain: serious errors in meta-analysis of placebo analgesia mechanism studies. *J. Clin. Epidemiol.* 59, 336–338. doi: 10.1016/j.jclinepi.2005.05.011

Hrobjartsson, A., and Gotzsche, P. C. (2010). Placebo interventions for all clinical conditions. *Cochrane Database Syst. Rev.* 20:CD003974.

Hui, K. K., Marina, O., Claunch, J. D., Nixon, E. E., Fang, J., Liu, J., et al. (2009). Acupuncture mobilizes the brain's default mode and its anti-correlated network in healthy subjects. *Brain Res.* 1287, 84–103. doi: 10.1016/j.brainres.2009.06.061

Irnich, D., and Beyer, A. (2002). [Neurobiological mechanisms of acupuncture analgesia]. *Schmerz* 16, 93–102.

Keltner, J. R., Furst, A., Fan, C., Redfern, R., Inglis, B., and Fields, H. L. (2006). Isolating the modulatory effect of expectation on pain transmission: a functional magnetic resonance imaging study. *J. Neurosci.* 26, 4437–4443. doi: 10.1523/jneurosci.4463-05.2006

Kirsch, I. (ed.) (1999). *How Expectancies Shape Experience*. Washington, D.C: American Psychological Association.

Koban, L., Jepma, M., Geuter, S., and Wager, T. D. (2017). What's in a word? How instructions, suggestions, and social information change pain and emotion. *Neurosci. Biobehav. Rev.* 81(Pt A), 29–42. doi: 10.1016/j.neubiorev.2017.02.014

Koyama, T., McHaffie, J. G., Laurienti, P. J., and Coghill, R. C. (2005). The subjective experience of pain: where expectations become reality. *Proc. Natl. Acad. Sci. U.S.A.* 102, 12950–12955. doi: 10.1073/pnas.0408576102

Langevin, H. M., Hammerschlag, R., Lao, L., Napadow, V., Schnyer, R. N., and Sherman, K. J. (2006). Controversies in acupuncture research: selection of controls and outcome measures in acupuncture clinical trials. *J. Altern. Comp. Med.* 12, 943–953. doi: 10.1089/acm.2006.12.943

Langevin, H. M., Wayne, P. M., Macpherson, H., Schnyer, R., Milley, R. M., Napadow, V., et al. (2011). Paradoxes in acupuncture research: strategies for moving forward. *Evid Based Comp. Alternat Med.* 2011:180805. doi: 10.1155/2011/180805

Le Bars, D. (2002). The whole body receptive field of dorsal horn multireceptive neurones. *Brain Res. Brain Res. Rev.* 40, 29–44. doi: 10.1016/s0165-0173(02)00186-8

Le Bars, D., and Cadden, S. W. (2007). "What is a wide dynamic cell?," in *The Senses: a Comprehensive Reference*, ed. A. Basbaum (London: Elsevier Churchill Livingstone), 331–338. doi: 10.1016/b978-012370880-9.00167-5

Le Bars, D., and Willer, J. C. (2002). Pain modulation triggered by high-intensity stimulation: implications for acupuncture analgesia? *Int. Congress Ser.* 1238, 11–29. doi: 10.1016/s0531-5131(02)00412-0

Le Bars, D., and Willer, J. C. (2007). "Diffuse noxious inhibitory controls (DNIC)," in *The Senses: a Comprehensive Reference*, ed. A. I. Basbaum (London: Elsevier Churchill Livingstone), 762–773.

Le Bars, D., Willers, J. C., De Broucker, T., and Villanueva, L. (1989). "Neurophysiological mechanisms involved in the pain-relieving effects of counterirritation and related techniques inclusing acupuncture," in *Scientific Bases of Acupuncture*, eds G. Stux and B. Pomeranz (Berlin: Springer), 79–112. doi: 10.1007/978-3-642-73757-2_5

Lee, I. S., Wallraven, C., Kong, J., Chang, D. S., Lee, H., Park, H. J., et al. (2015). When pain is not only pain: inserting needles into the body evokes distinct reward-related brain responses in the context of a treatment. *Physiol. Behav.* 140, 148–155. doi: 10.1016/j.physbeh.2014.12.030

Linde, K., Allais, G., Brinkhaus, B., Manheimer, E., Vickers, A., and White, A. R. (2009). Acupuncture for migraine prophylaxis. *Cochrane Database Syst. Rev.* 21:CD001218.

Linde, K., Niemann, K., and Meissner, K. (2010a). Are sham acupuncture interventions more effective than (other) placebos? a re-analysis of data from the cochrane review on placebo effects. *Forsch Komplementmed* 17, 259–264. doi: 10.1159/000320374

Linde, K., Niemann, K., Schneider, A., and Meissner, K. (2010b). How large are the nonspecific effects of acupuncture? a meta-analysis of randomized controlled trials. *BMC Med.* 8:75. doi: 10.1186/1741-7015-8-75

Linde, K., Streng, A., Jurgens, S., Hoppe, A., Brinkhaus, B., Witt, C., et al. (2005). Acupuncture for patients with migraine: a randomized controlled trial. *JAMA* 293, 2118–2125.

Lund, I., Näslund, J., and Lundeberg, T. (2009). Minimal acupuncture is not a valid placebo control in randomized controlled trials of acupuncture: a physiologist's perspective. *Comment. Chin. Med.* 4:1. doi: 10.1186/1749-8546-4-1

Lundeberg, T., Lund, I., Naslund, J., and Thomas, M. (2008). The emperors sham - wrong assumption that sham needling is sham. *Acupunct. Med.* 26, 239–242. doi: 10.1136/aim.26.4.239

Lundeberg, T., Lund, I., Sing, A., and Naslund, J. (2011). Is placebo acupuncture what it is intended to be? *Evid Based Comp. Alternat Med.* 2011:932407. doi: 10.1093/ecam/nep049

MacPherson, H., Vertosick, E. A., Foster, N. E., Lewith, G., Linde, K., Sherman, K. J., et al. (2017). The persistence of the effects of acupuncture after a course of treatment: a meta-analysis of patients with chronic pain. *Pain* 158, 784–793. doi: 10.1097/j.pain.0000000000000747

Madsen, M. V., Gotzsche, P. C., and Hrobjartsson, A. (2009). Acupuncture treatment for pain: systematic review of randomised clinical trials with acupuncture, placebo acupuncture, and no acupuncture groups. *BMJ* 338:a3115. doi: 10.1136/bmj.a3115

Maeda, Y., Kettner, N., Lee, J., Kim, J., Cina, S., Malatesta, C., et al. (2013). Acupuncture-evoked response in somatosensory and prefrontal cortices predicts immediate pain reduction in carpal tunnel syndrome. *Evid Based Comp. Alternat Med.* 2013:795906. doi: 10.1155/2013/795906

Maeda, Y., Kim, H., Kettner, N., Kim, J., Cina, S., Malatesta, C., et al. (2017). Rewiring the primary somatosensory cortex in carpal tunnel syndrome with acupuncture. *Brain* 140, 914–927. doi: 10.1093/brain/awx015

Mayer, D., Mayer, E. A., and Saper, C. B. (2000). "Biological mechanisms of acupuncture," in *Progress in Brain Research*, (London: Elsevier Churchill Livingstone), 122–132.

McGlone, F., Vallbo, A. B., Olausson, H., Loken, L., and Wessberg, J. (2007). Discriminative touch and emotional touch. *Can. J. Exp. Psychol.* 61, 173–183. doi: 10.1037/cjep2007019

McGlone, F., Wessberg, J., and Olausson, H. (2014). Discriminative and affective touch: sensing and feeling. *Neuron* 82, 737–755. doi: 10.1016/j.neuron.2014.05.001

Meissner, K., Fassler, M., Rucker, G., Kleijnen, J., Hrobjartsson, A., Schneider, A., et al. (2013). Differential effectiveness of placebo treatments: a systematic review of migraine prophylaxis. *JAMA Intern. Med.* 173, 1941–1951. doi: 10.1001/jamainternmed.2013.10391

Meissner, W., Weiss, T., Trippe, R. H., Hecht, H., Krapp, C., and Miltner, W. H. (2004). Acupuncture decreases somatosensory evoked potential amplitudes to noxious stimuli in anesthetized volunteers. *Anesth. Analg.* 98, 141–147. doi: 10.1213/01.ane.0000096191.07929.44

Melchart, D., Streng, A., Hoppe, A., Brinkhaus, B., Witt, C., Wagenpfeil, S., et al. (2005). Acupuncture in patients with tension-type headache: randomised controlled trial. *BMJ* 331, 376–382. doi: 10.1136/bmj.38512.405440.8f

Moffet, H. H. (2009). Sham acupuncture may be as efficacious as true acupuncture: a systematic review of clinical trials. *J. Altern. Comp. Med.* 15, 213–216. doi: 10.1089/acm.2008.0356

Molsberger, A. F., Boewing, G., Diener, H. C., Endres, H. G., Kraehmer, N., Kronfeld, K., et al. (2006a). Designing an acupuncture study: the nationwide, randomized, controlled, german acupuncture trials on migraine and tension-type headache. *J. Altern. Comp. Med.* 12, 237–245. doi: 10.1089/acm.2006.12.237

Molsberger, A. F., Streitberger, K., Kraemer, J., Brittinger, C. S., Witte, S., Boewing, G., et al. (2006b). Designing an acupuncture study: II. The nationwide, randomized, controlled German acupuncture trials on low-back pain and gonarthrosis. *J. Altern Comp. Med.* 12, 733–742. doi: 10.1089/acm.2006.12.733

Moore, A., and McQuay, H. (2005). Acupuncture: not just needles? *Lancet* 366, 100–101. doi: 10.1016/s0140-6736(05)66843-2

Musial, F., Choi, K. E., Gabriel, T., Ludtke, R., Rampp, T., Michalsen, A., et al. (2012). The effect of electroacupuncture and tramadol on experimental tourniquet pain. *Acupunct. Med.* 30, 21–26. doi: 10.1136/acupmed-2011-010094

Musial, F., and Weiss, T. (2014). The healing power of touch: the specificity of the 'unspecific' effects of massage. *Forsch Komplementmed* 21, 282–283. doi: 10.1159/000368449

Pariente, J., White, P., Frackowiak, R. S., and Lewith, G. (2005). Expectancy and belief modulate the neuronal substrates of pain treated by acupuncture. *Neuroimage* 25, 1161–1167. doi: 10.1016/j.neuroimage.2005.01.016

Park, J., White, A., Stevinson, C., Ernst, E., and James, M. (2002). Validating a new non-penetrating sham acupuncture device: two randomised controlled trials. *Acupunct. Med.* 20, 168–174. doi: 10.1136/aim.20.4.168

Petrovic, P., Kalso, E., Petersson, K. M., and Ingvar, M. (2002). Placebo and opioid analgesia– imaging a shared neuronal network. *Science* 295, 1737–1740. doi: 10.1126/science.1067176

Schafer, S. M., Geuter, S., and Wager, T. D. (2018). Mechanisms of placebo analgesia: a dual-process model informed by insights from cross-species comparisons. *Prog. Neurobiol.* 160, 101–122. doi: 10.1016/j.pneurobio.2017.10.008

Sprenger, C., Bingel, U., and Buchel, C. (2011). Treating pain with pain: supraspinal mechanisms of endogenous analgesia elicited by heterotopic noxious conditioning stimulation. *Pain* 152, 428–439. doi: 10.1016/j.pain.2010.11.018

Streitberger, K., and Kleinhenz, J. (1998). Introducing a placebo needle into acupuncture research. *Lancet* 352, 364–365. doi: 10.1016/s0140-6736(97)10471-8

Stux, G., Berman, B., and Pomeranz, B. (2003). *Basics of Acupuncture*. Berlin: Springer.

Theysohn, N., Choi, K. E., Gizewski, E. R., Wen, M., Rampp, T., Gasser, T., et al. (2014). Acupuncture-related modulation of pain-associated brain networks during electrical pain stimulation: a functional magnetic resonance imaging study. *J. Altern. Complement. Med.* 20, 893–900. doi: 10.1089/acm.2014.0105

Toroski, M., Nikfar, S., Mojahedian, M. M., and Ayati, M. H. (2018). Comparison of the cost-utility analysis of electroacupuncture and nonsteroidal

antiinflammatory drugs in the treatment of chronic low back pain. *J. Acupunct. Meridian Stud.* 11, 62–66. doi: 10.1016/j.jams.2018.01.003

Vickers, A. J., Cronin, A. M., Maschino, A. C., Lewith, G., MacPherson, H., Foster, N. E., et al. (2012). Acupuncture for chronic pain: individual patient data meta-analysis. *Arch. Intern. Med.* 172, 1444–1453. doi: 10.1001/archinternmed.2012.3654

Vickers, A. J., Cronin, A. M., Maschino, A. C., Lewith, G., Macpherson, H., Victor, N., et al. (2010). Individual patient data meta-analysis of acupuncture for chronic pain: protocol of the acupuncture trialists' collaboration. *Trials* 11:90.

Vickers, A. J., Vertosick, E. A., Lewith, G., MacPherson, H., Foster, N. E., Sherman, K. J., et al. (2017). acupuncture for chronic pain: update of an individual patient data meta-analysis. *J. Pain* 19, 455–474. doi: 10.1016/j.jpain.2017.11.005

Wager, T. D., and Atlas, L. Y. (2015). The neuroscience of placebo effects: connecting context, learning and health. *Nat. Rev. Neurosci.* 16, 403–418. doi: 10.1038/nrn3976

Wang, S. M., Kain, Z. N., and White, P. (2008). Acupuncture analgesia: i.the scientific basis. *Anesth Analg.* 106, 602–610. doi: 10.1213/01.ane.0000277493.42335.7b

Witt, C., Brinkhaus, B., Jena, S., Linde, K., Streng, A., Wagenpfeil, S., et al. (2005). Acupuncture in patients with osteoarthritis of the knee: a randomised trial. *Lancet* 366, 136–143.

Zhang, C. S., Tan, H. Y., Zhang, G. S., Zhang, A. L., Xue, C. C., and Xie, Y. M. (2015). Placebo devices as effective control methods in acupuncture clinical trials: a systematic review. *PLoS One* 10:e0140825. doi: 10.1371/journal.pone.0140825

Zhang, W. T., Jin, Z., Huang, J., Zhang, L., Zeng, Y. W., Luo, F., et al. (2003). Modulation of cold pain in human brain by electric acupoint stimulation: evidence from fMRI. *Neuroreport* 14, 1591–1596. doi: 10.1097/00001756-200308260-00010

Zhao, Z. Q. (2008). Neural mechanism underlying acupuncture analgesia. *Prog. Neurobiol.* 85, 355–375. doi: 10.1016/j.pneurobio.2008.05.004

Zubieta, J. K., Bueller, J. A., Jackson, L. R., Scott, D. J., Xu, Y., Koeppe, R. A., et al. (2005). Placebo effects mediated by endogenous opioid activity on mu-opioid receptors. *J. Neurosci.* 25, 7754–7762. doi: 10.1523/jneurosci.0439-05.2005

Zunhammer, M., Bingel, U., and Wager, T. D. (2018). Placebo effects on the neurologic pain signature: a meta-analysis of individual participant functional magnetic resonance imaging data. *JAMA Neurol.* 75, 1321–1330. doi: 10.1001/jamaneurol.2018.2017

Conflict of Interest: The author declares that the research was conducted in the absence of any commercial or financial relationships that could be construed as a potential conflict of interest.

frontiers in Neuroscience

ORIGINAL RESEARCH
published: 13 November 2019
doi: 10.3389/fnins.2019.01212

The Role of Tactile Stimulation for Expectation, Perceived Treatment Assignment and the Placebo Effect in an Experimental Nausea Paradigm

*Simone Aichner[1], Anja Haile[1], Verena Hoffmann[1], Elisabeth Olliges[1,2], Matthias H. Tschöp[3,4,5] and Karin Meissner[1,2]**

[1] Institute of Medical Psychology, Faculty of Medicine, LMU Munich, Munich, Germany, [2] Division of Health Promotion, Coburg University of Applied Sciences, Coburg, Germany, [3] Institute for Diabetes and Obesity, Helmholtz Diabetes Center, Helmholtz Zentrum München, Munich, Germany, [4] German Center for Diabetes Research (DZD), Munich, Germany, [5] Division of Metabolic Diseases, Department of Medicine, Technische Universität München, Munich, Germany

Introduction: Tactile stimulation during a placebo treatment could enhance its credibility and thereby boost positive treatment expectations and the placebo effect. This experimental study aimed to investigate the interplay between tactile stimulation, expectation, and treatment credibility for the placebo effect in nausea.

Methods: Ninety healthy participants were exposed to a 20-min vection stimulus on two separate days and were randomly allocated to one of three groups on the second day after the baseline period: Placebo transcutaneous electrical nerve stimulation (TENS) with tactile stimulation (n = 30), placebo TENS without tactile stimulation (n = 30), or no intervention (n = 30). Placebo TENS was performed for 20 min at a dummy acupuncture point on both forearms. Expected and perceived nausea severity and further symptoms of motion sickness were assessed at baseline and during the evaluation period. At the end of the experiment, participants in the placebo groups guessed whether they had received active or placebo treatment.

Results: Expected nausea decreased significantly more in the placebo groups as compared to the no treatment control group (interaction *day* × *group*, F = 6.60, p = 0.003, partial η^2 = 0.20), with equal reductions in the two placebo groups (p = 1.0). Reduced expectation went along with a significant placebo effect on nausea (interaction *day* × *group*, F = 22.2, $p < 0.001$, partial η^2 = 0.35) with no difference between the two placebo groups (p = 1.0). Twenty-three out of 29 participants in the tactile placebo group (79%) but only 14 out of 30 participants (47%) in the non-tactile placebo group believed that they had received the active intervention (p = 0.015). Bang's blinding index (BI) indicated random guessing in the non-tactile placebo group (BI = 0; 95% CI, −0.35 to 0.35) and non-random guessing in the direction of an "opposite guess" in the tactile placebo group (BI = −0.52; 95% CI, −0.81 to −0.22).

OPEN ACCESS

Edited by:
Younbyoung Chae,
Kyung Hee University, South Korea

Reviewed by:
Jose Pablo Ossandon,
Universität Hamburg, Germany
Yi-Hung Chen,
China Medical University, Taiwan

***Correspondence:**
Karin Meissner
karin.meissner@med.lmu.de

Specialty section:
This article was submitted to Perception Science, a section of the journal Frontiers in Neuroscience

Received: *12 February 2019*
Accepted: *28 October 2019*
Published: *13 November 2019*

Citation:
Aichner S, Haile A, Hoffmann V, Olliges E, Tschöp MH and Meissner K (2019) The Role of Tactile Stimulation for Expectation, Perceived Treatment Assignment and the Placebo Effect in an Experimental Nausea Paradigm. Front. Neurosci. 13:1212. doi: 10.3389/fnins.2019.01212

Conclusion: Tactile stimulation during placebo TENS did not further enhance positive treatment expectations and the placebo effect in nausea but increased the credibility of the intervention. Further trials should investigate the interaction between perceived treatment assignment, expectation, and the placebo effect during the course of a trial.

Keywords: placebo effect, expectation, nausea, motion sickness, tactile stimulation, acupuncture

INTRODUCTION

In randomized controlled trials (RCT), the specific effect of acupuncture compared with placebo acupuncture is usually small. An individual patient data meta-analysis with nearly 18.000 patients revealed standardized differences (SD) for the specific effect of acupuncture between 0.15 and 0.23 SD for various chronic pain conditions (Vickers et al., 2012). Compared to no treatment, however, the overall improvement after acupuncture is usually large (Linde et al., 2010a,b; Meissner et al., 2013). The small specific effect of acupuncture compared to the large overall effect indicates the involvement of "non-specific" factors, such as expectation and tactile stimulation, which contribute to the success of acupuncture treatment.

There is increasing evidence that positive treatment expectations influence the non-specific response to acupuncture treatment. In four large RCT of acupuncture, for example, patients with chronic pain conditions and high outcome expectations at baseline showed larger pain reduction at follow-up regardless of whether they were allocated to active acupuncture or placebo acupuncture (Linde et al., 2007). Research from the last decades clearly indicates that the effects of expectation, referred to as "placebo effects," are deeply rooted in our brains. Placebo effects in pain, for example, are accompanied by the activation of a specific pain modulating network that extends from cortical areas to the spinal cord (Geuter et al., 2017). Expectation can be formed via various mechanisms, including verbal suggestions and conditioning (Colloca and Miller, 2011). Also the non-verbal cues of a treatment, such as prizing, labeling, and dosing, can increase outcome expectations and thus the placebo effect (Meissner and Linde, 2018). Placebo effects have been demonstrated for various clinical conditions including nausea (Quinn and Colagiuri, 2014, 2016; Müller et al., 2016), depression and anxiety (Meyer et al., 2015; Peciña et al., 2015; Rutherford et al., 2016), Parkinson's disease (De la Fuente-Fernández et al., 2001; Benedetti et al., 2004; Lidstone et al., 2010), as well as for gastrointestinal and cardiovascular systems (Meissner, 2009, 2011; Meissner and Ziep, 2011; Meissner et al., 2011; Ronel et al., 2011; Meissner, 2014; Rief et al., 2017) and immune responses (Hadamitzky et al., 2018).

In addition to positive expectations, skin penetration during needling appears to contribute to the non-specific effects of acupuncture. A re-analysis of the individual patient data meta-analysis by Vickers et al. (2012) revealed a considerably smaller specific effect of acupuncture in RCTs with control groups using skin penetrating needles (SD acupuncture vs. control 0.17, 95% CI 0.11–0.23; $n = 9$) compared to control groups using non-penetrating needles (SD acupuncture vs. control 0.43, 95% CI 0.01–0.85; $n = 4$) (MacPherson et al., 2014). An update of the individual patient data meta-analysis by Vickers et al. (2018) further confirmed this finding, with smaller effects sizes for sham controlled trials that used a penetrating needle in the sham groups compared to trials that used non-penetrating or non-needle sham (difference in SD −0.30, 95% CI −0.60, −0.00, $p = 0.047$). The authors argue that this difference could be either due to the unblinding of patients in the control groups with non-penetrating needles, or to the physiologic effects of skin-penetrating placebo needles, which may have still some therapeutic activity against pain. They argue further that the possibility of unblinding is unlikely, since non-penetrating needles, such as the Streitberger needle, have been confirmed as credible placebos (MacPherson et al., 2014).

However, an imbalance due to differences in blinding could still occur: Patients receiving penetrating needles may be more prone to believe that they have received true acupuncture than patients receiving non-penetrating needles. An "opposite guess" – that is, a higher probability to guess "active treatment" than would be expected by chance (Bang et al., 2010) – could strengthen the outcome expectations of patients in the control groups of RCTs and thereby enhance the placebo effect. First support for this notion comes from experimental placebo studies, showing that "active" placebos that mimic the side effects of pharmacological drugs were more effective in reducing pain than placebos without such side effects (Bjorkedal and Flaten, 2011; Rief and Glombiewski, 2012).

To better understand the role of tactile stimulation, expectation, and perceived treatment assignment for the overall response to acupuncture point stimulation, we conducted a placebo study using an established experimental nausea design (Gianaros et al., 2001; Levine et al., 2006). We recently showed that a placebo transcutaneous electrical nerve stimulation (TENS) stimulation at a dummy point, which elicited slight tactile stimulation, induced a large placebo effect on experimentally induced nausea in comparison to a no-treatment control condition in female participants (Müller et al., 2016). In the present study, we focused on the role of tactile stimulation for the size of the placebo effect and included a second placebo group without tactile stimulation by the TENS device. We hypothesized that tactile stimulation during the placebo intervention would enhance the placebo effect in nausea due to the development of higher outcome expectations. With regard to blinding effectiveness, we expected that the tactile stimulation would lead more participants to believe that they had received the active treatment ("opposite guess") as compared to the placebo TENS intervention without tactile stimulation, for which we expected a "random guess" (Bang et al., 2010).

MATERIALS AND METHODS

Participants

Healthy adult participants between 18 and 50 years with a history of motion sickness [score ≥80 in Motion Sickness Susceptibility Questionnaire (MSSQ); Golding, 1998] were recruited. Further inclusion criteria were normal or corrected-to-normal vision and hearing, right-handedness, and normal weight (BMI 18–25 kg/m^2). Exclusion criteria comprised implanted devices (e.g., pacemaker, insulin pump) or metal implants, a history of diseases of the inner ear (e.g., Morbus Menière, acute hearing loss), blood-clotting disorders or a tendency for thromboembolic diseases, and the presence of skin disease, diabetes, cardiovascular disease, epilepsy, or cancer. Further exclusion criteria comprised surgery during the past 4 weeks, current pregnancy or breast feeding, alcohol or drug abuse, inability to imply with the specific instructions, the regular intake of drugs except of hormonal contraceptives, thyroid hormones, and anti-allergic drugs, and anxiety and/or depression scores above the clinically relevant cut-off, as assessed with the Hospital Anxiety and Depression Scale (Zigmond and Snaith, 1983). Participants, who fulfilled all inclusion criteria and none of the exclusion criteria, were invited to participate in a 20-min screening session, during which their susceptibility for the visual vection stimulus was tested. Participants, who developed at least moderate nausea (≥"5" on a 11-point NRS, with "0" indicating "no nausea" and "10" indicating "maximal tolerable nausea"), were invited to participate in the core experiment.

The study protocol was approved by the ethical committee of the Medical Faculty at Ludwig Maximilian University of Munich and was registered retrospectively at the German Clinical Trials Register (no. DRKS00015192). All participants provided written informed consent.

Study Design

The experiment consisted of a baseline session (day 1) and a testing session (day 2) on two separate days at least 24 h apart. On day 2 after the resting period, participants were randomly allocated to one of four treatment arms: placebo intervention with somatosensory stimulation (n = 30), placebo intervention without somatosensory stimulation (n = 30), no treatment (n = 30), or active treatment (n = 10; results not reported). The active treatment arm was implemented to avoid deceptive administration of the placebo treatment. All groups were stratified by sex (50% women, 50% men).

Experimental Procedure

Participants were tested on two separate days at least 24 h apart (median, 7 days) at the same daytime between 2:00 to 7:00 pm and were instructed to fast at least 3 h before the experiment. Nausea was induced through a standardized visual presentation of alternating black and white stripes with circular motion at 60°, which induces a circular vection sensation (Napadow et al., 2012). The visual stimulus was projected onto a semicylindrical and semitransparent screen placed around the volunteer at a distance of 30 cm to the eyes. Participants were asked to keep their eyes open and look straight ahead without fixating the stripes.

On both testing days upon arrival in the laboratory, participants were seated in a recliner and asked to fill out several questionnaires. Electrodes for psychophysiological assessments were placed, and an indwelling catheter was fixed at the forearm to allow for repeated blood drawings (results of physiological parameters will be reported elsewhere). On day 1, the session started with a 10-min baseline period, followed by a 10-min resting period and a 20-min presentation of the visual vection stimulus. The session ended with a 15 min resting period. On day 2 after the 10-min baseline period, participants were randomized to one of the experimental groups. The experimenter opened the first randomization envelope and delivered standardized information according to group allocation ("treatment" or "no treatment"). Then a medical assistant opened the second randomization envelope, placed the TENS electrodes according to group allocation and started the TENS device for 20 min, if applicable. After 10 min the visual stimulus was presented for 20 min. The experiment ended with a 15-min resting period. For security reasons, the vection stimulus was stopped on both testing days, if nausea ratings indicated severe nausea (ratings of 9 or 10 on 11-point NRS). **Table 1** summarizes the time course of the experiment as well as the different times of symptom assessment.

Interventions

Supplementary Table S1 shows the main characteristics of the interventions and the content of the verbal suggestions for each of the three study groups. In short, participants in the treatment groups were informed that the nausea treatment would consist of either an active treatment or a placebo treatment and that the active treatment would reduce nausea by electrical stimulation of an acupuncture point, while the placebo treatment would

TABLE 1 | Timeline of the experiment on day 1 and day 2 and time points of behavioral assessments.

		Randomization			
	Baseline	**Rest 1**	**Nausea 1**	**Nausea 2**	**Rest 2**
Minute	**1–10**	**11–20**	**21–30**	**31–40**	**41–55**
Visual stimulation (20 min)			ON	ON	
(Placebo) TENS intervention (20 min)		ON[a]	ON[a]		
Perceived nausea (NRS)	X[b]			X[c]	
Perceived dizziness (NRS)	X[b]			X[c]	
SSMS Questionnaire (score)	X[b]			X[c]	
Expected nausea (NRS)		X[d]			
Treatment guess (Verum/Placebo)					X[b]
Perceived treatment efficacy (NRS)					X[b]

NRS, 11-point numeric rating scale; SSMS, Subjective Symptoms of Motion Sickness. [a]Only day 2, according to group allocation. [b]Last minute. [c]Every minute (ratings were averaged prior to analysis). [d]Immediately after verbal suggestions and applying/testing the TENS device, if applicable.

consist of a placebo acupoint stimulation. Subjects were further informed that the best effects were to be expected when the treatment is begun before exposure to the nauseogenic stimulus (Ezzo et al., 2006). Participants in the no-treatment control group were informed about the rationale and value of a no-treatment control group.

All interventions were conducted using a programmable TENS device (Digital EMS/TENS unit SEM 42, Sanitas, Uttenweiler, Germany). In the placebo groups, two electrodes were attached proximal and distal to a generally accepted dummy point in the context of acupuncture research located on the ulnar side of both forearms (Witt et al., 2012). In the placebo group with somatosensory stimulation ("tactile placebo"), the superficial massage program of the TENS device was turned on for 20 min in order to induce a slight tingling sensation at the electrode site. In the placebo group without somatosensory stimulation ("non-tactile placebo"), electrodes were connected to the TENS device but the device was only allegedly turned on. The active treatment group received real TENS at the acupoint "PC6" (Lee and Fan, 2009) on both forearms for 20 min.

Randomization and Blinding

Random allocation was accomplished using sealed and numbered envelopes. A person not directly involved in the experiments prepared the randomization envelopes based on a computer-derived randomization list. The interventions were performed in a single-blind design. Participants in the no-treatment control group were necessarily unblinded.

Ratings and Questionnaires

Expected nausea intensity was rated on 11-point NRS, with "0" indicating "no expected nausea" and "10" indicating "maximal tolerable expected nausea." Perceived nausea and dizziness intensities were rated at baseline and every minute during the nausea period on 11-point NRSs, with "0" indicating "no nausea/dizziness" and "10" indicating "maximal tolerable nausea/dizziness." Symptoms of motion sickness were assessed using the "Subjective Symptoms of Motion Sickness" (SSMS) questionnaire (adapted from Graybiel et al., 1968), with scores of 0–3 assigned to responses of none, slight, moderate, and severe for symptoms of dizziness, headache, nausea/urge to vomit, tiredness, sweating, and stomach awareness, respectively. At the end of day 2, participants in the treatment groups were asked to guess whether they had received active or placebo treatment as well as to rate the perceived effectiveness of treatment on an 11-point NRS, with "0" indicating "not effective at all" and "10" indicating "highly effective." They were furthermore asked to rate on 11-point NRS, how sure they were about their treatment guesses, with "0" indicating "not sure at all" and "10" indicating "very sure." Bang's blinding index (BI) was used to estimate the proportion of participants who guess their treatment incorrectly beyond chance level. Random guess exists if the BI's confidence interval covers 0 (Bang et al., 2010).

Statistical Analyses

Sample size calculation was performed for baseline-adjusted nausea scores. Assuming a medium effect size partial eta-squared of 0.13 for the difference in baseline-adjusted nausea scores between the tactile and the non-tactile placebo group, 28 subjects per group would be needed to give 80% power to detect a significant difference (with a type 1 error of 5%) (calculated by G*Power Version 3.1.7). We increased the sample size to 30 per group to compensate for possible attrition rates. Statistical analyses were performed with SPSS statistics software (version 24, IBM).

Prior to the analyses, nausea and dizziness ratings were averaged for the evaluation period, which comprised minutes 11 to 20 of visual nausea induction. A period without placebo-TENS intervention was chosen in order to avoid distraction effects by tactile stimulation. Expected nausea as well as nausea, dizziness, and the SSMS sum score were subjected to separate 2 × 3 × 2 mixed-design analyses of variance (ANOVA), with day (day 1: baseline, day 2: intervention) as the within-subject factor and group (placebo TENS with tactile stimulation, placebo TENS without tactile stimulation, no treatment) and sex (male, female) as between-subject factors. Significant effects were followed-up by Bonferroni-corrected *post hoc* tests. For all statistical tests, a p-value of ≤ 0.05 (two-tailed) was considered statistically significant.

RESULTS

Sample

The flow of study participants is shown in **Figure 1**. In total, 494 volunteers were assessed for eligibility and 245 were invited to participate in the screening session to assess their susceptibility for the visual vection stimulus. 104 volunteers were included in the study, four of whom were excluded before randomization on Day 2. Hundred participants were randomized and completed the experiment. Analyses were based on the data from 90 participants assigned to placebo treatment or no treatment [45 males, 45 females; age ($M \pm SD$), 23.5 ± 3.2 years]. The experimental groups were comparable with regard to sociodemographic, physical and psychological characteristics (**Table 2**).

Nausea Expectation

The 2 × 3 × 2 mixed-design ANOVA indicated differential changes of expected nausea from day 1 to day 2 in the experimental groups (interaction *day* × *group*, $F = 6.60$, $p = 0.003$, partial $\eta^2 = 0.20$) without a difference between male and female participants (interaction *day* × *group* × *sex*, $F = 1.8$, $p = 0.564$, partial $\eta^2 = 0.02$). *Post hoc* tests indicated significantly lower levels of expected nausea in both placebo groups in comparison to the no treatment group (Bonferroni-corrected p-values 0.002 and 0.021 vs. no treatment for the tactile and the non-tactile placebo groups, respectively). The decrease in expected nausea did not differ between the tactile and the non-tactile placebo groups ($p = 1.0$) (**Table 3**).

Nausea and Dizziness

The 2 × 3 × 2 mixed-design ANOVA for baseline-adjusted nausea scores indicated a significant group-by-day interaction

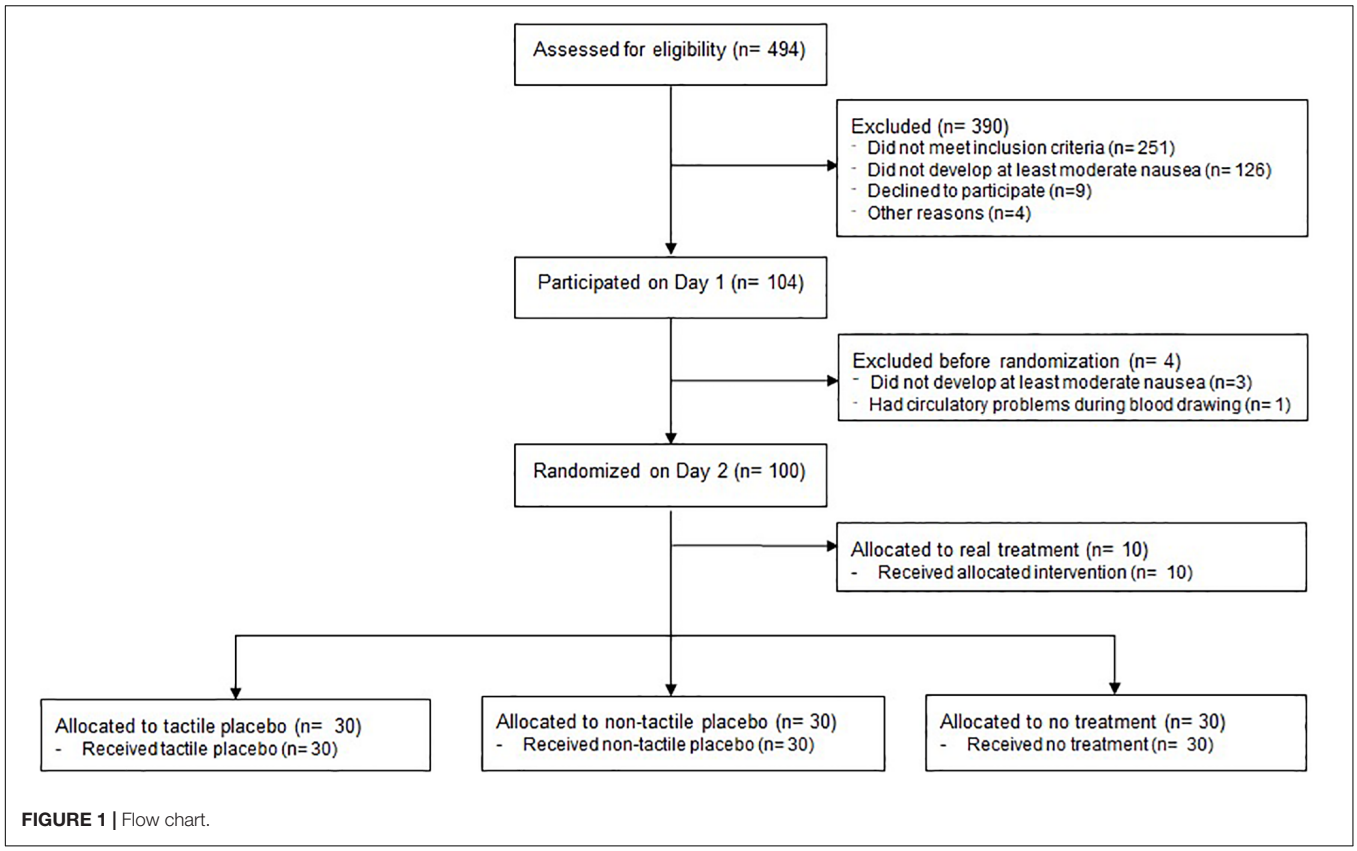

FIGURE 1 | Flow chart.

TABLE 2 | Sample characteristics at baseline.

	No treatment (*n* = 30)	Non-tactile placebo (*n* = 30)	Tactile placebo (*n* = 30)	*p**
Sex, *m/f*	15/15	15/15	15/15	1
Age, mean (*SD*)	23.5 (2.7)	23.8 (3.8)	23.1 (3.0)	0.69
Education (≥high school degree), *n* (%)	27 (90)	30 (100)	29 (97)	0.59
Non-smoker, *n* (%)	26	27	26	0.90
Body mass index	22.3 (2.7)	21.9 (2.2)	21.2 (2.0)	0.31
MSSQ, mean (*SD*)	130.3 (38.4)	139.8 (42.3)	134.5 (37.9)	0.65
HADS-anxiety, mean (*SD*)	4.0 (2.6)	3.8 (2.2)	4.2 (2.2)	0.75
HADS-depression, mean (*SD*)	1.4 (1.6)	1.5 (1.8)	2.0 (1.5)	0.10
STAI-trait anxiety, mean (*SD*)	38.8 (6.4)	38.1 (6.7)	37.4 (6.3)	0.61
PSQ-Stress, mean (*SD*)	31.1 (14.3)	30.9 (19.4)	28.7 (12.1)	0.81

*MSSQ, Motion Sickness Susceptibility Questionnaire; HADS, Hospital Anxiety and Depression Scale; STAI, State-Trait Anxiety Inventory; PSQ, Perceived Stress Questionnaire. *Results of χ^2 tests, Kruskal–Wallis tests, or univariate ANOVA, as appropriate.*

(F = 22.2, $p < 0.001$, partial η^2 = 0.35) with no evident sex difference (interaction *day* × *group* × *sex*, F = 1.0, p = 0.390, partial η^2 = 0.02). The decrease in baseline-adjusted nausea scores from day 1 to day 2 was significantly larger in the placebo groups as compared to the no treatment group, confirming the occurrence of a placebo effect in nausea (both Bonferroni-corrected p's < 0.001). The placebo effect did not differ between the two placebo groups (p = 1.0) (**Table 3**; **Figure 2**).

The 2 × 3 × 2 mixed-model ANOVA for baseline-adjusted dizziness scores likewise revealed a significant group-by-day interaction (F = 14.2, $p < 0.001$, partial η^2 = 0.25), without a difference between male and female participants (interaction *day* × *group* × *sex*, F = 1.7, p = 0.190, partial η^2 = 0.04). Significantly larger decreases of baseline-adjusted dizziness scores were observed in both placebo groups in comparison to the no treatment group (both Bonferroni-corrected p's < 0.001), while no differences between the two placebo groups occurred (p = 1.0) (**Table 3**).

Subjective Symptoms of Motion Sickness

The 2 × 3 × 2 mixed-design ANOVA for sum scores in the baseline-adjusted SSMS scores revealed a significant

TABLE 3 | Expected and perceived symptoms (day 1, day 2, and changes) in each experimental group.

	No treatment (n = 30)	Non-tactile placebo (n = 30)	Tactile placebo (n = 30)
Nausea expectation (NRS 0–10)			
Control day, mean (*SD*)	6.8 (2.2)	7.6 (1.3)	7.6 (1.0)
Intervention day, mean (*SD*)	7.0 (1.1)	5.6 (1.9)	5.2 (2.4)
Mean change (95% CI)	0.3 (−1.0; 1.6)	−2.1 (−3.3; −1.0)*	−2.8 (−4.0; −1.5)**
Baseline-adjusted nausea score (NRS 0–10)			
Control day, mean (*SD*)	5.6 (1.5)	6.0 (1.6)	5.2 (2.0)
Intervention day, mean (*SD*)	4.8 (1.8)	2.7 (2.1)	2.0 (2.0)
Mean change (95% CI)	−0.8 (−1.4; −0.2)	−3.2 (−3.9; −2.6)***	−3.2 (−3.8; −2.6)***
Baseline-adjusted dizziness score (NRS 0–10)			
Control day, mean (*SD*)	5.8 (1.8)	5.7 (1.9)	4.9 (1.8)
Intervention day, mean (*SD*)	5.1 (2.2)	3.1 (2.2)	2.4 (1.7)
Mean change (95% CI)	−0.7 (−1.2; −0.1)	−2.6 (−3.1; −1.9)***	−2.5 (−3.1; −1.9)***
Baseline-adjusted SSMS score (0–18)			
Control day, mean (*SD*)	6.9 (2.7)	6.6 (3.4)	5.8 (2.6)
Intervention day, mean (*SD*)	6.4 (2.6)	4.1 (2.2)	3.3 (2.2)
Mean change (95% CI)	−0.5 (−1.4; 0.4)	−2.5 (−3.7; −1.4)*	−2.5 (−3.5; −1.51)*

*NRS, numeric rating scale (0–10), average of 11 individual NRS ratings assessed during the target period on the control and intervention days; SSMS, Subjective Symptoms of Motion Sickness Questionnaire. *$p < 0.05$ (vs. no treatment, Bonferroni-corrected). **$p < 0.01$ (vs. no treatment, Bonferroni-corrected). ***$p < 0.001$ (vs. no treatment, Bonferroni-corrected).*

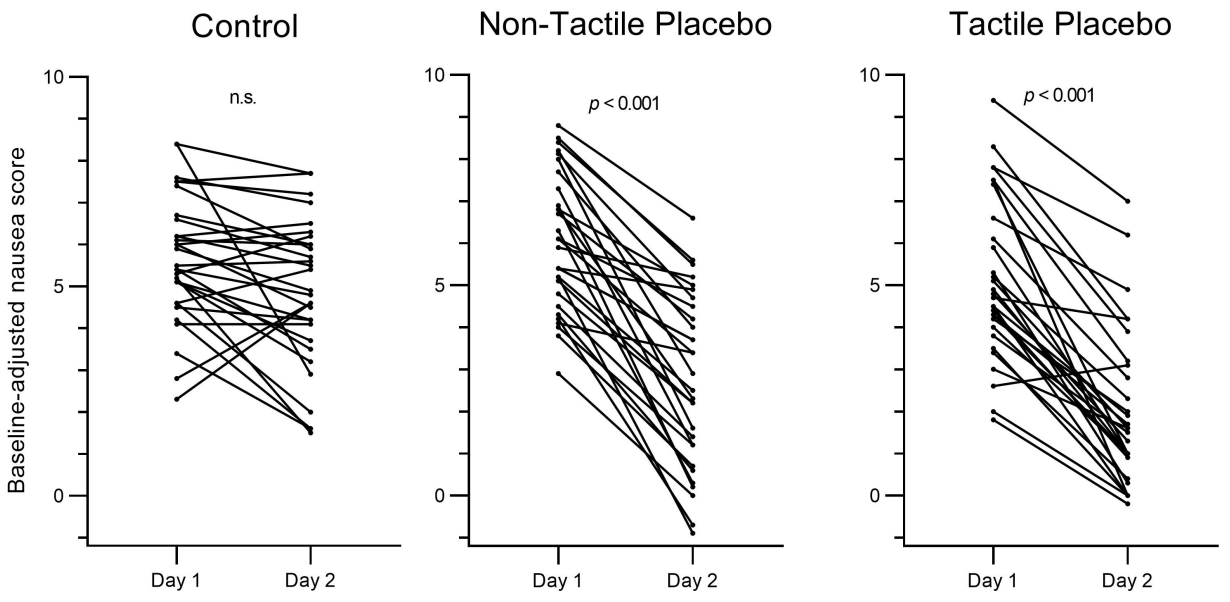

FIGURE 2 | Individual changes in baseline-adjusted nausea score from day 1 (control) to day 2 (intervention) in the control group, the non-tactile placebo group, and the tactile placebo group. Nausea was assessed on 11-point numeric rating scales.

group-by-day interaction (F = 7.9, p = 0.001, partial η^2 = 0.16), comparable in size for male and female participants (interaction *day* × *group* × *sex*, F = 1.1, p = 0.333, partial η^2 = 0.03). Bonferroni-corrected *post hoc* t-tests indicated significantly larger decreases of baseline-adjusted SSMS scores in both placebo groups in comparison to the untreated control group (p = 0.012 and 0.014 vs. untreated controls for the tactile and non-tactile placebo groups, respectively). Again, changes in baseline-adjusted SSMS scores did not differ between the two placebo groups (p = 1.0) (**Table 3**).

Perceived Treatment Effectiveness and Treatment Guesses in the Placebo Groups

Twenty-three out of 29 participants in the tactile placebo group (79%) believed that they had received the active intervention as compared to 14 out of 30 participants (47%) in the non-tactile placebo group, the difference was significant (χ^2 = 6.72, p = 0.015). Participants in the two placebo groups were equally sure about their treatment guesses (non-tactile placebo, 5.3 ± 2.6

(*mean* ± *SD*); tactile placebo: 5.9 ± 2.4; $Z = -1.12$, $p = 0.363$). Explorative analyses revealed no relationship between changes in baseline-adjusted nausea scores from day 1 to day 2 and treatment guess (guess "placebo," −3.0 ± 1.9; guess "verum," −3.5 ± 1.5; $F = 1.0$, $p = 0.313$).

At the end of the experiment, participants in the tactile placebo group rated the treatment as significantly more effective than did participants in the non-tactile placebo group (*mean* ± *SD*, 6.9 ± 2.2 vs. 5.7 ± 2.5; $Z = -1.99$, $p = 0.046$). At the same time, larger reductions in baseline-adjusted nausea scores from day 1 to day 2 correlated with higher effectiveness ratings in both placebo groups (non-tactile placebo, $r_s = -0.446$, $p = 0.013$; tactile placebo, $r_s = -0.402$, $p = 0.027$). An exploratory regression analysis on perceived treatment effectiveness with the factors "type of placebo" and "reduction in baseline-adjusted nausea" included as independent variables revealed that both factors contributed significantly to subjective effectiveness ($F = 7.2$, $p = 0.001$; type of placebo, $\beta = 0.257$, $p = 0.034$; reduction in baseline-adjusted nausea, $\beta = -0.377$, $p = 0.002$). These results suggest that ratings of perceived effectiveness are driven by both, perceived improvement and sensory characteristics of the placebo intervention.

Bang's Blinding Index in the Two Placebo Groups

Bang's BI in the non-tactile placebo group was 0 (95% CI, −0.35 to 0.35), indicating random guessing (**Table 4**). In the tactile placebo group Bang's BI was −0.52 (95% CI, −0.81 to −0.22), indicating non-random guessing in the direction of an "opposite guess," that is, the probability to guess "active treatment" was significantly higher than would be expected by chance.

DISCUSSION

In this randomized controlled placebo study, we aimed to vary the credibility of two placebo interventions by combining, or not combining it with tactile stimulation elicited by a TENS device. We hypothesized that 20 min of tactile stimulation would increase positive outcome expectations and thus the placebo effect. Results confirmed a large effect of the tactile stimulation by TENS on the credibility of the placebo treatment: Significantly more participants in the tactile placebo group believed that they had received the active intervention as compared to the non-tactile placebo group. In addition, the tactile placebo intervention was perceived as more effective. Neither expectations nor the placebo effect, however, differed between the two placebo groups.

TABLE 4 | Bang's blinding index for the non-tactile and tactile placebo groups.

Assignment	Guess, *n*			
	Active treatment	Placebo treatment	Don't know*	Total
Non-tactile placebo	14 (47%)	14 (47%)	2 (7%)	30
Tactile placebo	21 (72%)	6 (21%)	2 (7%)	29
Total	35	20	4	59

**Two participants in each placebo group indicated that they were "not sure at all" (NRS = "0") about their treatment guess and were re-assigned to category "don't know."*

The placebo effect as the difference between the placebo groups and the no-treatment control group was consistent for different outcome parameters and effect sizes were generally large (partial η^2, 0.16–0.35; Richardson, 2011). Results thus confirm the findings of our pilot study that placebo TENS induces a large placebo effect in experimentally induced nausea (Müller et al., 2016) and further extend them to male volunteers and to a placebo TENS intervention without tactile stimulation. The medical environment, in which the experiment took place – with many factors present that are known to boost placebo effects, such as a room full of sophisticated electrical equipment as well as prolonged interaction with the experimenters (Burke et al., 2019) – may have contributed to this large placebo effect.

As hypothesized, somatosensory stimulation during the placebo intervention increased blinding effectiveness: Bang's BI indicated random guessing in the non-tactile placebo group but non-random guessing in the direction of an opposite guess in the tactile placebo group. Our results thus lend support to the view that somatosensory stimulation during acupuncture point stimulation challenges the goal of patient blinding by enhancing the chance for a non-random guess. Given that most placebo acupuncture procedures are associated with random-guesses (Zhang et al., 2015), this discrepancy could result in a problematic blinding scenario with enhanced expectations and placebo effects in the true acupuncture groups (Bang et al., 2010; Chae et al., 2018). Contrary to our expectations, however, tactile stimulation by the TENS device during the placebo intervention did neither enhance outcome expectations nor the placebo effect during the evaluation period. Possibly, participants with opposite treatment guesses after the first placebo application may develop higher treatment expectations only with respect to subsequent placebo interventions. In a recent RCT in depression, for example, perceived treatment assignment affected symptom improvement only in the second half of the trial (Laferton et al., 2018). Furthermore, a large RCT in patients with chronic arm pain found no evidence that sham acupuncture was associated with an enhanced placebo effect during the 2 week placebo run-in period; however, sham acupuncture was significantly more effective than placebo pills during the further 6 weeks of the trial (Kaptchuk et al., 2006). Future studies are warranted to disentangle the putative interaction between expectation, perceived treatment assignment, and the placebo effect during the course of a trial.

Several possible limitations have to be considered. The medical setting of our experiment may have resulted in a ceiling effect, thereby preventing further enhancement of the placebo effect by tactile stimulation. Most acupuncture trials, however, are performed in comparable medical settings, emphasizing the external validity of our results. Furthermore, the gentle touch when placing the electrodes of the TENS device at the participants' skin could have initiated physiological responses by activating unmyelinated C tactile fibers in the body, resulting in feelings of calm and well-being as well as lower heart rate and blood pressure (Campbell, 2006; Kang et al., 2011;

Chae et al., 2018). Such physiological effects may have contributed to the improvement in the placebo groups independently from expectation. However, also the participants in the untreated control group received a variety of skin electrodes to measure the EEG, the EKG and the electrogastrogram and were provided with an indwelling catheter for repeated blood drawings during the experiment. Therefore, the gentle touch when placing the TENS electrodes was not unique to the placebo groups and the only difference between placebo and no treatment groups was the therapeutic meaning of placing the TENS electrodes. Finally, placing the TENS electrodes in the non-tactile placebo group also involved some amount of tactile stimulation and may thereby have enhanced the placebo effect. Compared with 20 min of somatosensory stimulation stimulation in the tactile TENS placebo group, however, somatosensory stimulation in the non-tactile TENS placebo group was considered to be only minor. The differential pattern of treatment guesses in the two placebo groups further supports the conceptual difference between the two placebo interventions.

CONCLUSION

Electrical stimulation during a placebo TENS intervention did not enhance the placebo effect in nausea but increased the credibility of the treatment. Further experimental trials are needed to investigate the putative interaction between perceived treatment assignment, expectation, and the placebo effect during the course of a trial.

DATA AVAILABILITY STATEMENT

The datasets generated for this study are available on request to the corresponding author.

ETHICS STATEMENT

All subjects gave written informed consent in accordance with the Declaration of Helsinki. The protocol was approved by the Ethics Committee of the Medical Faculty (LMU Munich) and was registered at the German Clinical Trials Register (no. DRKS00015192).

AUTHOR CONTRIBUTIONS

KM and MT designed the study. SA, AH, and VH conducted the experiment. KM, SA, and EO analyzed and interpreted the data. KM and SA drafted the manuscript. All authors revised the manuscript for critical intellectual content and approved the final version.

FUNDING

The study was supported by a research grant (ME-3675/1-1) from the German Research Foundation [Deutsche Forschungsgemeinschaft, DFG (FOR 1328)]. KM received additional financial support from the Theophrastus Foundation (Germany), and the Schweizer-Arau-Foundation (Germany). The funders had no role in study design, data collection or analysis, decision to publish, or in writing this manuscript.

SUPPLEMENTARY MATERIAL

The Supplementary Material for this article can be found online at: https://www.frontiersin.org/articles/10.3389/fnins.2019.01212/full#supplementary-material

REFERENCES

Bang, H., Flaherty, S. P., Kolahi, J., and Park, J. (2010). Blinding assessment in clinical trials: a review of statistical methods and a proposal of blinding assessment protocol. *Clin. Res. Regul. Aff.* 27, 42–51. doi: 10.3109/10601331003777444

Benedetti, F., Colloca, L., Torre, E., Lanotte, M., Melcarne, A., Pesare, M., et al. (2004). Placebo-responsive Parkinson patients show decreased activity in single neurons of subthalamic nucleus. *Nat. Neurosci.* 7:587. doi: 10.1038/nn1250

Bjorkedal, E., and Flaten, M. A. (2011). Interaction between expectancies and drug effects: an experimental investigation of placebo analgesia with caffeine as an active placebo. *Psychopharmacology* 215, 537–548. doi: 10.1007/s00213-011-2233-4

Burke, M. J., Kaptchuk, T. J., and Pascual-Leone, A. (2019). Challenges of differential placebo effects in contemporary medicine: the example of brain stimulation. *Ann. Neurol.* 85, 12–20. doi: 10.1002/ana.25387

Campbell, A. (2006). Role of C tactile fibres in touch and emotion–clinical and research relevance to acupuncture. *Acupunct. Med.* 24, 169–171. doi: 10.1136/aim.24.4.169

Chae, Y., Lee, Y.-S., and Enck, P. (2018). How placebo needles differ from placebo pills? *Front. Psychiatr.* 9:243. doi: 10.3389/fpsyt.2018.00243

Colloca, L., and Miller, F. G. (2011). How placebo responses are formed: a learning perspective. *Philos. Trans. R. Soc. Lond. B Biol. Sci.* 366, 1859–1869. doi: 10.1098/rstb.2010.0398

De la Fuente-Fernández, R., Ruth, T. J., Sossi, V., Schulzer, M., Calne, D. B., and Stoessl, A. J. (2001). Expectation and dopamine release: mechanism of the placebo effect in Parkinson's disease. *Science* 293, 1164–1166. doi: 10.1126/science.1060937

Ezzo, J. M., Richardson, M. A., Vickers, A., Allen, C., Dibble, S. L., Issell, B. F., et al. (2006). Acupuncture-point stimulation for chemotherapy-induced nausea or vomiting. *Cochrane Database Syst. Rev.* 2:CD002285. doi: 10.1002/14651858.CD002285.pub2

Geuter, S., Koban, L., and Wager, T. D. (2017). The cognitive neuroscience of placebo effects: concepts, predictions, and physiology. *Ann. Rev. Neurosci.* 40, 167–188. doi: 10.1146/annurev-neuro-072116-031132

Gianaros, P. J., Stern, R. M., Morrow, G. R., and Hickok, J. T. (2001). Relationship of gastric myoelectrical and cardiac parasympathetic activity to chemotherapy-induced nausea. *J. Psychosom. Res.* 50, 263–266. doi: 10.1016/s0022-3999(01)00201-x

Golding, J. F. (1998). Motion sickness susceptibility questionnaire revised and its relationship to other forms of sickness. *Brain Res. Bull.* 47, 507–516. doi: 10.1016/s0361-9230(98)00091-4

Graybiel, A., Wood, C. D., Miller, E. F., and Cramer, D. B. (1968). Diagnostic criteria for grading the severity of acute motion sickness. *Aerosp. Med.* 39, 453–455.

Hadamitzky, M., Sondermann, W., Benson, S., and Schedlowski, M. (2018). Placebo effects in the immune system. *Int. Rev. Neurobiol.* 138, 39–59. doi: 10.1016/bs.irn.2018.01.001

Kang, O. S., Chang, D. S., Lee, M. H., Lee, H., Park, H. J., and Chae, Y. (2011). Autonomic and subjective responses to real and sham acupuncture stimulation. *Auton. Neurosci.* 159, 127–130. doi: 10.1016/j.autneu.2010.07.027

Kaptchuk, T. J., Stason, W. B., Davis, R. B., Legedza, A. R., Schnyer, R. N., Kerr, C. E., et al. (2006). Sham device v inert pill: randomised controlled trial of two placebo treatments. *BMJ* 332, 391–397. doi: 10.1136/bmj.38726.603310.55

Laferton, J. A. C., Vijapura, S., Baer, L., Clain, A. J., Cooper, A., Papakostas, G., et al. (2018). Mechanisms of perceived treatment assignment and subsequent expectancy effects in a double blind placebo controlled RCT of major depression. *Front. Psychiatr.* 9:424. doi: 10.3389/fpsyt.2018.00424

Lee, A., and Fan, L. T. (2009). Stimulation of the wrist acupuncture point P6 for preventing postoperative nausea and vomiting. *Cochrane Database Syst. Rev.* 2:CD003281. doi: 10.1002/14651858.CD003281.pub3

Levine, M. E., Stern, R. M., and Koch, K. L. (2006). The effects of manipulating expectations through placebo and nocebo administration on gastric tachyarrhythmia and motion-induced nausea. *Psychosom. Med.* 68, 478–486. doi: 10.1097/01.psy.0000221377.52036.50

Lidstone, S. C., Schulzer, M., Dinelle, K., Mak, E., Sossi, V., Ruth, T. J., et al. (2010). Effects of expectation on placebo-induced dopamine release in Parkinson disease. *Arch. Gen. Psychiatr.* 67, 857–865. doi: 10.1001/archgenpsychiatry.2010.88

Linde, K., Niemann, K., and Meissner, K. (2010a). Are sham acupuncture interventions more effective than (other) placebos? A re-analysis of data from the cochrane review on placebo effects. *Forsch. Komplementmed.* 17, 259–264. doi: 10.1159/000320374

Linde, K., Niemann, K., Schneider, A., and Meissner, K. (2010b). How large are the nonspecific effects of acupuncture? A meta-analysis of randomized controlled trials. *BMC Med.* 8:75. doi: 10.1186/1741-7015-8-75

Linde, K., Witt, C. M., Streng, A., Weidenhammer, W., Wagenpfeil, S., Brinkhaus, B., et al. (2007). The impact of patient expectations on outcomes in four randomized controlled trials of acupuncture in patients with chronic pain. *Pain* 128, 264–271. doi: 10.1016/j.pain.2006.12.006

MacPherson, H., Vertosick, E., Lewith, G., Linde, K., Sherman, K. J., Witt, C. M., et al. (2014). Influence of control group on effect size in trials of acupuncture for chronic pain: a secondary analysis of an individual patient data meta-analysis. *PLoS One* 9:e93739. doi: 10.1371/journal.pone.0093739

Meissner, K. (2009). Effects of placebo interventions on gastric motility and general autonomic activity. *J. Psychosom. Res.* 66, 391–398. doi: 10.1016/j.jpsychores.2008.09.004

Meissner, K. (2011). The placebo effect and the autonomic nervous system: evidence for an intimate relationship. *Philos. Trans. R. Soc. Lond. B Biol. Sci.* 366, 1808–1817. doi: 10.1098/rstb.2010.0403

Meissner, K. (2014). Placebo responses on cardiovascular, gastrointestinal, and respiratory organ functions. *Handb. Exp. Pharmacol.* 225, 183–203. doi: 10.1007/978-3-662-44519-8-11

Meissner, K., Bingel, U., Colloca, L., Wager, T. D., Watson, A., and Flaten, M. A. (2011). The placebo effect: advances from different methodological approaches. *J. Neurosci.* 31, 16117–16124. doi: 10.1523/JNEUROSCI.4099-11.2011

Meissner, K., Fässler, M., Rücker, G., Kleijnen, J., Hróbjartsson, A., Schneider, A., et al. (2013). Differential effectiveness of placebo treatments: a systematic review of migraine prophylaxis. *JAMA Intern. Med.* 173, 1941–1951. doi: 10.1001/jamainternmed.2013.10391

Meissner, K., and Linde, K. (2018). Are blue pills better than green? How treatment features modulate placebo effects. *Int. Rev. Neurobiol.* 139, 357–378. doi: 10.1016/bs.irn.2018.07.014

Meissner, K., and Ziep, D. (2011). Organ-specificity of placebo effects on blood pressure. *Auton. Neurosci.* 164, 62–66. doi: 10.1016/j.autneu.2011.06.006

Meyer, B., Yuen, K. S., Ertl, M., Polomac, N., Mulert, C., Büchel, C., et al. (2015). Neural mechanisms of placebo anxiolysis. *J. Neurosci.* 35, 7365–7373. doi: 10.1523/JNEUROSCI.4793-14.2015

Müller, V., Remus, K., Hoffmann, V., Tschöp, M. H., and Meissner, K. (2016). Effectiveness of a placebo intervention on visually induced nausea in women–A randomized controlled pilot study. *J. Psychosom. Res.* 91, 9–11. doi: 10.1016/j.jpsychores.2016.09.012

Napadow, V., Sheehan, J. D., Kim, J., Lacount, L. T., Park, K., Kaptchuk, T. J., et al. (2012). The brain circuitry underlying the temporal evolution of nausea in humans. *Cereb. Cortex* 23, 806–813. doi: 10.1093/cercor/bhs073

Peciña, M., Bohnert, A. S., Sikora, M., Avery, E. T., Langenecker, S. A., Mickey, B. J., et al. (2015). Association between placebo-activated neural systems and antidepressant responses: neurochemistry of placebo effects in major depression. *JAMA Psychiatr.* 72, 1087–1094. doi: 10.1001/jamapsychiatry.2015.1335

Quinn, V. F., and Colagiuri, B. (2014). Placebo interventions for nausea: a systematic review. *Ann. Behav. Med.* 49, 449–462. doi: 10.1007/s12160-014-9670-3

Quinn, V. F., and Colagiuri, B. (2016). Sources of placebo-induced relief from nausea: the role of instruction and conditioning. *Psychosom. Med.* 78, 365–372. doi: 10.1097/PSY.0000000000000265

Richardson, J. T. E. (2011). Eta squared and partial eta squared as measures of effect size in educational research. *Educ. Res. Rev.* 6, 135–147. doi: 10.1016/j.edurev.2010.12.001

Rief, W., and Glombiewski, J. A. (2012). The hidden effects of blinded, placebo-controlled randomized trials: an experimental investigation. *Pain* 153, 2473–2477. doi: 10.1016/j.pain.2012.09.007

Rief, W., Shedden-Mora, M. C., Laferton, J. A., Auer, C., Petrie, K. J., Salzmann, S., et al. (2017). Preoperative optimization of patient expectations improves long-term outcome in heart surgery patients: results of the randomized controlled PSY-HEART trial. *BMC Med.* 15:4. doi: 10.1186/s12916-016-0767-3

Ronel, J., Mehilli, J., Ladwig, K. H., Blattler, H., Oversohl, N., Byrne, R. A., et al. (2011). Effects of verbal suggestion on coronary arteries: results of a randomized controlled experimental investigation during coronary angiography. *Am. Heart J.* 162, 507–511. doi: 10.1016/j.ahj.2011.06.016

Rutherford, B. R., Wall, M. M., Brown, P. J., Choo, T.-H., Wager, T. D., Peterson, B. S., et al. (2016). Patient expectancy as a mediator of placebo effects in antidepressant clinical trials. *Am. J. Psychiatr.* 174, 135–142. doi: 10.1176/appi.ajp.2016.16020225

Vickers, A. J., Cronin, A. M., Maschino, A. C., Lewith, G., MacPherson, H., Foster, N. E., et al. (2012). Acupuncture for chronic pain: individual patient data meta-analysis. *Arch. Intern. Med.* 172, 1444–1453. doi: 10.1001/archinternmed.2012.3654

Vickers, A. J., Vertosick, E. A., Lewith, G., MacPherson, H., Foster, N. E., Sherman, K. J., et al. (2018). Acupuncture for chronic pain: update of an individual patient data meta-analysis. *J. Pain* 19, 455–474. doi: 10.1016/j.jpain.2017.11.005

Witt, C. M., Meissner, K., Pach, D., Thiele, C., Ludtke, R., Ghadiyali, Z., et al. (2012). Stimulation of gastric slow waves with manual acupuncture at acupuncture points ST36 and PC6–a randomized single blind controlled trial. *Neurogastroenterol. Motil.* 24, 438–445. doi: 10.1111/j.1365-2982.2012.01877.x

Zhang, C. S., Tan, H. Y., Zhang, G. S., Zhang, A. L., Xue, C. C., and Xie, Y. M. (2015). Placebo devices as effective control methods in acupuncture clinical trials: a systematic review. *PLoS One* 10:e0140825. doi: 10.1371/journal.pone.0140825

Zigmond, A. S., and Snaith, R. P. (1983). The hospital anxiety and depression scale. *Acta Psychiatr. Scand.* 67, 361–370.

Conflict of Interest: The authors declare that the research was conducted in the absence of any commercial or financial relationships that could be construed as a potential conflict of interest.

frontiers in Cellular Neuroscience

ORIGINAL RESEARCH
published: 06 December 2019
doi: 10.3389/fncel.2019.00537

Electroacupuncture Pretreatment Alleviates Cerebral Ischemic Injury Through α7 Nicotinic Acetylcholine Receptor-Mediated Phenotypic Conversion of Microglia

Zhi Ma[1†], Zengli Zhang[2†], Fuhai Bai[2], Tao Jiang[1], Chaoying Yan[1] and Qiang Wang[1]*

[1] Department of Anesthesiology, Center for Brain Science, The First Affiliated Hospital of Xi'an Jiaotong University, Xi'an, China, [2] Department of Anesthesiology, Xijing Hospital, Fourth Military Medical University, Xi'an, China

Electroacupuncture (EA) pretreatment alleviates cerebral ischemic injury through α7 nicotinic acetylcholine receptor (α7nAChR). We attempted to investigate whether the phenotypic conversion of microglia was involved in the therapeutic effect of EA pretreatment in cerebral ischemia through α7nAChR. Adult male Sprague–Dawley (SD) rats were subjected to middle cerebral artery occlusion (MCAO) after EA or α7nAChR agonist *N*-(3*R*)-1-azabicyclo[2.2.2]oct-3-yl-furo[2,3-*c*]pyridine-5-carboxamide hydrochloride (PHA-543,613 hydrochloride) and antagonist α-bungarotoxin (α-BGT) pretreatment. Primary microglia were subjected to drug pretreatment and oxygen-glucose deprivation (OGD). The expressions of the classical activated phenotype (M1) microglia markers induced nitric oxide synthase (iNOS), interleukin-1β (IL-1β), and cluster of differentiation 86 (CD86); the alternative activated phenotype (M2) microglia markers arginase-1 (Arg-1), transforming growth factor-β1 (TGF-β1), and cluster of differentiation 206 (CD206); and the pro-inflammatory cytokines tumor necrosis factor-α (TNF-α), interleukin-6 (IL-6), and anti-inflammatory cytokines interleukin-4 (IL-4) and interleukin-10 (IL-10) in the ischemic penumbra or in the supernatant of primary microglia were analyzed. The infarction volume and neurological scores were assessed 72 h after reperfusion. The cell viability and lactate dehydrogenase (LDH) release of neurons co-cultured with microglia were analyzed using cell counting kit-8 (CCK-8) and LDH release assays. EA pretreatment decreased the expressions of M1 markers (iNOS, IL-1β, and CD86) and pro-inflammatory cytokines (TNF-α and IL-6), whereas it increased the expressions of M2 markers (Arg-1, TGF-β1, and CD206) and anti-inflammatory cytokines (IL-4 and IL-10) by activating α7nAChR. EA pretreatment also significantly reduced the infarction volume and improved the neurological deficit. The activation of α7nAChR in microglia relieved the inflammatory response of primary microglia subjected to OGD and attenuated the injury of neurons co-cultured with microglia. In conclusion, EA pretreatment alleviates cerebral ischemic injury through α7nAChR-mediated phenotypic conversion of microglia, which may be a new mechanism for the EA pretreatment-induced neuroprotection against cerebral ischemia.

Keywords: stroke, electroacupuncture, α7 nicotinic acetylcholine receptor, microglia, inflammation

OPEN ACCESS

Edited by:
Younbyoung Chae,
Kyung Hee University, South Korea

Reviewed by:
Nadine Ahmed Kerr,
University of Miami, United States
Marta Olah,
Columbia University Irving Medical Center, United States
Donald Stein,
Emory University, United States

****Correspondence:***
Qiang Wang
dr.wangqiang@139.com

† These authors have contributed equally to this work

Specialty section:
This article was submitted to Cellular Neuropathology, a section of the journal Frontiers in Cellular Neuroscience

Received: *14 March 2019*
Accepted: *19 November 2019*
Published: *06 December 2019*

Citation:
Ma Z, Zhang Z, Bai F, Jiang T, Yan C and Wang Q (2019) Electroacupuncture Pretreatment Alleviates Cerebral Ischemic Injury Through α7 Nicotinic Acetylcholine Receptor-Mediated Phenotypic Conversion of Microglia. Front. Cell. Neurosci. 13:537. doi: 10.3389/fncel.2019.00537

INTRODUCTION

Stroke is one of the leading causes of death worldwide (Mozaffarian et al., 2016). High mortality and disability after stroke significantly increase the financial burden of the society and threaten public health. In response to ischemic stroke, microglia in the ischemic penumbra are excessively activated and show two different phenotypes in the early and late stages after ischemic stroke. The classical activated phenotype (M1) microglia are immediately activated after ischemic stroke and release robust inflammatory cytokines, such as interleukin-1β (IL-1β), tumor necrosis factor-α (TNF-α), and induced nitric oxide synthase (iNOS), which contribute to neuronal apoptosis and aggravate brain injury (Denes et al., 2007; Hu et al., 2012; DeGracia, 2013; Garden, 2013; Wang et al., 2013). At later time points after ischemic stroke, M1 phenotype microglia converted to the alternative activated phenotype (M2) microglia, which release anti-inflammatory cytokines and neurotrophic substances and contribute to repair of injury and neuroprotection (Kawabori and Yenari, 2015; Zhai et al., 2017). It may be a potential therapeutic target for the treatment of ischemic stroke to facilitate the phenotypic conversion of microglia from M1 to M2.

Electroacupuncture (EA), as a combination of traditional acupuncture and electrotherapy, not only inherits the benefits of traditional acupuncture but also integrates with the physiological effects of electric stimulation (Napadow et al., 2005). Previous studies have reported that EA effectively ameliorates TNF-α and interleukin-6 (IL-6) expressions in activated microglia (Liu et al., 2016; Tang et al., 2016) and increased anti-inflammatory cytokines, such as interleukin-4 (IL-4) and interleukin-10 (IL-10) (Jiang et al., 2017). The α7 nicotinic acetylcholine receptor (α7nAChR) is highly expressed in the central nervous system (CNS) and plays an important role in cholinergic anti-inflammatory pathway. Studies have showed that activating α7nAChR in microglia and macrophage inhibits the release of NO and TNF-α (Lutz et al., 2014; Baez-Pagan et al., 2015), suggesting that α7nAChR might be a target to regulate microglial phenotypes. Our previous study found that activating α7nAChR reduced cerebral ischemic injury (Wang et al., 2012). Therefore, we investigated the roles of microglial α7nAChR in the phenotypic conversion of microglia and the neuroprotective effects of EA pretreatment against ischemic stroke.

MATERIALS AND METHODS

Animals

Male Sprague–Dawley (SD) rats (weighing 280–300 g) were obtained from the Experimental Animal Center of the Xi'an Jiaotong University (Xi'an, Shaanxi Province, China) and were maintained under a 12-h light–dark cycle, a temperature of 21 ± 2°C, and humidity of 60–70% for at least 1 week before any drug treatment or surgery was conducted. All animal experiments were approved by the Ethics Committee for Animal Experimental Center of the Xi'an Jiaotong University and were conducted according to the Chinese National Institutes of Health Guide for the Care and Use of Laboratory Animals[1].

Culture of Cells and Co-culture of Neuron–Microglia

Culture of cells and co-culture of neuron–microglia were performed as previously described (Zhang Z. et al., 2018). Briefly, mixed primary glial cultures were isolated from the cerebral cortex of 1-day-old SD pups. After the meninges and hippocampus were removed, the cortical tissues were subjected to enzymatic digestion and mechanical isolation. Then, the mixed cells were passed through a 70-μm nylon mesh cell strainer and were seeded into the poly-L-lysine-coated cell culture flask in Dulbecco's modified Eagle's medium (DMEM) containing 10% fetal bovine serum (FBS) and 1% antibiotics (penicillin and streptomycin). Cells were maintained in a humidified incubator at 37°C enriched with 5% CO_2 and fed every 3–5 days with fresh medium. After 14 days, microglia were harvested from the mixed glial cultures by mild shaking at 220 r/min for 1 h and were seeded into cell culture containers. The purity of the microglia was confirmed by Iba1 staining (**Supplementary Figure S1**).

Primary neurons were isolated from the cerebral cortices of E17–E19 rat embryos and were seeded into the poly-L-lysine-coated cell culture plates. Then, cells were cultured in Neurobasal medium (Gibco, Invitrogen Corp., Carlsbad, CA, United States) containing 2% B27, 1% glutamine, and 1% penicillin/streptomycin (Sigma–Aldrich, St. Louis, MO, United States). Cells were kept in a humidified incubator at 37°C enriched with 5% CO_2.

For indirect co-culture of neuron–microglia, the primary microglia (microglia:neurons = 1:2) were added to 0.4-μm pore sized Transwell inserts (Costar, United States) 2 days after the neurons were seeded into the 24-well plates. After the primary microglia and neurons were co-cultured for 2 days, the microglia and neurons were separated to receive drugs or oxygen-glucose deprivation (OGD) treatment. Then, the neurons and microglia were co-cultured again for 24 h.

Groups and Drug Treatment

In vivo, first, to observe the neuroprotection of EA pretreatment and whether EA pretreatment induced the phenotypic conversion of microglia from M1 to M2 after ischemia–reperfusion injury, rats were randomly divided into three groups: sham, middle cerebral artery occlusion (MCAO), and EA + MCAO. The rats in the EA + MCAO group received EA for five consecutive days and were then subjected to MCAO for 90 min 1 day after the last EA pretreatment. The infarction volume and neurological scores were assessed 72 h after reperfusion. The expressions of α7nAChR; M1 microglia markers iNOS, IL-1β, and cluster of differentiation 86 (CD86); and M2 microglia markers arginase-1 (Arg-1), transforming growth factor-β1 (TGF-β1), and cluster of differentiation 206 (CD206) in the ischemic penumbra

[1]https://grants.nih.gov/grants/olaw/Guide-for-the-Care-and-use-of-laboratory-animals.pdf

were analyzed. The pro-inflammatory cytokine TNF-α and anti-inflammatory cytokine IL-10 in the ischemic penumbra were analyzed. Second, to determine whether α7nAChR was associated with the phenotypic conversion of microglia and the neuroprotection of EA pretreatment after ischemia–reperfusion injury, rats were randomly divided into the following groups: sham, MCAO, *N*-(3*R*)-1-azabicyclo[2.2.2]oct-3-yl-furo[2,3-*c*]pyridine-5-carboxamide (PHA-543,613) + MCAO, vehicle + MCAO (saline), EA + MCAO, and sham, MCAO, EA + MCAO, α-bungarotoxin (α-BGT) + EA + MCAO, and vehicle + EA + MCAO (saline). Rats in the PHA-543,613 + MCAO group received intraperitoneal injection of PHA-543,613 (1.0 mg/kg, Tocris Bioscience, Bristol, United Kingdom) once a day for five consecutive days (Wang et al., 2012) and were then subjected to MCAO 24 h after the last injection. Rats in the α-BGT + EA + MCAO group received intracerebroventricular injection of α-BGT (0.5 μg/kg, Tocris Bioscience, Bristol, United Kingdom) for 30 min before the onset of EA for five consecutive days (Wang et al., 2012) and were then subjected to MCAO 24 h after the last EA treatment. The expressions of M1 microglia markers (iNOS, IL-1β, and CD86), M2 microglia markers (Arg-1, TGF-β1, and CD206), pro-inflammatory cytokine TNF-α, and anti-inflammatory cytokine IL-10 in the ischemic penumbra were accordingly analyzed. The infarction volume and neurological scores were assessed 72 h after reperfusion.

In vitro, to further confirm whether the α7nAChR in microglia was associated with the conversion of microglial phenotypes, α7nAChR agonist PHA-543,613 (100 μM) and antagonist α-BGT (10 nM) were used. Primary cultured microglia were randomly divided into five groups: control, OGD, PHA-543,613 + OGD, α-BGT + PHA-543,613 + OGD, and α-BGT + OGD. The PHA-543,613 (100 μM) was added into the cultured medium of microglia 24 h before OGD treatment, and the α7nAChR antagonist α-BGT (10 nM) was added to cells 30 min prior to PHA-543,613 to block the α7nAChR (Macpherson et al., 2014; Kimura et al., 2019). The M1 microglia markers (IL-1β and CD86) and M2 microglia markers (Arg-1 and CD206) were detected by western blot analysis and immunofluorescence staining. In addition, a neuron–microglia co-culture system was established to investigate the neuroprotection of α7nAChR in microglia. After the primary microglia and neurons were co-cultured for 2 days, the microglia were subjected to PHA-543,613 or α-BGT separately, and then the primary microglia and neurons were exposed to OGD for 4 and 1 h, respectively (Zhang Z. et al., 2018). The pro-inflammatory cytokines (TNF-α and IL-6) and anti-inflammatory cytokines (IL-4 and IL-10) in the supernatants of cultured microglia were detected by enzyme-linked immunosorbent assay (ELISA). The cell viability and lactate dehydrogenase (LDH) release of neurons were detected 24 h after the reintroduction of oxygen and glucose.

All drugs were administered as previously described (Wang et al., 2012; Macpherson et al., 2014; Kimura et al., 2019). All experiments followed the principles of randomization and double blindness.

Intracerebral-Ventricular Injection

The rats were anesthetized with isoflurane and fixed on a stereotaxic apparatus (Narishige, Tokyo, Japan). A scalp incision was made, and the bregma was exposed. The stereotaxic apparatus was located at bregma and punched in the position of 1.5 mm lateral and 1.0 mm posterior to bregma at the left hemisphere. A stainless steel 26-gauge cannula (C315G; Plastics One Inc., Roanoke, VA, United States) was slowly introduced through the hole into the left lateral ventricle (3.8 mm below the cerebral dura mater). The cannula was fixed by dental cement, and four stainless steel screws were secured to the skull and occluded. The rats were allowed to recover from the operation 3 days before the next treatment.

Electroacupuncture Pretreatment

Electroacupuncture was conducted as previously described (Li et al., 2012). Briefly, the rats were anesthetized, fixed on the animal thermostatic operating table, and maintained at 37.0 ± 0.5°C. The acupoint "Baihui (GV 20)," which is located at the intersection of the sagittal midline and the line linking the two ears, was stimulated using the Hwato Electronic Acupuncture Treatment Instrument (model no. SDZ-V, Suzhou Medical Appliances Co., Ltd., Suzhou, China) at an intensity of 1 mA and dense-disperse frequency of 2/15 Hz for 30 min per day for 5 days (Li et al., 2012).

Middle Cerebral Artery Occlusion

The focal cerebral ischemia model of rats was induced by MCAO as described previously (Wang et al., 2009). Briefly, the rats were anesthetized with isoflurane. The right internal carotid artery was separated and occluded using an intraluminal filament technique. Regional cerebral blood flow (rCBF) was monitored using a transcranial Doppler ultrasound flowmeter (PeriFlux System 5000; PERIMED, Stockholm, Sweden). The body temperature of the rats was maintained at 37.0–37.5°C. The rats were available if the rCBF showed a sharp drop to 20 and were recovered up to more than 80% of baseline (pre-ischemia) level. There were no significant differences in physiological parameters during EA pretreatment (at the onset of EA, 15 min after EA, and at the end of EA) or surgery (at the onset of ischemia, 60 min after the onset of ischemia, and 30 min after reperfusion) according to our previous study (Wang et al., 2012).

Neurobehavioral Evaluation

The neurological score was assessed 72 h after reperfusion using an 18-point neurobehavioral scoring system, which contained spontaneous activity, limb symmetry, forepaw outstretching, climbing, body proprioception, and response to vibrissae touch by another experimenter who was blind to the experimental groups as previously described (Garcia et al., 1995). The details of the score criterion are provided in **Supplementary Table S1**.

Infarct Measurement

The infarct measurement was assessed by 2,3,5-triphenyltetrazolium chloride (TTC; Sigma–Aldrich, St. Louis, MO, United States) staining. The brain sections were stained

for 15 min at 37°C, followed by overnight immersion in 4% paraformaldehyde. The stained sections were photographed, and the unstained areas were measured as the infarcted volume using an image analysis software (Adobe Photoshop 8.0 CS, Adobe Systems, San Jose, CA, United States) by an experimenter who was blind to the experimental groups. Infarct volume was quantified as follows: relative infarct volume = (contralateral area − ipsilateral non-infarct area)/contralateral area.

Oxygen-Glucose Deprivation

The cells were switched to a serum- and glucose-free medium and were then transferred into a humidified hypoxic chamber, which contained mixed gas (5% CO_2 and 95% N_2) for 15 min at room temperature. The chamber was then sealed and placed in a container at 37°C. The OGD was carried out for 4 h (microglia) or for 1 h (neurons). Following the OGD, cells were incubated with normal medium for an additional 24 h after the reintroduction of oxygen and glucose.

Assessment of Neuron Cell Viability

The survival of neuron cells was evaluated by cell counting kit-8 (CCK-8) (Seven Sea Biotech, China) 24 h after OGD. The procedures were strictly conducted according to the manufacturer's instructions. Briefly, after the CCK-8 solution was added to each well of the 24-well plates, neurons were incubated for 4 h at 37°C. Eventually, the absorbance was measured at 450 nm using a microplate reader (Infinite M200; TECAN, Männedorf, Switzerland).

Lactate Dehydrogenase Release Assay

The LDH-Cytotoxicity Colorimetric Assay Kit II (#K313-500; BioVision Inc., Milpitas, CA, United States) was used to detect cell injury 24 h after OGD. The LDH reaction mixture was mixed according to the manufacturer's instructions and added to a 96-well plate (100 μl per well). Then, 10 μl of cell-free supernatant of the samples was incubated with this reaction mixture for 30 min at 37°C. Finally, the absorbance was measured at 450 nm using a microplate reader (Infinite M200; TECAN, Männedorf, Switzerland).

Analysis of Inflammatory Factors

Enzyme-linked immunosorbent assay (R&D Systems, Minneapolis, MN, United States) was used to measure the levels of TNF-α and IL-10 in the ischemic penumbra, and also the levels of TNF-α, IL-4, IL-6, and IL-10 in the supernatants of cultured microglia according to the manufacturer's instructions.

Immunofluorescence Staining

Immunofluorescence staining was performed on frozen coronal sections of rat brains or on primary cultured microglia plated on cover slips. The rat brains were fixed with 4% paraformaldehyde. After fixation and concentration gradient dehydration, the brains were cut into 12-μm-thick sections using a Leica CM1900 frozen slicer. The cells were fixed with 4% paraformaldehyde for 30 min. The brain sections and cell cover slips were washed three times with phosphate-buffered saline (PBS) and then incubated overnight at 4°C in a humidified atmosphere with primary antibodies. The following primary antibodies were used: rabbit anti-iNOS antibody (1:100; Abcam, Cambridge, United Kingdom), rabbit anti-liver arginase antibody (1:100; Abcam, Cambridge, United Kingdom), rabbit anti-IL-1β antibody (1:50; Santa Cruz Biotechnology, Dallas, TX, United States), rabbit anti-α7nAChR antibody (1:50; Santa Cruz Biotechnology, Dallas, TX, United States), and goat anti-Iba1 antibody (1:50; Santa Cruz Biotechnology, Dallas, TX, United States) were used. The Alexa Fluor 488-labeled donkey anti-goat secondary antibody (1:200; Santa Cruz Biotechnology, Dallas, TX, United States), Alexa Fluor 594-labeled goat anti-rabbit secondary antibody (1:200; Santa Cruz Biotechnology, Dallas, TX, United States), and Alexa Fluor 488-labeled goat anti-rabbit secondary antibody (1:200; Santa Cruz Biotechnology, Dallas, TX, United States) were incubated for 2 h at room temperature in the dark. 4′,6-Diamidino-2-phenylindole (DAPI) (ZLI-9557, Zsbio) was used to stain nuclei. The sections were mounted with 50% glycerol. Finally, the sections were viewed and photographed using an Olympus BX51 (Japan) fluorescence microscope.

Western Blot Analysis

To determine the expressions of α7nAChR, iNOS, IL-1β, CD86, Arg-1, TGF-β1, and CD206 in the ischemic penumbra of rats or in the microglia, proteins were extracted and western blot analysis was performed. Briefly, the extracted proteins were separated by 10% sodium dodecyl sulfate–polyacrylamide gel electrophoresis (SDS-PAGE) and electrically transferred to polyvinylidene difluoride (PVDF) membranes. Then, the membranes were blocked in TBST containing 5% non-fat dry milk for 1 h at room temperature and were successively incubated with the dilute primary and secondary antibodies. The following primary antibodies were used: anti-α7nAChR rabbit antibody (1:50; Santa Cruz Biotechnology, Dallas, TX, United States), anti-iNOS rabbit antibody (1:500; Abcam, Cambridge, United Kingdom), anti-IL-1β rabbit antibody (1:200; Santa Cruz Biotechnology, Dallas, TX, United States), anti-CD86 rabbit antibody (1:500; Proteintech, United States), anti-liver arginase rabbit antibody (1:1,000; Abcam, Cambridge, United Kingdom), an anti-TGF-β1 rabbit antibody (1:1,000; GeneTex, Irvine, CA, United States), anti-CD206 rabbit antibody (1:500; Proteintech, United States), and an anti-tubulin rabbit antibody (1:1,000; Beijing ComWin Biotech Co., Ltd, Beijing, China). In addition, horseradish peroxidase-conjugated goat anti-rabbit secondary antibodies (1:10,000; Beijing ComWin Biotech Co., Ltd, Beijing, China) were used. Protein bands were visualized using the LI-COR Odyssey System (LI-COR Biotechnology, Lincoln, NE, United States). The relative changes in protein expression were expressed as the ratio of the integrated optical density (OD) of the target protein band to that of β-tubulin.

Statistical Analysis

GraphPad Prism 7.0 software was used for performing statistical analysis. Data were collected by two independent and blind investigators. Comparisons among multiple groups were

undertaken using one-way ANOVA followed by Tukey's *post hoc* test. Neurological scores were presented as medians and were analyzed using two-tailed Mann–Whitney *U*-tests, and the other values were presented as the mean ± SD. p-Value < 0.05 was considered statistically significant.

RESULTS

Electroacupuncture Pretreatment Ameliorated Cerebral Ischemia Injury and Upregulated Microglial α7 Nicotinic Acetylcholine Receptor Expression in Ischemic Penumbra After Stroke

The influence of EA pretreatment on cerebral ischemia injury and α7nAChR expression in the ischemic penumbra was evaluated 72 h after reperfusion (**Figure 1B**). As shown in **Figure 1**, EA pretreatment, compared with the MCAO group, significantly ameliorated the infarction volume (**Figures 1A,C**, $^{**}p < 0.01$) and increased the neurological scores after stroke, which mean that the neurological deficits had been improved (**Figure 1D**, $^{**}p < 0.01$). Moreover, the protein expression of α7nAChR in the ischemic penumbra was significantly increased in the EA group compared with the MCAO group (**Figure 1E**, $^{*}p < 0.05$). In addition, we detected the expression of α7nAChR in microglia by immunofluorescent double labeling of α7nAChR and Iba1 (microglial marker). It showed that EA pretreatment, compared with the MCAO group, upregulated microglial α7nAChR expression in the ischemic penumbra (**Figure 1F**). These results indicated that EA pretreatment exerted neuroprotective effects and reversed the effects of MCAO on the expression of α7nAChR in the ischemic penumbra of rats subjected to ischemia injury.

Electroacupuncture Pretreatment Induced the Phenotypic Conversion of Microglia From M1 to M2 and Relieved Inflammatory Response in the Ischemic Penumbra After Stroke

The time point of 72 h after ischemia–reperfusion was the key time point for microglial transformation from M1 to M2 (Zhai et al., 2017); thus, this specific time point was selected for subsequent experiments. At 72 h after ischemia–reperfusion, the expression of M1 microglia markers iNOS and IL-1β in the ischemic penumbra were significantly decreased in the EA + MCAO group compared with the MCAO group (**Figures 2A,B**, $^{**}p < 0.01$), whereas the expressions of M2 microglia markers Arg-1 and TGF-β1 were remarkably increased (**Figures 2C,D**, $^{**}p < 0.01$), which indicated that EA pretreatment induced the phenotypic conversion of microglia from M1 to M2. The pro-inflammatory cytokine TNF-α was significantly decreased and anti-inflammatory cytokine IL-10 was notably increased after EA pretreatment in the ischemic penumbra as detected by ELISA (**Figures 2E,F**, $^{*}p < 0.05$, $^{***}p < 0.001$).

The α7 Nicotinic Acetylcholine Receptor Was Involved in the Conversion of the Microglial Phenotype After Oxygen-Glucose Deprivation *in vitro*

We used primary microglia to further investigate whether the microglial phenotypic conversion was caused by the activation of α7nAChR in microglia. The purity of cultured primary microglia was confirmed by Iba1 staining (**Supplementary Figure S1**). The α7nAChR was expressed in the microglia (**Figure 3A**). Compared with the OGD group without drug treatment, pretreating microglia with 100 μM of α7nAChR agonist PHA-543,613 24 h before OGD treatment induced the phenotypic conversion of microglia from M1 to M2 as assessed by the expression of Arg-1 in microglia exposed to OGD injury (**Figure 3B**, $^{***}p < 0.001$); thus, the concentration of PHA-543,613 was chosen for the following experiments. PHA-543,613 pretreatment significantly attenuated M1 microglia markers IL-1β and CD86 protein expressions (**Figures 3C,D** and **Supplementary Figure S2C**, $^{**}p < 0.01$) and increased M2 microglia markers Arg-1 and CD206 expressions (**Figures 3E,F** and **Supplementary Figure S2C**, $^{***}p < 0.01$) in the microglia exposed to OGD. When the function of α7nAChR was blocked by adding its antagonist α-BGT to cells 30 min prior to PHA-543,613, PHA-543,613 pretreatment lost its influence on the expression of M1 and M2 microglia markers (**Figures 3C–F** and **Supplementary Figure S2C**, PHA-543,613 + OGD vs. α-BGT + PHA-543,613 + OGD). No significant differences were found between the OGD group and the α-BGT + PHA-543,613 + OGD group. These results suggested that microglial α7nAChR contributed to the phenotypic conversion of microglia.

Activating Microglial α7 Nicotinic Acetylcholine Receptor Relieved Inflammatory Response and Induced Neuroprotection Against Oxygen-Glucose Deprivation Injury *in vitro*

The levels of pro-inflammatory cytokines TNF-α and IL-6 and the levels of anti-inflammatory cytokines IL-10 and IL-4 in the supernatants of primary microglia were detected 24 h after the reintroduction of oxygen and glucose. The levels of TNF-α and IL-6 were significantly decreased whereas the levels of IL-4 and IL-10 were remarkably increased in the PHA-543,613 + OGD group when compared with the OGD group (**Figures 4A,B**, $^{*}p < 0.05$, $^{**}p < 0.01$, $^{***}p < 0.001$). After the function of α7nAChR was blocked by its antagonist α-BGT, the PHA-543,613 pretreatment lost its influence on the expressions of TNF-α, IL-6, IL-4, and IL-10 (**Figures 4A,B**; PHA-543,613 + OGD vs. α-BGT + PHA-543,613 + OGD). To further observe the neuroprotection of microglial α7nAChR, neurons and microglia were co-cultured. During the drug treatments and OGD, neurons and microglia were fully separated to avoid activating α7nAChR in neurons owing to the leakage of drugs through the 0.4-μm pore-sized membrane of the Transwell inserts. According to the CCK-8 cell viability assay, activation of α7nAChR in microglia

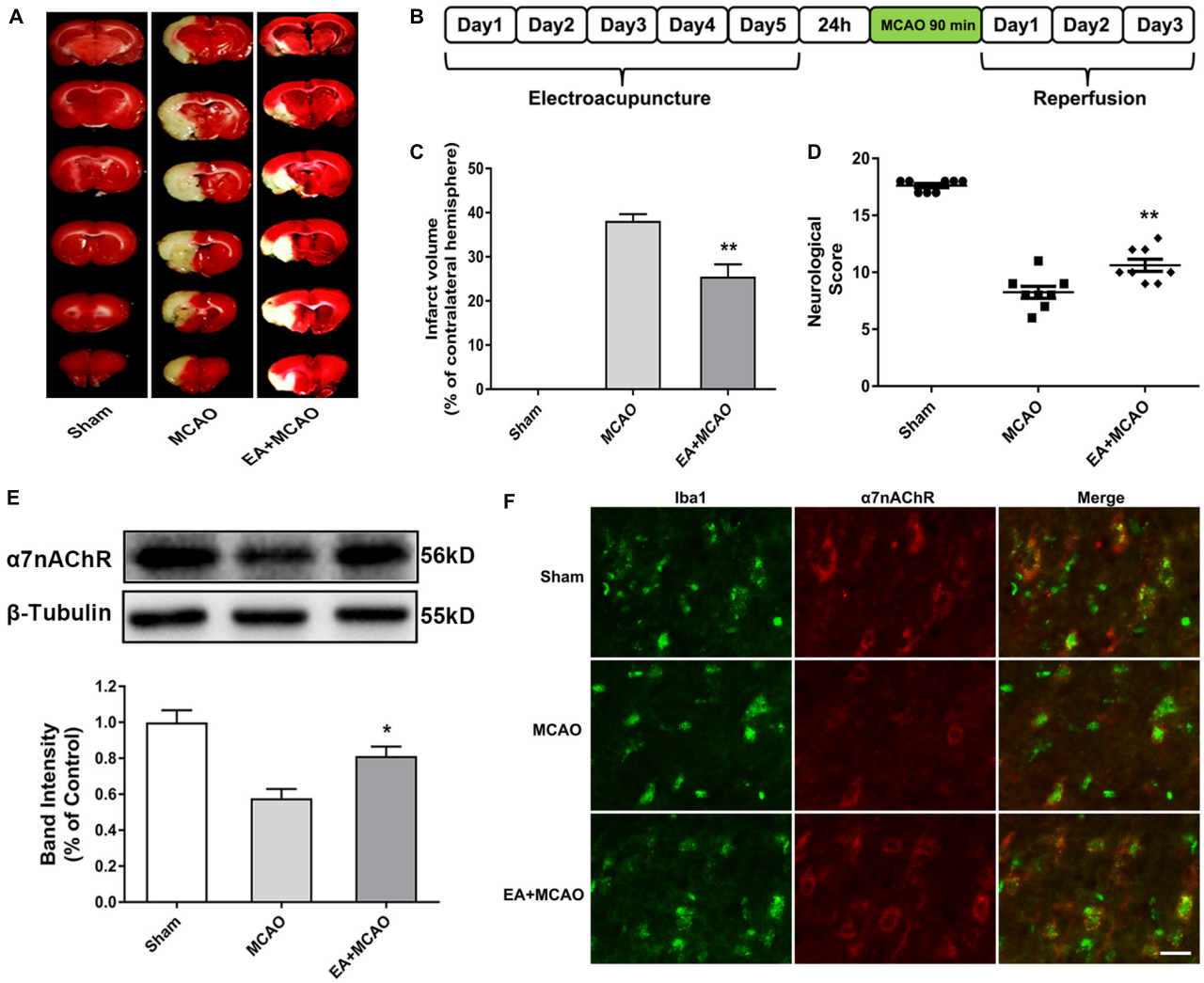

FIGURE 1 | Electroacupuncture (EA) pretreatment ameliorated cerebral ischemia injury and upregulated α7 nicotinic acetylcholine receptor (α7nAChR) expression in ischemic penumbra after stroke. **(A)** 2,3,5-Triphenyltetrazolium chloride (TTC) staining was used to measure infarct volume in coronal brain sections from sham, middle cerebral artery occlusion (MCAO), and MCAO + EA-treated rats at 72 h after reperfusion. **(B)** Schematic diagram of EA pretreatment. EA stimulation parameters: density-sparse wave of 2/15 Hz, current intensity of 1 mA, and 30 min/day for five consecutive days. **(C)** The percentages of infarct volume. The data were expressed as the mean ± *SD* and were analyzed by one-way ANOVA with Tukey's *post hoc* test. $n = 8$. $^{**}p < 0.01$ compared with the MCAO group. **(D)** Neurological deficit scores were evaluated 72 h after reperfusion. The data were expressed as the median and were analyzed by the Mann–Whitney *U*-test. $n = 8$. $^{**}p < 0.01$ compared with the MCAO group. **(E)** Western blot analysis of the expression level of α7nAChR protein in the ischemic penumbra 72 h after reperfusion. The data were expressed as the mean ± *SD* and were analyzed by one-way ANOVA with Tukey's *post hoc* test. $n = 5$. $^{*}p < 0.05$ compared with the MCAO group. **(F)** Representative immunofluorescence images showing the expression of α7nAChR in microglia in the ischemic penumbra after stroke. Microglial cells were labeled by Iba1 (microglia marker, green). $n = 5$. Scale bars = 20 μm.

significantly improved the viability of neurons compared with that in the OGD group (**Figure 4C**, $^{**}p < 0.01$). According to the LDH release assay, the levels of LDH release in the PHA-543,613 + OGD group were markedly lower than those in the OGD group (**Figure 4D**, $^{***}p < 0.001$). After the function of α7nAChR was blocked by its antagonist α-BGT, the PHA-543,613 pretreatment lost its influence on the viability and injury of neurons exposed to OGD (**Figures 4C,D**; PHA-543,613 + OGD vs. α-BGT + PHA-543,613 + OGD). No significant differences were observed between the OGD group and the α-BGT + PHA-543,613 + OGD group. These results indicated that activation of α7nAChR relieved inflammatory response and protected neurons from OGD injury.

Electroacupuncture Pretreatment Induced the Phenotypic Conversion of Microglia From M1 to M2 via α7 Nicotinic Acetylcholine Receptor After Stroke

The α7nAChR agonist PHA-543,613 and antagonist α-BGT were used to detect whether α7nAChR was associated with the phenotypic conversion of microglia *in vivo*. As illustrated

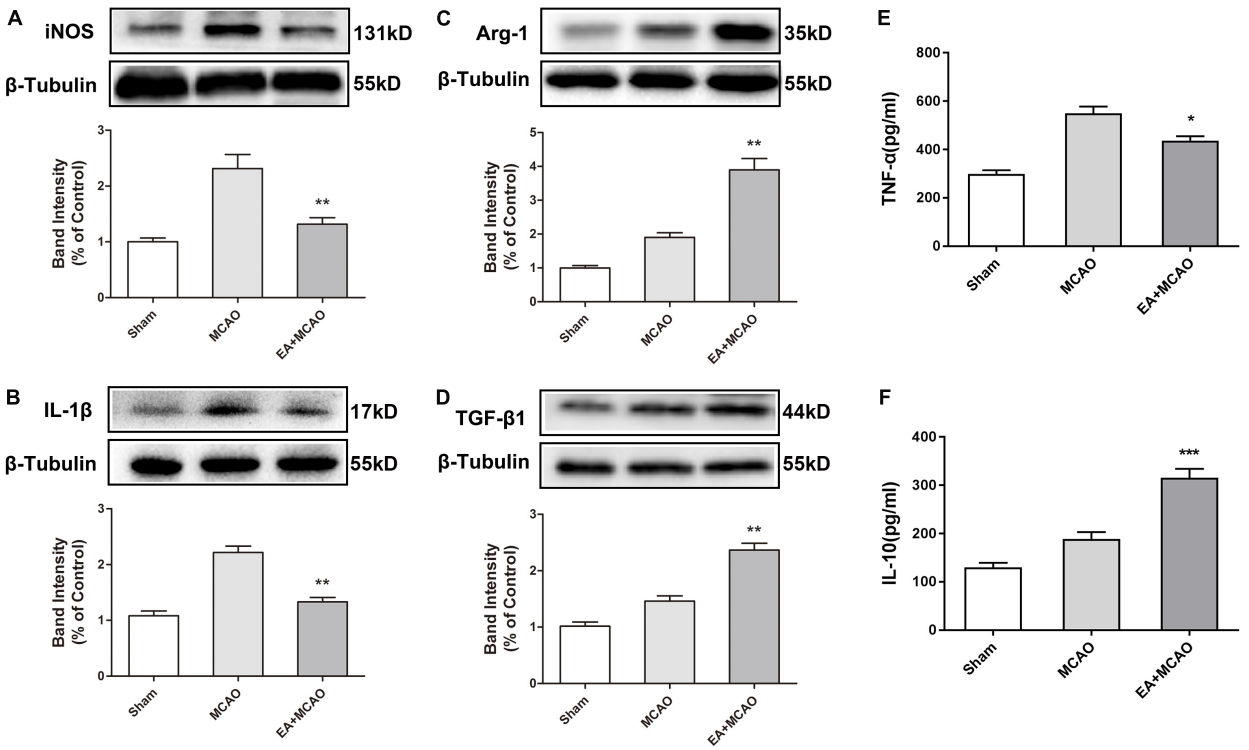

FIGURE 2 | Electroacupuncture (EA) pretreatment induced the phenotypic conversion of microglia from M1 to M2 and relieved inflammatory response in the ischemic penumbra after stroke. **(A–D)** Western blot analysis of the expression of M1 microglia markers nitric oxide synthase (iNOS) and interleukin-1β (IL-1β) as well as M2 microglia markers arginase-1 (Arg-1) and transforming growth factor-β1 (TGF-β1) in the ischemic penumbra 72 h after reperfusion. The data were expressed as the mean ± *SD* and were analyzed by one-way ANOVA with Tukey's *post hoc* test. $n = 5$. $^{**}p < 0.01$ compared with the MCAO group. **(E,F)** The levels of pro-inflammatory cytokine tumor necrosis factor-α (TNF-α) and anti-inflammatory cytokine interleukin-10 (IL-10). The data were expressed as the mean ± *SD* and were analyzed by one-way ANOVA with Tukey's *post hoc* test. $n = 5$. $^{*}p < 0.05$, $^{***}p < 0.001$ compared with the MCAO group.

in **Figure 5**, 72 h after ischemia–reperfusion, the expressions of M1 microglia markers iNOS, IL-1β, and CD86 in the ischemic penumbra were significantly reduced in the PHA-543,613 + MCAO group compared with the MCAO group (**Figure 5A** and **Supplementary Figure S2A**, $^{*}p < 0.05$, $^{**}p < 0.01$), whereas the expressions of M2 microglia markers Arg-1, TGF-β1, and CD206 were notably increased (**Figure 5B** and **Supplementary Figure S2A**, $^{*}p < 0.05$, $^{***}p < 0.001$). The EA and PHA-543,613 pretreatment had the same influence on the expression of iNOS, IL-1β, CD86, Arg-1, TGF-β1, and CD206 (**Figures 5A,B** and **Supplementary Figure S2A**). The expressions of M1 microglia markers iNOS, IL-1β, and CD86 in the ischemic penumbra were markedly increased in the α-BGT + EA + MCAO group compared with the EA + MCAO group (**Figure 5C** and **Supplementary Figure S2B**, $^{\#}p < 0.05$, $^{\#\#}p < 0.01$, $^{\#\#\#}p < 0.001$), whereas the expression of M2 microglia markers Arg-1, TGF-β1, and CD206 were significantly decreased (**Figure 5D** and **Supplementary Figure S2B**, $^{\#\#}p < 0.01$, $^{\#\#\#}p < 0.001$). The immunofluorescence assay revealed that the percentage of $iNOS^{+}/Iba1^{+}$ microglia in the ischemic penumbra of the EA + MCAO group was less than that in the MCAO group, and the percentage of $Arg\text{-}1^{+}/Iba1^{+}$ microglia in the ischemic penumbra of the EA + MCAO group was more than that in the MCAO group (**Figures 5E,F**, $^{***}p < 0.001$). After the function of α7nAChR was blocked by its antagonist α-BGT, the EA pretreatment lost its influence on the percentage of $iNOS^{+}/Iba1^{+}$ microglia and $Arg\text{-}1^{+}/Iba1^{+}$ microglia in the ischemic penumbra (**Figures 3E,F**, α-BGT + EA + MCAO vs. EA + MCAO). No significant differences were observed between the MCAO group and the α-BGT + EA + MCAO group. These findings suggested that EA pretreatment induced the phenotypic conversion of microglia from M1 to M2 via α7nAChR.

Electroacupuncture Pretreatment Relieved Inflammatory Response and Alleviated Cerebral Ischemia Injury via α7 Nicotinic Acetylcholine Receptor

The pro-inflammatory cytokine TNF-α and anti-inflammatory cytokine IL-10 in the ischemic penumbra 72 h after ischemia–reperfusion were measured by ELISA. The level of pro-inflammatory TNF-α was significantly decreased whereas the level of anti-inflammatory IL-10 was remarkably increased in the PHA-543,613 + MCAO group compared with the MCAO group (**Figures 6A,B**, $^{**}p < 0.01$, $^{***}p < 0.001$). The level of pro-inflammatory TNF-α was notably increased whereas the level of anti-inflammatory IL-10 was significantly decreased in the α-BGT + EA + MCAO group compared with the

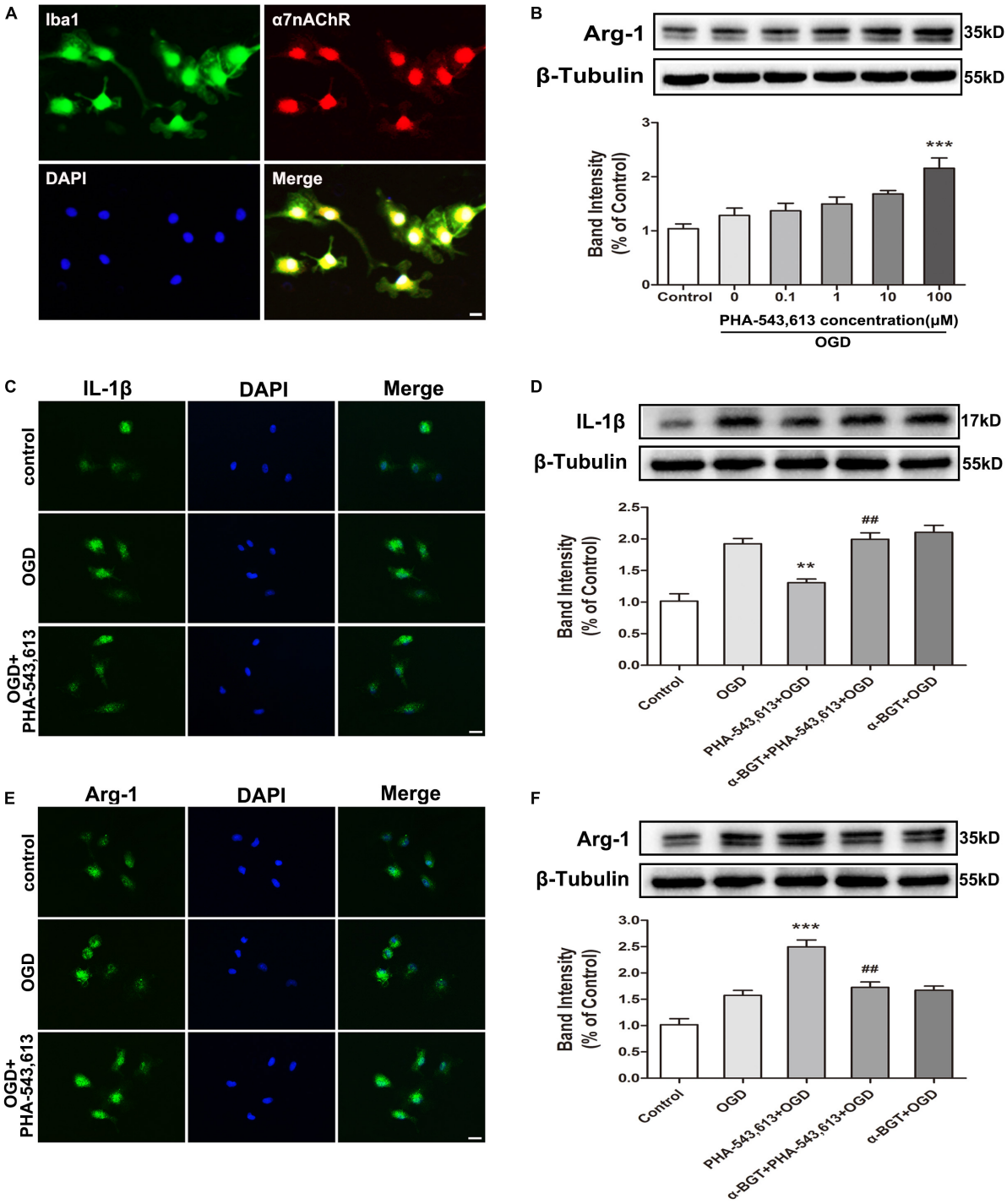

FIGURE 3 | α7 nicotinic acetylcholine receptor (α7nAChR) was involved in the modulation of the microglial phenotype after oxygen-glucose deprivation (OGD) *in vitro*. **(A)** Representative immunofluorescence images showing the expression of α7nAChR in primary microglia. Scale bar = 5 μm. **(B)** Western blot analysis of the expression levels of arginase-1 (Arg-1) protein in primary microglia exposed to different doses of PHA-543,613 24 h after the reintroduction of oxygen and glucose. The α7nAChR agonist PHA-543,613 was administrated 24 h before OGD. The data were expressed as the mean ± *SD* and were analyzed by one-way ANOVA with Tukey's *post hoc* test. The data were pooled from five independent experiments. $^{***}p < 0.001$ compared with the OGD group without drug treatment. **(C)** Immunofluorescence staining of M1 microglia marker IL-1β in primary microglia 24 h after the reintroduction of oxygen and glucose. The α7nAChR agonist PHA-543,613 (100 μM) was administrated 24 h before OGD. Scale bar = 5 μm. **(D)** Western blot analysis of the protein expression of IL-1β in primary microglia 24 h after the reintroduction of oxygen and glucose. The α7nAChR agonist PHA-543,613 (100 μM) was administrated 24 h before OGD. The α7nAChR antagonist α-BGT (10 nM) was administrated 30 min prior to PHA-543,613 to block the function of α7nAChR. The data were expressed as the mean ± *SD* and were analyzed

(Continued)

FIGURE 3 | Continued
by one-way ANOVA with Tukey's *post hoc* test. The data were pooled from five independent experiments. $^{**}p < 0.01$ compared with the OGD group, $^{\#\#}p < 0.01$ compared with the PHA-543,613 + OGD group. **(E)** Immunofluorescence staining of M2 microglia marker Arg-1 in primary microglia 24 h after the reintroduction of oxygen and glucose. Scale bar = 5 μm. **(F)** Western blot analysis of the protein expression of Arg-1 in primary microglia 24 h after the reintroduction of oxygen and glucose. The data were expressed as the mean ± *SD* and were analyzed by one-way ANOVA with Tukey's *post hoc* test. The data were pooled from five independent experiments. $^{***}p < 0.001$ compared with the OGD group, $^{\#\#}p < 0.01$ compared with the PHA-543,613 + OGD group.

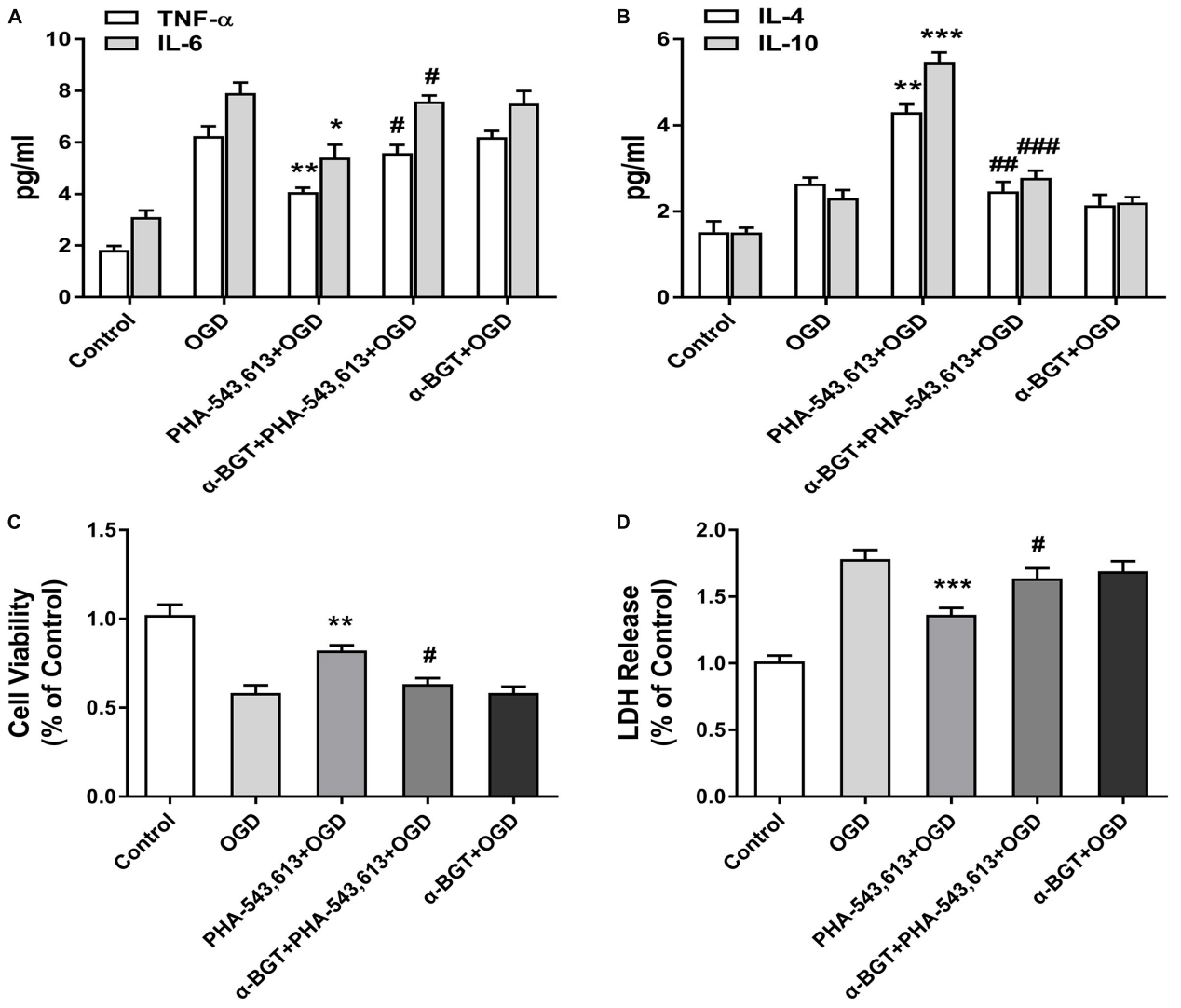

FIGURE 4 | Activating α7 nicotinic acetylcholine receptor (α7nAChR) in microglia relieved inflammatory response and induced neuroprotection against oxygen-glucose deprivation (OGD) injury *in vitro*. **(A)** The levels of the pro-inflammatory cytokines tumor necrosis factor-α (TNF-α) and interleukin-6 (IL-6) in the supernatants of primary microglia were detected by ELISA 24 h after the reintroduction of oxygen and glucose. The data were expressed as the mean ± *SD* and were analyzed by one-way ANOVA with Tukey's *post hoc* test. The data were pooled from five independent experiments. $^{*}p < 0.05$, $^{**}p < 0.01$ compared with the OGD group, $^{\#}p < 0.05$ compared with the PHA-543,613 + OGD group. **(B)** The levels of the anti-inflammatory cytokines IL-4 and IL-10 in the supernatants of primary microglia were detected by ELISA 24 h after the reintroduction of oxygen and glucose. The data were expressed as the mean ± *SD* and were analyzed by one-way ANOVA with Tukey's *post hoc* test. The data were pooled from five independent experiments. $^{**}p < 0.01$, $^{***}p < 0.001$ compared with the OGD group, $^{\#\#}p < 0.01$, $^{\#\#\#}p < 0.001$ compared with the PHA-543,613 + OGD group. **(C)** The cell viability of neurons co-cultured with microglia was detected by cell counting kit-8 (CCK-8) 24 h after the reintroduction of oxygen and glucose. The data were expressed as the mean ± *SD* and were analyzed by one-way ANOVA with Tukey's *post hoc* test. The data were pooled from five independent experiments. $^{**}p < 0.01$ compared with the OGD group, $^{\#}p < 0.05$ compared with the PHA-543,613 + OGD group. **(D)** The injury of neurons co-cultured with microglia was detected by lactate dehydrogenase (LDH) release assay 24 h after the reintroduction of oxygen and glucose. The data were expressed as the mean ± SD and were analyzed by one-way ANOVA with Tukey's *post hoc* test. The data were pooled from five independent experiments. $^{***}p < 0.001$ compared with the OGD group, $^{\#}p < 0.05$ compared with the PHA-543,613 + OGD group.

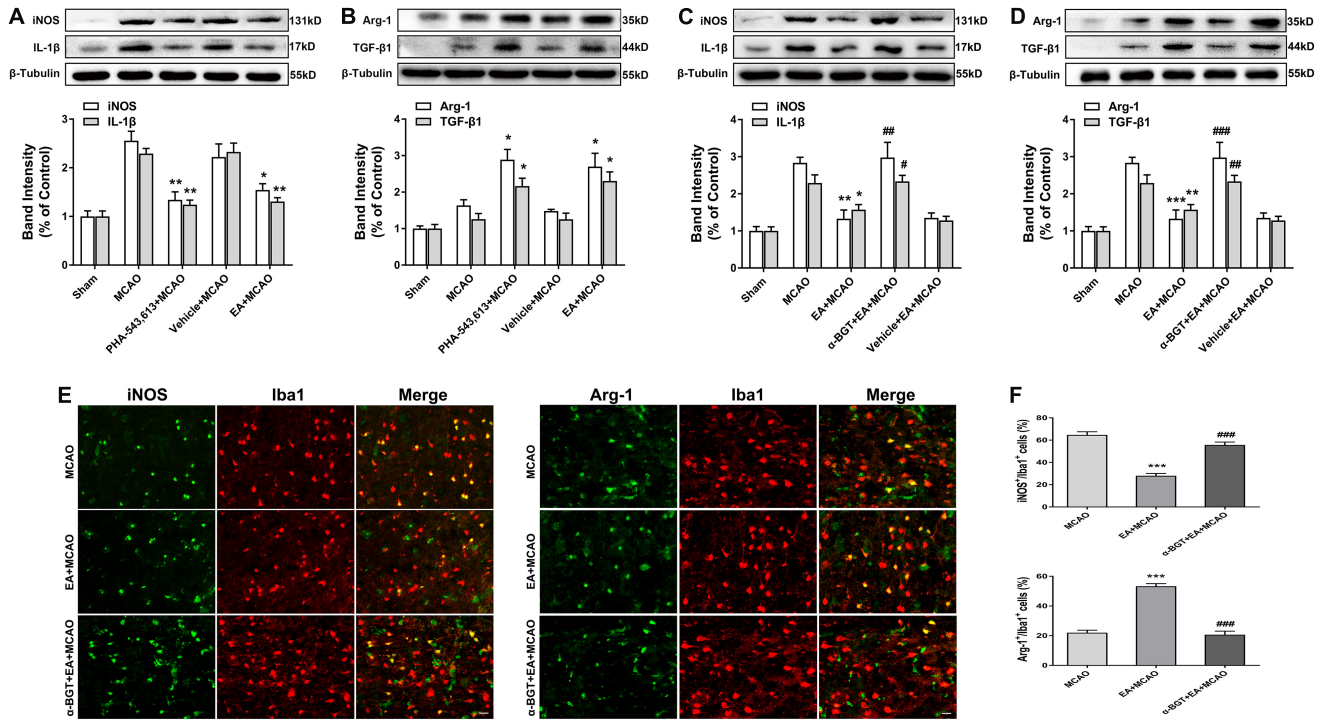

FIGURE 5 | Electroacupuncture (EA) pretreatment induced the phenotypic conversion of microglia from M1 to M2 via α7 nicotinic acetylcholine receptor (α7nAChR) after stroke. **(A)** Western blot analysis of the expression of M1 microglia markers nitric oxide synthase (iNOS) and interleukin-1β (IL-1β) in the ischemic penumbra 72 h after reperfusion. The data were expressed as the mean ± *SD* and were analyzed by one-way ANOVA with Tukey's *post hoc* test. $n = 5$. $^{*}p < 0.05$, $^{**}p < 0.01$ compared with the middle cerebral artery occlusion (MCAO) group. **(B)** Western blot analysis of the expression of M2 microglia markers arginase-1 (Arg-1) and transforming growth factor-β1 (TGF-β1) in the ischemic penumbra 72 h after reperfusion. The data were expressed as the mean ± *SD* and were analyzed by one-way ANOVA with Tukey's *post hoc* test. $n = 5$. $^{*}p < 0.05$ compared with the MCAO group. **(C)** Western blot analysis of the expression of M1 microglia markers iNOS and IL-1β in the ischemic penumbra 72 h after reperfusion. The data were expressed as the mean ± *SD* and were analyzed by one-way ANOVA with Tukey's *post hoc* test. $n = 5$. $^{*}p < 0.05$, $^{**}p < 0.01$ compared with the MCAO group, $^{\#}p < 0.05$, $^{\#\#}p < 0.01$ compared with the EA + MCAO group. **(D)** Western blot analysis of the expression of M2 microglia markers Arg-1 and TGF-β1 in the ischemic penumbra 72 h after reperfusion. The data were expressed as the mean ± *SD* and were analyzed by one-way ANOVA with Tukey's *post hoc* test. $n = 5$. $^{**}p < 0.01$, $^{***}p < 0.001$ compared with the MCAO group, $^{\#\#}p < 0.01$, $^{\#\#\#}p < 0.001$ compared with the EA + MCAO group. **(E)** Representative immunofluorescence images showing the expression of iNOS and Arg-1 in microglial cells. $n = 5$. Scale bar = 20 μm. **(F)** The percentage of $iNOS^{+}/Iba1^{+}$ and $Arg\text{-}1^{+}/Iba1^{+}$ cells. The data were expressed as the mean ± SD and were analyzed by one-way ANOVA with Tukey's *post hoc* test. $n = 5$. $^{***}p < 0.001$ compared with the MCAO group, $^{\#\#\#}p < 0.001$ compared with the EA + MCAO group.

PHA-543,613 + MCAO group (**Figures 6A,B**, $^{\#\#}p < 0.01$, $^{\#\#\#}p < 0.001$).

The infarct volume was significantly decreased and the neurological deficit was dramatically relieved in the PHA-543,613 + MCAO group compared with the MCAO group, whereas the infarct volume was increased and the neurological deficit was aggravated in the α-BGT + EA + MCAO group compared with the PHA-543,613 + MCAO group (**Figures 6C–E**, $^{**}p < 0.01$, $^{\#}p < 0.05$, $^{\#\#}p < 0.01$). No significant differences were observed between the MCAO group and the α-BGT + EA + MCAO group. These results further demonstrated that EA pretreatment displayed neuroprotective effect by regulating inflammatory response via α7nAChR.

DISCUSSION

In the present study, we investigated the roles of microglial α7nAChR in the neuroprotection of EA pretreatment against ischemic injury by *in vitro* and *in vivo* experiments. We found that EA pretreatment decreased the expression of M1 microglia markers (iNOS, IL-1β, and CD86) and pro-inflammatory cytokines (TNF-α and IL-6), whereas it increased the expression of M2 microglia markers (Arg-1, TGF-β1, and CD206) and anti-inflammatory cytokines (IL-4 and IL-10) in the ischemic penumbra and microglia by activating α7nAChR. EA pretreatment also significantly reduced the infarct volume and improved the neurological deficit. Activation of α7nAChR in microglia relieved the inflammatory response of primary microglia subjected to OGD and attenuated the injury of neurons co-cultured with microglia. Thus, although failing to completely cure stroke, EA pretreatment exerted neuroprotective effects against cerebral ischemic injury by promoting α7nAChR-mediated microglial phenotype conversion, suggesting a potential therapeutic target in the treatment of ischemic stroke.

Electroacupuncture confers strong neuroprotection against cerebral ischemic injury by inhibiting the inflammatory responses (Xiong et al., 2003; Wang et al., 2005, 2011;

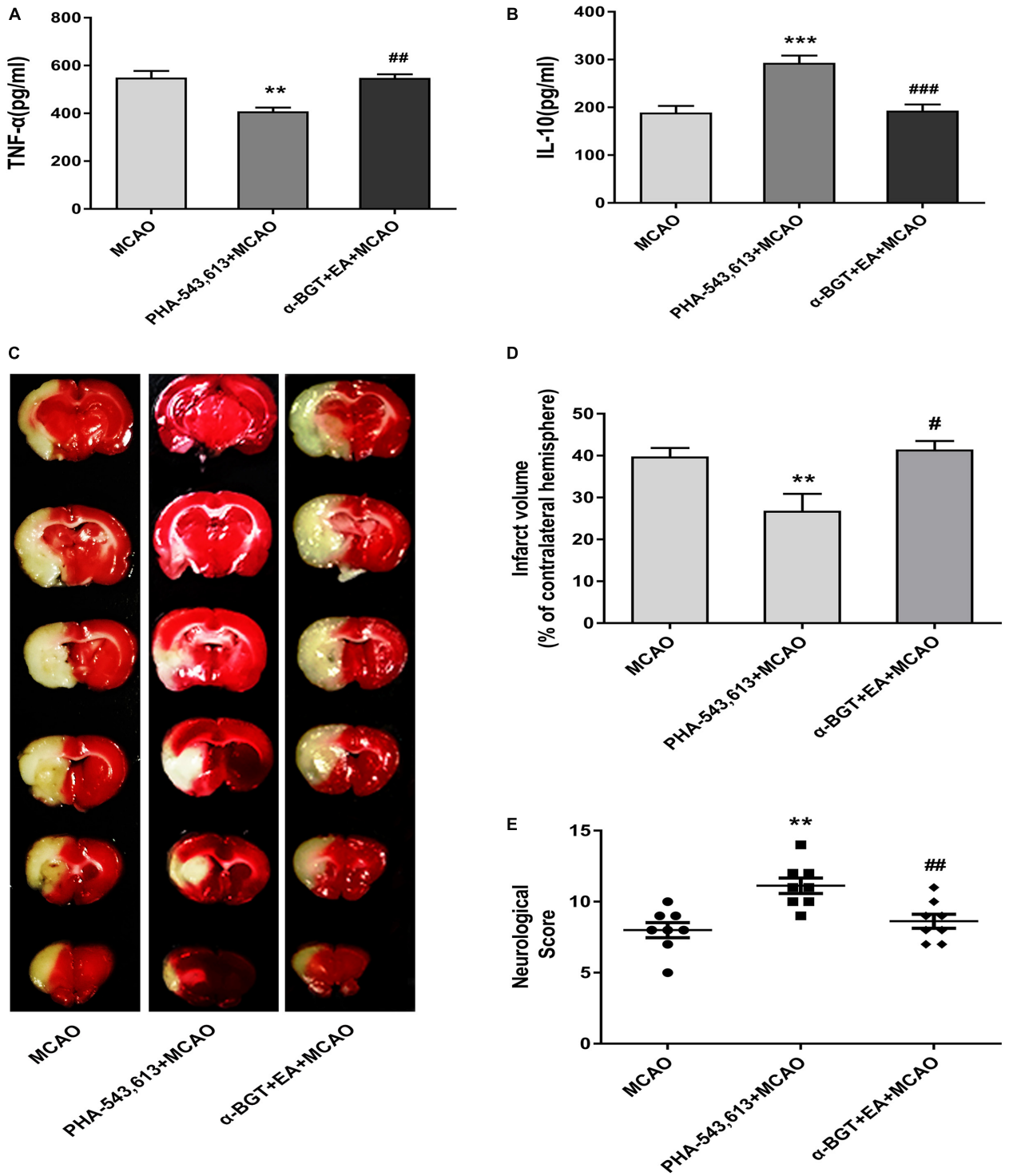

FIGURE 6 | EA pretreatment relieved inflammatory response and alleviated cerebral ischemia injury via α7 nicotinic acetylcholine receptor (α7nAChR). **(A,B)** The level of the pro-inflammatory cytokine tumor necrosis factor-α (TNF-α) and anti-inflammatory cytokine interleukin-10 (IL-10) in the ischemic penumbra was detected 72 h after reperfusion by ELISA. The data were expressed as the mean ± *SD* and were analyzed by one-way ANOVA with Tukey's *post hoc* test. $n = 5$. $^{**}p < 0.01$, $^{***}p < 0.001$ compared with the middle cerebral artery occlusion (MCAO) group, $^{\#\#}p < 0.01$, $^{\#\#\#}p < 0.001$ compared with the PHA-543,613 + MCAO group. **(C)** Representative photographs of brain slices showing the infarct volume assessed 72 h after reperfusion. **(D)** The percentages of infarct volume. The data were expressed as the mean ± *SD* and were analyzed by one-way ANOVA with Tukey's *post hoc* test. $n = 8$. $^{**}p < 0.01$ compared with the MCAO group, $^{\#}p < 0.05$ compared with the PHA-543,613 + MCAO group. **(E)** Neurological deficit scores were evaluated 72 h after reperfusion. The data were expressed as the median and were analyzed by the Mann–Whitney *U*-test. $n = 8$. $^{**}p < 0.01$ compared with the MCAO group, $^{\#\#}p < 0.01$ compared with the PHA-543,613 + MCAO group.

Hong et al., 2013; Zhu et al., 2013). A previous study has found that EA pretreatment suppresses the NF-κB signaling pathway by upregulating cylindromatosis to alleviate inflammatory injury after cerebral ischemia/reperfusion (Jiang et al., 2017). In addition, EA treatment inhibits microglia-mediated neuroinflammation through inactivation of p38 MAPK and MyD88, accompanied by the decrease of IL-1β, IL-6, and TNF-α after ischemic stroke (Liu et al., 2016). A randomized clinical trial provides evidences for the effectiveness of EA pretreatment on urinary leakage among women with stress urinary incontinence (Liu et al., 2017). In the current study, we demonstrated that EA pretreatment significantly decreased the expression of M1 microglia markers iNOS, IL-1β, and CD86, whereas it increased the expression of M2 microglia markers Arg-1, TGF-β1, and CD206 in the ischemic penumbra. Microglial cells are the pivotal mediators of neuroinflammation, performing functions by adopting different activation states, M1 phenotype with cytotoxic properties, and M2 phenotype with regeneration and repair (Colonna and Butovsky, 2017). The iNOS is transiently expressed during immune activation. Overproduction of NO by iNOS acts as a cytotoxic agent in pathological processes (Mukherjee et al., 2014). IL-1β is mainly produced by M1 microglia, expanding the microglia population in an autocrine manner and amplifying the production of inflammatory cytokines (Zhang C. J. et al., 2018). Arg-1 is expressed in the immune system and participates in a variety of inflammatory diseases by downregulation of nitric oxide synthesis, induction of fibrosis, and tissue regeneration (Munder, 2009). TGF-β1 has extensive immunomodulatory and anti-inflammatory properties and is abundantly produced in the ischemic penumbra by microglia (Islam et al., 2018). EA pretreatment transformed microglial phenotype from M1 to M2; thus, the expression of M1-related proteins decreased and M2-related proteins increased. Whether the inhibition of p38 MAPK-, MyD88-, and NF-κB-mediated signaling pathways is involved in the EA pretreatment-induced expression changes of iNOS, IL-1β, Arg-1, and TGF-β1 needs further investigation.

The α7nAChR is the pivotal receptor in the cholinergic anti-inflammatory pathway and is widely expressed in the CNS (Sharma and Vijayaraghavan, 2001; Gotti and Clementi, 2004; Shytle et al., 2004; Huston et al., 2006; De Jaco et al., 2017). Pharmacological stimulation of α7nAChR and stimulation of vagus nerve exert neuroprotective effects against cerebral ischemic injury (Kalappa et al., 2013; Parada et al., 2013; Jiang et al., 2014). Moreover, the α7nAChR signaling modulates the inflammatory phenotype of microglia in fetal brain, thereby providing a therapeutic approach for neuroinflammation *in utero* (Cortes et al., 2017). Consistent with these studies, we found that microglial α7nAChR played a key role in the neuroprotection of EA pretreatment against ischemic injury. In our study, activating α7nAChR in microglia promoted conversion of microglial phenotypes from M1 to M2 as assessed by the expression of M1 and M2 microglia markers, the pro-inflammatory cytokines (TNF-α and IL-6), and anti-inflammatory cytokines (IL-4 and IL-10) in the ischemic penumbra or in the supernatant of primary microglia. Furthermore, by establishing the microglia-neurons co-culture system, we found that activating α7nAChR in microglia increased neuronal cell viability and attenuated neuronal injury, which indicated that microglial α7nAChR exerted neuroprotection effects against OGD injury.

Microglial phenotypic transformation plays an important role in stroke, but the specific molecular mechanisms are not fully understood. A study has shown that cannabinoid receptors drive the acquisition of M2 polarization in microglia (Mecha et al., 2015). Inhibition of MyD88 signaling attenuates neuronal death in the hippocampus after status epilepticus in mice by skewing microglia/macrophage polarization (Liu et al., 2018). Our previous study found that activation or upregulation of triggering receptor expressed on myeloid cells 2 (TREM2) promoted the phenotypic conversion of microglia and thus decreased the number of apoptotic neurons in stroke mice (Zhai et al., 2017). Studies have also found that α7nAChR activation altered microglial phenotype by modulating intracellular iron load through α7nAChR-ferroportin signaling pathway, thus playing a neuroprotective role (Cortes et al., 2017). In addition, activation of the α7nAChR strongly inhibits the phosphorylation of p38 MAPK and upregulates phosphorylation of JAK2 and STAT3, thus transforming LPS-activated M1 microglia to the M2 phenotype (Zhang et al., 2017). Whether these pathways and signaling molecules are associated with the α7nAChR-mediated conversion of microglial phenotypes requires further clarification.

Our study includes some limitations. First, utilizing a rat model with a conditional knockout of the α7nAChR in microglia could better verify the effect of microglial α7nAChR. Second, as estrogen is an independent factor affecting the outcomes of stroke and the inflammatory signaling pathways, we failed to account for females. And long-term sensory or motor impairments detecting would be helpful to assess potential future therapies of EA pretreatment.

CONCLUSION

We found that EA pretreatment alleviated cerebral ischemic injury through the α7nAChR-mediated phenotypic conversion of microglia, which might be a new mechanism for EA pretreatment-induced neuroprotection against cerebral ischemia.

DATA AVAILABILITY STATEMENT

The raw data supporting the conclusions of this article will be made available by the authors, without undue reservation, to any qualified researcher.

AUTHOR CONTRIBUTIONS

Study supervision and study design was performed by QW. The study was conducted by ZM and ZZ. Data collection

and analysis were performed by FB, TJ, and CY. Writing and critical revision of the manuscript were performed by ZM, ZZ, and QW.

FUNDING

This work was supported by the National Natural Science Foundation of China (Grant Nos. 81473488 and 81774113) and the Overseas, Hong Kong and Macao Scholars Collaborative Researching Fund (Grant No. 81228022).

SUPPLEMENTARY MATERIAL

The Supplementary Material for this article can be found online at: https://www.frontiersin.org/articles/10.3389/fncel.2019.00537/full#supplementary-material

REFERENCES

Baez-Pagan, C. A., Delgado-Velez, M., and Lasalde-Dominicci, J. A. (2015). Activation of the macrophage alpha7 nicotinic acetylcholine receptor and control of inflammation. *J. Neuroimmune Pharmacol.* 10, 468–476. doi: 10.1007/s11481-015-9601-5

Colonna, M., and Butovsky, O. (2017). Microglia function in the central nervous system during health and neurodegeneration. *Annu. Rev. Immunol.* 35, 441–468. doi: 10.1146/annurev-immunol-051116-052358

Cortes, M., Cao, M., Liu, H. L., Moore, C. S., Durosier, L. D., Burns, P. (2017). alpha7 nicotinic acetylcholine receptor signaling modulates the inflammatory phenotype of fetal brain microglia: first evidence of interference by iron homeostasis. *Sci. Rep.* 7:10645. doi: 10.1038/s41598-017-09439-z

De Jaco, A., Bernardini, L., Rosati, J., and Tata, A. M. (2017). Alpha-7 nicotinic receptors in nervous system disorders: from function to therapeutic perspectives. *Cent. Nerv. Syst. Agents Med. Chem.* 17, 100–108. doi: 10.2174/1871524916666160729111446

DeGracia, D. J. (2013). A program for solving the brain ischemia problem. *Brain Sci.* 3, 460–503. doi: 10.3390/brainsci3020460

Denes, A., Vidyasagar, R., Feng, J., Narvainen, J., McColl, B. W., Kauppinen, R. A., et al. (2007). Proliferating resident microglia after focal cerebral ischaemia in mice. *J. Cereb. Blood Flow Metab.* 27, 1941–1953. doi: 10.1038/sj.jcbfm.9600495

Garcia, J. H., Wagner, S., Liu, K. F., and Hu, X. J. (1995). Neurological deficit and extent of neuronal necrosis attributable to middle cerebral artery occlusion in rats. Statistical validation. *Stroke* 26, 627–634.

Garden, G. A. (2013). Epigenetics and the modulation of neuroinflammation. *Neurotherapeutics* 10, 782–788. doi: 10.1007/s13311-013-0207-4

Gotti, C., and Clementi, F. (2004). Neuronal nicotinic receptors: from structure to pathology. *Prog. Neurobiol.* 74, 363–396. doi: 10.1016/j.pneurobio.2004.09.006

Hong, J., Wu, G., Zou, Y., Tao, J., and Chen, L. (2013). Electroacupuncture promotes neurological functional recovery via the retinoic acid signaling pathway in rats following cerebral ischemia-reperfusion injury. *Int. J. Mol. Med.* 31, 225–231. doi: 10.3892/ijmm.2012.1166

Hu, X., Li, P., Guo, Y., Wang, H., Leak, R. K., Chen, S., et al. (2012). Microglia/macrophage polarization dynamics reveal novel mechanism of injury expansion after focal cerebral ischemia. *Stroke* 43, 3063–3070. doi: 10.1161/strokeaha.112.659656

Huston, J. M., Ochani, M., Rosas-Ballina, M., Liao, H., Ochani, K., Pavlov, V. A., et al. (2006). Splenectomy inactivates the cholinergic antiinflammatory pathway during lethal endotoxemia and polymicrobial sepsis. *J. Exp. Med.* 203, 1623–1628. doi: 10.1084/jem.20052362

Islam, A., Choudhury, M. E., Kigami, Y., Utsunomiya, R., Matsumoto, S., Watanabe, H., et al. (2018). Sustained anti-inflammatory effects of TGF-β1 on microglia/macrophages. *Biochim. Biophys. Acta Mol. Basis Dis.* 1864, 721–734. doi: 10.1016/j.bbadis.2017.12.022

Jiang, J., Luo, Y., Qin, W., Ma, H., Li, Q., Zhan, J., et al. (2017). Electroacupuncture suppresses the NF-kappaB signaling pathway by upregulating cylindromatosis to alleviate inflammatory injury in cerebral ischemia/reperfusion rats. *Front. Mol. Neurosci.* 10:363. doi: 10.3389/fnmol.2017.00363

Jiang, Y., Li, L., Liu, B., Zhang, Y., Chen, Q., and Li, C. (2014). Vagus nerve stimulation attenuates cerebral ischemia and reperfusion injury via endogenous cholinergic pathway in rat. *PLoS One* 9:e102342. doi: 10.1371/journal.pone.0102342

Kalappa, B. I., Sun, F., Johnson, S. R., Jin, K., and Uteshev, V. V. (2013). A positive allosteric modulator of alpha7 nAChRs augments neuroprotective effects of endogenous nicotinic agonists in cerebral ischaemia. *Br. J. Pharmacol.* 169, 1862–1878. doi: 10.1111/bph.12247

Kawabori, M., and Yenari, M. A. (2015). The role of the microglia in acute CNS injury. *Metab. Brain Dis.* 30, 381–392. doi: 10.1007/s11011-014-9531-6

Kimura, I., Dohgu, S., Takata, F., Matsumoto, J., Kawahara, Y., Nishihira, M., et al. (2019). Activation of the α7 nicotinic acetylcholine receptor upregulates blood-brain barrier function through increased claudin-5 and occludin expression in rat brain endothelial cells. *Neurosci. Lett.* 694, 9–13. doi: 10.1016/j.neulet.2018.11.022

Li, X., Luo, P., Wang, Q., and Xiong, L. (2012). Electroacupuncture pretreatment as a novel avenue to protect brain against ischemia and reperfusion injury. *Evid. Based Complement. Alternat. Med.* 2012:195397. doi: 10.1155/2012/195397

Liu, J. T., Wu, S. X., Zhang, H., and Kuang, F. (2018). Inhibition of MyD88 signaling skews Microglia/macrophage polarization and attenuates neuronal apoptosis in the hippocampus after status epilepticus in mice. *Neurotherapeutics* 15, 1093–1111. doi: 10.1007/s13311-018-0653-0

Liu, W., Wang, X., Yang, S., Huang, J., Xue, X., Zheng, Y., et al. (2016). Electroacupunctre improves motor impairment via inhibition of microglia-mediated neuroinflammation in the sensorimotor cortex after ischemic stroke. *Life Sci.* 151, 313–322. doi: 10.1016/j.lfs.2016.01.045

Liu, Z., Liu, Y., Xu, H., He, L., Chen, Y., Fu, L., et al. (2017). Effect of electroacupuncture on urinary leakage among women with stress urinary incontinence: a randomized clinical trial. *JAMA* 317, 2493–2501. doi: 10.1001/jama.2017.7220

Lutz, J. A., Kulshrestha, M., Rogers, D. T., and Littleton, J. M. (2014). A nicotinic receptor-mediated anti-inflammatory effect of the flavonoid rhamnetin in BV2 microglia. *Fitoterapia* 98, 11–21. doi: 10.1016/j.fitote.2014.06.012

Macpherson, A., Zoheir, N., Awang, R. A., Culshaw, S., Ramage, G., Lappin, D. F., et al. (2014). The alpha 7 nicotinic receptor agonist PHA-543613 hydrochloride inhibits Porphyromonas gingivalis-induced expression of interleukin-8 by oral keratinocytes. *Inflamm. Res.* 63, 557–568. doi: 10.1007/s00011-014-0725-5

Mecha, M., Feliu, A., Carrillo-Salinas, F. J., Rueda-Zubiaurre, A., Ortega-Gutierrez, S., de Sola, R. G., et al. (2015). Endocannabinoids drive the acquisition of an alternative phenotype in microglia. *Brain Behav. Immun.* 49, 233–245. doi: 10.1016/j.bbi.2015.06.002

Mozaffarian, D., Benjamin, E. J., Go, A. S., Arnett, D. K., Blaha, M. J., Cushman, M., et al. (2016). Heart disease and stroke statistics-2016 update: a report from the american heart association. *Circulation* 133:e38-360. doi: 10.1161/cir.0000000000000350

Mukherjee, P., Cinelli, M. A., Kang, S., and Silverman, R. B. (2014). Development of nitric oxide synthase inhibitors for neurodegeneration and neuropathic pain. *Chem. Soc. Rev.* 43, 6814–6838. doi: 10.1039/c3cs60467e

Munder, M. (2009). Arginase: an emerging key player in the mammalian immune system. *Br. J. Pharmacol.* 158, 638–651. doi: 10.1111/j.1476-5381.2009.00291.x

Napadow, V., Makris, N., Liu, J., Kettner, N. W., Kwong, K. K., and Hui, K. K. (2005). Effects of electroacupuncture versus manual acupuncture on the human brain as measured by fMRI. *Hum. Brain Mapp.* 24, 193–205. doi: 10.1002/hbm.20081

Parada, E., Egea, J., Buendia, I., Negredo, P., Cunha, A. C., Cardoso, S., et al. (2013). The microglial alpha7-acetylcholine nicotinic receptor is a key element in promoting neuroprotection by inducing heme oxygenase-1 via nuclear factor erythroid-2-related factor 2. *Antioxid. Redox Signal.* 19, 1135–1148. doi: 10.1089/ars.2012.4671

Sharma, G., and Vijayaraghavan, S. (2001). Nicotinic cholinergic signaling in hippocampal astrocytes involves calcium-induced calcium release from

intracellular stores. *Proc. Natl. Acad. Sci. U.S.A.* 98, 4148–4153. doi: 10.1073/pnas.071540198

Shytle, R. D., Mori, T., Townsend, K., Vendrame, M., Sun, N., Zeng, J., et al. (2004). Cholinergic modulation of microglial activation by alpha 7 nicotinic receptors. *J. Neurochem.* 89, 337–343. doi: 10.1046/j.1471-4159.2004.02347.x

Tang, W. C., Hsu, Y. C., Wang, C. C., Hu, C. Y., Chio, C. C., and Kuo, J. R. (2016). Early electroacupuncture treatment ameliorates neuroinflammation in rats with traumatic brain injury. *BMC Complement. Altern. Med.* 16:470. doi: 10.1186/s12906-016-1457-6

Wang, G., Zhang, J., Hu, X., Zhang, L., Mao, L., Jiang, X., et al. (2013). Microglia/macrophage polarization dynamics in white matter after traumatic brain injury. *J. Cereb. Blood Flow Metab.* 33, 1864–1874. doi: 10.1038/jcbfm.2013.146

Wang, Q., Li, X., Chen, Y., Wang, F., Yang, Q., Chen, S., et al. (2011). Activation of epsilon protein kinase C-mediated anti-apoptosis is involved in rapid tolerance induced by electroacupuncture pretreatment through cannabinoid receptor type 1. *Stroke* 42, 389–396. doi: 10.1161/strokeaha.110.597336

Wang, Q., Peng, Y., Chen, S., Gou, X., Hu, B., Du, J., et al. (2009). Pretreatment with electroacupuncture induces rapid tolerance to focal cerebral ischemia through regulation of endocannabinoid system. *Stroke* 40, 2157–2164. doi: 10.1161/strokeaha.108.541490

Wang, Q., Wang, F., Li, X., Yang, Q., Li, X., Xu, N., et al. (2012). Electroacupuncture pretreatment attenuates cerebral ischemic injury through alpha7 nicotinic acetylcholine receptor-mediated inhibition of high-mobility group box 1 release in rats. *J. Neuroinflam.* 9:24. doi: 10.1186/1742-2094-9-24

Wang, Q., Xiong, L., Chen, S., Liu, Y., and Zhu, X. (2005). Rapid tolerance to focal cerebral ischemia in rats is induced by preconditioning with electroacupuncture: window of protection and the role of adenosine. *Neurosci. Lett.* 381, 158–162. doi: 10.1016/j.neulet.2005.02.019

Xiong, L., Lu, Z., Hou, L., Zheng, H., Zhu, Z., Wang, Q., et al. (2003). Pretreatment with repeated electroacupuncture attenuates transient focal cerebral ischemic injury in rats. *Chin. Med. J.* 116, 108–111.

Zhai, Q., Li, F., Chen, X., Jia, J., Sun, S., Zhou, D., et al. (2017). Triggering Receptor Expressed on Myeloid Cells 2, a Novel Regulator of Immunocyte Phenotypes, Confers Neuroprotection by Relieving Neuroinflammation. *Anesthesiology* 127, 98–110. doi: 10.1097/aln.0000000000001628

Zhang, C. J., Jiang, M., Zhou, H., Liu, W., Wang, C., Kang, Z., et al. (2018). TLR-stimulated IRAKM activates caspase-8 inflammasome in microglia and promotes neuroinflammation. *J. Clin. Invest.* 128, 5399–5412. doi: 10.1172/jci121901

Zhang, Q., Lu, Y., Bian, H., Guo, L., and Zhu, H. (2017). Activation of the α7 nicotinic receptor promotes lipopolysaccharide-induced conversion of M1 microglia to M2. *Am. J. Transl. Res.* 9, 971–985.

Zhang, Z., Qin, P., Deng, Y., Ma, Z., Guo, H., Guo, H., et al. (2018). The novel estrogenic receptor GPR30 alleviates ischemic injury by inhibiting TLR4-mediated microglial inflammation. *J. Neuroinflam.* 15:206. doi: 10.1186/s12974-018-1246-x

Zhu, X., Yin, J., Li, L., Ma, L., Tan, H., Deng, J., et al. (2013). Electroacupuncture preconditioning-induced neuroprotection may be mediated by glutamate transporter type 2. *Neurochem. Int.* 63, 302–308. doi: 10.1016/j.neuint.2013.06.017

Conflict of Interest: The authors declare that the research was conducted in the absence of any commercial or financial relationships that could be construed as a potential conflict of interest.

Advantages of publishing in Frontiers

OPEN ACCESS
Articles are free to read for greatest visibility and readership

FAST PUBLICATION
Around 90 days from submission to decision

HIGH QUALITY PEER-REVIEW
Rigorous, collaborative, and constructive peer-review

TRANSPARENT PEER-REVIEW
Editors and reviewers acknowledged by name on published articles

Frontiers
Avenue du Tribunal-Fédéral 34
1005 Lausanne | Switzerland

Visit us: www.frontiersin.org
Contact us: info@frontiersin.org | +41 21 510 17 00

REPRODUCIBILITY OF RESEARCH
Support open data and methods to enhance research reproducibility

DIGITAL PUBLISHING
Articles designed for optimal readership across devices

FOLLOW US
@frontiersin

IMPACT METRICS
Advanced article metrics track visibility across digital media

EXTENSIVE PROMOTION
Marketing and promotion of impactful research

LOOP RESEARCH NETWORK
Our network increases your article's readership